



University
of Glasgow

Ford, Laura Bernadette (2013) Characterising receptors for the chemokine CCL2, and their differential expression on dendritic cell subsets. PhD thesis

<http://theses.gla.ac.uk/4114/>

Copyright and moral rights for this thesis are retained by the author

A copy can be downloaded for personal non-commercial research or study, without prior permission or charge

This thesis cannot be reproduced or quoted extensively from without first obtaining permission in writing from the Author

The content must not be changed in any way or sold commercially in any format or medium without the formal permission of the Author

When referring to this work, full bibliographic details including the author, title, awarding institution and date of the thesis must be given.

Characterising receptors for the chemokine CCL2, and their differential expression on dendritic cell subsets

Laura Bernadette Ford

A thesis submitted to the College of Medicine, Veterinary and Life Sciences,
University of Glasgow in fulfilment of the requirements for the degree of Doctor
of Philosophy

March 2013

Institute of Infection, Immunity and Inflammation
University of Glasgow
120 University Place
Glasgow
G12 8TA

Summary

The generation of an effective immune response relies on the coordinated migration and interaction of cells of the immune system. Interactions between leukocytes and other cells occur within secondary lymphoid organs or at sites of inflammation. These interactions are tightly policed by a family of small chemotactic cytokines, or chemokines, that drive leukocyte migration.

Chemokines and their receptors are broadly divided into two functional groups, homeostatic and inflammatory. Typically homeostatic chemokines and their receptors regulate leukocyte migration to and within secondary lymphoid organs, whereas inflammatory chemokines and their receptors control migration of cells to sites of inflammation. However, this division is now blurred, as some inflammatory chemokine receptors also possess clear homeostatic roles. One such receptor is the chemokine receptor CCR2, which binds a number of inflammatory chemokines, including CCL2, CCL7 and CCL12. Further complexity is added to the chemokine biology field by the discovery of atypical chemokine receptors, which lack the capacity to signal in manner similar to conventional chemokine receptors, and are proposed to act as chemokine scavengers. The most frequently studied atypical chemokine receptor, D6, scavenges inflammatory chemokines, with a number of ligands overlapping with those of CCR2.

CCR2 has been reported to play a non-redundant role in the egress of Ly6C^{hi} monocytes from the bone marrow (BM) during homeostasis and inflammation. However, the role of CCR2 on other cell types has not been fully characterised and it is not known how much other CCR2⁺ cells may contribute to the role ascribed to CCR2 in several diseases, such as collagen-induced arthritis (CIA) and atherosclerosis. In addition, there is currently limited information about the leukocytic expression of D6, which can also bind CCL2. Although more information is available about CCR2, there are several conflicts reported between surface levels of CCR2 detected by antibody and transcript levels. To gain a true understanding of the function of these receptors in diseases it is crucial to have an accurate profile of CCR2 and D6 expression *in vivo* and subsequently determine the function of CCR2 and/or D6 on these cells. Therefore, the primary aim of this thesis was to generate a detailed profile of

CCR2 expression by leukocytes, focusing mainly on the spleen, but including lymph nodes (LNs), blood and BM.

In Chapter 3, I demonstrate that currently available anti-murine CCR2 antibodies are unreliable, as they were either unable to detect CCR2 or could only detect high levels of CCR2. I describe a novel technique using fluorescently labelled CCL2 (CCL2^{AF647}), which substantially enhanced CCR2 detection and enabled a detailed characterisation of D6 activity. Using this method, I present a comprehensive analysis of CCR2 and D6 expression on mouse leukocytes. CCR2 expression was primarily limited to myeloid cells, dendritic cells (DCs), and natural killer (NK) cells, with lymphoid cells having low levels of CCR2. Interestingly, my data illustrates that D6 expression is not as restricted as published data suggests, as several cell populations, such as plasmacytoid DCs (pDCs) and some monocyte populations were found to express both CCR2 and D6. Furthermore, I present preliminary evidence that suggests that CCR2 might exhibit cell-type specific responses to its ligands.

I also systematically analysed the cellular composition of lymphoid organs and the blood of CCR2 knock-out (KO) mice and compared it to age- and gender-matched wild-type (WT) controls. These studies revealed that CCR2 deletion only affected the distribution of cells of monocytic origin during homeostasis. In contrast, the results described in Chapter 4 demonstrated that systemic inflammation induced by lipopolysaccharide (LPS) affected the frequency of several populations possessing CCR2 activity, including Ly6C^{hi} monocytes and conventional DCs (cDCs). I also present data that suggests that LPS temporally regulates CCR2 and D6 activity in a cell type-specific manner.

In Chapter 5, I detail the identification of two subsets of pDCs, present in the spleen, BM, blood, and LNs that differ in their expression of CCR2 and D6. Both subsets were able to stimulate naïve T cell proliferation and responded to toll-like receptor 7 (TLR7) and TLR9 stimulation, in terms of interferon alpha (IFN α) production and expression of activation markers. However, transcriptomics and flow cytometry did reveal some notable differences between these two subsets and deficiency in D6 or CCR2 led to changes in the surface immunophenotype of pDCs at certain anatomical locations. I also demonstrate that pDCs are able to

migrate efficiently towards CCL2 *in vitro*, but that CCR2 was not required for the reported CCL2 dependent migration of pDCs to imiquimod-inflamed skin.

Taking these results together, I have established CCL2^{AF647} as a novel sensitive method of CCR2 detection, which facilitated the identification of two pDC subsets. Although I was unable to find a role for CCR2 on pDCs, further study might better define the function that CCR2, and D6, plays on pDCs. In Chapter 6 I discuss my findings, relating the results to published data and forming conclusions and hypotheses that can be examined further in future experiments.

Table of Contents

Summary.....	2
Table of Contents	5
List of Tables and Figures.....	9
Acknowledgements	11
Author's Declaration	12
Abbreviations.....	13
Chapter 1 – Introduction	17
1.1 Chemokines	18
1.1.1 Nomenclature and classification	19
1.1.2 Chemokine mediated control of cell movement.....	23
1.2 Chemokine receptors	28
1.2.1 Chemokine receptor signalling.....	29
1.2.2 Receptor desensitisation.....	33
1.3 Atypical Chemokine Receptors.....	33
1.4 Homeostatic versus inflammatory chemokines, and their roles in the immune system	35
1.4.1 Homeostatic chemokines.....	36
1.4.1.1 Structure and function of LNs.....	40
1.4.1.2 Structure and function of the spleen.....	46
1.4.2 Inflammatory chemokines and the innate immune system.....	50
1.5 Dendritic cells and their role in the immune system	51
1.5.1 Development of dendritic cells	51
1.5.2 cDCs.....	56
1.5.3 pDCs	60
1.5.3.1 Subsets of pDCs	61
1.5.3.2 Chemokine receptor expression.....	66
1.5.3.3 pDC function	69
1.6 Current understanding of CCL2 receptor expression and function	74
1.6.1 CCR2	74
1.6.1.1 CCR2 and neutrophils	74
1.6.1.2 CCR2 and monocytes	75
1.6.1.3 CCR2 in cDC biology.....	77
1.6.1.4 CCR2 and lymphocytes	78
1.6.1.5 CCR2 and disease.....	80
1.6.2 D6	81
1.7 Thesis Aims	86
Chapter 2 – Materials and Methods	88
2.1 Mice.....	88
2.2 Maintenance of Flt3L producing cell lines: Flt3L generation and isolation.....	88
2.3 Measurement of Flt3L by ELISA	89
2.4 LPS administration <i>in vivo</i>	89
2.5 Flt3L mediated expansion of DCs <i>in vivo</i>.....	89
2.6 Imiquimod administration <i>in vivo</i>	89
2.7 Preparation of single cell suspensions from lymphoid organs.....	90
2.8 Preparation of single cell suspensions from murine blood.....	90
2.9 Preparation of single cell suspension from human peripheral blood.....	91
2.10 Preparation of single cell suspensions from murine skin	91
2.11 Generation of BM-derived DCs.....	91
2.12 Flow cytometry.....	92

2.13	Conjugation of a fluorescent PE-Cy7 tandem dye to IL-17RB antibody.....	93
2.14	Staining of CCR2 using MC-21 antibody.....	93
2.15	Fluorescently labelled chemokines	94
2.16	Chemokine uptake assay	94
2.17	FACS purification of pDCs and cDCs.....	95
2.18	RNA preparation.....	95
2.19	Synthesis of complementary DNA (cDNA) from RNA	95
2.20	Microarray.....	96
2.21	QPCR	96
2.22	Co-culture of pDCs with naïve OTI or OTII T cells.....	97
2.23	Migration assays.....	97
2.24	<i>Ex vivo</i> stimulation of sorted pDCs to measure maturation of pDCs	98
2.25	<i>Ex vivo</i> stimulation of IFN α production by sorted pDCs.....	98
2.26	Measurement of IFN α production by ELISA	98
2.27	Cytospin preparation and staining	99
2.28	Statistical analyses.....	99
Chapter 3 – Using fluorescent CCL2 to detect CCR2 receptors.....		103
3.1	Currently available methods to detect CCR2	103
3.1.1	Examination of murine CCR2 detection by flow cytometry using commercially available anti-mouse CCR2 antibodies.....	105
3.1.2	Analysis of CCR2 detection by flow cytometry using a widely-used rat anti-mouse CCR2 monoclonal antibody, MC-21	105
3.1.3	Profiling CCR2 expression in murine lymphoid organs and blood using MC-21	107
3.2	Development of a sensitive method to detect CCR2	108
3.2.1	CCL2 ^{AF647} uptake assay can sensitively detect mouse CCR2 activity in cells from several lymphoid organs and the blood	110
3.3	Identification of cells carrying CCL2 receptor activity in mouse lymphoid tissue and blood	112
3.3.1	CCR2 activity in the spleen is predominantly restricted to cells of the innate immune system	112
3.3.2	Monocytes, CD11c ⁺ cells and pDCs possess CCR2 activity in the BM.....	115
3.3.3	CCR2 activity is predominantly restricted to monocytes, CD11c ⁺ cells and pDCs in the blood	116
3.3.4	CCR2 ⁺ cells are rare in resting PLNs.....	117
3.4	Effect of CCR2 deletion on the cellular composition of lymphoid organs and the blood	118
3.5	CCL2^{AF647} uptake assay detects CCL2 receptors in rat and human.....	119
3.6	Using CCL2^{AF647} uptake assay to determine CCR2 receptor specificity	121
3.6.1	Monitoring murine CCR2 activity in the presence of a competitor ligand.....	122
3.6.2	Establishing the effect of chemokine exposure on murine CCR2 activity.....	123
3.7	Summary	124
Chapter 4 – Impact of systemic inflammation on CCL2 receptor activity		145
4.1	Exploration of the dynamic changes in splenic leukocyte populations in response to systemic LPS administration and the affect of CCR2 deficiency	148
4.1.1	Splenic Ly6C ^{hi} monocytes.....	149
4.1.2	Splenic NK cells.....	150
4.1.3	Splenic neutrophils.....	151
4.1.4	Splenic MZ-B cells.....	151
4.1.5	Splenic pDCs	152
4.1.6	Splenic cDCs	153
4.2	Examination of the role of CCR2 in monocyte mobilisation during systemic inflammation.....	155
4.2.1	Evaluation of the role of CXCR2 on monocytes in the absence of CCR2.....	156

4.3	Summary	157
Chapter 5 – CCL2 receptors and pDCs		171
5.1	Detection of two subsets of pDCs based on CCR2 activity.....	171
5.2	Flt3L mediated <i>in vivo</i> expansion and <i>in vitro</i> generation of pDCs and their CCR2 activity	173
5.2.1	<i>In vitro</i> generation of pDCs.....	174
5.2.2	CCL2 receptor activity of <i>in vitro</i> BM-pDCs	175
5.2.3	<i>In vivo</i> expansion of pDCs.....	175
5.2.4	CCL2 receptor activity of <i>in vivo</i> expanded pDCs	176
5.3	Isolating CCL2 ^{hi} and CCL2 ^{lo} pDCs	177
5.4	Migration of pDCs in response to CCL2	177
5.5	Expression of known pDC markers by CCL2 ^{hi} and CCL2 ^{lo} pDCs.....	178
5.6	Morphology of CCL2 ^{hi} and CCL2 ^{lo} pDCs	182
5.7	<i>In vitro</i> function of the two subsets.....	183
5.7.1	T cell stimulatory capacity of CCL2 ^{hi} and CCL2 ^{lo} pDCs	183
5.7.1.1	Effect of pDC activation by TLR7 ligand on CD8 α ⁺ T cell stimulation	186
5.7.1.2	Establishing the impact of mCCL2 on pDC induced CD8 α ⁺ T cell proliferation.....	187
5.7.2	Analysing IFN α production by the two subsets.....	187
5.8	Determining transcriptional differences between CCL2 ^{hi} and CCL2 ^{lo} pDCs using transcriptomics	188
5.8.1	Experimental design	188
5.8.2	Performing the microarray.....	189
5.8.3	Examination of genes differentially expressed in CCL2 ^{hi} or CCL2 ^{lo} pDCs.....	191
5.8.4	Impact of culture on expression of genes identified as differentially expressed by CCL2 ^{hi} and CCL2 ^{lo} pDCs.....	192
5.8.5	Alterations in gene expression in pDCs as a result of culture with CCL2 ^{AF647}	193
5.8.6	Further analysis of gene differences between the two subsets.....	195
5.8.7	Effect of IL-13 on the activation of CCL2 ^{hi} and CCL2 ^{lo} pDC	197
5.8.8	Summary of microarray analysis	198
5.9	Strain dependent differences in the phenotype of pDCs.....	199
5.10	Investigating a role for CCR2 on pDCs during inflammation <i>in vivo</i>	201
5.10.1	Effect of CCR2 deficiency on pDCs during cutaneous inflammation.....	202
5.10.2	Effect of imiquimod on CCR2 activity of pDCs	202
5.11	Summary	203
Chapter 6 – Discussion.....		243
6.1	Introduction.....	243
6.2	Expression of CCR2 in steady-state animals.....	243
6.2.1	Antibody mediated detection of CCR2.....	244
6.2.2	Profiling CCL2 receptor activity using the CCL2 ^{AF647} assay.....	245
6.2.2.1	Myeloid cells.....	248
6.2.2.2	B cells.....	250
6.2.2.3	Populations A, B and C.....	251
6.2.2.4	Population D and CD11c ⁺ MHCII ⁻ cells	253
6.2.2.5	T cells	255
6.2.2.6	cDCs	256
6.3	Effect of systemic inflammation induced by LPS on CCR2 and D6 activity	259
6.4	Advantages and disadvantages of the CCL2 ^{AF647} assay	263
6.4.1	CCL2 ^{AF647} assay versus antibodies.....	263
6.4.2	CCL2 ^{AF647} assay versus knock-in reporter mice.....	269
6.5	Cellularity of lymphoid organs and blood in CCR2 KO	271
6.5.1	Steady-state	271
6.5.2	Systemic inflammation.....	272
6.5.2.1	Neutrophils.....	272
6.5.2.2	Monocytes.....	273

6.5.2.3	cDCs	274
6.6	CCL2 receptors and pDCs.....	277
6.6.1	Surface phenotype of CCL2 ^{hi} and CCL2 ^{lo} pDCs.....	278
6.6.2	CCR2- or D6-deficiency affects pDCs phenotype.....	281
6.6.3	Microarray analysis	283
6.7	What role does CCR2 play on pDCs?	286
6.8	Conclusions and future directions	290
Appendices		293
Appendix 1: List of genes examined for alterations in expression as an effect of incubation in Figure 5-26.		293
Appendix 2: List of published abstracts that I contributed to.		295
Appendix 3: Published work that I contributed to.		296
Appendix 4: List of my manuscripts in press or preparation.....		312
References		313

List of Tables and Figures

Chapter 1

Figure 1-1: Structure of the CC-chemokine ligand, CCL2.....	19
Table 1-1: Systematic nomenclature for chemokines.....	21
Figure 1-2: Leukocyte extravasation from blood vessels into underlying tissue.....	27
Figure 1-3: Chemokine receptor signalling cascade.....	32
Table 1-2: Atypical chemokine receptors and their ligands.....	35
Figure 1-4: Simplified diagram of LN structure.....	41
Figure 1-5: Simplified diagram of the structure of the spleen.....	47
Figure 1-6: Pathways of splenic DC development.	55
Table 1-3: Proposed expression of surface markers by developmentally immature and mature pDCs.	64

Chapter 2

Table 2-1: Antibodies and isotypes for flow cytometry of murine cells.....	100
Table 2-2: Antibodies and isotypes for flow cytometry of rat cells.....	101
Table 2-3: Antibodies and isotypes for flow cytometry of human cells.....	101
Table 2-4: Probes used in QPCR.....	102

Chapter 3

Figure 3-1: Antibody mediated CCR2 detection.	127
Figure 3-2: Testing the MC-21 anti-mouse CCR2 antibody.....	128
Figure 3-3: Further testing of the MC-21 anti-mouse CCR2 antibody.....	129
Figure 3-4: Detection of CCR2 expression using MC-21 antibody.	130
Figure 3-5: Using fluorescently labelled CCL2 to detect CCR2.....	131
Figure 3-6: mCCL22 competition is specific for D6 mediated uptake.....	132
Figure 3-7: CCL2 ^{AF647} uptake assay can detect CCR2 activity in multiple tissues.....	133
Figure 3-8: Competition of the CCR2 and D6 independent uptake in BM.	134
Figure 3-9: Characterisation of CCL2 receptor activity on murine splenic lymphocytes using CCL2 ^{AF647} ...	135
Figure 3-10: Characterisation of CCL2 receptor activity on murine splenic myeloid cells using CCL2 ^{AF647} .	136
Figure 3-11: Characterisation of CCL2 receptor activity on murine splenic DCs using CCL2 ^{AF647}	137
Figure 3-12: CCL2 receptor activity of murine BM cells as characterised by using CCL2 ^{AF647} assay.....	138
Figure 3-13: CCL2 receptor activity of murine blood cells as characterised by using CCL2 ^{AF647} assay.....	139
Figure 3-14: Characterisation of CCL2 receptor activity on murine LN cells using CCL2 ^{AF647}	140
Figure 3-15: Frequency of cell populations in WT and CCR2 KO.....	141
Figure 3-16: CCL2 ^{AF647} uptake assay can detect CCL2 receptor activity in other mammalian species.....	142
Figure 3-17: Effect of the presence of unlabelled CCR2 ligands on CCR2 activity of splenocytes, as measured by CCL2 ^{AF647}	143
Figure 3-18: Effect of chemokine exposure on CCR2 activity of splenocytes.....	144

Chapter 4

Figure 4-1: Effect of LPS on CCL2 receptor activity of splenic Ly6C ^{hi} monocytes.....	159
Figure 4-2: Effect of LPS on the frequency of splenic Ly6C ^{hi} monocytes.....	160
Figure 4-3: Effect of LPS on CCL2 receptor activity and frequency of splenic NK cells.	161
Figure 4-4: Effect of LPS on CCL2 receptor activity and frequency of splenic neutrophils.....	162
Figure 4-5: Effect of LPS on CCL2 receptor activity and frequency of splenic MZ-B cells.....	163
Figure 4-6: Effect of LPS on CCL2 receptor activity and frequency of splenic pDCs.....	164
Figure 4-7: Effect of LPS on CCL2 receptor activity of splenic CD11b ⁺ cDCs.....	165
Figure 4-8: Effect of LPS on CCR2 activity of splenic CD8 α ⁺ cDCs.....	166
Figure 4-9: Maturation of cDCs in response to LPS.....	167
Figure 4-10: Effect of LPS on splenic cDC frequencies.....	168
Figure 4-11: Effect of LPS on CCR2 activity and frequency of BM Ly6C ^{hi} monocytes.....	169
Figure 4-12: Assessment of the CXCR2 dependence of LPS induced monocyte mobilisation.....	170

Chapter 5

Table 5-1: Expected FCs when a gene is expressed at higher levels in CCL2 ^{hi} pDCs than CCL2 ^{lo} pDCs, and its expression is not affected by culture.	192
Table 5-2: Expected FCs when a gene is expressed at lower levels in CCL2 ^{hi} pDCs than CCL2 ^{lo} pDCs, and its expression is not affected by culture.	193
Figure 5-1: Detection of two subsets of splenic pDCs based on CCL2 ^{AF647} uptake.	205
Figure 5-2: Confirmation that the two subsets are truly pDCs.	206
Figure 5-3: Two subsets of pDCs can be defined by CCL2 ^{AF647} uptake in other lymphoid tissues.	207
Figure 5-4: Production of Flt3L by CHO-Flt3L and B16FL cells.	208
Figure 5-5: <i>In vitro</i> Flt3L expansion of pDCs.	209
Figure 5-6: Effect of <i>in vitro</i> Flt3L treatment on CCR2 activity of pDCs.	210
Figure 5-7: <i>In vivo</i> Flt3L expansion of pDCs.	211
Figure 5-8: Effect of <i>in vivo</i> Flt3L treatment on the two subsets of pDCs as defined by CCL2 ^{AF647} uptake.	212
Figure 5-9: Gating strategy for isolating splenic pDCs and the two subsets of pDCs.	213
Figure 5-10: Migration of pDCs in response to CCL2 <i>in vitro</i>	214
Figure 5-11: Expression of other chemokine receptors by splenic pDCs.	215
Figure 5-12: Expression of subset markers by splenic pDC CCL2 subsets.	216
Figure 5-13: Expression of activation markers by splenic pDC CCL2 subsets.	217
Figure 5-14: Morphology of the two subsets of pDCs.	218
Figure 5-15: Ability of pDCs to stimulate CD4 ⁺ T cell proliferation.	219
Figure 5-16: Ability of pDC subsets to stimulate CD4 ⁺ T cell proliferation.	220
Figure 5-17: Ability of pDCs to stimulate CD8 ⁺ T cell proliferation.	221
Figure 5-18: Ability of pDC subsets to stimulate CD8 ⁺ T cell proliferation.	222
Figure 5-19: R848 enhances the ability of pDCs to stimulate CD8 ⁺ T cell proliferation.	223
Figure 5-20: mCCL2 has no effect on the ability of pDCs to stimulate CD8 ⁺ T cell proliferation.	224
Figure 5-21: IFN α production by CCL2 ^{hi} and CCL2 ^{lo} pDCs.	225
Figure 5-22: Schematic representation of the potential effects of culture on gene expression.	226
Figure 5-23: RNA quantity and quality from sorted pDCs.	227
Figure 5-24: Gene differences between the two subsets of pDCs.	228
Figure 5-25: Effect of incubation on the expression of genes by pDCs.	229
Figure 5-26: Alteration in gene expression by pDCs, as a consequence of culture.	230
Figure 5-27: Final list of genes differences between the two pDC subsets.	231
Figure 5-28: Confirming differences in surface protein expression between the two pDC subsets, as detected by the microarray.	232
Figure 5-29: Effect of IL-13 on CpG-C induced CCL2 ^{hi} and CCL2 ^{lo} pDC activation.	233
Figure 5-30: Strain differences in the two subsets of pDCs based on CCL2 ^{AF647}	234
Figure 5-31: Strain differences in the expression of surface markers by total splenic pDCs in WT, D6 KO and CCR2 KO.	235
Figure 5-32: Strain differences in the expression of surface markers by total BM pDCs in WT, D6 KO and CCR2 KO.	236
Figure 5-33: No strain differences in the absolute number of splenic and BM pDCs.	237
Figure 5-34: Effect of imiquimod treatment on pDC numbers in the skin.	238
Figure 5-35: Effect of imiquimod treatment on inguinal LN pDCs.	239
Figure 5-36: Effect of imiquimod treatment on splenic pDCs.	240
Figure 5-37: Effect of imiquimod treatment on BM pDCs.	241
Figure 5-38: Effect of imiquimod treatment on blood pDCs.	242

Chapter 6

Table 6-1: CCR2 and D6 activity of splenic leukocyte populations.	247
Table 6-2: CCR2 and D6 activity of PLN leukocyte populations.	247
Table 6-3: CCR2 and D6 activity of BM leukocyte populations.	248
Table 6-4: CCR2 and D6 activity of blood leukocyte populations.	248

Acknowledgements

Firstly, I would like to thank my PhD supervisor, the newly ordained Prof. Rob Nibbs for his continued guidance and support throughout this project. I would also like to thank the Wellcome Trust for funding my studies. In addition, I would like to extend my thanks to Bill, Olwyn and Darren, especially Bill for all his words of encouragement during my first year.

For science-related help, I would like to extend special thanks to my lab mentor and friend, the ever-optimistic Chris. When science beat me down, your seemingly never ending optimism was contagious and convinced me time and time again that science was worth it. To my Serbo-Brit friend, Vuk thanks for your immeasurable help with my old adversary the Aria. When my patience failed me, you were always on hand to offer help and advice, plus takeaway and beer. Ellie, what can I say, meh! You've always been there to listen to my endless chat, science related or not. I consider you a life long friend. Ciao for now bella. I would also like to thank the current and past members of the Nibbs group, you made my time in work enjoyable and the long days less painful. It has been a pleasure to work with you all. I am also grateful for the help given to me by staff of the CRF, including, but not limited to, Joanne, Tony and Craig.

The unofficial motto for the University of Manchester, the university that I attended for my undergraduate degree, is "work hard; play hard." I must thank my friends in Glasgow for helping me to continue this culture. I have had many a laugh with all of you, in and outside of work, and you have all provided me with memories I shall cherish for years to come. My friends from home and Manchester, you have not been forgotten. I sometimes disappear, but yet you are always there for me. We have known each other for many years and I consider you all true friends.

Last but by no means least, I would like to extend my heartfelt thanks to my family. You have always provided me with support and a loving home to return/escape to. Without you none of this would have been possible.

Author's Declaration

I declare that, except where explicit reference is made to the contribution of others, that this thesis is the result of my own work and has not been submitted for any other degree at the University of Glasgow or any other institution.

Signature:

Printed name:

Abbreviations

The following abbreviations are used throughout this thesis:

aa	amino acid
AF647	alexafuor647
AIRE	autoimmune regulator
ANOVA	analysis of variance
APC	allophycocyanin
Ag	antigen
APCs	antigen-presenting cells
Arp2/3	actin related protein 2/3
β -ME	β -mercaptoethanol
B16FL	B16 melanoma line secreting Flt3L
BM	bone marrow
BM-pDC	BM derived pDCs
cAMP	cyclic adenosine monophosphate
CCL	CC chemokine ligand
CCR	CC chemokine receptor
CD	cluster of differentiation
cDC	conventional dendritic cell
Cdc42	cell division control protein 42 homolog
cDNA	complementary DNA
CDP	common DC progenitors
CFA	Complete Freund's adjuvant
CFSE	5-carboxyfluoresceindiacetate succinimidyl ester
CHO	Chinese hamster ovary
CHO-Flt3L	Flt3L from transfected CHO cell line
CIA	collagen-induced arthritis
CLP	common lymphoid progenitor
CM	conditioned media
CMP	common myeloid progenitor
CpG	cytosine phosphodiester guanine oligodeoxynucleotide
C-terminal	carboxy terminal
CXCL	CXC chemokine ligand
CXCR	CXC chemokine receptor
CX ₃ CL	CX₃C chemokine ligand
CX ₃ CR	CX₃C chemokine receptor
DAG	diacyl glycerol
°C	degrees Celsius
DC	dendritic cell
DNA	deoxyribonucleic acid
DSS	dextran sodium sulphate
DTR	diphtheria toxin receptor
EAE	experimental autoimmune encephalomyelitis
EDTA	ethylenediaminetetraacetic acid
ELISA	enzyme-linked immunosorbent assay
Erk	extracellular signal-regulated kinase
FACS	fluorescence activated cell sorting
FC	fold-change
FCS	foetal calf serum
FITC	fluorescein isothiocyanate

Flt3	Fms-like tyrosine kinase 3
Flt3L	Flt3 ligand
FMO	fluorescence minus one
FSC	forward scatter
GAG	glycosaminoglycan
GALT	gut associated lymphoid tissue
GC-RMA	GC-robust multi-array average
GDP	guanosine diphosphate
GM-CSF	granulocyte macrophage- colony stimulating factor
Δ MF1	geometric mean fluorescence intensity
GMP	granulocyte-monocyte progenitor
GFP	green fluorescent protein
GPCR	G-protein coupled receptor
GRK	G-protein coupled receptor kinase
GTP	guanosine triphosphate
h	human
HBSS	Hanks Balanced Salt Solution
HEPES	4-(2-hydroxyethyl)-1-piperazineethanesulfonic acid
HEK	human embryonic kidney
HEV	high endothelial venule
hi	high
hrs	hours
ICAM	intercellular adhesion molecule
ifitm	IFN induced transmembrane protein
IFN	interferon
Ig	Immunoglobulin
IL	interleukin
Immgen	Immunological Genome Project
iNOS	inducible nitric oxide synthase
inter	intermediate
i.p.	intraperitoneally
IP ₃	inositol triphosphate
IRF	IFN regulatory factor
i.v.	intravenously
JAK	Janus kinase
kD	kilodaltons
KO	knock-out
LCs	Langerhans cells
LFA1	leukocyte function-associated Ag 1
LN	lymph node
Lo	low
LPS	lipopolysaccharide
LT $\alpha_1\beta_2$	lymphotoxin $\alpha_1\beta_2$
LT β R	LT $\alpha_1\beta_2$ receptor
LTi	lymphoid tissue inducer
LTin	lymphoid tissue initiator
LTo	lymphoid tissue organiser
m	murine
MCMV	murine cytomegalovirus
MDP	macrophage DC precursors
MHCII	major histocompatibility complex class II
mins	minutes

µg	microgram
µl	microlitre
ml	millilitre
MLN	mesenteric LN
mM	millimolar
MMP	matrix metalloproteinase
mRNA	messenger RNA
MZ	marginal zone
ng	nanogram
NK cells	natural killer cells
nM	nanomolar
N-terminal	amino-terminal
OVA	ovalbumin
p	probability
PAK	p21-activated kinase
PALS	periarteriolar lymphoid sheath
PAMPs	pathogen-associated molecular patterns
PB	pacific blue
PBS	phosphate buffered saline
pDC	plasmacytoid DC
PDCA1	pDC Ag-1
PE	phycoerythrin
PerCP	peridinin-chlorophyll-protein
Phe	phenylalanine
PIP ₂	phosphatidylinositol bisphosphate
PI3K	phosphatidylinositol-3-kinase
PKC	protein kinase C
PLC	phospholipase C
PLN	peripheral LN
<i>plt/plt</i>	paucity of LN T cells mutation
PP	Peyer's patch
PRR	pattern recognition receptor
QPCR	quantitative polymerase chain reaction
R848	resiquimod
Rarg	retinoic acid receptor gamma
RFP	red fluorescent protein
rh	recombinant human
RIN	RNA integrity number
RMA	robust multi-array average
RNA	ribonucleic acid
RPM	revolutions per minute
RPMI	Roswell Park Memorial Institute-1640 medium
RQ	relative quantity
RT	room temperature
RT-PCR	reverse transcriptase-polymerase chain reaction
s.c.	subcutaneously
SD	standard deviation
secs	seconds
SLE	systemic lupus erythematosus
SN	supernatant
SOCS	suppressor of cytokine signalling
S1P	sphingosine-1-phosphate
S1P ₁	S1P receptor 1

Src	sarcoma
SSC	side scatter
STAT	signal transducer and activator of transcription
TCR	T cell receptor
Th	T helper
TipDC	TNF and iNOS producing DC
TLR	Toll-like receptor
TNF α	tumour necrosis factor alpha
TPA	12-O-tetradecanoylphorbol-13-acetate
TRAIL	TNF-related apoptosis-inducing ligand
Treg	regulatory T cell
Tyr	tyrosine
vs.	versus
WASP	Wiskott-Aldrich syndrome protein
WT	wild-type
XCL	XC chemokine ligand
XCR	XC chemokine receptor
xg	times gravity

Chapter 1 – Introduction

The immune system is at the forefront of defence against pathogens, the development of autoimmunity and immunopathology, and participates in the repair of damaged tissues. The ability to coordinate these responses requires a complex and highly organised system of cells and organs. The first line of defence against invading pathogens are organs, such as the skin and mucosal tissues, which act as physical barriers, protecting the body from initial injury or infection. A more coordinated response against pathogens is provided by the immune cells and organs of the lymphoid system.

The organs of the lymphoid system can be divided into primary and secondary lymphoid organs. Primary lymphoid organs, such as the bone marrow (BM) or thymus, are the sites of leukocyte generation, differentiation and maturation. Following their generation, naïve leukocytes leave these primary lymphoid organs and enter the blood. Several leukocyte populations, such as neutrophils (Eash et al., 2010) and monocytes (Serbina and Pamer, 2006), are dependent on members of the large family of *chemotactic cytokines*, known as chemokines, for their egress from the BM. Furthermore, CXCR4 and its ligand CXCL12 are involved in haematopoietic stem cell retention in the BM, as inhibition of the CXCL12-CXCR4 axis mobilises stem cells (Sharma et al., 2011). Chemokines and their receptors also play a role in the generation of naïve leukocytes by coordinating the migration of developmental precursors within the organ. For example, cell migration during T cell development in the thymus is dependent on several homeostatic chemokine receptors, particularly CCR7 and CCR9 (Misslitz et al., 2004; Förster et al., 2008; Nitta et al., 2008). Once in the periphery, leukocytes are guided by chemokines to secondary lymphoid organs, such as the spleen and lymph nodes (LNs). Alternatively they patrol the blood and tissues for pathogens. In response to a pathogen or sterile inflammation and tissue damage, leukocytes exhibit either a rapid response with low specificity or a highly specific response, and it is this distinction that divides the immune system into two branches: the innate and adaptive immune systems. The innate immune system provides a rapid response, which unlike the adaptive immune system is not antigen (Ag) specific, but is driven by the recognition of specific molecules on pathogens, known as pathogen associated molecular patterns (PAMPs). In contrast, the adaptive immune system is highly Ag specific. The

coordinated interaction between the innate and adaptive arms of the immune system is required to produce an effective immune response. Dendritic cells (DCs) are a critical component of this interaction. At sites of inflammation DCs take up Ag and mature as they migrate in a chemokine dependent manner to LNs via the lymphatics. Within the LN, chemokines direct the interaction of Ag loaded DCs with naïve T lymphocytes, and the subsequent interaction of T and B lymphocytes. The newly differentiated plasmablasts are located in the red pulp of the spleen and produce antibody (Mebius and Kraal, 2005). In contrast, activated T lymphocytes exit LNs and migrate to the original site of Ag encounter where they complement the existing response produced by cells of the innate immune system. This highly coordinated response allows for the eradication of pathogens. However, not all immune responses are beneficial, as activation of the immune system against harmless Ag, such as self-peptides, can be detrimental, leading to pathology. The immune system can discriminate between harmless and pathogenic Ags and in a process known as immune tolerance, lymphocytes are rendered non-reactive to harmless Ag or can develop into regulatory T cells that actively suppress immune responses. Allergic responses and autoimmune diseases, such as Crohn's disease are caused by a break in tolerance to a harmless Ag (Sartor, 2006). Therefore, tight regulation of immune responses is required to maintain a healthy pathogen-free host that does not develop destructive autoimmunity.

In this Introduction, I will describe the role that chemokines and their receptors play in the development and maintenance of lymphoid organs, with a more detailed account of their function in secondary lymphoid organs. I will also discuss the role of inflammatory chemokines and the innate immune system, providing a detailed review of the DC system. Finally, I will summarise the roles that the CCL2 chemokine receptors, CCR2 and D6, have been reported to play in the immune system. It is these chemokine receptors that form the focus of my thesis.

1.1 Chemokines

Chemokines are small secreted *chemotactic cytokines*, approximately 8-12 kDa in size (Allen et al., 2007). Primarily known for their ability to direct migration of immune cells, this is not their only role, being important for angiogenesis,

tumour metastasis, wound healing, development and maintenance of immune tissues, and response to infection (Raman et al., 2011). The majority of chemokines are secreted proteins, however two chemokines CXCL16 and CX₃CL1 are tethered to extracellular surfaces by mucin-like stalks. In fact the interaction of all chemokines with components of the extracellular matrix is a key aspect of their biology. Moreover, the membrane-bound chemokines can be cleaved to release soluble, diffusible protein (Murphy et al., 2000; Allen et al., 2007). Secreted and membrane-bound chemokines share similarities in their tertiary structure, despite variability in their primary amino acid (aa) sequence. The conserved tertiary structure of chemokines consists of a disordered N-terminus that contains signalling and receptor binding domains. The disordered N-terminus is followed by a long N-loop, β -sheets and a C-terminal α -helical tail (Figure 1-1) (Allen et al., 2007). This conserved structure is important for binding to chemokine receptors with variations in aa sequence, dictating receptor specificity.

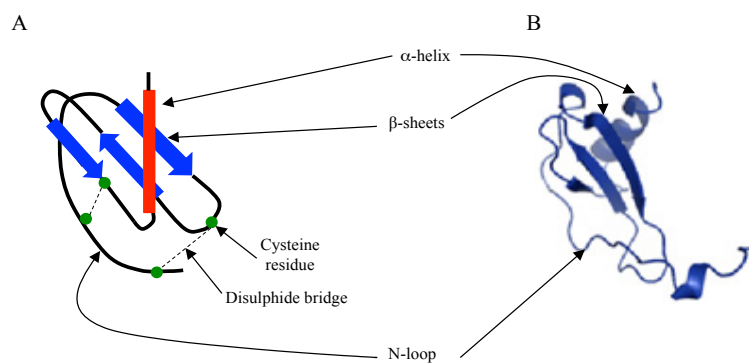


Figure 1-1: Structure of the CC-chemokine ligand, CCL2.

Schematic representation (A) and the crystal structure (B) of CCL2, illustrating the features of the conserved tertiary structure of chemokines. Schematic representation was adapted from (Deshmane et al., 2009) and the crystal structure was adapted from (Salanga and Handel, 2011).

1.1.1 Nomenclature and classification

In the late 90s, various bioinformatic and cloning strategies led to a large expansion of the number of identified chemokines (Murphy et al., 2000). Previously, they were identified in the culture media of stimulated cells. The proteins required for induction of directed cell migration were purified and sequencing of these proteins identified them as chemokines (Wells et al., 1998; Murphy et al., 2000). Historically, chemokines were named based on their identified functions, however this meant chemokines had several alternative names. Thus, within the chemokine research field there was a call for a more systematic nomenclature to be established. This standardised method to classify

chemokines is based on their structure, which is dictated by the number and spacing of conserved cysteine residues within their primary sequence (i.e. CC, CXC, CX₃C and XC). Furthermore, chemokines are numbered according to when the gene encoding the chemokine was first reported. There are four families of chemokines: CC chemokines, CXC chemokines, C chemokines and CX₃C, all members of which are listed in Table 1-1 (Murphy et al., 2000; Rossi and Zlotnik, 2000).

CC chemokines, like CXC and CX₃C chemokines, have four conserved cysteine residues, although some contain additional cysteine residues not present in other chemokines (e.g. CCL21). These four cysteine residues help in the retention of the functional tertiary structure, plus the similarity in structure within a chemokine family, because two disulphide bonds are formed between the first and third cysteine residues and between the second and fourth cysteines (Figure 1-1) (Rossi and Zlotnik, 2000). CC chemokines are the largest chemokine family and possess two adjacent cysteine residues near their N-terminus. Likewise, CXC chemokines possess two cysteine residues near their N-terminus, but these cysteine residues are separated by a single non-conserved aa. The CX₃C family has only one member, CX₃CL1 which has three non-conserved aas between its first two cysteine residues. Members of the C family of chemokines have only two conserved cysteine residues in the whole protein joined by one disulphide bond, which helps in the maintenance of the similar tertiary structure of this family of chemokines. These two cysteine residues correspond to the second and fourth cysteine residues in members of the other three chemokine families (Rossi and Zlotnik, 2000; Comerford and Nibbs, 2005; Charo and Ransohoff, 2006).

As Table 1-1 illustrates there is variability within the chemokine families between species. Several chemokines, such as CCL13 through to CCL16 exist in humans, but not in mice, whereas CCL9, CCL10 and CCL12 exist in mice, but not in humans (Murphy et al., 2000). Also, CCL8, a CCR2 ligand in humans, should really be considered as a different chemokine in mice because in this species it binds only CCR8 (Islam et al., 2011). There is also variation between individuals of the same species. For example, some chemokines, such as hCCL3, exist as different isoforms. The hCCL3 isoforms, CCL3 and CCL3L1, differ in their amino termini and they also have one aa change in the body of the protein (Mueller et

al., 2006). However, they are functionally distinct with clear differences in receptor specificity (Townson et al., 2002). Moreover, some individuals lack CCL3L1, whilst others have from 1 to 10 copies of this gene (Townson et al., 2002; Gonzalez et al., 2005). This is functionally significant in the context of HIV (Gonzalez et al., 2005). The large degree of redundancy within the chemokine system means that the significance of many of these differences has yet to be elucidated (Mestas and Hughes, 2004). However, it has been proposed that this apparent “redundancy” within the chemokine system provides robust outputs, even in the presence of genetic alterations (Mantovani, 1999). In contrast, the use of animals deficient in a chemokine receptor or ligand, such as CCR2 (Serbina and Pamer, 2006), CCR7 (Luther et al., 2000; Förster et al., 2008) and CXCR4 (Ma et al., 1998) has illustrated that some chemokine receptors play indispensable roles on specific cell populations. These roles shall be discussed later.

CXC Family Systemic Nomenclature	Alternative names	Receptor(s)
CXCL1	GRO α , KC	CXCR1, CXCR2
CXCL2	GRO β , MIP-2	CXCR2
CXCL3	GRO γ , DCIP-1	CXCR2
CXCL4	PF4	hCXCR3B
CXCL5	ENA-78, mGCP-2, LIX	CXCR2
hCXCL6	GCP-2	CXCR1, CXCR2
CXCL7	NAP-2	CXCR2
hCXCL8	IL-8	CXCR1, CXCR2
CXCL9	Mig	CXCR3, CCR3
CXCL10	IP-10	CXCR3, CCR3
CXCL11	I-TAC	CXCR3, CCR3
CXCL12	SDF-1	CXCR4
CXCL13	BCA-1, BLC	CXCR5
CXCL14	BRAK, Bolekine	Unknown
mCXCL15	Lungkine, WECH	Unknown
CXCL16	SCYB16, SR-PSOX	CXCR6

C Family Systemic Nomenclature	Alternative names	Receptor(s)
XCL1	Lymphotactin, SCM-1 α	XCR1
hXCL2	SCM-1 β	XCR1

CX ₃ C Family Systemic Nomenclature	Alternative names	Receptor(s)
CX ₃ CL1	Fractalkine, Neurotactin	CX ₃ CR1

CC Family Systemic Nomenclature	Alternative names	Receptor(s)
CCL1	I-309, TCA-3	CCR8
CCL2	MCP-1, JE, MACF	CCR2
CCL3	MIP-1 α S, MIP-1 α	CCR1, CCR5
hCCL3L1	MIP-1 α P, MIP-1 α	CCR1, CCR3, CCR5
CCL4	MIP-1 β	CCR5
hCCL4L1	MIP-1 β	CCR5
CCL5	RANTES	CCR1, CCR3, CCR5
mCCL6	C10, MRP-1	CCR1
CCL7	MCP-3, MARC	CCR1, CCR2, CCR3, CCR5
CCL8	MCP-2	hCCR2, hCCR3, mCCR8
mCCL9	MIP-1 γ , MRP-1, CCF18	CCR1
mCCL10	MIP-1 γ , MRP-1, CCF18	CCR1
CCL11	Eotaxin	CCR3, CXCR3
mCCL12	MCP-5	CCR2
hCCL13	MCP-4	CCR2, CCR3
hCCL14	HCC-1	CCR1
hCCL15	HCC-2, Lkn-1, MIP-1 δ	CCR1, CCR3
hCCL16	HCC-4, LEC, LCC-1	CCR1, CCR2, CCR5
CCL17	TARC	CCR4
hCCL18	DC-CK1, PARC	PITPNM3
CCL19	ELC, MIP-3 β , exodus-3	CCR7
CCL20	MIP-3 α , LARC, exodus-1	CCR6
CCL21	SLC, 6Ckine, exodus-2	CCR7
CCL22	MDC, STCP-1, ABCD-1	CCR4
hCCL23	MPIF-1	CCR1
CCL24	Eotaxin-2, MPIF-2	CCR3
CCL25	TECK	CCR9
hCCL26	Eotaxin-3	CCR1, CCR2, CCR3, CCR5, CX ₃ CR1
CCL27	C-TACK, PESKY, Eskine	CCR10
CCL28	MEC	CCR3, CCR10

Table 1-1: Systematic nomenclature for chemokines.

Chemokines listed according to the systemic nomenclature with their alternative names and receptor(s). Chemokines preceded with h indicates that the chemokine is present in humans, but not mice, whereas the prefix m designates chemokines present in mice, but not humans.

1.1.2 Chemokine mediated control of cell movement

Chemokines possess the ability to regulate and coordinate leukocyte migration and positioning within tissues. The regulation of leukocytes is the principal focus of my thesis, so my Introduction will focus on this key aspect of chemokine biology. The roles of chemokines in leukocyte migration can broadly be divided into two categories: firstly, chemokine-induced activation of integrins required for rapid leukocyte adhesion to endothelial surfaces and secondly, chemokine-induced rearrangements in the cells cytoskeleton via actin polymerisation, which is likely to be critical for interstitial navigation (Kinashi, 2005; Vicente-Manzanares et al., 2009; Schumann et al., 2010). Surface adhesion via chemokine-induced activation of integrins is critical for haptic movement, both random migration (haptokinesis) and migration along gradients of immobilised chemokine ligands (haptotaxis). It also plays a role in the induction of cell adhesion, such as occurs to leukocytes on endothelial surfaces. However, migration can also occur independently of firm adhesion, using soluble homogenous chemokine signals to trigger random migration (chemokinesis) or directed migration along soluble chemokine gradients (chemotaxis) (Schumann et al., 2010).

The extravasation of cells from the blood to tissues is a multi-step process, involving selectin-mediated rolling of cells, chemokine-induced integrin activation, integrin-induced cell arrest, and transmigration of cells across the endothelium (Handel et al., 2005) (Figure 1-2). This occurs continuously during homeostasis at many locations, most notably the high endothelial venules (HEVs) of LNs. During tissue inflammation, selectins are upregulated on endothelial cells in the tissue, which allows passing cells to roll along the endothelium. Sensing of chemokines presented by endothelial cells that are specific for chemokine receptors on the rolling cell leads to chemokine-induced integrin activation, which leads to cell arrest on the endothelium (Handel et al., 2005; Kinashi, 2005; Grailer et al., 2009). The role of chemokines in this simple paradigm has been expanded recently to demonstrate that leukocytes can migrate on endothelial cells after their arrest. For example, neutrophils have been reported to exhibit CXCR2 dependent haptotaxis, along an intravascular gradient of CXCR2 ligand presented on endothelial cells, towards a site of

inflammation (McDonald et al., 2010). Also, Ly6C^{lo} monocytes are constitutively motile on endothelial cells in a CX₃CR1 dependent manner (Auffray et al., 2007). Some chemokine receptors, such as CCR2, can mediate leukocyte transendothelial migration using chemokine ligands stored within vesicles underneath the plasma membrane of endothelial cells. Thus, in some cases transendothelial migration can occur even when the availability of chemokine presented on endothelial cells is low (Shulman et al., 2011).

The multiprocess of leukocyte extravasation can be summarised in several major steps (Figure 1-2) (Alon and Feigelson, 2002; Handel et al., 2005). First, leukocytes express L-selectin (also known as CD62L), which weakly binds to endothelial cells expressing L-selectin ligands, such as CD34. This mediates rolling of cells along the endothelial surface. Next, chemokines expressed and/or presented on glycosaminoglycans (GAGs) by endothelial cells bind to their appropriate chemokine receptor on the rolling leukocytes (Stein et al., 2000; Alon and Feigelson, 2002; Handel et al., 2005). Chemokine receptor engagement induces conformational changes in leukocyte integrin molecules, such as leukocyte function-associated Ag 1 (LFA1), leading to clustering on integrins, which are now in a high-affinity state (Stein et al., 2000; Alon and Feigelson, 2002). However, chemokine receptor activation is insufficient to induce robust integrin activation in the absence of shear flow/stress (Alon and Feigelson, 2009). These integrins interact with adhesion molecules (e.g. intercellular adhesion molecule (ICAM)-1) on the surface of endothelial cells, which leads to firm adhesion of the leukocyte to endothelial cell surface (Stein et al., 2000; Alon and Feigelson, 2002). The arrested leukocyte then accesses underlying inflamed tissue by migrating between (paracellular) or through (transcellular) endothelial cells, Figure 1-2 shows paracellular trans-migration (Förster et al., 2008).

The migration of cells into underlying tissues is facilitated by chemokine-induced polarisation of the actomyosin cytoskeleton (Kinashi, 2005; Vicente-Manzanares et al., 2009; Schumann et al., 2010). The leading edge of the cell has a concentrated expression of the appropriate chemokine receptor, and binding of further chemokine to the receptors facilitates coordinated integrin activation, which propel the cell forward through the endothelium towards the chemokine expressed in the inflamed tissue. This process has been extensively studied *in*

vitro, but it is still unclear whether true chemokine gradients exist within lymphoid tissues and inflamed tissues *in vivo* (Nieto et al., 1997). However, Schumann *et al.* have shown that a combination of immobilised CCL21, and soluble CCL19 and CCL21 gradients can direct DC migration within LNs (Schumann et al., 2010). Immobilised CCL21, in the absence of soluble CCL19 or CCL21 results in haptokinetic migration by DCs. In contrast, following truncation of anchoring residues of CCL21 by DCs, a soluble form of CCL21 is produced, which like soluble CCL19 can trigger chemotactic movement of DCs. Therefore, it has been reported that the directional CCR7 dependent migration of DCs within LNs after entry from the subcapsular sinus is a combined effect of immobilised CCL21 triggering integrin activation and cell adhesion, plus a soluble CCL19/CCL21 gradient providing directional cues (Schumann et al., 2010). CCR7 and its ligands have also been shown to be important for the intranodal motility of T cells, as in the absence of CCR7 or its ligands T cell motility was reduced (Worbs et al., 2007).

The extravasation of cells is heavily chemokine-dependent, as inhibition of chemokine receptor signalling via pertussis toxin treatment causes a subsequent inhibition in integrin activation, and blocks extravasation of cells (Cyster and Goodnow, 1995; Warnock et al., 1998). The presentation of chemokines on cell surfaces is intrinsic to their function in promoting extravasation of leukocytes into tissues. The majority of chemokines are soluble and secreted, but are bound to GAGS and presented on the surface of endothelial cells (Handel et al., 2005). GAGs are negatively charged polysaccharides that are covalently attached to a protein core forming proteoglycans that interact with several circulating proteins, including basic chemokines. However, other stromal components, such as the fibroblastic reticular cell network of the LN and spleen can present CCL21 and guide T cell migration within these secondary lymphoid organs (Bajénoff et al., 2006; Bajénoff et al., 2008). The interaction of chemokines with GAGs can lead to the generation of chemokine oligomers, and it is argued that the formation of oligomers and dimers may act to sequester ligands, thereby regulating the local chemokine concentration and availability (Lau et al., 2004; Comerford and Nibbs, 2005; Allen et al., 2007). GAGs can also protect bound chemokines from the action of proteases, such as matrix metalloproteinases (MMPs) and CD26. MMPs and CD26 cleave the N-termini of chemokines and

modulate their activity. MMP-mediated truncated CCL2, 7, and 13 lose their agonistic actions on CCR2 and CCR3 *in vitro*. However, they retain their ability to bind their respective receptors. Thus MMP cleavage converts them into antagonists, blocking binding of uncleaved ligands. Likewise, CD26 cleavage of CCL5 causes it to lose its agonist actions on CCR1 and CCR3, while retaining its ability to bind CCR5 (Comerford and Nibbs, 2005; Handel et al., 2005; Allen et al., 2007). Furthermore, GAGs may exhibit selectivity in their presentation of chemokines, thus discriminating which cell types are recruited (Middleton et al., 2002). By changing the concentration or availability of local chemokine monomers, GAGs, chemokine multimers and proteases can alter chemokine gradients, thus modifying the direction of cell migration and also which cells are recruited.

BLOOD

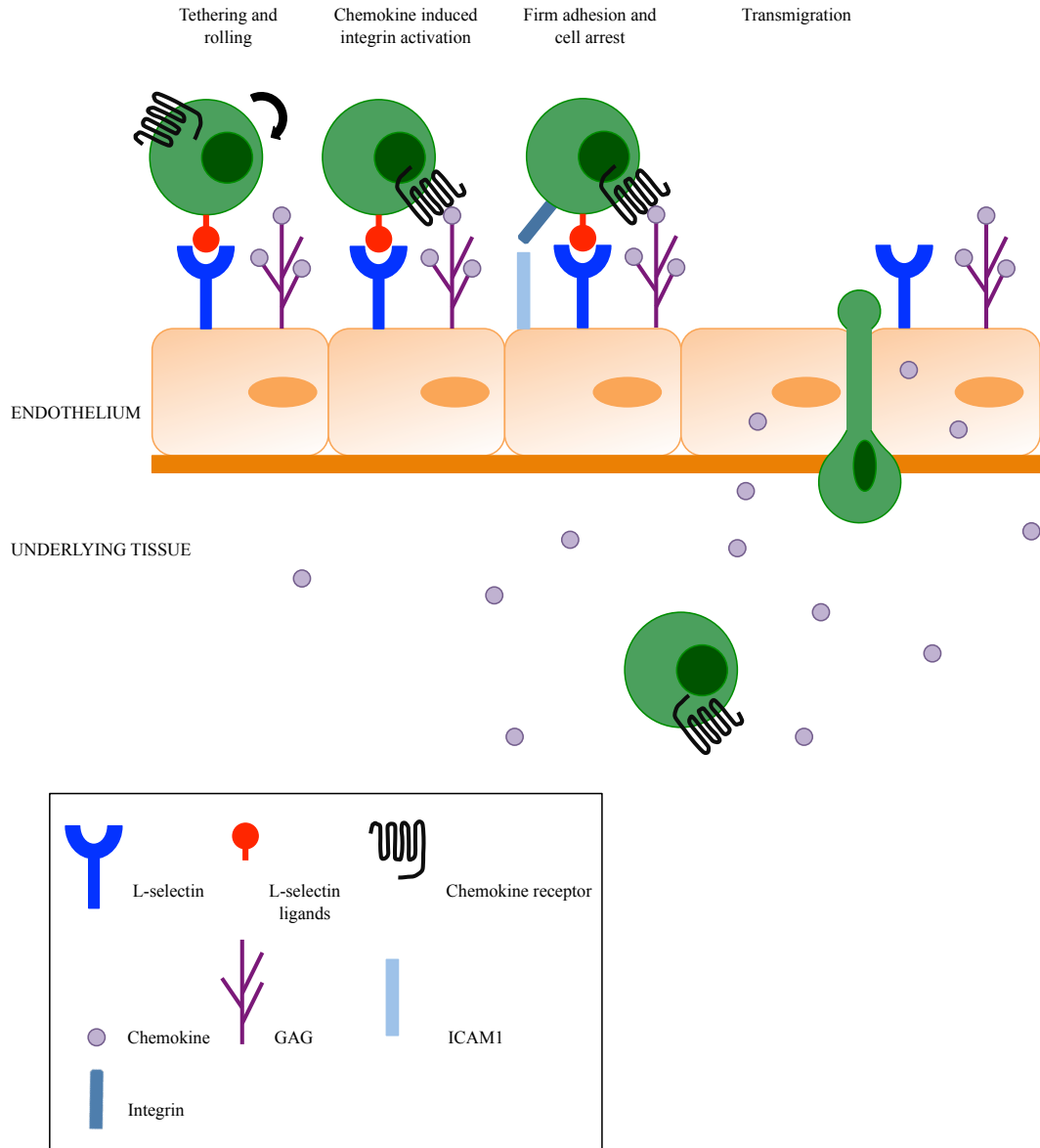


Figure 1-2: Leukocyte extravasation from blood vessels into underlying tissue.

Leukocyte extravasation is a multi-step process. Firstly selectin-mediated tethering of leukocytes in the bloodstream slows their movement, allowing them to roll along the endothelium. Rolling cells that express the appropriate chemokine receptor are activated by chemokines presented by GAGs on the endothelium surface. The chemokine-induced activation of cells leads to a high affinity integrin-mediated firm adhesion and arrest of cells. The cell transmigrates through the vascular endothelium and into the underlying tissue. Adapted from (Handel et al., 2005).

1.2 Chemokine receptors

Chemokine receptors are members of one of the most diverse class of surface receptor families, the G-protein coupled receptor (GPCR) superfamily. Like other GPCRs, chemokine receptors are seven transmembrane domain receptors that are coupled to heterotrimeric G-protein complexes. The C-terminus and three intracellular loops of the receptor face into the cytoplasm, and the G-protein is associated with the C-terminus (Murdoch and Finn, 2000). The presence of the canonical sequence DRYLAIV within their second intracellular loop is also important for G-protein coupling and signalling (Nibbs et al., 2003; Ulvmar et al., 2011). The N-terminus and three extracellular loops of the receptor are exposed outside of the cell (Murdoch and Finn, 2000). The binding of ligands to their respective receptors is proposed to be a two-site interaction. The N-terminus of the receptor is thought to bind to the N-loop of chemokine ligands, and the disordered N-terminal signalling domain of the ligand is thought to interact with the extracellular loops of the receptor and access the hole created by the seven transmembrane domains (Rajagopalan and Rajarathnam, 2006). The N-terminus of the receptor is rich in negatively charged residues and also contains sulphated tyrosine residues, both of which are essential in mediating high affinity ligand binding (Preobrazhensky et al., 2000; Rajagopalan and Rajarathnam, 2006). Upon ligand binding, the canonical DRYLAIV sequence found in the second intracellular loop of the receptor is vital for inducing intracellular signalling (Murphy et al., 2000; Rot and von Andrian, 2004).

Many chemokines are known to bind to more than one receptor, and several receptors are known to bind multiple ligands (Rot and von Andrian, 2004; Salanga et al., 2009). However, some chemokines still have no identified receptor (Table 1-1). Most receptors generally bind to ligands that are restricted to one class of chemokines, such as CC or CXC ligands. For example, CXCR bind CXC chemokines, CCR bind CC ligands, XCR1 binds C chemokines and CX₃CR1 binds CX₃CL1 (Murphy et al., 2000; Rossi and Zlotnik, 2000). There are some exceptions, as CXCR3 can be antagonised by CCL11, and CXCL9, 10 and 11 are all antagonists of CCR3 (Rot and von Andrian, 2004). Systematic nomenclature for chemokine receptors is based on the class of chemokine that they bind followed by a number depending on when they were first discovered.

1.2.1 Chemokine receptor signalling

Binding of a chemokine to its respective receptor initiates signalling events, starting with the activation of the associated G-protein. The heterotrimeric G-protein contains three subunits $G\alpha$, β and γ . There are four families of $G\alpha$ subunits, $G\alpha_s$, $G\alpha_{i/o}$, $G\alpha_{q/11}$ and $G\alpha_{12/13}$ all with several family members. Primarily $G\alpha_{i/o}$ subunits are responsible for regulating chemotaxis (Mellado et al., 2001; Rot and von Andrian, 2004; Cotton and Claing, 2009; Salanga et al., 2009). $G\alpha$ subunits in their inactive resting state are bound by guanosine diphosphate (GDP). Chemokine receptor activation by ligand binding leads to a conformational change of the intracellular domains of the receptor, and a resultant exchange of GDP for guanosine triphosphate (GTP). The heterotrimeric G-protein is destabilised by GTP binding, leading to the dissociation of the α subunit and a complex composed of β and γ subunits (Mellado et al., 2001; Rot and von Andrian, 2004; Cotton and Claing, 2009; Salanga et al., 2009). The system has an internal shut off switch because $G\alpha$ subunits have intrinsic GTPase activity that hydrolyses bound GTP, thereby reuniting the α subunit with the $\beta\gamma$ complex, and reforming the inactive heterotrimer (Figure 1-3) (Mellado et al., 2001; Rot and von Andrian, 2004).

Both the α subunit and the $\beta\gamma$ subunits complex mediate chemokine-induced signals. The targets of each of these subunits differ, with some overlap (Figure 1-3) (Mellado et al., 2001; Rot and von Andrian, 2004; Cotton and Claing, 2009). $G\alpha$ subunits control the activation of the GTPase RhoA (Cotton and Claing, 2009), which is involved in chemokine-induced rapid integrin activation and, as a consequence, leukocyte arrest (Giagulli et al., 2004). Furthermore, $G\alpha$ subunit triggers signal transduction by the Src kinase, which leads ultimately to the activation of a small GTPase Rac, which is involved in cell migration (Cotton and Claing, 2009). The $G\beta\gamma$ complex can lead to the activation of Rac through an alternative pathway initiating with the activation of the protein kinase PI3K. Rac activates two downstream effectors, WASP and PAK, which stimulate the actin related protein (Arp) 2/3, thereby inducing actin polymerisation (Rot and von Andrian, 2004). The $G\alpha$ subunit is also able to activate adenylate cyclase, leading to cAMP production, which ultimately results in the activation of Erk, which modulates cell migration (Cotton and Claing, 2009). Both the $G\alpha$ and $G\beta\gamma$

can activate two different pathways involving phospholipase C (PLC). Firstly the $G\alpha$ subunit activates PLC, which activates protein kinase C (PKC), leading to the activation of calmodulin, which enhances cell motility. In contrast the activation of PLC by $G\beta\gamma$ subunits complex leads to the cleavage of a phospholipid, PIP_2 generating two products DAG and IP_3 . IP_3 is involved in calcium mobilisation (Murphy et al., 2000; Mellado et al., 2001; Cotton and Claing, 2009). The role of calcium mobilisation in leukocyte migration is unclear. Some studies indicate that increased calcium mobilisation is required for chemotaxis, whereas T cells have been shown to migrate in response to CCR4 ligands independent of calcium mobilisation (Pettit and Fay, 1998; Cronshaw et al., 2006). Thus, many chemokine-induced signalling pathways induce cell migration, however in the absence of Cdc42 activation leukocytes fail to comprehend a directional chemokine gradient and instead exhibit random migration. It is only following activation of Cdc42, by either the $G\alpha$ or $G\beta\gamma$ subunits that migration becomes unidirectional. The $G\alpha$ subunit directly activates Cdc42 and $G\beta\gamma$ subunits complex indirectly activate Cdc42 via PAK1 (Rot and von Andrian, 2004; Cotton and Claing, 2009).

Chemokine induced migration of cells can also be regulated by suppressor of cytokine signalling (SOCS) proteins. SOCS proteins are a small family of 8 proteins that regulate signal transduction of cytokine signalling pathways. SOCS proteins have been shown to inhibit cell migration in response to chemokines, as SOCS1 and SOCS3 expression by a fibroblast cell line and HEK cells inhibited migration of the cells towards CCL11 (Stevenson et al., 2010). Overexpression of SOCS3 by a pro-B cell line inhibited CXCL12 induced polarisation of the cells. Furthermore, immature and mature B cells from SOCS3 deficient mice had increased CXCL12-induced adhesion (Le et al., 2007). In contrast to Stevenson *et al.* who found that expression of SOCS proteins inhibited migration of cells (Stevenson et al., 2010), Le *et al.* found that in the absence of SOCS3, immature B cells were retained in the BM (Le et al., 2007). Le *et al.* proposed that the enhanced adhesion properties of the B cells might impede CXCR4-dependent egress of B cells from the BM (Le et al., 2007).

Further complexity is added to chemokine receptor signalling, as the pathways induced and the subsequent outcome of activation depends on a variety of

factors, such as cell type, receptor and ligand. Earlier I mentioned a potential redundancy of chemokine receptors and ligands, however it is now proposed that different chemokines interacting with the same receptor may activate different signalling pathways (Murphy et al., 2000). The promiscuity of chemokine receptors and their ligands might exist to provide robust immune responses. Many pathogens attempt to subvert the chemokine system, therefore “redundancy” ensures robustness of response in the face of pathogen-mediated chemokine subversion (Finlay and McFadden, 2006). Furthermore, this area is complicated by the fact that chemokine receptors, like other GPCRs are subject to receptor dimerisation forming both homodimers and heterodimers, which may influence downstream signalling events (Salanga et al., 2009). Chemokine receptor dimerisation is reported to result in the association and activation of JAKs, which in turns leads to the phosphorylation and activation of STATs. STATs can then promote transcription of STAT responsive genes (Rodríguez-Frade et al., 1999; Mellado et al., 2001).

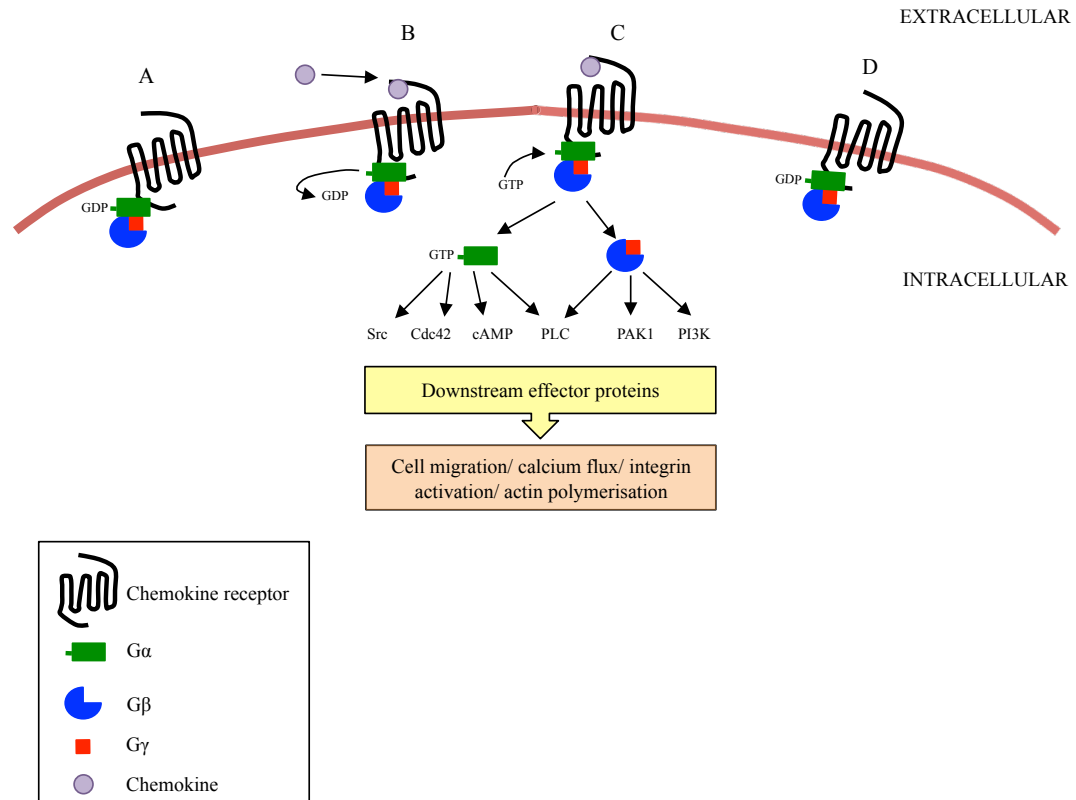


Figure 1-3: Chemokine receptor signalling cascade.

The 7 transmembrane chemokine receptor is associated with a heterotrimeric G-protein, consisting of α , β and γ subunits. (A) In a resting state the $G\alpha$ subunit is rendered inactive by the binding of GDP. (B) Upon ligand binding the intracellular domains of the chemokine receptor undergo a conformational change leading to the exchange of GDP for GTP. (C) Binding of GTP leads to the dissociation of the heterotrimeric protein from the receptor, as two entities the $G\alpha$ subunit and a $G\beta\gamma$ complex. Both the $G\alpha$ subunit and $G\beta\gamma$ complex lead to the initiation of signalling cascades, with some initial effector proteins shown, which result in cell migration, integrin activation, actin polymerisation and calcium mobilisation. (D) Intrinsic GTPase activity of the $G\alpha$ subunit hydrolyses GTP to GDP, leading the reunion of the $G\alpha$ subunit with the $G\beta\gamma$ complex, forming the inactive G-protein heterotrimer. The heterotrimer reassociates with a chemokine receptor. Adapted from (Rot and von Andrian, 2004; Cotton and Claing, 2009).

1.2.2 Receptor desensitisation

Typically following chemokine-mediated activation of a receptor, the receptor is internalised, whereupon it is either recycled back to the cell surface or targeted for lysosomal degradation. Recycling of the receptor allows it to bind more ligand and repeat the process again. By controlling the surface level of receptors, or the activity of the receptors, the strength and duration of the response can be altered (Rot and von Andrian, 2004; Cotton and Claing, 2009; Neel et al., 2009). Following prolonged ligand exposure, a receptor can become unresponsive to further ligand in a process known as receptor desensitisation. Desensitisation of receptors is controlled by phosphorylation of the receptor. G-protein-coupled receptor kinases (GRKs) phosphorylate the intracellular loops and/or C-terminus of ligand-bound receptors, which serve as binding sites for β -arrestin proteins. Binding of β -arrestins leads to steric hindrance of the G-protein interaction with the receptor, thereby preventing further activation of the receptor in response to additional ligand (Rot and von Andrian, 2004; Vroon et al., 2006; Premont and Gainetdinov, 2007; Cotton and Claing, 2009). Chemokine-induced receptor signalling can also be silenced by downregulation of the number of surface receptors. Binding of β -arrestin can stimulate clathrin-mediated receptor downregulation by targeting internalised receptors to endosomal compartments where they are degraded or resensitised (Neel et al., 2009). In contrast to their role in receptor desensitisation, GRKs may also contribute to signal transduction events, because although GRK6 deletion enhanced CXCR4 dependent migration of neutrophils to CXCL12, it decreased CXCR4 dependent migration of lymphocytes (Vroon et al., 2006; Cotton and Claing, 2009).

1.3 Atypical Chemokine Receptors

Some chemokine receptors appear not to be subject to desensitisation and are termed atypical chemokine receptors (Hansell et al., 2006; 2011b). There are now five identified atypical chemokine receptors (Table 1-2), which are unable to mediate signalling upon chemokine ligand binding in a manner similar to the “classical” chemokine receptors. Furthermore, this apparent lack of signalling capacity is accompanied by an inability to mediate chemotaxis in response to

chemokine ligand. The best-characterised atypical chemokine receptor D6 forms a main point of focus in my thesis, so this section focuses on D6 biology.

Following its cloning in 1997 (Bonini and Steiner, 1997; Nibbs et al., 1997a; 1997b), D6 was identified as a highly promiscuous receptor for proinflammatory CC chemokines, including, but not limited to CCL2-5, CCL11, CCL17 and CCL22. The ligand binding profile of human D6 has been better characterised than murine D6 (Mantovani et al., 2006; Graham, 2009; Hansell et al., 2011b). Ross Kinstrie tested all other chemokines on human D6 and none, other than those in Table 1-2, bound D6 (personal communication from Rob Nibbs). However, using cells transfected with murine D6 (Nibbs et al., 1997a) and also primary cells, such as innate-like B cells (Hansell et al., 2011b), murine D6 has also been shown to interact with many inflammatory CC chemokines. The ligand binding profiles of human and murine D6 are summarised in Table 1-2. The binding of any of its many ligands could not activate the conventional signalling pathways described earlier, nor could it drive chemotaxis (Mantovani et al., 2006; Graham, 2009; Hansell et al., 2011b). D6 possesses an altered DRYLAIV sequence, the sequence involved in G-protein coupling and signalling, in D6 it is changed to DKYLEIV (Nibbs et al., 1997a). Immunofluorescent staining or imaging of HEK293 cells transfected with human D6 has facilitated the analysis of the cellular distribution of D6. The majority of D6 is found in intracellular vesicles and cell surface protein only accounts for ~5% of D6 protein (Weber et al., 2004). D6 constitutively traffics to and from the cell surface irrespective of chemokine binding (Galliera et al., 2004; Weber et al., 2004). The precise mechanism of D6 internalisation remains to be fully understood, and conflicting findings exist in regards to its dependency on β -arrestins (Galliera et al., 2004; Weber et al., 2004; McCulloch et al., 2008). Chemokines that are bound to D6 are internalised with the receptor and upon entry into the acidic early endosomal compartment dissociate from the receptor and are targeted for degradation, whereas the receptor is returned to the cell surface. Upon return to the cell surface, D6 can bind more ligand, and in doing so functions as a chemokine scavenger, with its continuous recycling facilitating the destruction of high levels of chemokine ligands, such as CCL2 (Fra et al., 2003; Hansell et al., 2006; Mantovani et al., 2006; Graham, 2009). However, this feature is not restricted entirely to atypical chemokine receptors, as “classical” chemokine receptors possessing the DRYLAIV

sequence have also been reported to scavenge ligands (Hansell et al., 2006). Indeed, unchallenged mice lacking single “classical” chemokine receptors, such as CCR2 or CXCR2, have elevated levels of the ligands for these receptors, a phenomenon that is not seen in resting D6 deficient mice (Cardona et al., 2008). A more detailed discussion of D6 biology *in vivo* is included in section 1.6.2.

Atypical Chemokine Receptor	Chemokine Ligands
D6	CCL2, CCL3, hCCL3L1, CCL4, hCCL4L1, CCL5, hCCL7, hCCL8, CCL11, mCCL12, hCCL13, hCCL14, CCL17, CCL22, hCCL23, CCL24
DARC	hCCL2, hCCL5, hCCL7, hCCL11, hCCL13, hCCL14, hCCL17, hCXCL1, hCXCL2, hCXCL5, hCXCL6, hCXCL8, hCXCL11
CXCR7	CXCL11, CXCL12
CCX-CKR	CCL19, CCL21, CCL25, hCXCL13
mCCRL2 (hCRAM)	CCL19, CCL5

Table 1-2: Atypical chemokine receptors and their ligands.

Chemokines preceded with h indicates that this chemokine binds to the receptor in humans, but not mice, whereas the prefix m designates chemokines that bind to the receptor in mice, but not humans.

1.4 Homeostatic versus inflammatory chemokines, and their roles in the immune system

In addition to grouping chemokines based on the arrangement of their conserved cysteine residues, chemokines can be broadly divided into two functional groups, homeostatic or inflammatory chemokines. Homeostatic chemokines are constitutively expressed, i.e. continuously produced, whereas expression of inflammatory chemokines is induced principally during times of infection or injury. Homeostatic chemokines include CCL19, CCL21, CXCL12 and CXCL13 and have a fundamental role in the organisation and maintenance of secondary lymphoid organs. CCL2, CCL3, CCL5 and CXCL1 are examples of inflammatory chemokines, which mediate activation and recruitment of effector cells to sites of infection and injury (Murphy et al., 2000; Le et al., 2004; Rot and von Andrian, 2004; Allen et al., 2007). The division of chemokines as constitutive homeostatic or inducible inflammatory has become less clear and some homeostatic chemokines, such as CCL21 are also inducible at peripheral sites (Serra et al., 2004). Furthermore, some inflammatory chemokines now clearly have homeostatic and developmental roles. CCR2 is required for Ly6C^{hi} monocyte mobilisation from the BM both during homeostasis and following infection of the

host with *Listeria monocytogenes* (Serbina and Pamer, 2006). CCR2 has also been described to play a role in balancing bone mass, as animals deficient in CCR2 have an increase in their bone mass. The increase in bone mass is associated with alterations in the development and bone resorptive potential of osteoclasts (Binder et al., 2009). Furthermore, CXCR2 has been reported to control neutrophil emigration from the BM during acute inflammation, but also controls the positioning and proliferation of oligodendrocyte progenitor cells in the developing spinal cord (Veenstra and Ransohoff, 2012). Nonetheless, the homeostatic/inflammatory designation is still a useful way of characterising chemokines and summarising their functional significance.

1.4.1 Homeostatic chemokines

Homeostatic chemokines regulate the development of primary and secondary lymphoid organs during embryogenesis. CXCL12 is considered to be the primordial chemokine (i.e. the first chemokine to evolve), as during embryogenesis it is involved in the organisation of the primary lymphoid organ, the BM. It is constitutively produced by BM stroma, and, through its interaction with its receptor CXCR4, it triggers B cell progenitor proliferation (D'Apuzzo et al., 1997) and directs haematopoietic precursors to the BM during embryogenesis (Aiuti et al., 1997). In the absence of CXCL12 or CXCR4, mice die perinatally, suffering from defects in B cell lymphopoiesis, myelopoiesis and cerebellar development (Ma et al., 1998). CXCL12 and CXCR4 are highly conserved during evolution, indicative of critical functions maintained in all organisms. For example, migration of primordial germ cells in zebrafish is CXCR4 dependent, as reduced CXCL12 results in a migrational defect (Raz and Reichman-Fried, 2006; Boldajipour et al., 2008). Interestingly, the atypical chemokine receptor CXCR7 is crucial in directing the CXCR4-dependent migration of primordial germ cells. CXCR7 removes excess CXCL12 from undesirable locations, thereby aiding the generation and maintenance of a gradient of CXCL12. In the absence of CXCR7 cells still respond to CXCL12, but do not exhibit directional migration (Boldajipour et al., 2008; Wang et al., 2011). Likewise in mice, CXCR7 regulates CXCR4 protein levels on interneurons by taking up CXCL12. CXCR7 regulates CXCL12 levels, and by doing so can regulate the level of responsive CXCR4 on interneurons, as excess CXCL12 leads to desensitisation of CXCR4 and its degradation (Sánchez-Alcañiz et al., 2011). In the absence of either of these

receptors, mice had defects in interneuron positioning (Wang et al., 2011). Most mice deficient in CXCR7 die at birth, as CXCR7 deficiency has been associated with abnormal cardiac development. Mice with a conditional deletion of CXCR7 in endothelium presented with a similar phenotype as CXCR7 knock-out (KO) mice, illustrating that expression of the atypical chemokine receptor CXCR7 by endothelium cells is essential for normal cardiac development (Sierra et al., 2007).

Homeostatic chemokines, in particular CCR7 and CCR9, are involved in T cell development in the thymus. The thymus is a primary lymphoid organ that is surrounded by a capsule, underneath which lies the subcapsular zone, cortex, corticomedullary junction and medulla. Haematopoietic stem cell-derived precursors arrive in the thymus via blood vessels present at the corticomedullary junction (Nitta et al., 2008). Uehara *et al.* reported that CCR9 was crucial for T cell development, as repopulation of the thymus of lethally irradiated Rag mice (deficient in T and B cells) was less efficient with BM from CCR9 KO mice than WT (Uehara et al., 2002). However, CCR9 deficiency does not result in complete inhibition of precursor entry. It is the coordinated action of CCR7 and CCR9 that regulates entry of precursors into the thymus. In the absence of both these receptors there is a severe reduction in thymic precursors (Uehara et al., 2002; Liu et al., 2006; Krueger et al., 2010; Zlotoff et al., 2010). These precursors are double negative thymocytes that migrate outwards through the cortex to the subcapsular region of the thymus. CCR9, CCR7 and CXCR4 have also been reported to play a role in the migration of double negative thymocytes to the subcapsular region. CCR9 and CCR7 KO mice have decreased accumulation of double negative thymocytes near the subcapsular region (Miszlitz et al., 2004; Förster et al., 2008; Nitta et al., 2008). During their migration, these cells mature into double positive CD4⁺CD8⁺ thymocytes and undergo pre-T cell receptor (TCR) mediated selection (Nitta et al., 2008; Rodewald, 2008). Self-peptides are presented via major histocompatibility complex class II (MHCII) on thymic epithelial cells and thymic DCs. Cells are selected for survival or deletion based on the strength of the interaction between their TCR and the presented self-peptide. Weak interactions result in positive selection and cell survival, whereas a strong interaction leads to negative selection and deletion of cells by apoptosis. Clonal deletion of thymocytes with a strong TCR interaction to self-

peptide is not the only outcome for thymocytes. Reactive T cells can survive, but are rendered anergic i.e. can not be stimulated to react to the self-peptide (Hogquist et al., 1994; Palmer, 2003; Nitta et al., 2008). Alternatively, thymocytes can be induced to differentiate into regulatory T cells (Tregs). Tregs can suppress autoreactivity of cells in the periphery (Workman et al., 2009). The autoimmune regulator (*AIRE*) gene is expressed by thymic epithelial cells in the medulla and is involved in the expression of tissue specific self-peptides. Mice deficient in *AIRE* have been shown to develop autoimmunity (Heino et al., 1999; Metzger and Anderson, 2011). Furthermore, *AIRE* regulates the accumulation of thymic DCs in the medulla. The migration of thymic DCs into the medulla is *XCR1* dependent and medullary thymic epithelial cells express the chemokine ligand *XCL1*. *XCL1* deficient animals are defective in the accumulation of thymic DCs and in the generation of Tregs, and as a consequence are more susceptible to autoimmunity (Lei et al., 2011).

Double positive thymocytes that were positively selected, migrate into the medulla and undergo further maturation into single positive cells, either $CD4^+$ or $CD8^+$ (Förster et al., 2008; Nitta et al., 2008). Maturation of single positive cells in the medulla is accompanied by an increase in responsiveness to the *CCR7* ligands, *CCL19* and *CCL21* expressed by thymic epithelial cells in the medulla. Fully mature $CD4^+$ and $CD8^+$ T cells express high levels of *CCR7* (Ueno et al., 2004; Davalos-Miszlitz et al., 2007; Förster et al., 2008). The importance of *CCR7* for thymocyte migration in the medulla is demonstrated in *CCR7* KO animals and mice containing the spontaneous paucity of LN T cells mutation (*plt/plt*). *plt/plt* mice lack *CCL19* and *CCL21* in lymphoid organs, but due to the existence of two *CCL21* genes in mice, *CCL21* production in non-lymphoid organs, such as the lung, is intact (Luther et al., 2000; Förster et al., 2008). Both *CCR7* KO animals and *plt/plt* mice have decreased migration of thymocytes towards to the medulla. These mice also fail to negatively select thymocytes possessing TCRs reactive to self-peptides (Kwan and Killeen, 2004; Miszlitz et al., 2004; Ueno et al., 2004; Witt and Robey, 2004; Kurobe et al., 2006), thus *CCR7* KO animals have been shown to develop spontaneous autoimmunity and have exaggerated immune responses (Schneider et al., 2007; Förster et al., 2008). The egress of mature single positive thymocytes from the thymus is regulated by sphingosine-1-phosphate receptor 1 (*S1P₁*), which is upregulated in maturing single positive

thymocytes (Pappu et al., 2007; Zachariah and Cyster, 2009). Pappu *et al.* illustrated that targeted ablation of two kinases involved in the generation of S1P, the ligand for S1P₁ causes significant reduction in thymocyte egress from the thymus (Pappu et al., 2007).

The organisation of secondary lymphoid organs, such as LNs occurs via homeostatic chemokines that attract haematopoietic cells, such as lymphoid tissue inducer (LTi) cells to the site of future lymphoid organ development (Randall et al., 2008). The development of secondary lymphoid organs, such as LNs occurs through an interaction of a cell surface heterotrimer of lymphotoxin- $\alpha_1\beta_2$ (LT $\alpha_1\beta_2$) positive LTi and lymphoid tissue initiator (LTin) cells with the LT $\alpha_1\beta_2$ receptor (LT β R) positive lymphoid tissue organiser (LTo) cells (Ohl et al., 2003a; Mebius and Kraal, 2005; Randall et al., 2008). The ligation of LT β R triggers the differentiation of LTo cells that form a stromal cell matrix that produces CCL19, CCL21 and CXCL13 and express cell adhesion molecules VCAM-1 and ICAM-1. LTi cells express the integrin receptors for these cell adhesion molecules. These chemokines promote recruitment and clustering of LTi cells and the recruitment of mature lymphocytes to the developing lymphoid organ. In addition, homeostatic chemokines trigger expression of LT $\alpha_1\beta_2$ on the surface of LTi cells and mature lymphocytes, thereby creating a positive feedback loop in which engagement of LT β R triggers release of homeostatic chemokines that recruit further LT $\alpha_1\beta_2$ expressing cells (Ansel et al., 2000; Ansel and Cyster, 2001; Cupedo and Mebius, 2003; Luther et al., 2003; Randall et al., 2008).

The importance of CXCR5 and CCR7 ligands in the development of secondary lymphoid organs has been reported using mice lacking one or more of the ligands. Reports show that CXCL13 is the dominant chemokine ligand involved, as deletion of either CXCL13 or its receptor CXCR5 disrupts the formation of most peripheral LNs (PLNs) and Peyers's patches (PPs) in intestine. In contrast, CCR7 KO mice possess the majority of their PLNs (Ansel and Cyster, 2001; Ohl et al., 2003b). LTi cells express both CXCR5 and CCR7, thus the deletion of CCR7 and the CXCR5 ligand, CXCL13, leads to a more severe phenotype, suggesting that these two receptors have overlapping roles in the development of LNs (Luther et al., 2003; Ohl et al., 2003b). Interestingly, mesenteric LNs (MLNs) are retained in CCR7/CXCL13 double KO mice, suggesting other chemokine receptors, such as

CXCR4 are involved in the recruitment of LT_i cells during the development of MLNs (Luther et al., 2003). Furthermore, although still present, spleens in CCR7 KO, CXCL13 KO and CCR7/CXCL13 double KO mice are disorganised, lacking clearly defined red and white pulp areas (Ohl et al., 2003a; 2003b).

1.4.1.1 Structure and function of LNs

In addition to regulating the development of secondary lymphoid organs, homeostatic chemokines also support the maintenance of these highly organised and structured lymphoid tissues by controlling the migration of lymphocytes and DCs within the distinct areas of the organs (Rossi and Zlotnik, 2000).

LNs, as illustrated in Figure 1-4, are segregated into two principal areas: the cortex and the medulla. The cortex is further divided into an additional two areas, the T cell zone (paracortex) and the B cell zone, which consists of follicles and germinal centres. The medulla contains a network of lymphatic sinuses, called medullary sinuses which lymph drains into. Lymph enters LNs through the afferent lymphatic vessel and is channelled around the edge of LN in the subcapsular sinus, a hollow space below the fibrous capsule that surrounds the LN. Lymph also moves through trabecular sinuses towards medullary sinuses, located in the medulla of the LN (von Andrian and Mempel, 2003). LNs contain a fibroblastic reticular cell network, known as the conduit system. Fibroblastic reticular cells wrap around collagen fibres, and form channels that deliver lymph from the subcapsular sinus to T cell areas and direct to HEVs. The fibroblastic reticular cell network also acts as a filter of lymph, only allowing low molecular weight molecules, such as chemokines to enter the channels. The filtered lymph is transported via the conduit system to the HEVs, where lymph-borne chemokine can be transported into the lumen of HEVs and presented to attract blood-borne cells (Gretz et al., 2000; von Andrian and Mempel, 2003; Roozendaal et al., 2008). Lymph drains into the efferent lymphatic vessels and leaves the LN, providing an exit for lymphocytes. The majority of naïve lymphocytes enter the paracortex of LNs via HEVs. However, some memory T cells gain entry via the afferent lymphatics and the subcapsular sinus (von Andrian and Mempel, 2003).

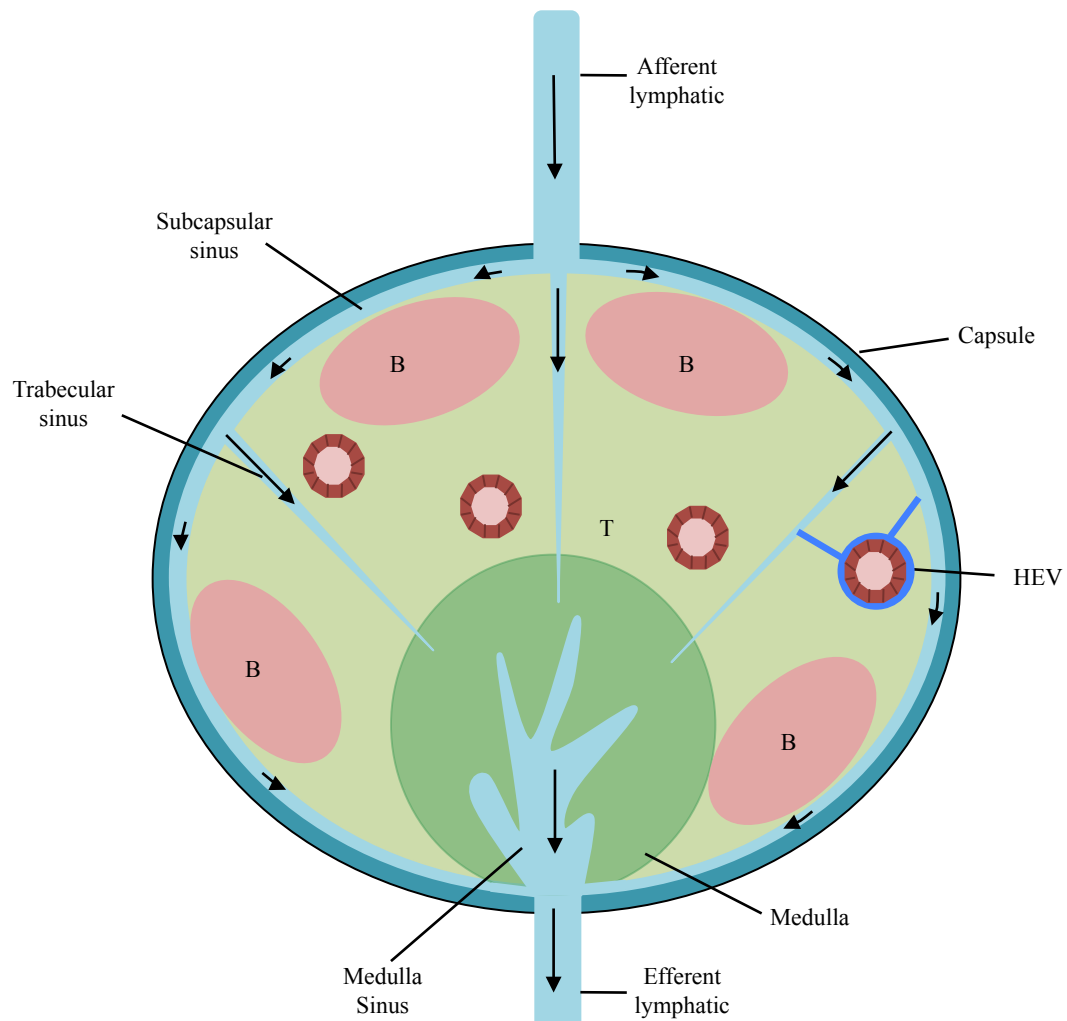


Figure 1-4: Simplified diagram of LN structure.

LNs are surrounded by a fibrous capsule underneath which lymph flows in the subcapsular sinus and the trabecular sinuses. The trabecular sinuses extend through the cortex towards the medulla, where they connect with the medullary sinuses, which drain into the efferent lymphatic vessel. The cortex is divided into two sections, the T cell zone, known as paracortex and the B cell area consisting of primary follicles and germinal centres. HEVs allow flow of venous blood into the LN, delivering blood-circulating lymphocytes to the LN. Also illustrated in dark blue, is an example of the flow of filtered lymph from the subcapsular sinus to HEVs via the channels formed by the fibroblastic reticular cell network. Adapted from (von Andrian and Mempel, 2003).

Entry of the majority of lymphocytes from the blood into LNs is coordinated in a manner similar to that depicted in Figure 1-2. The chemokine-induced integrin activation for T and B cell migration through HEVs into LN is CCR7 dependent in resting LNs (von Andrian and Mempel, 2003; Miyasaka and Tanaka, 2004; Förster et al., 2008; Worbs and Förster, 2009). Binding of CCR7 to its ligand mediates leukocyte extravasation through the HEV into the paracortical area of the LN, where CCR7 ligands are constitutively expressed (von Andrian and Mempel, 2003; Miyasaka and Tanaka, 2004; Förster et al., 2008).

The importance of CCR7 and its ligands in T cell migration has been illustrated using animals deficient in one or more of its ligands, or the receptor itself. LNs of *plt/plt* mice are smaller in size than wild-type (WT) animals and have a deficit in T cell numbers (Luther et al., 2000; Förster et al., 2008). Luther *et al.* demonstrated that HEVs express CCL21, but not CCL19, suggesting that CCL19 was not involved in recruitment of leukocytes into LNs from the blood (Luther et al., 2000). In accordance with these results, mice specifically deficient in CCL19 illustrated that CCL21 was sufficient for the organisation of T cell zones (Link et al., 2007). In contrast, Baekkevold *et al.* have reported that CCL19 protein can be transported from its site of production by LN stromal cells to the luminal side of HEVs and enables efficient T cell homing to LNs (Baekkevold et al., 2001). CCL19 also plays a non-redundant role in naïve T cell homeostasis that can not be compensated by CCL21 (Link et al., 2007). Naïve T cell homeostasis is highly dependent on the access of naïve T cells to LNs, as once in the T cell zone, naïve T cells receive survival signals provided by IL-7 produced by the fibroblastic reticular cell network. *In vitro* data also suggest that CCL19 is able to provide a survival signal to T cells, whereas CCL21 is not (Link et al., 2007). In addition to mediating efficient LN homing of T cells, CCR7 is required for T cell motility within LNs. In the absence of CCR7 signalling, either through deletion of CCR7 or its ligands, intranodal motility of CD4⁺ T cells is reduced. The transfer of WT CD4⁺ T cells and systemic administration of CCL21 restored motility of T cells in LNs of *plt/plt* mice (Worbs et al., 2007).

The LNs of CCR7 KO animals are also deficient in T cells however, the B cell compartment of LNs in these mice is relatively unaffected by the absence of CCR7 (Förster et al., 1999; von Andrian and Mempel, 2003; Worbs et al., 2007). This indicates that although B cells can use CCR7 to migrate into LNs they are

not dependent on it, as it has been shown that CXCR4 can contribute to B cell LN homing. Okada *et al.* reported that transfer of CXCR4 deficient B cells into *plt/plt* mice resulted in reduced B cell homing to LNs. In contrast, although B cell homing to PPs was reduced in the absence of CXCR4 and CCR7 signalling it was not as severe as in the LNs. However, B cells deficient in CXCR5 also had a deficiency in homing to PPs, which was further reduced by the absence of CXCR4 and CCR7 signalling. Therefore, B cell entry into PPs is dependent on CXCR4, CCR7 and CXCR5 (Okada *et al.*, 2002).

Entry of B cells into B cell follicles of LNs is mediated by CXCR5. CXCR5 ligand CXCL13 is expressed at high levels by stromal cells within the B cell follicles, named follicular DCs. Following activation, B cells downregulate CXCR5 and upregulate CCR7, which mediates their migration towards the T cell area. Also, a distinct T cell lineage, the follicular helper T cells, upon activation transiently downregulate CCR7 and upregulate CXCR5, mediating their mobilisation towards the B cell follicle (Fazilleau *et al.*, 2009). B cells present Ag on MHCII to follicular helper T cells, which mediate Ag specific activation of B cells, driving their proliferation, affinity maturation and antibody class switching of plasmablasts (Cyster, 1999; von Andrian and Mempel, 2003; Worbs *et al.*, 2007; Förster *et al.*, 2008). Furthermore, B cells are activated by intact Ag presented to them by follicular DCs (von Andrian and Mempel, 2003).

For all these processes to occur, naïve T cells need to be presented with an Ag peptide specific for their TCR. Ag presenting cells (APCs), in particular DCs, process and present Ag to T cells, mediating the initiation of the adaptive immune response, which is crucial in the defence against foreign pathogens (von Andrian and Mempel, 2003). Following activation of CD4⁺ T cells by engagement of their TCR with their specific Ag peptide presented in the context of MHCII, CD4⁺ T cells proliferate and differentiate into effector T helper (Th) cells, Th1, Th2, Th17, follicular Th cells or Tregs (Zhu *et al.*, 2010). The differentiation of T cells into effector Th cells is accompanied by a change in chemokine receptor expression, which can facilitate their homing to inflamed sites. Although chemokine receptor expression can not fully be coordinated with an individual lineage, Th1 cells have been reported to have high expression of CXCR3 and CCR5. Th2 cells have high expression of CCR3, CCR4, and CCR8 and human Th17 cells have high expression of CCR6 and CCR4 (Zhu and Paul, 2008). A proportion

of effector T cells also contributes to immunological memory. Memory T cells that persist after the resolution of inflammation or infection can broadly be divided into effector memory T cells or central memory T cells. Central memory T cells are CCR7⁺, whereas effector memory T cells are tissue resident, therefore express chemokine receptors other than CCR7 (Sallusto et al., 2004; Lanzavecchia and Sallusto, 2005).

Migration of activated effector T cells to peripheral sites can be associated with the expression of specific receptors that allow constitutive homing to specific inflamed tissues. Upregulation of these receptors is related to the LN in which the T cells are activated. CD4⁺ T cells activated in MLNs upregulate the gut homing integrin $\alpha 4\beta 7$ and the chemokine receptor CCR9, and are therefore highly responsive to CCL25, a chemokine ligand expressed by the epithelial cells of the small intestine (Campbell and Butcher, 2002). Upregulation of CCR9 and $\alpha 4\beta 7$ is induced by DCs in the gut associated lymphoid tissue (GALT), and specifically the vitamin A metabolite retinoic acid, produced by the GALT DCs, enhances expression of the two gut homing molecules. The production of retinoic acid from vitamin A is reported to be crucial to imprint gut homing specificity, as vitamin A deficiency in mice results in the depletion of T cells from gut lamina propria (Iwata et al., 2004). In contrast, the biologically active form of vitamin D₃ suppresses expression of the gut homing receptors, CCR9 and $\alpha 4\beta 7$ by activated T cells, and induces expression of CCR10. CCR10 facilitates the recruitment of activated T cells to the skin in response to CCL27 secreted by keratinocytes (Sigmundsdottir et al., 2007). Furthermore, naïve CD4⁺ T cells activated in the subcutaneous LNs upregulate CCR4 and CCR10 and home to skin. In a model of delayed type hypersensitivity, T cells were still efficient in their migration to inflamed skin in the absence or following the blockage of one of these receptors. Inhibition of T cell migration to the skin was only achieved in mice with no functional CCR4 or CCR10 (Reiss et al., 2001).

Ag reaches LNs by two routes. The first is by lymphatic drainage of peripheral tissues, which carries Ag to LNs where it can be taken up by an immature DC for Ag presentation. Alternatively, Ag is acquired and processed in peripheral tissues by immature DCs, the processed Ag is then carried to the draining LN by DCs. Entry of DCs into lymphatics from the tissues is CCR7 dependent. CCL21 is

produced by the lymphatic endothelial cells in peripheral tissues and coordinates DC migration into the lymphatics (Ohl et al., 2004). Delivery of DCs to the LN is also CCR7 dependent. DCs enter into the LN parenchyma by transmigrating through the floor of the subcapsular sinus in a CCR7 dependent manner. DCs deficient in CCR7 are retained in the subcapsular sinus (Braun et al., 2011). DC migration to the T cell zones is also CCR7 dependent, and as mentioned earlier is thought to be due to a combined effect of immobilised CCL21 and soluble CCL19/CCL21 (Schumann et al., 2010). Within the T cell zones, DCs can interact with naïve T cells. The interaction between incoming T cells and DCs bearing the Ag peptide specific for its TCR is impeded by competition by other T cells with irrelevant TCR specificity. To enhance the probability of the interaction occurring, naïve T cells within the paracortex undergo rapid migration in random directions (von Andrian and Mempel, 2003; Worbs et al., 2007; Förster et al., 2008; Worbs and Förster, 2009). T cells that do not encounter their specific Ag peptide leave the LN via the efferent lymphatic. Exit of T and B cells from LNs is regulated by S1P and its receptor S1P₁. S1P is expressed at higher levels in the blood and lymph than in the LN (Schwab and Cyster, 2007). The high levels of S1P in the blood means that S1P₁ is desensitised, facilitating lymphocyte extravasation into tissues with low S1P levels, such as LNs. Within S1P low LNs, S1P₁ is gradually resensitised and eventually is sufficiently active to drive departure of lymphocytes into the lymph. Activated T cells upregulate CD69, which downregulates S1P₁ expression, stopping responsiveness to S1P and cells are retained in the LN. A S1P-degrading enzyme, S1P lyase, maintains the low levels of S1P within LNs, which upon inhibition leads to an increase in S1P levels in LNs and lymphocyte egress from the LN is blocked (Schwab et al., 2005). Lymphocyte egress can also be blocked by treatment with the S1P₁ agonist, FTY720. *In vitro* studies have shown that binding of FTY720 to S1P₁ inactivates it, by triggering its internalisation and subsequent degradation of the receptor (Schwab and Cyster, 2007).

The role of DCs within the immune system shall be discussed in depth later in this Introduction in section 1.5.

1.4.1.2 Structure and function of the spleen

The spleen, as illustrated in Figure 1-5 is divided into two main anatomically discrete areas, the red pulp and the white pulp, each with their own specific functions (Mebius and Kraal, 2005; Cesta, 2006). The red pulp is enriched with venous sinuses and macrophages, both of which facilitate the red pulp's role as a blood filter and as a site for the removal of old erythrocytes. Macrophages destroy old or damaged erythrocytes, recycle released iron, and are also involved in the defence against blood-borne bacteria. After encountering bacteria, macrophages release molecules that inhibit iron uptake by the bacteria, thereby limiting their growth (Mebius and Kraal, 2005).



Figure 1-5: Simplified diagram of the structure of the spleen.

The spleen is divided into the red pulp and the white pulp, all of which is surrounded by a fibrous capsule. The white pulp is the lymphoid region of the spleen, which consists of the T cell containing area, the periarteriolar lymphoid sheath (PALS) and B cell follicles. The white pulp is surrounded by the marginal zone, which is separated from the white pulp by the marginal sinus. Adapted from (Mebius and Kraal, 2005).

The white pulp is the lymphoid region of the spleen, and as such is of principal relevance to thesis. It has a similar structure in many ways to LNs. However, the main differences between the two secondary lymphoid organs lie in how lymphocytes and Ag enter each organ, and the presence of a region called the marginal zone (MZ). Ag delivery to LNs occurs via the lymphatics, whereas the blood carries Ag to the spleen where it is delivered through the MZ to the white pulp (Ohl et al., 2003a; Mebius and Kraal, 2005). The MZ is a specialised feature of the spleen, it surrounds the white pulp, but is separated from the white pulp by cell lined space known as the marginal sinus. The white pulp surrounds arterial vessels that enter the spleen and is composed of two areas, the T cell-containing periarteriolar lymphoid sheath (PALS) and the B cell follicles (Ohl et al., 2003a; Mebius and Kraal, 2005; Cesta, 2006; Britschgi et al., 2008).

Lymphocyte entry into the white pulp via the MZ is integrin and chemokine-dependent. This process is thought to be mediated by a method similar to the transmigration of cells from the blood into underlying tissues, as depicted in Figure 1-2. A deficiency in CXCR5 or CCR7 reduces accumulation of B and T cells in the white pulp, respectively (Ohl et al., 2003a; Cyster, 2005; Mebius and Kraal, 2005).

There are also MZ bridging channels, narrow channels that extend between the red pulp and the white pulp, and into the PALS. They provide a bridge through the MZ and assist in the migration of cells from the red pulp into the white pulp (Mitchell, 1973; Mebius and Kraal, 2005). The MZ bridging channels are rich in fibroblastic reticular cells, which form a network that guides T cell migration into the PALS. Bajenoff *et al.* proposed that this migration is likely to be CCR7 dependent, as, similar to LN fibroblastic reticular cells, splenic fibroblastic reticular cells also produce CCL21. Furthermore, the introduction of WT T cells into WT and *plt/plt* mice illustrated that CCR7 ligands were required for T cell entry into PALS (Bajénoff et al., 2008). Blood-borne DCs enter the spleen via the MZ and the migration of DCs to the T cell zones of the spleen is also CCR7 dependent, as *plt/plt* mice have decreased numbers of DCs in their splenic T cell zones (Gunn et al., 1999). However, a population of CXCR5⁺ DCs that are located near B cell follicles have also been described, which are dependent on CXCL13 for their presence, as very few CXCR5⁺ DCs are detected in the spleen of CXCL13 deficient mice (Yu et al., 2002). Interestingly, León *et al.* have shown

that these CXCR5⁺ DCs are able to drive development of Th2 cells outside of the T cell zone in response to the intestinal nematode, *Heligmosomoides polygyrus* (León et al., 2012).

The spleen is also a key site for B cell maturation in mice. “Transitional” B cells from the BM enter the spleen and mature into either follicular B cells or MZ-B cells. Follicular B cells are the “classical” B cells that traffic around the body. MZ-B cells are long-lived resident cells of the MZ (Pillai et al., 2005; Pillai and Cariappa, 2009). Most B cells do not possess the appropriate adhesive properties that permit their retention in the MZ, but MZ-B cells express cannabinoid receptor 2, which positions and retains MZ-B cells in the MZ. Mice deficient in cannabinoid receptor 2 have decreased MZ-B cells within the MZ (Muppidi et al., 2011). Their unique location within the MZ allows MZ-B cells to respond rapidly to blood-borne pathogens, producing antibodies and participating in the early response against blood-borne Ag. These innate-like cells provide a bridge between the innate and adaptive immune system (Lopes-Carvalho and Kearney, 2004; Pillai et al., 2005; Pillai and Cariappa, 2009). MZ-B cells are limited to the MZ of the spleen, however other innate-like B cells, known as B1 B cells can be identified in body cavities (Martin and Kearney, 2000).

Migration of follicular B cells to the B cell follicles is CXCR5 dependent, as naïve B cells respond to CXCL13 expression by stromal cells in B cell follicles. In the absence of CXCR5, mice have a defect in follicle and germinal centre formation (Förster et al., 1996). Within the B cell follicle, B cells are activated by binding of Ag to their Ag-specific B cell receptor. Similar to the LN, activated B cells upregulate CCR7 and migrate towards the edge of the B cell follicle towards the PALS. A third GPCR, EBI2 is involved in B cell migration to the outer areas of follicles and the MZ bridging channel, as in its absence EBI2 deficient B cells accumulate in the centre of B cell follicles and decreased numbers of B cells are found at the periphery of the follicle (Gatto et al., 2011). T cells activated by DCs presenting the Ag peptide specific for their TCR, downregulate CCR7 and upregulate CXCR5, which facilitates their migration to the edge of B cell follicles. Activated CD4⁺ Th cells stimulate isotype switching of B cells and their differentiation into Ag specific plasmablasts (Ohl et al., 2003a; Mebius and Kraal, 2005; Cesta, 2006). Plasmablasts downregulate both CXCR5 and CCR7, and upregulate CXCR4, leading to their migration into the CXCL12 expressing red

pulp. The presence of plasmablasts and the later differentiated plasma cells in the red pulp facilitates the rapid entry of antibodies into the bloodstream (Hargreaves et al., 2001; MacLennan et al., 2003; Mebius and Kraal, 2005). Finally, similar to the lymphocyte egress from LNs, S1P and its receptor S1P₁ regulate T cell emigration from the spleen into the bloodstream (Mebius and Kraal, 2005; Schwab and Cyster, 2007).

1.4.2 Inflammatory chemokines and the innate immune system

The adaptive immune response, although not clarified as such has already been discussed, as primarily it is an Ag specific response by T and B cells. The activation of T and B cells occurs within the secondary lymphoid organs, and their migration to, and within, these specialised structures is regulated by homeostatic chemokines. However, pathogen invasion usually occurs at peripheral sites away from these specialised lymphoid structures. Therefore, cells of the innate immune system act as an “alarm” system, alerting lymphocytes in secondary lymphoid organs to the presence of pathogen in the periphery. Pathogen invasion can stimulate the production of inflammatory chemokines by tissue resident DCs, macrophages, parenchymal and stromal cells. These inflammatory chemokines are typically ligands of the inflammatory chemokine receptors, CCR1, CCR3, CCR5, CXCR2, CXCR3 and CCR2 (Rot and von Andrian, 2004). CCR2 forms the main focus of this PhD and will be discussed in greater depth below. Inflammatory chemokines recruit cells of the innate immune system, such as DCs, monocytes, neutrophils and natural killer (NK) cells to the site of infection. The innate immune system does not recognise specific antigenic peptides like the adaptive immune system, but it recognises molecules on the surface of invading organisms called PAMPs. Innate effector cells recognise PAMPs and host-derived damage-associated molecular patterns by pattern recognition receptors (PRRs) (Rot and von Andrian, 2004; Sabroe et al., 2008). Toll-like receptors (TLRs) are a family of PRRs that each recognise a specific PAMP or group of PAMPs. For example, TLR4 recognises, amongst other things, lipopolysaccharide (LPS) present in the cell wall of gram negative bacteria; TLR7 recognises single stranded RNA, a common feature of viruses, plus synthetic molecules such as imidazoquinolines; and TLR9 recognises bacterial unmethylated CpG oligodeoxynucleotide DNA (Edwards et al., 2003; Takeda et al., 2003). The innate immune system provides a rapid non-specific

response against the pathogen, and the subsequent adaptive immune response allows a targeted Ag specific response (Rot and von Andrian, 2004).

One of the most important links between the innate and adaptive immune system are DCs, and the role they play in the immune system is now discussed. These cells form a focus of my studies described in Chapter 5.

1.5 Dendritic cells and their role in the immune system

Up to this point, I have presented an oversimplified role of DCs within the immune system, stating only their importance in driving T cell activation. However, the DC system and its functions are complex, consisting of many DC populations defined by differences in their function, mode of activation, and location. The first major division that can be made is between conventional DCs (cDCs) and plasmacytoid DCs (pDCs). cDCs, as their name implies, perform all tasks commonly assigned to DCs, such as sampling Ag in tissues, and processing and presenting Ag peptide to naïve T cells in secondary lymphoid organs. The context of this presentation determines the outcome for T cells, i.e. whether they become activated, tolerised or anergic (Ardavín, 2003; Shortman and Naik, 2007; Tan and O'Neill, 2007). Activated pDCs are also thought to have Ag presenting function, but they are also professional type 1 interferon (IFN) producing cells (Asselin-Paturel et al., 2001; Tan and O'Neill, 2007). The functional properties of cDCs and pDCs will be discussed in greater depth below, but regardless of differences in their classification and roles, the development of both cDCs and pDCs is from common progenitors.

As splenic cDCs and pDCs form a key focus of my thesis, I will next outline in detail what is known about the splenic DC system, including their development, subsets and functions.

1.5.1 Development of dendritic cells

cDCs were thought to be entirely of myeloid origin. However as Figure 1-6 depicts, cDCs may also be of lymphoid origin (Ardavín et al., 1993; Ardavín, 2003). Initially the distinction between cDCs of lymphoid and myeloid origin was thought to be in the expression of CD8 α : lymphoid cDCs being CD8 α ⁺ and

myeloid cDCs $CD8\alpha^-$. However, although the resting splenic cDC compartment does indeed consist of $CD8\alpha^+$ and $CD8\alpha^-$ cDCs, they can both be of lymphoid and myeloid origin (Vremec and Shortman, 1997; Martín et al., 2000; Manz et al., 2001; Ardavin, 2003). Both cDCs and pDCs develop from haematopoietic stem cells that give rise to a multipotent progenitor, which in turn can give rise to both the common lymphoid progenitor (CLP) and common myeloid progenitor (CMP) (Figure 1-6). The CMP gives rise to the macrophage DC precursors (MDP) via the granulocyte-monocyte progenitor (GMP). Monocytes are progeny of MDPs, as are the common DC progenitors (CDP), which generate cDCs. (Naik et al., 2007; Wu and Liu, 2007; Sathe and Shortman, 2008; Liu et al., 2009). CLPs are also thought to form cDCs, however most data indicating that CLPs are also a parent population of cDCs is produced *in vitro* (Ardavin et al., 1993; Traver et al., 2000; Manz et al., 2001; Wu et al., 2001; Shortman and Naik, 2007). Thus, it is thought that most splenic cDCs are derived from CMPs (Traver et al., 2000; Wu et al., 2001; Liu and Nussenzweig, 2010).

There are few fully differentiated cDCs within the BM, as cDCs only complete their differentiation in the periphery. Thus, in the steady-state spleen, cDC precursors, known as pre-cDCs, can be found, that can give rise to both $CD8\alpha^+$ and $CD8\alpha^-$ cDCs, but not pDCs (Naik et al., 2006; 2007; Shortman and Naik, 2007; Liu et al., 2009). Naik *et al.* conducted a detailed profiling of the surface phenotype of pre-cDCs that distinguished them from monocytes and fully developed cDCs, as they were found to be $CD11c^{int}MHCII^-CD8\alpha^-Ly6C^+CD11b^{lo}$ (Naik et al., 2006). Pre-cDCs are committed to $CD8\alpha^+$ or $CD8\alpha^-$ cDC lineages via intermediary precursors that are $CD24^{hi}$ or $CD24^{lo}$, respectively (Naik et al., 2006; 2007; Shortman and Naik, 2007; Liu et al., 2009). These immature $CD8\alpha^+$ or $CD8\alpha^-$ cDCs are capable of some proliferation in homeostasis (Liu et al., 2007; Shortman and Naik, 2007). However, it is not the proliferation of these cells that is responsible for maintaining cDC numbers in the spleen. It is in fact, the pre-cDCs that achieve this feat (Kamath et al., 2000; Shortman and Naik, 2007). Splenic pre-cDCs are also responsive to the growth factor, fms-like tyrosine kinase-3 ligand (Flt3L), and in response to a decrease in splenic cDC numbers there is an increase in Flt3L in the blood, which triggers an increase in both the frequency and differentiation of pre-cDCs restoring splenic cDC populations (Hochweller et al., 2009). The Flt3L receptor, Flt3, is vital for DC development,

as Flt3 KO animals are deficient in pDCs and the majority of cDCs (McKenna et al., 2000). Both CLPs and CMPs are responsive to Flt3L as a proportion of each population expresses Flt3. Furthermore, Flt3L treatment of mice results in a dramatic expansion of cDCs and pDCs in secondary lymphoid organs (Mach et al., 2000; D'Amico and Wu, 2003; Karsunky et al., 2003; Naik et al., 2005b; 2007).

The developmental stages of pDCs are less well defined, but similar to cDCs they can be of both myeloid and lymphoid origin, with both CLPs and CMPs contributing to their development (Förster et al., 1999; von Andrian and Mempel, 2003; D'Amico and Wu, 2003; Worbs et al., 2007; Reizis, 2010).

Traditionally, pDCs are thought to be fully differentiated before leaving the BM, so pDCs can be found in low numbers in the BM, blood and spleen (Omatsu et al., 2005; Naik et al., 2005a). However, recent research suggests that there is also an intermediary precursor of pDCs that mainly exists in the BM, but is also found in low numbers in secondary lymphoid organs (Rossi and Zlotnik, 2000; Schlitzer et al., 2011; 2012). This precursor is proposed to be CCR9⁻, whereas fully differentiated pDCs are CCR9⁺. The CCR9⁻ precursors, like pre-cDCs, are derived from CDPs, but are different from pre-cDCs as they express pDC markers, such as pDC Ag 1 (PDCA1) and SiglecH (Schlitzer et al., 2011; 2012). CCR9⁻ precursors preferentially give rise to fully differentiated CCR9⁺ pDCs in the BM. CCR9⁻ pDCs have a higher proliferative capacity than CCR9⁺ pDCs. In addition to their capacity to generate fully differentiated pDCs in the BM, CCR9⁻ precursors present in the periphery can also give rise to cDCs, particularly the CD11b⁺CD8α⁻ cDC population and to a lesser extent the CD8α⁺CD11b⁻ cDC population (Schlitzer et al., 2011; 2012). This deviation from the pDC lineage is accompanied by the downregulation of transcription factors required for pDC differentiation, such as E2-2 and the E2-2 regulated transcription factors IRF8 and SpiB. Furthermore, there is a parallel upregulation of transcription factors, such as ID2 and PU.1 which control cDC development (Cisse et al., 2008; Ghosh et al., 2010; Reizis et al., 2011a; Schlitzer et al., 2011; 2012).

All of these populations are present in the steady-state spleen and it is only following injury or infection that pDCs, and cDCs, both CD8α⁺ and CD8α⁻ cDCs are fully activated (Ardavín, 2003; Shortman and Naik, 2007). Furthermore, in a steady-state spleen Ly6C^{hi} monocytes do not contribute to the splenic cDC

populations. However, in a challenged spleen or other tissue, Ly6C^{hi} monocytes can differentiate into inflammatory DCs (Tam and Wick, 2004; Naik et al., 2006; Shortman and Naik, 2007). For example, following infection with *Listeria monocytogenes*, Ly6C^{hi} monocytes differentiate into the inflammatory tumour necrosis factor alpha (TNF α) and inducible nitric oxide synthase (iNOS) producing DCs (TipDCs), identified as Ly6C⁺CD11b⁺CD11c⁺Mac3⁺ cells (Serbina and Pamer, 2006).

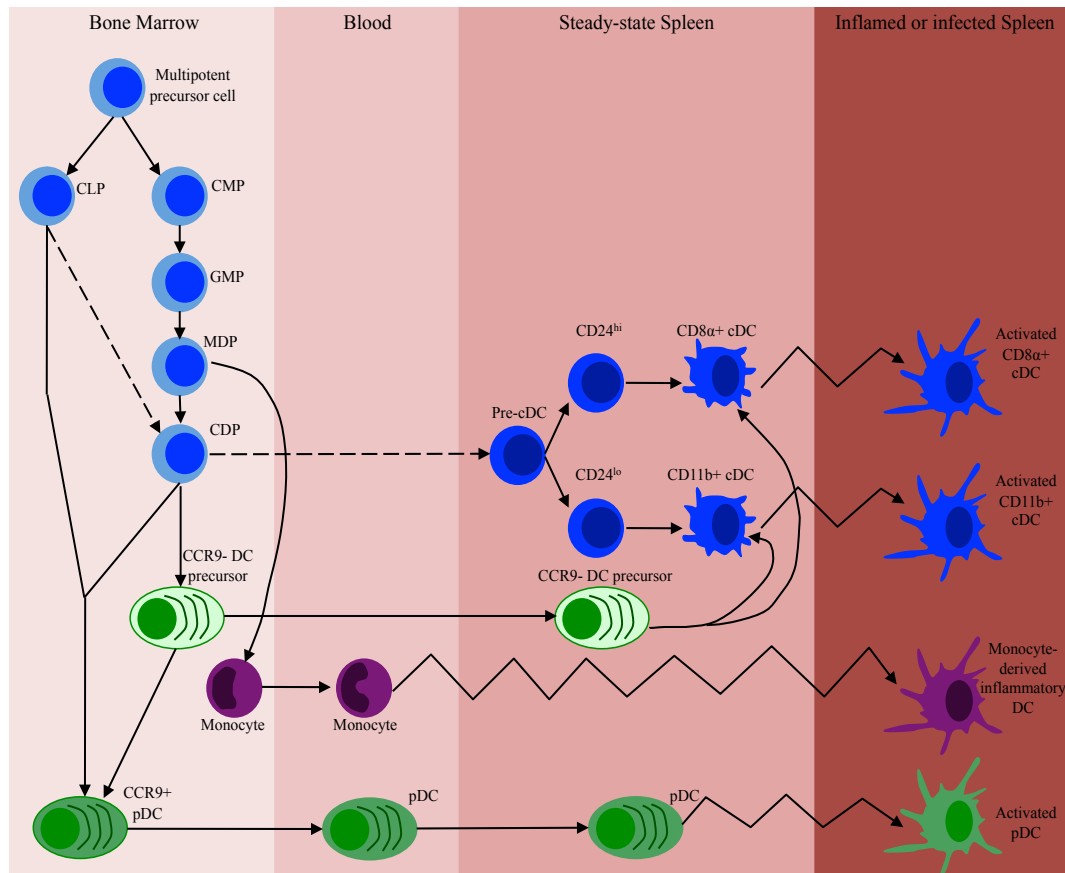


Figure 1-6: Pathways of splenic DC development.

In the BM a multipotent precursor cell can give rise to both the common lymphoid progenitor (CLP) and the common myeloid progenitor (CMP). CMPs differentiate to form the granulocyte-myeloid progenitor (GMP), from which the macrophage DC precursors (MDP) are formed. Following the downregulation of *c-kit*, MDPs become common DC progenitors (CDP). The CLP and the CDP generate fully differentiated pDCs that migrate into the blood and spleen. The CDP can also differentiate into a CCR9⁻ DC precursor that in the BM can form fully differentiated pDCs. Alternatively, in the periphery CCR9⁻ DC precursors generate CD11b⁺ and CD8 α ⁺ cDCs. Following infection or injury pDCs become activated. MDPs also differentiate into monocytes, which can give rise to inflammatory DCs, but not in the steady-state spleen, only following an inflammatory insult. In contrast to pDCs, cDCs are not fully differentiated on exit of BM, and a pre-cDC exists in the spleen. Pre-cDC population can be divided based on expression of CD24. CD24^{hi} and CD24^{lo} pre-cDCs generate immature CD8 α ⁺ and CD11b⁺ cDCs, respectively. Following infection or injury the immature CD8 α ⁺ and CD11b⁺ cDCs become activated. Dashed lines indicate relationships that are still a source of controversy. Adapted from (Shortman and Naik, 2007; Schlitzer et al., 2012).

1.5.2 cDCs

cDCs are resident cells that patrol peripheral tissue, and each tissue has specific cDC populations. Most cDCs in steady-state animals are immature, possessing a high capacity to sample their environment, internalise Ag and process it for presentation on MHC (Alvarez et al., 2008; Miloud et al., 2010). Immature cDCs express inflammatory chemokine receptors, such as CCR1, CCR2, CCR5 and CXCR1 (Sallusto et al., 1998; Sozzani et al., 1999; 2000). Upon an inflammatory insult, injury or infection, immature cDCs are recruited to the site by the recognition of inflammatory chemokine ligands for these receptors. Activation of TLRs by exposure to microbial stimuli or proinflammatory cytokines, such as IL-1 β and TNF α , results in maturation of cDCs (Allavena et al., 2000; Alvarez et al., 2008). cDC maturation is accompanied by a decrease in their capacity to internalise Ag, and a parallel increase in their ability to present Ag. Mature cDCs upregulate production of the Ag peptide presentation complex, MHCII, whilst immature cDCs have low surface levels of MHCII (Cella et al., 1997; Sallusto and Lanzavecchia, 2002; Wilson et al., 2003). Immature splenic cDCs have a rapid turnover rate and their activation is associated with increased turnover and a shortened lifespan. This might act to limit the duration of Ag presentation and, as a consequence, the T cell mediated immune responses to that Ag (Kamath et al., 2000; 2002). Furthermore, cDC maturation results in a switch in the chemokine expression profile, with downregulation of inflammatory chemokine receptors and upregulation of CCR7 (Dieu et al., 1998; Sallusto et al., 1998; Sozzani et al., 1999; 2000; Alvarez et al., 2008). CCR7 leads to recruitment of mature/maturing cDCs to the draining LN. DCs enter LNs through the afferent lymphatics and accumulate in the subcapsular sinus (Weinlich et al., 1998; von Andrian and Mempel, 2003; Ohl et al., 2004; Alvarez et al., 2008; Wendland et al., 2011). As discussed above (section 1.4.1.1), the emigration of cDCs from the sinus to the T cell zones is CCR7 dependent, and *plt/plt* animals have a deficit of cDCs in the T cell zones with cDCs trapped in the subcapsular sinus (Gunn et al., 1999; Alvarez et al., 2008; Braun et al., 2011).

The CCR7 dependent migration of cDCs from the periphery into LNs is an essential step in the development of peripheral tolerance (Worbs et al., 2006). Negative selection of self-reactive T cells in the thymus results in their deletion,

however not all cells specific for self-Ag are deleted and some escape into the periphery. cDCs are continuously exposed to self-Ag, such as apoptotic cells, which they can carry to LNs, and process and present to T cells. The activation of T cells specific for self-Ag could have deleterious effects, driving development of autoimmune diseases. Thus, cDCs are the driving force of peripheral tolerance, minimising the action of T cells specific for self-Ag by rendering them anergic or stimulating their differentiation into Tregs, thereby maintaining tolerance against self-Ags (Banchereau and Steinman, 1998; de St Groth, 2001; Lutz and Schuler, 2002; Steinman et al., 2003; Ohl et al., 2004).

Nakano *et al.* have reported that not all cDCs are dependent on CCR7 for their migration to LNs, as although there was a significant reduction in the number of all cDC subsets in a resting LN of a *plt/plt* mouse there was no effect on the number inflammatory DCs, identified as CD11c⁺CD11b⁺Gr1⁺ (Nakano et al., 2009). They reported that viral infection resulted in the accumulation of inflammatory DCs in LNs as a consequence of Ly6C^{hi} monocyte migration directly from the blood to the LN (Nakano et al., 2009). The extravasation of Ly6C^{hi} monocytes from the BM is highly CCR2 dependent (Serbina and Pamer, 2006) and consistent with these observations Nakano *et al.* observed a decrease in LN inflammatory DC accumulation in a CCR2 KO animal (Nakano et al., 2009). A similar decrease was not observed in CCL2 KO mice, indicating that CCL2 is not required for inflammatory DC accumulation (Nakano et al., 2009). Nakano *et al.* proposed that CCL8 is induced and that it is responsible for CCR2 dependent accumulation of inflammatory DCs, not CCL2 (Nakano et al., 2009). However, it is now known that CCL8 is not a CCR2 ligand in mice, but binds to CCR8 (Islam et al., 2011). A deficiency of either CCR2, or its ligands, CCL2 or CCL7, leads to a reduction in peripheral Ly6C^{hi} monocyte numbers. However, retention of Ly6C^{hi} monocytes in the BM was less pronounced in CCL2 KO mice, and low numbers of Ly6C^{hi} monocytes are found in the periphery, which might explain the presence of inflammatory DCs in these animals (Tsou et al., 2007). Therefore, recruitment of inflammatory DCs to LNs is likely to be CCR2 independent, and the decrease in LN accumulation of inflammatory DCs might be due to decreased Ly6C^{hi} monocytes in the blood of CCR2 deficient mice.

cDCs within the T cell zones produce CCR7 ligands, which induce extension of dendrites on the mature cDC (Cyster, 1999; Yanagawa, 2002; Mebius and Kraal,

2005). Mature activated cDCs also produce thromboxane A₂ that enhances random motility of T cells (von Andrian and Mempel, 2003; Kabashima et al., 2003). Both of these processes increase the probability of an encounter between a cDC and a cognate T cell. The interaction of T cells with cDCs, as described earlier, occurs in the T cell zones of LNs and spleen (von Andrian and Mempel, 2003; Mebius and Kraal, 2005). CCL21 is also found bound to the surface of LN cDCs. Chemokine-bearing cDCs mediate an initial chemokine-mediated tether between cDCs and T cells. This tether precedes synapse formation and does not support TCR signalling, but enhances the probability of an Ag dependent interaction between the tethered T cell and neighbouring cDCs presenting Ag specific for its TCR (Friedman et al., 2006). The Ag dependent contact between T cells and cDCs occurs via the immunological synapse, a specialised area containing adhesion molecules, MHCII and TCRs (Grakoui et al., 1999; Sallusto and Lanzavecchia, 2002). Activation and the full differentiation of naïve T cells requires three signals. Signal one is the recognition of MHCII presented Ag via the TCR. Signal two is provided by costimulatory molecules, such as CD80 and CD86. To support this process, maturing cDCs also upregulate costimulatory molecules and MHCII. Cytokines, such as IL-23 and IL-12 provide signal 3, determining the outcome of T cell activation, polarising T cells to an effector phenotype and influencing their homing properties. However, additional signals can be provided by molecules such as retinoic acid and Vitamin D3 (Hart, 1997; Banchereau et al., 2000; Sallusto and Lanzavecchia, 2002; Miloud et al., 2010). Activation of naïve T cells results in their proliferation in an IL-2 dependent manner and their differentiation into effector cells (Sallusto and Lanzavecchia, 2002; Liao et al., 2011). Effector cells comprise CD4⁺ Th cells, cytolytic CD8⁺ T cells, Tregs or memory cells. It is these memory T cells that provide a rapid response to previously encountered Ag. They can respond to low doses of Ag even in the absence of costimulatory molecules and do not require Ag presentation by DCs (Sallusto and Lanzavecchia, 2002; Sallusto et al., 2004).

Earlier in this Introduction, I described two routes for Ag delivery to LNs. The first, involves delivery of processed Ag from peripheral tissue by migratory mature cDCs. The second route of delivery is the lymphatic drainage of peripheral tissues, which carries Ag to LNs where it can be taken up by resident cDCs for Ag presentation. The majority of cDCs resident in secondary lymphoid

organs are reported to be immature and therefore possess a high capacity to capture Ag (Wilson et al., 2003). Resident cDCs can project extensions into the channels of the conduit system and pick up lymph-borne Ag (Rozenendaal et al., 2008). cDCs in the spleen are also exposed to systemic (blood-borne) Ag as well as local splenic Ag (von Andrian and Mempel, 2003; Mebius and Kraal, 2005). Thus, secondary lymphoid organ resident cDCs are most likely responsible for the development of an immune response against Ag delivered via lymph or blood to the lymphoid organs (Sixt et al., 2005).

The spleen contains several subsets of cDCs that can be distinguished based on their expression of CD8 α , CD11b and CD4. Splenic cDCs can be broadly divided into two groups: the CD8 α^+ cDCs, which are negative for CD11b, and CD11b $^+$ cDCs that are negative for CD8 α (Pulendran et al., 1997; Vremec and Shortman, 1997; Leenen et al., 1998; Vremec et al., 2000; Wilson et al., 2003). The CD11b $^+$ cDC population can be further subdivided into two subsets that are CD4 $^+$ or CD4 $^-$, both of which are located in the MZ of the spleen. Upon activation by inflammatory stimuli, such as LPS, they migrate into the T cell zone (Banchereau et al., 2000; Vremec et al., 2000; McLellan et al., 2002). The CD8 α^+ cDC subset are mainly located within the T cell zone regardless of their activation state (Wilson et al., 2003; Shortman and Heath, 2010). These two groups of cDCs differ in their expression of TLR, with CD8 α^+ cDCs possessing higher levels of expression of TLR3, and CD11b $^+$ cDCs having higher expression of TLR5 and 7 (Edwards et al., 2003). However, both subsets express TLR4, the receptor for LPS (Mazzoni and Segal, 2004) and following induction of systemic inflammation by LPS administration, both the CD8 α^+ and CD11b $^+$ cDCs have increased turnover rates (Kamath et al., 2000) and die by apoptosis (Zanoni and Granucci, 2010). Experiments conducted by Liu *et al.* using parabiotic mice have provided data suggesting that blood-borne DC progenitors replenish splenic and LN DC network (Liu et al., 2007). Earlier I also discussed the role of the Flt3L responsive splenic pre-cDCs in restoring cDC numbers (Hochweller et al., 2009).

CD8 α^+ and CD11b $^+$ cDCs show several functional differences. CD8 α^+ cDCs are able to cross prime CD8 $^+$ T cells by presenting exogenous Ag on MHC class I, but are less efficient than CD11b $^+$ cDCs at presenting Ag on MHCII (Haan et al., 2000; Shortman and Heath, 2010). The interaction of the cross-priming CD8 α^+ cDCs

with CD8⁺ T cells is mediated by the chemokine receptor XCR1 and its ligand XCL1. XCR1 reporter mice illustrated that XCR1 was exclusively expressed by CD8 α^+ cDCs, and CD8⁺ T cells produced XCL1, which stimulates XCR1 dependent chemotaxis of the CD8 α^+ cDCs. In the absence of XCL1, there was a decrease in the number of T cells reacting to Ag cross-presented by CD8 α^+ cDCs (Dorner et al., 2009). A population of splenic CD8 α^+ DCs have also been found to be positive for the expression of the C-type lectin langerin (Douillard et al., 2005; Kissenpfennig et al., 2005). Langerin is a marker of Langerhans cells, APCs which are found in the epidermis of skin (Kissenpfennig et al., 2005). Langerhans cells traffic to LNs via the dermal lymphatics in a CCR7 dependent manner (Gunn et al., 1999). Fluorescein isothiocyanate (FITC) painting of the epidermis of mice activates Langerhans cells resulting in an accumulation of FITC⁺ Langerhans cells in the LN. There are significantly fewer Langerhans cells in the LN of *plt/plt* mice (Gunn et al., 1999). Interestingly, following FITC painting Langerin⁺ cells in the spleen did not become FITC⁺. Similarly, a population of Langerin⁺ CD8 α^+ DCs has been reported in PLNs, which also do not become FITC⁺, but the “classical” Langerhans cells, identified as Langerin⁺CD8 α^- were FITC⁺ and their appearance in the PLNs was blocked by treatment with pertussis toxin. These results suggest that Langerhans cells within lymphoid organs might be segregated into two subpopulations: the blood-derived Langerin⁺CD8 α^+ DCs that do not migrate from the skin, and Langerin⁺CD8 α^- cells that migrate from the skin (Douillard et al., 2005; Kissenpfennig et al., 2005).

1.5.3 pDCs

pDCs come under scrutiny in a major part of the Results section of my thesis so in this section I will describe the identification of pDCs and their subsets, followed by chemokine receptor expression by pDCs and the roles these receptors might play in pDC migration. I will then present an overview of the role of pDCs within the immune system. The majority of studies described in this section were performed in mice; when human data is described this distinction will be made clear.

pDCs are rare cells (0.3-0.5% of lymphoid organs) that originate in the BM (Naik et al., 2005a; Reizis et al., 2011a). Although pDCs are classed as DCs they exhibit functional and morphological differences from cDCs. pDCs were originally

described as a minor subset of leukocytes, being found to have similar morphological properties to secretory lymphocytes (Asselin-Paturel et al., 2001; Bjorck, 2001; Nakano et al., 2001). In addition, their classification as plasmacytoid cells was due to similarities in morphology between pDCs and plasma B cells, and also by their expression of the B cell marker B220/CD45RA (Naik et al., 2005a; Reizis et al., 2011a). Furthermore, they were originally called plasmacytoid T cells due to their localisation within the T cell zones in human lymphoid tissue (Colonna et al., 2004; Liu, 2005). Likewise, murine splenic pDCs are mainly found within PALS, but can also be found in the red pulp (Asselin-Paturel et al., 2003; 2005; Umemoto et al., 2012). Murine pDCs have been shown to express low levels of MHCII and costimulatory molecules, in addition to low levels of CD11c, all molecules expressed at high levels on cDCs. pDCs are less efficient at T cell priming than cDCs, but can stimulate memory CD8⁺ T cells and effector Th1 cells (Colonna, 2003; Fonteneau et al., 2003). Furthermore, TLR7 and TLR9 activation of pDCs is reported to endow them with the ability to prime naïve T cells (Asselin-Paturel et al., 2001; Mouriès et al., 2008; Villadangos and Young, 2008). Another difference between cDCs and pDCs is in the turnover rate of these cells: cDCs turn over rapidly, whereas pDCs turn over relatively slowly. Potentially the most obvious distinction between these two dendritic cell types is a functional difference, as pDCs possess the ability to produce high levels of type I IFNs (IFN α/β) quickly in response to viral infections via stimulation through TLR7 and TLR9 (Naik et al., 2005a; Reizis et al., 2011a).

1.5.3.1 Subsets of pDCs

In addition to the complexity of their classification, a further complication of pDCs is in their identification. There is no specific pDC marker, even though the most commonly used marker, PDCA1, also known as BST2 or tethrin, is often mistakenly thought of as one. PDCA1 is also expressed on plasma cells and during activation can also be found on several other cell types, including cDCs (Asselin-Paturel et al., 2003; Blasius et al., 2006b). Thus, several cell surface markers are required to accurately identify pDCs. Typically used markers are B220, CD11c, MHCII, Siglech, and Ly6C (Colonna et al., 2004; Reizis et al., 2011a). Flow cytometry illustrated that Siglech was specifically expressed by pDCs in the BM, spleen, blood and LNs (Zhang et al., 2006; Blasius et al., 2006a). However, staining of tissues sections with anti-Siglech illustrated that a subset of MZ

macrophages in the spleen and medullary macrophages in LNs also expressed SiglecH (Zhang et al., 2006).

The lack of a pDC specific antibody has hampered investigations into pDC function *in vivo*, and as a consequence many studies establishing pDC function have been performed *ex vivo*. In the absence of a pDC specific antibody, pDCs can not be specifically ablated, as treatment with anti-PDCA1 or anti-CD11c results in the deletion of additional cell types. Mice deficient in PDCA1 have been generated, but in addition to the deletion of pDCs, plasma cell numbers are affected (Blasius et al., 2006b). Recently, a diphtheria toxin receptor (DTR)-mediated conditional SiglecH KO has been generated (SiglecH-DTR). Following treatment with a single dose of diphtheria toxin, pDCs in the spleen, MLNs and BM of SiglecH-DTR mice were completely ablated, while there were no changes in the proportions of cDCs or other leukocytes. Tissue section staining illustrated that localisation of MZ macrophages was not affected in diphtheria toxin treated SiglecH-DTR mice (Takagi et al., 2011).

Both PDCA1 and SiglecH have been described to modulate pDC function. PDCA1 has been reported to limit viral spread and infection by preventing viral release from infected cells. Therefore, PDCA1 deficient animals were expected to have increased viral titres following infection, however they were shown to have decreased IFN α and decreased viral titres in lungs following intranasal infection with influenza B virus. There was an increase in the number of CD8⁺ virus specific T cells within the infected lungs of PDCA1 KO mice (Swiecki et al., 2012). Interestingly, in addition to being located on the cell surface, PDCA1 is found in the Golgi apparatus and has been reported to regulate IFN α production. Binding of PDCA1 by anti-PDCA1 antibodies has been reported to cause a decrease in CpG induced IFN α production by splenic pDCs (Blasius et al., 2006b). Blasius *et al.* have also reported that incubation of purified splenic pDCs with anti-SiglecH antibodies caused a reduction in CpG induced IFN α secretion (Blasius et al., 2004). Furthermore, subcutaneous (s.c.) administration of CpG and SiglecH antibody resulted in a decrease in the level of IFN α present in the serum, with no effect on pDC numbers (Blasius et al., 2004). In sharp contrast, Zhang *et al.* reported no effect on IFN α production following addition of SiglecH antibody to BM derived pDCs (Zhang et al., 2006).

The use of Siglech-DTR mice, which are actually deficient in Siglech transcript and surface protein has revealed that in the absence of Siglech, pDCs have altered developmental processes. They had higher levels of PDCA1 and CD11c, and produced more IFN α and IL12p40 than WT pDCs following treatment with CpG (Takagi et al., 2011). The absence of Siglech and ablation of pDCs was shown to enhance Ag specific CD4⁺ T cell responses, as untreated Siglech-DTR and pDC ablated animals had increased Ag specific division of OTII OVA specific T cells compared to WT animals. The increase in Ag specific division was accompanied by a parallel decrease in the ability of pDC-ablated animals to induce Treg generation (Takagi et al., 2011). Siglech can also function as an endocytic receptor mediating Ag uptake. OVA conjugated to anti-Siglech antibodies was internalised, processed and cross-presented on MHC class I to CD8⁺ T cells (Zhang et al., 2006). Takagi *et al.* also showed *in vivo* that a deficiency in pDCs or an absence of Siglech led to a decrease in Ag specific division of OTI OVA specific CD8⁺ T cells, which was overcome by reconstitution with WT pDCs (Takagi et al., 2011). Collectively, these results illustrate that pDCs can mediate Ag specific T cell responses, and that Siglech is involved in cross-presentation of Ag and regulates the generation of effector T cells and Tregs (Zhang et al., 2006; Takagi et al., 2011).

Following the identification of pDCs using a combination of the above markers, several groups have recently described subsets of pDCs based on the expression of one or more surface proteins. It has also been proposed that the expression of these markers may indicate different stages of pDC development, rather than discrete subsets. The expression of these markers by putative immature and mature pDCs is summarised in Table 1-3. Kamogawa-Schifter *et al.* identified two subsets of pDCs based on the expression of a single marker, Ly49Q (Kamogawa-Schifter et al., 2005). Ly49Q is a type II C-type lectin and is a member of the Ly49 family of mouse NK receptors. However, it is not found on NK cells, NKT cells or T cell subsets, but is preferentially expressed on Gr1⁺ cells, including monocytes, neutrophils and pDCs (Omatsu et al., 2005; Toyama-Sorimachi et al., 2004). Both Ly49Q⁺ and Ly49Q⁻ pDCs have been identified in the BM. However, these cells were only classified as B220⁺CD11c⁺ before gating for Ly49Q. The B220⁺CD11c⁺ population can actually contain multiple cell types, such as NK-like cells and cDC progenitors. Nevertheless, both Ly49Q⁺ and Ly49Q⁻

populations produced high levels of IFN α in response to stimuli, indicating that they contained pDCs (Kamogawa-Schifter et al., 2005). Recent publications contradict the classification of two subsets of pDCs based on Ly49Q expression, and have identified Ly49Q as a marker of pDC maturation (Omatsu et al., 2005; Toma-Hirano et al., 2007). Toma-Hirano *et al.* and Omatsu *et al.* have both found that peripheral pDCs express Ly49Q, whereas Ly49Q⁻ pDCs in the BM acquire expression of the marker before migrating to the periphery. Both groups conclude that Ly49Q⁻ pDCs are an earlier developmental stage of pDCs that differentiate into the mature Ly49Q⁺ pDCs found in the spleen and LNs (Omatsu et al., 2005; Toma-Hirano et al., 2007).

Surface Marker	Immature	Mature
Ly49Q	-	+
CD4	-	+
CD9	+	-
CCR9	-	+

Table 1-3: Proposed expression of surface markers by developmentally immature and mature pDCs.

Another group has proposed that the developmental stages of pDCs can be defined by CD4 expression with CD4⁻ pDCs maturing into CD4⁺ pDCs (O’Keeffe et al., 2002; Naik et al., 2005a). O’Keeffe *et al.* transferred purified CD4⁺ and CD4⁻ pDCs from the spleen of a Ly5.2⁺ mouse into a normal, non-irradiated and non-stimulated Ly5.1⁺ mouse and found that CD4⁻ pDCs acquired expression of CD4 (O’Keeffe et al., 2002). Similarly, Omatsu *et al.* found that there was a parallel acquisition of CD4 with Ly49Q expression by the mature pDC population (Omatsu et al., 2005). CpG induced activation of pDCs resulted in the downregulation of CD4 expression (O’Keeffe et al., 2002). Recent research has defined three subpopulations of pDCs based on expression of CD8 α and CD8 β : CD8 α ⁻ β ⁻, CD8 α ⁺ β ⁻, and CD8 α ⁺ β ⁺. The three subsets are mature unactivated pDCs, as defined by their expression of Ly49Q and the absence of activation markers. It was also shown that, in a model of allergic lung inflammation, CD8 α ⁺ populations had tolerogenic properties, both inducing generation of FoxP3⁺ Tregs and preventing the development of airway hyperreactivity (Lombardi et al., 2012). Lombardi *et al.* also demonstrated that activation of pDCs via TLR7 or TLR9 did

not alter their expression of CD8 α or CD8 β (Lombardi et al., 2012), which is in contrast to O’Keeffe *et al.* who showed that activation of pDCs was associated with upregulation of CD8 α (O’Keeffe et al., 2002). Lastly, Björck *et al.* have described two developmental stages of pDCs based on the expression of CD9 (Björck et al., 2011). CD9⁺ pDCs were purified from the BM and labelled with 5-Carboxyfluorescein diacetate succinimidyl ester (CFSE) and injected into a non-irradiated and non-stimulated recipient and after 4 days were found to lose CD9 expression. The majority of BM pDCs were CD9⁺ and following their migration and differentiation into developmentally mature pDCs in the periphery lost CD9 expression (Björck et al., 2011). The CD9⁺ subset was CD4⁻ and the CD9⁻ subset was CD4⁺ (Björck et al., 2011). This supports the conclusion drawn from the work by the O’Keefe group, as they determined the CD4⁻ subset to be a precursor of CD4⁺ pDCs (O’Keeffe et al., 2002).

When describing the developmental stages of pDCs, all groups looked at the IFN α producing capabilities of these cells either by enzyme-linked immunosorbent assay (ELISA) or by monitoring intracellular IFN α . O’Keeffe *et al.* measured IFN α by ELISA following stimulation of pDCs with CpG for 14 hours (hrs) (O’Keeffe et al., 2002). Omatsu *et al.* (Omatsu et al., 2005) and Björck *et al.* (Björck et al., 2011) monitored intracellular IFN α levels following 5 or 9 hrs stimulation with CpG, respectively. All groups found that the two subsets had the ability to produce IFN α in response to bacterial CpG stimulation (O’Keeffe et al., 2002; Omatsu et al., 2005; Toma-Hirano et al., 2007), except Björck *et al.* who showed that the CD9⁻ pDCs only produced minimal levels of IFN α (Björck et al., 2011). Interestingly, most groups showed that the developmentally more “immature” pDC subset, CD4⁻ or CD9⁺, are the cells responsible for producing the majority of IFN α in response to *Staphylococcus aureus* extract or influenza virus, respectively (Björck et al., 2011); O’Keeffe et al., 2002). This would indicate that the developmentally immature pDCs are responsible for the majority of IFN α production in response to viral infections and that mature (CD4⁺CD9⁻) pDCs produce minimal levels of IFN α (O’Keeffe et al., 2002; Björck et al., 2011). It has also been proposed that these mature peripheral pDCs promote immune tolerance (Björck et al., 2011). However, research using the Ly49Q marker to determine maturation has, in fact, suggested that the reverse is true. The developmentally immature Ly49Q⁻ pDCs that differentiate to acquire the

maturation marker Ly49Q, actually produce less IFN α/β and inflammatory cytokines (IL-6 and IL-12) than the mature Ly49Q⁺ pDCs (Omatsu et al., 2005; Toma-Hirano et al., 2007). Thus, there remain some contradictions over the function of developmentally mature and immature pDCs.

In brief, identification of pDCs requires a range of cell surface markers (Colonna et al., 2004; Reizis et al., 2011a). Gating strategies typically use a combination of pDC “specific” markers, such as PDCA1 (Asselin-Paturel et al., 2003; Blasius et al., 2006b) and SiglecH (Zhang et al., 2006; Blasius et al., 2006a), and markers expressed by other cell types, such as B220, CD11c and Ly6C (Colonna et al., 2004; Reizis et al., 2011a). Furthermore, developmentally mature pDCs can theoretically be distinguished from immature pDCs by differences in expression of several markers (Table 1-3). Mature pDCs are proposed to be Ly49Q⁺, CD4⁺, CD9⁻, CD8 α ⁺ and CCR9⁺, whereas immature pDCs are Ly49Q⁻, CD4⁻, CD9⁺ and CCR9⁻ (O’Keeffe et al., 2002; Omatsu et al., 2005; Björck et al., 2011; Lombardi et al., 2012). This division might be oversimplified, as no study has examined the expression of all five markers on splenic pDCs. The majority of research has illustrated that both immature and mature pDCs can produce IFN α , but there is debate over which pDC developmental stage has the superior ability to produce IFN α (O’Keeffe et al., 2002; Omatsu et al., 2005; Björck et al., 2011).

1.5.3.2 Chemokine receptor expression

Despite the current controversy regarding the identification and function of the maturation states of pDCs, they have been assigned several key roles *in vivo*. In addition, several lines of evidence suggest that pDC subset location and function is critically dependent on chemokine receptor expression. pDCs have been shown to express a variety of chemokine receptors, both inflammatory (CCR2, CCR5 and CXCR3) and homeostatic (CCR9, CXCR4 and CCR7) (Wendland et al., 2007; Randolph et al., 2008; Seth et al., 2011). Several groups have investigated the role of many of these chemokine receptors in pDC migration. For example, CCR9 is responsible for the migration of pDCs into the intestine, in both homeostatic and inflammatory conditions. pDCs are largely absent from the intestine of an animal deficient in CCR9, but pDC numbers in secondary lymphoid organs are unaffected (Wendland et al., 2007). In the BM, Björck *et al.* have shown that the two developmental pDC stages, the CD9⁺ and CD9⁻, are also CCR9⁻ and CCR9⁺,

respectively (Björck et al., 2011). CD9⁻CCR9⁺ pDCs were reported to be mature peripheral pDCs that secrete low levels of IFN α in response to viral infection. It also appears that it is the precursor CCR9⁻ population of pDCs that is responsible for the secretion of proinflammatory cytokines, such as TNF α and IL-6 (Björck et al., 2011). In support of these observations, Schlitzer *et al.* have recently identified a pDC precursor in the BM and in secondary lymphoid organs that is CCR9⁻ (Schlitzer et al., 2011). Upon CpG stimulation, the precursor CCR9⁻ pDCs secreted higher levels of IFN α , IL-12 and IL-6 than CCR9⁺ pDCs (Schlitzer et al., 2011). Hadeiba *et al.* also report that the majority of peripheral pDCs are CCR9⁺ (Hadeiba et al., 2008). This group found that CCR9 was rapidly downregulated in response to activation by TLR7 or TLR9 ligands, while co-stimulatory molecules and MHCII were upregulated. Interestingly, it was found that both the CCR9⁺ and CCR9⁻ populations could both produce IFN α in similar quantities in response to CpG (Hadeiba et al., 2008). However, a consistency between the two groups was in the description of CCR9⁺ pDCs being responsible for the tolerogenic properties associated with pDCs (Hadeiba et al., 2008; Björck et al., 2011; Schlitzer et al., 2011). The tolerogenic role of pDCs is thought to occur due to their induction of Tregs that secrete the anti-inflammatory cytokine, IL-10 (Colonna et al., 2004; Ito et al., 2007; Baba et al., 2009; Matta et al., 2010). Hadeiba *et al.* demonstrated that CCR9⁺ pDCs suppressed the frequency of IL-17 producing effector T cells, thereby decreasing the clinical severity of allogeneic graft versus host disease. CCR9⁺ pDCs induced the development of FoxP3⁺ Tregs cells, which also contributed to the reduction in disease severity (Hadeiba et al., 2008).

Other chemokine receptors have also been ascribed roles in pDC migration. Until very recently, CCR7 had only been shown to mediate migration of pDCs in *in vitro* chemotaxis assays, but it has now been shown to facilitate pDC extravasation into LNs through HEVs (Seth et al., 2011). Originally, this role was thought to be accomplished by CCR5, which was one of the few identified receptors that could mediate a chemotactic response resulting in the mobilisation of pDCs to an inflamed LN vessel (Colonna et al., 2004; Randolph et al., 2008; Sozzani et al., 2010; Seth et al., 2011). However, Seth *et al.* showed that although CCR7 was present in minute levels on naïve cells, it was highly upregulated on pDCs following their activation with TLR ligands (Seth et al.,

2011). Interestingly, CCR7 KO animals, regardless of their activation status, display reduced LN pDC numbers due to impairment in the mobilisation of CCR7 deficient pDCs. Conversely, BM and splenic pDC numbers were not affected by the absence of CCR7. This would indicate that, similar to naïve T cells, pDCs may also demonstrate increased integrin affinity in response to CCR7 signalling, which facilitates effective adhesion and migration across HEVs (Seth et al., 2011). Results produced in our lab by Elinor Anderson also show that mice deficient in CCX-CKR, the atypical chemokine receptor for CCL19, CCL21 and CCL25, have a deficit in pDC numbers restricted to their MLNs (Anderson, 2011).

pDCs have been shown to constitutively migrate into the splenic white pulp using a combination of CCR7 and CXCR4 to traverse MZ bridging channels (Umemoto et al., 2012). Another inflammatory chemokine receptor reported to mediate pDC migration *in vivo* is CXCR3 which has been shown to mediate murine pDC migration across HEVs during times of inflammation (Yoneyama et al., 2004). In addition, intravenous (i.v.) administration of CpG leads to the migration of some pDCs into the MZ, and the formation of pDCs clusters in both the MZ and T cell zones of the spleen. The initial migration and clustering of pDCs was shown to be dependent on CXCR3 and CXCR4, and at later time points was entirely CCR7 dependent (Asselin-Paturel et al., 2005).

In contrast to the previously discussed chemokine receptors, CCR2 has yet to be designated an *in vivo* role in pDC migration. Investigations using human pDCs have suggested that CCR2 is non-functioning in *in vitro* migration assays (Colonna et al., 2004). Interestingly, it has been reported that although most murine BM pDCs express CCR5 and CXCR3, only ~25% express CCR2 (according to staining with anti-CCR2 antibody MC-21) (Wendland et al., 2007), indicating that CCR2 might have a role on a specific subset of pDCs. However, Wendland *et al.* also demonstrated that a significantly higher proportion of Flt3L expanded splenic pDCs expressed CCR2 compared to BM pDCs from an untreated animal (Wendland et al., 2007). Baba *et al.* have shown that the absence of CCR2 or CCR5 does not affect thymic pDCs numbers (Baba et al., 2009). However, recruitment of pDCs to sites of imiquimod induced skin inflammation has been reported to be dependent on the CCR2 ligand, CCL2 (Drobits et al., 2012).

1.5.3.3 pDC function

pDCs have been described to have a variety of functions, with the majority of their functions reliant on their ability to produce high levels of IFN α/β following TLR7 or TLR9 activation (Gibson et al., 2002; Colonna et al., 2004; Fuchsberger et al., 2005). TLR7 and TLR9 are expressed intracellularly and recognise single stranded viral RNA and DNA that is transported to the endosomal compartments upon infection of a cell with virus (Edwards et al., 2003; Colonna et al., 2004; Fuchsberger et al., 2005). IFN α has well-characterised, direct anti-viral effects, including inhibition of viral replication and upregulation of IFN-stimulated genes, such as *ribonuclease L*, which also combat viral replication. Thus, pDCs have a vital role in immune defence against viral infections (Borrow et al., 2010). In addition, they have been described to function in tissue repair following acute injury (Colonna et al., 2004; Smit et al., 2006; Gilliet et al., 2008; Gregorio et al., 2010; Cervantes-Barragan et al., 2012). For example, although pDCs can be found in the majority of secondary lymphoid organs in low numbers, they are actually absent from most peripheral tissues, including normal skin. However, following injury to the skin, pDCs are rapidly recruited to the injury site (Gilliet et al., 2008; Gilliet and Lande, 2008; Gregorio et al., 2010). Human pDCs have been shown to respond to CXCR3 ligands, and production of CXCR3 ligands is induced by skin injury. Therefore, it has been proposed that CXCR3 might play a role in pDC recruitment to sites of inflammation (Vanbervliet et al., 2003; Gregorio et al., 2010). Chemerin, the ligand for chemokine-like receptor 1, has also been assigned a role in pDC recruitment to inflamed skin. Chemerin is constitutively produced in an inactive form by keratinocytes and endothelial cells in healthy skin. It is only following its activation by C-terminal cleavage by serine proteases that chemerin can stimulate pDC recruitment to inflamed skin. It has been hypothesised that skin injury might stimulate protease release from damaged keratinocytes (Vermi et al., 2005; Gregorio et al., 2010).

Gregorio *et al.* have demonstrated, using a tape strip model of skin injury, that the infiltration of pDCs is rapid, occurring within 24 hrs after injury. This was transient, as pDC numbers were dramatically reduced within 48 hrs, and returned to the low levels found in healthy skin (Gregorio et al., 2010). The infiltrated pDCs produce high levels of IFN α/β , in response to TLR7 and TLR9 stimulation, and contribute to wound healing. Interference with the IFN α/β

pathway, either through inhibition of IFN α/β receptor signalling or in mice lacking the receptor for these cytokines, led to an impairment in wound healing due to a delay in wound re-epithelisation (Gregorio et al., 2010; Guiducci et al., 2010). Furthermore, the inflammatory response was profoundly affected in the absence of the IFN α/β receptor. There was a deficiency in IL-6, IL-17 and IL-22 expression in injured skin, thereby demonstrating the pivotal role of IFN α/β produced by infiltrating pDCs in early inflammatory responses (Gregorio et al., 2010; Guiducci et al., 2010).

Interestingly, in this model of skin injury, the groups concluded that the stimulus for pDC activation via TLR7 and TLR9 was actually host derived nucleic acids (Gilliet and Lande, 2008; Gregorio et al., 2010; Guiducci et al., 2010). This was a consequence of the induction of a cathelicidin peptide, which forms a complex with the self RNA and DNA released upon cell damage and transports them to the endosomes containing TLR7 and TLR9. However, although cathelicidin was sufficient to promote IFN α/β , it was not essential (Gilliet and Lande, 2008; Gregorio et al., 2010; Guiducci et al., 2010). The chronic activation of pDCs by nucleic acids can lead to the development of autoimmune diseases of the skin. For example, the thickening of the epidermal layer, characteristically found in psoriatic lesions, is thought to occur as a consequence of IFN α/β production from chronically activated pDCs leading to the expansion of autoimmune T cells (Anandarajah and Ritchlin, 2004). In summary it is clear that IFN-producing pDCs, whether characterised as mature or immature, have a major role in the induction of skin inflammation. Somewhat paradoxically, these same cells may have a major role in the resolution of inflammation, as they can substantially aid wound healing processes. Both these contrasting roles are likely dependent on continuous recruitment of pDCs with IFN-producing potential from the BM into the blood (Anandarajah and Ritchlin, 2004; Gilliet and Lande, 2008; Gregorio et al., 2010; Guiducci et al., 2010).

The chronic activation of pDCs has also been associated with other autoimmune diseases, in particular systemic lupus erythematosus (SLE). A dominant feature of SLE is the formation of immune complexes that are deposited in different parts of the body. Immune complexes are mainly formed by an interaction of autoantibodies with self-nucleic acids that are released from dying cells.

Autoantibodies are produced from autoreactive B cells that become activated as a consequence of a breakdown in tolerance to nuclear self-Ags. The deposition of the immune complexes triggers immune reactions leading to inflammation and detrimental tissue damage, particularly in the kidneys (Banchereau and Pascual, 2006; Pascual et al., 2006; Mangini et al., 2007; Rönnblom and Pascual, 2008; Santiago-Raber et al., 2009). pDCs are thought to play a pivotal role in the development of SLE, due to their recognition of self-nucleic acids via TLR7/9. This can lead to their chronic activation of pDCs and secretion of copious amounts of IFN α/β . IFN α/β has several fundamental roles in the initiation and exacerbation of the disease (Banchereau and Pascual, 2006; Pascual et al., 2006; Mangini et al., 2007; Rönnblom and Pascual, 2008; Santiago-Raber et al., 2009). Firstly, it has DC inducing properties, in that it triggers the unregulated differentiation of monocytes into cDCs. These cDCs capture autoAg and present it to CD4⁺ and CD8⁺ T cells, thereby promoting the loss of tolerance and the development of autoimmunity (Banchereau and Pascual, 2006; Pascual et al., 2006; Mangini et al., 2007). Furthermore, IFN α/β are thought to have direct and indirect actions on B cell function. Foremost, the development of autoreactive T cells via the effects of IFN α/β helps to promote the development of autoreactive B cells into plasma cells. IFN α/β can act directly on these plasma cells, promoting the production of autoantibodies and leading to the generation of immune complexes (Banchereau and Pascual, 2006; Pascual et al., 2006; Mangini et al., 2007).

Crucially, it is important to understand that although pDCs may contribute to the generation of autoimmune diseases, their immunosuppressive properties may balance some of these effects. For example, pDC induction of Tregs is beneficial in reducing the occurrence of autoreactive T cells. However, this property may contribute to pathogenesis in some cases. Indeed, pDCs are known for their ability to induce tolerance to tumour cells, thereby aiding tumour generation and growth (Wei et al., 2005; Sisirak et al., 2012). In spite of this, they can also facilitate protective responses against tumour cells (Matta et al., 2010). The deciding factor in this balance between tolerance and protection against tumours is thought to be the activation state of pDCs. Resting pDCs are thought to induce tumour tolerance via their induction of Tregs, whereas TLR7/9 activated pDCs can induce tumour regression (Colonna et al., 2004; McKenna et

al., 2005; Swiecki and Colonna, 2010). Topical treatment of mice with an imiquimod containing cream, Aldara, leads to a TLR7 and IFN α/β dependent regression of tumours. Tumour regression was coordinated with an increase in pDC numbers, which expressed CD8 α . There was also an increase in the number of NK cells and CD8 $^+$ T cells within the tumour, however the absence of either of these populations had no effect on tumour regression, whereas depletion of pDCs enhanced tumour growth. The cytotoxicity of pDCs corresponded with their expression of CD8 α , as TLR7 activation of pDCs by imiquimod treatment led to upregulation of the cytolytic molecules, TNF-related apoptosis-inducing ligand (TRAIL) and granzyme B. Thus, imiquimod treatment leads to tumour regression as a direct consequence of TLR7 mediated activation of pDCs, with NK cells and T cells having minimal roles (Palamara et al., 2004; Drobits et al., 2012). In contrast, TLR9 mediated activation of pDCs has been shown to cause tumour regression in a CD8 $^+$ T cell- and NK cell-dependent fashion (Liu et al., 2008). However, Sorrentino *et al.* have described a role of TLR9 activated pDCs in generating tolerance to tumours (Sorrentino et al., 2010). This apparent discrepancy might be explained by differences in the tumour model used in these studies; tumour tolerance was described using a lung carcinoma model, whereas tumour regression was illustrated in a model of melanoma. Furthermore, TLR9 activation was induced by two different classes of CpG: tolerance was induced using CpG type B (CpG-B) and regression was induced using CpG type A (CpG-A) (Liu et al., 2008; Sorrentino et al., 2010). There are three classes of CpGs, type A, B and C. CpG-A induces potent IFN α/β production by pDCs; CpG-B induces pDC activation, in terms of expression of costimulatory molecules and MHCII; and CpG type C (CpG-C) induces a combination of the two effects (Krug et al., 2001a; Kerkmann et al., 2003). Thus, differences in the role of pDCs in tumour defence or tolerance might be explained by alterations in the precise nature of the activation of pDCs.

I have highlighted some of the protective and inductive roles for pDCs in a variety of scenarios, but their most imperative role is in the defence against viral pathogens, acting as a vital link between the innate and adaptive immune systems (Swiecki and Colonna, 2010). Production of IFN α/β by activated pDCs promotes cytotoxicity in NK cells and CD8 $^+$ T cell and stimulates their production of the proinflammatory cytokine IFN γ , aiding in defence against viruses (Colonna

et al., 2004; Guillerey et al., 2012). Furthermore, $\text{IFN}\alpha/\beta$ can regulate the production of the Th1 inducing cytokine IL-12, thereby modulating polarisation of naïve CD4^+ T cells. Low levels of $\text{IFN}\alpha/\beta$ lead to IL-12 production by both cDCs and pDCs, polarising naïve CD4^+ T cells to a Th1 phenotype, although high levels of $\text{IFN}\alpha/\beta$ inhibit IL-12 production by cDCs (Asselin-Paturel et al., 2001; Colonna et al., 2004). Activated pDCs also produce the proinflammatory cytokine IL-6, which stimulates the differentiation of B cells into antibody-producing plasma cells (Jego et al., 2003; Colonna et al., 2004). In addition, as already discussed, pDCs can induce development of Tregs, which can lead to tolerance against tumours (Colonna et al., 2004; McKenna et al., 2005; Matta et al., 2010; Sorrentino et al., 2010; Swiecki and Colonna, 2010). However, pDC induced Treg generation has also been shown to dampen autoimmune T cell responses, leading to protection against the development of experimental autoimmune encephalomyelitis (EAE) (Irla et al., 2010). EAE was induced in mice with a pDC specific deficiency in MHCII expression by immunisation with the encephalitogenic myelin oligodendrocyte glycoprotein (35-55) peptide, in combination with Complete Freund's adjuvant (CFA). In the absence of MHCII expression by pDCs, mice had impaired expansion of Ag-specific Tregs, which was associated with exacerbation of EAE in these animals (Irla et al., 2010).

In summary, the varying functions of pDCs are largely dependent on their activation by TLR7/9, and subsequent $\text{IFN}\alpha$ production (Gibson et al., 2002; Colonna et al., 2004; Fuchsberger et al., 2005). $\text{IFN}\alpha$ has direct anti-viral effects and therefore functions as part of the innate immune system. Furthermore, $\text{IFN}\alpha$ provides a link between the innate and adaptive immune system, promoting cytotoxicity in NK cells and CD8^+ T cells, thereby generating an effective immune response against viral pathogens (Colonna et al., 2004; Guillerey et al., 2012). However, activation of pDCs is not always beneficial, as their chronic activation can be detrimental and has been associated with the development of pathologies, such as SLE (Banchereau and Pascual, 2006; Pascual et al., 2006; Mangini et al., 2007) and psoriasis (Anandarajah and Ritchlin, 2004). In addition, pDCs have been described to possess conflicting roles in tumour generation. Activated pDCs, in most cases, induce tumour regression, whereas resting pDCs are thought to induce tolerance to tumour cells, promoting tumour growth (Colonna et al., 2004; McKenna et al., 2005; Swiecki and Colonna, 2010).

Therefore, in addition to generating an effective inflammatory response against pathogenic organisms and tumours, pDCs may also play a role in the maintenance of peripheral tolerance to harmless self-Ag. For instance, mature CCR9⁺ pDCs have been described to possess tolerogenic properties, which facilitate the induction of Tregs (Hadeiba et al., 2008; Björck et al., 2011; Schlitzer et al., 2011).

1.6 Current understanding of CCL2 receptor expression and function

The expression and function of the two CCL2 receptors, CCR2 and D6 are a key focus point in my thesis. Therefore, in this section I will provide an overview of the current understanding of the roles of CCR2 and D6 in the immune system.

1.6.1 CCR2

Expression of CCR2 has been reported on numerous cell types, including Ly6C^{hi} monocytes (Serbina and Pamer, 2006), cDCs (Lewis et al., 2011) and pDCs (Wendland et al., 2007). In addition, other cell populations, such as NK cells (Saederup et al., 2010), neutrophils (Maus et al., 2003) and T cells (Mack et al., 2001) have been reported to express CCR2, however this is a source of controversy. The role of CCR2 differs depending on the cell, organ, or inflammatory environment. A cell system that has been extensively studied, in regards to its expression and the role of CCR2, is the phagocytic system. The phagocytic system of cells includes neutrophils, monocytes, DCs and macrophages.

1.6.1.1 CCR2 and neutrophils

Neutrophils and monocytes both arise from the same precursor in the BM, the GMP, however they both exhibit differential cell division properties, as mature neutrophils take longer to generate than monocytes (Gordon and Taylor, 2005; Sugimoto et al., 2006; Gabrilovich et al., 2012). GMPs are CCR2⁺ (Si et al., 2010), but there is controversy surrounding the expression of CCR2 by neutrophils. Souto *et al.* showed that neutrophils in steady-state mice were CCR2⁻, but that these cells upregulated CCR2 during chronic inflammation and that this was crucial for tissue infiltration in a model of sepsis (Souto et al.,

2011). Similarly migration of neutrophils into postischaemic tissue has also been reported to be CCR2 dependent (Reichel et al., 2006). In contrast, Maus *et al.* reported that neutrophils do not express CCR2, and LPS-induced neutrophil migration was CCR2 independent. However, neutrophil accumulation within pulmonary tissue in response to LPS was increased in the presence of CCL2. Furthermore, absence of CCR2 led to decreased neutrophil accumulation. This decrease in accumulation was coincident with a CCR2 dependent decrease in monocyte mobilisation into pulmonary tissue, and the presence of monocytes led to accelerated and amplified accumulation of neutrophils. Thus, accumulation of neutrophils in inflamed lung tissue was proposed to be mediated by the CCR2 dependent recruitment of monocytes (Maus et al., 2003).

1.6.1.2 CCR2 and monocytes

There are two subsets of monocytes that can be separated by their expression of the surface marker Ly6C. Ly6C^{hi} monocytes express low levels of the chemokine receptor CX₃CR1 and high levels of CCR2. The second subset of monocytes, Ly6C^{lo}, expresses much lower levels of Ly6C, high levels of the CX₃CR1, and lower levels of CCR2. There is a third subset of monocytes that are classed as Ly6C^{inter}, due to their intermediate expression of this marker (Sunderkötter et al., 2004; Serbina and Pamer, 2006; Tacke and Randolph, 2006). The Ly6C^{inter} monocytes are thought to have an intermediate phenotype, i.e. between that of Ly6C^{hi} and Ly6C^{lo} monocytes. They are produced from Ly6C^{hi} monocytes, by the downregulation of CCR2 and Ly6C after inflammation has been resolved, and these cells are thought to mature into Ly6C^{lo} monocytes. Ly6C^{lo} monocytes have a longer half life than Ly6C^{hi} monocytes and can be found in both resting and inflamed tissues (Geissmann et al., 2003; Auffray et al., 2009b). Using mice with a targeted replacement of CX₃CR1 by a green fluorescent protein (GFP) reporter (Jung et al., 2000), CX₃CR1^{hi}Ly6C^{lo} monocytes have been shown to patrol blood vessels in resting animals by crawling on the luminal side of the endothelium (Auffray et al., 2007; 2009b). In contrast, Ly6C^{hi} monocytes are recruited from the BM and into tissues in response to inflammation or infection in a highly CCR2 dependent manner, and are thus classified as inflammatory monocytes. CCR2 is usually considered as an inflammatory chemokine receptor, although the dependence of Ly6C^{hi} monocytes on CCR2 for their egress from the BM during homeostasis demonstrates that CCR2 also has key homeostatic roles

(Sunderkötter et al., 2004; Serbina and Pamer, 2006; Tacke and Randolph, 2006).

The BM has always been assumed to be the main source of monocytes during inflammation. However, very recently Swirski *et al* has presented evidence of a splenic Ly6C^{hi} monocyte reservoir. This reservoir consists of clusters of monocytes in the cords of the subcapsular red pulp. However, CCR2 does not appear to be so critical for the mobilisation of these cells during inflammation. Swirski and coworkers demonstrated that in response to myocardial infarction there was a loss of monocytes from the spleen, gain in blood and no change in BM. The same was true in WT and CCR2 KO mice, indicating CCR2 independent migration from the spleen. Thus, CCR2 is required for monocyte mobilisation from the BM, but not the spleen (Swirski et al., 2009). The migration of monocytes into inflamed LNs has also been reported to be dependent on CCL2. Skin inflammation results in the production of CCL2, which drains into LNs via the lymphatics. HEVs have been reported to present CCL2 on their luminal side, which mediates extravasation of blood-borne monocytes into LNs. The number of monocytes in the draining LN of a CCL2 KO animal was significantly lower, but could be rescued by the administration of CCL2 (Palframan et al., 2001).

CCR2⁺ monocytes have been shown to have important roles in many disease models, particularly in defence against pathogens. CCR2 KO mice have enhanced susceptibility to the intracellular pathogen *Listeria monocytogenes*. This is due to the lack of TipDCs in the spleen. Ly6C^{hi} monocytes give rise to these inflammatory DCs, thus retention of Ly6C^{hi} monocytes in the BM of CCR2 KO mice leaves them susceptible to this infection (Serbina and Pamer, 2006; Serbina et al., 2008). Furthermore, the CCR2-dependent recruitment of Ly6C^{hi} monocytes is involved in the defence against viral pathogens, such as murine cytomegalovirus (MCMV) infection. The induction of IFN α/β production by pDCs was shown to be crucial for the CCR2 dependent release of monocytes from the BM in response to MCMV infection. IFN α/β stimulated production of CCR2 ligands by F4/80⁺ cells in the BM, and, in the absence of CCR2, monocytes were retained in the BM and unable to mount a protective response in the infected liver (Hokeness et al., 2005; Crane et al., 2009).

1.6.1.3 CCR2 in cDC biology

Chiu *et al.* have reported that CCR2 is important for the maturation of cDCs. They induced localised immune responses in the lungs of mice by challenging them with beads coated with *Mycobacterium bovis* protein Ag or *Schistosoma mansoni* egg Ag and found that in the absence of CCR2, cDCs in the lungs of Ag challenged mice had significantly decreased MHCII and CD40 expression (Chiu *et al.*, 2004). BM derived DCs from CCR2 KO mice were also shown to have reduced expression of the costimulatory molecules, CD80 and CD86 compared to WT counterparts (Fiorina *et al.*, 2008; Jimenez *et al.*, 2010). However, differences in the cellularity of the BM of WT and CCR2 KO mice e.g. numbers of Ly6C^{hi} monocytes (Serbina and Pamer, 2006) are likely to have influenced this result because the cellular composition of the BM derived DC cultures would have been different from the start. However, Fiorina *et al.* also showed that cDCs from the spleen of CCR2 KO animals also have reduced expression of CD80, but not CD86 (Fiorina *et al.*, 2008). CCR2 dependent maturation has been hypothesised to act through the transcription factor NF- κ B because the inhibition of NF- κ B blocks cDC maturation and the expression of costimulatory molecules. Jimenez *et al.* proposed a model where the interaction of CCR2 with its ligand, CCL2, induces the activation of NF- κ B, thereby influencing cDC maturation (Jimenez *et al.*, 2010).

CCR2 is involved in the migration of cDCs to inflammatory sites rather than their migration into LNs, which is CCR7 dependent (Sallusto *et al.*, 1998). In contrast, CCR2 has been reported to participate in Langerhans cell migration from inflamed skin to the draining LN. The density of Langerhans cells in the skin of CCR2 KO mice was normal, but the migration of Langerhans cells to the draining LN was diminished in the absence of CCR2 (Sato *et al.*, 2000). Langerhans cells in resting animals are generated and maintained locally by precursors in the epidermis. However, following their depletion by localised skin inflammation, inflammatory Ly6C^{hi} monocytes can replenish the population of Langerhans cell precursors (Ginhoux *et al.*, 2006; Shortman and Naik, 2007). However, it has also been reported that the migration of Langerhans cells from the skin to the draining LNs is not actually CCR2 dependent, but in fact activation of NF- κ B by CCR2 signalling pathways leads to local production of the CCR7 ligand, CCL19 (Jimenez *et al.*, 2010). Thus, CCR2 deficiency not only leads to cDC maturation

defects, but is also associated with decrease CCL19 production, and thus CCR7-dependent migration of Langerhans cells.

1.6.1.4 CCR2 and lymphocytes

The absence of CCR2 results in several other phenotypes. For example, CCR2 KO mice have impaired cytokine responses after bacterial infection, exhibiting a deficit in IL-12 production. This deficit has been observed in LN cells, splenocytes and BM derived DCs following LPS stimulation, and is attributed to decreased production of this cytokine by cDCs (Boring et al., 1997; Peters et al., 2000; Jimenez et al., 2010). IL-12 is required for polarisation of T cell responses to a Th1 phenotype, resulting in the production of T cells capable of releasing the proinflammatory cytokine IFN γ . Thus, in addition to IL-12, CCR2 KO animals produce significantly less IFN γ than WT mice. However, there is no reported difference in the levels of Th2 cytokines detected indicating that CCR2 is only needed for a successful Th1 response (Boring et al., 1997; Peters et al., 2000; Chiu et al., 2004). The deficit in Th1 responses by CCR2 KOs has been reported to be as a consequence of the absence of IL-12 producing inflammatory DCs in CCR2 deficient animals (Nakano et al., 2009). As discussed earlier in section 1.5.2, inflammatory DCs are derived from Ly6C^{hi} monocytes. In the absence of CCR2, Ly6C^{hi} monocytes are retained in the BM leading to a subsequent decrease in the accumulation of inflammatory DCs in LNs (Serbina et al., 2008; Nakano et al., 2009). The accumulation of inflammatory DCs in inflamed LNs and Th1 responses were not affected by the absence of CCL2 (Nakano et al., 2009). CCL2 deficient animals also retain Ly6C^{hi} monocytes in the BM, but it is less pronounced than in CCR2 KO animals (Tsou et al., 2007). Therefore, low numbers of Ly6C^{hi} monocytes might still be present in the periphery of CCL2 deficient animals, and as a consequence appropriate numbers of inflammatory DCs might be expected to be found in inflamed LNs.

The polarisation of T cells to an effector phenotype can be influenced by the presence of inflammatory chemokines at the time of their activation. The presence of CCL3 induces effector Th1 cells, whereas CCL2 induces Th2 cells (Luther and Cyster, 2001; Rot and von Andrian, 2004). Therefore, in the absence of CCL2 the Th2 response is diminished and mice are susceptible to infection by a range of pathogens (Boring et al., 1997; deSchoolmeester et al., 2003). For

example, the expulsion of helminth nematodes, such *Trichuris muris* is highly dependent on Th2 polarised immune responses. In the absence of CCL2, worms were not expelled (deSchoolmeester et al., 2003).

Interestingly, although CCR2 can affect T cell activity, there is some controversy over the expression of CCR2 by naïve T cells. Although CCR2 mRNA has been found in naïve T cells, there are conflicting results about surface protein expression. Mack *et al.*, using an anti-CCR2 antibody MC-21, found that both naïve CD8⁺ and CD4⁺ T cells expressed CCR2 (Mack et al., 2001). In contrast, the use of the CCR2-red fluorescent protein (RFP) reporter mice illustrated that although T cells possessed CCR2 at the transcript level, no CCR2 was detected on their surface (Saederup et al., 2010). Activated T cells have been shown to express CCR2, both at the transcript level and antibody mediated detection of surface CCR2 (Nansen et al., 2000; Mack et al., 2001; Peters et al., 2004).

Inngjerdingen *et al.* have also presented a clear example of CCR2 expression being upregulated by cell activation. CCR2 expression was higher on activated human NK cells, than on nonactivated (Inngjerdingen et al., 2001). They also showed that CCR2, even though at lower levels on nonactivated NK cells, was still active, demonstrated by chemotaxis of these cells in response to CCL2, although the response was less robust than activated cells (Inngjerdingen et al., 2001). CCR2-RFP reporter mice illustrated that although murine NK cells were positive for RFP, they were reported not to possess surface CCR2 based on staining with anti-CCR2 MC-21 antibody (Saederup et al., 2010). However, CCL2 has been shown to mediate NK cell recruitment *in vivo*. Morrison *et al.* have reported that neutralisation of CCL2 leads to a decrease in NK cell recruitment to fungal infected lungs (Morrison et al., 2003). Thus, activation of NK cells and T cells might be associated with their upregulation of CCR2. In contrast, B cells have been reported to downregulate CCR2 expression following maturation, as measured by monitoring CCR2 mRNA. Activation of CCR2 on immature B cell did not mediate their recruitment to inflamed areas, but actually antagonised immature B cell migration to B cell follicles (Flaishon et al., 2004).

1.6.1.5 CCR2 and disease

CCR2 has been described to function on a variety of cell types, both myeloid and lymphoid, therefore it is not surprising in addition to its roles in the defence against bacterial and viral pathogens, CCR2 has been described to function in a variety of immunopathologies. In particular monocyte migration has been shown to be involved in the development of atherosclerosis, as CCR2 and CX₃CR1 mediated migration of Ly6C^{hi} and Ly6C^{low} monocytes respectively, leads to the development of macrophage derived foam cells (Lucas and Greaves, 2001; Tacke et al., 2007). The CCR2 dependent recruitment of monocytes to the central nervous system is crucial for the development of EAE, as CCR2 KO animals are resistant to EAE development (Gaupp et al., 2003; Mildner et al., 2009; Prinz and Priller, 2010). CCR2 has also been described to have both protective and disease-promoting effects on the development and progression of collagen-induced arthritis (CIA). During the initiation phase of CIA, blockade of CCR2 using the anti-CCR2 antibody MC-21 led to a decreased clinical score, as CCR2 influences the Ag specific activation of T cells (Brühl et al., 2004), which might be associated with the earlier discussed CCR2 KO inflammatory DC deficit (Nakano et al., 2009). In contrast, during the progressive stage of the disease, blockade of CCR2 enhances clinical score, which correlates with a decrease in the number of Tregs. This decrease was specifically limited to a CCR2⁺ subpopulation of Tregs, which suppressed activation of other T cells and B cells (Brühl et al., 2004).

The pivotal role CCR2 and its ligands play in monocyte mobilisation, and the role that these cells play in numerous diseases have highlighted CCR2 and CCL2 as potential therapeutic targets. Merck developed a CCR2 inhibitor, MK-0812, which has entered into clinical trials for rheumatoid arthritis and multiple sclerosis. However, in a phase II clinical rheumatoid arthritis trial, MK-0812 treated patients failed to show any significant improvements compared to the placebo group (Horuk, 2009). Vergunst *et al.* also reported no clinical improvement of rheumatoid arthritis following treatment with a CCR2 blocking antibody (MLN1202) (Vergunst et al., 2008). Likewise, infusions of human anti-CCL2 antibody (ABN912) did not result in clinical improvement of rheumatoid arthritis (Haringman et al., 2006). ChemoCentryx also developed a CCR2 antagonist, CCX140, which is being tested in numerous inflammatory and metabolic

diseases. A phase II clinical trial in patients with Type 2 diabetes mellitus has been completed and indicated CCX410 treatment results in a decrease in fasting plasma glucose levels (Xia and Sui, 2009).

In summary, CCR2 expression appears to be mainly limited to cells of the innate immune system and their BM precursors, particularly Ly6C^{hi} monocytes (Sallusto et al., 1998; Serbina and Pamer, 2006). However, low levels of CCR2 have been detected on some lymphocyte populations (Mack et al., 2001). The absence of CCR2 has a profound effect on Ly6C^{hi} monocytes. Ly6C^{hi} monocytes are highly dependent on CCR2 for their emigration from the BM during homeostasis and inflammation. The deficit in peripheral Ly6C^{hi} monocytes in CCR2 KO animals leaves them susceptible to infection *Listeria monocytogenes*, due to a decrease in inflammatory monocyte derived TipDCs (Serbina and Pamer, 2006). The absence of CCR2 is not always detrimental, as the absence of peripheral Ly6C^{hi} monocytes in CCR2 KO mice renders them resistant to EAE development (Gaupp et al., 2003; Mildner et al., 2009; Prinz and Priller, 2010). CCR2, amongst over inflammatory chemokine receptors, has been reported to facilitate the migration of cDCs to sites of inflammation. Following their maturation cDCs downregulate CCR2 and upregulate CCR7 (Sallusto et al., 1998). Interestingly, CCR2 deficiency reportedly affects the maturation state of cDCs, as CCR2 signalling led to NF- κ B induced cDC maturation (Jimenez et al., 2010). Collectively, these data suggest that regardless of its classification as an inflammatory chemokine receptor, CCR2 plays vital roles both in homeostasis and inflammation.

1.6.2 D6

Most information about cell-type specific expression of D6 has been generated in human samples using an anti-human D6 antibody. First assessment of D6 expression came from Northern blotting, which showed placenta to be by far the site of highest D6 expression in humans (Nibbs et al., 1997b). Nibbs *et al.* have also reported D6 expression by lymphatic endothelium in human skin, gut and LN afferent lymphatics, but D6 was absent from lymphatics in other organs (Nibbs et al., 2001). D6 has also been shown to be expressed by human trophoblasts (Martinez de la Torre et al., 2007; Madigan et al., 2010), hepatocytes and some leukocytes populations, such as mast cells, and macrophages (Hansell et al.,

2011a). D6 has also been detected on human blood pDCs, B cells and cDCs (McKimmie et al., 2008). The absence of a reliable anti-murine D6 antibody means that there is limited information available about D6 expression by mouse leukocytes. However, the use of a chemokine internalisation assay facilitated the detection of D6 activity on murine innate-like B cells, including B cells in the colon (Bordon et al., 2009), splenic MZ-B cells and B1 B cells in various tissues (Hansell et al., 2011b).

As discussed earlier, D6 is considered to be an atypical chemokine receptor, due to its inability to signal using the “classical” signalling pathways and its ability to scavenge large amounts of ligands without becoming desensitised. The proposed function of D6 in regulating inflammatory chemokine levels and as a consequence modulating *in vivo* inflammatory responses was established by studies investigating the affect of D6 deletion in the progression and resolution of a number of models of inflammation (Fra et al., 2003; Bonecchi et al., 2004; Hansell et al., 2011b). Lee *et al.* have proposed that it is not the D6 dependent regulation of inflammatory chemokine levels at peripheral sites of inflammation, but its ability to regulate the level of inflammatory chemokines on the lymphatic surfaces that might explain the inability of D6 deficient animals to resolve inflammatory responses (Lee et al., 2011). D6 was reported to regulate accumulation of inflammatory leukocytes at sites of peripheral inflammation and in the draining LNs by clearing inflammatory chemokines from lymphatic surfaces. In the absence of D6, lymphatic endothelial cells present inflammatory chemokines, which leads to an accumulation of cells in the draining LNs and lymphatic congestion. Lymphatic congestion leads to impaired migration of cells, including APCs from peripheral sites of inflammation, therefore hindering the development of an effective immune response (Lee et al., 2011). Recently D6 has also been suggested to indirectly modulate the function of other chemokine receptors expressed by D6⁺ cells. The CXCR5 dependent migration of innate-like B1 B cells to CXCL13 was enhanced in the absence of D6 (Hansell et al., 2011b).

Aberrant inflammatory responses in the absence of D6 have been observed in two different models of cutaneous skin inflammation. In one study skin inflammation was induced by the s.c. injection of CFA, which leads to the development of cutaneous lesions. A significantly greater proportion of D6 KO animals developed lesions that were graded as moderate to severe than WT

animals. D6 KO animals also had a significant increase in necrotic tissue at the injection site, and the draining LNs of D6 KOs had increased cellularity and levels of inflammatory chemokines compared to WT (Martinez de la Torre et al., 2007). More convincingly, Jamieson *et al.* induced cutaneous skin inflammation by repeated topical application of a phorbol ester irritant, TPA. TPA application caused production of TNF α that induced production of inflammatory chemokines that drive leukocyte infiltration. D6 KO animals were found to have significantly higher levels of inflammatory chemokines, supporting the role of D6 in the clearance of inflammatory chemokines. Repeated application of TPA to WT animals induced moderate inflammation that was rapidly resolved. In contrast, D6 deficient animals had a prolonged and exaggerated response developing a psoriatic like pathology (Jamieson et al., 2005).

Nibbs *et al.* demonstrated that D6 deficient mice were more susceptible to the development of papillomas in a chemical carcinogen model of tumourigenesis (Nibbs et al., 2007). Furthermore, deletion of D6 was sufficient to render previously resistant mouse strains susceptible to papilloma formation. Mouse strains that are susceptible to papilloma formation were shown to have increased tumour burdens in the absence of D6 (Nibbs et al., 2007). In addition, transgenic overexpression of D6 in keratinocytes in the epidermis of transgenic mice altered their susceptibility to papilloma formation; susceptible mouse strains were more resistant to papilloma formation. Furthermore, TPA induced inflammation was more rapidly resolved in transgenic animals overexpressing D6. This study suggested that increased inflammatory chemokine levels and delayed resolution of TPA-induced inflammation in D6 KO animals were associated with their enhanced susceptibility to tumour development (Nibbs et al., 2007).

The progression of several other diseases has been found to be altered in D6 deficient animals, such as allergic lung inflammation (Whitehead et al., 2006), and *Mycobacterium tuberculosis* infection (Di Liberto et al., 2008). D6 deficient animals had increased disease severity in each of these models (Whitehead et al., 2006; Di Liberto et al., 2008). In a murine model of myocardial infarction, deletion of D6 resulted in adverse cardiac remodelling (Cochain et al., 2012). The aberrant response in each of these diseases could be linked to elevated inflammatory chemokine levels and increased infiltration of inflammatory cells

(Whitehead et al., 2006; Di Liberto et al., 2008; Cochain et al., 2012). Likewise, D6 deficiency and the associated increase in inflammatory chemokines and inflammatory infiltrate has been suggested to cause increased rate of foetal loss during inflammation (Martinez de la Torre et al., 2007). D6 has also been reported to inhibit resorption of embryos transferred into allogeneic recipients (Madigan et al., 2010). Therefore, expression of D6 by trophoblasts in the placenta might have key roles in foetal survival during inflammation (Martinez de la Torre et al., 2007; Madigan et al., 2010).

There are conflicting reports of the role of D6 in dextran sodium sulphate (DSS)-induced model of colitis. Our group found that D6 deficient mice had reduced disease severity (Bordon et al., 2009), whereas Vetrano *et al.* reported that D6 deficient animals presented with increased disease severity (Vetrano et al., 2010). A further contradiction between the two studies was that Vetrano *et al.* illustrated that D6 KO mice had increased production of inflammatory chemokines and leukocyte recruitment to inflamed mucosa (Vetrano et al., 2010), while Bordon *et al.* showed no difference in inflammatory chemokine production by WT and D6 KO (Bordon et al., 2009). Furthermore, Bordon *et al.* found that D6 deficient inflamed colons had elevated numbers of IL-17A secreting $\gamma\delta$ T cells compared to WT animals, with a corresponding increase in IL-17A levels. The decreased susceptibility was linked to the increase IL-17A levels, as blockade of IL-17A increased disease severity in D6 KO mice (Bordon et al., 2009). A consistency between the two groups is that both showed that D6 mRNA was upregulated in inflamed colons (Bordon et al., 2009; Vetrano et al., 2010). The discrepancies in these two studies might be explained by differences in the setup of the disease models. Both groups scored animals for 8 days after the start of DSS administration. However, Bordon *et al.* induced colitis with a lower dose of DSS over a shorter time-scale than Vetrano and co-workers (Bordon et al., 2009; Vetrano et al., 2010). Vetrano *et al.* added 3% DSS to the drinking water of animals for 7 days (Vetrano et al., 2010), whereas Bordon *et al.* added 2% DSS to their drinking water for 5 days, followed by 3 days with normal drinking water (Bordon et al., 2009). The DSS model of colitis is also markedly affected by local animal housing conditions, most likely because it affects the intestinal microflora of the animals. The contradictions within these studies mean that the

exact requirement for D6 in DSS-induced colitis is unclear and requires more investigation.

Savino *et al.* reported an increase in the number of Ly6C^{hi} monocytes that accumulate in the spleen of D6 deficient animals following inflammation. Subcutaneous administration of the inflammatory agent CFA led to an accumulation of Ly6C^{hi} monocytes in the spleens of D6 KO animals greater than that observed in WT animals. Furthermore, Savino *et al.* illustrated that the accumulation of Ly6C^{hi} monocytes in the spleen of D6 KO animals was CCR2 dependent. D6 KO animals were irradiated and reconstituted with BM from WT, D6 KO or CCR2 KO animals prior to CFA treatment. The accumulation of Ly6C^{hi} monocytes was observed in animals reconstituted with BM from WT and D6 KO animals, but not CCR2 KO animals (Savino *et al.*, 2012). Ly6C^{hi} monocytes from D6 KO animals were reported to have enhanced immunosuppressive activity, as measured by decreased disease severity in a model of graft versus host disease and decreased proliferation of CD8⁺ T cells upon culture *in vitro* with monocytes from D6 KO animals compared to WT (Savino *et al.*, 2012).

It has been proposed that in addition to the atypical chemokine receptor D6, which can scavenge CCL2, CCR2 also possesses some scavenging function, as it too can be rapidly recycled back to the plasma membrane and maintain high responsiveness to ligands (Volpe *et al.*, 2012). The absence of CCR2 leads to sustained high CCL2 levels at sites of inflammation (Tylaska *et al.*, 2002; Maus *et al.*, 2005). In WT animals the levels of CCL2 gradually decrease over the course of inflammation, whereas in CCR2 KO animals the levels actually increase (Tylaska *et al.*, 2002). Thus, CCR2 dependent recruitment of monocytes may limit further recruitment of monocytes by sequestering CCL2 and returning the inflamed tissue to steady-state (Maus *et al.*, 2005).

In summary, the majority of D6 expression data has been produced by analysing human tissues. Studies in the murine system have been hampered by the lack of a reliable anti-D6 antibody. However, recently using a chemokine internalisation assay, D6 receptor activity has been detected on murine innate-like B cells, including B cells in the colon, MZ-B cells and B1 B cells (Bordon *et al.*, 2009; Hansell *et al.*, 2011b). D6 is a promiscuous receptor that binds many inflammatory CC chemokines. Several groups have proposed that D6 serves as a

scavenger for inflammatory chemokines and as a consequence modulates inflammatory responses (Fra et al., 2003; Hansell et al., 2006; Mantovani et al., 2006; Graham, 2009). Consistent with this hypothesis, D6 deletion is associated with aberrant inflammatory responses (Jamieson et al., 2005; Whitehead et al., 2006; Di Liberto et al., 2008; Cochain et al., 2012). Therefore, D6 appears to be important for the resolution of inflammation.

1.7 Thesis Aims

Two CCL2 receptors, CCR2 and D6, have been implicated in the progression and regulation of several diseases through their ability to control leukocyte migration. With my group's interest in chemokine regulation, at the outset of the project I was initially interested in examining how CCR2 contributes to the regulation of its ligands through chemokine scavenging, and the mechanisms that are responsible for this form of feedback control during inflammation. When considering the regulation of CCR2 ligands, it is important to consider the activity of D6 alongside those of CCR2 because this molecule, as discussed in the previous sections, binds many of the CCR2 ligands and is proposed to act as a 'professional' chemokine scavenger. The relative contribution of CCR2 and D6 to chemokine regulation was considered an important aim. We specifically wanted to conduct these experiments using homogenous populations of primary leukocytes purified from mice because (i) it was considered more physiological than using transfected cell systems; (ii) leukocytes are easy to isolate in bulk with high purity; and (iii) it would allow us to use equivalent cell preparations from animals lacking CCR2 or D6 to identify the receptor(s) responsible for scavenging. To facilitate this work, therefore, we first needed to confidently identify suitable cell preparations expressing and possibly co-expressing CCR2 and D6. However, primarily due to the lack of antibodies specific for mouse D6, there was limited understanding at the time of which cells express D6 and whether this atypical chemokine receptor could be co-expressed with CCR2. CCR2 had been more widely investigated and the impact of CCR2 deficiency on steady state and inflammation-driven leukocyte trafficking had been extensively reported. CCR2 protein expression in the mouse had been primarily assessed using a rat anti-mouse CCR2 antibody produced by Mack and colleagues (Mack et al., 2001), although commercial sources of anti-CCR2 antibodies were also available. Rat monoclonal antibodies often cross-react non-specifically with

mouse cells, and careful control experiments are required, but surprisingly, CCR2 deficient cells had rarely been used as controls in published studies using this antibody. Moreover, there were contradictions and inconsistencies in the anti-CCR2 flow cytometry data in literature, and between flow cytometry data and transcript analysis of CCR2 expression. This has led to uncertainty about whether certain cell types, such as neutrophils, can express CCR2 and this could clearly affect the interpretation of results generated using CCR2 deficient mice. Thus, at the beginning of the project, we felt that not only was our understanding of D6 expression by mouse leukocytes somewhat limited, but also that a comprehensive flow cytometric characterisation of CCR2 expression by mouse leukocytes was required. Therefore, I initially aimed to:

- 1) Use available anti-mouse CCR2 antibodies, alongside other chemokine receptor detection techniques under development in the group, to provide a hitherto unavailable, carefully controlled, and robust description of the expression of D6 and CCR2 by mouse leukocytes.

The data generated from these experiments, and the techniques developed to generate these data (all of which are reported in Chapter 3), altered the direction of my project away from its original focus on chemokine scavenging and allowed me to set the following subsequent aims:

- 2) To explore whether the novel receptor detection techniques I developed can be used to examine receptor specificity and to detect CCL2 receptors on leukocytes from other mammalian species (Chapter 3);
- 3) To define the impact of CCR2 deletion on the cellularity of lymphoid organs before and during systemic LPS challenge (Chapters 3 & 4);
- 4) To reveal the dynamics of CCL2 receptor regulation in response to transient systemic inflammation (Chapter 4);
- 5) To define the function of CCR2 on pDCs and examine whether differential expression of CCR2 defines two functionally distinct pDC subsets (Chapter 5).

Chapter 2 – Materials and Methods

2.1 Mice

WT, D6 KO, CX₃CXR1^{GFP/+}, CD200R1 KO, CCR2 KO, OTII and OTI TCR transgenic mice, all on a C57BL/6 background, were bred at the Central Research Facility, University of Glasgow. Alternatively, WT animals on a C57BL/6 background were obtained from Harlan UK (Bicester, Oxon). The generation of CCR2 KOs (Boring et al., 1997), D6 KOs (Jamieson et al., 2005), CX₃CXR1^{GFP/+} (Jung et al., 2000), CD200R1 KO (Boudakov et al., 2007), OTII (Murphy et al., 1990) and OTI (Hogquist et al., 1994) mice has been described. OTI and OTII animals possess CD8 or CD4 T cells with TCR specific for OVA peptides, respectively. OTI mice have CD8 TCR specific for OVA peptide 257-264 and OTII animals have CD4 TCR specific for OVA peptide 323-339, both of which need to be complexed to MHC I or MHC II, respectively. In all experiments, age-matched male littermate cohorts at 8-12 weeks of age were used. All mice were housed under specific pathogen-free conditions in the animal facility at the Central Research Facility, University of Glasgow, UK. OTI mice were maintained in filter-top cages. All procedures were performed in accordance with United Kingdom Home Office regulations, and under the auspices of Project and Personal Licences.

2.2 Maintenance of Flt3L producing cell lines: Flt3L generation and isolation

CHO-Flt3L cells (a kind gift from the Simon Milling Laboratory, University of Glasgow, UK) and B16FL (kindly provided by Oliver Pabst, Medizinischen Hochschule Hannover, Germany) are two cell lines engineered to stably produce murine Flt3L. Both CHO-Flt3L cells (Naik et al., 2010) and B16FL (a murine melanoma tumour cell line) (Mach et al., 2000) were maintained in T75 flasks in RPMI 1640 supplemented with 10 U/ml penicillin/streptomycin, 0.2 mM L-glutamine, 10% Foetal Calf Serum, and 26.3 nM β-Mercaptoethanol (β-ME) (all purchased from Invitrogen, Paisley, UK). Cells were harvested at 70-80% confluency twice a week and cell culture conditioned media (CM) containing Flt3L was harvested from cultures when cells reached confluency, typically every 3 days. CM was filtered using a 0.2 μm pore filter and syringe.

2.3 Measurement of Flt3L by ELISA

The amount of Flt3L in CMs was determined by ELISA according to the manufacturer's instructions (R&D Systems, Abingdon, UK). In brief, following the addition of assay diluent to each well, samples, controls or standards were added to wells and incubated for 2 hours (hrs) at room temperature (RT). After washing with the supplied wash buffer, Mouse Flt3L conjugate was added to each well and incubated at RT for 2 hrs. Plates were then washed and the substrate solution was added to each well and incubated for 30 minutes (mins) at RT before stop solution was applied. The optical density of each well at 450 nm was determined using a Sunrise microplate reader (Tecan, Reading, UK) and sample Flt3L concentrations calculated from the standard curve obtained.

2.4 LPS administration *in vivo*

Age-matched animals were treated intravenously (i.v.) with either 100 μ l sterile PBS (Invitrogen) or 15 μ g LPS *E. coli* (serotype 0111.B4; Sigma Aldrich, Dorset, UK) in 100 μ l sterile PBS, 24, 48 or 72 hrs before tissues were harvested.

Alternatively, 3 hrs prior to the i.v. injection of PBS or LPS, mice were injected intraperitoneally (i.p.) with either 100 μ l sterile PBS or 0.3 mg/kg CXCR2 antagonist, SB225002 (Cambridge Bioscience, Cambridge, UK).

2.5 Flt3L mediated expansion of DCs *in vivo*

In vivo expansion of pDCs was achieved by the administration of 10 μ g human recombinant Flt3L (rhFlt3L) (kindly provided by the Simon Milling Laboratory, University of Glasgow, UK) in 100 μ l sterile PBS i.p. for 9 consecutive days. Mice were sacrificed on the 10th day. Alternatively, pDCs were expanded using murine Flt3L produced by B16FL cells. Mice were s.c. transplanted with $\sim 2 \times 10^6$ B16FL cells and tumour growth was monitored over a period of 10-14 days until sacrifice.

2.6 Imiquimod administration *in vivo*

The dorsal skin of age-matched animals was topically treated once daily with either ~ 10 - 12 μ l of AldaraTM 5% imiquimod cream (Meda AB, Takeley, UK) or

control aqueous cream B.P. (Boots, Nottingham, UK) for 7 days before tissues were harvested on the 8th day.

2.7 Preparation of single cell suspensions from lymphoid organs

Spleens and LNs were collected, cut into approximately 5 mm³ pieces and digested with 0.1 mg/ml Collagenase D (Roche, Burgess Hill, UK) in Hank's balanced salt solution medium (HBSS) (Invitrogen) for 45 mins at 37°C in a cell shaker. The use of the term peripheral LNs (PLNs) is in reference to a pooled collection of the cervical, axillary, brachial, inguinal and popliteal LNs. The BM was prepared by harvesting femurs and flushing the BM from the bones with complete RPMI (RPMI 1640 supplemented with 10 U/ml penicillin/streptomycin, 0.2 mM L-glutamine, and 10% Foetal Calf Serum (FCS) [all Invitrogen]) using a syringe and a 26-gauge needle. Single cell suspensions were prepared in complete RPMI by the gentle mechanical disruption of tissues and passing through a 40 µm nylon mesh (Cadisch, London, UK). Cells were subsequently washed by centrifugation at 400xg for 5 mins at 4°C and resuspended in complete medium. Red blood cell lysis was performed on both spleen and BM samples using Red Blood Cell Lysis Buffer (Sigma Aldrich) for 1 min at RT followed by washing with complete RPMI for 5 mins at 4°C. Cells were resuspended in complete medium and viable cell counts were performed using a Neubauer haemocytometer and phase contrast microscope. Cell suspensions were kept on ice until required.

2.8 Preparation of single cell suspensions from murine blood

Blood was harvested from animals by terminal cardiac puncture using a 1 ml syringe and a 25-gauge needle, which prior to collection had been flushed with 0.5 M ethylenediaminetetraacetic acid (EDTA) pH8.0 dissolved in distilled H₂O (kind gift from Chris Hansell, University of Glasgow, UK). The amount of blood retrieved was recorded. Red blood cell lysis was performed using ammonium chloride (Stemcell Technologies, Manchester, UK) at a ratio of 9:1 ammonium chloride to blood. The cells in ammonium chloride were vortexed and incubated on ice for 10 mins. Cells were then washed twice by centrifugation at 400xg with

complete RPMI for 5 mins at 4°C. Cells were resuspended in complete medium and viable cell counts were performed using a Neubauer haemocytometer and phase contrast microscope. Cell suspensions were kept on ice until required.

2.9 Preparation of single cell suspension from human peripheral blood

50 ml of blood was collected from healthy donors. 4 ml of Histopaque (Sigma Aldrich) was added to a 15 ml Falcon Tube (BD Biosciences, Oxford, UK). 10 ml of blood was gently layered on top of the Histopaque. The solution was centrifuged for 20 mins at 2100 RPM at RT with the acceleration and break set to the lowest setting. The lymphocyte layer was harvested and washed three times in complete RPMI by centrifugation at 400xg for 5 mins at 4°C. Cells were resuspended in complete medium and viable cell counts were performed using a Neubauer haemocytometer and phase contrast microscope. Cell suspensions were kept on ice until required.

2.10 Preparation of single cell suspensions from murine skin

Murine dorsal skin was excised and cut into small ~5 mm³ pieces and digested using 0.1 mg/ml Collagenase D (Roche) in HBSS (Invitrogen) for 1.5 hrs at 37°C in a cell shaker. After the incubation, 0.2% (w/v) Dispase (Invitrogen) was added and cells were incubated for a further 20 mins at 37°C in a cell shaker. Following digestion of the skin, a single cell suspension was prepared by passing pieces of skin through a 70 µm nylon mesh (Cadisch). Cells were subsequently washed twice in complete medium by centrifugation for 5 mins at 4°C and resuspended in complete medium.

2.11 Generation of BM-derived DCs

BM was harvested as described in section 2.7, and used for the differentiation of BM-derived pDCs (BM-pDCs). 2x10⁶ BM cells per ml were incubated at 37°C in 5% CO₂ and cultured for 7 to 10 days in RPMI 1640 medium supplemented with 10% FCS, penicillin/streptomycin, 4 mM L-Glutamine, and 26.3 nM β-ME. Medium was conditioned with 1-100 ng/ml Flt3L, either rhFlt3L, or CM from the CHO-Flt3L

cell line or the B16FL tumour cell line. Medium was replaced every 2-3 days. BM-DCs were harvested by gentle washing of the plates.

2.12 Flow cytometry

Cells were washed by centrifugation at 400xg at 4°C for 5 mins in ice cold FACS buffer (1X PBS, 1% FCS, 0.02% NaNH₃ and 5 mM EDTA), suspended at 1-2 x10⁶ cells per well in a 96-well round bottomed plate (Corning Limited, New York, USA). Cells were treated with Fc block (Anti-CD16/CD32) (BD Biosciences) diluted 1:100 in FACS buffer at 4°C for 15 mins prior to antibody staining. Treatment with Fc Block is used to minimise non-specific binding. Cells were washed by centrifugation at 400xg at 4°C for 5 mins, supernatant (SN) was removed and cells were stained for 15 mins with fluorescein isothiocyanate (FITC), phycoerythrin (PE), allophycocyanin (APC), efluor450 (e450), pacific blue (PB), Horizon V450 (V450), peridinin chlorophyll protein complex (PerCP), AlexaFluor647 (AF647), PE-Cy7 conjugate, PE-Cy5 conjugate, APC-Cy7 conjugate, alexafluor700 (AF700) or biotin-conjugated antibodies specific for selected cell markers (antibodies targeted against cell markers; murine Table 2-1; rat Table 2-2 and human Table 2-3). Antibodies were purchased from BD Biosciences; eBioscience (Hatfield, UK); Miltenyi-Biotec (Surrey, UK); R&D Systems; MBL (Woburn, USA); Novus Biologicals (Cambridge, UK); Epitomics (Burlingame, USA); Biolegend (Cambridge, UK) or AbD Serotec (Kidlington, UK), as indicated. Some of the anti-rat antibodies were generated in house and were kindly provided by the Simon Milling laboratory (University of Glasgow, UK). Biotin-conjugated antibodies were detected by the addition of one of a variety of streptavidin antibodies conjugated with a fluorescent dye (BD Biosciences). All FACS antibodies were used at 1:200, unless stated otherwise, in FACS buffer. All incubations were performed in 50 µl of FACS buffer at 4°C in the dark. After 15 mins at 4°C, with appropriate stains, the cells were washed twice with FACS buffer. Dead cell exclusion was performed in the majority of experiments using the cell viability dye ViaProbe (BD Biosciences). 10 µl of ViaProbe in 100 µl of FACS buffer was added to each well and incubated for 10 mins. Following ViaProbe staining of dead cells, an additional 100-200 µl FACS buffer was added. Alternatively, fixable viability dyes (eBiosciences) were used prior to the antibody staining steps, according to manufacturer's instructions. Concisely,

cells were washed twice in PBS, resuspended at $1-10 \times 10^6$ cells per ml in PBS and $1 \mu\text{l}$ of fixable viability dye per ml was added. The cells were vortexed immediately and incubated for 30 mins at 4°C . Cells were washed in FACS buffer and stained according to the above protocol.

Stained cell preparations were acquired using either a Miltenyi MACSQuant or BD LSRII. Unstained cells and cells stained with only one fluorescent antibody were used to establish acquisition parameters. Retrieved data was analysed using FlowJo software (Treestar inc., OR, USA). To aid analysis, fluorescent minus one (FMOs) samples were prepared, these cells were stained with all antibodies bar one, which was substituted with an appropriate isotype. This technique allows for confident determination of true populations of stained cells.

2.13 Conjugation of a fluorescent PE-Cy7 tandem dye to IL-17RB antibody

The Lightning-Link™ PE-Cy7 Tandem Conjugation kit (Innova Biosciences, Cambridge, UK) was used according to manufacturer's instructions to attach a PE-Cy7 fluorescent tandem dye to the anti-murine IL-17RB antibody supplied by Andrew McKenzie (University of Cambridge, UK). $1 \mu\text{l}$ of the supplied LL-modifier reagent was added to $10 \mu\text{g}/10 \mu\text{l}$ antibody and mixed gently. The $11 \mu\text{l}$ of antibody/LL-modifier mix was added to a vial of Lightning-Link™ mix and resuspended gently by pipetting the mixture up and down. The mixture was left for 3 hrs in the dark at RT. Following completion of the incubation period, $1 \mu\text{l}$ of the supplied LL-Quencher FD reagent was added, and subsequent to a 30 min incubation period the antibody was used according to staining protocol described in section 2-12.

2.14 Staining of CCR2 using MC-21 antibody

Cells were washed by centrifugation at $400 \times g$ at 4°C for 5 mins in ice cold FACS buffer, resuspended at $1-2 \times 10^6$ cells per well in a 96-well round bottomed plate. Following further centrifugation cells were incubated in 10% heat-inactivated mouse serum (kindly provided by Chris Hansell, University of Glasgow, UK) in PBS for 1 hr at 4°C . Cells were then washed three times in FACS buffer. The cells were then stained with 2.5, 5 or $10 \mu\text{g}/\text{ml}$ MC-21 anti-CCR2 (a kind gift from the

Matthias Mack Laboratory, Regensburg, Germany) or the appropriate isotype (Rat IgG2b κ) for 1 hr at 4°C. Subsequent to a further three wash steps, cells were stained with biotinylated polyclonal anti-rat IgG (1:100) (BD Biosciences) for 30 mins at 4°C. Cells were then washed another three times and stained with the streptavidin-APC for 15 mins at 4°C. Lastly, cells were washed three more times and then stained for other surface markers as indicated in section 2-12.

2.15 Fluorescently labelled chemokines

Almac (Craigavon, UK) chemically synthesise endotoxin free human chemokines labelled with AF647. Chemical synthesis of chemokines ensures high purity products with precise aa sequences. CCL2 and CCL5 selectively labelled at or near their C-terminus with a single AF647 molecule were used in this project.

CCL2^{AF647}: QPDAINAPVT CCYNFTNRKI SVQRLASYRR ITSSKCPKEA VIFKTIVAKE
ICADPKQKWV QDSMDHLDKQ TQTPK(AF647)T-OH

CCL5^{AF647}: SPYSSDTTPC CFAYIARPLP RAHIKEYFYT SGKCSNPAVV FVTRKNRQVC
ANPEKKWVRE YINSLEK(AF647)S

In the case of each chemokine AF647 was incorporated at the indicated position at a molar ratio of dye:chemokine of 1:1. Targeted labelling of chemokines at their C-terminus leaves the N-terminus, which is important for the biological function of chemokines, unmodified.

2.16 Chemokine uptake assay

Cells (1-2x10⁶ cells/ 50 μ l) in binding buffer (complete RPMI with 20 mM 4-(2-hydroxyethyl)-1-piperazineethanesulfonic acid (HEPES) pH7.2 [Invitrogen]) were incubated in a 96-well polypropylene plate (NUNC, Fisher Scientific, Leicestershire, UK) with 25 nM CCL2^{AF647} or CCL5^{AF647} with or without competition at 37°C for 60 mins in the dark. Competition, unless indicated otherwise, refers to the addition of 10-fold molar excess of unlabelled chemokine ligand (PeproTech, London, UK) to the binding buffer. Alternatively, prior to incubation with CCL2^{AF647}, cells were incubated for 30 mins with 0-250 nM of unlabelled chemokine ligand. Cells were washed in binding buffer by centrifugation at

400xg for 5 mins at 4°C, and incubated in binding buffer containing 25 nM CCL2^{AF647} for 60 mins at 37°C. Subsequent to the 60 min incubation period with CCL2^{AF647}, cells were washed and stained for surface markers as indicated in section 2-12.

2.17 FACS purification of pDCs and cDCs

pDCs and cDCs from the spleen of B16FL treated tumour bearing WT animals were purified using a BD FACS Aria. Following preparation of a single cell suspension as described above, cells were either immediately Fc Blocked and stained for pDCs, or this was delayed until after the chemokine uptake assay was performed. The pDCs were gated as live, B220⁺CD11c⁺Ly6C⁺CD11b⁻SiglecH⁺ and cells were sorted as total pDCs. Alternatively, pDCs were divided into two subsets, CCL2^{hi} and CCL2^{lo} and each subset sorted. B220⁻CD11c⁺ cells were sorted and classified as cDCs. Subsequent to sorting the purity of the sorted cells was tested and was routinely >95%.

2.18 RNA preparation

Following purification, cells were centrifuged at 400xg for 5 mins at 4°C and the SN completely removed. Samples were resuspended in 350 µl RLT buffer provided in the RNeasy Mini Kit (Qiagen, Crawley, UK). The cell lysates were homogenised by passing 5-10 times through a 20-gauge needle attached to a 1 ml syringe. The homogenised cell lysates were then stored at -80°C. RNA was isolated the following day according to the RNeasy Mini Kit instruction manual. The optional on-column DNase digestion step was performed using the RNase-Free DNase Set (Qiagen). Each sample was stored at -80°C until used.

2.19 Synthesis of complementary DNA (cDNA) from RNA

cDNA was reverse-transcribed from 200 ng of RNA using the AffinityScriptTM Multiple Temperature cDNA Synthesis Kit (Agilent Technologies Limited, Wokingham, UK), according to manufacturer's instructions. Concisely, 200 ng RNA was added to 0.5 µg oligo (dT) primer and the total volume adjusted to 15.7 µl in RNase-free water. Samples were incubated at 65°C for 5 min, then 21°C for 10 mins. When the reaction had been cooled to RT, the final volume of the

reaction was adjusted to 20 μl by the addition of 4.3 μl of a cocktail containing 1X AffinityScript RT Buffer, 2 mM dNTP mix, 20 U RNase Block Ribonuclease Inhibitor and 1 μl of AffinityScript Multiple Temperature RT. In controls, AffinityScript Multiple Temperature RT was replaced by 1 μl of RNase-free water. Samples were incubated for 5 mins at 42°C, followed by 1 hr incubation at 55°C and then 70°C for 15 mins. Samples were stored at -20°C until they were used for Quantitative Polymerase Chain Reaction (QPCR).

2.20 Microarray

RNA extracted from sorted total pDCs, CCL2^{hi} and CCL2^{lo} pDCs was sent to the Glasgow University Polyomics Facility. The facility determined the RNA concentration using a Thermo Fisher Nanodrop 1000TM Spectrophotometer (Thermo Fisher Scientific, Loughborough, UK). The facility used the RNA 6000 Nano kit (Agilent Technologies Limited) to determine the RNA integrity using an Agilent Bioanalyzer 2100 (Agilent Technologies Limited). The RNA samples were loaded and run on a Gene 1.0 ST array (Affymetrix, High Wycombe, UK), which analysed ~28,000 genes within the mouse genome, including exons. Analysis of the ensuing results was performed using software from Partek Genomic Suite (Partek Incorporated, Saint Louis, USA) and heat-maps were generated using GeneSpring version 12.0 (Agilent Technologies Limited).

2.21 QPCR

Equal amounts of cDNA were added to a 384-well MicroAmp® Fast Optical Reaction Plate (Applied Biosystems, Paisley, UK) in triplicate per biological sample. The final total of each well was adjusted to 10 μl with 1X TaqMan® Universal PCR Master Mix, No AmpErase® UNG (Applied Biosystems), 0.5 μl of 20X appropriate probe (Applied Biosystems) (see Table 2-4 for list of probes) and RNase-free water. All assays contain sequence-specific unlabelled primers plus a TaqMan® probe labelled with a fluorescent FAMTM dye. Plates were loaded into a 7900HT Fast Real-Time PCR System machine (Applied Biosystems) and incubated for 10 mins at 95°C followed by 40 cycles of 15 secs at 95°C, and 1 min at 60°C. Relative quantity (RQ) values were determined for each sample using RQ Manager software (Applied Biosystems).

2.22 Co-culture of pDCs with naïve OTI or OTII T cells

cDCs, or pDCs, either CCL2^{hi}, CCL2^{lo} or total pDCs, purified from the spleens of B16FL tumour bearing mice, were incubated in complete RPMI supplemented with 50 μ M β -ME, plus varying amounts of total OVA protein (Calbiochem, Nottingham, UK) for 3 hrs at 37°C with or without 1 μ g/ml R848 (kind gift from the Simon Milling laboratory, University of Glasgow, UK). Following the incubation period, cells were washed twice in media by centrifugation at 400xg for 5 mins at 4°C. Naïve T cells from the LNs and spleen of OTI or OTII mice were sorted using a BD FACS Aria, as CD8 α ⁺CD62L⁺ or CD4⁺CD62L⁺ T cells, respectively. Purified T cells were spun at 400xg for 5 mins at 4°C, washed in PBS, and resuspended at 10x10⁶ cells per ml in PBS. 1 μ l of 5 mM stock CFSE (eBioscience) was added per ml of cells, and cells were incubated in the dark for 3-4 mins at 37°C. Upon completion of incubation period, cells were washed in PBS and resuspended at 1x10⁶ cells per ml. 100 μ l of the T cell suspension was added to either cDC or pDC containing wells. In some experiments 1, 12.5 or 25 nM mCCL2 (PeproTech) was added to the culture media. Cells were incubated for 3 days, before restaining according to section 2-12. Data were acquired on a BD LSRII.

2.23 Migration assays

Total pDCs, purified from the spleens of B16FL treated mice, were resuspended at 1x10⁶ cells per ml in chemotaxis buffer (RPMI supplemented with 0.5% bovine serum albumin [Sigma Aldrich] and 25 mM HEPES, pH7.2 [Invitrogen]). 600 μ l of chemotaxis buffer was added to the middle 12 wells of a 24 Transwell plate following the removal of the provided 5.0 μ m pore polycarbonate membrane insert (Corning Limited). Plates were incubated at 37°C for 10 mins. The wells were then spiked with 0-50 nM unlabelled murine CCL2 (PeproTech) diluted in chemotaxis buffer. Following, the gentle lowering of the filters into the media filled wells, the plate was once again incubated at 37°C for 10 mins, to allow some chemokine to adhere to the filter. 100 μ l of the cell suspension (1x10⁵ cells) was added to the upper well and the plate was returned to the 37°C incubator for 3 hrs. The cells were then retrieved from the lower well and stained according to section 2-12. Cells were resuspended in 200 μ l FACS buffer and data were acquired from a set volume of sample on a Miltenyi MACSQuant.

2.24 *Ex vivo* stimulation of sorted pDCs to measure maturation of pDCs

CCL2^{hi} and CCL2^{lo} pDCs, purified from the spleens of B16FL tumour bearing mice, were resuspended at 1×10^6 per ml in complete RPMI supplemented with $50 \mu\text{M}$ β -ME. 1×10^5 cells were added to each well and incubated with $5 \mu\text{g/ml}$ CpG-C (Source BioScience LifeSciences, Nottingham, UK) with 0, 0.1 or $1 \mu\text{g/ml}$ recombinant murine IL-13 (R&D Systems) for 18 hrs at 37°C . Subsequent to the completion of the incubation period, cells were centrifuged at 400xg for 5 mins at 4°C . Cells were then restained according to section 2-12 and data were acquired on a BD LSRII.

2.25 *Ex vivo* stimulation of IFN α production by sorted pDCs

CCL2^{hi} and CCL2^{lo} pDCs, purified from the spleens of mice carrying B16FL tumours, were resuspended at 1×10^6 per ml in complete RPMI supplemented with $50 \mu\text{M}$ β -ME. 1×10^5 cells were added to each well and incubated with either media alone, $10 \mu\text{g/ml}$ CpG-A (Source BioScience LifeSciences), or $10 \mu\text{g/ml}$ R848 for 8 hrs at 37°C . Subsequent to the completion of the incubation period, cells were centrifuged at 400xg for 5 mins at 4°C . Following of which SN was harvested and frozen at -80°C until required. Cells were also harvested and RNA extracted as described in section 2-17.

2.26 Measurement of IFN α production by ELISA

The amount IFN α in the SN from section 2-24 was determined by ELISA according to the manufacturer's instructions (PBL Interferon Source, New Jersey, USA). Following the preparation of samples, controls or standards diluted in sample buffer (PBL Interferon Source) they were added to each well, and incubated for 1 hr at RT with shaking 450 RPM. The plate was then transferred to 4°C and incubated for 20-24 hrs. After washing four times with the supplied wash buffer (PBL Interferon Source), horseradish peroxidase solution (PBL Interferon Source) was added to each well and incubated at RT for 2 hrs with shaking 450 RPM. Plates were then washed four times and the substrate solution (PBL Interferon Source) was added to each well and incubated for 15 mins at RT before stop

solution (PBL Interferon Source) was applied. The optical density of each well was determined within 5 mins of stop solution being added at 450 nm using a Sunrise microplate reader (Tecan) and sample IFN α concentrations calculated from the standard curve obtained.

2.27 Cytospin preparation and staining

5×10^4 CCL2^{hi} or CCL2^{lo} pDCs, purified from the spleens of B16FL treated mice, were centrifuged at 400xg for 5 mins at 4°C and resuspended in 70 μ l PBS. Alternatively, cells were stimulated with CpG-C according to section 2-23. Upon assembling of the poly-L-lysine slide (VWR, Lutterworth, UK), filter card (Thermo Fisher Scientific) and funnel in the clip, cells were pipetted into the funnel. The cells were centrifuged for 6 mins at 450 RPM at RT. Slides were allowed to dry and stained using Rapid Romanowsky staining kit (Raymond A Lamb Limited, Eastbourne, UK), according to manufacturer's instructions. In brief, slides were immersed in fixative solution (contains Thiazine dye in methanol) for 30 secs and transferred without rinsing or drying to solution B (contains Eosin Y) for 15-30 secs. The slide was slowly agitated whilst in solution B, by gently immersing and withdrawing the slide. Again without washing or rinsing, this staining procedure was repeated with solution C (contains Methylene Blue). Slides were washed in distilled H₂O and allowed to dry. Slides were then mounted using DPX mountant for microscopy (VWR) and examined under an Olympus BX41 microscope and Cell^B Software (Olympus, Essex, UK).

2.28 Statistical analyses

Results are shown as means \pm 1 standard deviation (SD) unless otherwise stated. Normal distribution was tested where appropriate using the D'Agostino and Pearson omnibus normality test. Groups were compared using a Student's unpaired two-tailed t test, one-way ANOVA with Tukey post-test, two-way ANOVA with Bonferroni post-test or Mann-Whitney test. Values of $p < 0.05$ were considered to be statistically significant.

Antigen	Clone	Isotype	Supplier	Dilution
Ly6C	AL-21	RatIgM κ	BD Biosciences	1:200
I-A/I-E	M5/114.15.2	RatIgG2b κ	eBioscience	1:500
Gr1	RB6-8C	RatIgG2b κ	eBioscience	1:200
CD86	GL1	RatIgG2a κ	eBioscience	1:200
CD3	17A2	RatIgG2b κ	eBioscience	1:200
CD11b	M1/70	RatIgG2b κ	BD Biosciences	1:200
CD4	GK1.5	RatIgG2b κ	eBioscience	1:200
PDCA1	JF05-12C.4.1	RatIgG2b κ	Miltenyi-Biotec	1:11
CD49b	DX5	RatIgM κ	eBioscience	1:200
CD11c	N418	Armenian Hamster IgG	eBioscience	1:200
F4/80	BM8	RatIgG2a κ	eBioscience	1:200
$\gamma\delta$	eBioGL3	Armenian Hamster IgG	eBioscience	1:200
CD8 α	53-6.7	RatIgG2a κ	eBioscience	1:200
B220	RA3-6B2	RatIgG2a κ	eBioscience	1:250
CD115	AFS98	RatIgG2a κ	eBioscience	1:200
SiglecH	eBio440c	RatIgG2b κ	eBioscience	1:200
CCR9	242503	RatIgG2b κ	R&D Systems	1:50
CD62L	MEL-14	RatIgG2a κ	eBioscience	1:200
LPAM-1	DATK32	RatIgG2a κ	eBioscience	1:200
OX40L	RM134L	RatIgG2b κ	eBioscience	1:200
CD9	eBioKMC8	RatIgG2a κ	eBioscience	1:200
CCR7	4B12	RatIgG2a κ	eBioscience	1:200
CD69	H1.2F3	Armenian Hamster IgG	eBioscience	1:200
IL-17RB	D9.2	MouseIgG1 κ	Andrew McKenzie	1:200
Ly49Q	2E6	RatIgG2a κ	MBL	1:200
CCR2		Polyclonal	Novus Bio.	1:10
CCR2	E68	Rabbit Monoclonal IgG	Epitomics	1:10
CCR2	MC-21	RatIgG2b κ	Matthias Mack	1:100
CD19	eBio1D3	RatIgG2a κ	eBioscience	1:200
CD107b	M3/84	RatIgG1 κ	eBioscience	1:100
NK1.1	PK136	MouseIgG2a κ	eBioscience	1:200
CD25	7D4	RatIgM κ	BD Biosciences	1:200
CD200R1	OX-90	RatIgG2a κ	AbD Serotec	1:100
CD312a1	13MOKA	RatIgG2a κ	eBioscience	1:100
ICOS-L	HK5.3	RatIgG2a κ	eBioscience	1:200
CD45	30-F11	RatIgG2b κ	eBioscience	1:200

Table 2-1: Antibodies and isotypes for flow cytometry of murine cells.

Antigen	Clone	Supplier	Dilution
MHCII	OX-6	BD Biosciences	1:400
CD4	OX-35	BD Biosciences	1:400
CD45R	His24	BD Biosciences	1:200
CD11b	OX-42	BD Biosciences	1:200
CD43	W3/13	In house	1:200
CD45RA	OX-33	Biolegend	1:200
Ig κ	OX-12	Biolegend	1:200
CD45RC	OX-22	In house	1:200
TCR $\alpha\beta$	R73	In house	1:200
Ig λ	MRL-61	Biolegend	1:200

Table 2-2: Antibodies and isotypes for flow cytometry of rat cells.

Antigen	Clone	Supplier	Dilution
CD14	M5E2	Biolegend	1:20
CD3	UCHT1	Biolegend	1:100
CD56	MEM-188	Biolegend	1:25
CD15	W6D3	Biolegend	1:25
CD19	HIB19	Biolegend	1:100
CD123	6H6	Biolegend	1:20
CD304	BDCA-4	Miltenyi Biotech	1:20
MHCII	L243	Biolegend	1:40

Table 2-3: Antibodies and isotypes for flow cytometry of human cells.

Target Gene	Abbreviation	Assay ID
cysteinyl leukotriene receptor 1	Cysltr1	Mm00445433_m1
G protein-coupled receptor 174	Gpr174	Mm01238430_m1
Eph receptor B2	Ephb2	Mm01181021_m1
chemokine (C-C motif) receptor 2	Ccr2	Mm00438270_m1
PHD finger protein 17	Phf17	Mm00552321_m1
guanylate binding protein 4	Gbp4	Mm00657752_m1
cytochrome c oxidase, subunit VI a, polypeptide 2	Cox6a2	Mm00438295_g1
retinoic acid receptor, gamma	Rarg	Mm00441091_m1
mitogen-activated protein kinase kinase kinase 14	Map3k14	Mm00444166_m1
interferon regulatory factor 7	IRF7	Mm00516788_m1
glyceraldehyde 3-phosphate dehydrogenase	GAPDH	4352932E

Table 2-4: Probes used in QPCR.

Chapter 3 – Using fluorescent CCL2 to detect CCR2 receptors

3.1 Currently available methods to detect CCR2

In the Introduction, I discussed the role that chemokines and their receptors play in homeostasis and inflammation. I provided details about the known roles of CCR2 in diseases, such as atherosclerosis (Lucas and Greaves, 2001; Tacke et al., 2007), CIA (Brühl et al., 2004) and EAE (Gaupp et al., 2003; Mildner et al., 2009; Prinz and Priller, 2010). In many cases the role of CCR2 was identified by using animals deficient in the receptor, with a lack of CCR2 causing disease to be either abrogated or augmented. In addition, observed alterations in cell frequencies in analysed tissues of CCR2 KOs provided information about the dependency of specific cell populations on CCR2 for their migration. However, in the case of many murine chemokine receptors, including CCR2 and D6, there is limited information available about their expression, mainly due to poor sensitivity of available reagents. The original aim of this project was to determine how CCR2 and D6 contribute to the regulation of their ligands through chemokine scavenging. To achieve this aim, a comprehensive flow cytometric characterisation of CCR2 and D6 expression by mouse leukocytes was required.

Methods that are currently available to detect CCR2, in addition to other chemokine receptors, are limited to either antibodies targeted against the receptor, RT-PCR or knock-in reporter mice. Two CCR2 reporter mice have been generated. Serbina *et al.* generated a CCR2-GFP reporter mouse using bacterial artificial chromosomes carrying the gene encoding *enhanced GFP* under the control of the CCR2 promoter (Serbina et al., 2009). The CCR2-RFP reporter mice were generated by Saederup *et al.* and have the first 279 base pairs of the amino terminus of the CCR2 opening reading frame replaced with an expression cassette containing cDNA encoding RFP (Saederup et al., 2010). These methods all suffer from limitations. RT-PCR only provides information about receptor transcript levels, and although RT-PCR on a single cell basis is possible, it is technically challenging and difficult to use to look at large mixed populations of cells. Moreover, the transcript level does not necessarily reflect the level of functional protein. Reporter mice provide further scope for the analysis of CCR2 expression as they facilitate analysis of CCR2 expression by individual cells using

flow cytometry and tissue sections. However, the GFP/RFP levels merely reflect CCR2 transcript levels - positivity for GFP/RFP does not necessarily indicate expression of CCR2 protein. Indeed, some RFP⁺ cells were not found to express CCR2 at the cell surface (Saederup et al., 2010). This is one of several caveats that need to be considered when thinking about the validity of knock-in reporter mice. Therefore, a method of protein detection is preferable in many cases. Anti-CCR2 antibodies also facilitate the analysis of CCR2 expression by single cells using flow cytometry. Furthermore, at the beginning of this project the CCR2-RFP reporter mice had yet to be generated and thus were not available to the scientific community. Consequently, as the only remaining option, our focus turned to the use of antibodies to specifically detect CCR2. It was known at the time of initiating our study that antibodies targeted against chemokine receptors have proven in many cases to be unreliable. Most antibodies targeted against murine chemokine receptors are less efficient than the human equivalents, with some antibodies failing to detect the receptor of interest or having low sensitivity for their target (Hansell et al., 2011b). This is in part due to the fact that mice are the usual animals of choice for inoculation with immunogen to generate monoclonal antibodies targeted against chemokine receptors. In addition, many antibodies are not generated against the entire protein, but a selective peptide, which may be obscured when the protein is in its native, folded conformation. Furthermore, chemokine receptors are subject to post-translational modifications, which alter the binding affinity and functions of the receptor, which could interfere with antibody binding. For example, the N-terminus of chemokine receptors is thought to be decorated by glycosylation, and tyrosine residues are often sulphated (Preobrazhensky et al., 2000; Gutiérrez et al., 2004). This phenomenon may be cell-type specific resulting in the antibody recognising the receptor better on one cell-type than another. Regardless of these constraints I tested a range of available anti-mouse CCR2 antibodies and, crucially, included CCR2 KO mice as negative controls. In addition, I used a novel chemokine receptor detection technique that has been optimised in our lab that uses fluorescently labelled chemokine to detect cells bearing CCR2 and/or D6. The data from these experiments, which are described below, altered the direction of my project from the original focus on chemokine scavenging, and my subsequent aims were to explore the regulation, specificity and function of CCR2 receptors on the identified cell populations.

3.1.1 Examination of murine CCR2 detection by flow cytometry using commercially available anti-mouse CCR2 antibodies

I first assessed the ability of two commercially available anti-CCR2 antibodies to detect murine surface CCR2 protein, one monoclonal and the second polyclonal. The monoclonal antibody from Epitomics was generated in rabbits and a synthetic peptide corresponding to the N-terminal residues of human CCR2 was used as the immunogen. It was stated to have immunoreactivity to both human and murine CCR2. The polyclonal antibody from Novus Biologicals was generated in goats and a synthetic peptide (SHSLFTRSIQELDEGATTPYDYDDGEPG), which corresponds to the N-terminal residues of murine CCR2, was used as the immunogen. The BM is a rich source of CCR2⁺ cells, particularly Ly6C^{hi} monocytes, which are known to be highly dependent on CCR2 for their emigration from the BM. CCR2 KO animals have a deficit in peripheral Ly6C^{hi} monocytes due to their retention within the BM in the absence of CCR2 (Serbina and Pamer, 2006; Tsou et al., 2007). Therefore, due to the large number of CCR2⁺ cells within the BM, both antibodies were tested at a range of concentrations and incubation times on BM cells. However, both failed to detect CCR2 in WT BM when compared to background level in CCR2 KO BM (Figure 3-1).

3.1.2 Analysis of CCR2 detection by flow cytometry using a widely-used rat anti-mouse CCR2 monoclonal antibody, MC-21

Following the failure of the two commercial antibodies to detect murine CCR2, I tested the most commonly used anti-mouse CCR2 antibody (clone MC-21) generated in the laboratory of Matthias Mack (Mack et al., 2001). The MC-21 antibody is considered to be the gold standard for CCR2 detection in mice, with many published conclusions being based on the results generated with this antibody (Maus et al., 2002; Peters et al., 2004; Saederup et al., 2010). Unlike the commercially available antibodies, MC-21 is a rat antibody targeted against murine CCR2 protein. The antibody is a monoclonal antibody, which means it only recognises a single epitope on murine CCR2. The coding region of murine CCR2 was amplified and inserted into a vector that was used to transfect CHO cells, which were then used to immunise rats (Mack et al., 2001). The staining method reported in the original paper was followed, with the reported concentration 5 µg/ml (1:100), plus two further concentrations, 10 µg/ml (1:50)

or 2.5 $\mu\text{g}/\text{ml}$ (1:200) being used. WT cells were also analysed with the isotype control antibody used in previous studies using MC-21, RatIgG2b κ (Mack et al., 2001). The isotype control antibody was also used at 2.5 $\mu\text{g}/\text{ml}$, 5 $\mu\text{g}/\text{ml}$ or 10 $\mu\text{g}/\text{ml}$. MC-21 mediated CCR2 detection was assessed in the spleen, BM and blood of WT mice by flow cytometry. Importantly, cells from CCR2 KO mice stained with MC-21 were used as controls (Figure 3-2). Following gating of cells based on their size and granularity properties using forward scatter (FSC) and side scatter (SSC), live cells were gated on the basis of being ViaProbe negative and the relative anti-CCR2 immunoreactivity detected by MC-21 was determined on WT and CCR2 KO cells. In the three tested tissues and with all concentrations of MC-21, total live WT cells appeared to have specific CCR2 immunoreactivity when compared to WT cells stained with the isotype control used at the same concentration as MC-21. However, MC-21 stained CCR2 KO cells had similar immunoreactivity to WT cells in all tissues tested, except in the blood when a 1:100 dilution of MC-21 was used and BM when a 1:200 dilution was used. Nevertheless, when comparing flow cytometry plots of MC-21 immunoreactivity on WT and CCR2 KO there were some noticeable differences (Figure 3-3). Live cells were divided into six populations based on their expression of Ly6C and MC-21 immunoreactivity. The relative frequency of each of these populations was determined in the spleen (Figure 3-3B), BM (Figure 3-3C) and blood (Figure 3-3D) of WT and CCR2 KO animals, in addition to WT isotype control samples. The majority of cells possessing high MC-21 immunoreactivity also expressed high levels of Ly6C, and consistent with published observations (Serbina and Pamer, 2006), these cells were absent in the periphery of CCR2 KO animals. As discussed in the Introduction, Ly6C^{hi} monocytes are highly dependent on CCR2 for their mobilisation from the BM (Sunderkötter et al., 2004; Serbina and Pamer, 2006; Tacke and Randolph, 2006), thus it is likely that MC-21 is detecting CCR2 on monocytes in the BM of WT animals. In contrast, in the spleen and blood the observed decrease in CCR2 detection might be explained by a loss of CCR2 protein and/or the loss of Ly6C^{hi} monocytes from CCR2 KO animals. In the majority of cell populations, the isotype control gave fewer positive cells when compared to both WT and CCR2 KO samples. There were, however, few statistical differences between WT and CCR2 KO MC-21 stained samples. In fact, in some populations, such as the spleen Ly6C⁻MC-21/Iso^{lo} (Figure 3-3A) and BM Ly6C⁺MC-21/Iso^{lo} (Figure 3-3B) there was a higher proportion of cells with MC-21

immunoreactivity present in CCR2 KO samples than WT or isotype control. This suggests that MC-21 is subject to non-specific binding (i.e. binding to something other than CCR2). Therefore, despite providing some detection of CCR2, these results indicate that MC-21 has a high level of non-specific background staining, demonstrating the importance of using CCR2 KOs as controls.

3.1.3 Profiling CCR2 expression in murine lymphoid organs and blood using MC-21

I next investigated which cells might be responsible for the limited CCR2 specific staining noted in Figure 3-3. To determine relative background level of staining on different cell types in the spleen (Figure 3-4A), BM (Figure 3-4C) and blood (Figure 3-4E), I compared the level of CCR2 detection with 5 µg/ml MC-21 on WT and CCR2 KO cells to staining of WT cells with the isotype. Comparison of MC-21 stained WT cells to isotype control WT samples in histogram overlays of each splenic cell population indicated that all WT cells, excluding neutrophils, possessed MC-21 immunoreactivity (Figure 3-4A). In contrast, in the BM (Figure 3-4C) and blood (Figure 3-4E) comparison of histogram overlays of MC-21 stained WT cells to isotype control WT samples indicated that Ly6C^{hi} monocytes and neutrophils both possessed MC-21 immunoreactivity. However, comparison of MC-21 stained WT to CCR2 KO samples, indicated that only Ly6C^{hi} monocytes in each tissue had an appreciable level of MC-21 immunoreactivity specific for CCR2, although low levels of CCR2-specific MC-21 immunoreactivity were detected on splenic pDCs, CD11b⁺ cDCs and perhaps NK cells. The high background level of staining with MC-21 became even more apparent when the number of MC-21⁺ cells within each population in WT and CCR2 KO samples was quantified. Quantification of the results, considering anything above the isotype stained WT cells to be positive, illustrated that there were no statistical differences in the proportions of MC-21⁺ cells detected in any splenic cell population of WT and CCR2 KO animals (Figure 3-4B). Trends in the data suggested decreased MC-21 immunoreactivity in Ly6C^{hi} monocytes of CCR2 KO animals compared to WT, which was significant in the BM (Figure 3-4D) and blood (Figure 3-4F), but not in the spleen. Furthermore, in each tissue no statistical differences were found in the proportion of MC-21⁺ neutrophils detected in WT and CCR2 KO samples.

Collectively, these results indicate that the tested commercially available anti-mouse CCR2 antibodies were unable to detect CCR2. Furthermore, in my hands, the commonly used MC-21 was also limited in its ability to detect CCR2. It did, however, detect some CCR2, but it was predominantly restricted to Ly6C^{hi} monocytes. The large shift in signal detected in WT animals over the background isotype level indicated high levels of CCR2. However, in the majority of cell populations a large proportion of this signal was not in fact true CCR2 detection, as it was also present in stained CCR2 KO samples. Thus, accurate CCR2 detection using MC-21 can only be achieved by comparing staining in WT and CCR2 KO animals, and the isotype staining in the case of MC-21 is not a particularly useful control.

3.2 Development of a sensitive method to detect CCR2

The commercial antibodies that I tested were unable to detect CCR2 and, although MC-21 did detect CCR2, it provided poor distinction of CCR2⁺ cells in all cell populations except Ly6C^{hi} monocytes. Furthermore, MC-21 should be used with caution, as without the appropriate CCR2 KO controls, false positives might be generated. Typically an isotype control would be used to establish what anti-CCR2 reactivity is specific. However, in many cases this staining would still be present in CCR2 KO cells. It is for this reason a new assay needed to be developed that would allow reliable identification of CCR2⁻, CCR2^{lo} and CCR2^{hi} cells. Our lab has optimised a novel approach using fluorescently labelled chemokines to detect cells bearing chemokine receptors (Figure 3-5). In brief, a single cell suspension is incubated with fluorescent chemokine for 1 hr at 37°C, with or without an unlabelled competitor chemokine ligand, and following immuno-staining for cell surface markers, cells are analysed by flow cytometry. This method does not measure binding of fluorescent chemokine to surface chemokine receptor, but actually provides information about the ‘activity’ of the receptor, as fluorescent chemokine must bind and be internalised by the receptor to be detectable in subsequent flow cytometry. Receptor internalisation is generally seen as a key part of the signalling cascade of these molecules, so ligand internalisation probably indicates when the receptor is competent for signalling. Using CCL2^{AF647} or CCL22^{AF647}, this method has been used to detect cells expressing the atypical chemokine receptor D6. In these

experiments, much CCL2^{AF647} uptake was D6-independent (Bordon et al., 2009; Hansell et al., 2011b).

Since both CCR2 and D6 can bind CCL2, suitable controls need to be included to discriminate between CCR2 and D6 dependent uptake of CCL2^{AF647} (Figure 3-5). Comparison of CCL2^{AF647} uptake by WT and CCR2 KO should identify cells capable of CCR2 dependent uptake of CCL2^{AF647}. Similarly, D6 KO animals can be used to define D6-specific uptake. However, to discriminate between CCR2 and D6 dependent uptake and non-specific uptake by WT or CCR2 KO cells, competition of CCL2^{AF647} uptake with unlabelled murine CCL22 (mCCL22), a D6 specific ligand is used. Any observed decrease in CCL2^{AF647} uptake in the presence of mCCL22 is indicative of D6 activity, as D6 is the only known receptor to bind both CCL2 and CCL22. As confirmation that any decrease in CCL2^{AF647} uptake as a consequence of competition with mCCL22 was truly D6 dependent, and was not simply due to the addition of unlabelled chemokine, competition with a non-D6 ligand, such as mCCL19 is included. The lab had previously conducted some profiling of D6 activity, which indicated that in resting mice D6 activity was predominantly restricted to innate-like B cells i.e. MZ-B cells and B1 B cells (Hansell et al., 2011b). Thus, in the first experiments, CCL2^{AF647} uptake was plotted against CD19, a lineage specific marker of B cells (Figure 3-6). By comparing uptake in WT and CCR2 KO animals, it was clear that the vast majority of CCR2 dependent uptake was limited to CD19⁺ cells. However, there was a small population of CD19^{lo} cells that possessed CCR2 dependent uptake of CCL2^{AF647}, highlighted in Figure 3-6A by the yellow box. The detection of CCR2 dependent uptake by CD19^{lo} cells was not entirely unexpected, as CCR2 has previously been shown to be expressed by immature B cells (Flaishon et al., 2004) and plasma cells (Delogu et al., 2006). It was likely that the observed uptake was by plasmablasts or plasma cells, as maturation of B cells into plasma cells is accompanied by a downregulation of CD19 (Cascalho et al., 2000) and the cells were CD19^{lo}. Surprisingly, both the CD19⁺ and CD19^{lo} populations in CCR2 KO mice possessed significant levels of D6 dependent uptake, as indicated by competition with mCCL22 (Figure 3-6B). Thus, D6 activity is not restricted to B cells as first thought from WT/D6 KO comparisons (Hansell et al., 2011b), however D6 dependent uptake may have been hard to detect in these experiments due to the high levels of CCR2 dependent uptake of CCL2^{AF647}. In contrast, competition

with mCCL19, a ligand that does not bind CCR2 or D6 did not cause a significant reduction in CCL2^{AF647} uptake in the CCR2 KO by either CD19⁺ or CD19⁻ cells (Figure 3-6B). This illustrates that the large majority of uptake remaining in CCR2 KO samples, is truly D6 dependent and is not as a consequence of non-specific inhibition of CCL2^{AF647} uptake by the presence of an excess of unlabelled chemokine.

The CCL2^{AF647} assay relies on the ability of either CCR2 or D6 to internalise CCL2^{AF647}. Therefore, the assay can only detect active receptor, and provides information about the 'activity' of the receptor. However, it may be argued that using a method to detect only active chemokine receptor is restrictive, in that 'inactive' receptors would not be identified using this method. In theory, with a simple modification to the assay (incubation at 4°C) it could also be used to measure surface levels of CCR2, irrespective of the ability of CCR2 to internalise or its activity on these cells. Another member of the lab, Chris Hansell (personal communication) has performed the assay incubating cells with CCL2^{AF647} at 4°C instead of 37°C to prevent receptor internalisation (Hurson, 2011). This allows measurement of binding of CCL2^{AF647} to surface receptors. However, the fluorescence detected by flow cytometry is much lower than with incubations at 37°C and receptor detection is very poor. Therefore, throughout this thesis, incubations were performed at 37°C and for this reason CCR2 and D6 detection is referred to in terms of 'activity' rather than expression or binding.

3.2.1 CCL2^{AF647} uptake assay can sensitively detect mouse CCR2 activity in cells from several lymphoid organs and the blood

The internalisation assay was next used to characterise CCR2 dependent uptake of CCL2^{AF647} in the spleen (top row), BM (middle row) and blood (bottom row) (Figure 3-7). Use of the MC-21 anti-CCR2 antibody indicated that CCR2 expression was predominantly limited to Ly6C^{hi} monocytes, thus here I plotted Ly6C against CCL2^{AF647} uptake, which would facilitate the examination of CCL2^{AF647} uptake by both Ly6C⁺ and Ly6C⁻ cells. In comparison to data generated with MC-21 (Figure 3-3), there were much larger flow cytometry shifts when using CCL2^{AF647}, indicating that the CCL2^{AF647} assay had improved sensitivity compared to anti-murine CCR2 antibodies. Live cells were divided into 5 populations based on Ly6C expression and CCL2^{AF647} uptake. The majority of

CCR2 dependent activity was by Ly6C⁺ cells, however some cells within the Ly6C⁻ fraction also exhibited CCR2 dependent uptake. Of note is the Ly6C^{hi}CCL2^{AF647-hi} population present in all WT tissues, but absent in CCR2 KO, as there was a significant reduction in the number of live cells detected in this gate (Figure 3-7B-D). Ly6C⁺ cells from the spleen and BM of CCR2 KOs also had some D6 dependent uptake, as remaining uptake in the BM Ly6C⁺CCL2⁺ population and splenic Ly6C⁺CCL2^{lo} was sensitive to the addition of mCCL22. However, the majority of D6 dependent uptake was restricted to Ly6C⁻ cells. These results indicate that the prevalent receptor responsible for CCL2^{AF647} uptake in all three tissues is CCR2, with D6 responsible for a minor proportion of uptake. D6 appears to have a greater role in the spleen, which corresponds with D6 being a marker of MZ-B cells and B1 B cells. MZ-B cells are restricted to the spleen and B1 B cells are more abundant in this organ than in BM or blood (Hansell et al., 2011b).

A deficiency in CCR2 clearly led to a major reduction in CCL2^{AF647} uptake, and competition with mCCL22 resulted in maximum reduction of CCL2^{AF647} uptake in the spleen. However, in the BM and blood there was a population of Ly6C⁺ cells that were still positive for CCL2^{AF647} uptake in CCR2 KO even in the presence of excess mCCL22 (Figure 3-7). These cells appeared to have CCR2 and D6 independent uptake of CCL2^{AF647}. It was hypothesised that these cells may express another receptor that can uptake CCL2^{AF647}. To investigate this possibility, CCL2^{AF647} uptake by BM cells was competed with a range of CC chemokine ligands, including mCCL2 and other mouse inflammatory chemokines (Figure 3-8). CCL2^{AF647} is based on human CCL2, so the use of mCCL2 would assess whether uptake is by a mouse CCL2 receptor. The majority of these ligands are D6 ligands, except mCCL7, mCCL8, mCCL19 and mCCL21. mCCL7 and mCCL8 were originally thought to be ligands of D6 (Graham, 2009). However recent work by Hansell *et al.* demonstrated that mCCL7 and mCCL8 are not D6 ligands, as they were both unable to block D6 dependent uptake of CCL2^{AF647} by B1 B cells (Hansell et al., 2011b). All D6 ligands used were able to marginally reduce CCL2^{AF647} uptake by BM cells compared to non-D6 ligands, but no tested ligand was able to completely compete the CCR2 and D6 independent uptake. Thus, these cells have some D6 activity, but remaining uptake is not due to a mouse CCL2 receptor, or other mouse receptors, such as CCR1, CCR2, CCR4, CCR5, CCR7 and CCR8 (Islam et al., 2011). The cells might therefore be

exhibiting a form of non-specific uptake of CCL2^{AF647}, perhaps pinocytosis, or be internalising CCL2^{AF647} via another unidentified receptor.

3.3 Identification of cells carrying CCL2 receptor activity in mouse lymphoid tissue and blood

Most information on CCR2 expression has been provided using MC-21. Since the CCL2^{AF647} assay appears to give improved sensitivity of CCR2 detection compared to MC-21, earlier profiling experiments using this antibody may have led to an unintentional disregard of some CCR2^{lo} cell populations. Also, as discussed earlier, the use of this antibody with the isotype alone and no CCR2 KO control can lead to the generation of false positive CCR2⁺ populations. Consequently, having begun to establish the CCL2^{AF647} uptake assay as a sensitive and reliable way to detect CCR2 activity, I performed a detailed profiling of CCR2 expressing cells in lymphoid organs and blood. Furthermore, as a by-product of the assay design, I anticipated that I would also generate data on the activity of D6 on the same cell populations analysed for CCR2. This could prove to be advantageous as perhaps, similar to CXCR7 and CXCR4, D6 and CCR2 might have roles in regulating one another when co-expressed on the same cell (Hartmann et al., 2008; Salanga et al., 2009). Moreover, my data described so far has already indicated that D6 activity is not restricted to innate-like B cells, at least in the context of CCR2 deficiency.

3.3.1 CCR2 activity in the spleen is predominantly restricted to cells of the innate immune system

The spleen contains several lymphoid and myeloid cell subsets. By comparing internalisation of CCL2^{AF647} in WT and CCR2 KO with or without mCCL22 competition, I established the receptor responsible for CCL2^{AF647} uptake by a variety of splenic lymphocytic (Figure 3-9), myeloid (Figure 3-10) and DC populations (Figure 3-11). These cells were all identified on the basis of their expression of various standard markers, according to the literature. In most cases, a range of markers are required to definitely identify cell populations, as although some markers are considered to identify distinct lineages, there is some overlap. Macrophages were identified using the myeloid cell markers F4/80 and CD11b (Lloyd et al., 2008). pDCs were identified using CD11b and a

combination of other markers: B220, CD11c and Ly6C (Asselin-Paturel et al., 2003). CD11c is typically considered to be a DC marker, however other cell types, such as macrophages, germinal centre B cells and granulocytes, also express CD11c (Hume, 2008). Thus, cDCs were identified as CD11c^{hi} MHCII^{hi} cells (Ghosh et al., 2010) and to avoid potential contamination of the cDC populations the majority of lymphocytes were excluded from the analysis. A combination of antibodies used to identify T cells (anti-CD3), B cells (anti-CD19) and NK cells (anti-NK1.1) were all conjugated to a similar fluorophore as the viability dye, which facilitated the removal of these cells from the analysis at the time of live/dead cell gating. The two subsets of cDCs were delineated using CD11b and CD8 α (Vremec and Shortman, 1997; Wilson and O'Neill, 2003). NK cells were identified using anti-CD49b (clone DX5), which, unlike the NK1.1 cell marker recognises NK cells in all mouse strains (Arase et al., 2001).

First, I examined the activity of the CCL2 receptors, CCR2 and D6 on a number of splenic lymphocyte populations (Figure 3-9). In contrast to MC-21 staining, WT NK cells were found to have significant levels of CCR2 mediated uptake of CCL2^{AF647} (Figure 3-9A). WT T cells, both $\gamma\delta^+$ T cells (Figure 3-9B) and TCR $\alpha\beta^+$ T cells, CD4⁺ and CD8 α^+ (Figure 3-9C), had low levels of CCR2 activity. B cells, as expected were the only lymphocyte population that were found to have D6 dependent uptake with approximately 14% of CCR2 KO cells taking up CCL2^{AF647} (Figure 3-9D). With a more detailed gating strategy to delineate MZ-B cells from within the total B cell gate, it was found that approximately 68% of CCR2 KO MZ-B cells possess D6 activity. These results support published observations stating that within the spleen MZ-B cells are the principal cells with D6 dependent CCL2^{AF647} uptake (Hansell et al., 2011b). The remaining CD21⁻ B cell population (Figure 3-9D) did, however still possess significant levels of D6 specific uptake in CCR2 KOs, which might be explained by the previously identified D6⁺ B1 B cells (Hansell et al., 2011b).

Next, I focused on myeloid cells (Figure 3-10). Ly6C^{hi} monocytes, identified as Ly6C^{hi}CD11b⁺Gr1^{lo} (Sunderkötter et al., 2004; Serbina and Pamer, 2006), were found to have high CCR2 activity in WT animals, having the highest proportion of CCL2⁺ cells (~85%) of all cell populations tested. Furthermore, competition with mCCL22 had no effect on CCL2^{AF647} uptake by CCR2 KO cells, indicating an

absence of D6 on Ly6C^{hi} monocytes (Figure 3-10A). Macrophages had low, but significant levels of CCR2 activity in WT animals, and also D6 dependent uptake in CCR2 KO samples (Figure 3-10B). Some populations clearly lack CCR2 or D6 activity, for example neutrophils, identified as Ly6C⁺Gr1^{hi}CD11b⁺ (Panopoulos et al., 2006; Daley et al., 2008), because WT neutrophils did not internalise more CCL2^{AF647} than CCR2 KO neutrophils in the presence or absence of mCCL22 (Figure 3-10A).

The final splenic cell populations to be examined for CCR2 and D6 activity were DCs (Figure 3-11). In contrast to MC-21 staining, CD11b⁺ cDCs (Figure 3-11A), CD8 α ⁺ cDCs (Figure 3-11B) and pDCs (Figure 3-11B) from WT animals were found to have significant levels of CCR2 mediated uptake of CCL2^{AF647}. Approximately 46% of pDCs were found to have strong CCR2 activity, and were also found to have significant levels of D6 activity, as mCCL22 resulted in a further reduction of CCL2^{AF647} by CCR2 KO cells. There was no evidence of D6 activity on either of the CCR2 KO cDC populations. The gated CD11c⁺MHCII⁻ population of cells in Figure 3-11A also possessed significant levels of CCR2 activity. The identity of this population is uncertain, but initial investigations suggest that the population contains a mix of several cell types. These observations shall be discussed in more detail in the Discussion.

In accordance with earlier results the vast majority of cell populations internalised CCL2^{AF647} in a CCR2 mediated fashion, with only a few cell populations in the spleen of CCR2 KOs having any evidence of low D6 activity i.e. macrophages (Figure 3-10) and pDCs (Figure 3-11). The majority of splenic CCR2 dependent uptake was by myeloid cells and DCs, with limited uptake by lymphoid cells except NK cells. As illustrated in the Introduction, CCR2 has been described to have roles in the mobilisation of numerous cell populations, including CD11b⁺ cDCs (Osterholzer et al., 2009), NK cells (Morrison et al., 2003) and monocytes (Serbina and Pamer, 2006). Conversely, a functional role of CCR2 on pDCs, to my knowledge, has yet to be elucidated and it was striking that these cells could be clearly divided into CCL2^{hi} and CCL2^{lo} subsets. Moreover, the apparent presence of D6 activity on these cells was also unexpected.

3.3.2 Monocytes, CD11c⁺ cells and pDCs possess CCR2 activity in the BM

A somewhat less detailed profiling of CCR2 activity was also conducted in the BM (Figure 3-12). Monocytes and neutrophils were gated based on their expression of Ly6C, CD11b, Gr1 and CD115. Ly6C⁺CD11b⁺ cells were examined for Gr1 and CD115 expression (Figure 3-12A). Mature neutrophils express high levels of Gr1 and are CD115⁻, whereas monocytes are Gr1^{lo}CD115⁺ (Sunderkötter et al., 2004; Serbina and Pamer, 2006; Rose et al., 2011). Once more, Ly6C^{hi} monocytes were found to have the highest CCR2 activity of all cell types analysed, with ~98% of WT cells being very positive for CCR2 dependent CCL2^{AF647} uptake. In contrast to splenic Ly6C^{hi} monocytes, CCR2 KO BM Ly6C^{hi} monocytes possessed weak but significant levels of D6 activity. Neutrophils were predominantly negative for CCR2 activity. However, there was a small population of neutrophils that were CCL2⁺, which might be explained by a small contamination with Ly6C^{hi} monocytes or cell doublets. There was also a population of Ly6C⁺CD11b⁺ cells that were Gr1^{hi}CD115⁺, highlighted by the green box in Figure 3-12A. Analysis of the physical properties of the Gr1^{hi}CD115⁺ cells (shown at the top of Figure 3-12A in green) illustrated that the cells were very large, being larger than both monocytes and neutrophils, suggesting that these 'cells' might be cell doublets.

A further 3 populations of cells, Populations A, B and C were identified in the BM by their expression of CD11b, Gr1, CD115 and Ly6C (Figure 3-12A). All 3 populations were Gr1^{lo}CD11b⁺, but differed in their expression of Ly6C and CD115. Population A was Gr1^{lo}CD11b⁺CD115⁺Ly6C^{lo}. The expression of CD115 and the physical properties of these cells (shown in light blue at the top of Figure 3-12A) suggested that they are of monocytic origin. Furthermore, Population A cells were very positive for CCR2 uptake, and CCR2 KO Population A possessed significant levels of D6 activity. Populations B and C were both Gr1^{lo}CD11b⁺CD115⁻ differing only in their expression of Ly6C. Population B was Ly6C⁺, whereas Population C was Ly6C^{lo}. Populations B and C also had unique physical properties that could be used to segregate the two populations. Population B (shown in yellow at the top of Figure 3-12A) were found to have similar properties to monocytes, as they were larger than lymphocyte populations. The physical properties of Population C (shown in purple at the top of Figure 3-12A) indicated that these are very large granular cells. Populations B

and C did not possess significant levels of CCR2 or D6 activity, but both populations from WT animals did internalise very low levels of CCL2^{AF647} in a CCR2 dependent manner. The identity of Populations A, B and C shall be discussed in more detail in the Discussion.

The assay also illustrated that BM B cells, delineated as B220⁺CD11c⁻ cells, were largely negative for CCR2 and D6 dependent uptake of CCL2^{AF647} (Figure 3-12B). Similar to splenic pDCs, WT BM pDCs were found to have significant levels of CCR2 mediated uptake of CCL2^{AF647} and showed CCL2^{hi} and CCL2^{lo} subsets, and CCR2 KO pDCs also possessed significant levels of D6 activity (Figure 3-12B). However, the level of D6 activity on BM pDCs appeared to be substantially higher than that found on splenic pDCs (Figure 3-11B). CD11c⁺ cells also had significant CCR2 and D6 activity. CD11c is expressed by a range of cells including DCs, macrophages, B cells and granulocytes (Hume, 2008). I therefore, chose not to name the CD11c⁺ population cDCs as it may contain others cell types too and insufficient markers were present to allow them to be more definitively assigned.

3.3.3 CCR2 activity is predominantly restricted to monocytes, CD11c⁺ cells and pDCs in the blood

I next assessed the cells that were responsible for CCR2 mediated uptake of CCL2^{AF647} in the blood (Figure 3-13). As with the spleen and BM, Ly6C^{hi} monocytes were the cells highest for CCR2 activity, with ~95% of WT cells showing CCR2 dependent CCL2^{AF647} uptake (Figure 3-13A). Similar to neutrophils in all other tissues tested, blood neutrophils were predominantly CCR2⁻. The blood also contained the Ly6C⁺CD11b⁺CD115⁺Gr1^{hi} population of cells (Figure 3-13A) that were previously identified in the BM (Figure 3-12A). The physical properties of these cells, shown at the top of Figure 3-13 in green, also indicated that they too might be doublets. Furthermore, as with BM samples, the blood contained the three cell populations of uncertain identity, Populations A, B and C (Figure 3-13A). Population A had significant levels of CCR2 activity, however in contrast to Population A in the BM, the population was much more heterogeneous and possessed no detectable D6 activity in the absence of CCR2. The percentage of CCL2⁺ cells within Population A (50%) was also dramatically lower than that observed in the BM (85%). In stark contrast to Population B in

the BM, the blood WT Population B had significant levels of CCR2 activity, comparable to that of Ly6C^{hi} monocytes. Population C in both the BM and blood did not possess significant levels of CCR2 or D6 activity, but a small proportion of cells internalised very low levels of CCL2^{AF647} in a CCR2 dependent manner. The physical properties of each of these cell populations in the blood were consistent with the previous observations in the BM (Figure 3-12A) e.g. Populations A and B were of similar size to monocytes, whilst Population C were large and granulocytic in appearance (Figure 3-13A). As mentioned above, these three populations of cells will be discussed in more detail in the Discussion.

Similar to data generated in the BM, B cells in the blood were largely negative for CCR2 and D6 dependent uptake of CCL2^{AF647}, while WT B220⁻CD11c⁺ cells possessed significant levels of CCR2 activity (Figure 3-13B). However, there was no significant D6 activity detected in B220⁻CD11c⁺ cells of CCR2 KO animals, although histogram overlays suggested that mCCL22 did have a minor effect on CCL2^{AF647} uptake. pDCs in the blood also possessed D6 and significant CCR2 activity, with clear CCL2^{hi} and CCL2^{lo} subsets identifiable (Figure 3-13B). The level of pDC D6 activity was comparable to that in the BM and was higher than the levels detected in splenic pDCs.

3.3.4 CCR2⁺ cells are rare in resting PLNs

CCR2 activity was next profiled on lymphocyte and myeloid cell subsets in the PLNs of WT animals, using CCR2 KO animals as controls (Figure 3-14). Similar to the spleen, $\gamma\delta^+$ T cells in the PLNs had low, but significant levels of CCR2 activity (Figure 3-14A). In contrast to the spleen, T cells (CD3⁺) were negative for CCR2 activity (Figure 3-14A) and B cells from CCR2 KO animals were negative for D6 activity (Figure 3-14B). This apparent lack of D6 activity can be explained by the low abundance of D6 expressing B1 B cells and the absence of MZ-B cells in the LNs (Hansell et al., 2011b). cDCs gated as CD11c⁺ were further divided into two populations based on their level of MHCII expression (Cella et al., 1997; Wilson et al., 2003) (Figure 3-14C). MHCII^{hi} cells, defined as migratory cDCs, were negative for both CCR2 and D6, whereas a subset of resident cDCs defined by their low MHCII expression showed CCR2 dependent uptake of CCL2^{AF647}. pDCs are also CD11c⁺ and MHCII^{lo}, and are likely to be included in the resident cDC gate, and therefore may account for some, if not all, of the CCR2 dependent

uptake. The CCR2 activity of PLN pDCs will be examined in more detail in Chapter 5. In contrast to all other tissues, no D6 activity was detected on any population in resting PLNs.

3.4 Effect of CCR2 deletion on the cellular composition of lymphoid organs and the blood

CCR2 plays a pivotal role in the migration of several cell types during inflammation, including cell populations that I have identified as having CCR2 activity, such as NK cells (Morrison et al., 2003), cDCs (Osterholzer et al., 2005) and Ly6C^{hi} monocytes (Serbina and Pamer, 2006). Ly6C^{hi} monocytes have also been shown to be highly dependent on CCR2 for their emigration from the BM into the blood during homeostasis, as a lack of CCR2 leads to the retention of Ly6C^{hi} monocytes in the BM (Geissmann et al., 2003; Serbina and Pamer, 2006). Therefore, I next sought to determine if CCR2 deletion affected the cellularity of secondary lymphoid organs, blood and BM, as perhaps akin to Ly6C^{hi} monocytes, other CCR2⁺ populations require CCR2 for their mobilisation into blood and seeding of secondary lymphoid organs during homeostasis (Figure 3-15).

Consistent with published observations (Serbina and Pamer, 2006), there was a significant deficit in peripheral monocytes in the spleen and blood of the CCR2 KO mice, which coincided with a significant increase in monocytes in the BM of CCR2 KOs (Figure 3-15). There were no apparent effects of CCR2 deletion on the frequency of any other identified cell populations in the spleen or BM (Figure 3-15A and B). The absence of CCR2 affected the frequency of blood Population B, as there was a significant reduction in the CCR2 KOs (Figure 3-15C). However, there was no corresponding increase in the BM of CCR2 KOs (Figure 3-15B). No cell population in the blood, other than Ly6C^{hi} monocytes and Population B, was affected by a deficit in CCR2 (Figure 3-15C). The frequency of migratory cDCs, resident cDCs and $\gamma\delta^+$ T cells present in PLNs were not affected by the absence of CCR2. However, there was an increase in B cell frequency in the PLNs of CCR2 KOs, and a decrease in the frequency of T cells (Figure 3-15D).

In summary, I have definitively identified numerous cell populations within the secondary lymphoid organs, BM and blood that possess CCR2 activity. CCR2

activity was mainly limited to myeloid cells and DCs, both cDCs and pDCs. I was able to define two populations of pDCs with respect to CCR2 activity, and there was clear evidence of D6 activity in CCR2 KO pDCs. There was also variation in CCL2 receptor activity between pDCs from different anatomical locations. Furthermore, two populations of cells identified in the blood, Populations A and B were found to have high levels of CCR2 activity. Interestingly, although these populations were also identified in the BM, only Population A possessed CCR2 activity in the BM. In each tissue, CCR2 was the receptor responsible for the majority of CCL2^{AF647} uptake. In addition, in all tissues except PLNs, significant levels of D6 activity were also detected on a few cell populations, such as MZ-B cells and pDCs in CCR2 KOs. The frequency of all but a few CCR2⁺ populations were relatively unaffected by deletion of CCR2. The frequency of Ly6C^{hi} monocytes was profoundly affected in the BM, spleen and blood of CCR2 KOs. Furthermore, the frequency of Population B in the blood was significantly reduced in the absence of CCR2. Lastly, T cell frequency was significantly reduced whilst B cell frequency was significantly increased in the PLNs of CCR2 KOs. The reason for this alteration in lymphocyte subsets is not clear and was not investigated further.

3.5 CCL2^{AF647} uptake assay detects CCL2 receptors in rat and human

Having demonstrated that the CCL2^{AF647} uptake assay could be used to reliably and sensitively detect CCR2 and D6 activity on cells from murine spleen, BM, PLNs and blood, I assessed whether the uptake assay would work to detect CCL2 receptors in other species. The ability of the reagents I used to work across species would present a further advantage of the assay over antibodies, which are often species restricted in terms of reactivity. As stated earlier, the fluorescent CCL2 used in the assay is human CCL2, yet it can be used to detect CCR2 and D6 activity of murine cells. This is due to the fact that chemokines have highly conserved primary and tertiary structures (Allen et al., 2007). Thus, human and murine CCL2 are structurally very similar, providing a likely explanation for the cross-reactivity of human CCL2^{AF647} with murine CCR2 and D6. This is very common with chemokines, and chemokines from one species can usually bind and activate receptors from another species. To determine if CCL2^{AF647} could be used to detect CCL2 receptors in species other than the

mouse, I tested the assay using single cell suspensions of both rat spleen (Figure 3-16A) and human peripheral blood (Figure 3-16B). Similar to the chemokine ligands, chemokine receptors are also highly conserved between species (Murphy et al., 2000), and although CCR2 and D6 genes are present within the rat genome there is little known about their expression or chemokine binding profiles in the rat. Therefore, I do not refer to CCL2^{AF647} uptake by rat splenocytes in terms of CCR2 or D6, but as CCL2 receptors. However, I used competition with mCCL22 to try and identify D6 activity on rat splenocytes, and rat CCL2 (rCCL2) was used to demonstrate that uptake was receptor-mediated rather than non-specific uptake. It is not known whether mCCL22 is active on rat CCL2 binding receptors, however no rat CCL22 was available for purchase.

First, I characterised uptake of CCL2^{AF647} by four rat splenic populations: CD4⁺ cDCs, pDCs, neutrophils and monocytes (Figure 3-16A). Earlier I discussed the use of CD11c as a marker for DCs, but stated that other cells also express it (Hume, 2008). However, its use, in combination with a number of other markers, is key in the identification of DCs in mice. The identification of DCs within the rat is hindered by the lack of a functioning anti-CD11c antibody or an equivalent lineage marker. Thus, complex gating strategies that rely on the exclusion of the majority of lymphocyte populations are employed to identify DC subsets in this species (Hubert et al., 2006). To identify monocyte and neutrophil populations I employed gating strategies similar to those that have been described elsewhere (Yrlid et al., 2006).

Similar to the mouse, the majority of rat neutrophils did not internalise CCL2^{AF647} (Figure 3-16A). However, there was a small population of neutrophils with CCL2 receptor activity. I think these are likely to be contaminating monocytes, as their CCL2^{AF647} uptake profile appears similar to that of monocytes. In the other three populations (pDCs, monocytes and CD4⁺ cDCs), much of the uptake was competable with rCCL2, indicating uptake by a rat receptor capable of binding rat CCL2. Addition of mCCL22 had no effect on the ability of the cells to internalise CCL2^{AF647}, indicating that mCCL22 may not be active on rat D6 or that rat D6 is not expressed in the cells examined. pDCs and monocytes were found to have high levels of receptor mediated CCL2^{AF647} internalisation, while only a small number of CD4⁺ cDCs had low levels. In contrast to murine pDCs, all rat pDCs appeared to be CCL2⁺. CD43⁻ monocytes are considered to be the rat

equivalent of the murine Ly6C^{hi} monocytes, possessing high levels of CCR2 (Yrlid et al., 2006). However, in contrast to murine monocytes, I found a proportion of rat monocytes that did not possess CCL2 receptor activity (Figure 3-16A).

The assay was also tested on human peripheral blood leukocytes (Figure 3-16B). Uptake was competed with an excess of hCCL2 or hCCL22, as human D6 is known to bind both hCCL2 and hCCL22, whilst human CCR2 binds hCCL2 but not hCCL22 (Bonecchi et al., 2004). Monocytes and pDCs were found to have high levels of CCR2, demonstrated by inhibition of CCL2^{AF647} uptake with hCCL2 with no corresponding decrease with competition with hCCL22. As in mice, but in contrast to rats, there was heterogeneity amongst human pDCs with respect to CCR2 activity. In stark contrast to mouse splenic NK cells, very few human peripheral blood NK cells showed evidence of CCR2 activity. B cells had no CCR2 mediated uptake of CCL2^{AF647}. The presence of hCCL22 did not modulate CCL2^{AF647} uptake, indicating that there is unlikely to be any active D6 present on any of these cells.

Collectively these results indicate that a single reagent, CCL2^{AF647}, works in three mammalian species. Work conducted by Amanda Guth (Colorado State University, USA) also suggests that the assay works with cells isolated from dogs (personal communication). Therefore, I propose that the CCL2^{AF647} assay might work in all mammalian species. This presents a distinct advantage of the assay over antibody mediated detection, as reliable anti-CCR2 antibodies are not available in many mammalian species, and, as I have shown, the available anti-mouse CCR2 antibodies are of limited sensitivity and reliability.

3.6 Using CCL2^{AF647} uptake assay to determine CCR2 receptor specificity

In the process of establishing CCL2^{AF647} as a reliable detection method of CCR2, I have shown the assay to be capable of detecting both high and low levels of CCR2 on a range of cells in different tissues. I next set out to assess the ability of the assay to monitor receptor specificity, by assessing CCR2 mediated CCL2^{AF647} uptake in the presence of unlabelled ligands. By pre-incubating cells with unlabelled CCR2 ligands, or by competing CCL2^{AF647} uptake with unlabelled

CCR2 ligands, I was able to characterise CCR2 specificity and the impact of prior exposure of CCR2 ligands on subsequent CCR2 activity.

3.6.1 Monitoring murine CCR2 activity in the presence of a competitor ligand

Having consistently shown the inhibition of D6 dependent CCL2^{AF647} uptake by co-incubation with an excess of unlabelled mCCL22, I assessed the effect of co-incubating unlabelled CCR2 ligands on CCR2 activity in the CCL2^{AF647} uptake assay. Mouse CCL8 was originally considered to be a CCR2 ligand, but it is now known to be a CCR8 ligand rather than binding CCR2 (Hansell et al., 2011b; Islam et al., 2011), so it was not included in my experiments. CCL3 was included as a negative control, as similar to CCL22, it is also a D6 ligand and should have little, if any, CCR2 binding activity. Splenocytes from WT mice were incubated with CCL2^{AF647} in the presence or absence of 25 nM unlabelled mCCL2, mCCL3, mCCL7 or mCCL12, and CCL2^{AF647} uptake was assessed (Figure 3-17A). CCR2 deficient splenocytes incubated with CCL2^{AF647} without a competitor chemokine were included as a negative control. Each competitor ligand generated a unique profile in terms of uninhibited CCL2^{AF647} uptake. CCL2^{AF647} uptake was blocked in the presence of unlabelled mCCL2 and within the Ly6C⁻ population was actually more effective than CCR2 deletion because it inhibited uptake by MZ-B cells. Similarly, although mCCL3 had little effect on CCL2^{AF647} uptake by Ly6C⁺ cells it did cause a reduction in CCL2^{AF647} uptake by Ly6C⁻ cells. Competition with mCCL7 and mCCL12 caused a reduction in CCL2^{AF647} uptake by Ly6C^{hi} cells, but had differential effects on Ly6C⁻ cells. This is consistent with mCCL12 being a ligand of D6, whilst mCCL7 is not (Hansell et al., 2011b).

In the earlier profiling experiments, Ly6C^{hi} monocytes were consistently found to have the highest CCR2 activity. Therefore, I measured CCR2 activity on splenic Ly6C^{hi} monocytes in response to co-incubation with varying concentrations of several unlabelled murine CCR2 ligands (Figure 3-17B). Within the same sample I was able to measure CCR2 activity of splenic Ly6C⁻CD11b⁺ cells (Figure 3-17C). Representative histograms of CCL2^{AF647} uptake in CCR2 KO and WT monocytes, in the presence of increasing concentrations of mCCL2, mCCL7 or mCCL12, illustrate that as the concentration of the competitor ligands increases, there is a parallel decrease in CCL2^{AF647} uptake. mCCL3 had minimal effects on CCR2

mediated uptake of CCL2^{AF647} as expected. At higher concentrations of the competitor ligands, mCCL2 appeared to cause the greatest inhibition of CCL2^{AF647} uptake. However, on quantification, there were no significant differences between mCCL2, mCCL7 and mCCL12 in their ability to inhibit CCL2^{AF647} uptake, but mCCL3 was significantly inferior at all tested concentrations than mCCL2. Furthermore, at the highest concentration of competitor ligands (25 nM), CCL2^{AF647} uptake was comparable to that in the CCR2 KO, particularly in the case of mCCL2. These results demonstrate that the three ligands are equal in their capacity to compete CCR2 dependent CCL2^{AF647} uptake by Ly6C^{hi} monocytes. In contrast, although mCCL2 showed a dose response curve for inhibition of CCL2^{AF647} uptake by Ly6C^{hi}CD11b⁺ cells, mCCL7 and mCCL12 were less effective.

3.6.2 Establishing the effect of chemokine exposure on murine CCR2 activity

Having demonstrated the ability of the assay to confirm the specificity of murine CCR2, I next assessed whether prior exposure of CCR2 to unlabelled ligands affected its activity. The underlying principle to this experiment extends from another aspect of chemokine receptor dynamics, known as desensitisation. Chemokine receptor desensitisation, as discussed in the Introduction, is a process by which a receptor becomes refractory to further stimulation by a chemokine ligand after an initial exposure to chemokine. Thus, on exposure to ligand, the chemokine receptor can become unresponsive to further chemokine ligands. Splenocytes from WT mice were pre-incubated with varying concentrations of unlabelled CCR2 ligands, or the negative control mCCL3, prior to exposure to CCL2^{AF647} (Figure 3-18). CCR2 deficient splenocytes without prior exposure to unlabelled CCR2 ligands, but incubated with CCL2^{AF647} were used as a negative control. Similar to the co-incubation data, each unlabelled chemokine generated unique profiles of uncompleted CCL2^{AF647} uptake (Figure 3-18A). Representative histograms of CCL2^{AF647} uptake in Ly6C^{hi} monocytes following exposure to unlabelled mCCL2, mCCL7 or mCCL12, indicate that as the concentration of ligand increases, CCL2^{AF647} uptake decreases (Figure 3-18B). Pre-incubation with mCCL3 had no effect on CCR2 mediated uptake of CCL2^{AF647}. By comparing the effect of each ligand on CCL2^{AF647} uptake, mCCL2 was found to be the most effective at inhibiting uptake at the majority of concentrations tested, causing a significant decrease in uptake when compared to mCCL3,

mCCL7 and mCCL12. Also, at the highest concentration tested, mCCL2 inhibited uptake to levels similar to the background levels observed in the CCR2 KO. mCCL7 and mCCL12 although not as effective as mCCL2 appeared to have similar profiles to each other. This result was more striking in Ly6C^{hi}CD11b⁺ cells, as mCCL7 and mCCL12 were unable to inhibit CCL2^{AF647} uptake at all concentrations, except the highest concentration (250 nM) where minimal inhibition was achieved (Figure 3-18C).

Taken these results together they detail a sensitive technique that is capable of monitoring downregulation of receptor activity, as a consequence of receptor desensitisation. They give preliminary insights into the responsiveness of CCR2, as competition of CCL2^{AF647} binding to CCR2 required only low concentrations of unlabelled ligand, whereas over ten-fold higher concentrations of unlabelled ligand were required to fully desensitise CCR2. In addition, these results suggest that although each ligand can inhibit CCL2^{AF647} uptake, they differ in their capacity to desensitise CCR2. Furthermore, these results also suggest that the interaction of CCR2 with its ligands are cell-type specific, as although mCCL7 and mCCL12 were able to desensitise CCR2 on Ly6C^{hi} monocytes, they were unable to do so on Ly6C^{hi}CD11b⁺ cells.

3.7 Summary

In this chapter, I have detailed how several anti-mouse CCR2 antibodies are either incapable of detecting CCR2, or can only facilitate the detection of high levels of CCR2. With MC-21, careful controls are essential, with cells from CCR2 KO mice serving as a better control than isotype control antibodies. I described the use of a novel sensitive assay to detect CCR2 and demonstrate some of the advantages of the assay over currently available methods. Firstly, with appropriate controls it can be used to detect both CCR2 and D6. Furthermore, other members of the group have used this assay with other fluorescently labelled chemokines to detect other chemokine receptor activity on cells, in single cell suspensions from other tissues, including the gut and lung. These tissues, particularly the gut, have provided further challenges when using antibodies, as they have an even greater background signal, yet the chemokine assays can be used to profile receptor activity (Bordon et al., 2009; Hansell et al., 2011b). The assay can also be used to detect receptor activity in multiple

species, providing yet another advantage over the use of antibodies, particularly in the rat where antibody reagents are scarce. In addition, the assay has also facilitated the monitoring of CCR2 receptor specificity, and the receptiveness of CCR2 to desensitisation with unlabelled chemokines.

These results present a detailed profiling of CCR2 activity on leukocytes in some of the major murine lymphoid organs. In all organs tested, CCR2 was the major receptor mediating CCL2^{AF647} uptake, with D6 playing a minor role. The cell populations that were found to be responsible for the majority of CCR2 dependent uptake were of either a myeloid cell origin or DCs, with monocytes always being the population with highest CCR2 activity. Furthermore, I identified three Gr1^{lo}CD11b⁺ populations, present in the blood and BM, that I named Population A, B and C. These populations differed in their expression of Ly6C and CD115. Population A was the only one of the three populations to express CD115 and possessed significant levels of CCR2 activity in the BM and blood. In contrast, Populations B and C were CD115⁻ and no CCR2 activity was evident on either population in the BM. However, Population B in the blood possessed significant CCR2 activity. The identity of these populations is uncertain, but in the discussion I speculate over their possible origin (sections 6.2.2.3 and 6.5.2.3).

One of the striking results from these profiling experiments is that in all populations, other than Ly6C^{hi} monocytes, there is only a percentage of each cell population that takes up CCL2^{AF647} in a CCR2 dependent fashion. Furthermore, in contrast to results I generated with MC-21, several cell populations that were thought to be negative for CCR2 or express low levels of CCR2, were found to be CCR2⁺, including NK cells, CD8 α ⁺ cDCs, pDCs and CD11b⁺ cDCs. Chemokine receptors are often able to define functionally distinct leukocytes subsets, therefore these results provide new insight into CCR2 expression and potentially undiscovered roles for CCR2 *in vivo*.

The absence of CCR2 is known to lead to deficiencies in peripheral Ly6C^{hi} monocytes, as they are retained in the BM and clearly require CCR2 for their release (Serbina and Pamer, 2006). My results support these observations, as there were decreased Ly6C^{hi} monocytes in the spleen and blood of the CCR2 KO, with a corresponding increase in the BM. My results also showed that the

absence of CCR2 led to alterations in the frequency of only a few of the other identified CCR2⁺ populations. T cells in PLNs and blood Population B cells were significantly reduced in the CCR2 KO. In contrast, there was an increase in the frequency of B cells present in the PLNs of the CCR2 KO.

The findings in this chapter are discussed in greater detail in the Discussion section. Having optimised and detailed the use of the CCL2^{AF647} assay to accurately detect CCR2, in the next chapter I explore the consequence of *in vivo* LPS treatment on the CCR2 and D6 activity of the described CCR2/D6⁺ populations. Furthermore, having established that CCR2 deletion affects the frequency of a number of the CCR2⁺ populations, I explore the effect of systemic inflammation on the frequency of splenic CCR2⁺ populations.

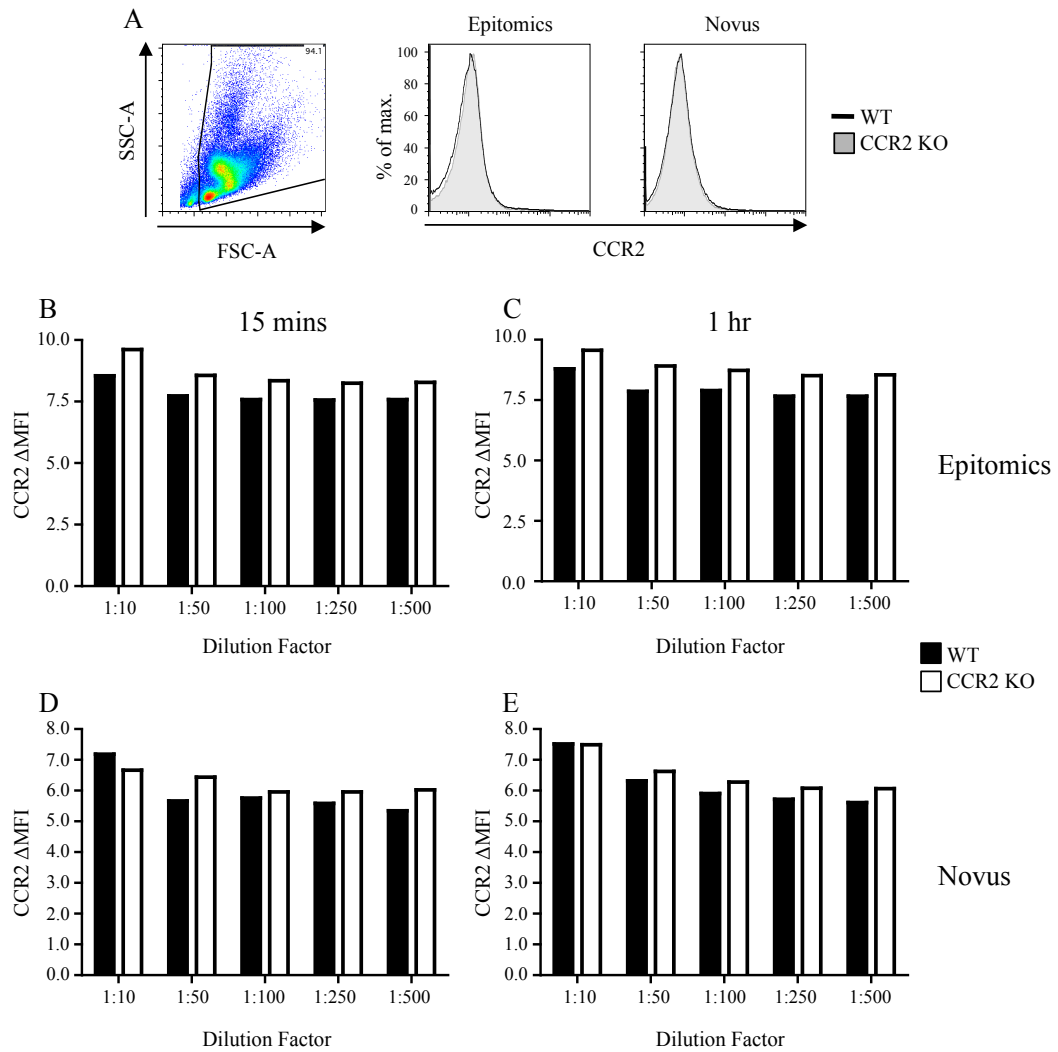


Figure 3-1: Antibody mediated CCR2 detection.

BM cells derived from WT (black line) and CCR2 KO (shaded grey area) were stained with commercial anti-CCR2 antibodies. Epitomics anti-CCR2 antibody was tested at 718 μ g/ml (1:10), 143.6 μ g/ml (1:50), 71.8 μ g/ml (1:100), 28.72 μ g/ml (1:250) and 14.36 μ g/ml (1:500) and incubated with BM cells for either 1 hr or 15 mins. Novus biologicals antibody was tested on BM cells at 100 μ g/ml (1:10), 20 μ g/ml (1:50), 10 μ g/ml (1:100), 4 μ g/ml (1:250) and 2 μ g/ml (1:500) for either 1 hr or 15 mins. (A) Staining following a 1 hr incubation with the highest tested concentration of each antibody on cells gated based on FSC and SSC properties. (B-E) CCR2 geometric mean fluorescence intensity (Δ MFI) was determined for each dilution of the Epitomics (B&C) and Novus (D&E) antibodies for both WT (black bars) and CCR2 KO (white bars) BM cells following staining for the two different incubation periods, 15 mins (B&D) and 1 hr (C&E). n=1.

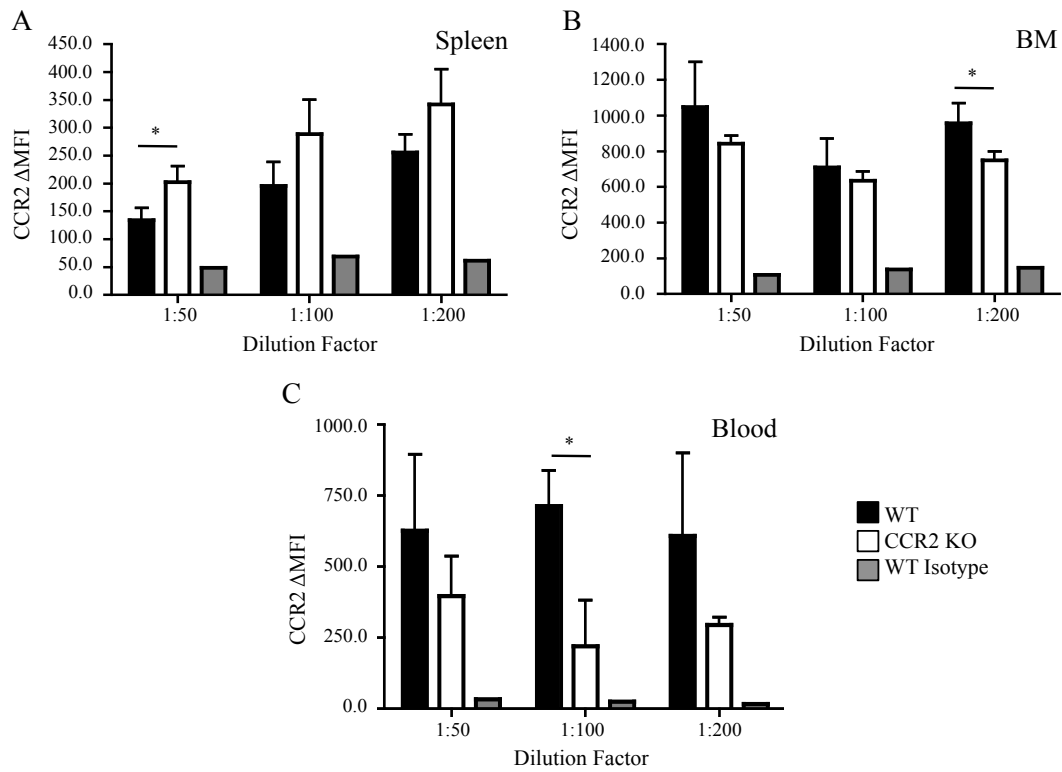
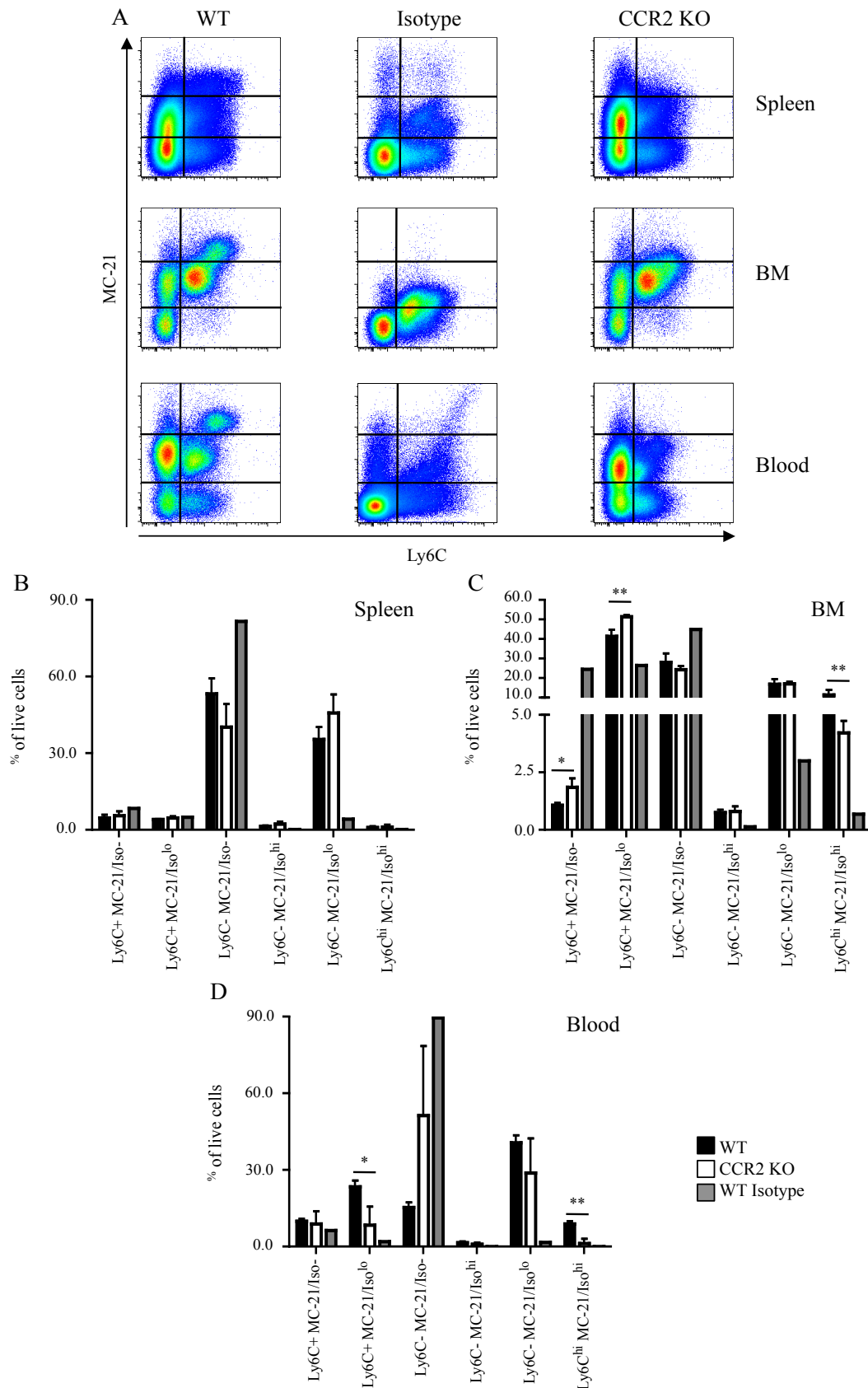


Figure 3-2: Testing the MC-21 anti-mouse CCR2 antibody.

Live cells from the spleen (A), BM (B), or blood (C) isolated from WT and CCR2 KO mice were stained with 2.5 $\mu\text{g}/\text{ml}$ (1:200), 5 $\mu\text{g}/\text{ml}$ (1:100) or 10 $\mu\text{g}/\text{ml}$ (1:50) MC-21 anti-CCR2 antibody or WT cells were stained with isotype control antibody. Graphical representation of the calculated CCR2 geometric mean fluorescence intensity (ΔMFI) of WT cells (black bars) or CCR2 KO (white bars) or WT cells stained with isotype (grey bars). Data are from three individual mice per genotype (mean + SD), except the isotype result that was generated from a single mouse. Data were analysed by unpaired T-test comparing WT to CCR2 KO at each dilution $p < 0.05$ *.



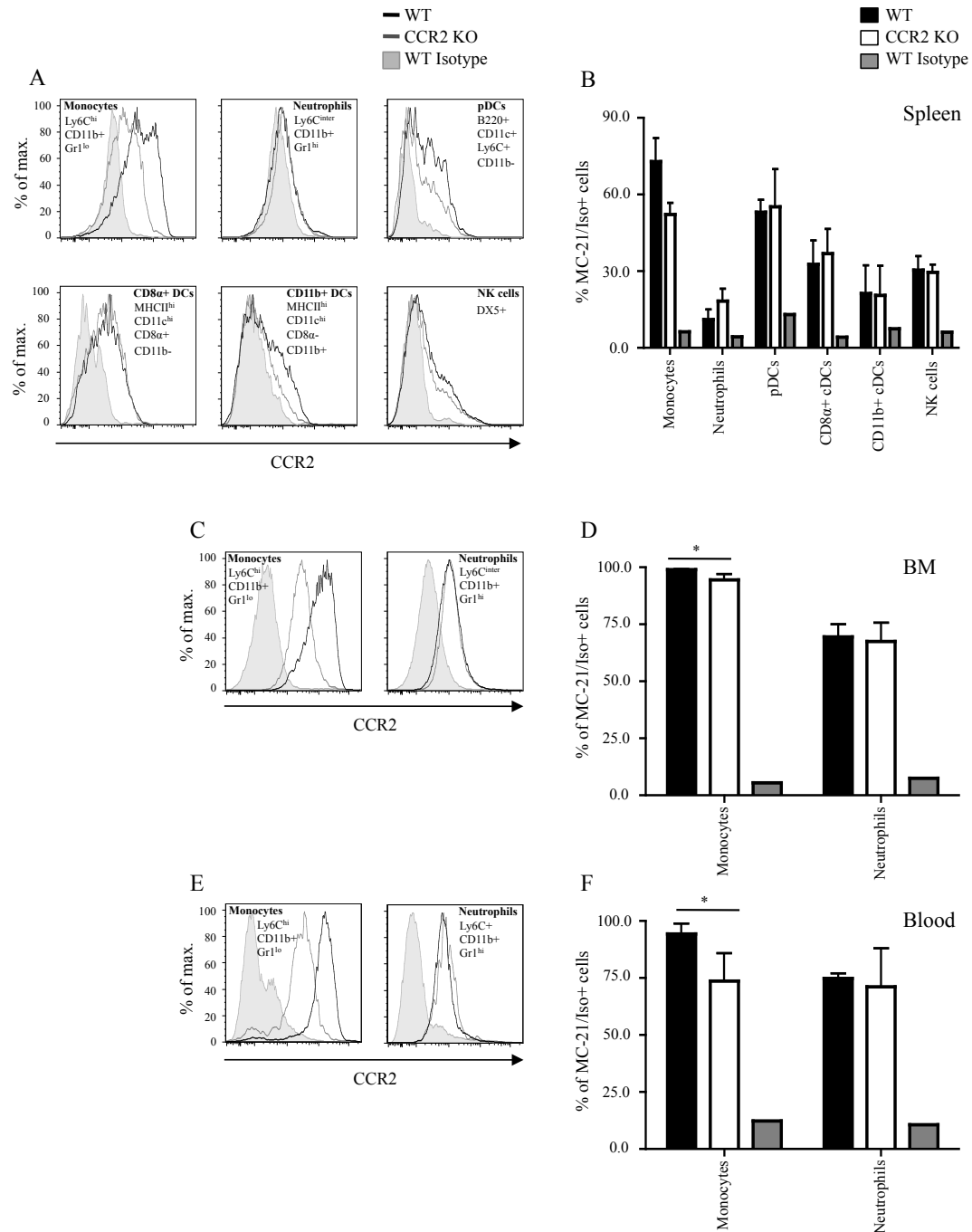


Figure 3-4: Detection of CCR2 expression using MC-21 antibody.

Specific cell populations in the spleen (A&B), BM (C&D) and blood (E&F) were identified by FACS, according to specific lineage markers as indicated. The level of CCR2 expression was assessed using the MC-21 antibody (black line) and compared to isotype controls (shaded grey area) or CCR2 KO stained with MC-21 (grey line) and is shown in representative histograms. The proportion of cells positive for staining with MC-21 (MC-21/Iso⁺) was determined for each population by considering anything above the isotype control to be positive. The proportion of MC-21/Iso⁺ cells within each population was calculated for WT, CCR2 KO and isotype control samples in the spleen (B), BM (D) and blood (F). Data are from three individual mice per genotype, except the isotype result, which was generated from a single WT mouse (mean + SD). Data were analysed by unpaired T-test comparing WT to CCR2 KO $p < 0.05$ *.

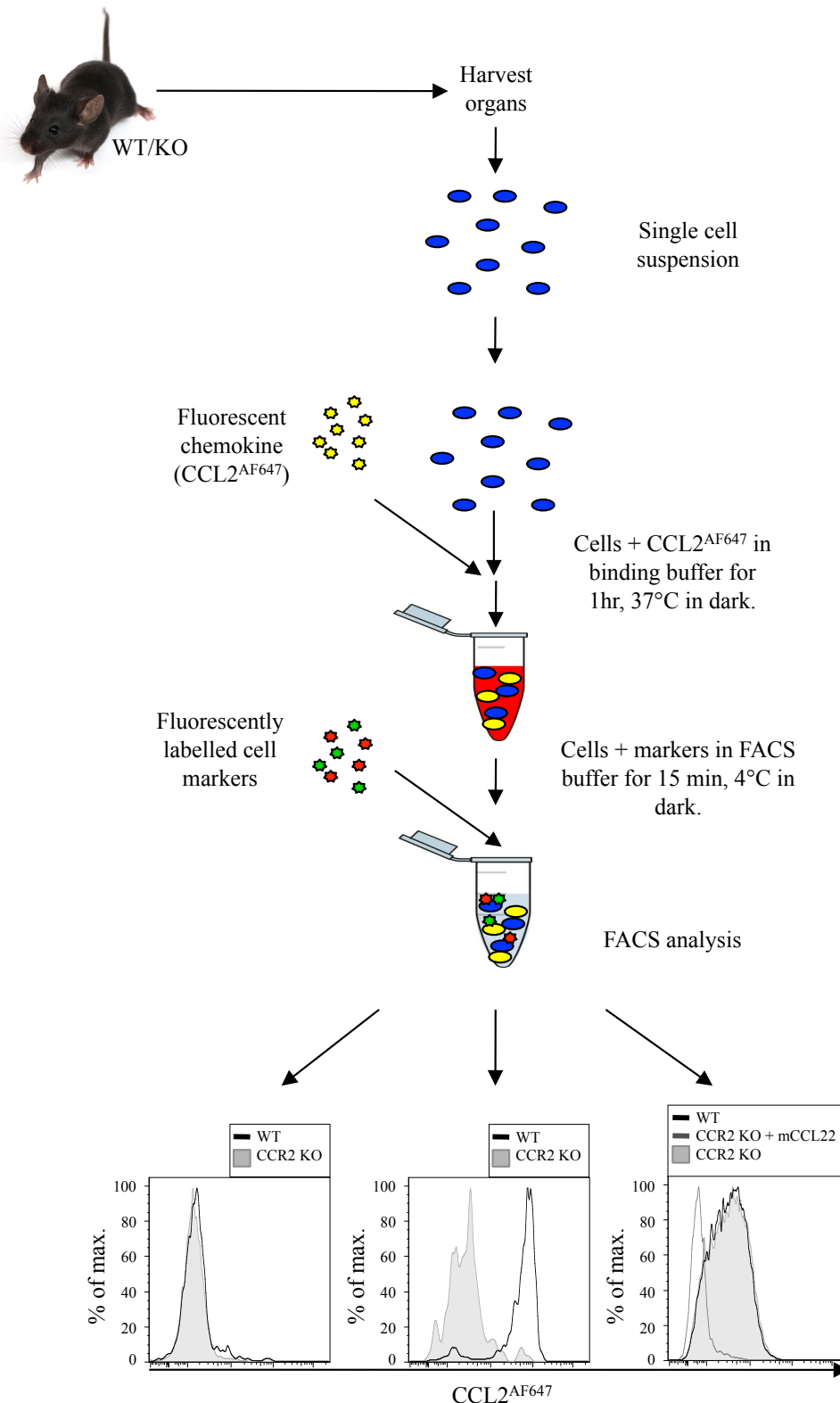


Figure 3-5: Using fluorescently labelled CCL2 to detect CCR2.

CCL2^{AF647} is incubated with a single cell suspension of cells generated from the tissue of choice for 1 hr at 37°C. Cells are subsequently stained with fluorescently labelled antibodies against cell surface markers and analysed using flow cytometry. Using a combination of samples from WT (black line) and CCR2 KO (shaded grey area) animals the receptor responsible for the uptake of CCL2^{AF647} can be determined. The histograms illustrate typical results that may be generated with the assay when either no CCR2 dependent uptake (left hand panel) or CCR2 dependent uptake (middle panel) is observed. Furthermore, in most cases a control competition sample which refers to the addition of a 10-fold molar excess of unlabelled murine CCL22 (mCCL22) was included (grey line). In addition to CCR2, the atypical chemokine receptor D6 can also bind CCL2^{AF647}. The addition of mCCL22 (right hand panel) can confirm that uptake is in fact due to D6, as D6 is the only receptor that binds to CCL2 and CCL22.

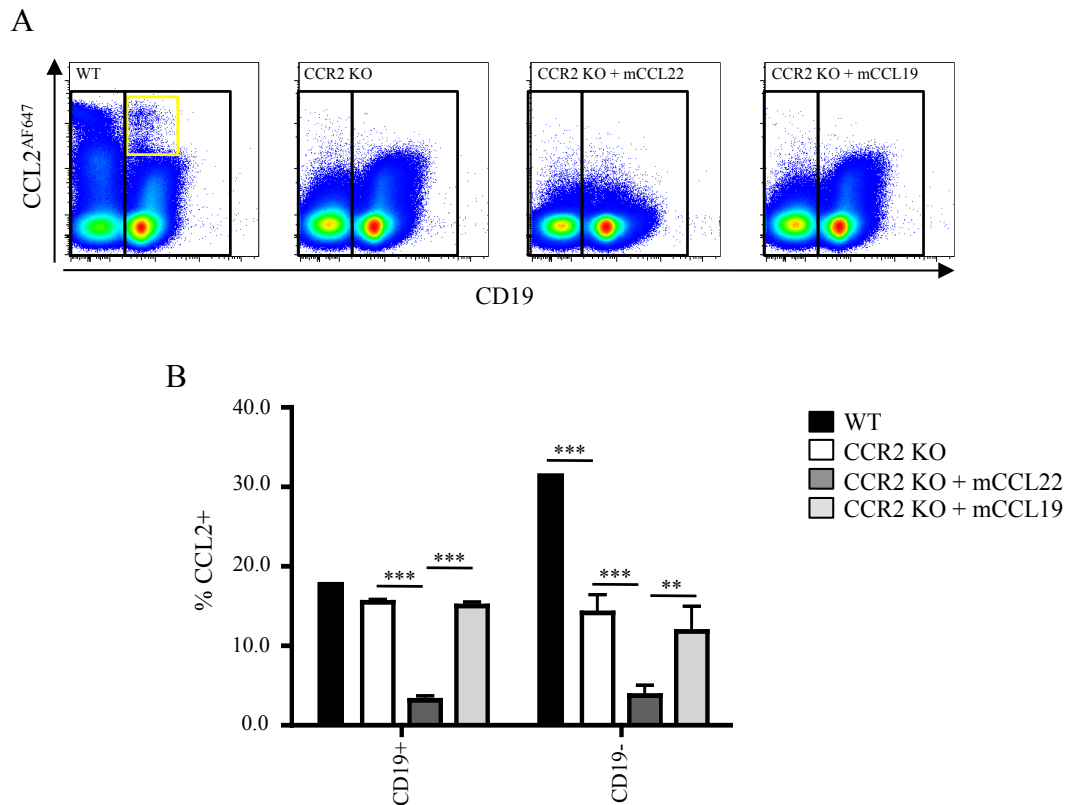
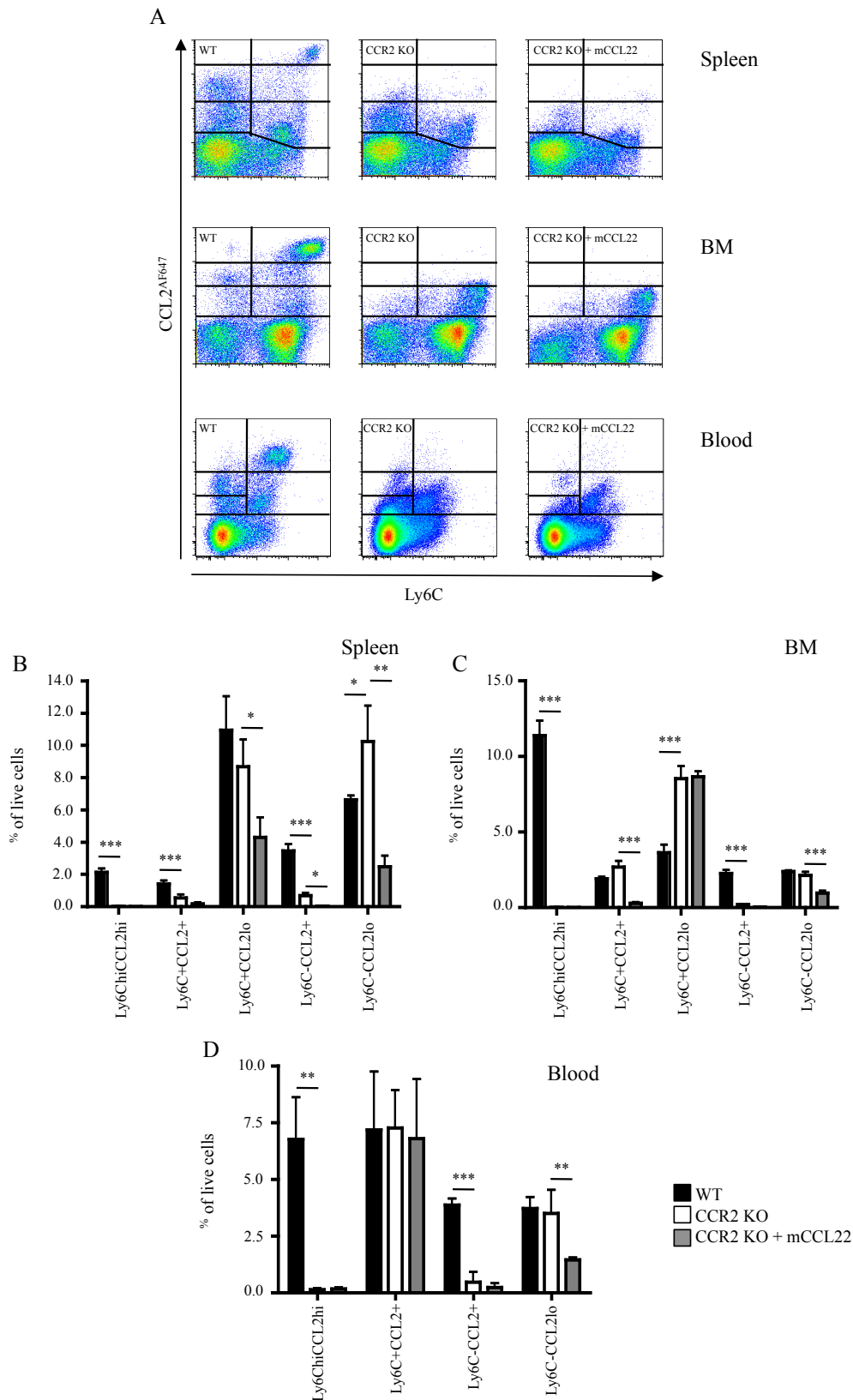


Figure 3-6: mCCL22 competition is specific for D6 mediated uptake.

(A) Splenocytes isolated from WT (far left hand panel) or CCR2 KO (left hand panel) animals were incubated with CCL2^{AF647} without competition. CCL2^{AF647} uptake in CCR2 KO splenocytes was also competed with 10-fold molar excess of mCCL22 (right hand panel) or mCCL19 (far right hand panel). Yellow box indicates the presence of a CD19^{lo} population that possesses CCR2 dependent uptake. (B) The proportion of CCL2⁺ cells within CD19⁺ and CD19⁻ populations, as gated in (A) were calculated for WT, CCR2 KO and competition samples. Data are from three individual mice per genotype (mean + SD). Data were analysed by one-way ANOVA with Tukey post-test $p < 0.01$ ** and $p < 0.001$ ***.



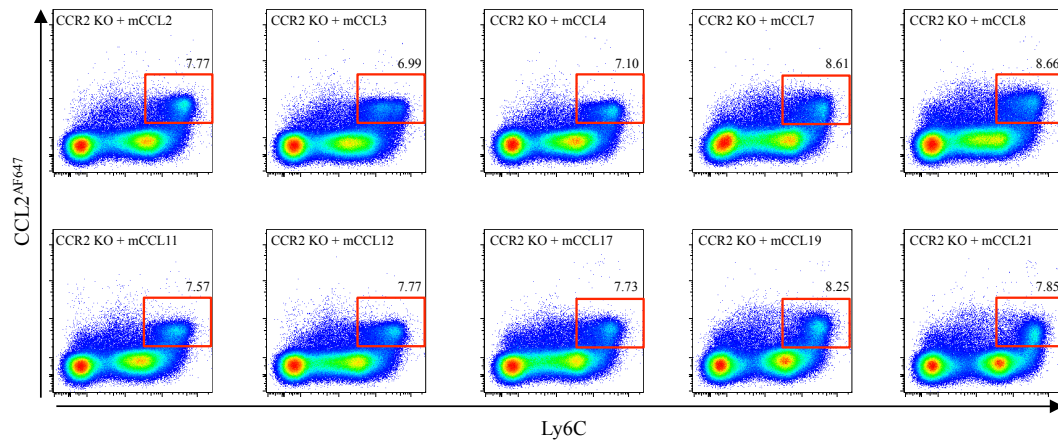


Figure 3-8: Competition of the CCR2 and D6 independent uptake in BM.

Cells isolated from CCR2 KO BM were incubated with an excess of a range of murine CC chemokines ligands at 10-fold molar excess. Representative plots of CCL2^{AF647} uptake in BM of CCR2 KO animals with competition. Red boxes indicate the CCR2 and D6 independent uptake and the proportion of live cells within each box is indicated. Plots are representative of three biological replicates.

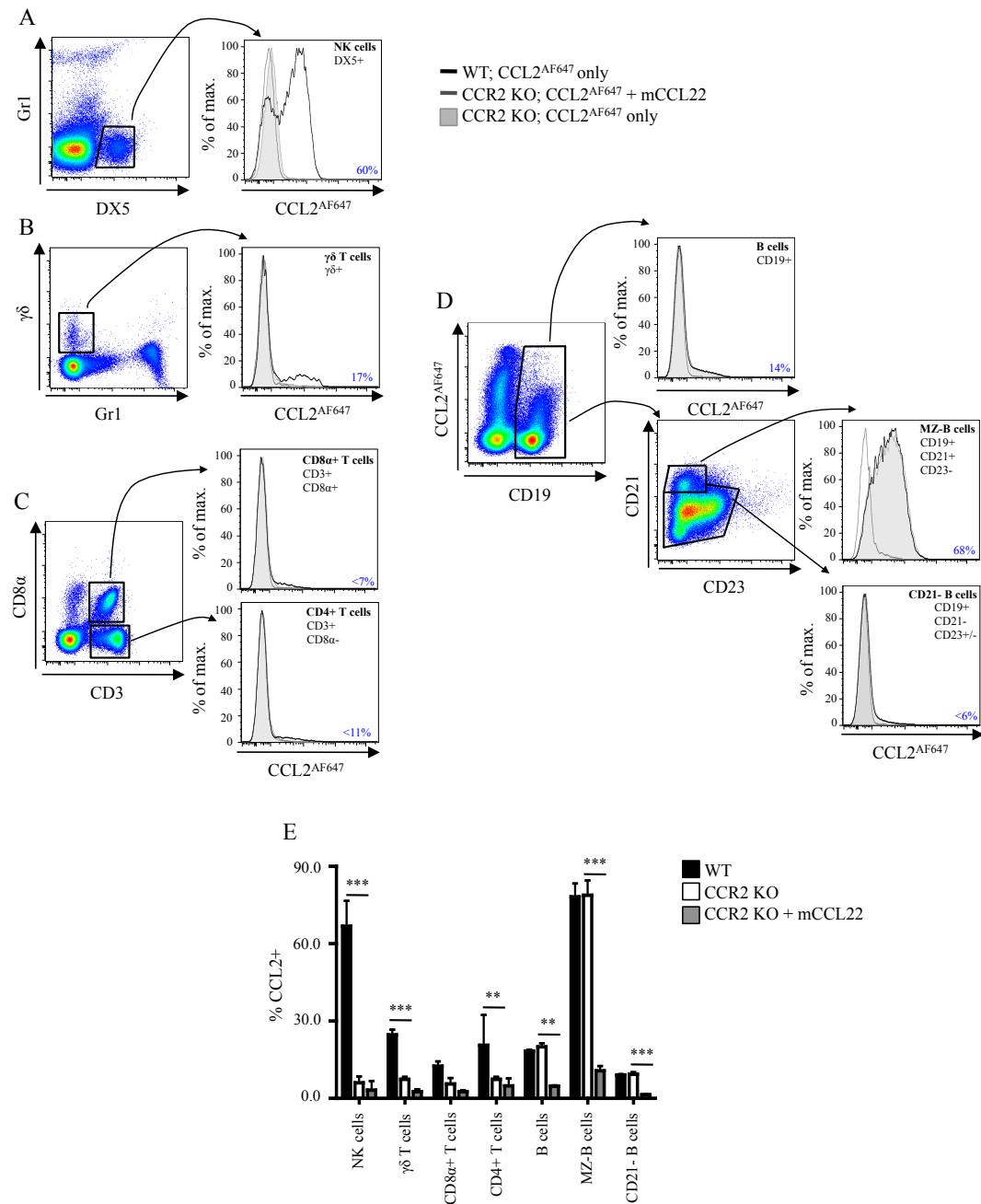


Figure 3-9: Characterisation of CCL2 receptor activity on murine splenic lymphocytes using CCL2^{AF647}.

Murine NK cells (A), $\gamma\delta^+$ T cells (B), CD8 α^+ and CD4⁺ T cells (C) and B cells, including MZ-B cells and CD21⁻ B cells (D) were gated as depicted in the left hand panels of the figure. Representative histograms of WT (black line) and CCR2 KO (shaded grey area) cells incubated with CCL2^{AF647} alone, or CCL2^{AF647} uptake in CCR2 KO competed with 10-fold molar excess mCCL22 (grey line) are shown for each gated population. Proportion of CCL2⁺ cells is illustrated in histograms for each cell population, calculated by subtracting % CCL2⁺ cells in CCR2 KO + mCCL22 samples from WT samples. (E) The proportion of CCL2⁺ cells within each population was calculated by considering anything above CCR2 KO + mCCL22 sample to be positive. Data are from 3 or more individual mice per genotype (mean + SD). Data were analysed by one-way ANOVA with Tukey post-test $p < 0.01$ ** and $p < 0.001$ ***.

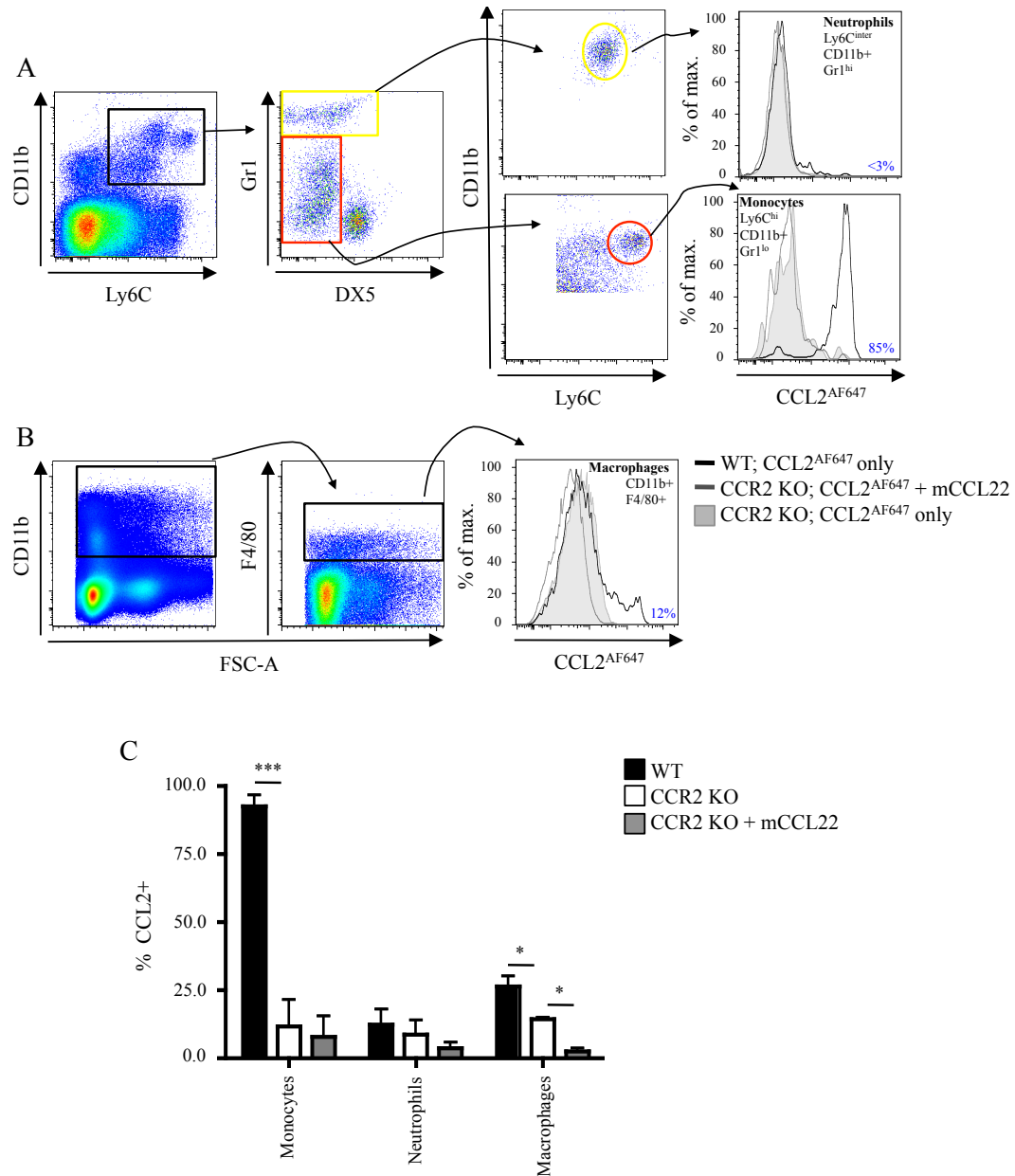


Figure 3-10: Characterisation of CCL2 receptor activity on murine splenic myeloid cells using CCL2^{AF647}.

Murine neutrophils and monocytes (A) and macrophages (B) were gated as depicted in the left hand plots of the figure. Representative histograms of WT (black line) and CCR2 KO (shaded grey area) cells incubated with CCL2^{AF647} alone, or CCL2^{AF647} uptake in CCR2 KO competed with 10-fold molar excess mCCL22 (grey line). Proportion of CCL2⁺ cells is illustrated in histograms for each cell population, calculated by subtracting % CCL2⁺ cells in CCR2 KO + mCCL22 samples from WT samples. (C) The proportion of CCL2⁺ cells within each population was calculated by considering anything above CCR2 KO + mCCL22 sample to be positive. Data are from 3 or more individual mice per genotype (mean + SD). Data were analysed by one-way ANOVA with Tukey post-test p < 0.05 * and p < 0.001 ***.

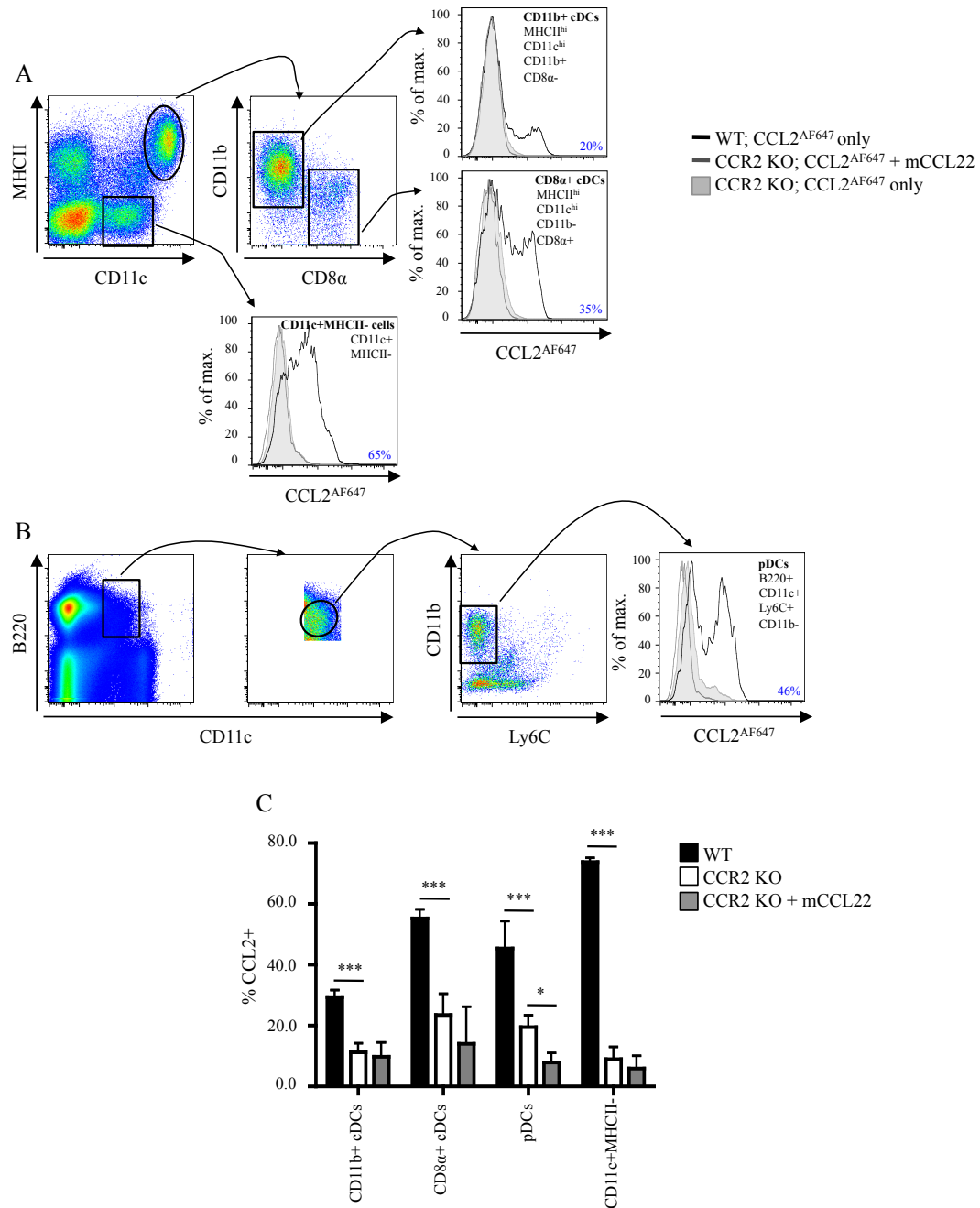


Figure 3-11: Characterisation of CCL2 receptor activity on murine splenic DCs using CCL2^{AF647}.

CD11b⁺ cDCs, CD8α⁺ cDCs, and CD11c⁺MHCII⁻ cells (A) and pDCs (B) were gated as depicted in the left hand panels of the figure. Both cDC populations and the CD11c⁺MHCII⁻ were gated following the exclusion of dead cells, CD19⁺, NK1.1⁺ and CD3⁺ cells. Representative histograms of WT (black line) and CCR2 KO (shaded grey area) cells incubated with CCL2^{AF647} alone, or CCL2^{AF647} uptake in CCR2 KO competed with 10-fold molar excess mCCL22 (grey line). Proportion of CCL2⁺ cells is illustrated in histograms for each cell population, calculated by subtracting % CCL2⁺ cells in CCR2 KO + mCCL22 samples from WT samples. (C) The proportion of CCL2⁺ cells within each population was calculated by considering anything above CCR2 KO + mCCL22 sample to be positive. Data are from 3 or more individual mice per genotype (mean + SD). Data were analysed by one-way ANOVA with Tukey post-test p<0.05 * and p<0.001 ***.

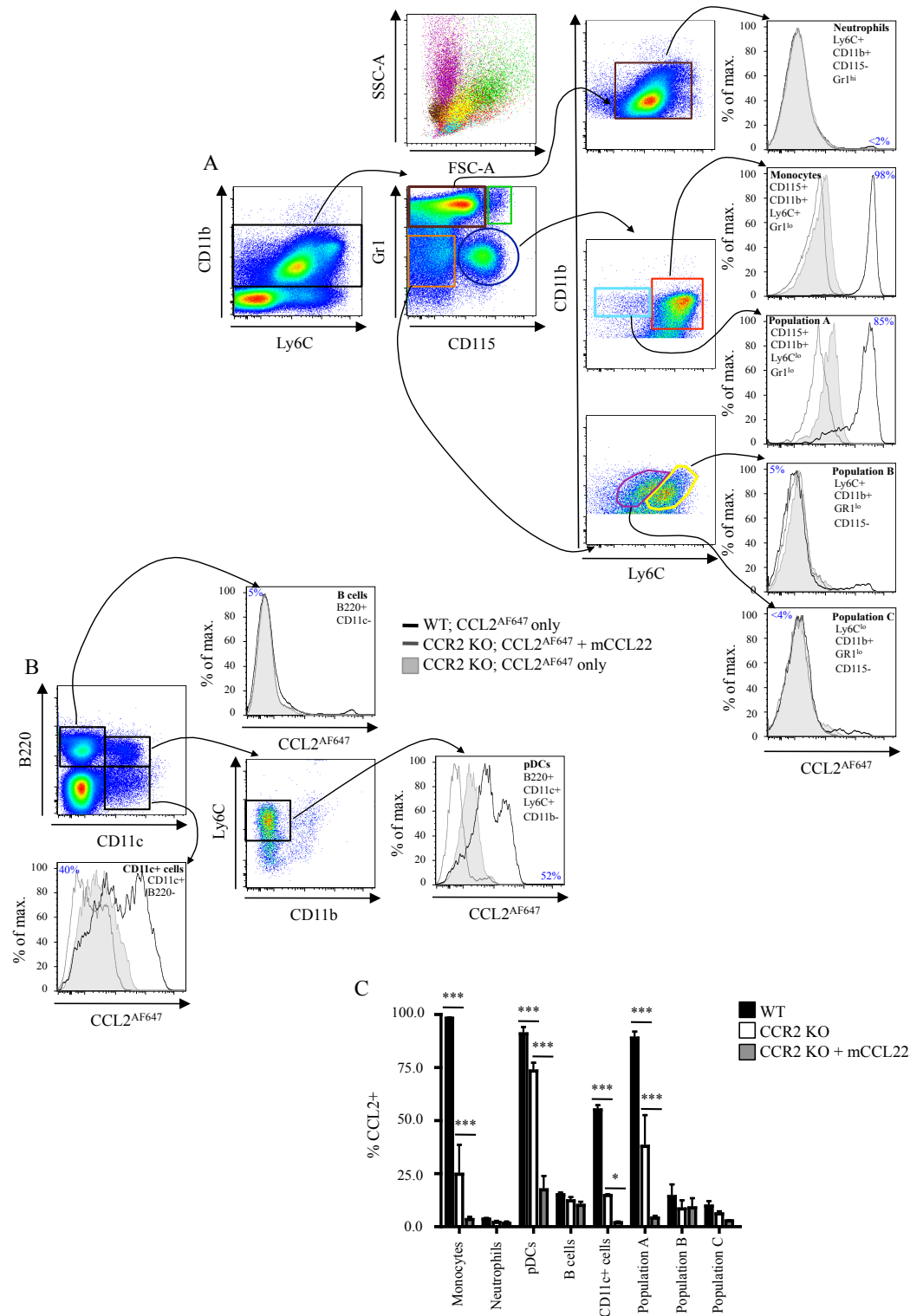


Figure 3-12: CCL2 receptor activity of murine BM cells as characterised by using CCL2^{AF647} assay.

Murine BM neutrophils, monocytes, Gr1^{hi}CD115⁺ cells, Populations A, B and C (A), B cells, CD11c⁺ cells and pDCs (B) were gated as depicted in the left hand plots of the figure. Representative histograms of WT (black line) and CCR2 KO (shaded grey area) cells incubated with CCL2^{AF647} alone, or CCL2^{AF647} uptake in CCR2 KO competed with 10-fold molar excess mCCL22 (grey line). Proportion of CCL2⁺ cells is illustrated in histograms for each cell population, calculated by subtracting % CCL2⁺ cells in CCR2 KO + mCCL22 samples from WT samples. Physical properties of monocytes (red), neutrophils (brown), Population A (light blue), Population B (yellow), Population C (purple) and the Gr1^{hi}CD115⁺ population (green) are shown in (A). (C) The proportion of CCL2⁺ cells within each population was calculated by considering anything above CCR2 KO + mCCL22 sample to be positive. Data are from 3 or more individual mice per genotype (mean + SD). Data were analysed by one-way ANOVA with Tukey post-test p<0.05 * and p<0.001 ***.

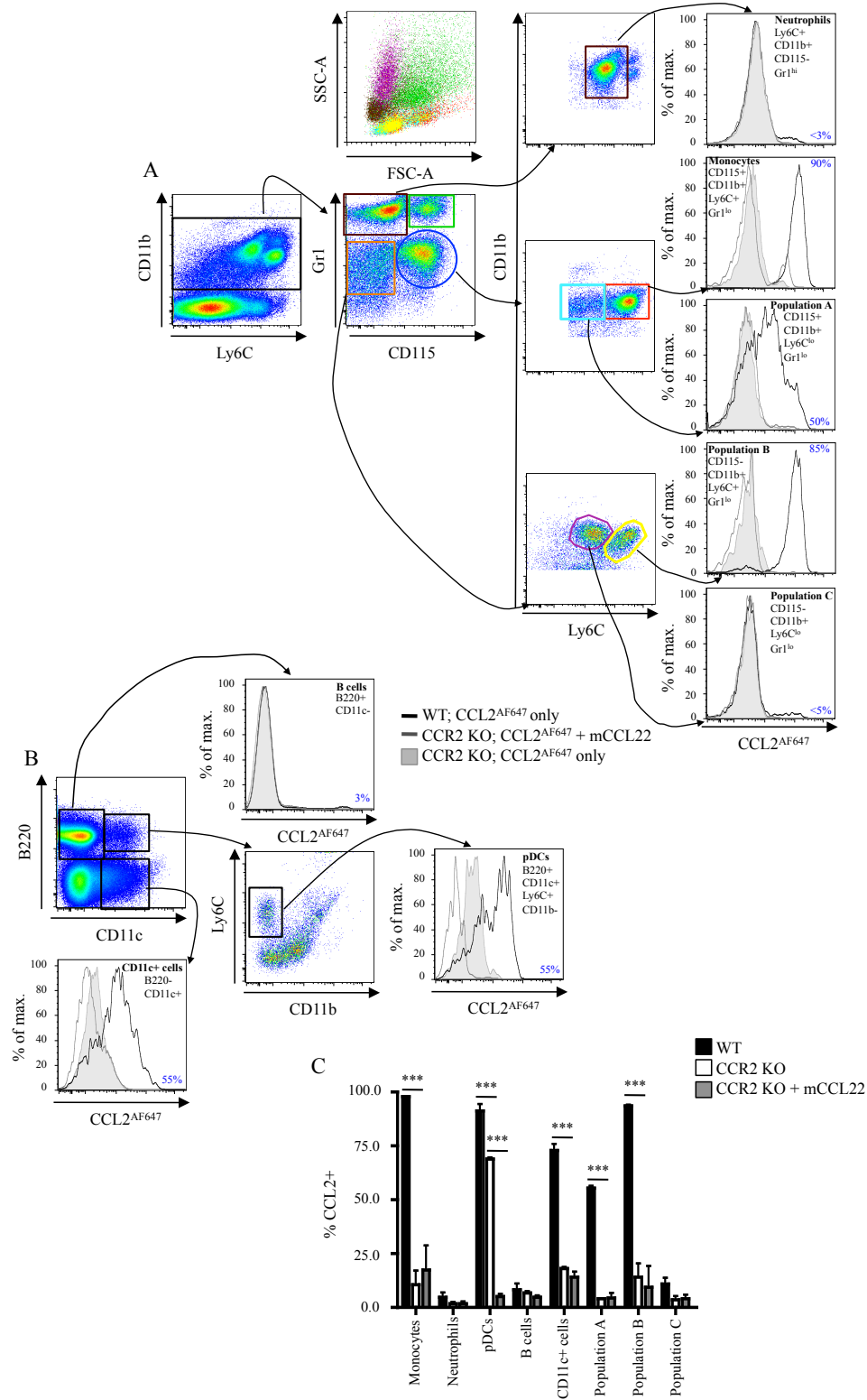


Figure 3-13: CCL2 receptor activity of murine blood cells as characterised by using CCL2^{AF647} assay.

Murine blood neutrophils, monocytes, Gr1^{hi}CD115⁺ cells, Populations A, B and C (A), B cells, CD11c⁺ cells and pDCs (B) were gated as depicted in the left hand plots of the figure. Representative histograms of WT (black line) and CCR2 KO (shaded grey area) cells incubated with CCL2^{AF647} alone, or CCL2^{AF647} uptake in CCR2 KO competed with 10-fold molar excess mCCL22 (grey line). Proportion of CCL2⁺ cells is illustrated in histograms for each cell population, calculated by subtracting % CCL2⁺ cells in CCR2 KO + mCCL22 samples from WT samples. Physical properties of monocyte (red), neutrophils (brown), Population A (light blue), Population B (yellow), Population C (purple) and the Gr1^{hi}CD115⁺ population (green) are shown in (A). (C) The proportion of CCL2⁺ cells within each population was calculated by considering anything above CCR2 KO + mCCL22 sample to be positive. Data are from 3 or more individual mice per genotype (mean + SD). Data were analysed by one-way ANOVA with Tukey post-test p<0.001 ***.

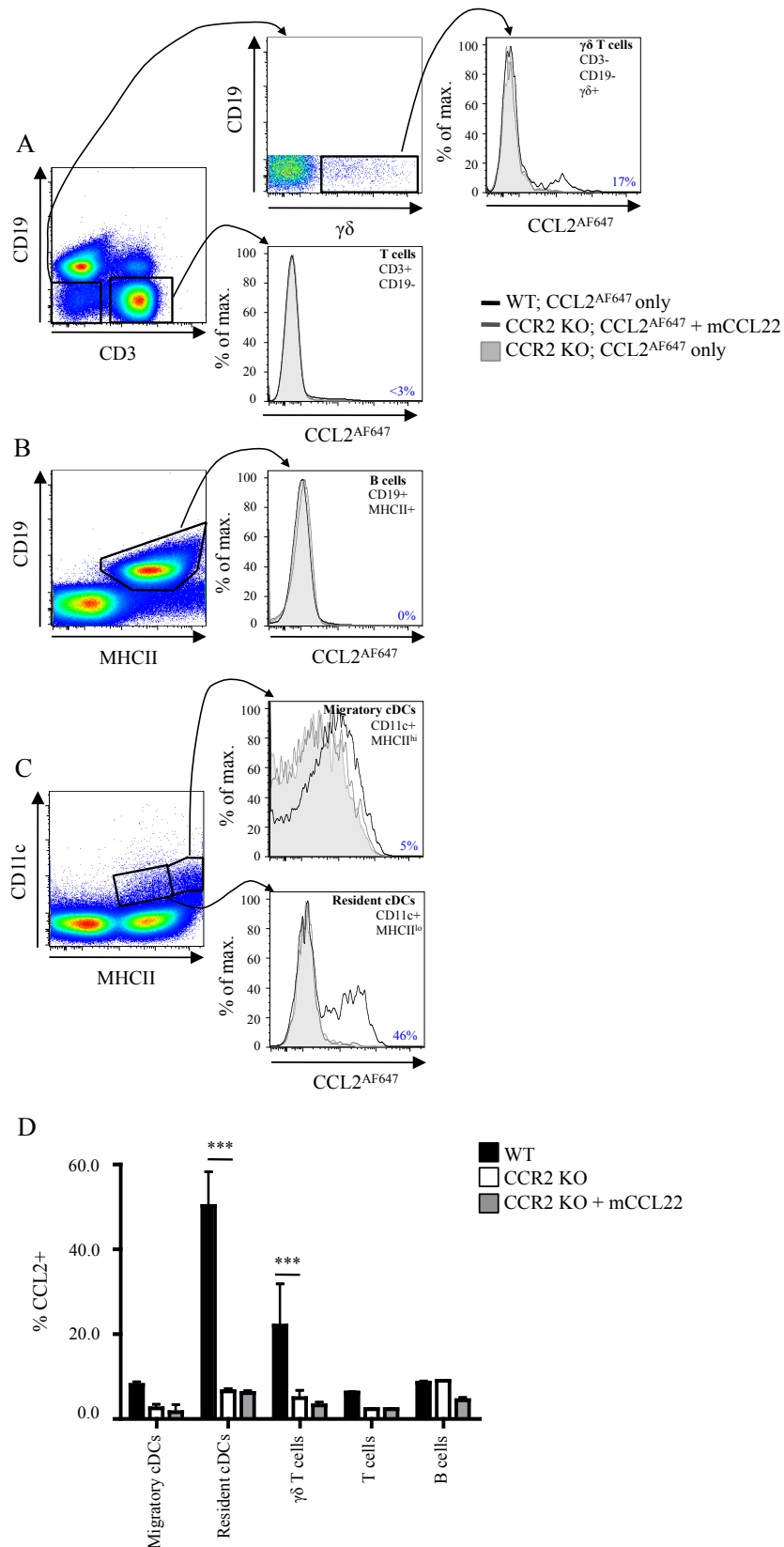


Figure 3-14: Characterisation of CCL2 receptor activity on murine LN cells using CCL2^{AF647}. Murine LN $\gamma\delta^+$ T cells and TCR $\alpha\beta$ CD3⁺ T cells (A), B cells (B), and migratory and resident cDCs (C) were gated as depicted in the left hand panels of the figure. Representative histograms of WT (black line) and CCR2 KO (shaded grey area) cells incubated with CCL2^{AF647} alone, or CCL2^{AF647} uptake in CCR2 KO competed with 10-fold molar excess mCCL22 (grey line). Proportion of CCL2⁺ cells is illustrated in histograms for each cell population, calculated by subtracting % CCL2⁺ cells in CCR2 KO + mCCL22 samples from WT samples. (D) The proportion of CCL2⁺ cells within each population was calculated by considering anything above CCR2 KO + mCCL22 sample to be positive. Data are from 3 or more individual mice per genotype (mean + SD). Data were analysed by one-way ANOVA with Tukey post-test p < 0.001 ***.

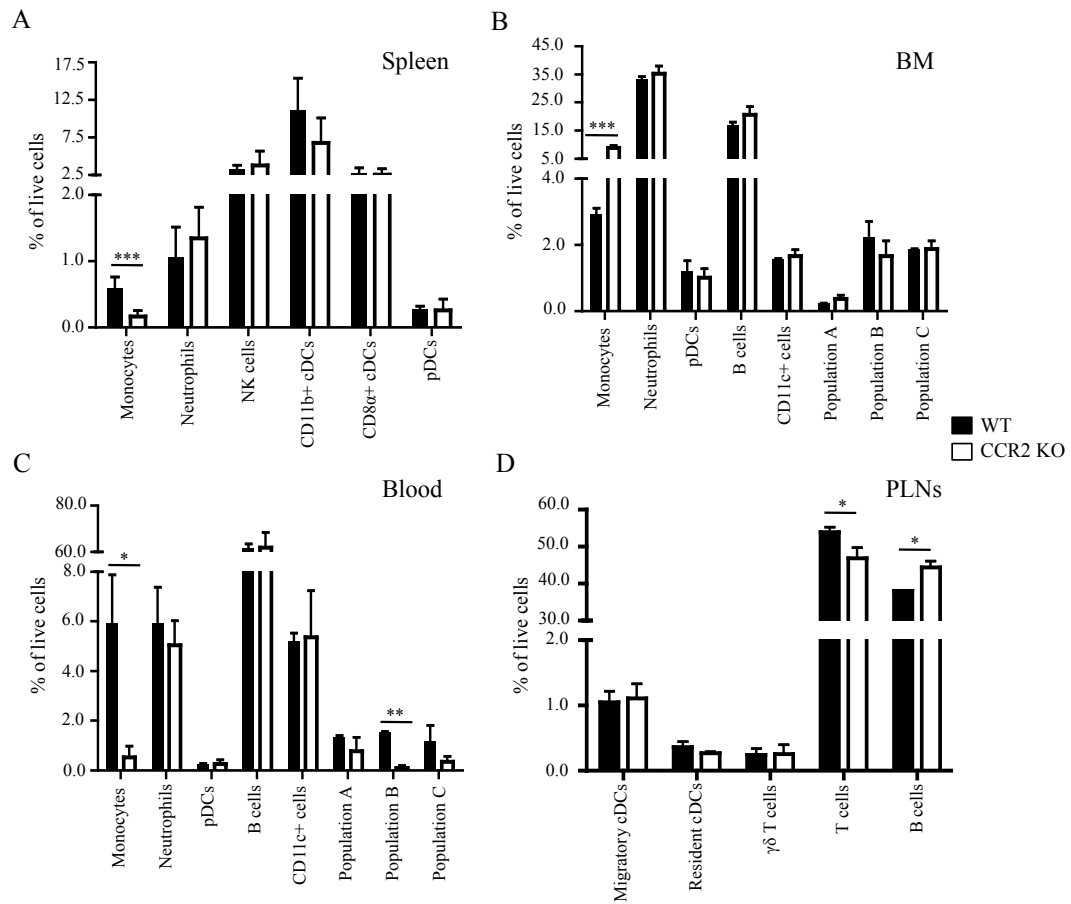
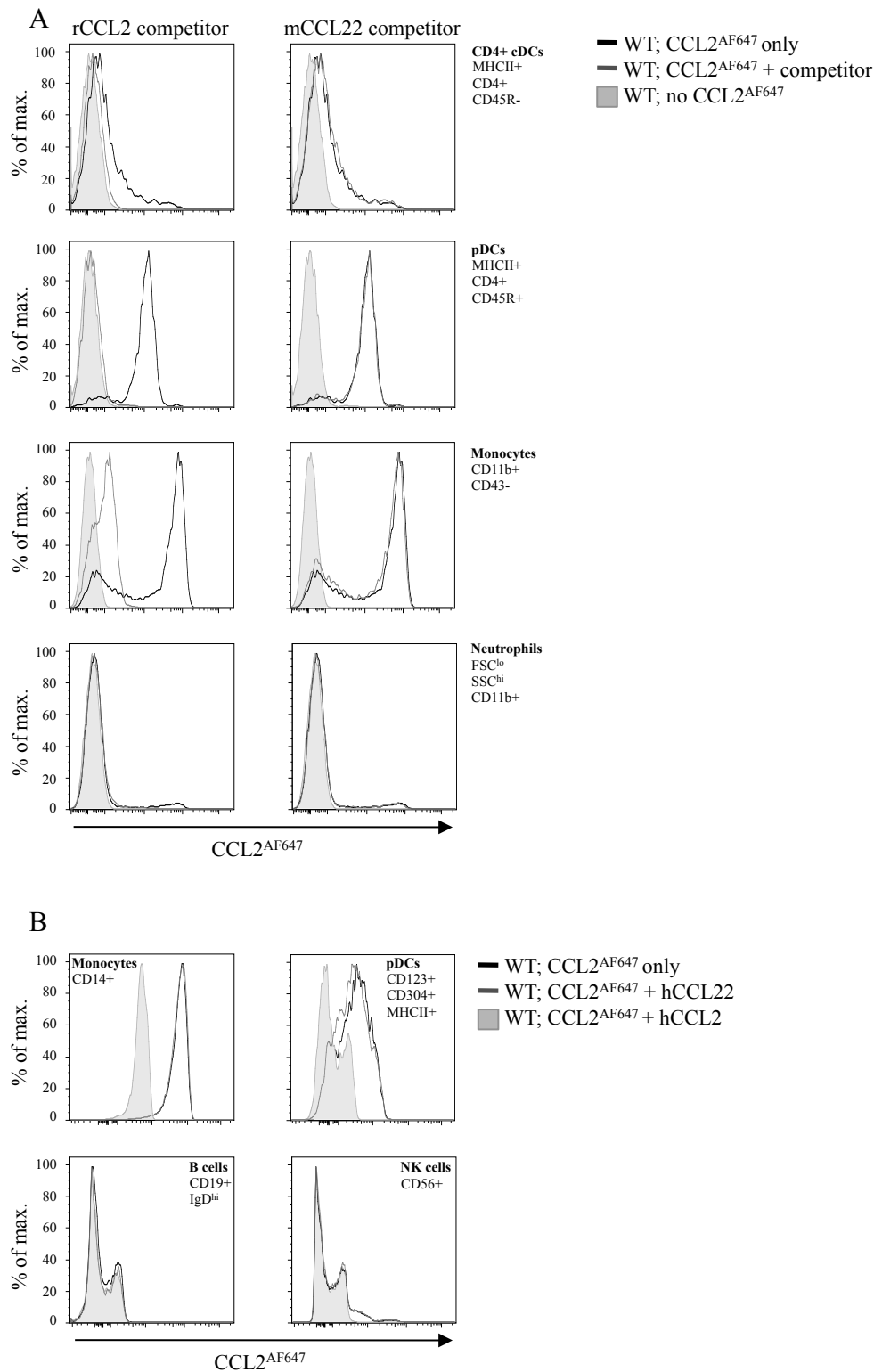


Figure 3-15: Frequency of cell populations in WT and CCR2 KO.

Single cell suspensions from WT (black bars) and CCR2 KO (white bars) spleen (A), BM (B), blood (C) and PLNs (D) were analysed for the frequency of individual cell populations. Populations were gated as dictated as per Figures 3-9 to 3-14. Data are from 3 or more individual mice per genotype (mean + SD). Data were analysed by unpaired T-test $p < 0.05$ *, $p < 0.01$ ** and $p < 0.001$ ***.



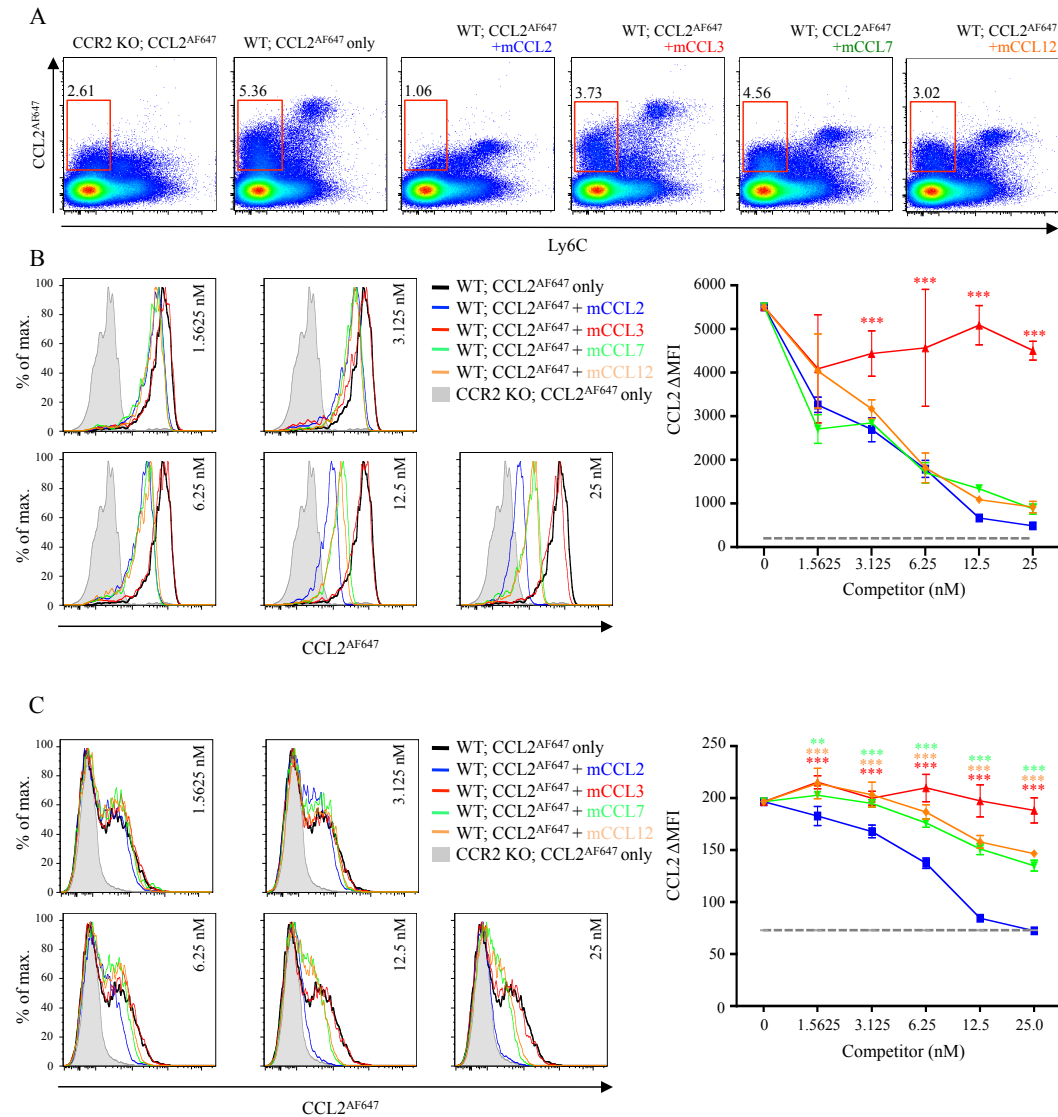


Figure 3-17: Effect of the presence of unlabelled CCR2 ligands on CCR2 activity of splenocytes, as measured by CCL2^{AF647}.

Single cell suspensions of WT and CCR2 KO murine splenocytes were incubated with 25 nM CCL2^{AF647} with or without competition. Competition refers to the addition of 1.5625 – 25 nM of murine CCL2, CCL3, CCL7 or CCL12. (A) Representative plots of CCL2^{AF647} uptake by CCR2 KO and WT splenocytes without competition, and WT splenocytes with competition with 25 nM mCCL2, mCCL3, mCCL7 or mCCL12. Red boxes highlight CCL2^{AF647} uptake by Ly6C^{hi} cells and the proportion of live cells within the gate is shown. Monocytes gated as Ly6C^{hi}, CD11b⁺ and Gr1^{lo} (B) and Ly6C^{hi}CD11b⁺ cells (C) were analysed for CCR2 activity. Representative histograms of CCL2^{AF647} uptake are shown. CCR2 KO without competition (shaded grey area), WT with competition with murine chemokines, CCL2 (blue line), CCL3 (red line), CCL7 (green line) and CCL12 (orange line). For each condition CCL2 geometric mean fluorescence intensity (ΔMFI) was calculated, n=3 except for CCR2 KO alone controls where n=1 (dotted grey line) (mean ±SD). Data were analysed by two-way ANOVA with Bonferroni post-test. Statistics were generated by comparing individual concentrations of each chemokine to competition with the same concentration of CCL2 p<0.01 ** and p<0.001 ***.

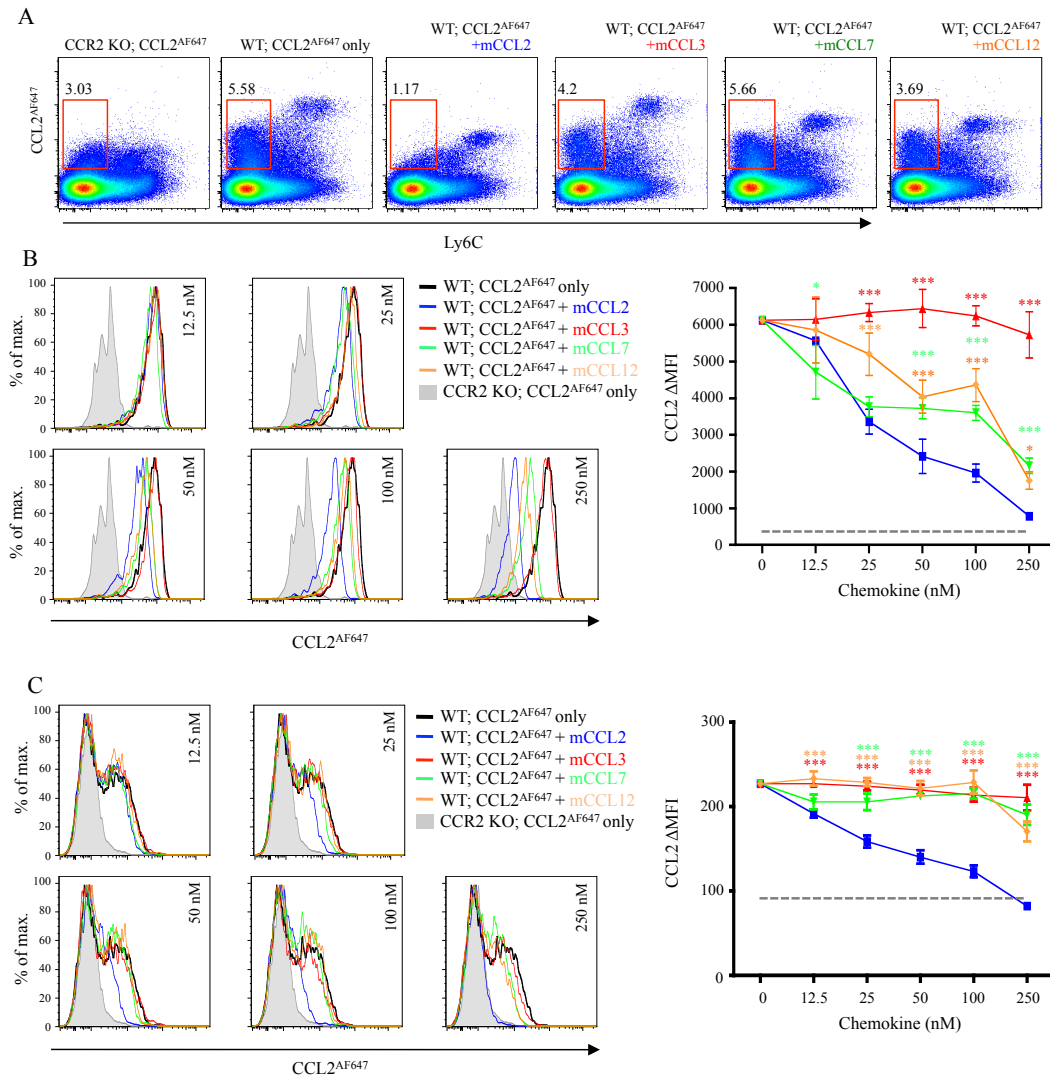


Figure 3-18: Effect of chemokine exposure on CCR2 activity of splenocytes.

Single cell suspensions of WT and CCR2 KO murine splenocytes were incubated with CCL2^{AF647} subsequent to incubation with an unlabelled chemokine. Pre-incubation refers to the prior exposure of splenocytes with 0 – 250 nM of murine CCL2, CCL7 or CCL12 before washing in binding buffer and then incubation with 25 nM CCL2^{AF647}. (A) Representative plots of CCL2^{AF647} uptake by CCR2 KO without prior exposure to ligand, and WT splenocytes with or without prior exposure to 250 nM mCCL2, mCCL3, mCCL7 or mCCL12. Red boxes highlight CCL2^{AF647} uptake by Ly6C^{hi} cells and the proportion of live cells within gate is shown. Monocytes gated as Ly6C^{hi}, CD11b⁺ and Gr1^{lo} (B) and Ly6C^{hi} CD11b⁺ cells (C) were analysed for CCR2 activity. Representative histograms of CCL2^{AF647} uptake are shown. CCR2 KO without prior exposure (shaded grey area), WT without prior exposure (black line), and WT exposed to unlabelled murine chemokines, CCL2 (blue line), CCL3 (red line), CCL7 (green line) and CCL12 (orange line). For each condition CCL2 geometric mean fluorescence intensity (ΔMFI) was calculated, n=3 except for CCR2 KO alone controls where n=1 (dotted grey line) (mean ±SD). Data were analysed by two-way ANOVA with Bonferroni post-test. Statistics were generated by comparing individual concentrations of each chemokine to competition with the same concentration of CCL2 p<0.05* and p<0.001 ***.

Chapter 4 – Impact of systemic inflammation on CCL2 receptor activity

CCR2 exerts key homeostatic functions, but both CCR2 and D6 are receptors for chemokines produced at high levels during times of inflammation (Serbina and Pamer, 2006; Hansell et al., 2011b). Consequently, these receptors play major roles during inflammatory responses (Fra et al., 2003; Bonecchi et al., 2004; Serbina et al., 2008; Nakano et al., 2009; Hansell et al., 2011b). In Chapter 3 I have presented data offering a comprehensive analysis of CCR2 bearing cells *in vivo* and the impact of CCR2 deletion on these cell populations. In this chapter I examine the effect of systemic inflammation on CCL2 receptor activity and on the size of these populations in the presence and absence of CCR2. As a simple model of systemic inflammation in mice, I used intravenous (i.v.) injection of *E. coli* LPS.

LPS is a potent proinflammatory agent that upon injection into an experimental animal induces systemic inflammation. Furthermore, the early expression of CCL2, a ligand for both CCR2 and D6, has been reported to positively predict the development of LPS induced systemic inflammation (Juskewitch et al., 2012). There is extensive literature on the effects of LPS, both *in vivo* and *in vitro* derived data. For example, LPS induced inflammation *in vivo* can affect the cellular composition of lymphoid organs. It has been reported to cause a reduction in splenic cDC numbers (De Smedt et al., 1996), as a consequence of increased cell turnover and a shortened lifespan (Kamath et al., 2000), as activated cDCs are subject to apoptotic cell death (Zanoni et al., 2009). In contrast, neutrophils and macrophages accumulate in the spleen of LPS treated animals (Chandra et al., 2008). These are all cells of the innate immune system, which have been described to possess TLR4, the receptor for LPS. However, a cell does not necessarily need to express TLR4 in order to respond to LPS, as LPS can have indirect effects on cells. For example, the differentiation of naïve T cells, which possess little or no TLR4 can be indirectly mediated by LPS induced activation of cDCs (Rahman et al., 2009; Jin et al., 2012). However, the maturation state of a cell can also change their responsiveness to LPS, as effector CD4⁺ T cells can be directly activated by LPS (González-Navajas et al., 2010; Jin et al., 2012). Therefore, a broad range of cells including myeloid, lymphoid and DCs should be able to respond to LPS either directly or indirectly.

LPS treatment has also been shown *in vitro* and *in vivo* to affect the expression of CCR2. The surface level of CCR2 on human monocytes is known to be affected by LPS mediated activation of TLR4 *in vitro* (Xu et al., 2000; Parker et al., 2004). Zhou *et al.* have also shown that CCR2 expression, both transcript and surface protein are downregulated by murine monocytes in response to LPS *in vivo* (Zhou et al., 1999). However, these data were derived using an anti-CCR2 antibody, which, as I have shown in Chapter 3, suffers from poor sensitivity and as a consequence, an inability to detect low levels of CCR2. This has meant that, in many cases, CCR2 downregulation is only measured at the transcript level. Due to their high expression of CCR2, Ly6C^{hi} monocytes are the usual cell of choice for studying CCR2 function and regulation. My results in Chapter 3, also illustrated that Ly6C^{hi} monocytes had significantly higher CCR2 activity than other cell populations. CCR2 may behave differently on other cell populations, perhaps only playing roles in their migration under specific inflammatory conditions, being subject to different regulation, or even having different specificity for chemokines. Indeed, this is what my data in Figures 3-17 and 3-18 suggest. Therefore, by only using a population of cells that has high levels of CCR2 to examine its function and regulation we might form conclusions that are inaccurate for other CCR2⁺ populations.

Furthermore, in Chapter 3, I demonstrated that several of the populations bearing CCL2 receptors, such as pDCs and BM Ly6C^{hi} monocytes, showed evidence of possessing both CCR2 and D6 activity. Specific chemokine receptors, when co-expressed by individual cells, can modulate the function of the other receptor. The co-expression of CXCR4 and CXCR7 leads to the formation of heterodimers and leads to enhanced migration of cancer cells (Décaillot et al., 2011). D6 has also been shown to affect the function of CXCR5 on innate-like B cells, leading to a decrease in migration in response to the CXCR5 ligand, CXCL13 (Hansell et al., 2011b). Perhaps similar to D6 on innate-like B cells, the presence of D6 on a CCR2⁺ population might also be important for CCR2 function on these cells. Furthermore, the dynamics of CCR2 and D6 regulation by LPS, in whole animals, is not known.

Therefore in order to establish the effects of LPS on both the activity of CCL2 receptors and the size of the CCL2⁺ populations, I performed a time-course of LPS induced inflammation in WT and CCR2 KO animals. This time-course was

performed in collaboration with Chris Hansell, who was examining the effects of LPS on splenic B cell populations. A low dose of LPS (15 µg per mouse) was chosen, as it was reported to affect some of the CCR2 expressing populations, such as cDCs (De Smedt et al., 1998; Zanoni et al., 2009). WT and CCR2 KO animals were either treated i.v. with 100 µl of sterile PBS or 15 µg of LPS dissolved in 100 µl of sterile PBS. Spleens and BM were harvested 24 or 48 hrs after PBS treatment, or 24, 48 or 72 hrs after LPS administration. These time-points were chosen because LPS induces a rapid and transient inflammation and we believed that these time-points would facilitate the examination of the induction and resolution phases of inflammation. CCL2 has been reported to be a predictive marker of the development of systemic inflammation by LPS (Juskewitch et al., 2012), therefore high levels of CCL2 might correlate with the early time-points of the time-course, and thus CCR2 might be desensitised and unable to bind and internalise CCL2^{AF647}. In contrast, I expected that expression of the atypical chemokine receptor, D6, by cell populations, such as MZ-B cells and pDCs to be relatively unaffected by LPS treatment and D6 would facilitate the scavenging of inflammatory chemokines, including CCL2, which might aid in the resolution of LPS induced inflammation.

Furthermore, based on published data (Ulich et al., 1991), I expected that LPS would cause a rapid recruitment of neutrophils into the spleen. My data in Chapter 3, suggests that their recruitment would be CCR2 independent, as these cells were not found to possess CCR2 activity (Figure 3-10). In contrast, I hypothesised that recruitment of Ly6C^{hi} monocytes (and/or other CCR2⁺ populations) will be reduced in CCR2 KOs. However, I expected the frequency of Ly6C^{hi} monocytes in the spleen of WT animals to be increased following LPS induced inflammation, as Chandra *et al.* reported increased number of splenic macrophages 24 hrs after LPS treatment (Chandra et al., 2008). I also expected there to be decreased numbers of splenic cDCs at the later time-points in LPS time-course, due to their increased turnover rate (Kamath et al., 2000).

4.1 Exploration of the dynamic changes in splenic leukocyte populations in response to systemic LPS administration and the affect of CCR2 deficiency

I monitored CCL2 receptor activity and the abundance of the several CCL2⁺ populations over the duration of a LPS time-course, in both the spleen (Figure 4-1 to 4-10) and the BM (Figure 4-11), in parallel with Chris Hansell who assessed CCL2 receptor activity in B cells. His data are included here with permission, for comparative purposes (Figure 4-5). Splenic cDC maturation was also examined (Figure 4-9). Uptake of CCL2^{AF647} was measured in WT and CCR2 KO samples with or without competition with mCCL22. In previous experiments I only examined D6 activity in CCR2 KO animals by competing CCL2^{AF647} uptake by CCR2 KO cells with mCCL22. This provides information about D6 activity only in the absence of CCR2. The absence of CCR2 might conceivably affect expression or the activity of D6: perhaps D6 is only expressed or detectable when CCR2 is absent. By including WT samples with mCCL22 competition I hoped to establish whether D6 activity was detectable in the presence of CCR2. The frequency of CCL2⁺ populations was determined at each time-point in the LPS time-course and all data are presented as a proportion of live cells rather than as an absolute number of cells. Therefore, I can not describe alterations in the number of particular cell types, but these data do provide information about any increase or decrease in the proportion of live splenocytes that are a particular cell type. There were, however, no dramatic differences in the total number of cells retrieved from WT and CCR2 KO tissues.

I will describe the data generated for each CCL2⁺ cell population individually, but as all cell types were analysed simultaneously, and as a consequence all cell data are linked, I will first describe some broad observations that were true for the majority of cell types. All cell populations found to possess CCR2 activity in PBS control mice had a reduction in CCR2 dependent CCL2^{AF647} uptake 24 hrs after LPS administration. In contrast, LPS did not cause a reduction in D6 dependent CCL2^{AF647} uptake by the few cell populations that were found to possess D6 activity in resting CCR2 KO animals, such as MZ-B cells, pDCs and BM Ly6C^{hi} monocytes. CCR2 activity was restored or upregulated at later time-points in the LPS time-course in all CCL2⁺ cell populations other than pDCs. 72 hrs after LPS treatment pDCs exhibited a switch in the receptor responsible for CCL2^{AF647}

uptake, as all CCL2^{AF647} uptake at this time-point was not mediated by CCR2, but by D6. Furthermore, in every cell population, including CCR2⁻ neutrophils, D6 activity was upregulated in CCR2 KO cells 48 hrs after LPS. However, this activity was not detectable in the majority of WT cell populations at 48 hrs. There now follows a more detailed description of the data for each individual cell type analysed.

4.1.1 Splenic Ly6C^{hi} monocytes

Ly6C^{hi} monocytes had high levels of CCR2 dependent uptake of CCL2^{AF647} in PBS treated mice, which was reduced substantially 24 hrs after LPS treatment, but not completely lost (Figure 4-1). Quantification of the number of CCL2⁺ Ly6C^{hi} monocytes revealed a significant reduction in the number of CCL2⁺ cells in CCR2 KO compared to WT at all time-points as expected (Figure 4-1C). Furthermore, there was a significant reduction in the number of CCL2⁺ cells in WT samples at 24 hrs. However, there were still significant levels of CCR2 dependent uptake remaining. By 48 and 72 hrs after LPS treatment, CCL2 Δ MFI (Figure 4-1B) and the percentage of CCL2⁺ cells were restored to levels comparable to PBS controls (Figure 4-1C), indicating restoration of CCR2 dependent uptake. In contrast to histogram overlays that suggested evidence of D6 activity in both WT and CCR2 KO samples (Figure 4-1A), there were no statistically significant levels of D6 activity detected at any time-point, except in KO Ly6C^{hi} monocytes 48 hrs after LPS treatment (Figure 4-1C).

The decrease in CCR2 activity at 24 hrs might be explained by partial desensitisation or downregulation of CCR2, or by changes in the frequency of Ly6C^{hi} monocytes present in the spleen. However, the decrease in CCL2⁺ Ly6C^{hi} monocytes detected at 24 hrs could not be correlated with a decrease in the proportion of live WT splenocytes that were Ly6C^{hi} monocytes (Figure 4-2A). At later time-points in the LPS time-course there is a significant increase in Ly6C^{hi} monocytes as a percentage of total cells in the spleen of WT animals compared to PBS treated mice ($p < 0.01$). Furthermore, as expected CCR2 KO animals had a deficit in peripheral Ly6C^{hi} monocytes in PBS-treated mice, however 24 hrs after LPS treatment this deficit was rescued, as a comparable proportion of spleen cells were Ly6C^{hi} monocytes in WT and CCR2 KO spleens. The increase in the frequency of Ly6C^{hi} monocytes as a proportion of live splenocytes in CCR2 KO

animals is highlighted in Figure 4-2B and C. However, the splenic CCR2 KO Ly6C^{hi} monocyte deficit was restored by 48 hrs after LPS administration, and a greater proportion of splenocytes were Ly6C^{hi} monocytes in WT compared to CCR2 KOs at 48 and 72 hrs (Figure 4-2A).

Thus, LPS transiently downregulates, but does not completely remove CCR2 activity on Ly6C^{hi} monocytes, and rescues the Ly6C^{hi} monocyte deficit in CCR2 deficient mice, but both parameters are rapidly restored. It is also notable that even at 24 hrs after LPS administration, there is more CCR2 activity on Ly6C^{hi} monocytes than on most other CCR2 expressing cells in resting mice (see Chapter 3 and following results).

4.1.2 Splenic NK cells

Similar to Ly6C^{hi} monocytes, the large majority of CCL2^{AF647} uptake by splenic NK cells was CCR2 dependent in PBS and LPS treated WT mice. Furthermore, like Ly6C^{hi} monocytes, CCL2 Δ MFI data suggested decreased CCL2^{AF647} uptake 24 hrs after LPS treatment (Figure 4-3B). There was, however, no significant reduction in the number of CCL2⁺ NK cells at this time-point, and significant levels of CCR2 activity were still detectable (Figure 4-3C). At 48 and 72 hrs there was a dramatic increase in CCL2^{AF647} uptake by WT cells, which was also CCR2 dependent. Furthermore, histogram overlays suggested evidence of D6 activity in CCR2 KO NK cells at 48 and 72 hrs, and low levels of D6 activity in WT NK cells at 48 hrs (Figure 4-3A). In contrast, CCL2 Δ MFI data demonstrated significant levels of D6 activity only in WT NK cells at 48 and 72 hrs (Figure 4-3B). However, quantification of the number of CCL2⁺ NK cells indicated that a proportion of CCR2 KO NK cells possessed D6 activity and it was limited to the 48 hr time-point (Figure 4-3C). These results suggest that WT and CCR2 KO NK cells possess low, but significant levels of D6 activity 48 hrs after LPS administration.

LPS also appeared to affect the frequency of splenic NK cells, as there was a significant reduction in the frequency of total NK cells in the spleen of WT ($p < 0.05$) and CCR2 KO ($p < 0.01$) animals, 24 hrs after LPS treatment compared to PBS controls (Figure 4-3D). However, there was no change in the proportion of NK cells that were CCL2⁺, which suggests that both CCL2⁺ and CCL2⁻ NK cells must be reduced (Figure 4-3C). The decrease in splenic NK cell frequency might

be explained by NK cells leaving the spleen and entering the blood, or by cell death. If the decrease in frequency is due to their exit from the spleen, this mobilisation does not appear to be CCR2 dependent as the decrease was also present in CCR2 KO animals. Furthermore, the proportions of splenic NK cell were restored at later time-points to levels comparable to PBS controls, but it was not due to CCR2 dependent processes, as it was also found in the CCR2 KO. Therefore, CCR2 does not appear to be involved in regulating NK cell abundance in the spleen before or after LPS treatment. Thus, LPS induces downregulation of CCR2 activity on NK cells, and reduces their abundance as a proportion of live splenocytes, but by 48 hrs these cells reappear and show enhanced CCR2 activity.

4.1.3 Splenic neutrophils

Interestingly, neutrophils possessed no CCR2 or D6 dependent uptake in homeostasis, but were found to uptake CCL2^{AF647} 48 and 72 hrs after LPS treatment (Figure 4-4). This uptake was CCR2 independent, as it was still present in the CCR2 KO samples. Competition of uptake in both WT and CCR2 KO samples with the D6 ligand, mCCL22 demonstrated that uptake was in fact due to D6. The increase in D6 activity might be explained by the upregulation of D6 activity on the original splenic neutrophil population or infiltration of “new” neutrophils possessing D6 activity. There was a significant increase in the frequency of splenic neutrophils 48 hrs after LPS ($p < 0.001$), before returning to levels comparable to PBS control at 72 hrs (Figure 4-4D). The frequency of CCR2 KO splenic neutrophils followed similar trends, although there was a significant increase in the proportion of live splenocytes that were neutrophils in CCR2 KO animals compared to WT 24 hrs after LPS treatment ($p < 0.001$). Therefore, neutrophils did not display any dependence on CCR2 for infiltration into the spleen, but rather their abundance in spleen early after LPS treatment was somewhat suppressed by CCR2.

4.1.4 Splenic MZ-B cells

MZ-B cells in a resting animal do not possess CCR2 activity and all CCL2^{AF647} uptake is D6 dependent, as shown in Chapter 3. Unlike the observed loss of CCR2 activity by Ly6C^{hi} monocytes and NK cells 24 hrs after LPS treatment, D6 activity

on MZ-B cells was maintained (Figure 4-5). 48 and 72 hrs after LPS administration D6 mediated uptake of CCL2^{AF647} was dramatically increased over the PBS control, as indicated by an increase in the CCL2 Δ MFI of MZ-B cells (Figure 4-5B). There was also a corresponding significant increase in the frequency of CCL2⁺ MZ-B cells at 48 hrs, but there was no parallel increase at 72 hrs (Figure 4-5C). The increase in CCL2⁺ MZ-B cells might be explained by an overall increase in the splenic MZ-B cell frequency, however statistical analysis showed no significant increase in MZ-B cell frequency at any time-point when compared to PBS control (Figure 4-5D). Furthermore, there was no statistically significant effect of CCR2 deletion on the frequency of splenic MZ-B cells (Figure 4-5D).

4.1.5 Splenic pDCs

Like Ly6C^{hi} monocytes and NK cells, pDCs also had a significant reduction in CCR2 activity at 24 hrs, but like MZ-B cells appeared to maintain D6 mediated CCL2^{AF647} uptake, albeit at much lower levels than MZ-B cells (Figure 4-6). By 48 hrs pDCs had restored some CCR2 dependent uptake of CCL2^{AF647}, and CCR2 KO samples also possessed significant levels of D6 activity (Figure 4-6C). CCL2^{AF647} uptake was restored 72 hrs after LPS treatment to levels comparable to the PBS control, as demonstrated by both CCL2 Δ MFI data (Figure 4-6B) and percentage of CCL2⁺ cells (Figure 4-6C). Surprisingly however, this uptake was also present in CCR2 KO pDCs. Competition of CCL2^{AF647} uptake with mCCL22 in both WT and CCR2 KO samples indicated that uptake was predominantly D6 dependent, as there was a significant reduction in CCL2^{AF647} uptake in the presence of mCCL22, although substantially more non-specific uptake of CCL2^{AF647} was also observed. Furthermore, unlike resting mice, it was no longer possible to distinguish CCL2^{hi} and CCL2^{lo} populations of pDCs.

The frequency of splenic pDCs was relatively unaffected by LPS treatment, or by CCR2 deletion (Figure 4-6D). Therefore, CCR2 did not appear to play a role in controlling pDC abundance in the spleen during homeostasis or inflammation. Furthermore, consistent with Ly6C^{hi} monocytes and NK cells, LPS induces downregulation of CCR2 activity on pDCs, and similar to MZ-B cells there was no effect of LPS on D6 activity 24 hrs after LPS. In contrast to all other populations possessing CCR2 activity, pDCs did not restore CCR2 activity by 72 hrs, but both WT and CCR2 KO pDCs significantly upregulated D6 activity.

4.1.6 Splenic cDCs

Uptake of CCL2^{AF647} by CD11b⁺ cDCs in PBS control WT animals (Figure 4-7) was CCR2 dependent and had nearly completely disappeared by 24 hrs after LPS treatment. At 48 and 72 hrs CCL2^{AF647} uptake was significantly increased in CD11b⁺ cDCs over that of PBS controls, and this uptake was dependent on CCR2, and due primarily to an increase in the proportion of cells that were CCL2⁺. There was no evidence of D6 activity in WT CD11b⁺ cDCs at any time-point. In contrast, CD11b⁺ cDCs from CCR2 KO animals possessed very weak D6 activity 48 hrs after LPS treatment, which was lost by 72 hrs.

CD8 α ⁺ cDCs in PBS control WT animals possessed both CCR2 and very low levels of D6 activity (Figure 4-8). D6 activity was not present in CCR2 KO animals in PBS controls. Like CD11b⁺ cDCs, 24 hrs after LPS treatment there was a near complete loss of CCL2^{AF647} uptake, which was restored to levels comparable to PBS control by 48 hrs. Furthermore, WT and CCR2 KO CD8 α ⁺ cDCs possessed low, but significant levels of D6 activity 48 hrs after LPS treatment. D6 activity in both WT and CCR2 KO CD8 α ⁺ cDCs was lost by 72 hrs and all CCL2^{AF647} uptake by WT CD8 α ⁺ cDCs at this time-point was CCR2 dependent.

As mentioned earlier, LPS is known to mediate CCR2 downregulation via TLR4 activation (Zhou et al., 1999; Xu et al., 2000; Parker et al., 2004). However, an alternative theory to explain the downregulation of CCR2 activity 24 hrs after LPS treatment is that LPS activates cells, such as cDCs resulting in their maturation. Maturation of DCs can effect expression of chemokine receptors (Sallusto et al., 1998; Vecchi et al., 1999), thus I monitored expression of CD86, an activation marker on both cDC subsets (Figure 4-9). The downregulation of CCR2 activity by cDCs 24 hrs after LPS treatment was inversely correlated with their acquisition of the activation marker CD86. cDCs in resting animals had minimal levels of CD86 expression, which was significantly increased in WT and CCR2 KO samples at the 24 hrs time-point. CD86 expression was returned to PBS control levels by 48 and 72 hrs.

Alternatively, the reduction in CCR2 activity might be explained by migration of cDCs from the spleen or apoptosis of the cells. Zanoni *et al.* reported that 24 and 48 hrs after LPS treatment there was a marked reduction in the number of

cDCs within the spleen (Zanoni et al., 2009). Furthermore, they demonstrated that LPS induced activation of cDCs was associated with their death by apoptosis. My data support this observation as 48 hrs after LPS administration there was a dramatic decrease in the frequency of cDCs in the spleen of WT and CCR2 KO animals and these cells were even less abundant at 72 hrs (Figure 4-10). However, at 24 hrs the frequencies of both cDC subsets were unaffected by LPS treatment in WT animals, but there was a significant decrease in the frequency of both CD11b⁺ and CD8 α ⁺ cDCs in CCR2 KOs compared to WT animals (highlighted in Figure 4-10C). Interestingly, decreased cDC numbers at 48 and 72 hrs was associated with the restoration of CCR2 activity by CD8 α ⁺ cDCs (Figure 4-8) or upregulation of CCR2 dependent CCL2^{AF647} uptake in the case of CD11b⁺ cDCs (Figure 4-7). These results suggest that a significantly lower number of cDCs when compared to PBS control were responsible for the high levels of CCR2 activity observed at the later time-points.

Collectively these results clearly indicate that the dynamics of the CCL2 receptor activity post LPS treatment are influenced by cell type and the receptor mediating the activity. CCR2 activity was typically downregulated 24 hrs after LPS administration. In contrast, there was no reduction in D6 dependent CCL2^{AF647} uptake by MZ-B cells and pDCs at this time-point. CCR2 activity was restored or upregulated 48 and 72 hrs after LPS administration, in all CCL2⁺ cell populations, other than pDCs. Strikingly, all CCL2^{AF647} uptake by WT and CCR2 KO pDCs 72 hrs after LPS treatment was D6 dependent. Furthermore, neutrophils, which do not possess any CCR2 or D6 dependent CCL2^{AF647} in PBS controls or 24 hrs after LPS, were found to significantly upregulate D6 activity on a small number of cells at 48 hrs and most notably at 72 hrs. Interestingly, regardless of their expression of CCR2 or D6 in resting animals, all cell populations in CCR2 KO animals were found to internalise CCL2^{AF647} in a D6 dependent manner 48 hrs after LPS.

During homeostasis the frequency of the majority of splenic CCL2⁺ cell populations, except Ly6C^{hi} monocytes, were unaffected by the absence of CCR2. However, the frequency of Ly6C^{hi} monocytes and cDCs were drastically and reciprocally affected by the absence of CCR2 during inflammation with the

Ly6C^{hi} monocyte defect seen in resting CCR2 KO mice being transiently rescued and a cDC deficit emerging.

4.2 Examination of the role of CCR2 in monocyte mobilisation during systemic inflammation

I have already discussed the fundamental role CCR2 plays in the mobilisation of monocytes from the BM. Several groups and my own results have demonstrated the scarcity of peripheral Ly6C^{hi} inflammatory monocytes in CCR2 KO mice and their coincident increase in the BM of these animals (Figure 3-15), illustrating the requirement of CCR2 for monocyte mobilisation during homeostasis (Geissmann et al., 2003; Serbina and Pamer, 2006). Furthermore, CCR2 is necessary for monocyte emigration from the BM during infections, such as with *Listeria monocytogenes* (Serbina and Pamer, 2006) or *Leishmania amazonensis* (Strauss-Ayali et al., 2007) and inflammation (Geissmann et al., 2003). However, my data suggest that LPS injection rescues the CCR2 KO Ly6C^{hi} monocyte mobilisation defect (Figure 4-2). Therefore, I next sought to establish if systemic inflammation induced by LPS also affected the CCR2 activity and frequency of Ly6C^{hi} monocytes within the BM (Figure 4-11). Similar to splenic Ly6C^{hi} monocytes, BM Ly6C^{hi} monocytes had high levels of CCR2 activity, which were substantially reduced 24 hrs after LPS treatment (Figure 4-11B). However, there was no significant reduction in the proportion of CCL2⁺ BM Ly6C^{hi} monocytes that were present at 24 hrs. There were still significant levels of CCR2 mediated uptake of CCL2^{AF647} present at this time-point (Figure 4-11C). CCR2 dependent uptake of CCL2^{AF647} uptake was restored by 48 and 72 hrs after LPS treatment.

In contrast to splenic Ly6C^{hi} monocytes (Figure 4-1), there was evidence of D6 activity in PBS treated CCR2 KO control animals. Furthermore, there was no reduction in D6 dependent CCL2^{AF647} uptake by CCR2 KO BM Ly6C^{hi} monocytes at 24 hrs, and D6 activity was also maintained at 48 hrs. However by 72 hrs there was no evidence of D6 activity and all uptake was CCR2 dependent (Figure 4-11C). mCCL22 was also able to significantly reduce CCL2^{AF647} uptake by WT BM Ly6C^{hi} monocytes in PBS treated mice, and 48 and 72 hrs after LPS treatment, indicative of D6 activity (Figure 4-11A and B).

The retention of Ly6C^{hi} monocytes in the BM of resting CCR2 KO animals is well established (Serbina and Pamer, 2006). Accordingly, I have found that resting CCR2 KO animals have a greater proportion of live BM cells that are Ly6C^{hi} monocytes compared to WT animals (Figures 3-15 and 4-11D). However, there was a significant reduction ($p < 0.001$) in the frequency of Ly6C^{hi} monocytes in CCR2 KO BM 24 hrs after LPS administration. CCR2 KO animals had similar proportions of Ly6C^{hi} monocytes in the BM as WT animals (Figure 4-11D). This decrease in Ly6C^{hi} monocyte frequency could be correlated with the earlier described restoration of peripheral Ly6C^{hi} monocytes in CCR2 KOs 24 hrs after LPS treatment (Figure 4-2). At later time-points the proportion of Ly6C^{hi} monocytes in CCR2 KO BM was restored to levels comparable to PBS treated CCR2 KO controls. In contrast to resting animals there was no difference in the proportion of Ly6C^{hi} monocytes present in BM of WT and CCR2 KOs, as there was a significant increase ($p < 0.001$) in the proportion of Ly6C^{hi} monocytes in WT BM 48 hrs after LPS administration.

4.2.1 Evaluation of the role of CXCR2 on monocytes in the absence of CCR2

Due to other research conducted in the lab, which demonstrated that BM Ly6C^{hi} monocytes express another inflammatory chemokine receptor CXCR2, I proposed that, in the absence of CCR2, CXCR2 might play a role in the release of Ly6C^{hi} monocytes from the BM during LPS induced inflammation. CCR2 KO animals were treated with a CXCR2 antagonist, SB225002 (Bento et al., 2008) followed by LPS 3 hrs later (Figure 4-12). The absolute number of Ly6C^{hi} monocytes and neutrophils were determined in both the spleen and the BM 24 hrs after SB225002 treatment. Neutrophils are a rich source of CXCR2 and are highly dependent on CXCR2 for their mobilisation from the BM into the periphery (Eash et al., 2010), thus a decrease in BM neutrophil numbers was used as a positive control to determine if the CXCR2 antagonist worked. As Figure 4-12B shows, LPS treatment results in a significant reduction of BM neutrophils, with a parallel increase in splenic neutrophils. Prior treatment with SB225002 appeared to result in a lower proportion of neutrophils emigrating from the BM and thus a smaller increase in splenic neutrophil numbers, although neither result was statistically significant. The results do, however suggest that the CXCR2 antagonist did function in diminishing CXCR2 activity. The same was true with

Ly6C^{hi} monocytes: LPS caused significant mobilisation of BM monocytes into the periphery, but SB225002 had no significant effects on this LPS induced mobilisation (Figure 4-12C).

These results have demonstrated that LPS can induce CCR2 independent mobilisation of Ly6C^{hi} monocytes from the BM into the periphery. Furthermore, this mobilisation appears not to be CXCR2 dependent.

4.3 Summary

In this chapter, I have established that induction of systemic inflammation using a low dose of LPS alters the frequency of several of the CCL2⁺ populations, including monocytes and cDCs. Furthermore, one of the significant findings that arose by studying the effects of LPS on Ly6C^{hi} monocytes was that 24 hrs after LPS administration the peripheral deficit in Ly6C^{hi} monocytes in CCR2 KO animals was rescued, as LPS induced CCR2 independent mobilisation of BM monocytes. However, in a few preliminary experiments I was unable to confirm the mechanism for this emigration.

LPS induced inflammation resulted in a significant downregulation of CCR2 activity on all analysed CCL2⁺ populations by 24 hrs after treatment, but did not affect D6 activity. However, in CCR2^{hi} populations, such as Ly6C^{hi} monocytes and NK cells, although LPS did cause a reduction in CCR2 dependent CCL2^{AF647} uptake there were still significant levels of CCR2 activity detectable, according to the calculated percentage of CCL2⁺ cells present. At later time-points CCR2 activity had been restored to the baseline level in PBS controls or was significantly increased above baseline, in all CCL2⁺ populations except pDCs. By 72 hrs of treatment pDCs did not re-establish CCR2 activity, but demonstrated high levels of the atypical chemokine receptor, D6. Several of the CCL2⁺ populations in CCR2 KO animals acquired D6 activity, but in many cases it was limited to 48 hrs after LPS administration. Furthermore, MZ-B cells and neutrophils, both of which do not exhibit any CCR2 dependent CCL2^{AF647} uptake, significantly upregulated D6 activity at 48 hrs in both WT and CCR2 KO animals.

This comprehensive profiling of CCR2 activity led to the establishment of CCR2 activity on splenic pDCs. I have demonstrated approximately half of pDCs are

CCL2^{hi}, and although LPS had no effect on splenic pDC frequency, it did affect their CCR2 activity, as well as their D6 activity. As briefly discussed earlier, a role for CCR2 or D6 on pDCs has yet to be described. Thus, in the next chapter I perform an in depth analysis of CCR2 on pDCs and examine potential functional and transcriptional differences between CCL2^{hi} and CCL2^{lo} pDCs. In short, I examine whether the presence or absence of CCR2 activity defines functionally distinct subsets of pDCs.

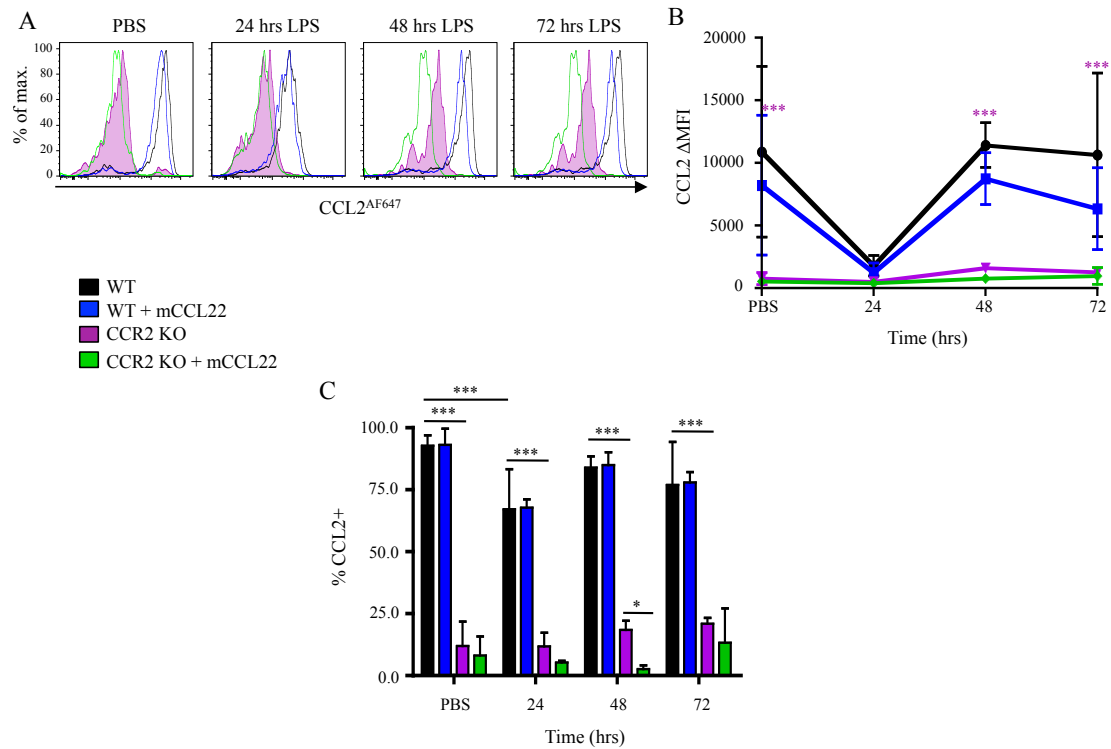


Figure 4-1: Effect of LPS on CCL2 receptor activity of splenic Ly6C^{hi} monocytes.

WT and CCR2 KO animals were treated i.v. with PBS for 24 or 48 hrs, or LPS for 24, 48 and 72 hrs. Splenocytes from WT and CCR2 KO animals were incubated with CCL2^{AF647} with or without mCCL22 competition. (A) Representative histogram of CCL2^{AF647} uptake by Ly6C^{hi} monocytes, gated as described in Figure 3-10 (Ly6C^{hi}CD11b⁺Gr1^{lo}), from WT (black line) and CCR2 KO cells (shaded purple area) without competition, and WT (blue line) and CCR2 KO (green line) samples with mCCL22 competition. (B) CCL2 geometric mean fluorescence intensity (ΔMFI) of WT (black line) and CCR2 KO (purple line) incubated with CCL2^{AF647} without competition. CCL2^{AF647} uptake in WT (blue line) and CCR2 KO (green line) splenic Ly6C^{hi} monocytes competed with a 10-fold molar excess of mCCL22. (C) Proportion of Ly6C^{hi} monocytes that were CCL2⁺. Data were generated from three or more individual mice per genotype (mean ± SD). Data were analysed by either one-way ANOVA with Tukey post-test or two-way ANOVA with Bonferroni post-test p<0.05 * and p<0.001 ***. Statistical significant in (B) is shown between WT to CCR2 KO by * symbols.

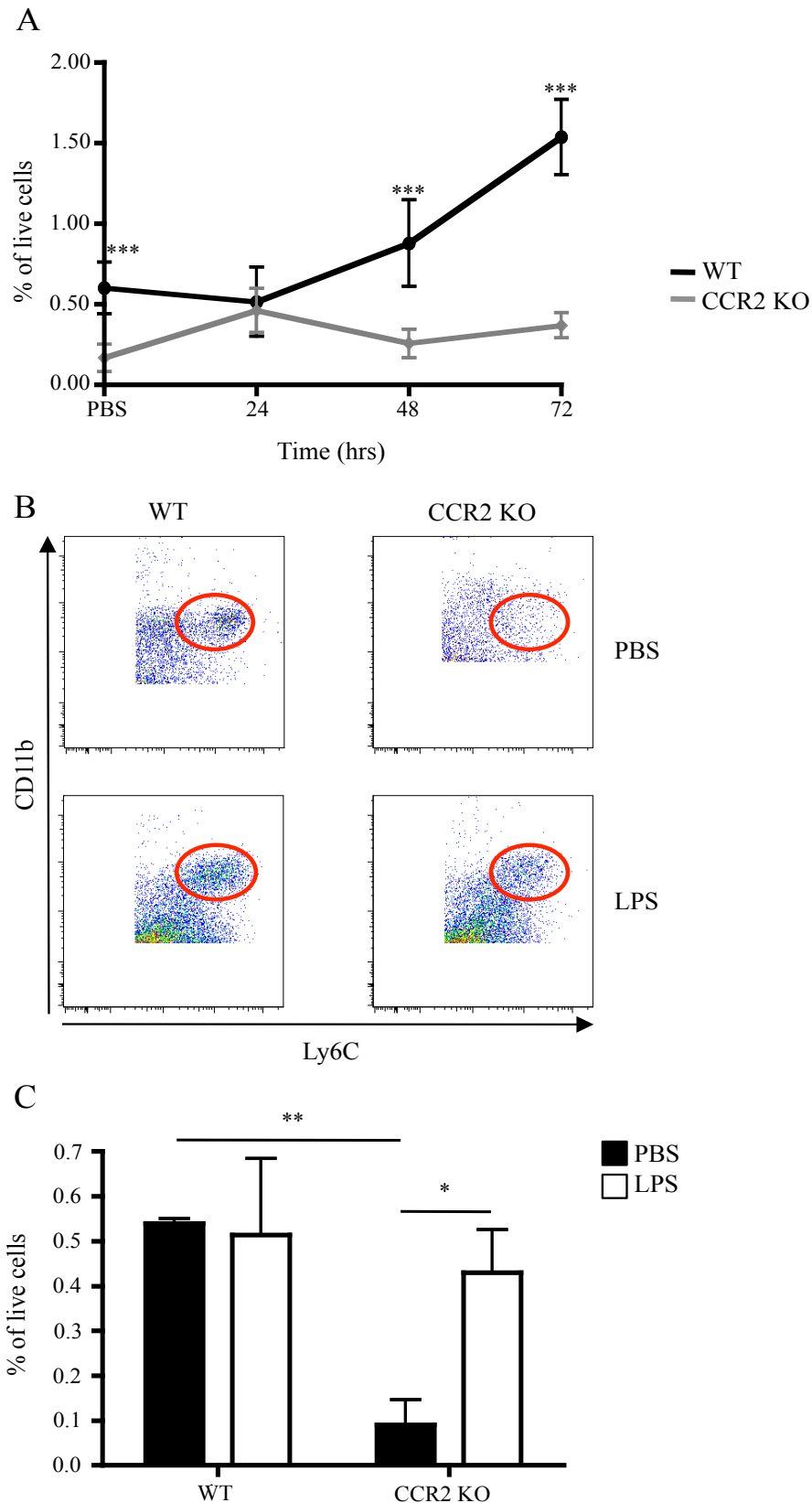


Figure 4-2: Effect of LPS on the frequency of splenic Ly6C^{hi} monocytes.

WT (black line) and CCR2 KO (grey line) animals were treated i.v. with PBS for 24 or 48 hrs, or LPS for 24, 48 and 72 hrs. (A) Frequencies of Ly6C^{hi} monocytes, gated as depicted in Figure 3-10 (Ly6C^{hi}CD11b⁺Gr1^{lo}) over the LPS time-course. (B&C) WT and CCR2 KO animals were treated i.v. with PBS or LPS for 24 hrs. (B) Illustration of the reduction of peripheral Ly6C^{hi} monocytes in the spleen of CCR2 KO and their restoration in CCR2 KO following LPS treatment. (C) Frequency of monocytes as determined by gating as depicted in Figure 3-10 in PBS control animals (black bars) or following 24 hrs of LPS (white bars). Data were generated from three or more individual mice per genotype (mean \pm SD). Data were analysed by two-way ANOVA with Bonferroni post-test $p < 0.05$ *, $p < 0.01$ ** and $p < 0.001$ ***.

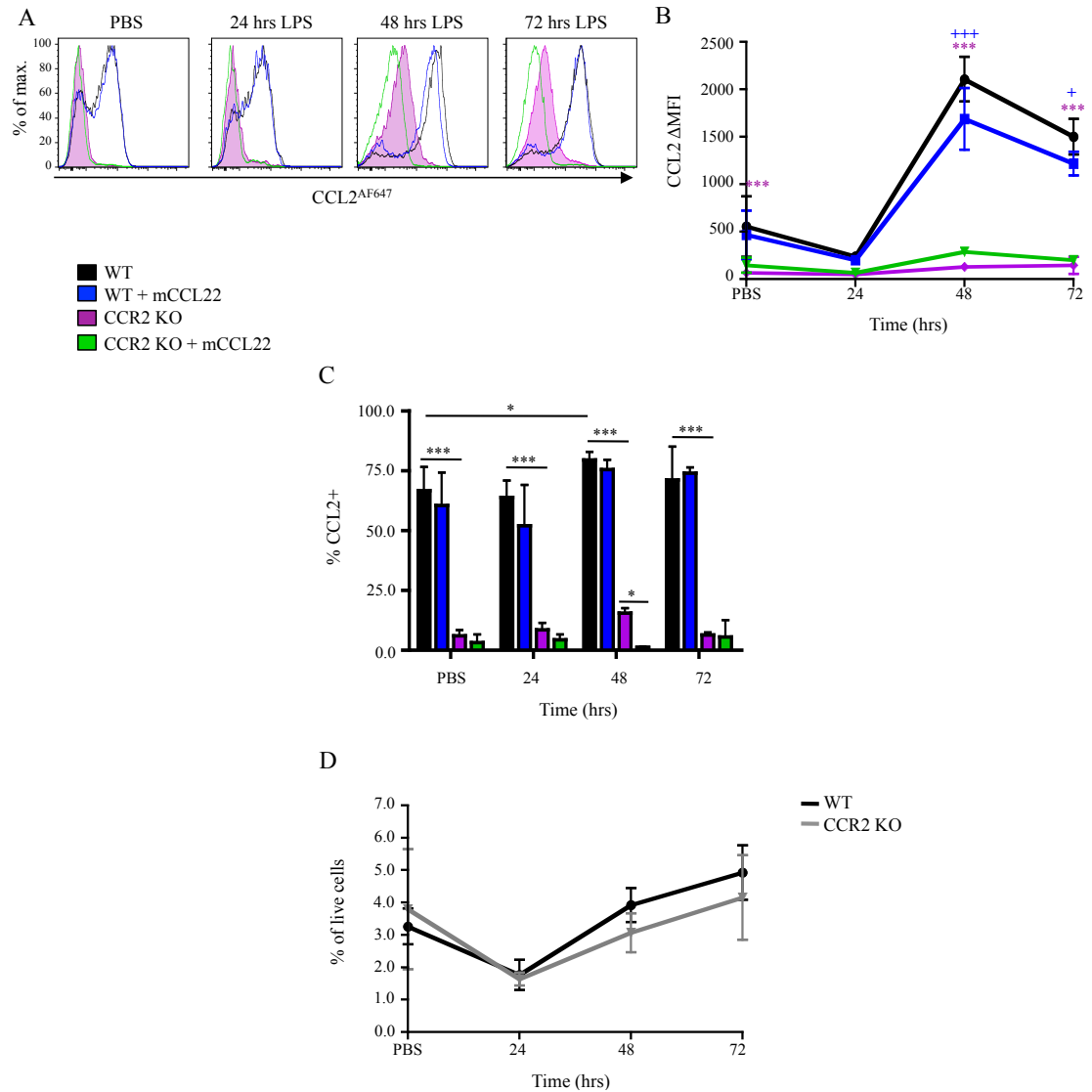


Figure 4-3: Effect of LPS on CCL2 receptor activity and frequency of splenic NK cells.

WT and CCR2 KO animals were treated i.v. with PBS for 24 or 48 hrs, or LPS for 24, 48 and 72 hrs. Splenocytes from WT and CCR2 KO animals were incubated with CCL2^{AF647} with or without mCCL22 competition. (A) Representative histogram of CCL2^{AF647} uptake by NK cells, gated as described in Figure 3-9 (DX5⁺), from WT (black line) and CCR2 KO cells (shaded purple area) without competition, and WT (blue line) and CCR2 KO (green line) samples with mCCL22 competition. (B) CCL2 geometric mean fluorescence intensity (Δ MFI) of WT (black line) and CCR2 KO (purple line) incubated with CCL2^{AF647} without competition. CCL2^{AF647} uptake in WT (blue line) and CCR2 KO (green line) splenic NK cells competed with a 10-fold molar excess of mCCL22. (C) Proportion of NK cells that were CCL2⁺. (D) Frequencies of NK cells over the LPS time-course. Data were generated from three or more individual mice per genotype (mean \pm SD). Data were analysed by either one-way ANOVA with Tukey post-test or two-way ANOVA with Bonferroni post-test $p < 0.05$ * and $p < 0.001$ ***. Statistical significant in (B) is shown between WT to CCR2 KO by * symbols and WT to WT with mCCL22 by + symbols.

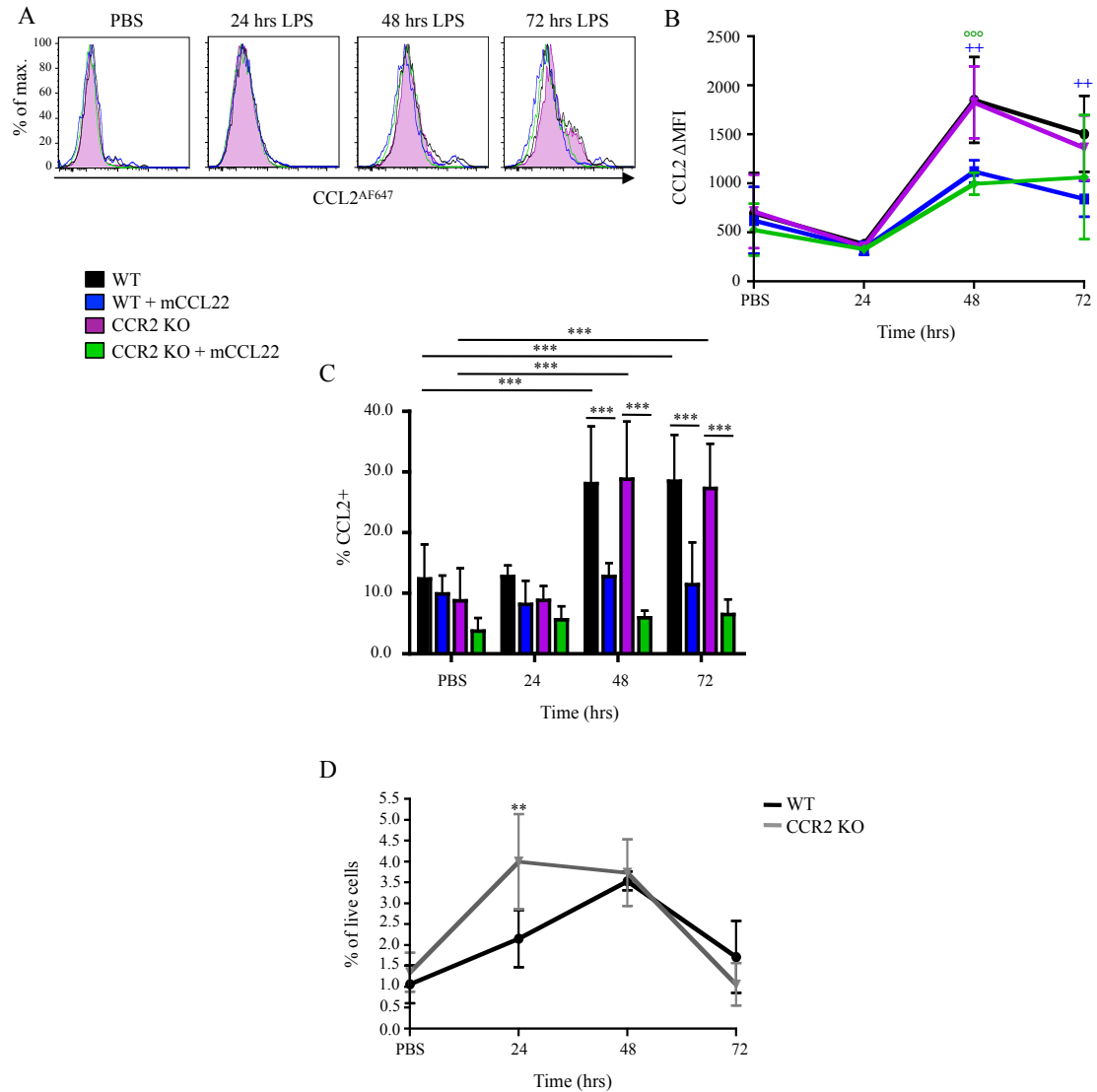


Figure 4-4: Effect of LPS on CCL2 receptor activity and frequency of splenic neutrophils.

WT and CCR2 KO animals were treated i.v. with PBS for 24 or 48 hrs, or LPS for 24, 48 and 72 hrs. Splenocytes from WT and CCR2 KO animals were incubated with CCL2^{AF647} with or without mCCL22 competition. (A) Representative histogram of CCL2^{AF647} uptake by neutrophils, gated as described in Figure 3-10 (Ly6C^{inter}CD11b⁺Gr1^{hi}), from WT (black line) and CCR2 KO cells (shaded purple area) without competition, and WT (blue line) and CCR2 KO (green line) samples with mCCL22 competition. (B) CCL2 geometric mean fluorescence intensity (ΔMFI) of WT (black line) and CCR2 KO (purple line) splenic neutrophils incubated with CCL2^{AF647} without competition. CCL2^{AF647} uptake in WT (blue line) and CCR2 KO (green line) splenic neutrophils competed with a 10-fold molar excess of mCCL22. (C) Proportion of neutrophils that were CCL2⁺. (D) Frequencies of neutrophils over the LPS time-course. Data were generated from three or more individual mice per genotype (mean ± SD). Data were analysed by either one-way ANOVA with Tukey post-test or two-way ANOVA with Bonferroni post-test $p < 0.01$ ** and $p < 0.001$ ***. Statistical significant in (B) is shown between WT to WT with mCCL22 by + symbols and CCR2 KO to CCR2 KO with mCCL22 by ° symbols.

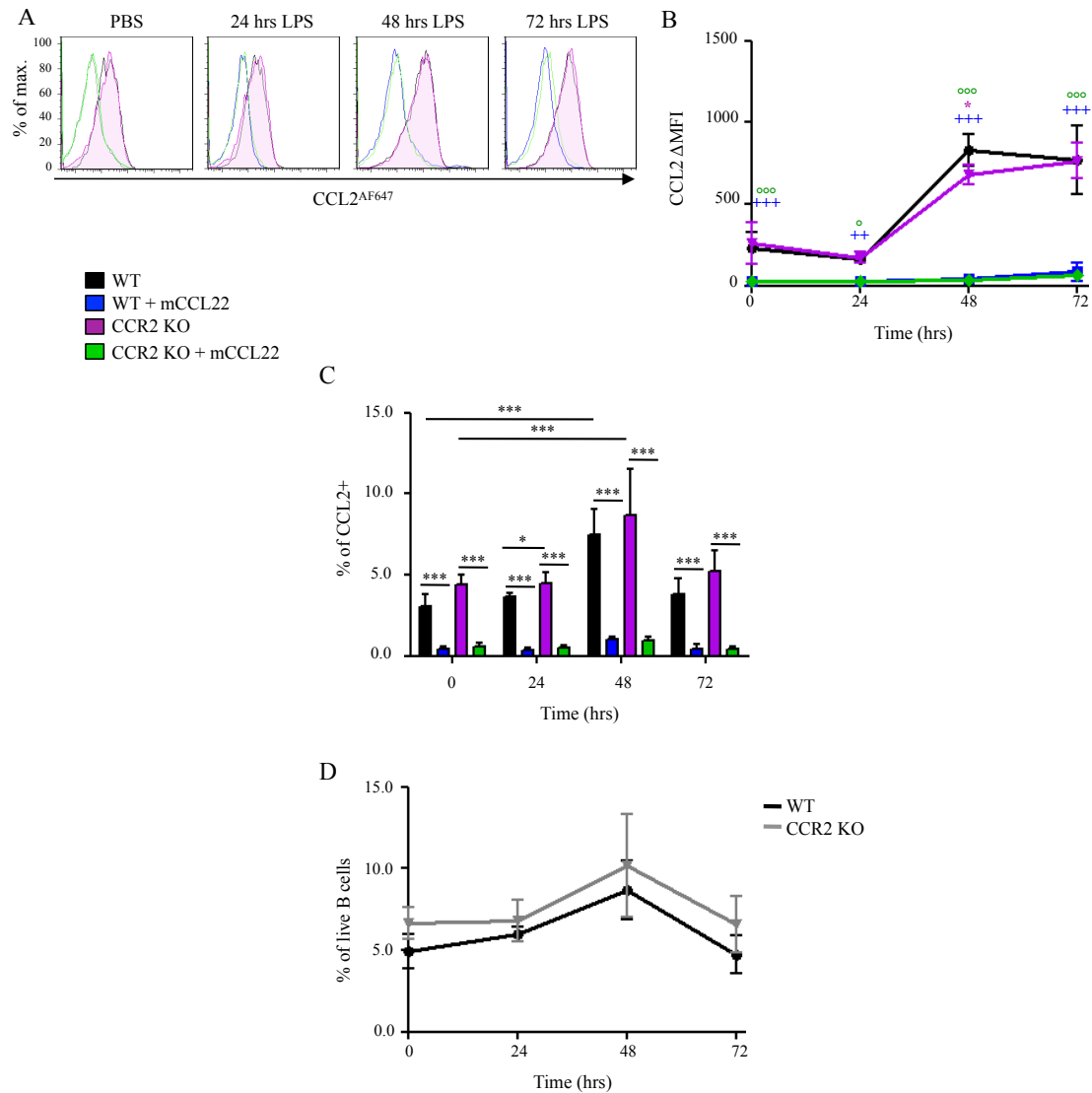


Figure 4-5: Effect of LPS on CCL2 receptor activity and frequency of splenic MZ-B cells. WT and CCR2 KO animals were treated i.v. with PBS for 24 or 48 hrs, or LPS for 24, 48 and 72 hrs. Splenocytes from WT and CCR2 KO animals were incubated with CCL2^{AF647} with or without mCCL22 competition. (A) Representative histogram of CCL2^{AF647} uptake by MZ-B cells, gated as CD19⁺IgM^{hi}IgD^{lo}CD21⁺, from WT (black line) and CCR2 KO cells (shaded purple area) without competition, and WT (blue line) and CCR2 KO (green line) samples with mCCL22 competition. (B) CCL2 geometric mean fluorescence intensity (ΔMFI) of WT (black line) and CCR2 KO (purple line) incubated with CCL2^{AF647} without competition. CCL2^{AF647} uptake in WT (blue line) and CCR2 KO (green line) splenic MZ-B cells competed with a 10-fold molar excess of mCCL22. (C) Proportion of MZ-B cells that were CCL2⁺. (D) Frequencies of MZ-B cells as a proportion of live B cells over the LPS time-course. Data were generated from three or more individual mice per genotype (mean ± SD). Data were analysed by either one-way ANOVA with Tukey post-test or two-way ANOVA with Bonferroni post-test $p < 0.05$ *, $p < 0.01$ ** and $p < 0.001$ ***. Statistical significant in (B) is shown between WT to CCR2 KO by * symbols, WT to WT with mCCL22 by + symbols and CCR2 KO to CCR2 KO with mCCL22 by ° symbols. These data were provided by Chris Hansell.

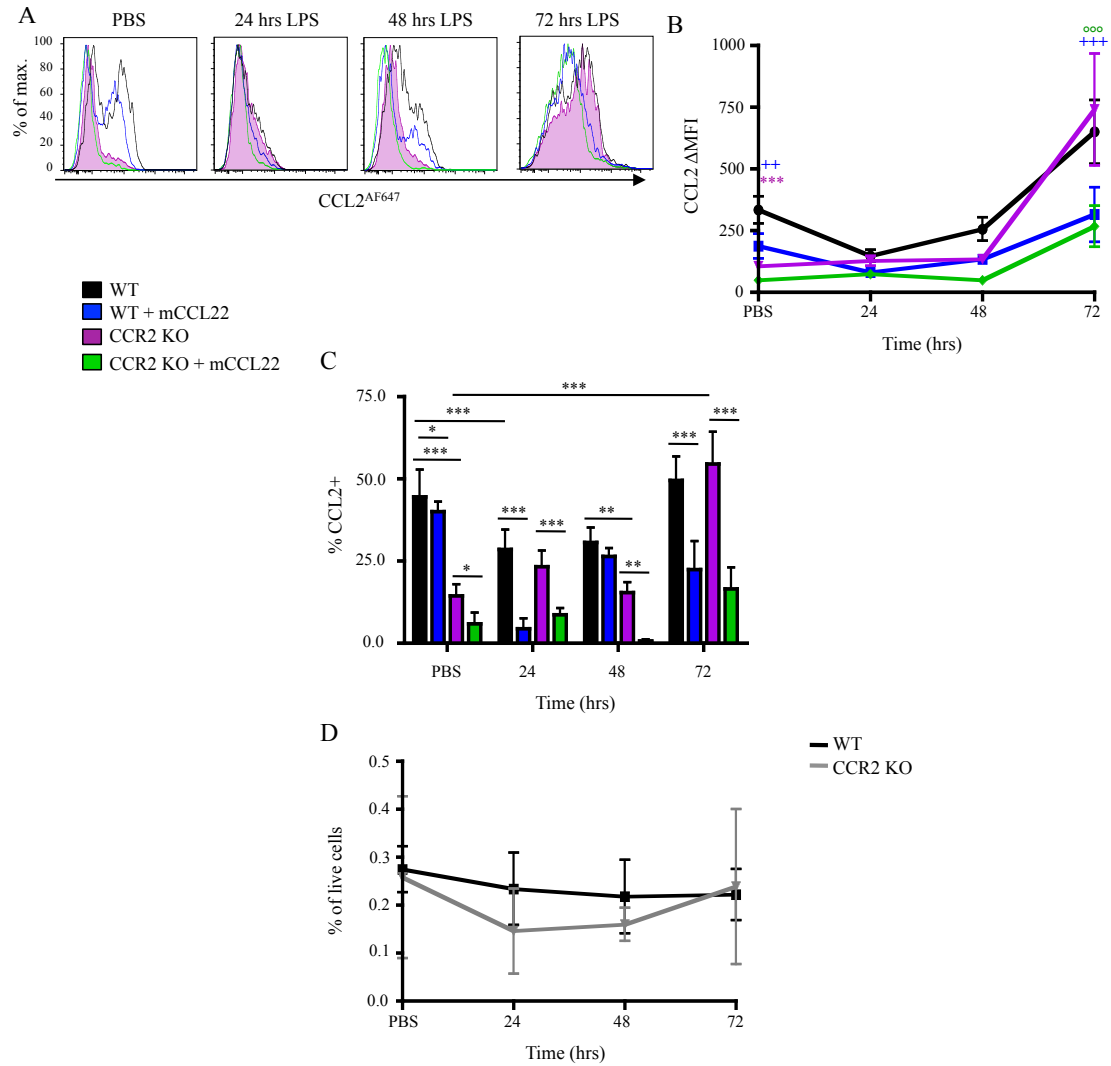


Figure 4-6: Effect of LPS on CCL2 receptor activity and frequency of splenic pDCs.

WT and CCR2 KO animals were treated i.v. with PBS for 24 or 48 hrs, or LPS for 24, 48 and 72 hrs. Splenocytes from WT and CCR2 KO animals were incubated with CCL2^{AF647} with or without mCCL22 competition. (A) Representative histogram of CCL2^{AF647} uptake by pDCs, gated as described in Figure 3-11 (B220⁺CD11c⁺Ly6C⁺CD11b⁻), from WT (black line) and CCR2 KO cells (shaded purple area) without competition, and WT (blue line) and CCR2 KO (green line) samples with mCCL22 competition. (B) CCL2 geometric mean fluorescence intensity (ΔMFI) of WT (black line) and CCR2 KO (purple line) incubated with CCL2^{AF647} without competition. CCL2^{AF647} uptake in WT (blue line) and CCR2 KO (green line) splenic pDCs competed with a 10-fold molar excess of mCCL22. (C) Proportion of pDCs that were CCL2⁺. (D) Frequencies of pDCs over the LPS time-course. Data were generated from three or more individual mice per genotype (mean ± SD). Data were analysed by either one-way ANOVA with Tukey post-test or two-way ANOVA with Bonferroni post-test $p < 0.05$ *, $p < 0.01$ ** and $p < 0.001$ ***. Statistical significant in (B) is shown between WT to CCR2 KO by * symbols, WT to WT with mCCL22 by + symbols and CCR2 KO to CCR2 KO with mCCL22 by ° symbols.

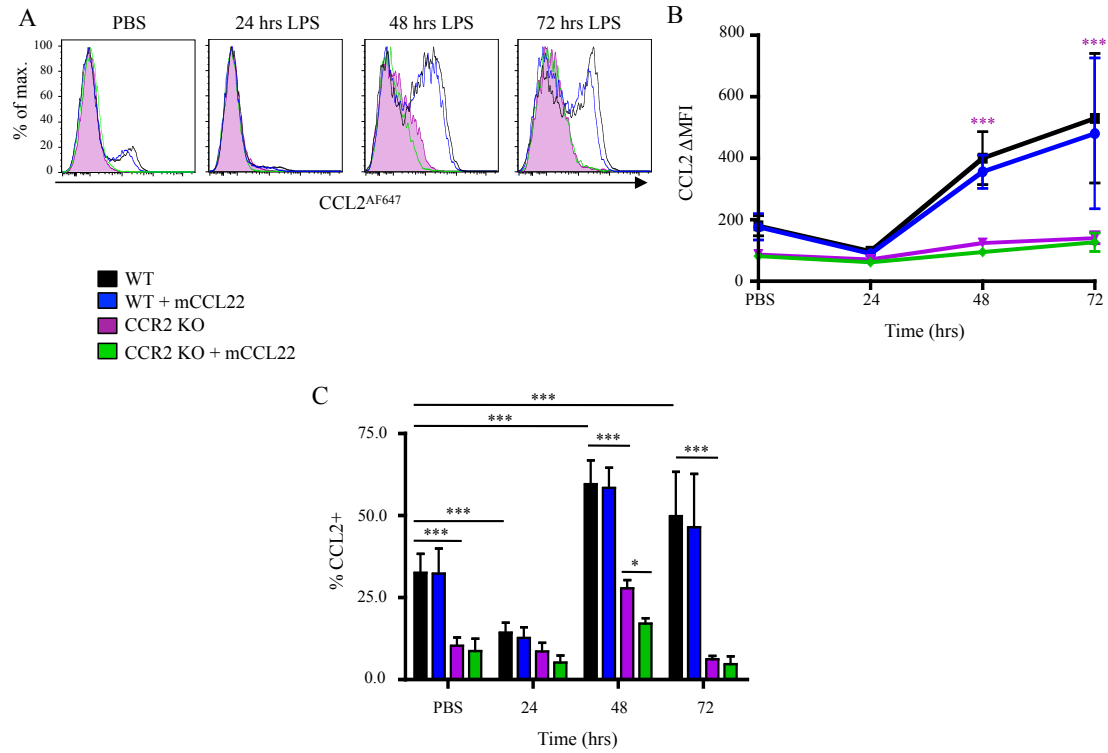


Figure 4-7: Effect of LPS on CCL2 receptor activity of splenic CD11b⁺ cDCs.

WT and CCR2 KO animals were treated i.v. with PBS for 24 or 48 hrs, or LPS for 24, 48 and 72 hrs. Splenocytes from WT and CCR2 KO animals were incubated with CCL2^{AF647} with or without mCCL22 competition. (A) Representative histogram of CCL2^{AF647} uptake by CD11b⁺ cDCs, gated as described in Figure 3-11 (MHCII^{hi}CD11c^{hi}CD11b⁺CD8α⁻), from WT (black line) and CCR2 KO cells (shaded purple area) without competition, and WT (blue line) and CCR2 KO (green line) samples with mCCL22 competition. (B) CCL2 geometric mean fluorescence intensity (ΔMFI) of WT (black line) and CCR2 KO (purple line) incubated with CCL2^{AF647} without competition. CCL2^{AF647} uptake in WT (blue line) and CCR2 KO (green line) splenic CD11b⁺ cDCs competed with a 10-fold molar excess of mCCL22. (C) Proportion of CD11b⁺ cDCs that were CCL2⁺. Data were generated from three or more individual mice per genotype (mean ± SD). Data were analysed by either one-way ANOVA with Tukey post-test or two-way ANOVA with Bonferroni post-test p<0.05 * and p<0.001 ***. Statistical significant in (B) is shown between WT to CCR2 KO by * symbols.

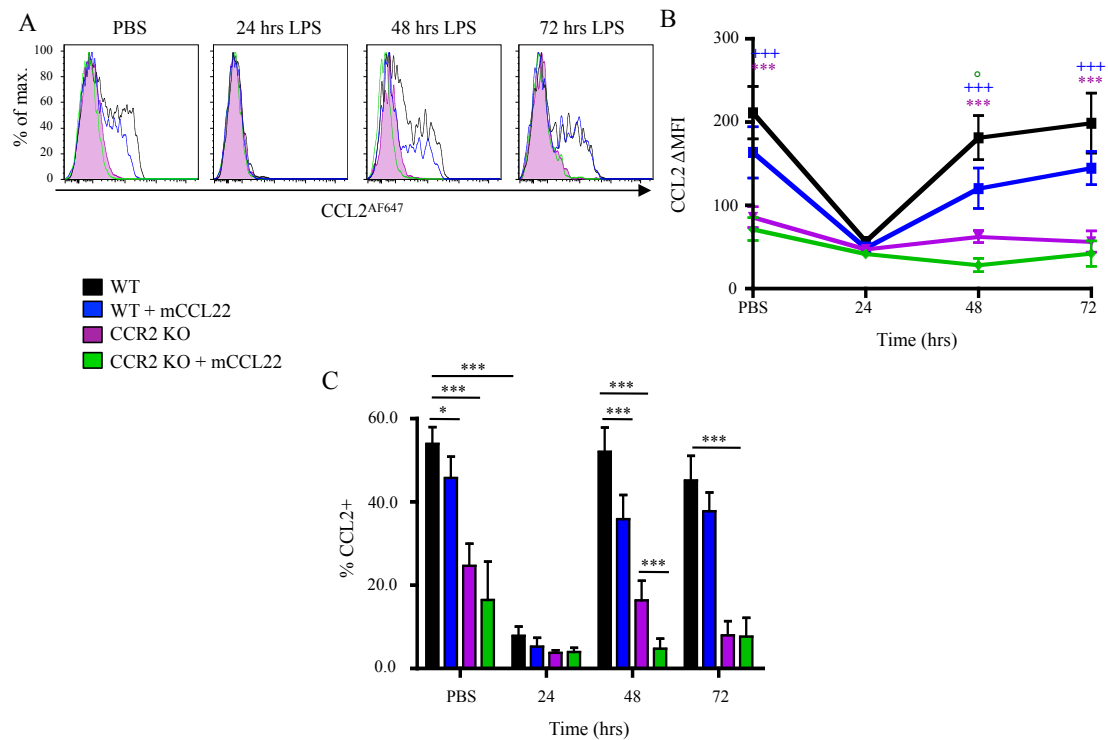


Figure 4-8: Effect of LPS on CCR2 activity of splenic CD8 α^+ cDCs.

WT and CCR2 KO animals were treated i.v. with PBS for 24 or 48 hrs, or LPS for 24, 48 and 72 hrs. Splenocytes from WT and CCR2 KO animals were incubated with CCL2^{AF647} with or without mCCL22 competition. (A) Representative histogram of CCL2^{AF647} uptake by CD8 α^+ cDCs, gated as described in Figure 3-11 (MHCII^{hi}CD11c^{hi}CD11b^{lo}CD8 α^+), from WT (black line) and CCR2 KO cells (shaded purple area) without competition, and WT (blue line) and CCR2 KO (green line) samples with mCCL22 competition. (B) CCL2 geometric mean fluorescence intensity (Δ MFI) of WT (black line) and CCR2 KO (purple line) incubated with CCL2^{AF647} without competition. CCL2^{AF647} uptake in WT (blue line) and CCR2 KO (green line) splenic CD8 α^+ cDCs competed with a 10-fold molar excess of mCCL22. (C) Proportion of CD8 α^+ cDCs that were CCL2⁺. Data were generated from three or more individual mice per genotype (mean \pm SD). Data were analysed by either one-way ANOVA with Tukey post-test or two-way ANOVA with Bonferroni post-test $p < 0.05$ * and $p < 0.001$ ***. Statistical significant in (B) is shown between WT to CCR2 KO by * symbols, WT to WT with mCCL22 by + symbols and CCR2 KO to CCR2 KO with mCCL22 by ° symbols.

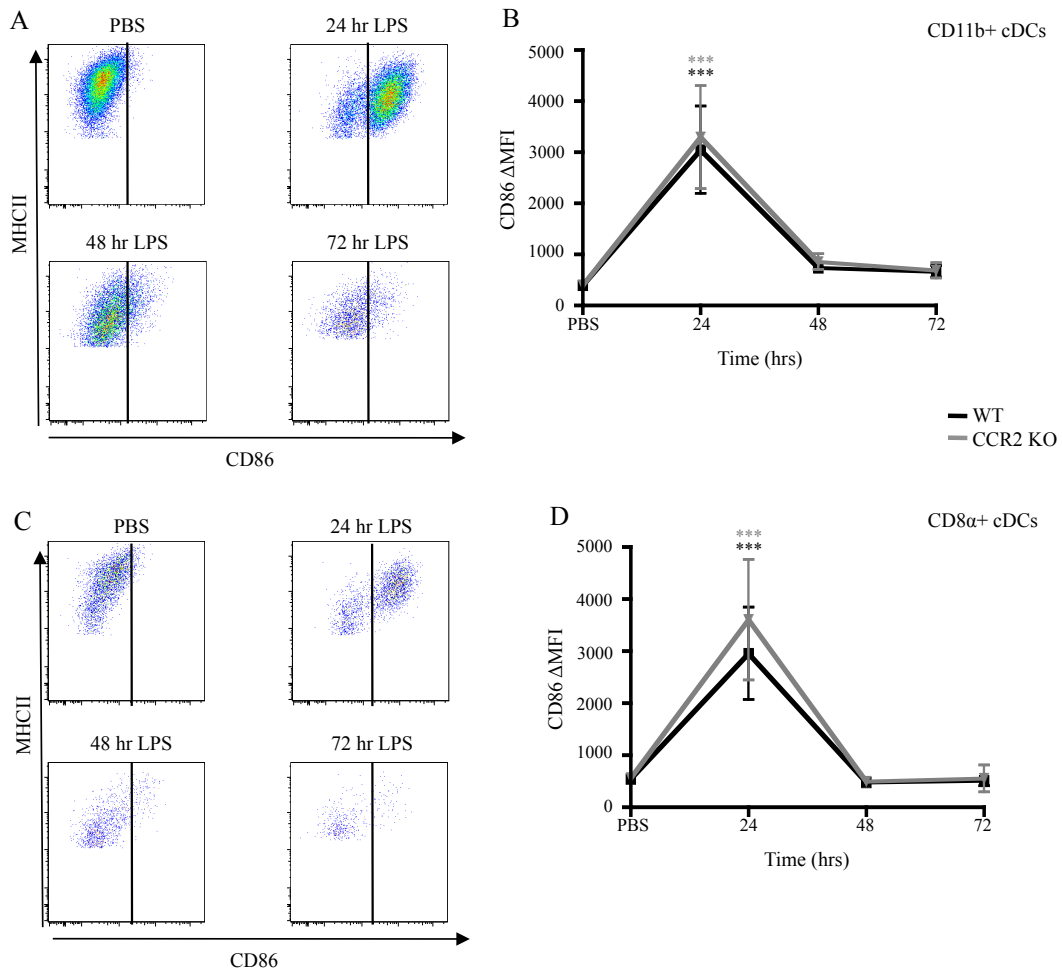


Figure 4-9: Maturation of cDCs in response to LPS.

WT (black line) and CCR2 KO (grey line) animals were treated i.v. with PBS for 24 or 48 hrs, or LPS for 24, 48 and 72 hrs and the expression of the activation marker CD86 by CD11b⁺ cDCs (A&B) and CD8α⁺ cDCs (C&D) was examined, gated as described in Figure 3-11. Representative plots of CD86 expression by WT CD11b⁺ cDCs (A) and CD8α⁺ cDCs (B). CD86 geometric mean fluorescence intensity (ΔMFI) of CD11b⁺ cDCs (C) and CD8α⁺ cDCs (D) was monitored over the time-course. Gating of the two populations has been described in Figure 3-11. Data were generated from five or more individual mice per genotype (mean ± SD). Data were analysed by two-way ANOVA with Bonferroni post-test comparing each time point in the individual murine strains p<0.001 ***.

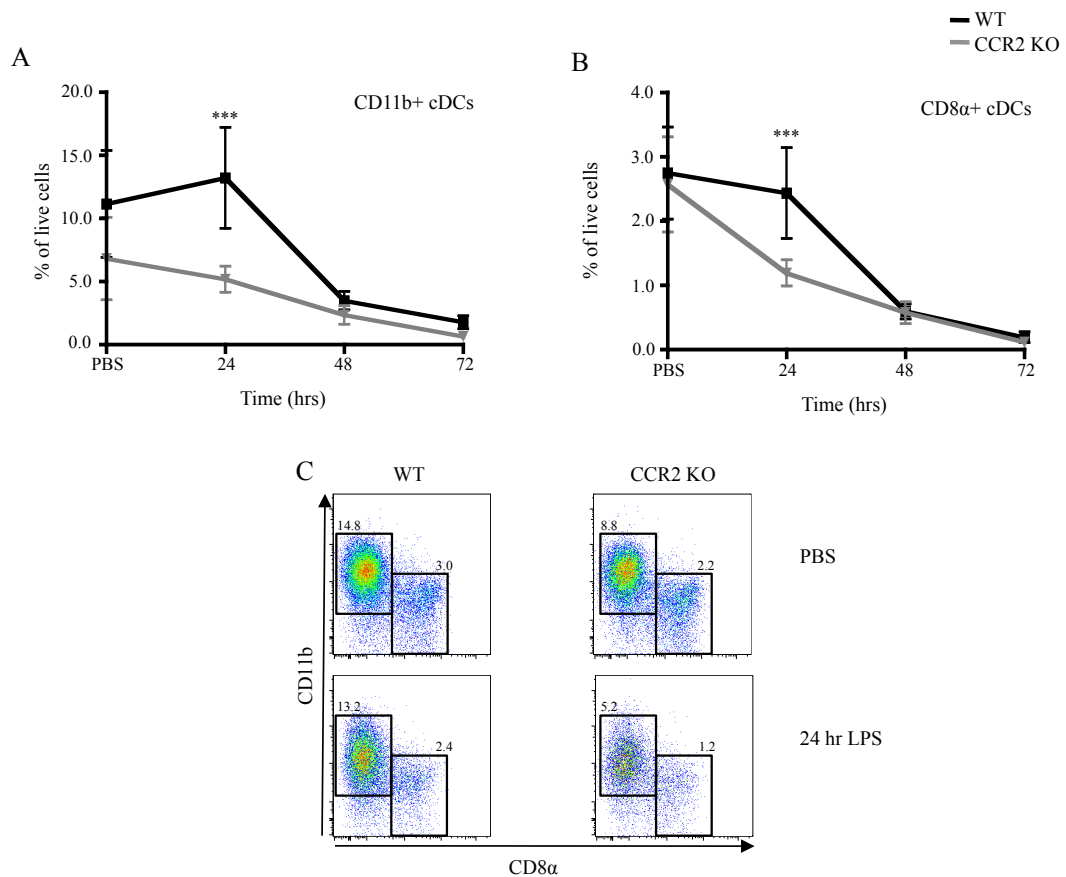


Figure 4-10: Effect of LPS on splenic cDC frequencies.

WT (black line) and CCR2 KO (grey line) animals were treated i.v. with PBS for 24 or 48 hrs, or LPS for 24, 48 and 72 hrs. Frequencies of (A) CD11b⁺ cDC and (B) CD8α⁺ cDC, gated as depicted in Figure 3-11. Data were generated from five or more individual mice per genotype (mean ± SD). Data were analysed by two-way ANOVA with Bonferroni post-test $p < 0.001$ ***. (C) Illustration of the decrease in CD11b⁺ cDCs and CD8α⁺ cDCs numbers following a pre-gate for CD11c^{hi}MHCII^{hi} cells in the spleen of CCR2 KO mice 24 hrs after LPS administration. Numbers in each gate represent proportion of live cells within the gate.

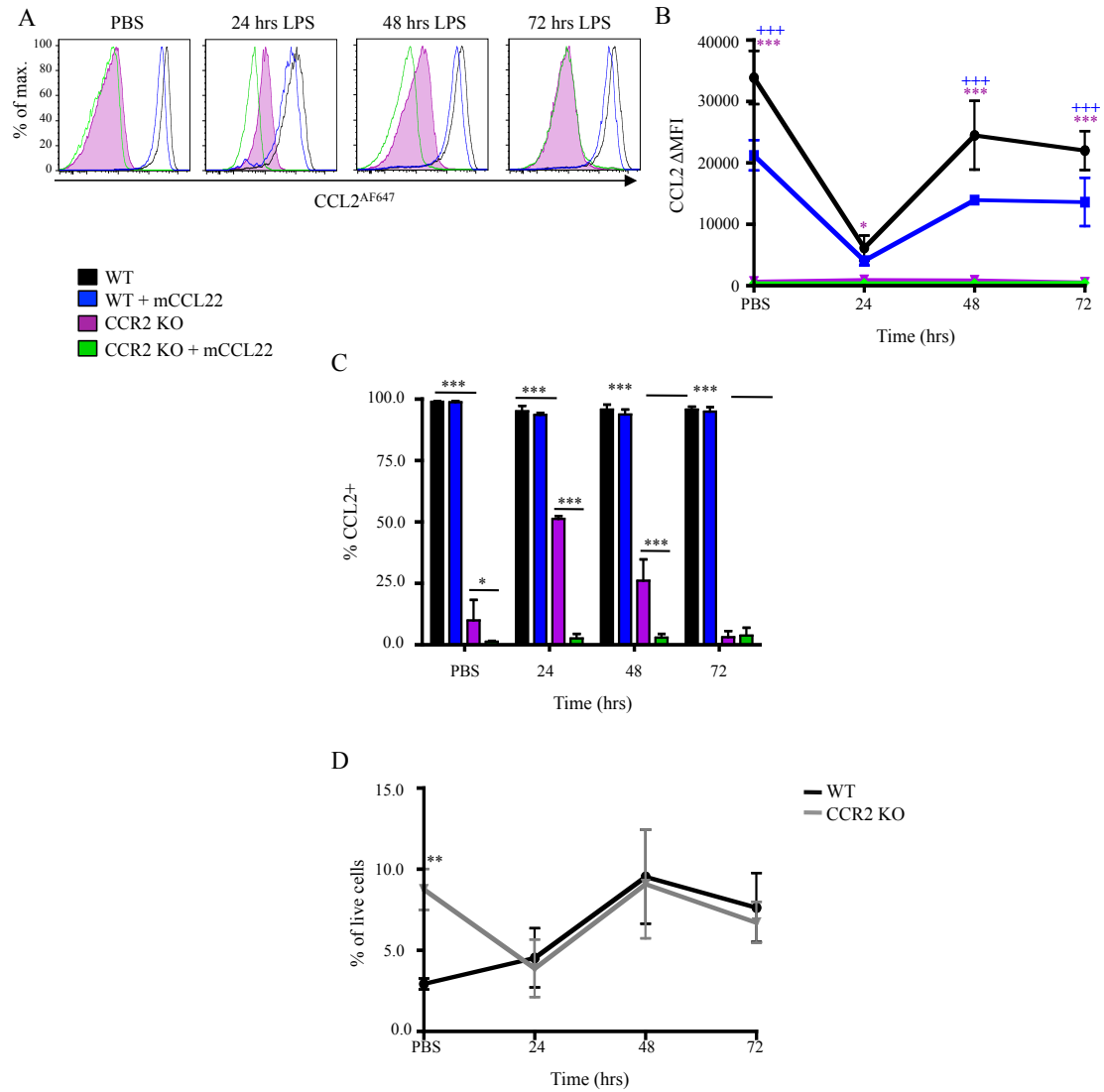


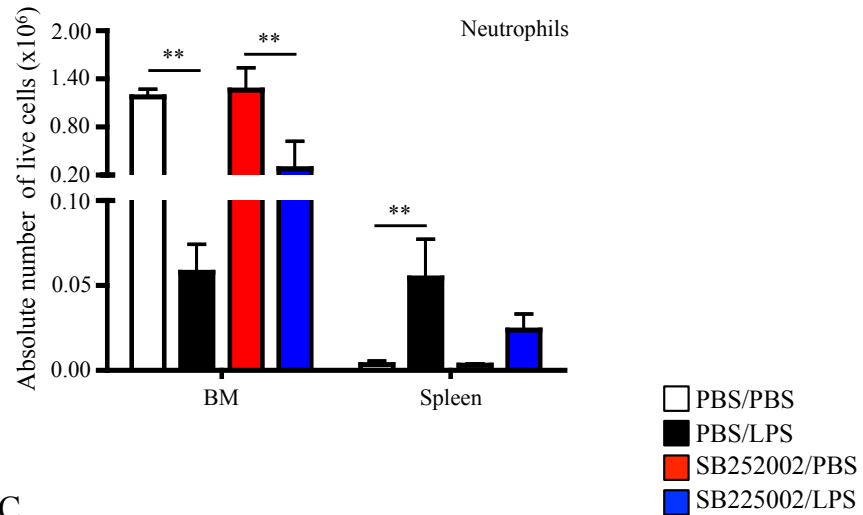
Figure 4-11: Effect of LPS on CCR2 activity and frequency of BM Ly6C^{hi} monocytes.

WT and CCR2 KO animals were treated i.v. with PBS for 24 or 48 hrs, or LPS for 24, 48 and 72 hrs. BM cells from WT and CCR2 KO animals were incubated with CCL2^{AF647} with or without mCCL22 competition. (A) Representative histogram of CCL2^{AF647} uptake by BM Ly6C^{hi} monocytes, gated as described in Figure 3-12 (CD115⁺CD11b⁺Ly6C⁺Gr1^{lo}), from WT (black line) and CCR2 KO cells (shaded purple area) without competition, and WT (blue line) and CCR2 KO (green line) samples with mCCL22 competition. (B) CCL2 geometric mean fluorescence intensity (ΔMFI) of WT (black line) and CCR2 KO (purple line) incubated with CCL2^{AF647} without competition. CCL2^{AF647} uptake in WT (blue line) and CCR2 KO (green line) BM Ly6C^{hi} monocytes competed with a 10-fold molar excess of mCCL22. (C) Proportion of BM Ly6C^{hi} monocytes that were CCL2⁺. (D) Frequencies of Ly6C^{hi} monocytes over the LPS time-course. Data were generated from three or more individual mice per genotype (mean ± SD). Data were analysed by either one-way ANOVA with Tukey post-test or two-way ANOVA with Bonferroni post-test $p < 0.05$ *, $p < 0.01$ ** and $p < 0.001$ ***. Statistical significant in (B) is shown between WT to CCR2 KO by * symbols and WT to WT with mCCL22 by + symbols.

A



B



C

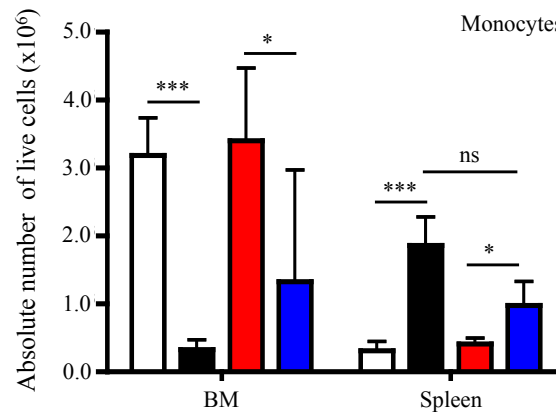


Figure 4-12: Assessment of the CXCR2 dependence of LPS induced monocyte mobilisation. (A) CCR2 KO animals were treated i.p. with 0.3 mg/kg CXCR2 antagonist SB225002 or PBS for 3 hrs. Mice were then treated i.v. with PBS or LPS for 21 hrs. (B) Absolute number of neutrophils in BM and spleen, as determined by gating as depicted in Figure 3-10 ($CD115^-CD11b^+Ly6C^+Gr1^{hi}$) and 3-9 ($Ly6C^{inter}CD11b^+Gr1^{lo}$), respectively. (C) Absolute number of monocytes in BM and spleen, as determined by gating as depicted in Figure 3-10 ($CD115^+CD11b^+Ly6C^+Gr1^{lo}$) and 3-9 ($Ly6C^{hi}CD11b^+Gr1^{lo}$), respectively. Animals were treated with PBS i.p. and then i.v. (white bars), PBS i.p. and then LPS i.v. (black bars), SB225002 i.p. then PBS i.v. (red bars) and SB225002 i.p. and LPS i.v. (blue bars). For each condition, $n=3$ (mean + SD). Data were analysed by one-way ANOVA with Tukey post-test $p<0.05$ *, $p<0.01$ ** and $p<0.001$ ***.

Chapter 5 – CCL2 receptors and pDCs

In recent years research on pDCs has intensified. As discussed in the Introduction they have now been accredited with a variety of roles, including anti-viral (Naik et al., 2005a; Reizis et al., 2011a) and tumour responses (Wei et al., 2005; Matta et al., 2010), and, although less efficient than cDCs, mature pDCs possess the ability to prime and cross-prime naïve T cells (Asselin-Paturel et al., 2001; Colonna et al., 2004; Villadangos and Young, 2008). Many of these roles have been assigned to particular subsets of pDCs, which are delineated by surface markers. For example, the expression of CCR9 by pDCs is reported to be associated with tolerogenic properties of these cells (Hadeiba et al., 2008; Björck et al., 2011; Schlitzer et al., 2011), and several other potential subsets of pDCs have been described based on expression of markers, such as CD9 (Björck et al., 2011) and CD8 α (Lombardi et al., 2012). These studies demonstrate the existence of functionally distinct subsets of pDCs that are identifiable by differences in expression of a single marker. Moreover, the homing capabilities of pDCs, and indeed all other immune cells, are critical for them to exert their functions in specific tissues or tissue compartments, or at specific times (e.g. homeostasis or inflammation). Therefore, it is interesting that a proportion of pDCs have been found to possess CCR2 and D6 activity. The increased sensitivity of the CCL2^{AF647} assay, in addition to its ability to examine the activity of both CCR2 and D6, means that this is one of the first times that pDCs have been reliably described to possess CCR2, and certainly the first time that they have been shown to have D6 activity. To my knowledge, CCR2 and D6 have not been assigned a role on pDCs. Thus, in this results chapter I aim to characterise the two pDC subsets, CCL2^{hi} and CCL2^{lo}, both functionally and genetically.

5.1 Detection of two subsets of pDCs based on CCR2 activity

First, in Figure 5-1, using splenocytes as an example, I describe the gating strategy, by which two subsets of pDC based on CCL2^{AF647} uptake, have been identified so far. pDCs were identified as B220⁺CD11c⁺Ly6C⁺CD11b⁻, and although other cell populations may express one or more of these markers, pDCs are the only population that have this pattern of expression (Asselin-Paturel et al., 2003). Many groups have identified pDCs, as B220⁺CD11c⁺ cells, including no

further markers. However, examination of Ly6C and CD11b illustrates that gating as simply B220⁺CD11c⁺ would include numerous cell populations (Blasius et al., 2007). B220⁺CD11c⁺ cells excluding pDCs, (i.e. B220⁺CD11c⁺Ly6C⁺/CD11b⁺ cells) were gated and called Population D. Similar to pDCs, this population possessed high levels of CCR2 activity and also weak D6 activity (Figure 5-1). This gating strategy did not include a marker that is considered to be pDC specific, such as PDCA-1 or SiglecH (Asselin-Paturel et al., 2003; Zhang et al., 2006; Blasius et al., 2006a; 2006b). Thus, further characterisation was required. Following the gating as described in Figure 5-1, the expression of PDCA1 and SiglecH was determined on CCL2^{hi}, CCL2^{lo} pDCs, and Population D (Figure 5-2A). Both CCL2^{hi} and CCL2^{lo} subsets expressed high levels of both PDCA1 and SiglecH, illustrating that they are truly pDCs. In contrast, Population D did not express either PDCA1 or SiglecH. This indicates that only B220⁺CD11c⁺ cells that are Ly6C⁺ and CD11b⁻ are in fact pDCs. The identity of Population D is uncertain, but it is likely to include a subset of NK cells that have been identified as B220⁺CD11c⁺NK1.1⁺CD11b⁺ (Blasius et al., 2007). As further confirmation of the lineage of the two CCL2 subsets of pDCs, pDCs were identified by a more simple gating strategy that is frequently published, PDCA1⁺CD11c⁺ (Figure 5-2B). Within the PDCA1⁺CD11c⁺ population the two subsets based on CCL2 uptake were present. Thus, these data confirm the existence of two subsets of pDCs based on CCL2^{AF647} uptake in spleen. Furthermore, in Chapter 3 and Figure 4-6, I proved that CCL2^{AF647} uptake was primarily, but not exclusively CCR2 dependent, as there was evidence of D6 on splenic, BM and blood pDCs.

I next determined whether pDCs elsewhere in the lymphoid system could be delineated into two subsets based on CCL2^{AF647} (Figure 5-3). By using the CCL2^{AF647} assay I was able to establish that pDCs in all tissues tested could be segregated into CCL2^{hi} and CCL2^{lo} populations, with the relative proportion of CCL2^{hi} pDCs in each tissue indicated in the histograms. In the spleen, PLNs, MLNs and blood, CCL2^{hi} contributed approximately 50% of the pDC population, whereas the proportions of CCL2^{hi} to CCL2^{lo} pDCs appeared to be altered in BM, with a lower number of CCL2^{hi} pDCs detected. In each tissue the majority of uptake was CCR2 dependent, but there was also evidence of D6 expression in CCR2 KO pDCs. Furthermore, examination of WT pDCs for D6 activity indicated that in the spleen and BM, both CCL2^{hi} and CCL2^{lo} pDCs possessed D6 activity,

whereas in the blood, MLNs and PLNs only CCL2^{lo} pDCs possessed D6 activity. Notably, pDCs in the BM and blood had greater overall CCL2 receptor activity in both WT and CCR2 KO mice than pDCs in spleen and LNs.

Thus, two subsets of pDCs can be identified on CCR2 activity in the spleen, blood, MLNs, PLNs and BM. The key objective in the remainder of my thesis was therefore to assess if CCR2 expression defines two functionally distinct pDC subsets and explore the indispensable roles played by CCR2 on these cells.

5.2 Flt3L mediated *in vivo* expansion and *in vitro* generation of pDCs and their CCR2 activity

pDCs represent only a low number of splenic cells, comprising only ~0.3% of the splenic populations. They are also rare cells in blood, BM and LNs (Reizis et al., 2011a). As both the CCL2^{hi} and CCL2^{lo} subsets of pDCs comprise approximately 50% of pDCs this would equate to less than 0.15% of splenic cells. Most functional studies require large numbers of purified cells, thus the low cell numbers present a challenge when working with these cells. Therefore, in order to further characterise the two pDC subsets identified, in addition to conducting functional studies using these cells, larger numbers of cells were required than could be purified from resting mice. The vast majority of pDC research is conducted using human peripheral blood pDCs. Alternatively, in the murine system, pDC numbers can be expanded *in vivo* and *in vitro* by using Flt3L. As described in the Introduction, Flt3L plays a pivotal role in the generation of pDCs in the BM, driving differentiation of a DC progenitor to the pDC lineage (Naik et al., 2005a; Reizis et al., 2011a). Many groups have described the generation of large numbers of pDCs *in vitro* by using Flt3L to drive differentiation of BM cells into pDCs (Brawand et al., 2002; Gilliet et al., 2002; Naik et al., 2005b; 2010). Another method used to expand murine pDCs *in vivo* is the treatment of animals with Flt3L or inoculation (s.c.) with Flt3L secreting tumours (Maraskovsky et al., 1996; Mach et al., 2000). Thus, I next performed some pilot experiments to explore the effect of *in vitro* and *in vivo* Flt3L to identify the optimal method to expand pDCs, while retaining their segregation into CCL2^{hi} and CCL2^{lo} subsets.

5.2.1 *In vitro* generation of pDCs

The generation of BM-derived pDCs (BM-pDCs) using Flt3L has been extensively described (Gilliet et al., 2002; Naik et al., 2005b). In the majority of these papers, the Flt3L used was either recombinant human (rh) Flt3L, or present in conditioned media (CM) from cell lines that have been engineered to stably produce murine Flt3L. CHO-Flt3L and B16FL, two cell lines containing Flt3L expression constructs, were obtained from the Simon Milling Laboratory (University of Glasgow, U.K.) and Oliver Pabst (Medizinischen Hochschule Hannover, Germany), respectively, and the amount of Flt3L generated from these cell lines was measured by ELISA (Figure 5-4). Both cell lines produced substantial quantities of Flt3L.

Next, these Flt3L-containing CM, along with rhFlt3L, were tested for their ability to generate BM-pDC over a range of concentrations and incubation times (Figure 5-5). In this first experiment, the frequency of generated pDCs was not determined, only the frequency of live cells. In accordance with published observations (Seth et al., 2011), rhFlt3L was a poor differentiator of BM-DCs, as the proportion of total live cells was never higher than 8% at all concentrations and time-points tested (Figure 5-5A). Treatment of BM cells with CM from CHO-Flt3L and B16FL resulted in an increase in number of live cells compared to rhFlt3L (Figure 5-5B&C). Furthermore, this appeared to have a concentration dependent effect, with the two highest concentrations, 50 ng/ml and 100 ng/ml Flt3L generating the greatest frequency of live cells. Therefore, in the next experiment I incubated BM cells with the two most effective concentrations of CHO-Flt3L or B16FL CM (50 or 100 ng/ml) and determined the absolute number of pDCs produced 7-10 days after setting up the cultures (Figure 5-5D&E). The number of BM-pDC produced using B16FL Flt3L gradually decreased over the time-course, with the highest number of BM-pDC being produced at day 7 with 100 ng/ml. In contrast, Flt3L from CHO-Flt3L produced higher numbers of BM-pDC at day 8. In fact, 100 ng/ml Flt3L from CHO-Flt3L appeared to produce higher numbers of BM-pDC than Flt3L from B16FL, at all times tested. The same was true with 50 ng/ml Flt3L from CHO-Flt3L except at day 7, where 100 ng/ml of Flt3L from B16FL produced a higher number of BM-pDC. In terms of absolute numbers, the optimum condition for BM-pDC production was 100 ng/ml Flt3L from CHO-Flt3L. It produced $\sim 6 \times 10^6$ live BM-pDC from 1×10^7 BM cells. These

experiments were only pilot studies, so only one data point was generated for each condition and no statistical analyses were conducted. However, they showed that BM-pDCs could be successfully generated in high numbers *in vitro*.

5.2.2 CCL2 receptor activity of *in vitro* BM-pDCs

I analysed CCL2 receptor activity of BM-pDCs at day 8, 9 or 10 of culture with either Flt3L containing CM from CHO-Flt3L (Figure 5-6A) or B16FL (Figure 5-6B). At all conditions tested, BM-pDCs internalised CCL2^{AF647} in a predominantly CCR2 dependent manner, as illustrated by competition with mCCL2, that was far less apparent when using mCCL22. mCCL22 competition did cause some reduction in CCL2^{AF647} uptake, mainly with CHO-Flt3L treated cells, but also at day 8 and 9 of culture with B16FL treatment, indicative of D6 activity in these cells. There also appeared to be an effect on the relative proportions of CCL2^{hi} and CCL2^{lo} pDCs observed *in vivo*, with a higher proportion of CCL2^{hi} pDCs being found at day 8. Furthermore, at later points of culture there were alterations in the profiles of uptake, with diminished CCL2^{AF647} uptake observed. There was also a lot of variation between pDCs derived with different Flt3L sources, particularly in the ability of mCCL2 to compete CCL2^{AF647} uptake. Thus, although encouraging, these results led to some concerns about the potential reproducibility of generating CCR2-expressing pDCs *in vitro*. Moreover, it was felt that *in vivo* expanded pDCs might represent a more physiological source of pDCs. Thus, this method was next explored.

5.2.3 *In vivo* expansion of pDCs

I tested two commonly used methods to expand the number of pDCs *in vivo* (Figure 5-7). Due to the expense and limited availability of rhFlt3L, experiments using this reagent were conducted in collaboration with Calum Bain and Vuk Cerovic (University of Glasgow) who required the treatment to be done in CX₃CR1^{GFP/+} mice. As discussed in the Introduction, CX₃CR1^{GFP/+} mice are reporter mice with a targeted replacement of CX₃CR1 by a GFP reporter. They are frequently used to explore the role of Ly6C^{lo} monocytes and macrophages (Jung et al., 2000; Auffray et al., 2007; 2009a). Calum Bain and Vuk Cerovic were interested in the macrophage and DC populations in the gut and MLNs of the CX₃CR1^{GFP/+} mice, and I was able to analyse pDCs in spleen, blood and PLNs.

Thus, CX₃CR1^{GFP/+} mice were treated i.p. for 10 days with rhFlt3L and the absolute number of pDCs in secondary lymphoid organs and blood was determined. Alternatively, WT mice were injected s.c. with ~2x10⁶ B16FL tumour cells. As described in the original paper that details the generation and use of B16FL cells, they have the ability to form a pigmented melanoma that spontaneously secretes murine Flt3L resulting in an increase in the number of peripheral DCs (Mach et al., 2000). 13 days after injection of cells, the absolute number of pDCs and B220⁻CD11c⁺ cells were determined in the spleen, blood and PLN. The treatment of WT or CX₃CR1^{GFP/+} animals with B16FL or rhFlt3L, respectively, resulted in a marked increase in the frequency of pDCs in the spleen (Figure 5-7A), blood (Figure 5-7B) and PLNs (Figure 5-7C), as illustrated by representative plots. Furthermore, as Flt3L treatment does not result in a specific expansion of pDCs (it also expands cDCs populations), these plots show a dramatic increase in B220⁻CD11c⁺ cells, a population which includes cDCs. Although images are not shown, treatment with either form of Flt3L resulted in splenomegaly, and thus upon calculation of absolute cell numbers there was a dramatic increase in the number of pDCs and B220⁻CD11c⁺ cells in the spleen (Figure 5-7A), blood (Figure 5-7B) and PLNs (Figure 5-7C).

5.2.4 CCL2 receptor activity of *in vivo* expanded pDCs

I also analysed the CCL2 receptor activity of splenic (Figure 5-8A) and PLN pDCs (Figure 5-8B) from B16FL or rhFlt3L treated WT mice. In both tissues, regardless of method of pDC expansion, there was uptake of CCL2^{AF647}. The proportion of CCL2^{hi} and CCL2^{lo} pDCs was determined in spleen (Figure 5-8C) and PLNs (Figure 5-8D) in untreated and Flt3L treated animals. In the spleen there appeared to be no effect of Flt3L treatment on the ratio of CCL2^{hi} to CCL2^{lo} pDCs, with both populations contributing ~50% of pDCs. The same was true for PLN pDCs, however trends suggested that treatment with rhFlt3L resulted in an increase in CCL2^{lo} pDCs to ~60% and a concomitant decrease in CCL2^{hi} pDCs. No statistics are available for this observation, due to the low number of biological replicates in this experiment. Nonetheless, it is clear that Flt3L treatment leads to an expansion of pDCs *in vivo* and that these cells broadly retain the CCL2^{AF647} uptake profiles of untreated mice.

To conclude, I found that Flt3L treatment *in vitro* generated large numbers of BM-pDCs and *in vivo* resulted in a dramatic increase in the number of pDCs. Furthermore, *in vivo* treatment with Flt3L had minor, if any, effects on the CCR2 activity of pDCs, as there was no obvious perturbation to the ratio of CCL2^{hi} and CCL2^{lo} pDCs. In contrast, although *in vitro* generated BM-pDCs possessed CCR2 activity, the activity appeared diminished at later points in culture and results between cultures were highly variable. While BM-pDCs represent a useful model for the generation of a large number of cells, the results can be difficult to correlate to a biological system. Analysis of *in vivo* expanded pDC populations allows the assessment of pDC development and function *in situ* under more physiologically relevant conditions. Taking all this into account, when large numbers of pDCs were required in the following work they were expanded by *in vivo* treatment with Flt3L. Furthermore, due to the limited availability and substantial cost of rhFlt3L, pDC numbers were routinely expanded by treating animals with B16FL cells. Throughout, I routinely generated large numbers of pDCs that consistently showed CCL2^{AF647} uptake profiles that were very similar to untreated control animals.

5.3 Isolating CCL2^{hi} and CCL2^{lo} pDCs

To perform transcriptional and functional comparisons between the CCL2^{hi} and CCL2^{lo} pDCs, I devised a sorting strategy that would facilitate the isolation of either total pDCs, which were not subject to exposure of CCL2^{AF647}, or CCL2^{hi} and CCL2^{lo} pDCs using a BD FACS Aria (Figure 5-9A). Total splenic pDCs from a B16FL treated animal were identified using several parameters, including the pDC specific marker SiglecH. Alternatively, after incubation with CCL2^{AF647} for 1 hr, CCL2^{hi} and CCL2^{lo} pDCs were gated and sorted. Purity checks were habitually run following sorting of cells and, as Figure 5-9B illustrates, purity was routinely between 90-95%.

5.4 Migration of pDCs in response to CCL2

The CCL2/CCR2 pathway has been shown to mediate migration of a range of cell types, such as monocytes (Geissmann et al., 2003; Serbina and Pamer, 2006), mast cells (Collington et al., 2010) and dendritic cells (Osterholzer et al., 2008; Jimenez et al., 2010). To my knowledge, the studies demonstrating CCR2

dependent migration of pDCs all have used human pDCs from peripheral blood (Penna et al., 2001; Kohrgruber et al., 2004). Thus, I examined whether murine pDCs also respond chemotactically to mCCL2. Sorted total pDCs from the spleen of B16FL tumour bearing mice clearly had a chemotactic response to mCCL2 in *in vitro* transwell migration assays (Figure 5-10). Total pDCs were used, as exposure to CCL2^{AF647} would be expected to desensitise CCR2 to further exposure of mCCL2 in the migration assay. As the concentration of mCCL2 increased there was a parallel increase in the absolute number of migrated pDCs. There were, however some cells that migrated in the absence of mCCL2, but there were significantly more migrated pDCs in the presence of mCCL2 at all concentrations tested. Thus, mouse pDCs respond chemotactically to CCL2 gradients *in vitro*.

5.5 Expression of known pDC markers by CCL2^{hi} and CCL2^{lo} pDCs

Next, I tried to establish whether expression of markers known to be capable of subdividing pDCs correlated with the two pDC subsets I had defined by CCL2^{AF647} uptake. Current pDC literature allowed me to identify a list of surface markers that pDCs are known to express, and which, in many cases, have been used to characterise subsets of pDCs. Thus, using flow cytometry I determined their expression on the two CCL2 pDC subsets in untreated controls (i.e. mice not carrying B16FL tumours) (Figures 5-11 to 5-13).

First, I examined the expression of other chemokine receptors by the two subsets (Figure 5-11). CCR9 is a homing receptor for pDCs to the small intestine (Wendland et al., 2007), and both CCR2 subsets expressed CCR9. However, there was a small population of CCL2^{hi} pDCs that did not express CCR9, thus there were significantly more CCL2^{lo} pDCs present that expressed CCR9. This is potentially interesting as pDC progenitors and non-tolerogenic pDCs are reportedly CCR9⁻ (Hadeiba et al., 2008; Björck et al., 2011; Schlitzer et al., 2011; 2012). Furthermore, by using a reporter CX₃CR1^{GFP/+} mouse, I was able to determine that both subsets expressed the GFP reporter and so probably express CX₃CR1. This chemokine receptor has been reported by others to be expressed by pDCs, also using GFP reporter mice (Schlitzer et al., 2011). Notably CCL2^{hi} pDCs had significantly higher expression of GFP than CCL2^{lo} pDCs, albeit only being marginally higher in CCL2^{hi} cells. Surprisingly, both subsets were negative

for the chemokine receptor CCR7, which has been reported to be expressed by pDCs at low levels and induced by their activation. It has also been shown to be vital for their migration to PLNs (Seth et al., 2011). As a control for staining with the anti-CCR7 antibody I examined all live splenic cells for CCR7 immunoreactivity, the majority of which will be T and B lymphocytes that are known to express CCR7. I found that all were negative for anti-CCR7 immunoreactivity (Figure 5-5E). This indicates that the CCR7 antibody failed to detect CCR7, highlighting the problem, discussed earlier in Chapter 3, with antibodies targeted against mouse chemokine receptors being unreliable detection reagents.

Other groups have reported that CCR5 is involved in pDC transmigration across HEVs into LNs (Diacovo et al., 2005) and also in pDC migration to inflammatory sites (Penna et al., 2001). Commercially available anti-mouse CCR5 antibodies had been rigorously tested in our lab by others, but failed to provide consistent detection of CCR5 (Ross Kinstrie and Rob Nibbs personal communication). Thus, I attempted to examine CCR5 activity on splenic pDCs using a CCL5^{AF647} uptake assay (Figure 5-11C&D). CCL5 can be bound by several receptors, including CCR1, CCR3, CCR5 and D6, therefore in order to determine CCR5 specific uptake several controls needed to be included. Competition of CCL5^{AF647} uptake with an excess of CCL5 demonstrates that uptake is mediated by one or more of the CCL5 binding receptors, whereas competition with excess CCL4 demonstrates CCR5 or D6 involvement, due to their exclusive ability to bind to both CCL5 and CCL4. Histogram overlays (Figure 5-11A) and the CCL5 Δ MFI data (Figure 5-11D) suggested that competition with mCCL4 caused a significant reduction in CCL5^{AF647} uptake, indicating either CCR5 or D6 activity. I have already shown evidence of D6 activity on these cells, thus D6 might be the receptor exclusively responsible for this uptake. In contrast, all CCL5^{AF647} uptake was competed with mCCL5. Thus, the uptake not competed by mCCL4 was probably mediated by CCR3 or CCR1, which bind mCCL5 but not CCL4. Notably, pDCs were homogeneous in these assays, and distinct subsets were not observed. So high CCR2 expression is unlikely to correlate with absence or presence of CCL5 receptors.

In addition to examining expression of chemokine receptors, I examined expression of integrins that aid the migration of cells *in vivo* (Figure 5-12).

CD62L is reportedly crucial for the transmigration of pDCs into PLNs (Nakano et al., 2001; Diacovo et al., 2005), but my data suggest very low, if any, expression in both subsets. However, there was a statistically significant decrease in CD62L expression by CCL2^{lo} pDCs compared to CCL2^{hi}, which might indicate a lower capacity to transmigrate into PLNs. However, previous data suggest that CCL2^{hi} and CCL2^{lo} pDCs are as abundant in PLNs as they are in spleen and blood (Figure 5-3). The subsets were also found to have very low levels of expression of the integrin $\alpha 4\beta 7$, which is involved in pDC migration to the small intestine and MLNs (Hadeiba et al., 2008).

pDCs have been described as possessing tolerogenic properties. However, only a subset of pDCs are reported to be tolerogenic (Matta et al., 2010). Several groups have identified a tolerogenic pDC subset by differences in expression of CD8 α (Lombardi et al., 2012), and CCR9 (Hadeiba et al., 2008). Tolerogenic pDCs are reported to express CD8 α and also CCR9 (Hadeiba et al., 2008; Lombardi et al., 2012). Nearly all pDCs in both CCL2 subsets have already been found to express CCR9 (Figure 5-11), although the CCL2^{hi} subset appears to be a mixed population as it contains CCR9⁺ and CCR9⁻ pDCs. Interestingly, it also contained a very small population of CD8 α ⁻ cells, however there were no statistically significant differences in the proportion of CCL2^{hi} and CCL2^{lo} pDCs expressing CD8 α and a large fraction of pDCs could be classified as CD8 α ⁺ (Figure 5-12).

As discussed in the Introduction, several markers, such as CD4 (O'Keeffe et al., 2002), Ly49Q (Kamogawa-Schifter et al., 2005) and CD9 (Björck et al., 2011) can be used to delineate immature and mature pDCs. I next sought to determine whether the CCL2^{hi} and CCL2^{lo} subsets differed in their maturation status (Figure 5-12). Immature BM pDCs are thought to acquire Ly49Q before migrating into the periphery (Omatsu et al., 2005; Toma-Hirano et al., 2007), therefore it should be expected that all splenic pDCs should be Ly49Q⁺. However, the two subsets of pDCs defined by CCR2 activity were negative for Ly49Q. Likewise, newly formed BM pDCs are CD9⁺ and lose CD9 expression upon migration into the periphery and become mature CD9⁻ pDCs (Björck et al., 2011). This suggests that all splenic pDCs should be CD9⁻, however the two subsets were found to express low levels of CD9. These data conflict as the lack of Ly49Q expression indicates that the splenic pDC subsets are immature pDCs, whereas the low levels of CD9 suggest

that only a fraction of the splenic pDCs are immature, with the majority of cells being mature CD9⁻ pDCs. CD4 is also defined as a maturation marker, with CD4⁻ pDCs being precursors to the mature CD4⁺ pDCs (O'Keefe et al., 2002).

Therefore, the CD4 expression data offers support to the CD9 data, as both subsets differentially expressed CD4, indicating the presence of both immature and mature pDCs.

To confirm that the low or lack of expression of markers was accurate and not due to a failure of the antibodies to detect their targets, I examined expression of CD62L, $\alpha 4\beta 7$ and Ly49Q in all live splenocytes (Figure 5-12C). This should serve as a positive control, as some cells within the spleen should be positive for the tested markers. For example, splenic Gr1⁺ cells, such as neutrophils and monocytes have been reported to express Ly49Q (Toyama-Sorimachi et al., 2004). Antibodies against CD62L and $\alpha 4\beta 7$ bound to a subset of cells to a greater extent than isotype control antibodies, suggesting they have the capacity to recognise their Ag on cells. This was not the case with the anti-Ly49Q antibody. This might indicate that it can not reliably detect Ly49Q protein.

In Chapter 4, I described the correlation of CCR2 downregulation with expression of the activation marker CD86 on cDCs. Therefore the differences in CCR2 activity by the two subsets could be due to differences in their activation status. However, the two subsets were essentially negative for the activation markers OX40L, CD69, and CD86, showing that the difference in CCR2 activity was not a consequence of differences in activation (Figure 5-13). The failure to detect the expression of either activation marker on pDCs might be explained by the antibodies failing to reliably detect the surface marker, similar to the CCR7 antibodies (Figures 5-11E and 5-12C). However, this is unlikely because in a naïve animal i.e. an animal not undergoing an inflammatory response, there would be very few activated cells. Anti-CD86 showed some specific staining when 'all live cells' were examined (Figure 5-32C). Although I did not have a positive control of activated cells within this experiment, I, and other members of the lab, have successfully used the anti-CD86 and anti-CD69 antibodies in experiments involving other cell types, so they are able to detect their respective targets. Thus, the weak staining on pDCs, in this case is probably an

accurate representation of the very low expression of the activation markers by resting pDCs.

In summary, the expression of no known pDC subset marker fully segregated the two subsets delineated by CCR2 activity in WT animals, and the data indicates that there are no major differences in the maturation or activation of these two subsets. CD8 α and CD4 split the two CCL2 subsets into CD8 $\alpha^+/-$ and CD4 $^+/-$. CCR9 was also able to segregate the CCL2^{hi} population into two subsets (CCR9⁺ and CCR9⁻), albeit it to a lesser extent than CD8 α and CD4, because CCR9⁻ pDCs were very rare in the spleen.

5.6 Morphology of CCL2^{hi} and CCL2^{lo} pDCs

Next, I wished to explore functional and transcriptional differences between CCL2^{hi} and CCL2^{lo} pDCs. First, following the isolation of CCL2^{hi} and CCL2^{lo} pDCs from the spleens of B16FL tumour bearing mice, the gross morphology of resting or activated cells was determined by light microscopy (Figure 5-14). As Figure 5-14 illustrates there were no major differences in the morphology of the cells. Both CCL2^{hi} and CCL2^{lo} pDCs appeared lymphocytic in morphology, round cells with large nuclei to cytoplasm ratio and unruffled plasma membranes. Approximately 50% of CCL2^{lo} pDCs did however appear to have several vacuoles present in their nuclei. The morphology of the two pDC subsets was also determined following stimulation with CpG-C. CpG-C is a type C oligonucleotide that is recognised by TLR9 and is capable of stimulating both maturation and IFN α/β production by pDCs (Berghöfer et al., 2007). After stimulation for 18 hrs with CpG-C, both subsets appear to be slightly larger in size, with a more irregular shape and ruffled membranes.

Thus, I have been unable to find any major morphological differences between the two subsets before or after activation. However, in resting cells some CCL2^{lo} pDCs appeared to have vacuoles present in their nuclei, which might be explained by dying cells or nuclear blebbing. However, this observation was not pursued and instead I examined the functional properties of CCL2^{lo} and CCL2^{hi} pDCs.

5.7 *In vitro* function of the two subsets

Functionally distinct subsets of pDCs have been delineated by the expression of a single marker. For example, CCR9 expression is reportedly associated with a tolerogenic subpopulation of pDCs (Hadeiba et al., 2008; Björck et al., 2011; Schlitzer et al., 2011), although it is notable that in my hands nearly all pDCs are CCR9⁺. Therefore, my next aim was to see if CCR2 expression correlated with specific functional attributes of pDCs. To accomplish this, I performed a series of *ex vivo* experiments to illuminate any functional differences between the two pDC subsets that I had identified based on differential CCR2 activity.

5.7.1 T cell stimulatory capacity of CCL2^{hi} and CCL2^{lo} pDCs

As pDCs, like all APCs, possess both MHC class I and II and therefore the ability to present Ag to T cells (Reizis et al., 2011a), I aimed to establish the ability of the two pDC subsets to process and present Ag to naïve T cells. First, I determined the optimal conditions to drive proliferation of naïve OVA specific CD4⁺ and CD8 α ⁺ T cells (Figure 5-15 and 5-17). To do this, total pDCs or B220⁻ CD11c⁺ cells were sorted from the spleens of mice carrying B16FL tumours. B220⁻ CD11c⁺ splenocytes will be highly enriched for cDCs, and are referred to as cDCs here after, but they will contain other cell types (see Figure 3-11). The associated purities are shown in Figure 5-15A. In all these experiments cDCs were used as a positive control to confirm that the T cells were capable of proliferation in response to Ag-specific activation. To establish optimum conditions for pDC driven naïve T cell proliferation, different ratios of total pDCs were incubated with increasing concentrations of OVA, washed extensively and incubated with 1x10⁵ naïve TCR transgenic OVA-specific CD4⁺ T cells (OTII) (Figure 5-15B) or CD8 α ⁺ T cells (OTI) (Figure 5-17). These T cells were labelled with CFSE, and the number of T cells undergoing more than 3 divisions was calculated by examining CFSE dilution. In the absence of OVA, there were a minimal number of T cells that had divided. Incubation of DCs with OVA, stimulated T cell division, but as the concentration of OVA was increased from 1 to 5 mg/ml there were nominal increases on the number of naïve CD4⁺ T cells that had divided in the presence of pDCs (Figure 5-15B). In contrast, as the concentration of OVA was increased there was a parallel increase in the number of naïve CD8 α ⁺ T cells that had divided in the presence of pDCs (Figure 5-17).

Furthermore, proliferation rates of both CD4⁺ and CD8 α ⁺ reduced as the ratio of pDCs to T cells decreased. Therefore, in subsequent experiments with CD4⁺ or CD8 α ⁺ T cells, the optimal conditions of 3 mg/ml OVA with a 1:1 ratio of pDCs to T cells were used.

Notably, under these optimal conditions, cDCs were far more effective at priming T cells with over 80% of CD4⁺ and CD8 α ⁺ T cells divided, compared to 30% of CD4⁺ T cells and 75% of CD8 α ⁺ T cells with pDCs at a 1:1 ratio. Strikingly cDCs were far more effective than pDCs when present at low numbers in cultures. Even at a 1:128 DC:T cell ratio, cDCs were able to induce T cell proliferation comparable to pDCs at highest dilutions tested (Figures 5-15 and 5-17). Thus, pDCs are clearly much less effective inducers of naïve CD4⁺ T cell proliferation than cDCs, but when present in high numbers pDCs do seem to possess the ability to cross-present Ag to naïve CD8 α ⁺ T cells.

Next, I examined the ability of CCL2^{hi} and CCL2^{lo} pDC subsets to process and present Ag to naïve OVA-specific CD4⁺ T cells (Figure 5-16) and stimulate naïve CD4⁺ T cell proliferation. Figure 5-16B shows representative histograms of CFSE dilution, which show that cDCs caused high levels of T cell proliferation, whereas both CCL2^{hi} and CCL2^{lo} pDCs produced low amounts. When the number of T cells that had undergone more than 3 divisions was quantified (Figure 5-16C) this result becomes even more apparent, over 40% of the CD4⁺ T cells in the presence of cDCs had undergone more than 3 divisions, while less than 5% of CD4⁺ T cells had undergone more than 3 divisions when cultured with either CCL2^{hi} or CCL2^{lo} pDCs. In spite of these low numbers of divided T cells, there was a significant decrease in the number of divided T cells when naïve CD4⁺ T cells were incubated with CCL2^{lo} pDCs than CCL2^{hi} pDCs. However, when the frequency of T cells in each division was quantified, there was no significant difference between the two subsets, and the majority of T cells remained undivided (Figure 5-16D).

As the purity checks in Figure 5-16A show there were small numbers of B220⁻ CD11c⁺ cells, which may be cDCs present in each CCL2^{hi} and CCL2^{lo} subset sample. Although only a very low number of these cells were present in pDC cultures they might be responsible for the low amounts of T cell proliferation

observed. If cDCs contributed only 1% of cells contaminating pDC cultures they would still represent ~1000 cells in the culture. Notably, a 1:128 ratio of cDCs to T cells (i.e. less than 1000 cDCs in the culture) produced similar proliferation observed as at 1:1 ratio of pDCs to T cells (Figure 5-15). It is therefore possible that pDCs, at least in my hands, do not process and present OVA at all to CD4⁺ T cells, and the proliferation observed was a consequence of cDC contamination. The ability of pDCs to present Ag and prime naïve CD4⁺ T cells is a source of controversy (Sapozhnikov et al., 2007; Kool et al., 2011), but, regardless of this, it is clear from my data that purified CCL2^{hi} and CCL2^{lo} pDCs did not differ substantially in their ability to prime CD4⁺ T cells.

Next, I analysed the ability of the two subsets of pDCs to cross-present OVA to naïve TCR transgenic Ag-specific CD8 α ⁺ T cells (Figure 5-18). In contrast to CD4⁺ T cell priming, both pDC subsets were capable of inducing high levels of CD8 α ⁺ T cell proliferation as shown by CFSE dilution (Figure 5-18A). However, approximately 20% of T cells remained undivided in cultures with either pDC subset. In contrast, in cultures of CD8 α ⁺ T cells with cDCs there were much lower numbers of undivided T cells. Accordingly, the frequency of T cells that had undergone more than three divisions was higher in cDCs (Figure 5-18B). There were no differences in the number of T cells that had undergone more than 3 divisions when cultured with CCL2^{hi} or CCL2^{lo} pDCs (Figure 5-18B). Likewise, when the frequency of T cells in each division was quantified there was also no difference between the two pDC subsets (Figure 5-18C).

Figure 5-18D shows the proportion of DCs and T cells in the culture after day 3. These plots show, as expected, that all B220⁻CD11c⁻ cells were the added transgenic CD8 α ⁺ T cells. More importantly these plots show that there were very few contaminating B220⁻CD11c⁺ cDCs in all pDC cultures, which could not account for the high level of CD8 α ⁺ T cells proliferation (Figure 5-17). Thus, the majority of the observed proliferation in the pDC cultures was likely due to pDCs rather than contaminating cDCs, although contributions by non-pDCs cannot be completely excluded.

There is a discrepancy in the percentage of T cells, both CD4⁺ and CD8 α ⁺ that divided when incubated with total pDCs or the two subsets of pDCs. I found that

a much high proportion of CD4⁺ T cells (~30%) and CD8 α ⁺ T cells (~75%) divided when cultured with total pDCs than sorted CCL2^{hi} and CCL2^{lo} pDCs. CCL2^{hi} and CCL2^{lo} pDCs only caused ~5% of CD4⁺ T cells (Figure 5-16C) and ~50% of CD8 α ⁺ T cells to proliferate (Figure 5-18B). Thus, incubation at 37°C with CCL2^{AF647} may affect pDCs ability to present OVA to T cells. Importantly, the decrease in T cell priming efficiency was also observed with cDCs in the same experiments, even though they were not exposed to CCL2^{AF647}. One possible explanation could be that in order to retrieve adequate numbers of CCL2^{hi} and CCL2^{lo} pDCs there was a considerable lengthening of the sort time (the sort took over 12 hrs, twice as long as a sort for total pDCs), which could negatively impact the viability of sorted cells.

5.7.1.1 Effect of pDC activation by TLR7 ligand on CD8 α ⁺ T cell stimulation

I next examined whether activation of the two pDC subsets affected their ability to present Ag and stimulate T cell proliferation (Figure 5-19). I concentrated on naïve CD8 α ⁺ T cells because pDCs stimulated a higher proliferative response in these cells compared to naïve CD4⁺ T cells. As Figures 5-19A and 5-19B illustrate, in the presence of the TLR7 agonist R848, there was a significant increase in the frequency of divided T cells. Importantly, there were no differences in the T cell stimulatory capacity between the two pDC subsets in the presence or absence of R848 stimulation (Figure 5-19B). I then calculated the frequency of T cells in each division when stimulated with CCL2^{hi} (Figure 5-19C) or CCL2^{lo} pDCs (Figure 5-19D) with or without R848 activation. Both subsets presented similar trends in that there was a significant reduction in the number of cells in division 0 and 1 in the presence of R848 and an increase in the number of cells in the later divisions, particularly divisions 4, 5 and 6. A relatively minor difference between the subsets was that R848 stimulated CCL2^{lo} pDC samples had significantly more T cells that had undergone 5 or 6 divisions than in the absence of R848, whereas the increase present in CCL2^{hi} samples was not significant. However, there were no other obvious differences between the two subsets and the data firmly indicate that R848 stimulated CCL2^{hi} or CCL2^{lo} pDCs do not differ substantially in their ability to stimulate naïve CD8 α ⁺ T cell proliferation.

5.7.1.2 Establishing the impact of mCCL2 on pDC induced CD8 α^+ T cell proliferation

In light of the observed differences in CCR2 activity between the two subsets, I monitored the effect of continuous exogenous mCCL2 exposure on the ability of the two pDC subsets to induce CD8 α^+ T cell proliferation (Figure 5-20). Either 0, 12.5 or 25 nM of exogenous mCCL2 was added to the co-culture of pDCs with CD8 α^+ T cells. Representative histograms of CFSE dilution illustrate that there were no major differences in the induction of T cell proliferation between the two subsets and mCCL2 had no effect. Also, when the number of CD8 α^+ T cells that had undergone more than 3 divisions was calculated there were no differences between the two subsets, and mCCL2 had no effect on the CD8 α^+ T cell stimulatory capacity of the two subsets.

To summarise, these results indicate that FACS-purified pDCs from the spleens of B16FL tumour bearing mice are unable to, or have limited ability to, process and present OVA to naïve CD4 $^+$ T cells. They are, however, able to stimulate proliferation of OVA specific naïve CD8 α^+ T cells. CCR2 activity did not segregate with any differences in the CD8 α^+ T cell stimulatory capacity of pDCs, either in steady-state or after activation by the TLR7 agonist R848. Furthermore, the addition of exogenous mCCL2 did not affect the ability of either pDC subset to stimulate CD8 α^+ T cell proliferation. While these results do not exclude the possibility that CCR2 expression may affect other pDC functions, they conclusively demonstrate that CCR2 expression/activity has no impact on the ability of pDCs to present Ag, at least *in vitro*.

5.7.2 Analysing IFN α production by the two subsets

One key role of pDCs is in defence against viral infections, executed following their activation by TLR7/9 and subsequent mass IFN α/β production (Gibson et al., 2002; Björck et al., 2011). Thus, I next assessed the ability of the two subsets (purified from the spleens of B16FL treated mice) to produce IFN α in response to the TLR7 agonist, R848 and a TLR9 agonist, CpG type A (CpG-A) (Figure 5-21). CpG-As are known for their propensity to induce pDCs to produce large amounts of IFN α . In accordance with this, both CCL2 hi and CCL2 lo pDCs produced copious amounts of IFN α when stimulated with CpG-A. Stimulation

with R848 also caused IFN α production, but it was significantly lower than with CpG-A. There were no significant differences between the subsets in their ability to produce IFN α in response to TLR7/9 activation in this experimental setup.

Collectively, considering marker expression, morphology, T cell activation and IFN α production, I have shown that there are no substantial functional differences between CCL2^{hi} and CCL2^{lo} pDCs.

5.8 Determining transcriptional differences between CCL2^{hi} and CCL2^{lo} pDCs using transcriptomics

Other than possibly CCR2, and subtle changes in expression of CCR9 and CX₃CR1, my analysis to this point had failed to establish any major differences in surface protein expression between CCL2^{hi} and CCL2^{lo} pDC subsets. Nevertheless, only a minor number of markers were tested, so I decided to more broadly examine transcriptional differences between the two subsets. Thus, a comparison between CCL2^{hi} and CCL2^{lo} pDCs was performed by using microarray technology.

5.8.1 Experimental design

The primary objective of this study was to compare the transcriptional profiles of CCL2^{hi} and CCL2^{lo} pDCs. However, to isolate these subsets it would be necessary to incubate splenocytes with CCL2^{AF647} for 1 hr at 37°C prior to sorting the cells. It was theorised that this incubation could result in alterations in the gene expression profile of the cells as a result of, for example, CCR2 signalling, differentiation, or cell death. Thus, it was felt at the outset of the experiment that it was important to try to control for this. To do this, I chose to use total pDCs purified from B16FL treated mice, without incubating them *ex vivo* at 37°C or exposing them to CCL2^{AF647}. In brief, following the preparation of a single cell suspension, cells were stained, total pDCs purified and RNA for the microarray was isolated from the cells. It was hypothesised that if genes were identified as differentially expressed between CCL2^{hi} and CCL2^{lo} pDCs, subsequent comparisons of CCL2^{hi} pDCs to total pDCs, and CCL2^{lo} pDCs to total pDCs, would give an indication of whether gene expression had been modulated by culture. To assist with this analysis, it is important to consider that ~50% of total pDCs have high CCR2 activity and ~50% have low CCR2 activity. Thus, if a gene was

found to be expressed higher in CCL2^{hi} pDCs than CCL2^{lo} pDCs, then, if its expression was unaffected by culture, we would expect that transcripts for this gene would be higher in CCL2^{hi} pDCs than total pDCs, and lower in CCL2^{lo} pDCs than total pDCs. A graphical representation of this is displayed in Figure 5-22A. Similarly, if a gene was found to be expressed at lower levels in CCL2^{hi} than CCL2^{lo} pDCs, then, if its expression was unaffected by culture, we would expect that this gene would be lower in CCL2^{hi} pDCs than total pDCs, and higher in CCL2^{lo} pDCs than total pDCs (Figure 5-22B). However, if a gene was differentially expressed between CCL2^{hi} and CCL2^{lo} pDCs, but its expression had been affected by culture, then a different profile would be expected when CCL2^{hi} or CCL2^{lo} pDC expression was compared to total pDCs (Figure 5-22C&D). For example, if a gene was found to be expressed higher in CCL2^{hi} pDCs than CCL2^{lo} pDCs, but had been upregulated by culture in both subsets, then we would expect transcripts for this gene to be higher in CCL2^{hi} pDCs and CCL2^{lo} pDCs when compared to total pDCs (Figure 5-22C). Similarly, if a gene was found to be expressed at lower levels in CCL2^{hi} pDCs than CCL2^{lo} pDCs, but had been downregulated by culture in both subsets, then we would expect transcripts for this gene to be lower in CCL2^{hi} and CCL2^{lo} pDCs than total pDCs (Figure 5-22D). Thus, by comparing CCL2^{hi} and CCL2^{lo} pDCs to total pDCs, we hoped that we would be able to get an indication of the impact of culture on the expression of each individual gene.

5.8.2 Performing the microarray

Total pDCs, CCL2^{hi} and CCL2^{lo} pDCs were sorted from the spleens of B16FL tumour bearing mice, RNA was extracted and it was sent to the Glasgow University Polyomics Facility for analysis. Each sample was tested for RNA concentration and integrity (Figure 5-23). RNA integrity number (RIN) is a software algorithm, which assigns a value to each RNA sample based on the presence or absence of degradation products. The optimal value for RIN is 10, which indicates that RNA is intact and has not been digested by RNase enzymes resulting in smaller fragments of RNA that can effect downstream applications, in this case microarray (Schroeder et al., 2006). As the table in Figure 5-23 illustrates, all samples had good RNA integrity, although unfortunately due to a malfunction of one of the RNA 6000 Nano kits, no values were retrieved for the CCL2^{hi} 3 and CCL2^{lo} 3 samples. Furthermore, the ratio of 260/280 gives

information in regards to RNA purity with the optimal value being 2.1. A high level of protein contamination of the RNA sample will result in a lower 260/280 value being calculated. Thus, as values in Figure 5-23 illustrate all samples were relatively pure.

Based on this analysis, it was decided to proceed with the microarray. The Mouse Gene 1.0 ST Array from Affymetrix was chosen, as it comprises probes that target exons of over 28,000 known genes and requires low amounts of RNA, working with as low as 100 ng of RNA. Each gene on the chip is represented by 27 probes that are distributed across the full length of the gene. These probes are in set pairs, each pair consisting of a perfect match and a mismatch oligonucleotide. As the name implies, the perfect match probe matches exactly the sequence of the gene, whereas the mismatch probe differs by a single central base substitution. Mismatch probes facilitate the identification of background noise caused by non-specific hybridisation compared to specific hybridisation. Non-specific binding is only one of the many variations that microarrays are subject to, with variation deriving from differences in samples, differences in chips, and the hybridisation between chips (Jiang et al., 2008). Therefore, normalisation of data is required to correct for these sources of standard variation. First, the data were subject to GC-RMA normalisation, which facilitates background correction. GC-RMA is an improved version of the robust multi-array average (RMA) method. RMA is an algorithm that corrects for non-specific binding by using only the intensity values generated by the perfect match probes. The data is then subject to normalisation, resulting in approximately the same distribution of perfect match probe values across all chips. The intensity values from all the perfect match probes for an individual gene are then summarised to give a single intensity value for the gene, which correlates with the amount of mRNA present for the corresponding gene (Irizarry et al., 2003). GC-RMA builds on the RMA method, as it also accounts for non-specific hybridisation by normalising probes for their GC content. Each perfect match probe will have different levels of GC content. GC is stickier and can lead to non-specific binding and a higher level of background than a probe that is AT rich. Therefore, the perfect match probe intensities are corrected for their GC content by adjusting the value according to a mismatch probe with the same GC content. This generates a normalised signal intensity for each gene. Pawel

Herzyk, Glasgow University Polyomics Facility, helped in the selection of the appropriate array, in addition to processing and normalising the data.

Furthermore, Dr. Herzyk also calculated the fold change (FC) between the CCL2^{hi}, CCL2^{lo} and total pDC samples using the normalised values for each gene. He also performed a large scale one-way ANOVA to calculate the differences between the samples with Storey multiple-testing correction.

5.8.3 Examination of genes differentially expressed in CCL2^{hi} or CCL2^{lo} pDCs

Before the microarray data was interpreted to establish differences in gene expression between the two subsets, some restrictions were applied that would minimise the chance of false positives. I applied a cut off of a FC of 1.5 between the CCL2^{hi} and CCL2^{lo} pDCs. Therefore, the CCL2^{hi} or CCL2^{lo} pDCs must express a gene 1.5x more than the other subset in order for it to be included. A further restraint was applied to the data, in that the calculated p-value for the FC had to be $p < 0.005$, which upon correction for multiple-testing correlates to a q-value of 0.344 generating a false discovery rate of 34.4%. Using these limits, a list of genes that were potentially differentially expressed between CCL2^{hi} and CCL2^{lo} pDCs was generated and is represented as a heat-map in Figure 5-24. This initial characterisation revealed a number of things. First, it was noticeable that CCL2^{lo} pDCs expressed less CCR2 than CCL2^{hi} pDCs. Furthermore, several of the genes expressed at higher levels in CCL2^{lo} pDCs have been suggested to have roles in tumour growth suppression, such as *rhobtb2* (Mao et al., 2009), *phf17* (Zhou et al., 2005) and *ephb2* (Kandouz et al., 2010). Also, in the CCL2^{hi} pDCs, interferon induced transmembrane proteins (*ifitm*) 1 and 3 were upregulated compared to CCL2^{lo} pDCs. These proteins are thought to contribute to viral defence (Huang et al., 2011). The list also showed that pDC enriched genes, such as *E2-2* and *pacsin1* (Ghosh et al., 2010; Reizis et al., 2011a) were not differentially expressed between the two subsets and that markers that were earlier assessed by flow cytometry, and D6 and other chemokine receptors were not differentially expressed at the level of mRNA transcripts.

5.8.4 Impact of culture on expression of genes identified as differentially expressed by CCL2^{hi} and CCL2^{lo} pDCs

I next determined whether incubation with CCL2^{AF647} at 37°C had any discernible effects on the expression of the genes shown in Figure 5-24. As discussed above, by comparing the calculated FCs in expression of a gene between the three groups of pDCs i.e. CCL2^{hi} pDCs vs. CCL2^{lo} pDCs, CCL2^{hi} pDCs vs. total pDCs and CCL2^{lo} pDCs vs. total pDCs, it was possible to establish whether incubation had substantially affected the expression of the gene of interest (Figure 5-25).

If we assume that cells with low and high CCR2 activity are present at roughly equal proportions in the total pDC preparation (not an unreasonable assumption based on work presented earlier in this thesis), then, based on the observed FC between CCL2^{hi} and CCL2^{lo} pDCs, it is possible to estimate the expected FC when CCL2^{hi} pDCs vs. total pDCs and CCL2^{lo} pDCs vs. total pDC comparisons are made, if there had been no effect of culture on gene expression. This is summarised in Table 5-1.

CCL2 ^{hi} pDCs vs. total pDCs Expected FC, if no affect of culture	CCL2 ^{lo} pDCs vs. total pDCs Expected FC, if no affect of culture	CCL2 ^{hi} pDCs vs. CCL2 ^{lo} pDCs Observed FC
1.20x - 1.33x	0.67x - 0.80x	1.50x - 2.00x
1.33x - 1.42x	0.57x - 0.67x	2.00x - 2.50x
1.42x - 1.50x	0.50x - 0.57x	2.50x - 3.00x
1.50x - 1.56x	0.44x - 0.50x	3.00x - 3.50x

Table 5-1: Expected FCs when a gene is expressed at higher levels in CCL2^{hi} pDCs than CCL2^{lo} pDCs, and its expression is not affected by culture.

When this is considered, some genes in Figure 5-25, such as *ifitm1*, *card10*, *map3k14* and particularly *jup*, clearly showed higher FC in CCL2^{hi} pDCs vs. total pDCs and CCL2^{lo} pDCs vs. total pDCs than anticipated. This indicates that these genes are upregulated to the same extent in both CCL2^{hi} and CCL2^{lo} pDCs during culture. In contrast, two genes showed a somewhat lower FC in CCL2^{hi} pDCs vs. total pDCs than predicted. These genes were *cd200r1* and, most notably, *ccr2*. With a FC in CCR2 expression between CCL2^{hi} and CCL2^{lo} pDCs of 3.26, if there had been no impact of culture and assuming that cells with low and high CCR2

activity are present at roughly equal proportions in the total pDC preparation, then a FC of 1.53 would be expected for the CCL2^{hi} pDCs vs. total pDC comparison and of 0.47 for CCL2^{lo} pDCs vs. total pDCs. The actual values were 0.82 and 0.25, respectively. One interpretation of these observations is that culture in CCL2^{AF647} leads to a reduction in CCR2 transcripts in both CCL2^{hi} and CCL2^{lo} pDCs.

A similar analysis can be undertaken for the genes that are lower in CCL2^{hi} pDCs than CCL2^{lo} pDCs (Figure 5-25B). With the assumptions outlined above, the predicted FC in CCL2^{hi} pDCs vs. total pDCs and CCL2^{lo} pDCs vs. total pDCs, based on the observed FC in CCL2^{hi} pDCs vs. CCL2^{lo} pDCs are shown in Table 5-2.

CCL2 ^{hi} pDCs vs. total pDCs	CCL2 ^{lo} pDCs vs. total pDCs	CCL2 ^{hi} pDCs vs. CCL2 ^{lo} pDCs
Expected FC, if no affect of culture	Expected FC, if no affect of culture	Observed FC
0.62x - 0.80x	1.20x - 1.38x	0.67x - 0.45x

Table 5-2: Expected FCs when a gene is expressed at lower levels in CCL2^{hi} pDCs than CCL2^{lo} pDCs, and its expression is not affected by culture.

Many genes expressed at lower levels in CCL2^{hi} pDCs than CCL2^{lo} pDCs behave roughly as expected and give similar profiles in the graph in Figure 5-25B. However, some genes, most notably *ppargc1a*, give greater FC in CCL2^{hi} pDCs vs. total pDCs and CCL2^{lo} pDCs vs. total pDCs than expected, suggesting that they are upregulated in both subsets by culture. Others, such as *ppm1e* and *rhobtb2*, had somewhat lower FC in CCL2^{hi} pDCs vs. total pDCs and CCL2^{lo} pDCs vs. total pDCs, so may be downregulated in both subsets as a result of culture.

5.8.5 Alterations in gene expression in pDCs as a result of culture with CCL2^{AF647}

Next, I specifically examined whether there were expression differences apparent in the microarray data of genes other than those analysed in Figures 5-24 and 5-25 that could be attributable to incubation of the pDCs in CCL2^{AF647} at 37°C. This was done by comparing expression of all genes between CCL2^{hi} pDCs and total pDCs (the former had been incubated at 37°C and exposed to CCL2^{AF647}, while the latter had been purified straight from a single cell

suspension of splenocytes from mice carrying B16FL tumours). When setting the p-value as <0.005 , large numbers of genes showed a >2 -fold increase or decrease in expression in CCL2^{hi} pDCs compared to total pDCs (~250 and ~150 genes, respectively). With almost all these genes, similar FCs were seen when CCL2^{lo} pDCs were compared with total pDCs (data not shown). Thus, incubation caused substantial changes in gene expression in pDCs, but it appeared to have similar effects on both subsets. For purposes of simplification, only genes that showed a >3 -fold increase or decrease in expression in CCL2^{hi} pDCs compared to total pDCs are shown in Figure 5-26. All these genes with their respective FCs are shown in Appendix 1. Of these, many genes were more highly expressed in CCL2^{hi} pDCs than total pDCs, but a few were expressed at lower levels in CCL2^{hi} compared to total pDCs. One transcript, *hspb1*, was 20-30-fold more abundant in cultured pDCs than freshly-isolated cells, while others, such as *il1r2*, *vdr*, *bag2* and *tnfsf9*, were >5 -fold higher in cultured pDCs. Some genes showed differential expression between CCL2^{hi} and CCL2^{lo} pDCs of >1.5 FC, but these had been excluded from preceding analyses because they had p-values that were too high.

To get some indication of what might be happening to the pDCs during culture, I examined data publicly available through the Immunological Genome Project (Immgen) (<http://www.immgen.org>). The Immgen database contains expression data for all genes by a large number (>250) of purified primary immune cell types (Bezman et al., 2011; Benoist et al., 2012; Malhotra et al., 2012; Miller et al., 2012). I specifically looked at expression of the genes I had identified by first using the 'Dendritic Cells' section of this database with a view to assessing their expression by pDCs. This section contains data for pDCs from spleen and LNs, along with data from a large array of other DC subtypes, such as splenic and LN cDCs, lung and intestinal DC subsets, and skin-derived Langerhans cells (LCs). Remarkably, most of the genes that were >3 -fold higher in cultured pDCs than fresh total pDCs were barely expressed by pDCs, but they were abundant in other DC subsets. Moreover, when I looked at other non-DC cell types on the Immgen database, it was apparent that many of these genes were in fact restricted to DCs. This is depicted in Figure 5-26 where the genes are colour coded according to the cell type they were found to have highest expression of the gene: blue represents genes reported to be expressed at high levels by LCs, red by the several cDC subsets and black by cell types other than cDCs, LCs and

pDCs. Furthermore, genes expressed at higher levels in pDCs than LCs are shown in pink and genes with similar expression levels between pDCs and LCs are shown in green. These results suggest that the majority of genes affected by culture were those reported to be expressed specifically at high levels by LCs and cDCs, and most were weakly, or not expressed at all, by pDCs. Since I had purified pDCs to near homogeneity for the microarray study, it is possible that this reflects some form of differentiation of these cells to LC/cDC-like cells in culture. This will be discussed further in the Discussion in Chapter 6.

Thus, incubation at 37°C with CCL2^{AF647} appears to affect expression of many genes in pDCs, and this needs to be considered when interpreting transcriptional differences between CCL2^{hi} and CCL2^{lo} pDCs. However, it appears that both subsets were similarly affected by incubation. Moreover, with a few notable exceptions, the transcript level of most of the genes differentially expressed between CCL2^{hi} and CCL2^{lo} pDCs does not appear to be substantially altered by culture.

5.8.6 Further analysis of gene differences between the two subsets

Due to time constraints, not all the genes in the initial list (Figure 5-24) could be subject to further analysis. Therefore, additional restrictions needed to be applied. The Immgen database was again used to determine the reported expression levels of each gene in pDCs. Any gene that was not expressed at an appreciable level in pDCs, according to Immgen, was removed from the list. This generated a much shorter list of pDC-expressed genes (Figure 5-27A). Similar to the earlier list it consisted of a range of genes that encode for transcription factors, signalling molecules and cell surface receptors, including CCR2.

Next, the microarray results needed to be subjected to quality control. I selected a number of genes from the list in Figure 5-27 that had a broad range of expression in pDCs i.e. low and highly expressed genes according to Immgen. Each of these genes was specifically chosen for their low p-values and/or high FC. Furthermore, a relatively even distribution of genes upregulated in either the CCL2^{hi} or the CCL2^{lo} pDCs was maintained, as 6 genes were selected that were upregulated in either the CCL2^{hi} or CCL2^{lo} subset. Several of the selected

genes were also chosen for their described roles. For example, *gbp4* was selected for the reported effects it possesses in regulating type 1 IFN production by targeting *irf7* (Hu et al., 2011). *cox6a2* was included due to its high expression in pDCs, being one of the most pDC specific genes that was differentially expressed between the two subsets. *rarg* was chosen as it has been demonstrated that an absence of *rarg* can lead to a decrease in pDC numbers in the spleen (personal communication by Stephanie Houston, University of Glasgow). *phf17* has been described as possessing tumour suppression properties (Zhou et al., 2005), which is in contrast to the described role of pDCs that can suppress the immune response to tumours by rendering the immune system tolerogenic (Kim et al., 2007). Furthermore, several of the genes, such as *il17rb*, *il13ra1* and *cd200r1* were all chosen because they are surface receptors with potential immunoregulatory roles. As one of the receptors for IL-25 (IL-17E), IL-17RB has been associated with the development of IL-25 induced pulmonary inflammation (Rickel et al., 2008). IL-13 has been reported to reduce human pDC responsiveness to CpG, as in its presence CpG activated pDCs had lower expression of the activation markers CD83 and CD86 (Tel et al., 2010). CD200 the ligand of CD200R1 can influence an immune response by controlling polarisation of cytokine production, and its aberrant expression is associated with autoimmune diseases, such as SLE (Li et al., 2012). Furthermore, pDCs can be induced to release IFN α as a consequence of CD200R1 engagement by CD200-expressing cells (Manlapat et al., 2007).

Quality control checks were run on the list of genes in Figure 5-27B by quantifying their expression in CCL2^{hi} and CCL2^{lo} pDCs using QPCR. The QPCR was conducted using cDNA produced from the same RNA that was sent for microarray. However, there was a malfunction in the QPCR and all results produced were 'flagged' and an accurate reading for expression could not be determined (results not shown). There was insufficient time to generate further pDC samples, so as an alternate means to validate the microarray data, I examined the expression of a select few genes that encode surface receptor proteins by FACS, such as IL-13Ra1 and CD200R1 (Figure 5-28). Following gating of total pDCs in B16FL treated animals, the expression of CD200R1 and IL-13Ra1 on CCL2^{hi} and CCL2^{lo} pDCs was determined. Comparison of CD200R1 and IL-13Ra1 staining of WT cells to the appropriate isotype stain (Figure 5-28A) illustrates

that there is staining of both CCL2^{hi} and CCL2^{lo} pDCs with each antibody. When these results were quantified there was no difference in the calculated CD200R1 Δ MFI of CCL2^{hi} and CCL2^{lo} pDCs. There was however a significant increase in the IL-13Ra1 Δ MFI of CCL2^{hi} pDCs compared to CCL2^{lo} pDCs, which was consistent with the microarray data in Figure 5-27. Next it was theorised that treatment with Flt3L may have affected the expression of CD200R1 or IL-13Ra1 from levels that would be detected in an untreated WT animal. Therefore, I determined the frequency of CCL2^{hi} and CCL2^{lo} pDCs that expressed CD200R1 in WT B16FL treated and untreated animals, in addition to untreated CD200R1 KO animals (Figure 5-28C). The CD200R1 KO was included as an additional control to confirm true antibody staining in the WT animals. The number of CCL2^{lo} pDCs with CD200R1 immunoreactivity was significantly higher in untreated WT than B16FL treated, but CD200R1 staining was also detected on both subsets of pDCs in the CD200R1 KO. This once again highlights the problems with antibodies targeted against surface receptors. I also established the frequency of CCL2^{hi} and CCL2^{lo} pDCs in a B16FL treated or untreated WT that express IL-13Ra1 (Figure 5-28D). Consistent with the earlier observation, IL-13Ra1 expression was lower in CCL2^{lo} pDCs in both treated and untreated animals, however there was only a small proportion of both CCL2 subsets that were IL-13Ra1⁺. Flt3L treatment does however appear to cause a significant reduction in IL-13Ra1 expression by CCL2^{hi} and CCL2^{lo} pDCs.

In an initial experiment I also tried to examine IL-17RB expression by the two subsets with no success. IL-17RB antibodies are unavailable commercially but were obtained from Andrew McKenzie's lab (University of Cambridge, UK) (Ballantyne et al., 2007). The conjugation of the antibody to a fluorophore failed and due to time constraints further attempts were not conducted.

5.8.7 Effect of IL-13 on the activation of CCL2^{hi} and CCL2^{lo} pDC

Taking into account the results illustrating that IL-13Ra1 is differentially expressed between the two pDC subsets, I next tested the effect exogenous IL-13 had on CpG-C induced pDC activation (Figure 5-29). Previous results have shown that IL-13 modulated TLR9 induced activation of human pDCs as measured by the expression of activation markers (Tel et al., 2010). It was found that incubation of both CCL2^{hi} and CCL2^{lo} pDCs (isolated from spleens of B16FL

tumour bearing mice) with CpG-C resulted in the division of both subsets into a further two populations based on SiglecH expression, one being high and one low for SiglecH (Figure 5-29A). The SiglecH^{hi} and SiglecH^{lo} populations were then examined for expression of the activation markers CD86 and ICOS-L (Figure 5-29B&C). The expression of both activation markers was found to be restricted to the SiglecH^{hi} populations of both CCL2^{hi} and CCL2^{lo} pDCs, with the SiglecH^{lo} population having similar expression of the activation markers as unstimulated total pDCs. The addition of IL-13 had no effect on the activation of the SiglecH^{hi} populations of both CCL2^{hi} and CCL2^{lo} subsets, as determined by the expression of CD86 (Figure 5-29D) and ICOS-L (Figure 5-29E). There was no difference in the relative proportions of SiglecH^{hi} and SiglecH^{lo} pDCs in the two CCL2 subsets. Furthermore, IL-13 had no effect on the frequency of SiglecH^{hi} and SiglecH^{lo} pDCs (Figure 5-29F). There was also no difference in the survival of cells, as there were similar frequencies of live CCL2^{hi} and CCL2^{lo} pDCs, which were also unaffected by IL-13 (Figure 5-29G).

5.8.8 Summary of microarray analysis

In brief summary, this section of my thesis has shown that some transcriptional differences exist between CCL2^{hi} and CCL2^{lo} pDCs, but it is clear that these two subsets do not differ dramatically at the level of gene expression. Importantly, they confirmed that CCL2^{hi} pDCs have higher levels of CCR2 transcripts than the CCL2^{lo} pDCs. Furthermore, higher IL-13Ra1 transcript levels were detected in the CCL2^{hi} pDC subsets. Antibody staining of IL-13Ra1 surface protein also helped to confirm the existence of a small difference in IL-13Ra1 expression by the two CCL2 subsets, as although there was only a low proportion of pDCs that were IL-13Ra1⁺, CCL2^{hi} pDCs had significantly more IL-13Ra1 on their surface. However, addition of IL-13 to cultures had no effect on CpG-induced activation. Furthermore, these data suggest that the two pDC subsets do not differ in viability or in their ability to mature in response to CpG. The microarray data will be discussed in more detail in Chapter 6.

5.9 Strain dependent differences in the phenotype of pDCs

The *in vitro* analyses demonstrated that CCL2^{hi} and CCL2^{lo} pDCs were very similar phenotypically in many assays. However, the development, phenotype and function of pDCs *in vivo* might be influenced by CCR2 deficiency. Thus, I next compared pDCs from WT and CCR2 KO mice. D6 KO mice were also included in the analysis. These animals were available, and my results have provided evidence for D6 expression by pDCs. First, I examined CCL2^{AF647} uptake by WT, D6 KO and CCR2 KO pDCs in a range of tissues (Figure 5-30). Previously, I have shown that the majority of CCL2^{AF647} uptake by pDCs is CCR2 dependent. Furthermore, I also demonstrated that both WT and CCR2 KO pDCs possessed D6 activity (Figure 5-3). Therefore, it was expected that in the absence of CCR2, pDCs would only internalise a little CCL2^{AF647} due to the presence of D6. D6 KO pDCs were expected to have profiles similar to WT pDCs i.e. large amount of CCR2 dependent CCL2^{AF647} uptake, but it would be reduced in comparison to WT pDCs due to the absence of D6 dependent CCL2^{AF647} uptake. As expected in all tested tissues, CCR2 KO pDCs internalised little CCL2^{AF647}, due to the deficiency in CCR2 mediated CCL2^{AF647} uptake (Figure 5-30). Unexpectedly, in the first experiment, all D6 KO pDCs in every tested tissue appeared to be CCL2^{hi} (Figure 5-30 left hand FACS panel). However, on repeating the experiments, I found that this phenotype was not always present, and approximately 50% of the time D6 KO pDCs had profiles similar to WT animals (Figure 5-30 right hand FACS panel). In the case of D6 KO splenic pDCs these profiles have been observed in 4 independent experiments, normal uptake profiles (i.e. similar to WT pDC) were found in 5 animals, whereas the abnormal profile (i.e. all pDCs are CCL2^{hi}) was found in 7 animals. The reason for this striking difference between D6 KO mice is unclear. It does, however, mean that data produced using D6 KO pDCs need to be interpreted with caution.

I next sought to determine whether there were any strain differences in the expression of the majority of the markers discussed in section 1.5 (Figure 5-31 and Figure 5-32). The percentage of pDCs that were positive for expression of each marker in WT, CCR2 KO and D6 KO was determined in the spleen (Figure 5-31A) and BM (Figure 5-32A). In the spleen the only tested markers that showed any strain dependent differences in expression were CD8 α , CD62L, CCR7 and

CD69. The most striking difference was with CD8 α . CD8 α was expressed by significantly fewer pDCs in D6 KO compared to WT, whereas CCR7 was expressed by significantly more pDCs in the D6 KO. CD62L and CD69 were both expressed at very low levels, but differences between the mouse strains were still present. CD62L was expressed by significantly more pDCs in the D6 KO and CD69 was expressed by significantly fewer pDCs in D6 KO and CCR2 KO, compared to WT. These differences were highlighted in histogram overlays in Figure 5-31B, illustrating the higher expression of CD62L and lower expression of CD8 α by splenic D6 KO pDCs compared to WT and CCR2 KO. Also, illustrated is the increase in CD69 expression by WT pDCs compared to D6 KO and CCR2 KOs. Quantification of the Δ MFI of each of these markers supported the observed strain differences, and showed the dramatic decrease in CD8 α expression by D6 KO pDCs (Figure 5-31C). Earlier in Figure 5-11, I demonstrated that the anti-CCR7 antibody failed to detect CCR7 on WT splenic pDCs or on total live splenocytes. The spleen is a rich source of T and B lymphocytes, which are known to express CCR7, therefore I reported that the antibody was unreliable. However, the antibody mediated detection of CCR7 on splenic D6 KO pDCs and representative histogram overlays showed the presence of a CCR7^{hi} population within the D6 KO that was absent in the other strains. In contrast, when CCR7 expression was examined on total live splenocytes it again failed to detect CCR7 by T or B lymphocytes (Figure 5-31B). Therefore the anti-CCR7 antibody is an unreliable method to detect CCR7 and the significant increase in 'CCR7 expression' by D6 KO splenic pDCs is unclear.

When the expression of these markers was analysed on BM pDCs there were some notable differences between the strains (Figure 5-32), and within strains when compared to the profile generated by splenic pDCs (Figure 5-31A). Similar to splenic pDCs, few WT and CCR2 KO BM pDCs expressed CD9, but dramatically a significant and much higher proportion of D6 KO BM pDCs were found to express CD9. As with splenic pDC data, CD62L was expressed at low levels, but significantly more pDCs in the D6 KO expressed CD62L, compared to WT and CCR2 KO. The same was true for CCR7, but for the aforementioned reasons this result is questionable. However, in contrast to the spleen data, there were no detectable differences in CD8 α expression. Furthermore, a higher proportion of WT pDCs expressed the activation markers, CD69 and CD86, but expression of

both of these markers, as shown in histogram overlays and Δ MFI was very low in all three strains. A significantly greater proportion of WT pDCs expressed the gut homing integrin $\alpha 4\beta 7$, but there a significant reduction in the proportion of pDCs expressing the gut homing chemokine receptor, CCR9 in WT animals, compared to D6 KO and CCR2 KOs. CCR9 Δ MFI data suggested that the increase in the proportion of pDCs in D6 KO BM expressing CCR9 was due to an increase in CCR9 expression by CCR9⁺ cells. In contrast, the increase in CCR9⁺ CCR2 KO pDCs appeared to be because of the absence of CCR9⁻ pDCs, as nearly 100% of CCR2 KO pDCs were CCR9⁺. There were also some strain dependent differences observed in CCR2 KO BM pDCs in regards to CD4 expression. There was a significant increase in the number of CCR2 KO BM pDCs that expressed CD4 compared to both WT and D6 KO. These differences are highlighted in Figure 5-32B, where representative histograms show the strain differences in expression of the discussed markers. Furthermore, calculation of the Δ MFI of each of the markers further emphasised some of the striking differences in expression by BM pDCs from the different mice strains, in particular CD9 expression by D6 KO pDCs (Figure 5-32C).

Finally, examination of absolute number of splenic and BM pDCs in WT, CCR2 KO and D6 KO animals (Figure 5-33) illustrated that the deletion of either CCR2 or D6 had no apparent effects on pDC numbers.

These results have illustrated that in mice lacking CCR2 or D6 there are some unexpected differences in the expression of certain surface markers, most strikingly CD9 in the D6 KO BM pDCs. However, interpretation of the D6 KO data requires caution because of the marked variability in results of CCL2^{AF647} uptake assays. The results described above were generated from three D6 KO mice, one of which had the abnormal CCL2^{AF647} uptake profile. Further experiments are required to assess the reproducibility of the findings, dissect the mechanisms responsible, and define their impact on pDC function.

5.10 Investigating a role for CCR2 on pDCs during inflammation *in vivo*

In Chapter 3, I showed that there was no difference in the frequency of pDCs between WT and CCR2 KO animals in the spleen, BM and blood (Figure 3-15).

Furthermore, in Figure 5-33 I determined the absolute number of BM and splenic pDCs in WT and CCR2 KO animals and found no significant differences. These results indicate that CCR2 is not required for steady-state pDC migration to spleen or for their emigration from the BM.

5.10.1 Effect of CCR2 deficiency on pDCs during cutaneous inflammation

As CCR2 only appeared to have a minor role in pDC migration during homeostatic conditions, I next tested whether CCR2 plays a role in pDC migration during inflammation. It is known that imiquimod treatment leads to skin inflammation and the recruitment of pDCs to the site of inflammation reportedly in a CCL2 dependent manner (Palamara et al., 2004; Drobits et al., 2012). Imiquimod is a TLR7 agonist that has potent anti-viral and anti-tumour effects (Gibson et al., 2002). Thus, I determined the absolute number of pDCs in the skin of WT and CCR2 KO animals subsequent to their daily treatment for 7 days with cutaneous application of imiquimod (Figure 5-34). Unexpectedly, there was a significant increase in the number of pDCs that migrated to the skin of CCR2 KO animals than that of WT animals, indicating that CCR2 is not required for pDC migration to the skin. However, this increase in pDC numbers in the skin could be explained by a dependence on CCR2 for pDC escape from the skin into draining LNs. Therefore, I next determined the absolute number of pDCs in the draining inguinal LNs in WT and CCR2 KO, but found no difference in pDCs numbers between these two strains (Figure 5-35). I also examined the effect of imiquimod treatment on pDC numbers in other immune compartments. There was no difference in the absolute number of splenic pDCs between the two strains, but imiquimod treatment appeared to cause a decrease in the number of splenic pDCs (Figure 5-36). Trends in data suggest that imiquimod treatment might cause a decrease in BM pDC numbers, with a corresponding increase in the blood of CCR2 KOs (Figures 5-37 and 5-38). However, the results were not significant according to statistical analysis and further repeat experiments will be required.

5.10.2 Effect of imiquimod on CCR2 activity of pDCs

In addition to determining the absolute number of pDCs within the tissues, I also examined the effect of imiquimod treatment on the CCR2 activity of pDCs. In

the inguinal LN (Figure 5-35), spleen (Figure 5-36) and BM (Figure 5-37) the proportion of CCL2^{hi} and CCL2^{lo} pDCs was perturbed, as they no longer constituted ~50% of the total pDC population. There was only ~25% CCL2⁺ pDCs in WT samples, which was still significantly higher than in CCR2 KO, indicating some residual CCR2 dependent uptake by WT pDCs. The WT and CCR2 KO pDCs also possessed D6 activity, demonstrated by competition with mCCL2. There was an increase in the proportion of CCL2^{lo} pDCs in WT samples, but there were still significantly more CCL2^{lo} pDCs in the CCR2 KO. Blood samples followed similar trends to the other tissues in that pDCs possessed CCR2 and D6 dependent uptake, but the ratio of CCL2^{hi} and CCL2^{lo} pDCs was relatively unaltered, with CCL2^{hi} pDC contributing ~45% of total pDCs (Figure 5-38).

In summary, although pDCs migrate to CCL2 *in vitro*, I have been unable to find an indispensable *in vivo* role for CCR2 on pDCs in the models used.

5.11 Summary

The data in this chapter have demonstrated that two subsets of pDCs based on CCL2 uptake are identifiable. These were present in all tested lymphoid tissues and possessed both CCR2 and D6 activity. I found that although Flt3L could induce the formation of BM-derived pDCs *in vitro* there were variations in the CCR2 activity of the cells at the different time-points and with the different sources of Flt3L. Therefore, following initial pilot experiments I successfully used B16FL cells to increase pDC numbers by approximately 10-fold *in vivo*, with no effects on CCR2 activity, as both CCL2^{hi} and CCL2^{lo} pDC subsets were still present. The resultant increase in pDC numbers as a consequence of Flt3L treatment facilitated sorting of reasonable numbers of CCL2^{hi} and CCL2^{lo} pDCs, which could be examined for transcriptomic and functional differences. Comparisons of the two subsets at the transcript level illustrated that CCR2 was differentially expressed, but there was no difference in D6 transcript levels between the two subsets. Several other genes were also differentially expressed by the two CCL2 subsets, such as *il13ra1*. However, IL-13 did not affect the activation of either pDC subset. Furthermore, these results showed that although incubation at 37°C with CCL2^{AF647} did affect expression of many genes, only a few genes that were differentially expressed by the two CCL2 subsets were affected.

There were no significant functional differences between the two subsets, both subsets possessed similar capacities to produce IFN α in response to TLR7/9 agonists. Furthermore, both subsets were able to process and present Ag to naïve CD8 α^+ T cells, and to a limited extent CD4 $^+$ T cells. In addition, activation of pDC by R848 treatment resulted in an increase in the ability of both subsets to stimulate CD8 α^+ T cell proliferation. However, exogenous CCL2 had minimal effects on the ability of the CCL2 hi and CCL2 lo subsets to stimulate CD8 α^+ T cell proliferation.

My results suggest that CCR2 may have a role in pDC migration, as I have shown that the CCL2/CCR2 pathway can mediate migration of total pDCs *in vitro*. However, pDCs showed no dependence on CCR2 for their emigration from the BM or into peripheral tissues in a resting animal. Furthermore, imiquimod induced inflammation resulted in an increase in pDC migration to the skin, which was CCR2 independent. Interestingly, although imiquimod treatment resulted in downregulation of CCR2 activity on pDCs there appeared to be no effect on D6 activity, as it was still present in pDCs in all tested tissues. Furthermore, examination of the surface phenotype of pDCs in WT, D6 KO and CCR2 KO animals illustrated strain dependent differences in expression of several markers, in particular D6 deletion led to a substantial increase in CD9 expression by BM pDCs. These apparent chemokine receptor dependent changes in surface immunophenotype clearly merit further investigation.

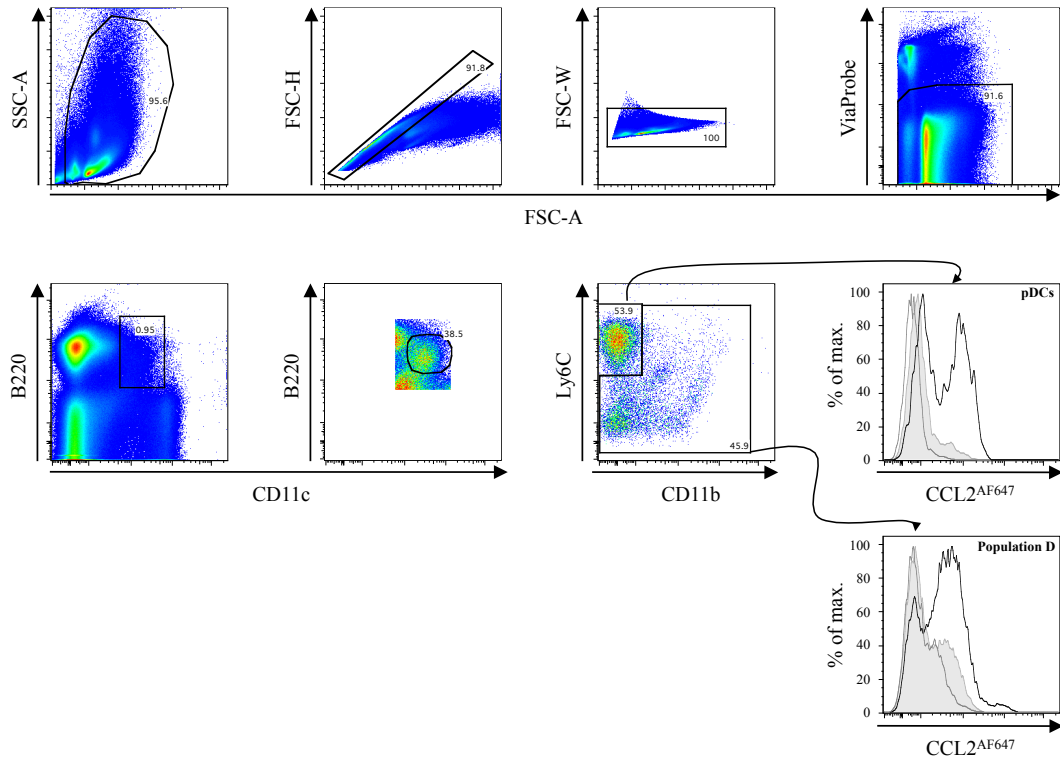


Figure 5-1: Detection of two subsets of splenic pDCs based on CCL2^{AF647} uptake.

Following exclusion of doublets, live splenocytes were gated as B220⁺CD11c⁺. Subsequently, a more stringent B220⁺CD11c⁺ gate was applied. B220⁺CD11c⁺ cells were then gated as Ly6C⁺ and CD11b⁻ (pDCs). The remaining B220⁺CD11c⁺ cells, excluding pDCs were also gated (Population D). CCL2^{AF647} uptake was then examined within these populations. Representative histograms of WT (black line) and CCR2 KO (shaded grey area) cells incubated with CCL2^{AF647} alone, or CCL2^{AF647} uptake in CCR2 KO competed with 10-fold molar excess mCCL22 (grey line). The CCL2^{AF647} histogram overlays of pDCs are the same as ones shown in Figure 3-11. Plots are representative of a minimum of three biological replicates.

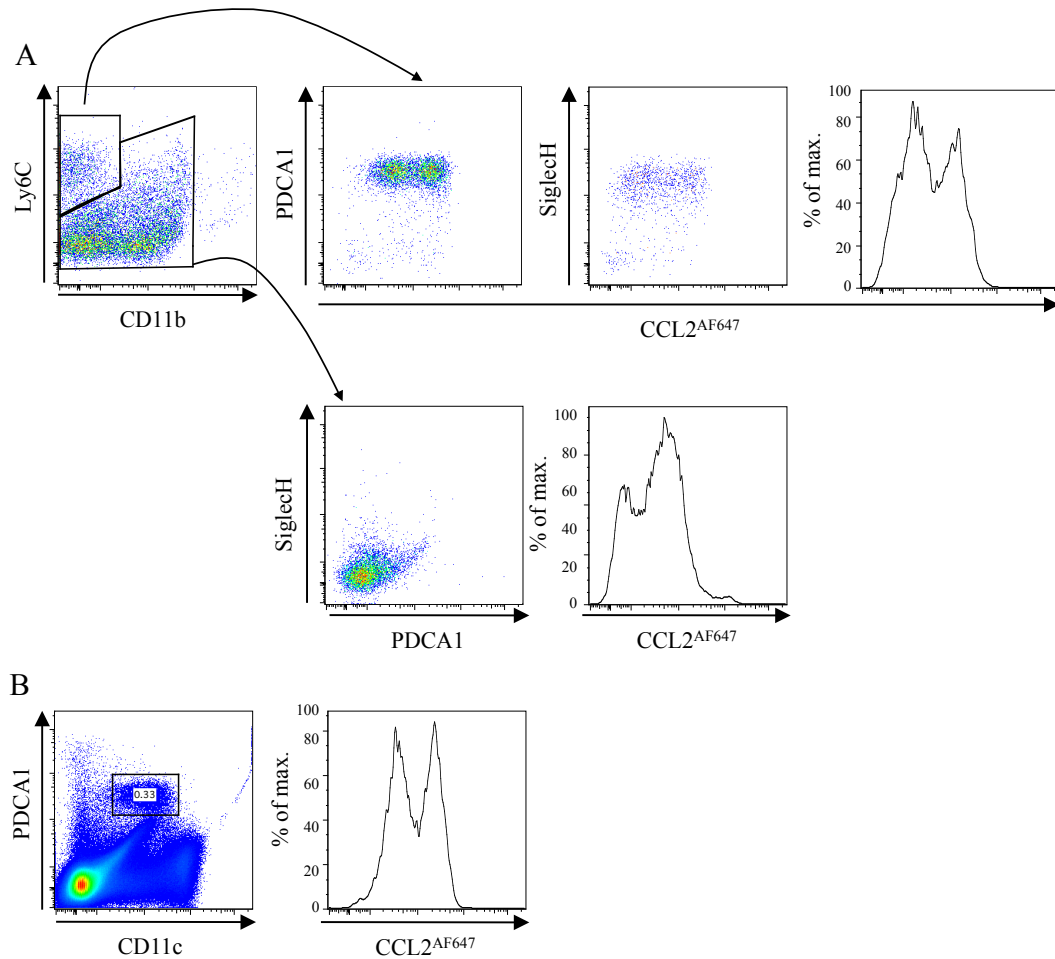


Figure 5-2: Confirmation that the two subsets are truly pDCs.

(A) Splenic pDCs and Population D were gated as described in Figure 5-1, and the two pDC subsets based on CCL2^{AF647} and Population D were examined for the expression of two pDC specific markers, PDCA1 and SiglecH. (B) Following exclusion of doublets, live splenocytes were gated as PDCA1⁺CD11c⁺. CCL2^{AF647} uptake was then examined within this population. Plots are representative of a minimum of three biological replicates.

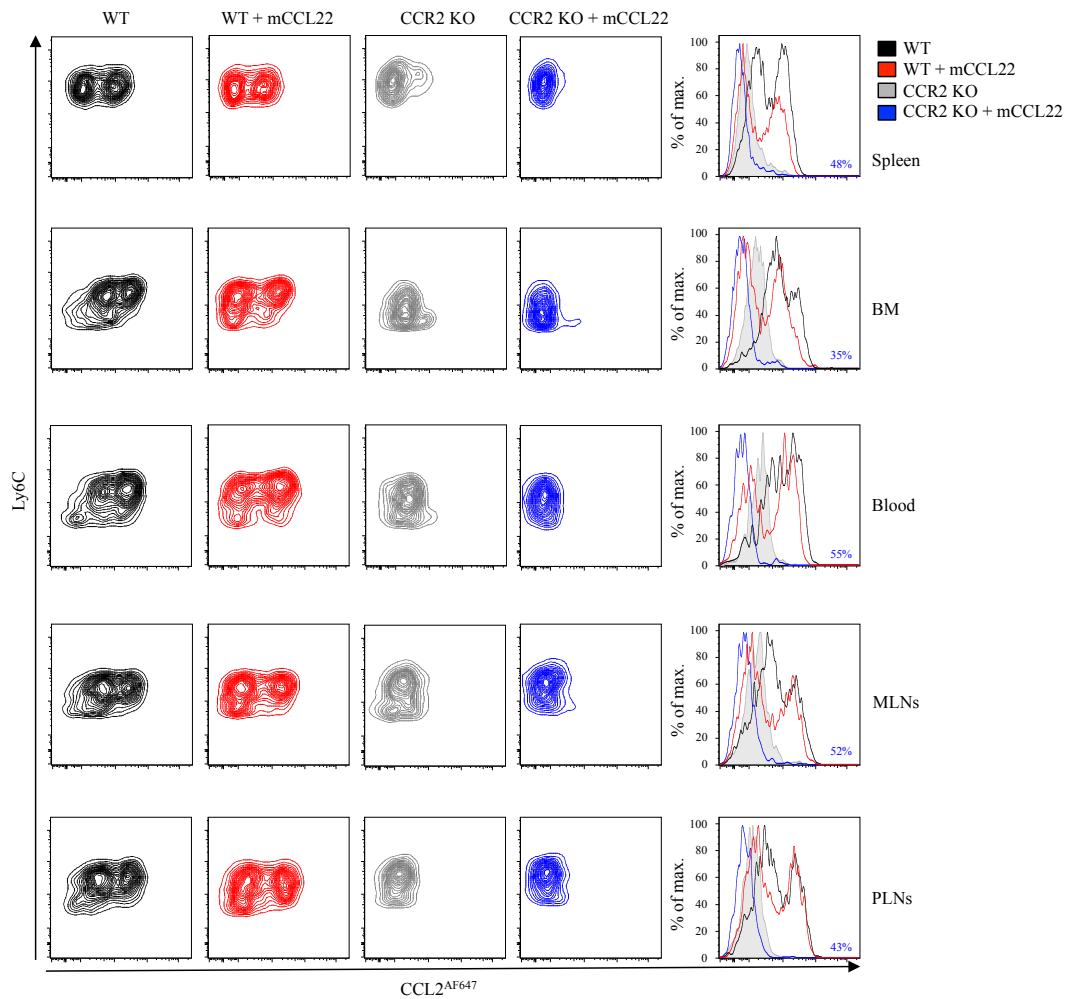


Figure 5-3: Two subsets of pDCs can be defined by CCL2^{AF647} uptake in other lymphoid tissues.

pDCs from the spleen, BM, blood, MLNs and PLNs of WT and CCR2 KO were gated as described in Figure 5-1, and analysed for uptake of CCL2^{AF647}. WT (black) and CCR2 KO (grey) cells incubated with CCL2^{AF647} alone, or CCL2^{AF647} uptake was competed with 10-fold molar excess mCCL22 in WT (red) or CCR2 KO (blue). Representative contour plots from each mouse strain and histogram overlays show CCL2^{AF647} uptake by pDCs. The proportion of CCL2^{hi} cells is shown in each histogram. Plots are representative of a minimum of three biological replicates.

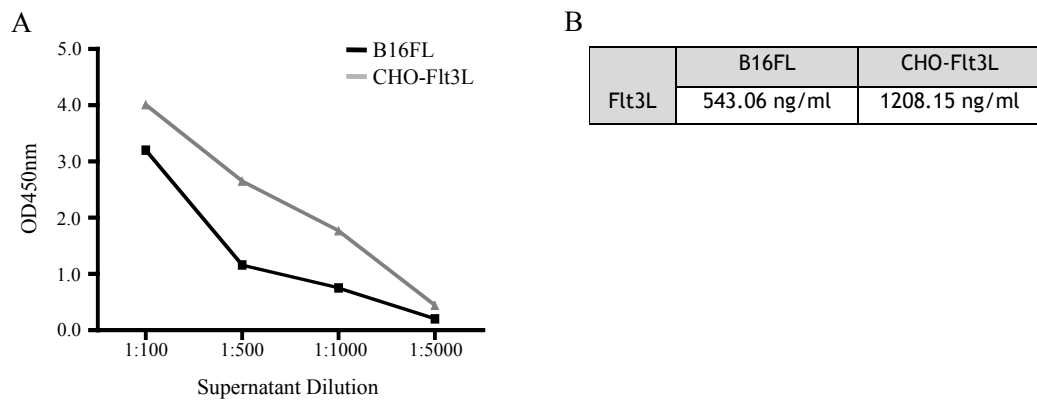


Figure 5-4: Production of Flt3L by CHO-Flt3L and B16FL cells.

(A) Conditioned media retrieved from cultures of B16FL (black line) and CHO-Flt3L (grey line) cells were assessed for Flt3L content by ELISA after dilution. (B) Concentration of Flt3L in conditioned media as determined by ELISA in A by comparison to a standard curve.

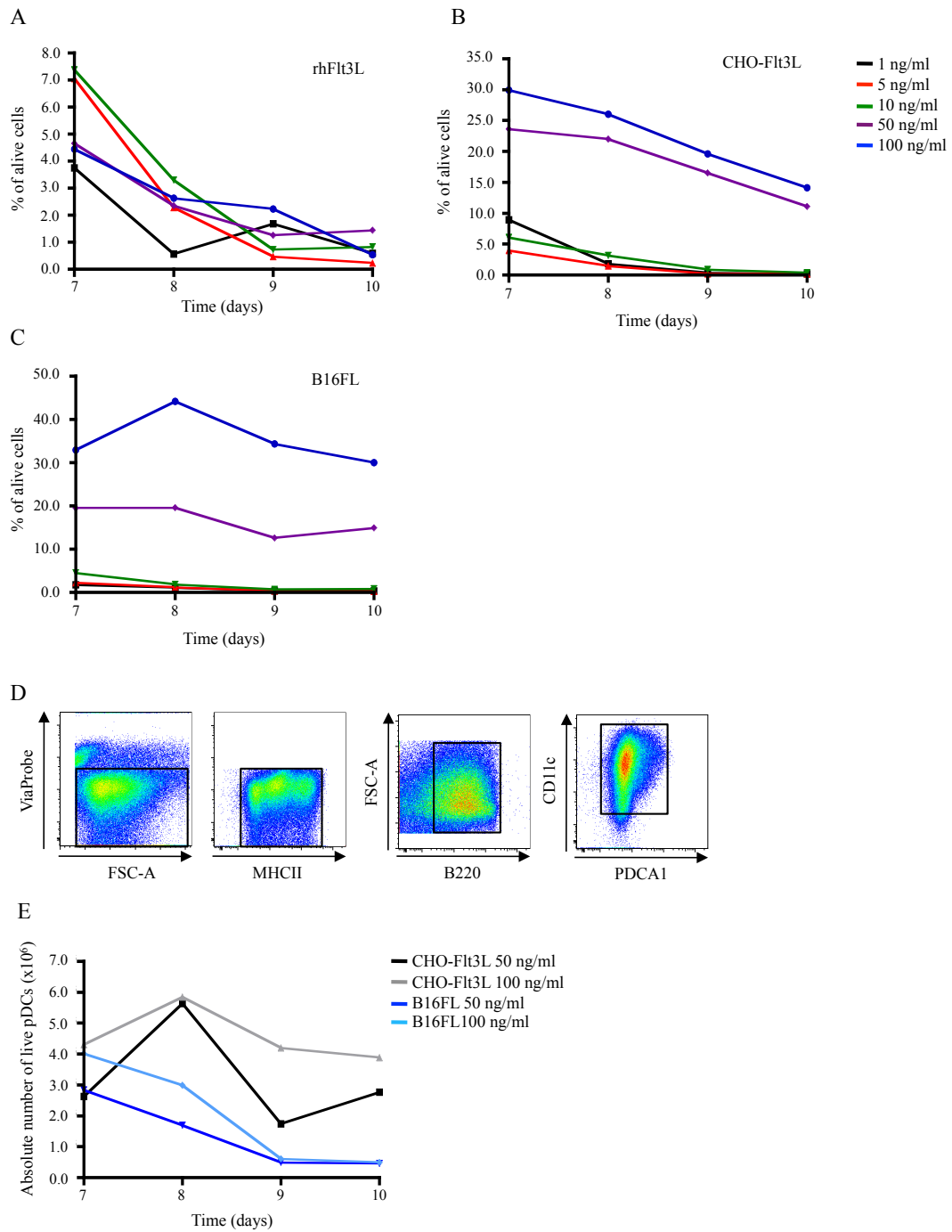


Figure 5-5: *In vitro* Flt3L expansion of pDCs.

(A-C) 2×10^6 BM cells per condition were incubated for 7-10 days in the presence of varying concentrations of rhFlt3L (A), CHO-Flt3L (B) or B16FL (C). The frequency of total live cells (i.e. ViaProbe negative cells) was determined for each condition, 1 ng/ml (black line), 5 ng/ml (red line), 10 ng/ml (green line), 50 ng/ml (purple line) and 100 ng/ml (blue line). (D&E) 1×10^7 BM cells per condition were incubated for 7-10 days in the presence of either 50 ng/ml CHO-Flt3L (black line), 100 ng/ml CHO-Flt3L (grey line), 50 ng/ml B16FL (dark blue line) or 100 ng/ml B16FL (light blue line). The absolute number of live BM-pDCs, gated as indicated in (D) was determined for each condition.

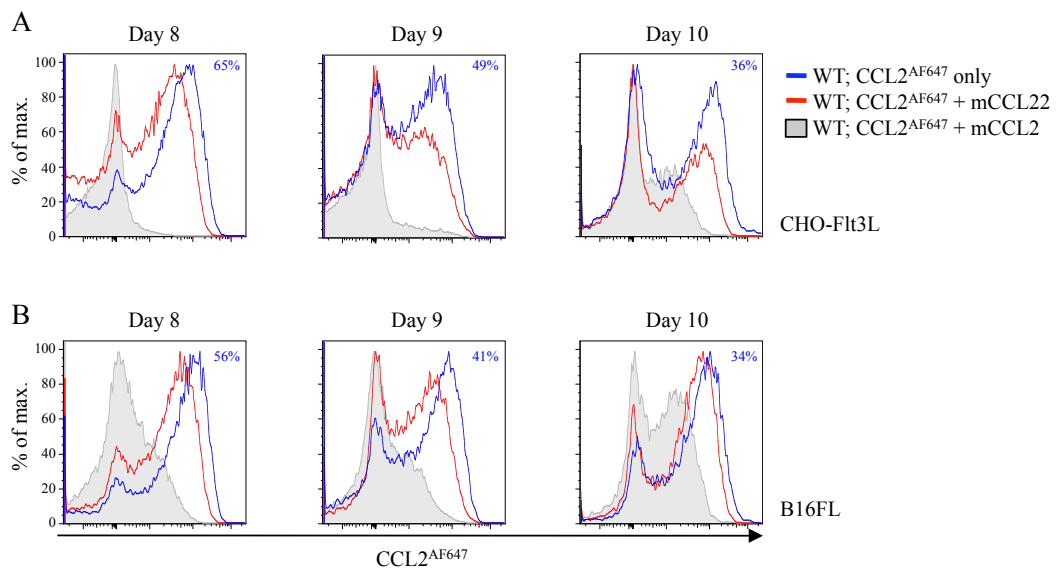


Figure 5-6: Effect of *in vitro* Fit3L treatment on CCR2 activity of pDCs.

CHO-Fit3L (A) or B16FL (B) WT BM-pDCs at day 8, day 9 or day 10 of culture with 100 ng/ml Fit3L (gated as described in Figure 5-5), were analysed for uptake of CCL2^{AF647}. Histogram overlays show CCL2^{AF647} uptake by pDCs with no competition (blue line), or CCL2^{AF647} uptake competed with 10-fold molar excess of either mCCL22 (red line) or mCCL2 (shaded grey area). The percentage of CCL2^{hi} cells in each culture is indicated in each histogram.

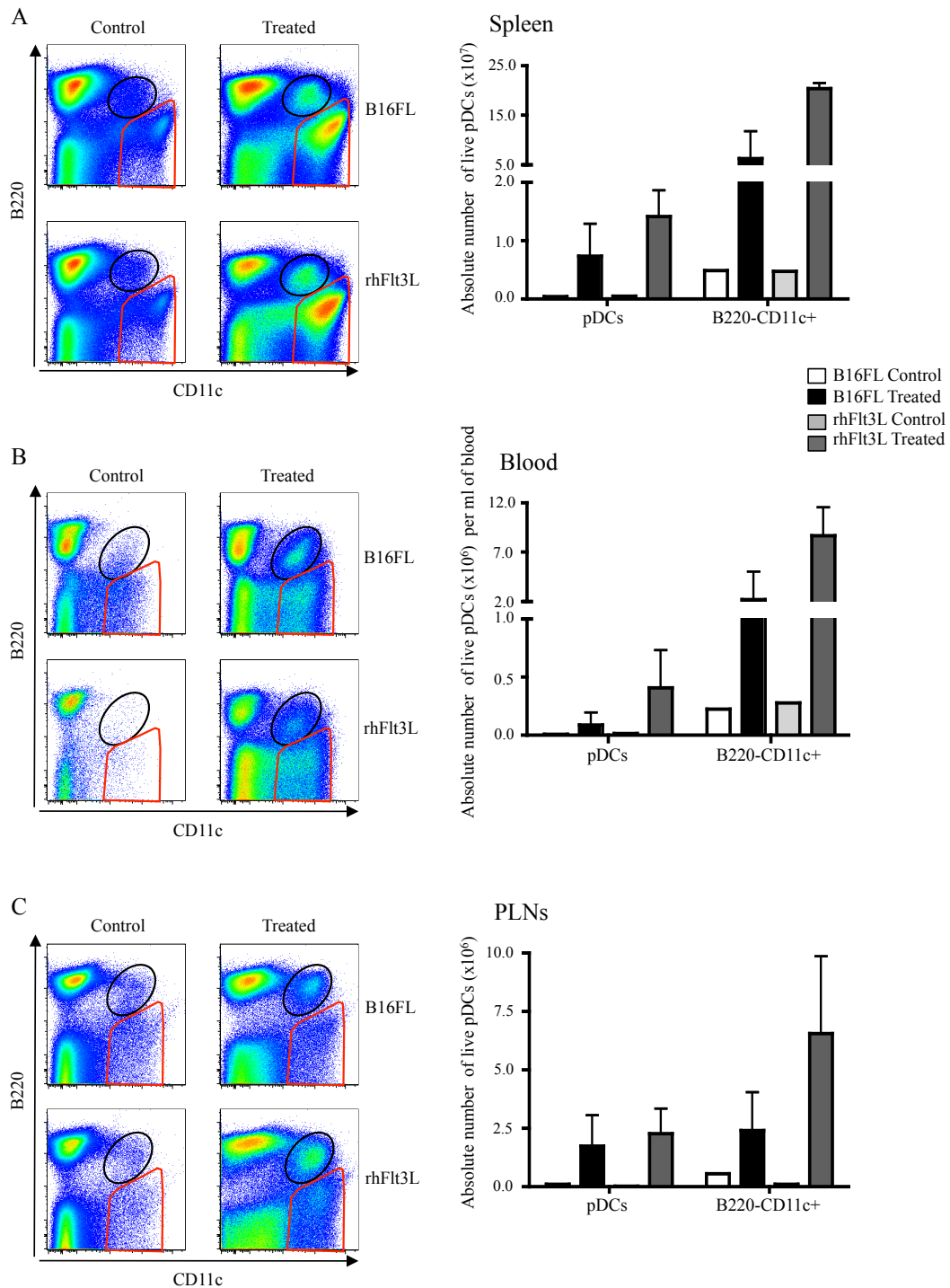


Figure 5-7: *In vivo* Flt3L expansion of pDCs.

WT animals were left untreated (B16FL control) or injected s.c. with 2×10^6 B16FL tumour cells (B16FL treated) and were sacrificed 13 days later. $CX_3CR1^{GFP/+}$ mice were injected i.p. with $10 \mu\text{g}$ rhFlt3L (rhFlt3L treated) or PBS (rhFlt3L control) for 10 consecutive days. Representative plots illustrate the increase in pDC proportions (black gate) and $B220^-CD11c^+$ cells (red gate) in the spleen (A), blood (B) and PLNs (C), with the calculated absolute cell numbers shown. pDCs in rhFlt3L control or treated animals were gated as depicted in Figure 5-1. pDCs in B16FL control or treated animals were also gated as described in Figure 5-1, however they were also gated as SiglecH⁺. For each control, only one mouse was used and for each treated condition $n = 2$ (mean + SD).

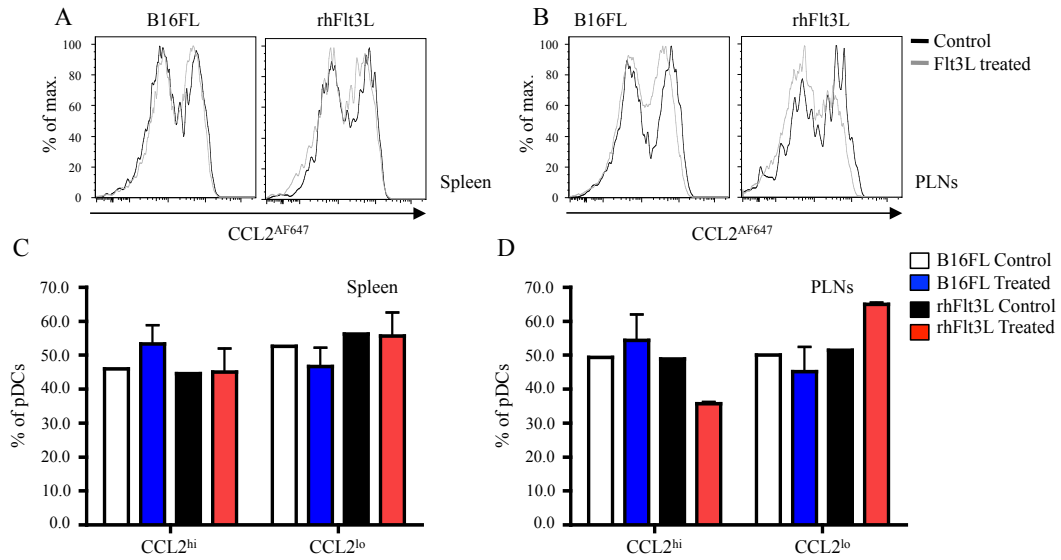


Figure 5-8: Effect of *in vivo* Flt3L treatment on the two subsets of pDCs as defined by CCL2^{AF647} uptake.

WT animals were left untreated (B16FL control) or injected s.c. with 2×10^6 B16FL tumour cells (B16FL treated) and harvested 13 days later. CX₃CR1^{GFP/+} mice were injected i.p. with 10 μ g rhFlt3L (rhFlt3L treated) or PBS (rhFlt3L control) for 10 consecutive days. Splenic (A) and PLN (B) pDCs (gated as described in Figure 5-7) were analysed for uptake of CCL2^{AF647}. Histogram overlays show CCL2^{AF647} uptake by pDCs in control animals (black line) or Flt3L treated, B16FL or rhFlt3L (grey lines). (C&D) The frequency of CCL2^{hi} and CCL2^{lo} pDCs was determined in control and treated animals, and plotted as a frequency of live pDCs. B16FL Control (white bars), B16FL Treated (blue bars), rhFlt3L Control (black bars) and rhFlt3L Treated (red bars). For each control, only one mouse used and for each treated condition, n = 2 (+ SD).

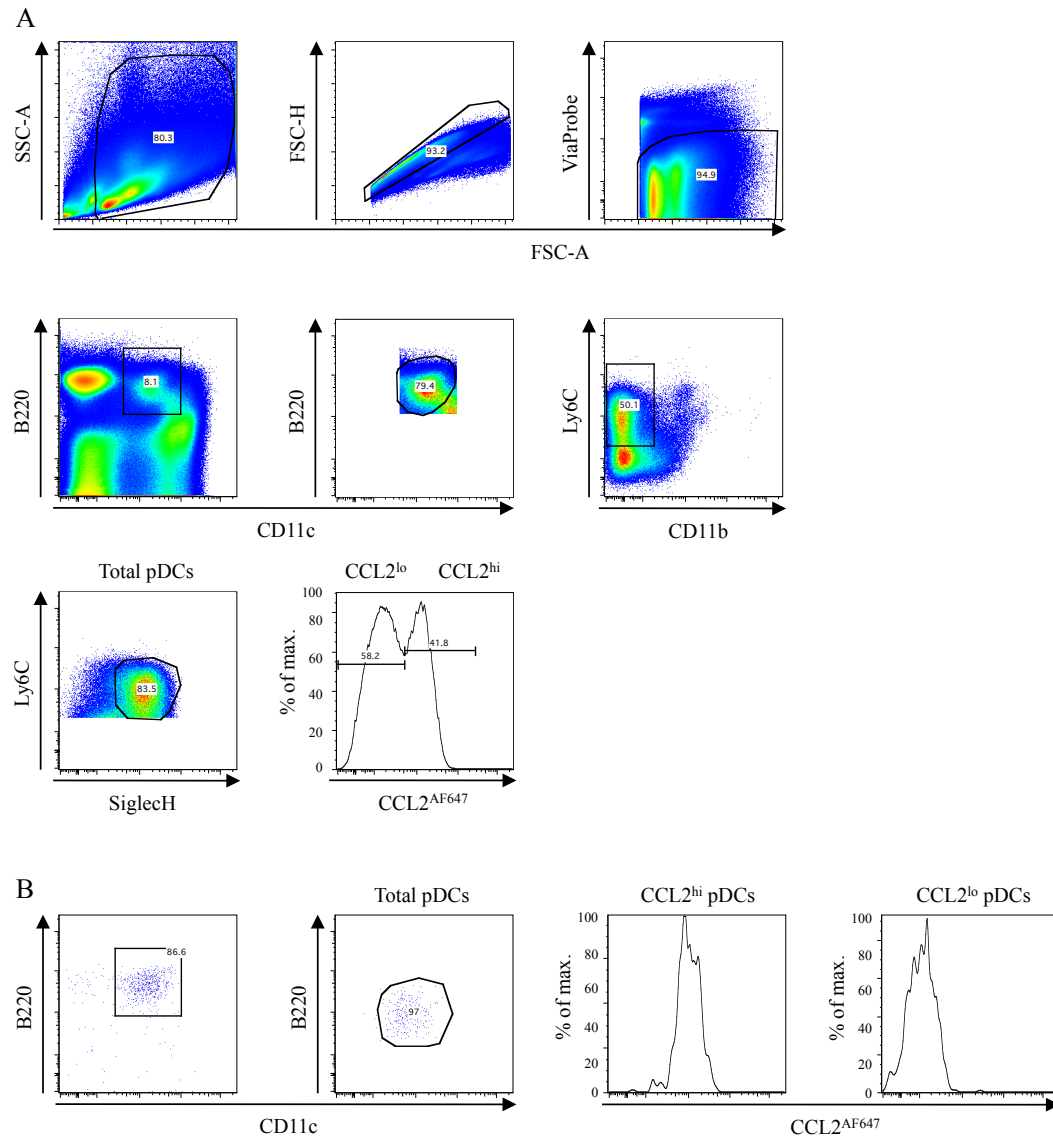


Figure 5-9: Gating strategy for isolating splenic pDCs and the two subsets of pDCs.

(A) Following exclusion of doublets, live cells were gated as $B220^+CD11c^+$. Subsequently, a more stringent $B220^+CD11c^+$ gate was applied. $B220^+CD11c^+$ cells were then gated as $Ly6C^+$ and $CD11b^-$. They were then examined for SiglecH expression and gated as $SiglecH^+$ (named total pDCs). CCL2^{AF647} uptake was then examined within this population, with the subsequent populations being named CCL2^{hi} pDCs or CCL2^{lo} pDCs. (B) An example of the typical purities gained following a sort for the two subsets of pDCs.

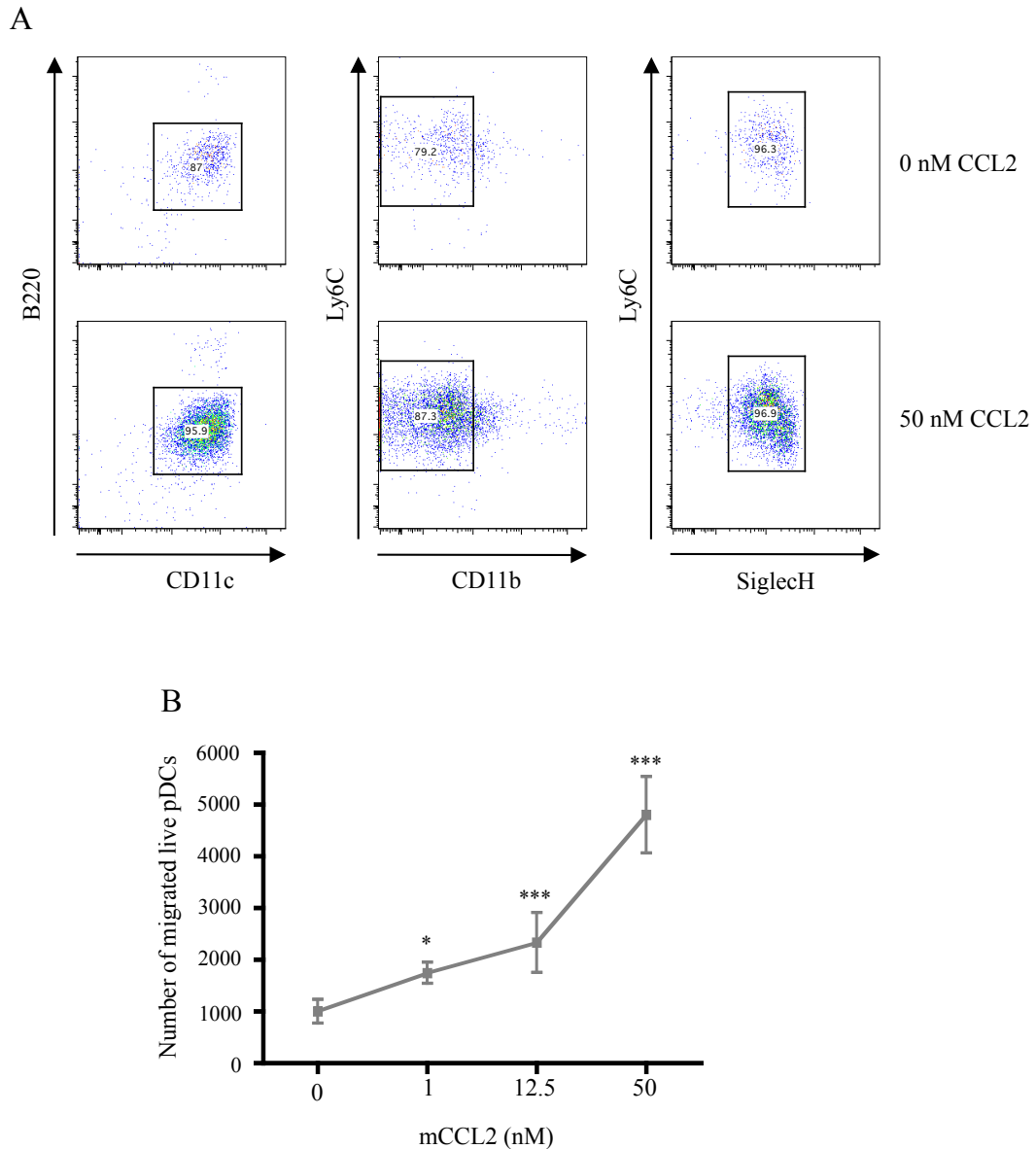


Figure 5-10: Migration of pDCs in response to CCL2 *in vitro*.

Total pDCs from WT animals carrying B16FL tumours were sorted according to the gating strategy depicted in Figure 5-9. 1×10^5 pDCs were incubated on the top of a chemotactic chamber above varying concentrations of unlabelled mCCL2 (0, 1, 12.5 and 50 nM) for 3 hrs. The number of migrated cells at each concentration was recorded by FACS. (A) Representative plots of flow cytometry of migrating cells in response to 0 nM and 50 nM mCCL2. (B) Graphical representation of absolute number of pDCs that migrated in response to increasing levels of mCCL2. Results were generated from two independent experiments with 3 or 5 technical replicates per experiment (mean \pm SD). Data were analysed by one-way ANOVA with Tukey post-test comparing migration at all concentrations to that observed at 0 nM CCL2 i.e. media alone $p < 0.05$ * and $p < 0.001$ ***.

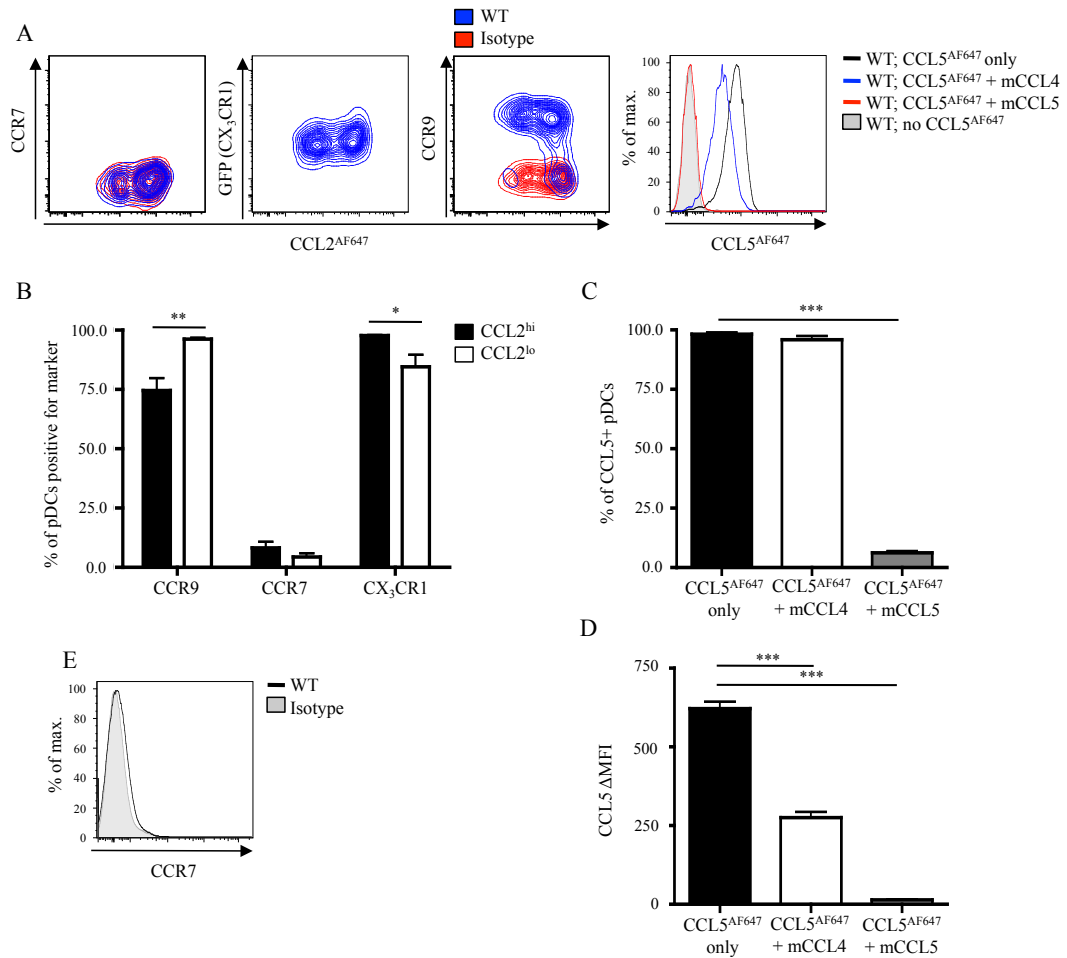


Figure 5-11: Expression of other chemokine receptors by splenic pDCs.

pDCs from the spleen of WT animals (gated as described in Figure 5-1) were analysed for uptake of either CCL2^{AF647} or CCL5^{AF647} and expression of other chemokine receptors known to be expressed by pDCs. (A) Representative contour plots from WT spleen stained with antibody (blue) or appropriate isotype (red). For CX₃CR1 detection, a CX₃CR1^{GFP/+} mouse was used. Representative histogram overlays show CCL5^{AF647} uptake by pDCs with no competition (black line) or CCL5^{AF647} uptake competed with 10-fold molar excess of either murine CCL4 (blue line) or murine CCL5 (red line). A further control of cells incubated with only binding buffer is shown (shaded grey area). (B) The frequency of CCL2^{hi} (black bars) and CCL2^{lo} pDCs (white bars) expressing each marker. (C) The proportion of cells taking up CCL5^{AF647} with no competition (black bar) or competed with 10-fold molar excess of either mCCL4 (white bar) or mCCL5 (grey bar). (D) CCL5 geometric mean fluorescence intensity (ΔMFI) of WT splenic pDCs. CCL5^{AF647} with no competition (black bar) or competed with 10-fold molar excess of either mCCL4 (white bar) or mCCL5 (grey bar). Data were analysed by unpaired T-test (B) or one-way ANOVA with Tukey post-test (C&D) $p < 0.05$ * and $p < 0.01$ ** $n = 3$ (mean + SD). (E) Illustration of CCR7 staining in all live cells. Plots are representative of a minimum of three biological replicates.

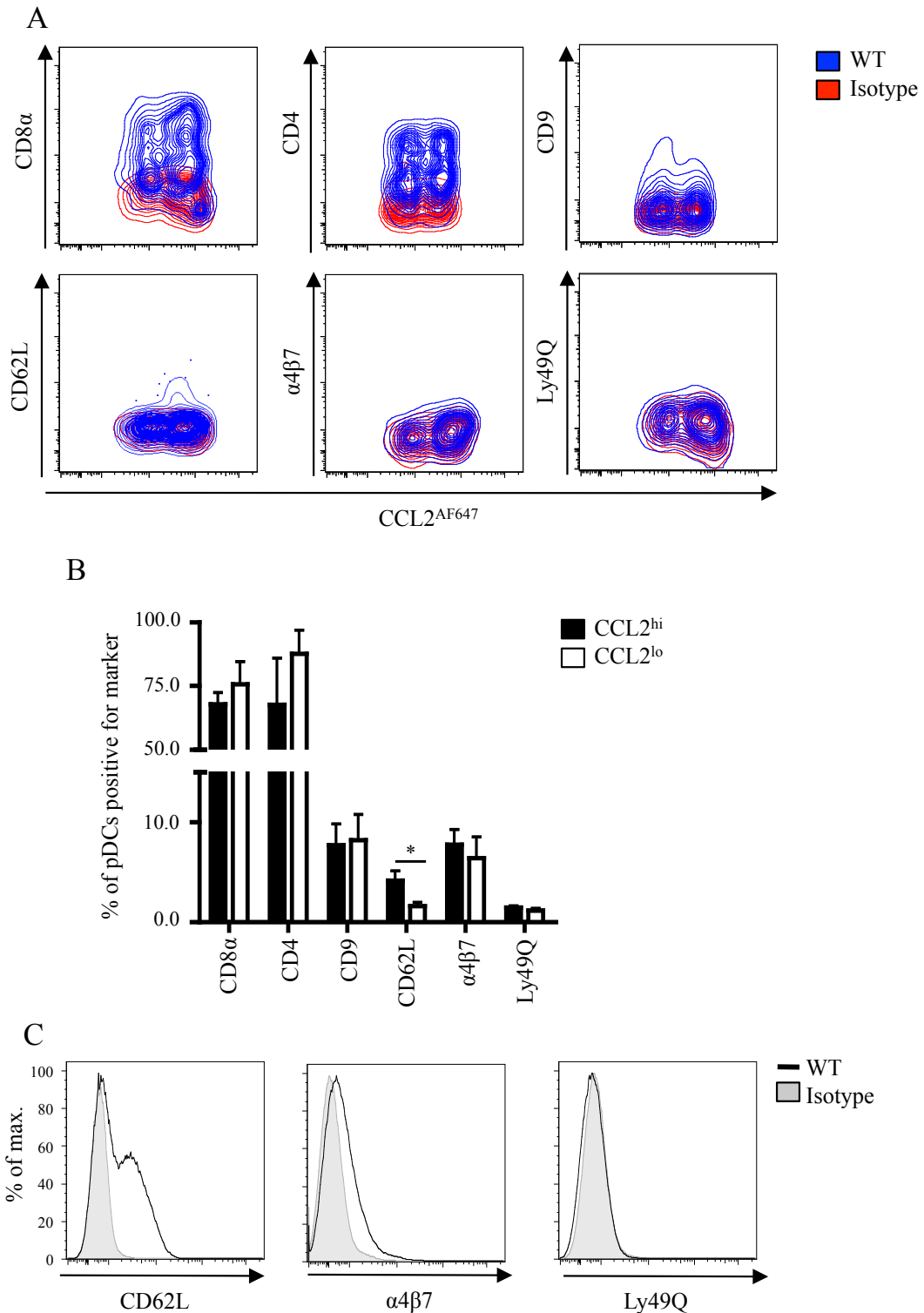


Figure 5-12: Expression of subset markers by splenic pDC CCL2 subsets.

pDCs from the spleen of WT animals (gated as described in Figure 5-1), were analysed for uptake of CCL2^{AF647} and expression of markers known to delineate two subsets of pDCs. (A) Representative contour plots from WT spleen stained with antibody (blue) or appropriate isotype (red). (B) The frequency of CCL2^{hi} (black bars) and CCL2^{lo} pDCs (white bars) expressing each marker was determined. $n=3$ (mean + SD). Data were analysed by unpaired T-test $p<0.05$ *. (C) Illustration of CD62L, $\alpha 4\beta 7$ and Ly49Q staining in all live cells. Plots are representative of a minimum of three biological replicates.

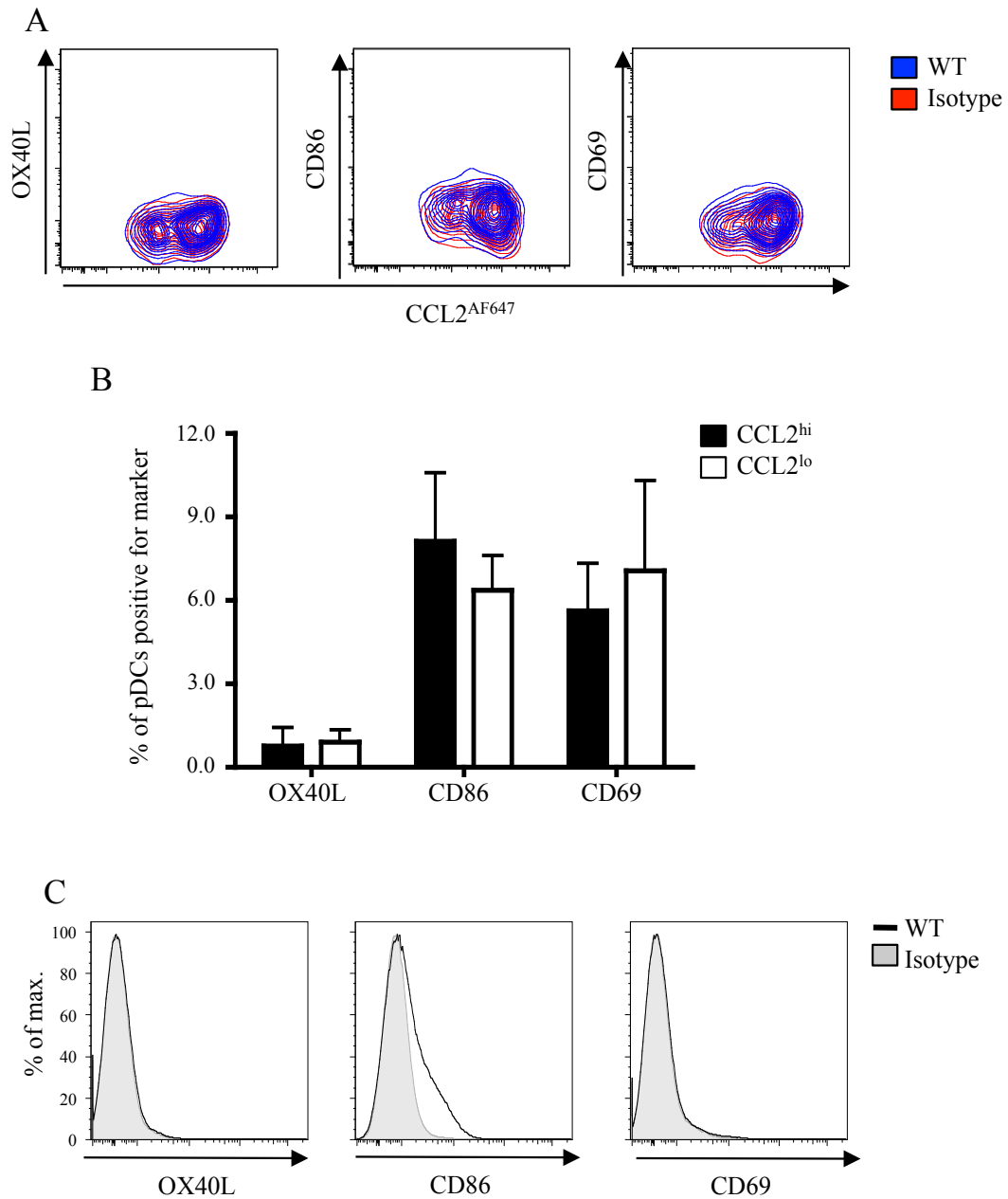


Figure 5-13: Expression of activation markers by splenic pDC CCL2 subsets.

pDCs from the spleen of WT animals (gated as described in Figure 5-1), were analysed for uptake of CCL2^{AF647} and expression of activation markers. (A) Representative contour plots from WT spleen stained with antibody (blue) or appropriate isotype (red). (B) The frequency of CCL2^{hi} (black bars) and CCL2^{lo} pDCs (white bars) expressing each marker. $n=3$ (mean + SD). Data were analysed by unpaired T-test. (C) Illustration of OX40L, CD86 and CD69 staining in all live cells. Plots are representative of a minimum of three biological replicates.

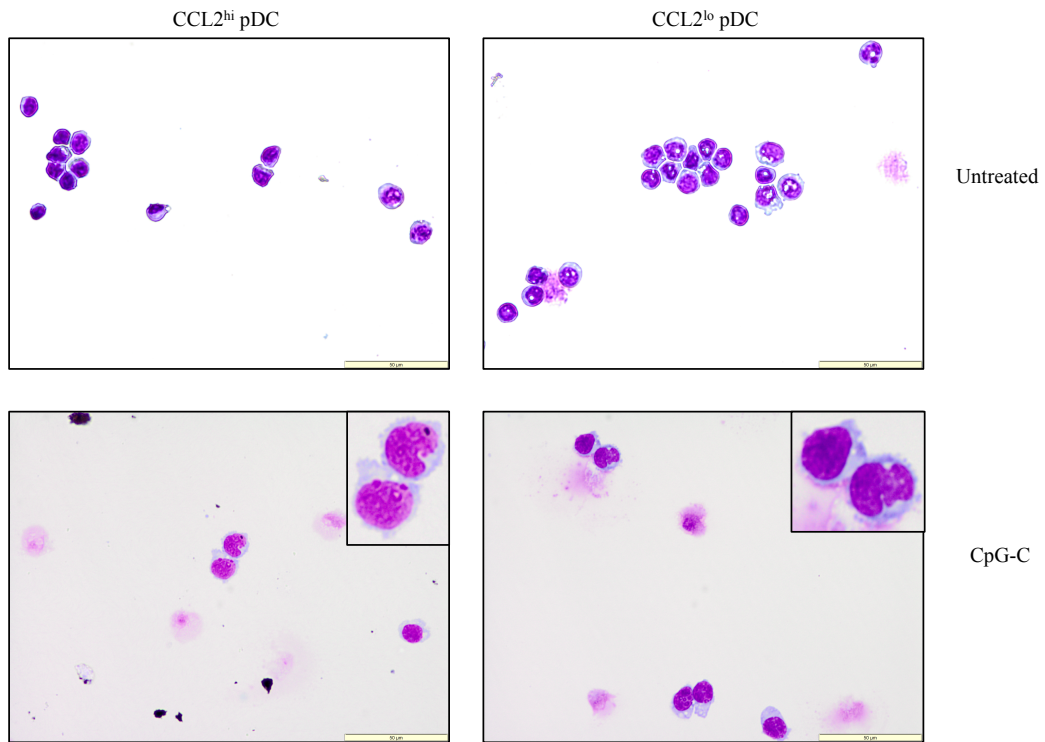


Figure 5-14: Morphology of the two subsets of pDCs.

~ 5×10^4 CCL2^{hi} or CCL2^{lo} pDCs were sorted from the spleen of B16FL tumour bearing WT mice, as described in Figure 5-9. Cells were left untreated or activated in the presence of 5 µg/ml CpG-C for 18 hrs. Cytospins were prepared, fixed and stained using the Rapid Romanowsky staining kit. Images were taken with a 40X objective using Olympus BX41 microscope and Cell^B software.

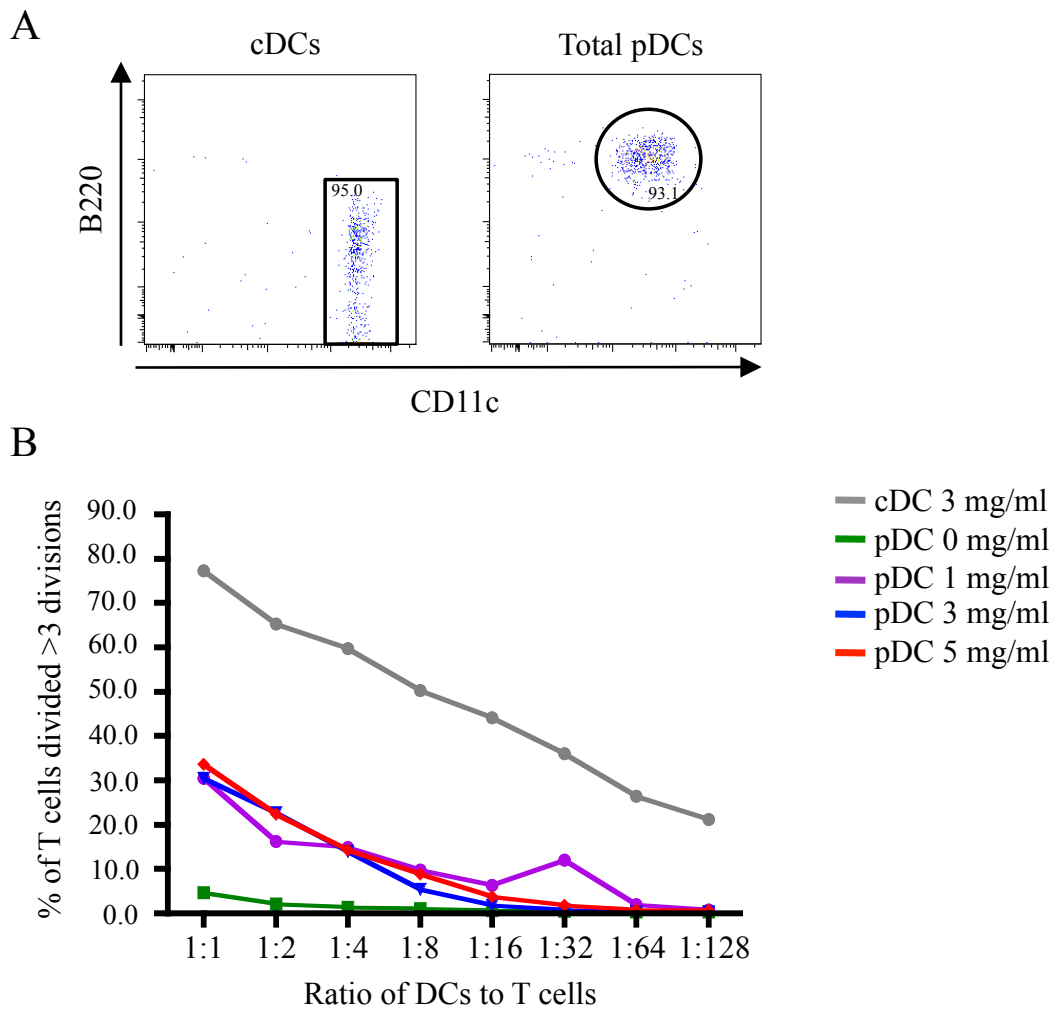


Figure 5-15: Ability of pDCs to stimulate CD4⁺ T cell proliferation.

Splenic pDCs were sorted from B16FL treated animals as indicated in Figure 5-9. Likewise, cDCs were also sorted from B16FL treated animals as B220⁺CD11c⁺ cells. Naïve CD4⁺CD62L⁺ OVA specific T cells were sorted from the spleen and LNs of OTII animals. DCs were cultured with total OVA protein for 3 hrs prior to the addition of 1×10^5 CFSE labelled T cells to each well. (A) Representative plots showing purities of sorted populations. (B) cDCs were cultured with 3 mg/ml, whereas total pDCs were cultured with varying amounts of OVA protein, 0 mg/ml (green line), 1 mg/ml (purple line), 3 mg/ml (blue line) and 5 mg/ml (red line). The ratio of DCs to T cells was decreased with the number of CFSE labelled T cells always remaining as 1×10^5 . The frequency of T cells divided is the number of T cells that have divided more than three divisions, according to CFSE dilution $n=1$.

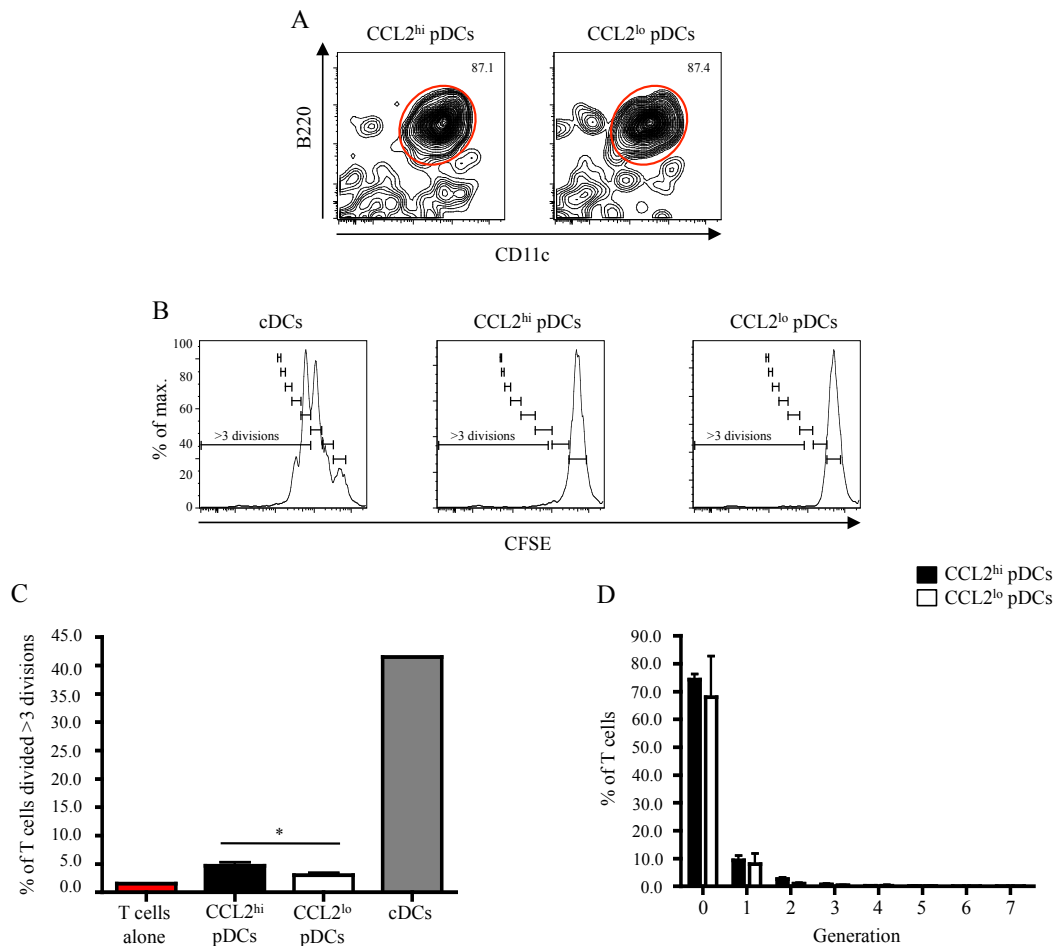


Figure 5-16: Ability of pDC subsets to stimulate CD4⁺ T cell proliferation.

CCL2^{hi} and CCL2^{lo} pDCs were sorted from B16FL treated animals as indicated in Figure 5-9. Likewise, cDCs were also sorted from B16FL treated animals as B220⁻CD11c⁺ cells. Naïve CD4⁺CD62L⁺ OVA specific T cells were sorted from the spleen and LNs of OTII animals. 1×10^5 DCs were cultured with 3 mg/ml total OVA protein for 3 hrs prior to the addition of 1×10^5 CFSE labelled T cells to each well. (A) Representative plots showing purities of sorted populations. (B) Representative CFSE dilution plots generated with cDCs (right hand panel), CCL2^{hi} pDCs (middle panel) or CCL2^{lo} pDCs (right hand panel) cultured with 3 mg/ml OVA. Gating is shown for each generation of divisions, plus the gating for more than three divisions. (C) Frequency of T cells divided more than three divisions when co-cultured with CCL2^{hi} pDCs (black bars), CCL2^{lo} pDCs (white bars), cDCs (grey bars) or T cells alone (red bars) at a ratio of 1:1 cultured with 3 mg/ml OVA. (D) The frequency of T cells in each generation of divisions when cultured with CCL2^{hi} pDCs (black bars) and CCL2^{lo} pDCs (white bars). Data were analysed by unpaired T-test (C) or two-way ANOVA with Bonferroni post-test (D) $p < 0.05$ ** $n = 3$ (mean + SD).

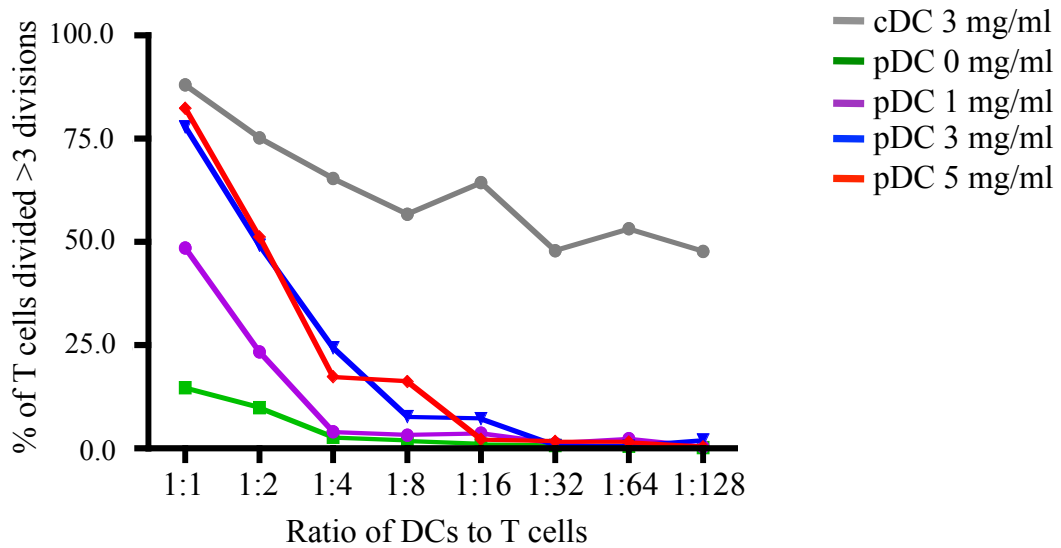


Figure 5-17: Ability of pDCs to stimulate CD8 α^+ T cell proliferation.

Splenic pDCs were sorted from B16FL treated animals as indicated in Figure 5-9. Likewise, cDCs were also sorted from B16FL treated animals as B220⁻CD11c⁺ cells. Naïve CD8 α^+ CD62L⁺ OVA specific T cells were sorted from the spleen and LNs of OTI animals. DCs were cultured with total OVA protein for 3 hrs prior to the addition of 1×10^5 CFSE labelled T cells to each well. cDCs were cultured with 3 mg/ml, whereas total pDCs were cultured with varying amounts of OVA protein, 0 mg/ml (green line), 1 mg/ml (purple line), 3 mg/ml (blue line) and 5 mg/ml (red line). The ratio of DCs to T cells was decreased with the number of CFSE labelled T cells always remaining as 1×10^5 . The frequency of T cells divided is the number of T cells that have divided more than three divisions, according to CFSE dilution $n=1$.

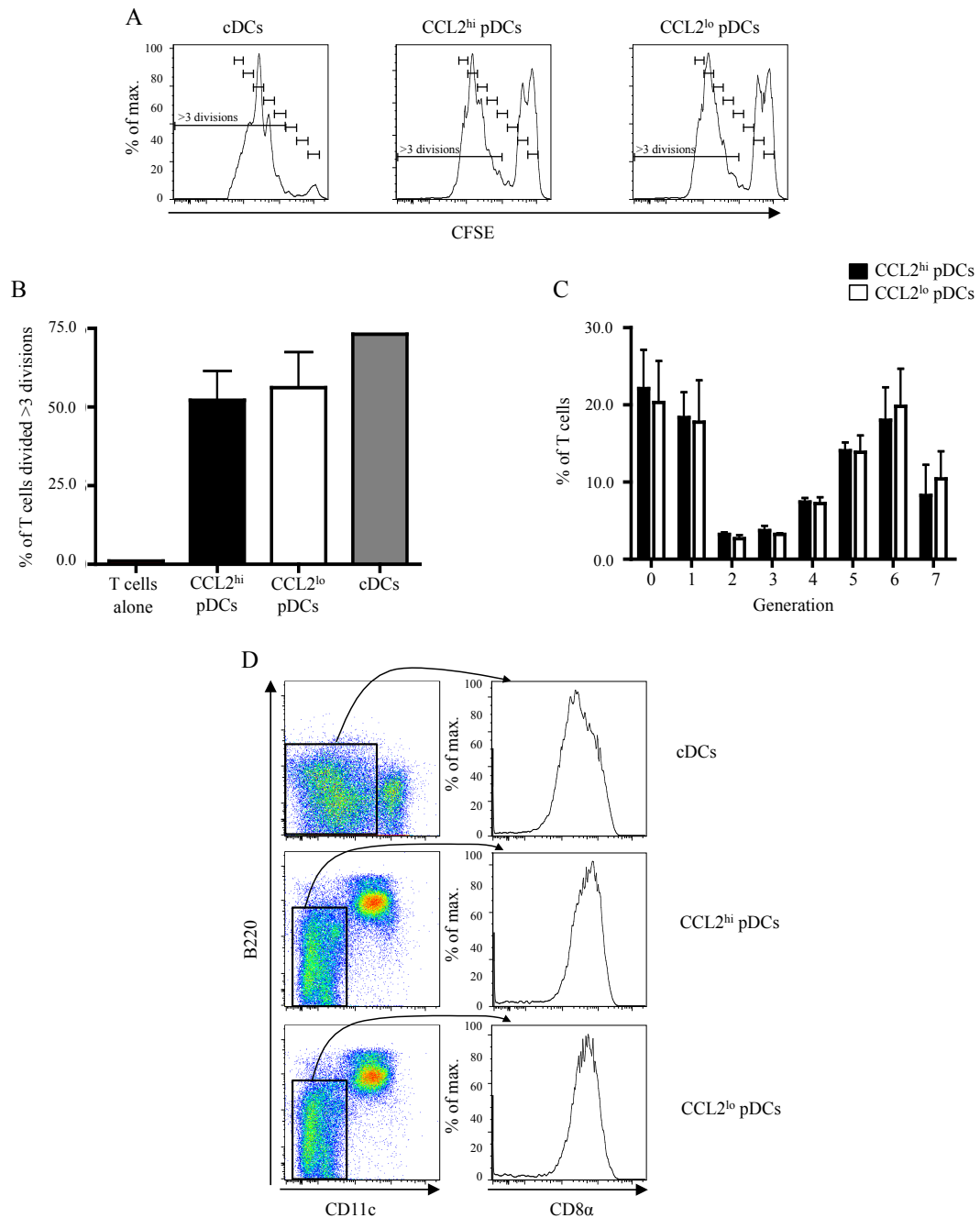


Figure 5-18: Ability of pDC subsets to stimulate CD8 α ⁺ T cell proliferation.

CCL2^{hi} and CCL2^{lo} pDCs were sorted from B16FL treated animals as indicated in Figure 5-9. Likewise, cDCs were also sorted from B16FL treated animals as B220⁺CD11c⁺ cells. Naïve CD8 α ⁺CD62L⁺ OVA specific T cells were sorted from the spleen and LNs of OTI animals. 1×10^5 DCs were cultured with 3 mg/ml total OVA protein for 3 hrs prior to the addition of 1×10^5 CFSE labelled T cells to each well. (A) Representative CFSE dilution plots generated with cDCs (right hand panel), CCL2^{hi} pDCs (middle panel) or CCL2^{lo} pDCs (right hand panel) cultured with 3 mg/ml OVA. Gating is shown for each generation of divisions, plus the gating for more than three divisions. (B) Frequency of T cells divided more than three divisions when co-cultured with CCL2^{hi} pDCs (black bars), CCL2^{lo} pDCs (white bars), cDCs (grey bars) or T cells alone (red bars) at a ratio of 1:1 cultured with 3 mg/ml OVA. (C) The frequency of T cells in each generation of divisions when cultured with CCL2^{hi} pDCs (black bars) and CCL2^{lo} pDCs (white bars). (D) Representative plots showing all cells present at the end of the 3 day culture of T cells with cDCs, CCL2^{hi} pDCs or CCL2^{lo} pDCs, illustrating that all B220⁺CD11c⁻ cells are CD8 α ⁺. Data were analysed by unpaired T-test (B) or two-way ANOVA with Bonferroni post-test (C) n=3 (mean + SD).

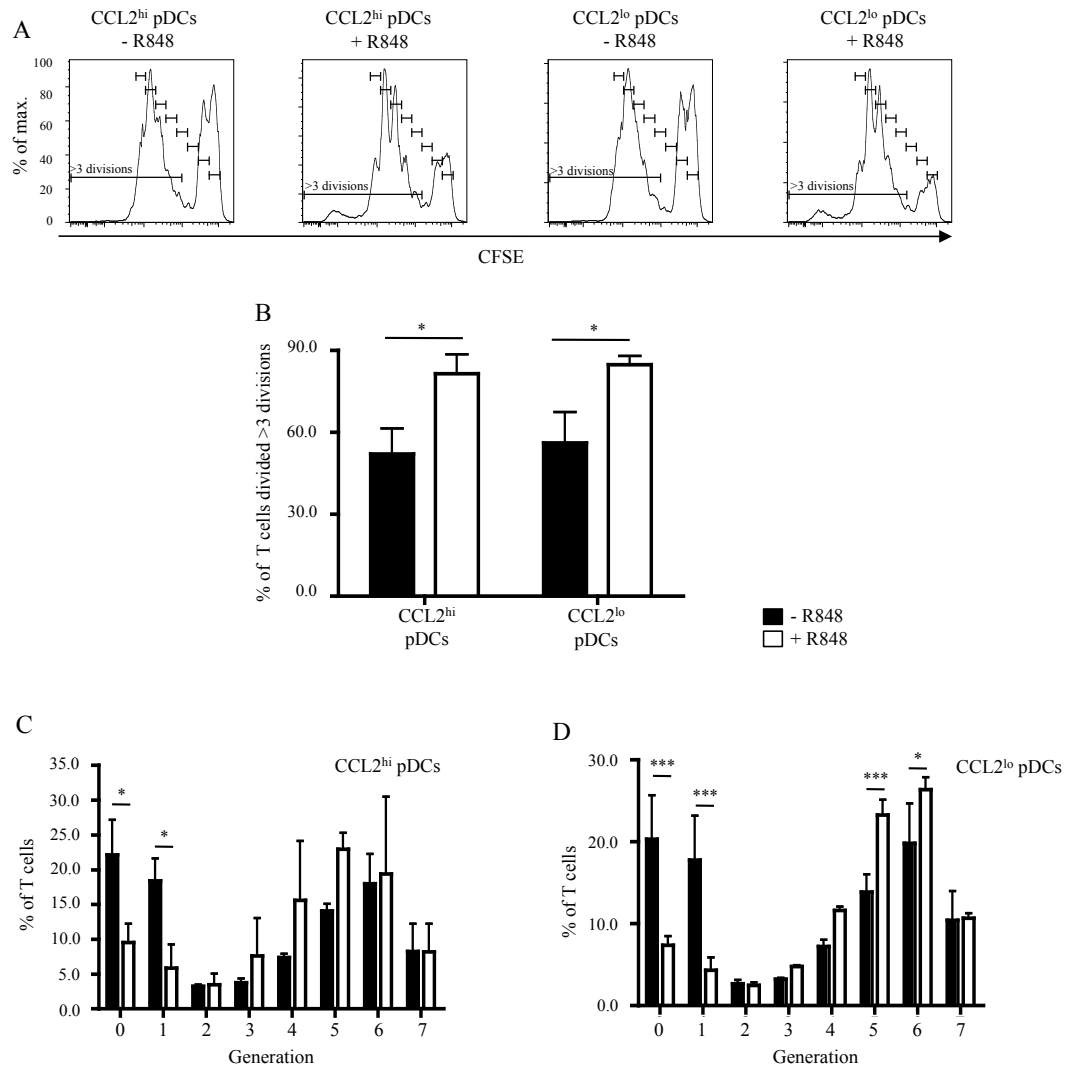


Figure 5-19: R848 enhances the ability of pDCs to stimulate CD8 α ⁺ T cell proliferation.

CCL2^{hi} and CCL2^{lo} pDCs were sorted from B16FL treated animals as indicated in Figure 5-9. Naïve CD8 α ⁺CD62L⁺ OVA specific T cells were sorted from the spleen and LNs of OTI animals. pDCs were cultured with 3 mg/ml OVA protein for 3 hrs with or without 1 μ g/ml R848 prior to the addition of 1×10^5 CFSE labelled T cells to each well. (A) Representative plots of CFSE dilution generated with CCL2^{hi} and CCL2^{lo} pDCs with or without 1 μ g/ml R848. (B) Frequency of T cells divided more than three divisions when co-cultured with CCL2^{hi} pDCs or CCL2^{lo} pDCs cultured with 3 mg/ml OVA with R848 (white bars) or without R848 (black bars) at a ratio of 1:1 (pDC:T cells). (C&D) The frequency of T cells in each generation of divisions when cultured with CCL2^{hi} pDCs (C) and CCL2^{lo} pDCs (D) with R848 (white bars) or without R848 (black bars). n=3 (mean + SD). Data were analysed by unpaired T-test (B) or two-way ANOVA with Bonferroni post-test (C&D) $p < 0.05$ * and $p < 0.001$ ***.

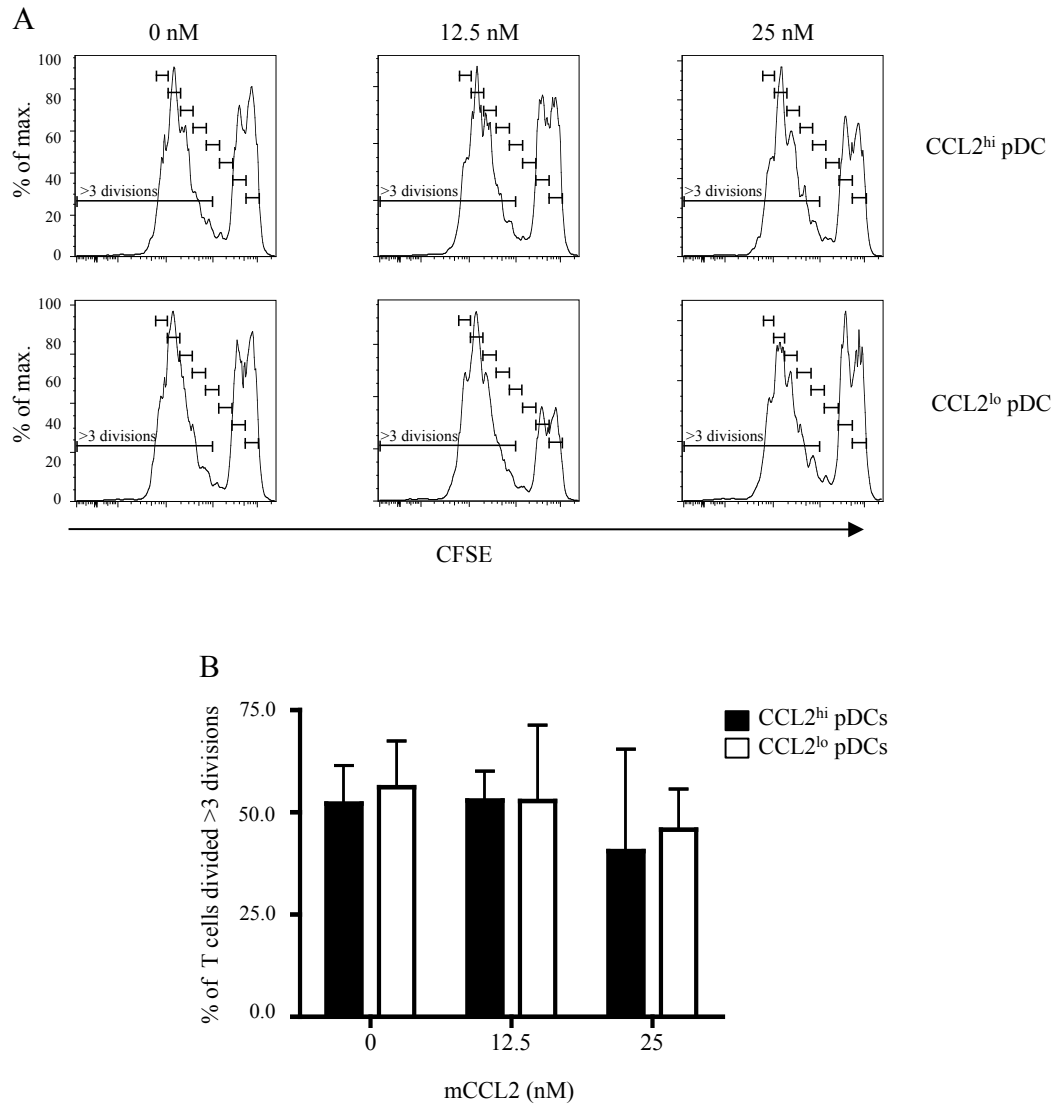


Figure 5-20: mCCL2 has no effect on the ability of pDCs to stimulate CD8 α^+ T cell proliferation.

CCL2^{hi} and CCL2^{lo} pDCs were sorted from B16FL treated animals as indicated in Figure 5-9. Naïve CD8 α^+ CD62L⁺ OVA specific T cells were sorted from the spleen and LNs of OTI animals. pDCs were cultured with 3 mg/ml OVA protein for 3 hrs prior to the addition of 1×10^5 CFSE labelled T cells to each well. 0-25 nM unlabelled murine CCL2 was then added to the culture for 72 hrs. (A) Representative plots of CFSE dilution generated with CCL2^{hi} (top row) and CCL2^{lo} pDCs (bottom row) with 0 nM, 12.5 nM or 25 nM mCCL2 added to the culture media. (B) Frequency of T cells divided more than three divisions when co-cultured with a ratio of 1:1 CCL2^{hi} pDCs (black bars) or CCL2^{lo} pDCs (white bars) to T cells with 0, 12.5 or 25 nM unlabelled mCCL2 n=3 (mean + SD). Data were analysed by two-way ANOVA with Bonferroni post-test.

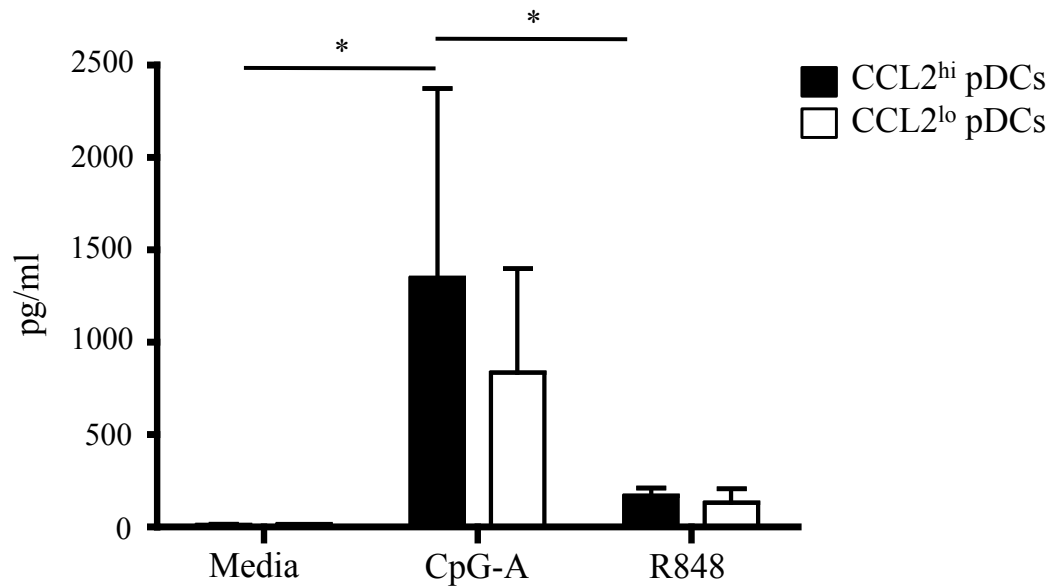


Figure 5-21: IFN α production by CCL2^{hi} and CCL2^{lo} pDCs.

CCL2^{hi} and CCL2^{lo} pDCs were sorted from B16FL treated animals as indicated in Figure 5-9. 1×10^5 pDCs were incubated with media alone, 10 $\mu\text{g/ml}$ CpG-A or 10 $\mu\text{g/ml}$ R848 for 8 hrs at 37°C. Cytokine production was assessed by ELISA and results show the mean IFN α production in pg/ml (n=3-9 from three independent experiments, mean + SD). Data were analysed by two-way ANOVA with Bonferroni post-test $p < 0.05$ *.

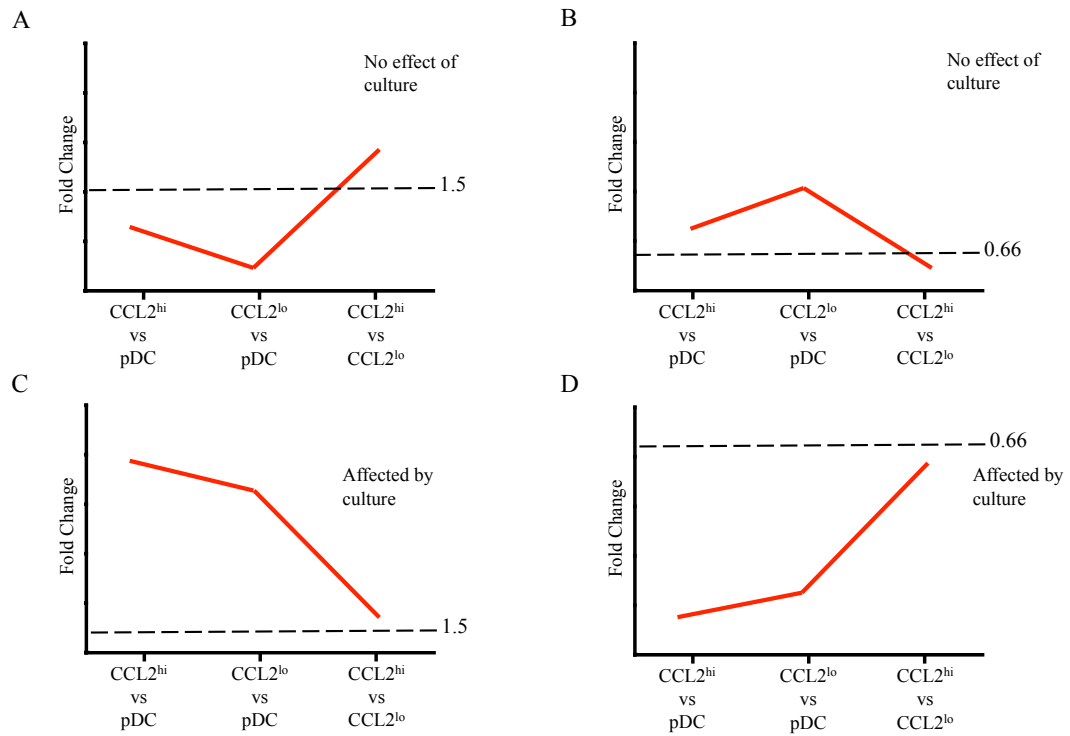
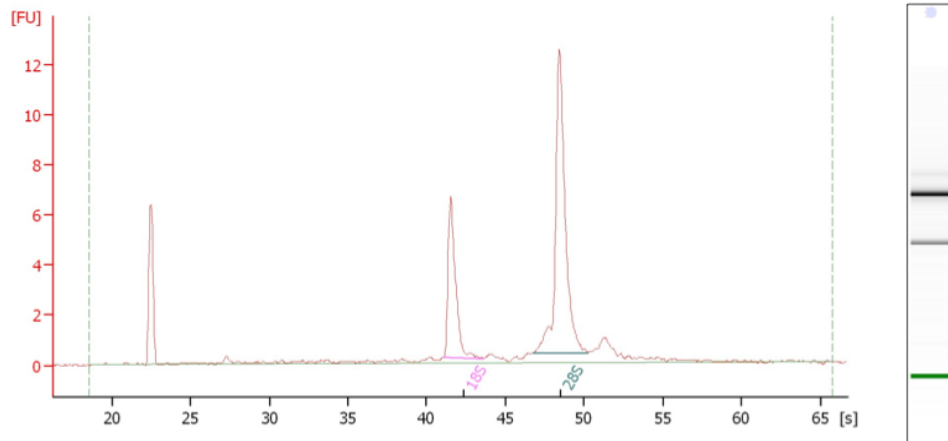


Figure 5-22: Schematic representation of the potential effects of culture on gene expression. The potential profiles generated by plotting FC differences between CCL2^{hi} pDCs vs. total pDCs, CCL2^{lo} pDCs vs. total pDCs and CCL2^{hi} pDCs vs. CCL2^{lo} pDCs for each individual gene might be similar to one of the four graphical representations shown. (A&B) illustrate profiles that might be produced if the expression level of a gene was not affected by the incubation step, but was expressed at higher levels in CCL2^{hi} (A) and CCL2^{lo} pDCs (B). Profiles similar to those represented in (C) and (D) might be produced if expression of a gene found to be differentially expressed between CCL2^{hi} and CCL2^{lo} pDCs, but which had been affected by culture.

A



B

	Concentration (ng/ μ l)	260/280	RNA Integrity Number (RIN)
pDC 1	44.48	2.07	9.8
pDC 2	46.23	2.15	10
pDC 3	42.28	2.21	10
pDC 4	29.78	2.21	10
CCL2 ^{hi} 1	34.52	2.21	10
CCL2 ^{hi} 2	17.34	2.36	9.9
CCL2 ^{hi} 3	13.70	2.12	X
CCL2 ^{lo} 1	46.29	2.12	10
CCL2 ^{lo} 2	16.85	2.50	9.5
CCL2 ^{lo} 3	33.60	2.19	X

Figure 5-23: RNA quantity and quality from sorted pDCs.

$\sim 2 \times 10^6$ pDCs were sorted from the spleens of B16FL tumour bearing mice, as designated in Figure 5-9, as either total pDCs (named pDCs 1-4), CCL2^{hi} pDCs (CCL2^{hi} 1-3) or CCL2^{lo} pDCs (CCL2^{lo} 1-3). RNA was extracted from the sorted cells and sent to the Glasgow University Polyomics Facility for analysis. (A) An example of a plot retrieved upon test of RNA integrity using the RNA 6000 Nano kit with 1 μ l of RNA. (B) Table illustrating the concentration of each RNA sample, plus the 260/280 ratio and RIN. Crosses are present in the CCL2^{hi} 3 and CCL2^{lo} 3 samples because there was a malfunction of the chip, and no values could be retrieved.

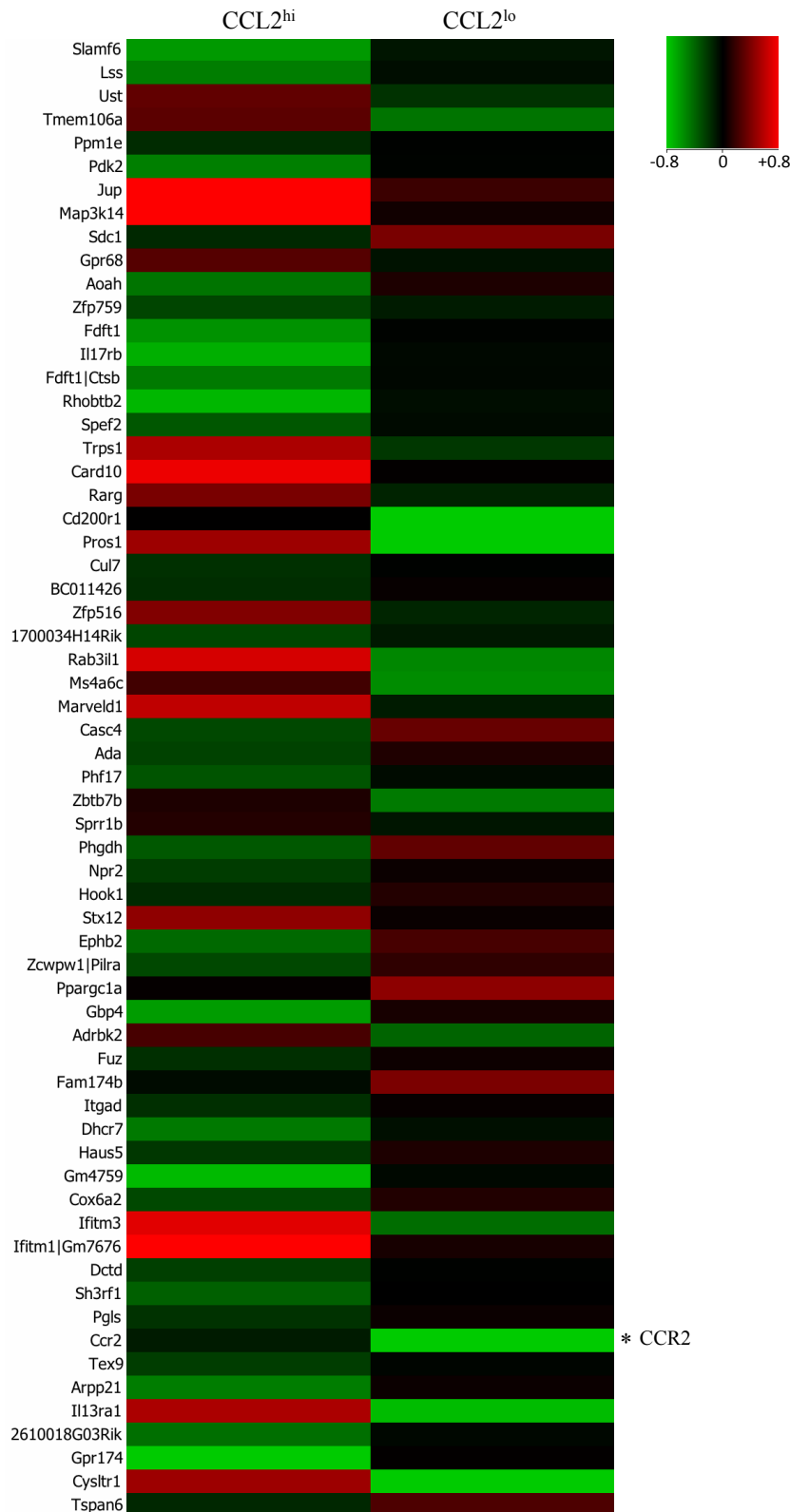
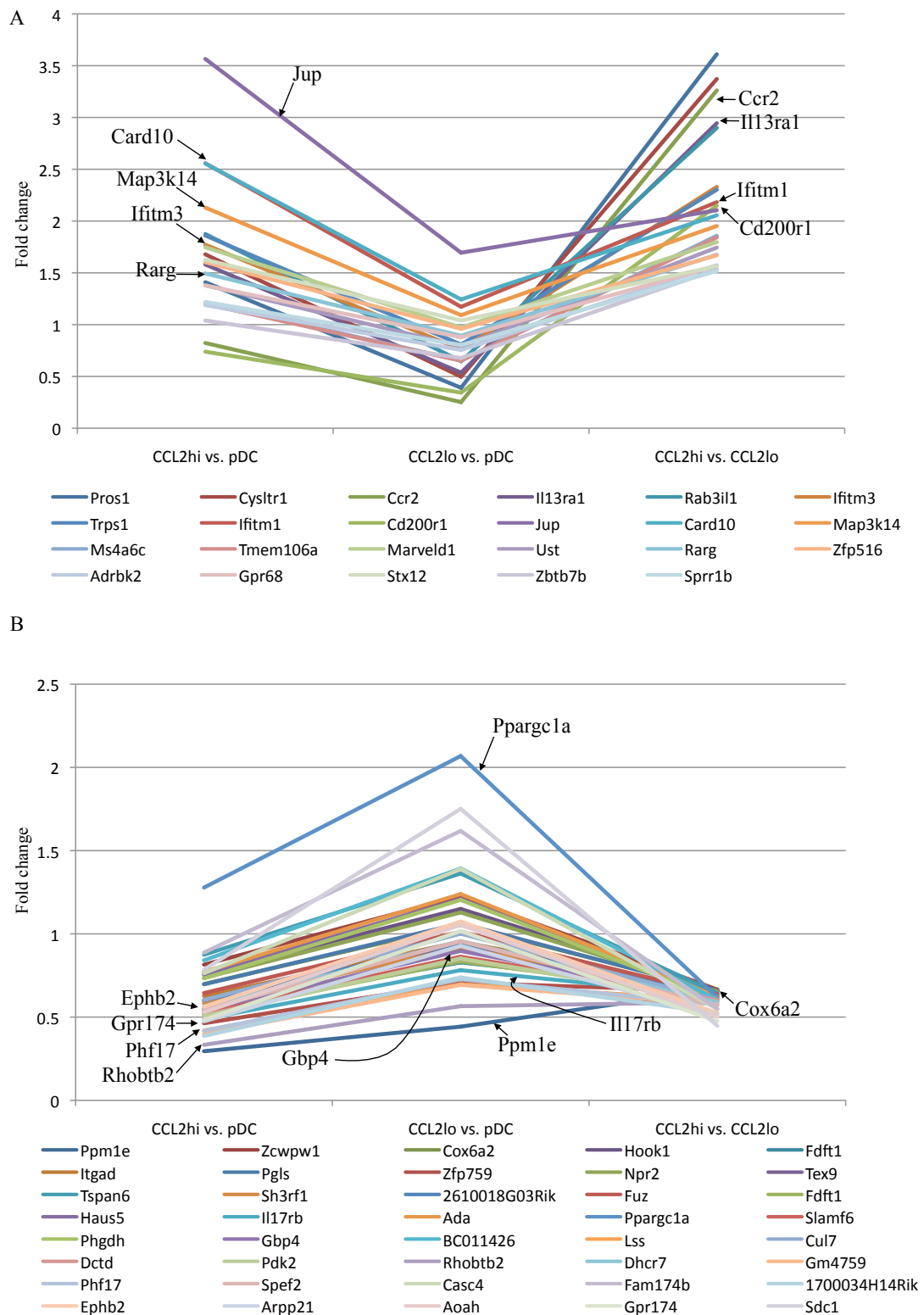


Figure 5-24: Gene differences between the two subsets of pDCs.

The RNA samples from Figure 5-23 were subject to GC-RMA normalisation. The normalised values for each gene were used to calculate the FC in expression between the CCL2^{hi} and CCL2^{lo} samples. The samples were compared by one-way ANOVA with Storey's multiple test correction. The data had restrictions applied to the resulting values, a standard cut-off of FC <-1.5 or >1.5 between CCL2^{hi} and CCL2^{lo} pDCs samples. A further cut-off was added to the p-value p<0.005, which correlates to a q-value of 0.344. The heat-map shows normalised signal intensity of the gene. The expression value of each gene is mapped to a colour-intensity value, low relative expression shown in green and high relative expression in red.



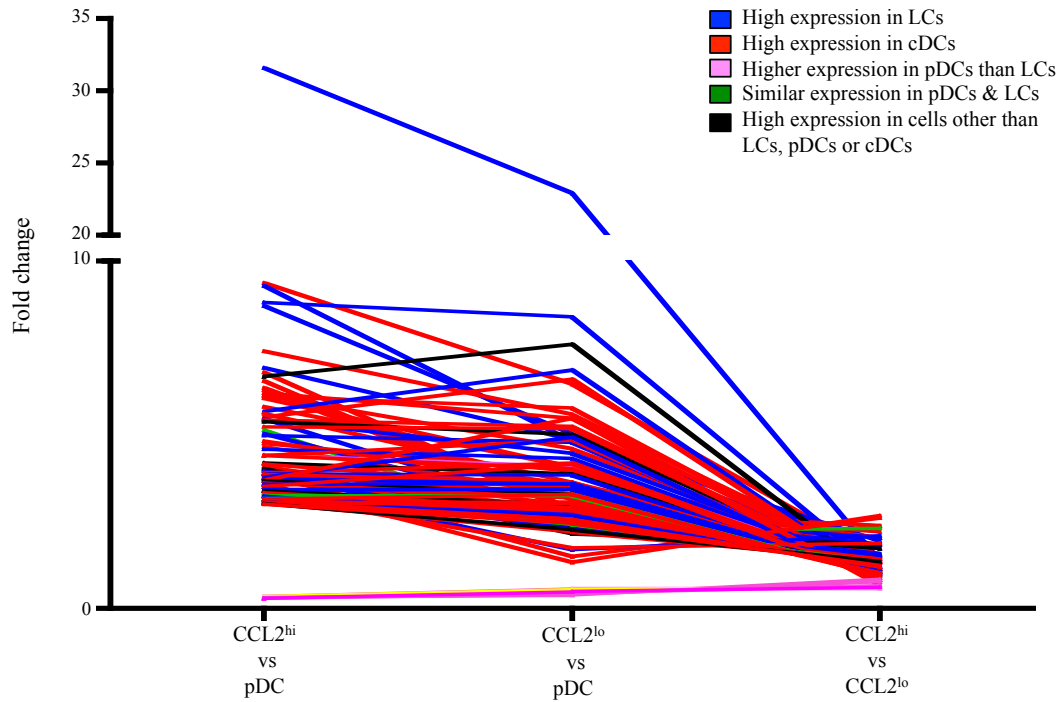


Figure 5-26: Alteration in gene expression by pDCs, as a consequence of culture.

The FC differences between CCL2^{hi} pDC vs. total pDCs, CCL2^{lo} pDCs vs. total pDCs and CCL2^{hi} vs. CCL2^{lo} pDCs were plotted for all genes with a FC of <-3.0 or >3.0 between the CCL2^{hi} pDCs and total pDCs. A further cut-off was added to the p-value $p < 0.005$. A negative FC was plotted as a fraction, e.g. 1/- FC. Each gene was examined for its relative expression in cell types using Immgen. Genes with high expression in Langerhans cells (LCs) are shown in blue, high expression in cDCs (red) and high expression in cells other than LCs, pDCs and cDCs (black). Furthermore, genes that were expressed at a higher level in pDCs than LCs are shown in pink and genes with similar expression in pDCs and LCs are shown in green. The list of genes is shown in Appendix 1.

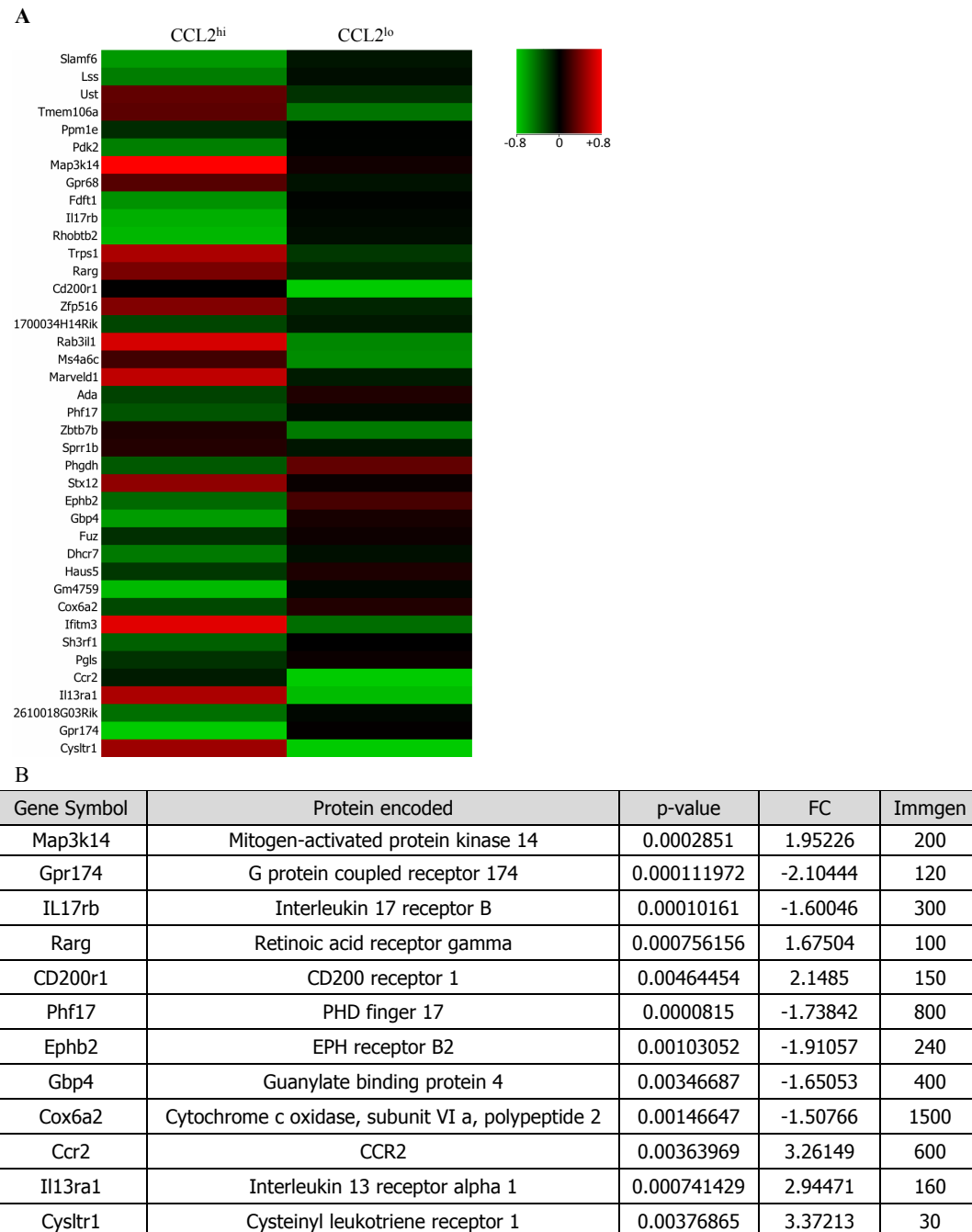


Figure 5-27: Final list of genes differences between the two pDC subsets.

Subsequent to the analysis and restrictions applied to the samples as described in Figure 5-24, the apparent expression level of each gene in pDCs was determined according to Immgen. Genes that were not found to be expressed in pDCs, according to Immgen, were removed from the list in Figure 5-24, generating what shall be referred to as the final list of genes. (A) The heat-map shows normalised signal intensity of the gene. The expression value of each gene is mapped to a colour-intensity value, low relative expression shown in green and high relative expression in red. (B) Table illustrating the final list of genes selected as quality controls for the microarray results. One-way ANOVA was used to compare differences between CCL2^{hi} and CCL2^{lo} pDCs and the generated p-values and FC are indicated for each gene. In addition, the final column of the table illustrates an approximate value for the expression of each gene in pDCs according to Immgen. The values according to Immgen are post-normalisation expression values that have been subject to stringent quality control checks. Furthermore, microarray technology can produce background signals, thus Immgen performed statistical analysis to generate probabilistic thresholds of expression. According to Immgen values >120 have a ≥95% probability of being accurate, 50-120 is equal to ~50% probability of being accurate and <47 is equivalent to ≥95% probability of the gene being silent (http://www.immgen.org/Protocols/ImmGen%20QC%20Documentation_ALL-DataGeneration_0612.pdf).

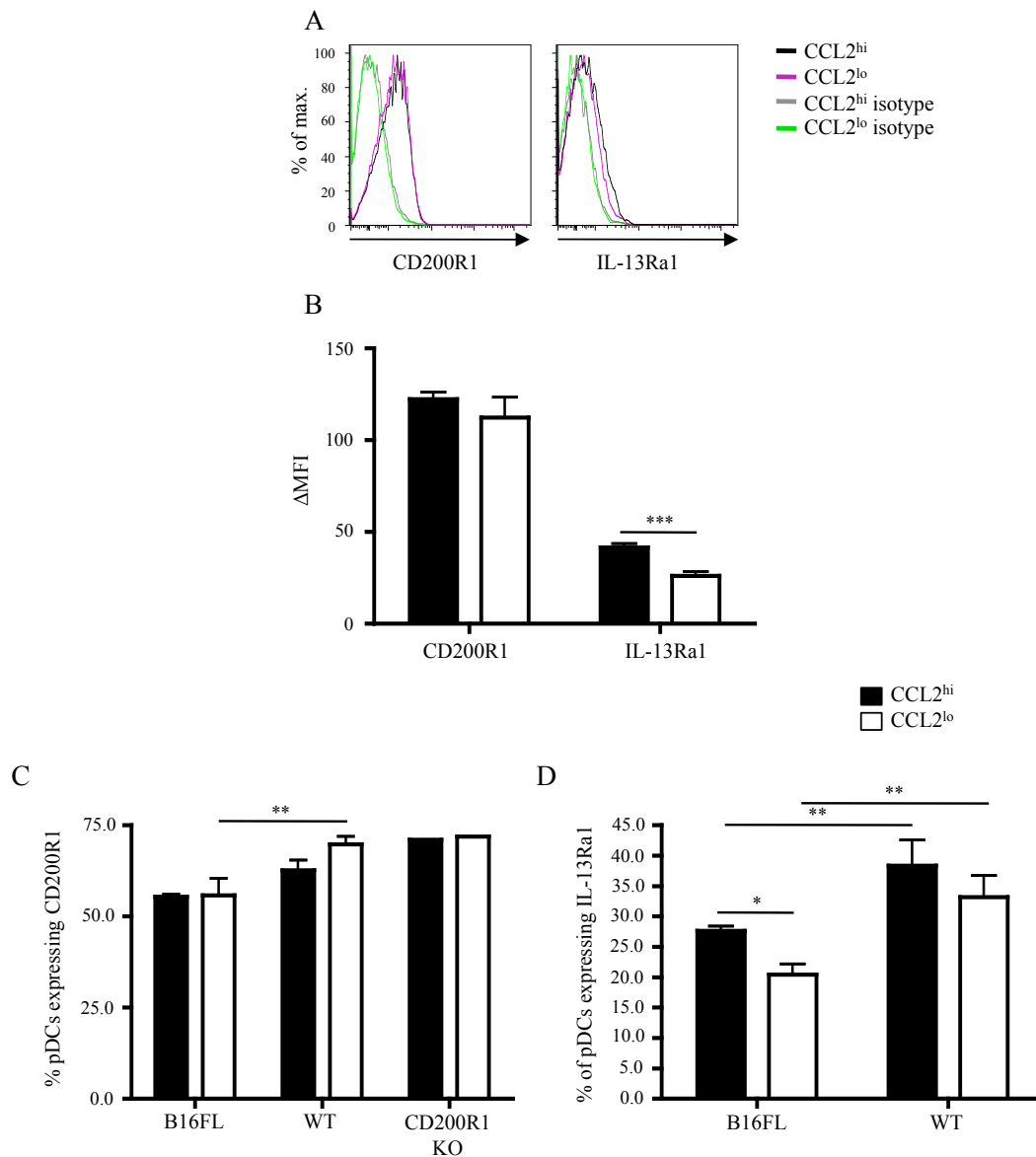
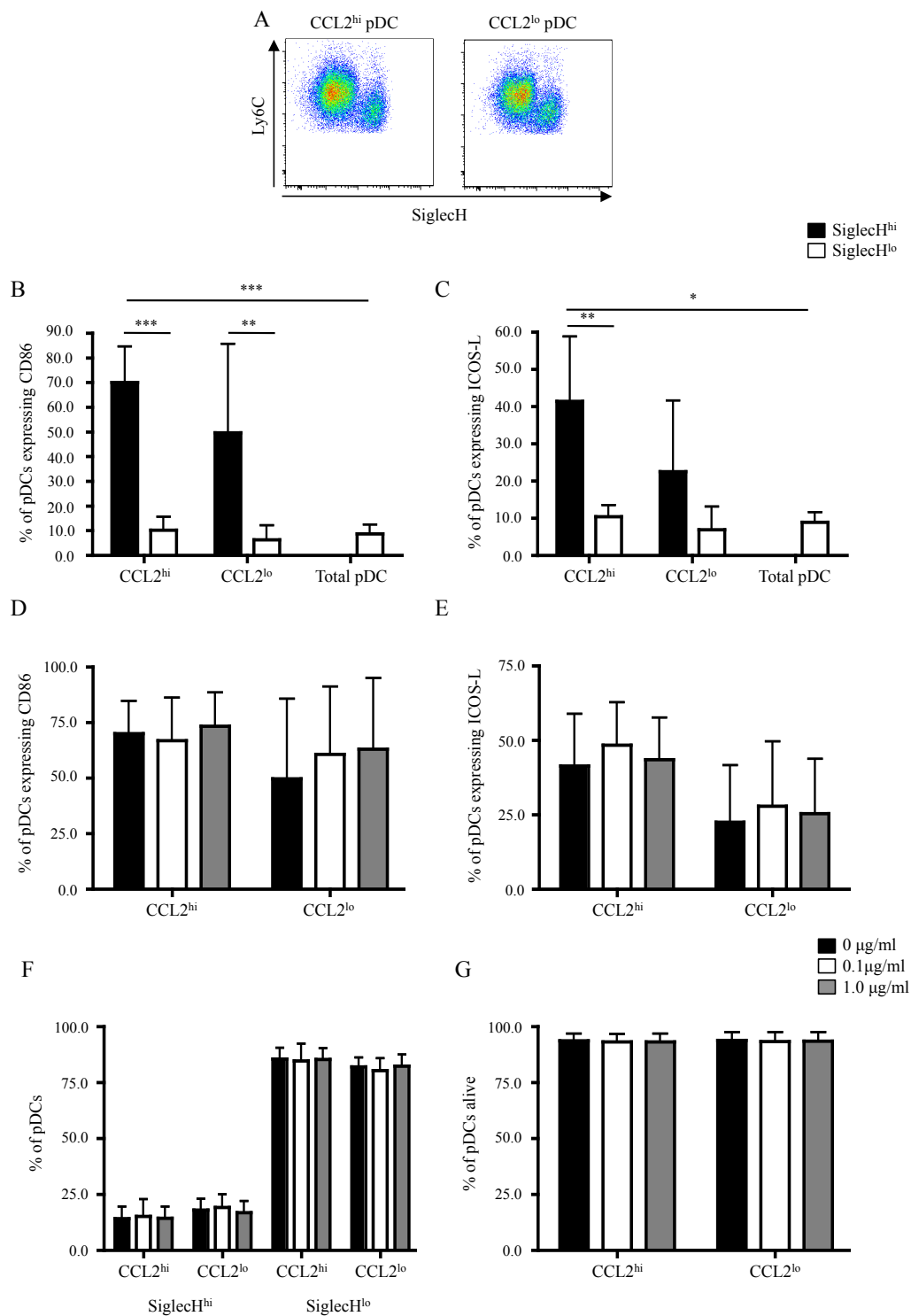


Figure 5-28: Confirming differences in surface protein expression between the two pDC subsets, as detected by the microarray.

pDCs from the spleen of B16FL treated WT animals (gated as described in Figure 5-1) were analysed for uptake of CCL2^{AF647} and expression of CD200R1 and IL-13Ra1. (A) Representative histograms showing staining of CD200R1 and IL-13Ra1 in CCL2^{hi} (black line) and CCL2^{lo} (purple line) pDC subsets, with appropriate isotype staining of CCL2^{hi} (grey line) and CCL2^{lo} (green line) pDC subsets. (B) Graphical representation of the calculated geometric mean fluorescence intensity (ΔMFI) of CD200R1 and IL-13Ra1 expression by B16FL treated WT animals. (C) Frequency of CCL2^{hi} and CCL2^{lo} pDCs in B16FL WT, untreated WT and untreated CD200R1 KO animals expressing CD200R1, as determined by flow cytometry. (D) Frequency of CCL2^{hi} and CCL2^{lo} pDCs in B16FL WT and untreated WT animals expressing IL-13Ra1, as determined by flow cytometry. Data are representative of a minimum of three biological replicates (mean + SD). Data were analysed by either unpaired T-test (B) or two-way ANOVA with Bonferroni post-test (C&D) $p < 0.05$ *, $p < 0.01$ ** and $p < 0.001$ ***.



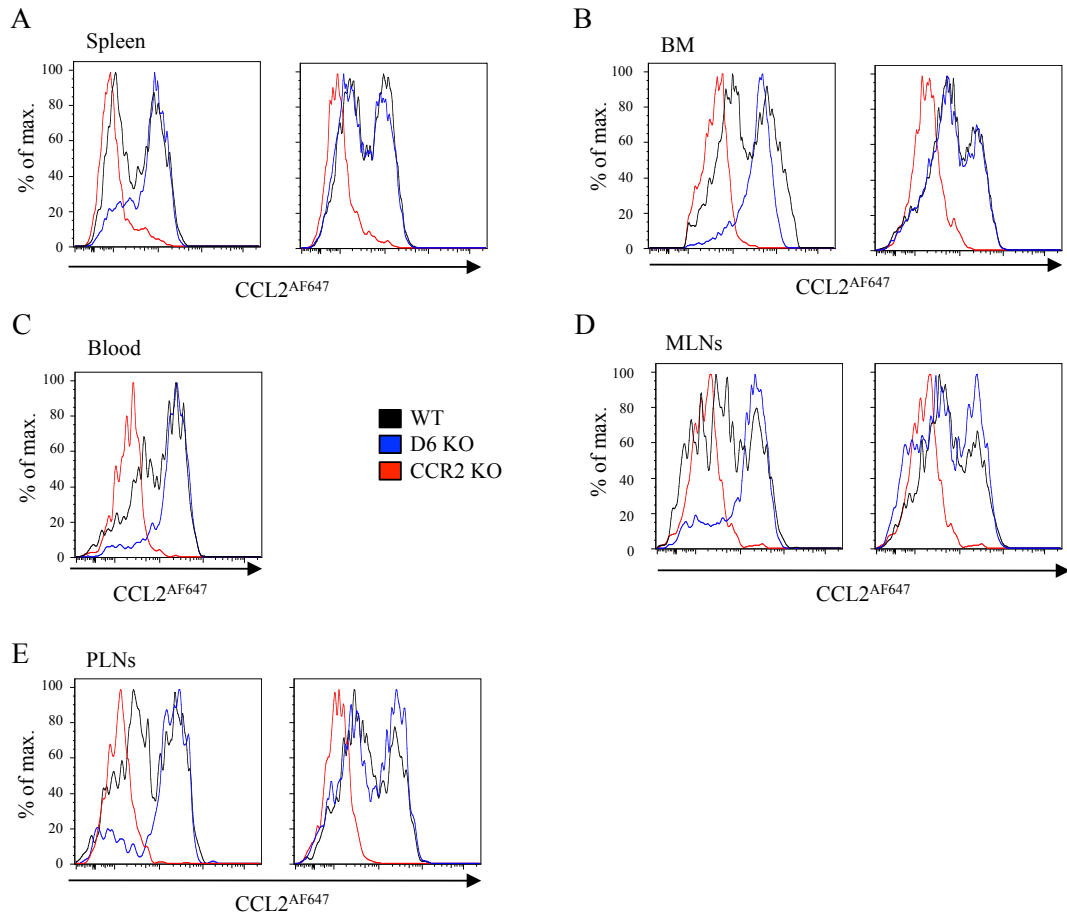


Figure 5-30: Strain differences in the two subsets of pDCs based on $CCL2^{AF647}$.

pDCs from the spleen (A), BM (B), blood (C), MLNs (D) and PLNs (E) of WT (black), D6 KO (blue) and CCR2 KO (red) were gated as described in Figure 5-1, and analysed for uptake of $CCL2^{AF647}$. In some tissues there are two histogram overlays shown illustrating the two different phenotypes in $CCL2^{AF647}$ uptake in D6 KO. Plots are representative of a minimum of three biological replicates.

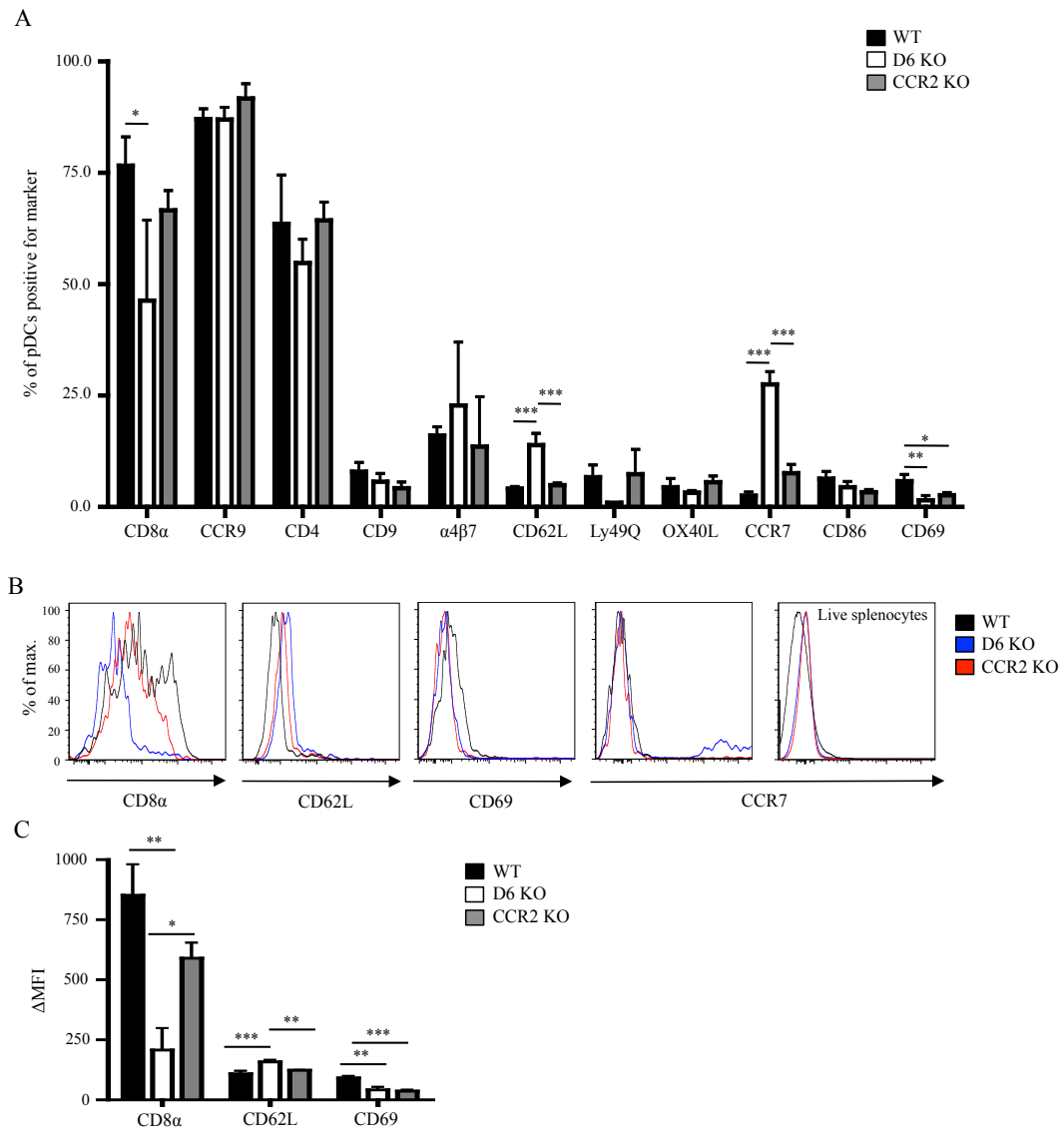


Figure 5-31: Strain differences in the expression of surface markers by total splenic pDCs in WT, D6 KO and CCR2 KO.

pDCs from spleen were gated as described in Figure 5-1. (A) The frequency of live pDCs expressing markers was determined by using FMOs to set the negative gate. FMOs consisted of the pDC stain described in Figure 5-1, plus the isotype for the marker of interest. Any signal detected above the FMO samples was considered positive. (B) Representative histogram overlays of the surface markers that were found to be differentially expressed by splenic pDCs from WT (black), D6 KO (blue) and CCR2 KO (red). Also included is CCR7 expression by all live splenocytes. (C) Geometric mean fluorescence intensity (Δ MFI) of markers with significant differences in expression between the mice strains in (A). $n=3$ (mean + SD). Data were analysed by one-way ANOVA with Tukey post-test $p<0.05$ *, $p<0.01$ ** and $p<0.001$ ***.

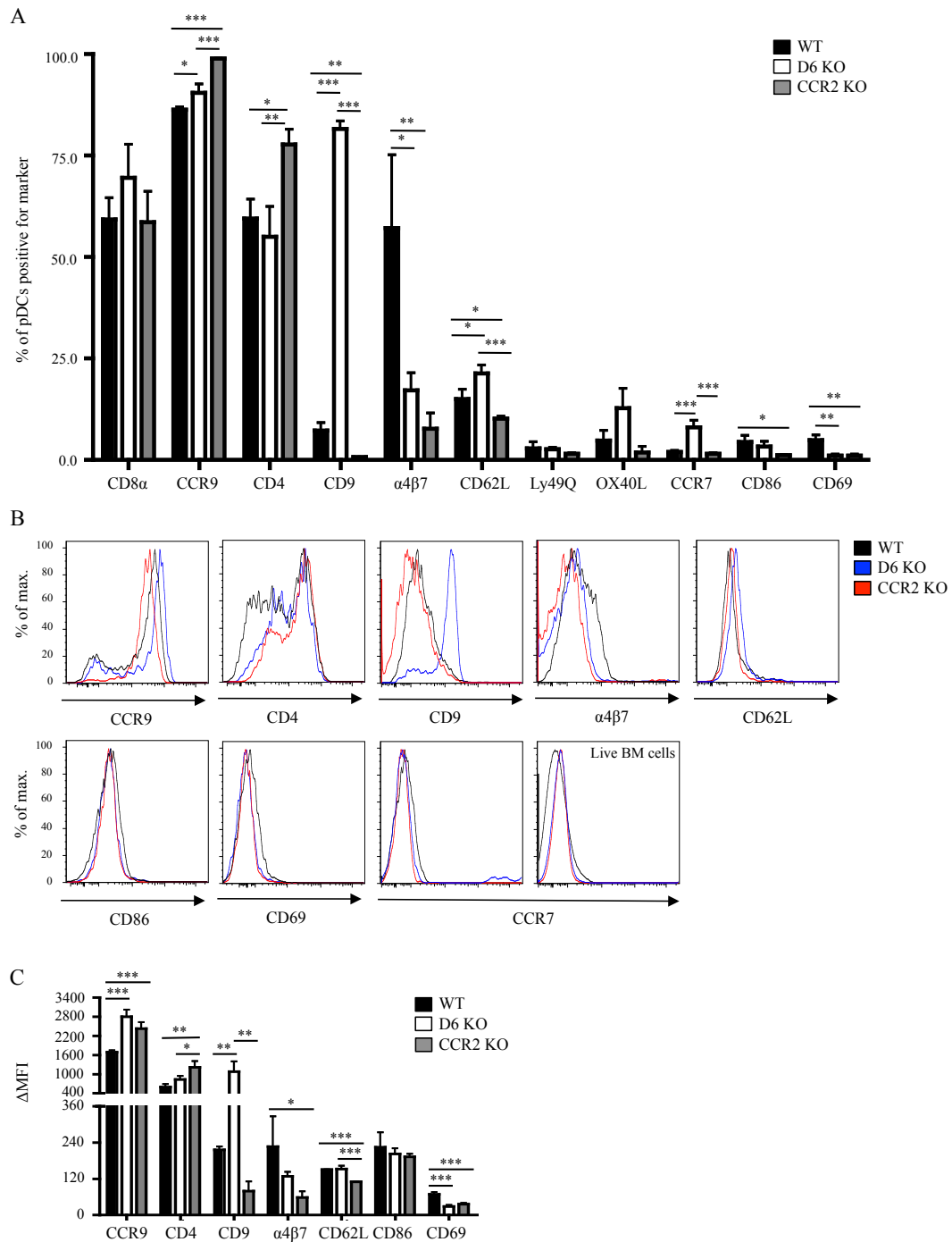


Figure 5-32: Strain differences in the expression of surface markers by total BM pDCs in WT, D6 KO and CCR2 KO.

pDCs from BM were gated as described in Figure 5-1. (A) The frequency of live pDCs expressing markers was determined by using FMOs to set the negative gate. FMOs consisted of the pDC stain described in Figure 5-1, plus the isotype for the marker of interest. Any signal detected above the FMO samples was considered positive. (B) Representative histogram overlays of the surface markers that were found to be differentially expressed by BM pDCs from WT (black), D6 KO (blue) and CCR2 KO (red). Also included is CCR7 expression by all live BM cells. (C) Geometric mean fluorescence intensity (Δ MFI) of markers with significant differences in expression between the mice strains in (A). $n=3$ (mean + SD). Data were analysed by one-way ANOVA with Tukey post-test $p < 0.05$ *, $p < 0.01$ ** and $p < 0.001$ ***.

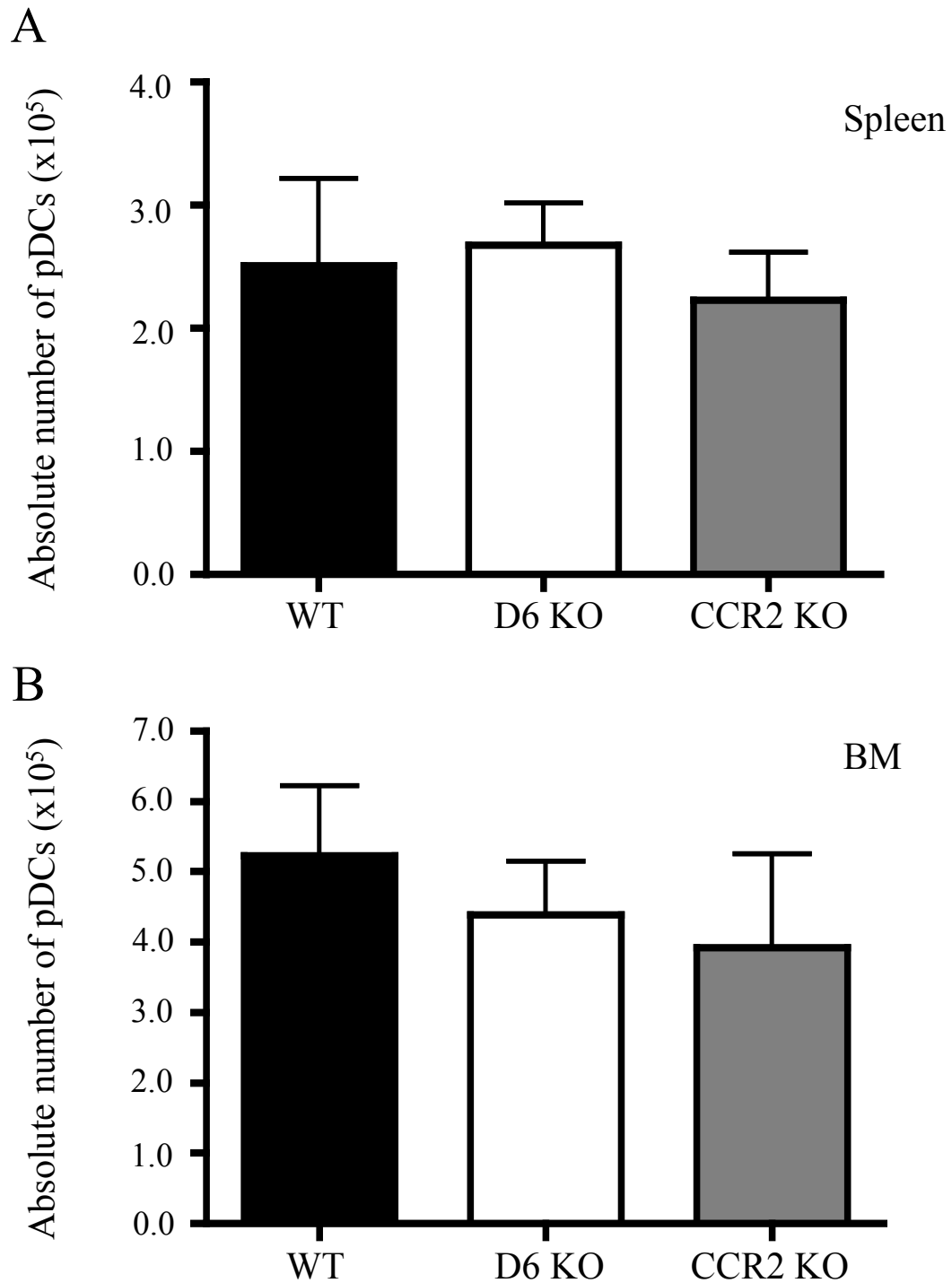


Figure 5-33: No strain differences in the absolute number of splenic and BM pDCs.

The absolute number of splenic (A) and BM (B) pDCs was determined in untreated WT, D6 KO and CCR2 KO animals ($n=3-6$ mean + SD). pDCs were gated as depicted in Figure 5-9. Data were analysed by one-way ANOVA with Tukey post-test.

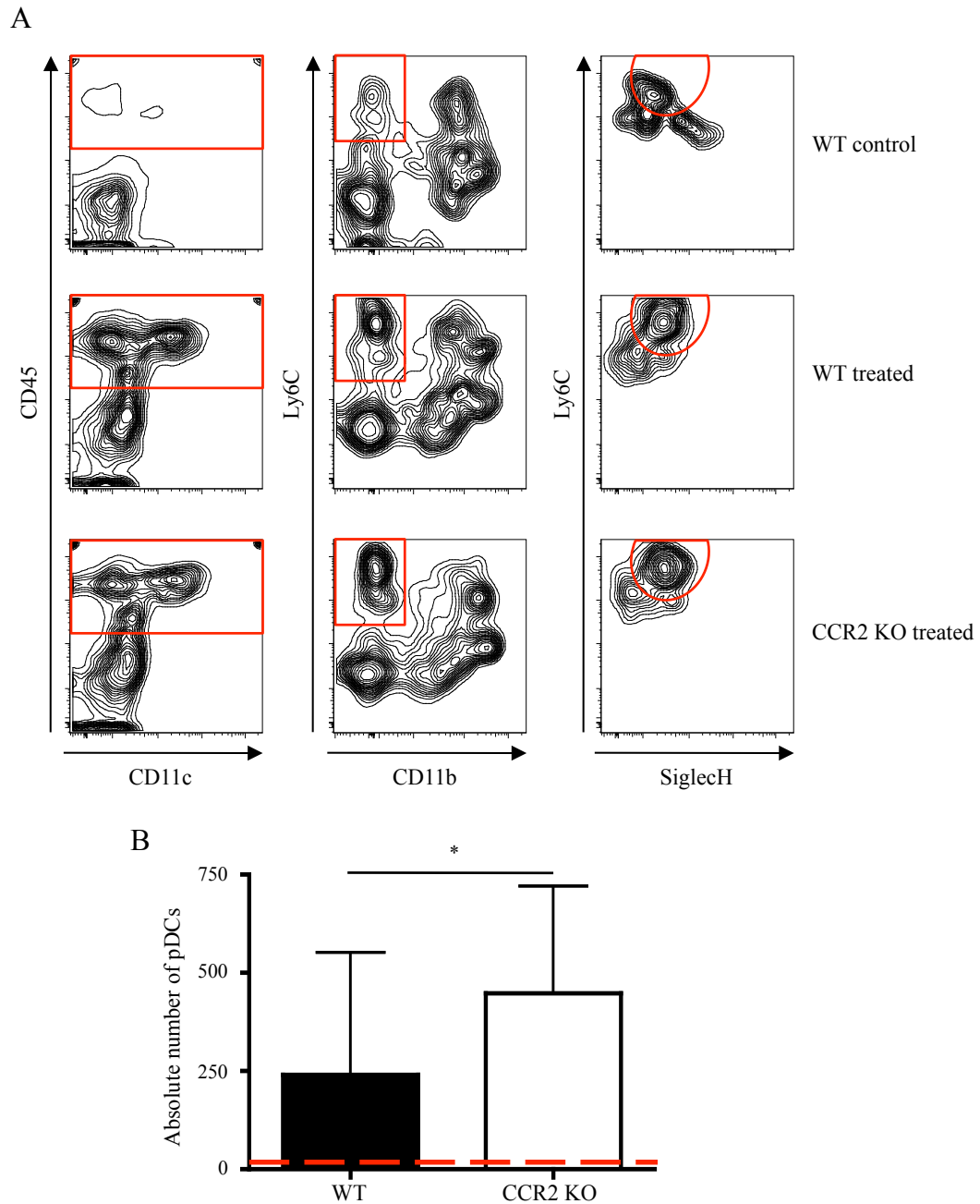


Figure 5-34: Effect of imiquimod treatment on pDC numbers in the skin.

The dorsal skin of WT and CCR2 KO animals was treated topically with imiquimod for 7 days before harvest on the 8th day. (A) Following exclusion of doublets, live cells were gated as CD45⁺, then Ly6C⁺CD11b⁻ and finally SiglecH⁺. Representative plots of pDC gating in WT control (untreated) animals and imiquimod treated animals. (B) The absolute number of skin pDCs was determined in imiquimod treated WT and CCR2 KO animals, and the red line illustrates absolute number of pDCs in the skin of a WT control animal (n=5-9 mean + SD). Data were analysed by Mann Whitney T test p<0.05 *.

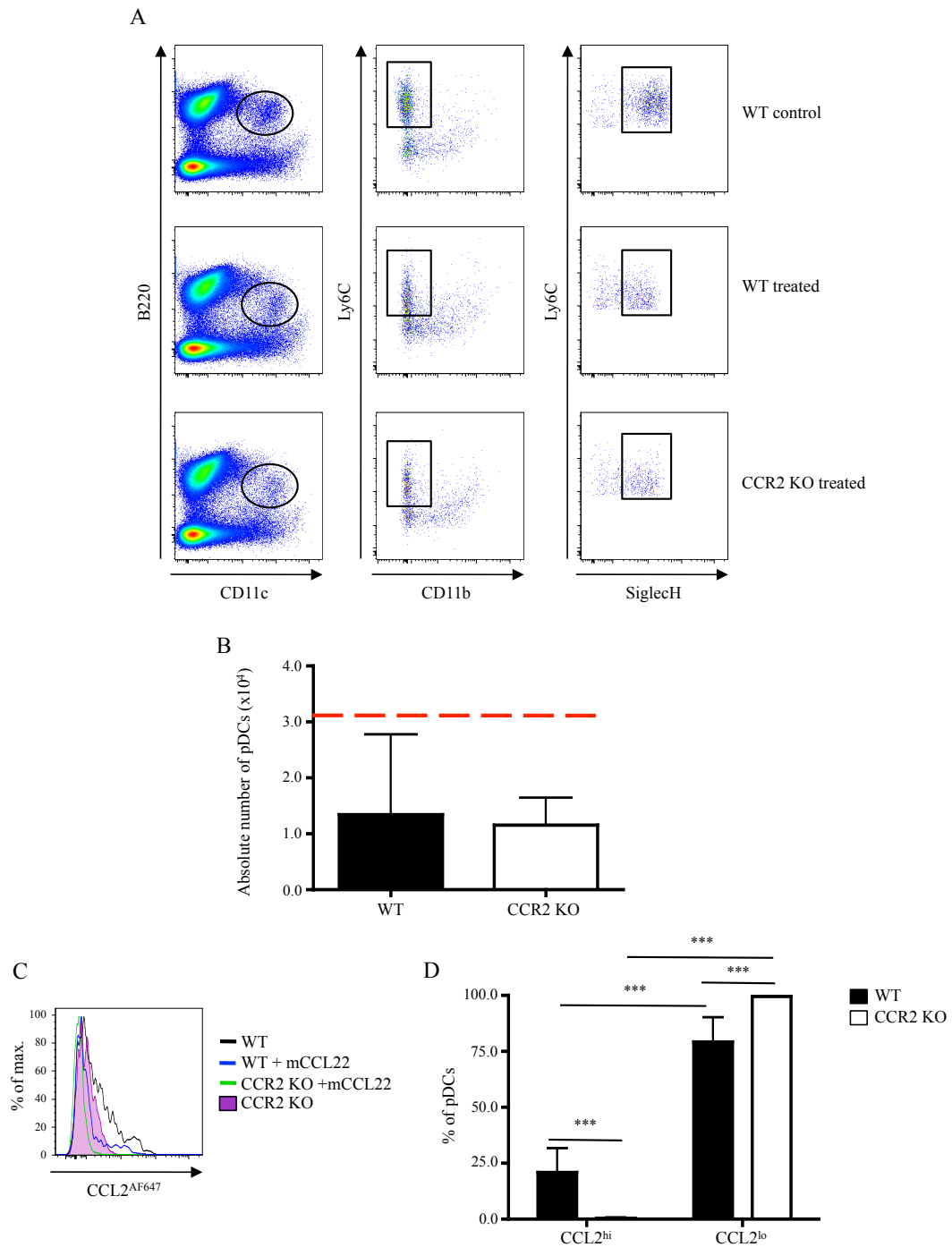


Figure 5-35: Effect of imiquimod treatment on inguinal LN pDCs.

The dorsal skin of WT and CCR2 KO animals was treated topically with imiquimod for 7 days before harvest on the 8th day. (A) Following exclusion of doublets, live cells were gated as B220⁺CD11c⁺, Ly6C⁺CD11b⁻ and finally SiglecH⁺. (A) Representative plots of pDC gating in WT control (untreated) animals and imiquimod treated animals. (B) The absolute number of inguinal LN pDCs was determined in imiquimod treated WT and CCR2 KO animals, and the red line illustrates absolute number of pDCs in the inguinal LNs of a WT control animal. (C) Representative histograms of CCL2^{AF647} uptake by pDCs from imiquimod treated WT (black line) and CCR2 KO cells (shaded purple area without competition, and WT (blue line) and CCR2 KO (green line) samples competed with 10-fold molar excess of mCCL22. (D) The proportion of CCL2^{hi} and CCL2^{lo} pDCs was determined (n=9 mean + SD). Data were analysed by Mann Whitney T-test (B) or two-way ANOVA with Bonferroni post-test (D) p<0.001 ***.

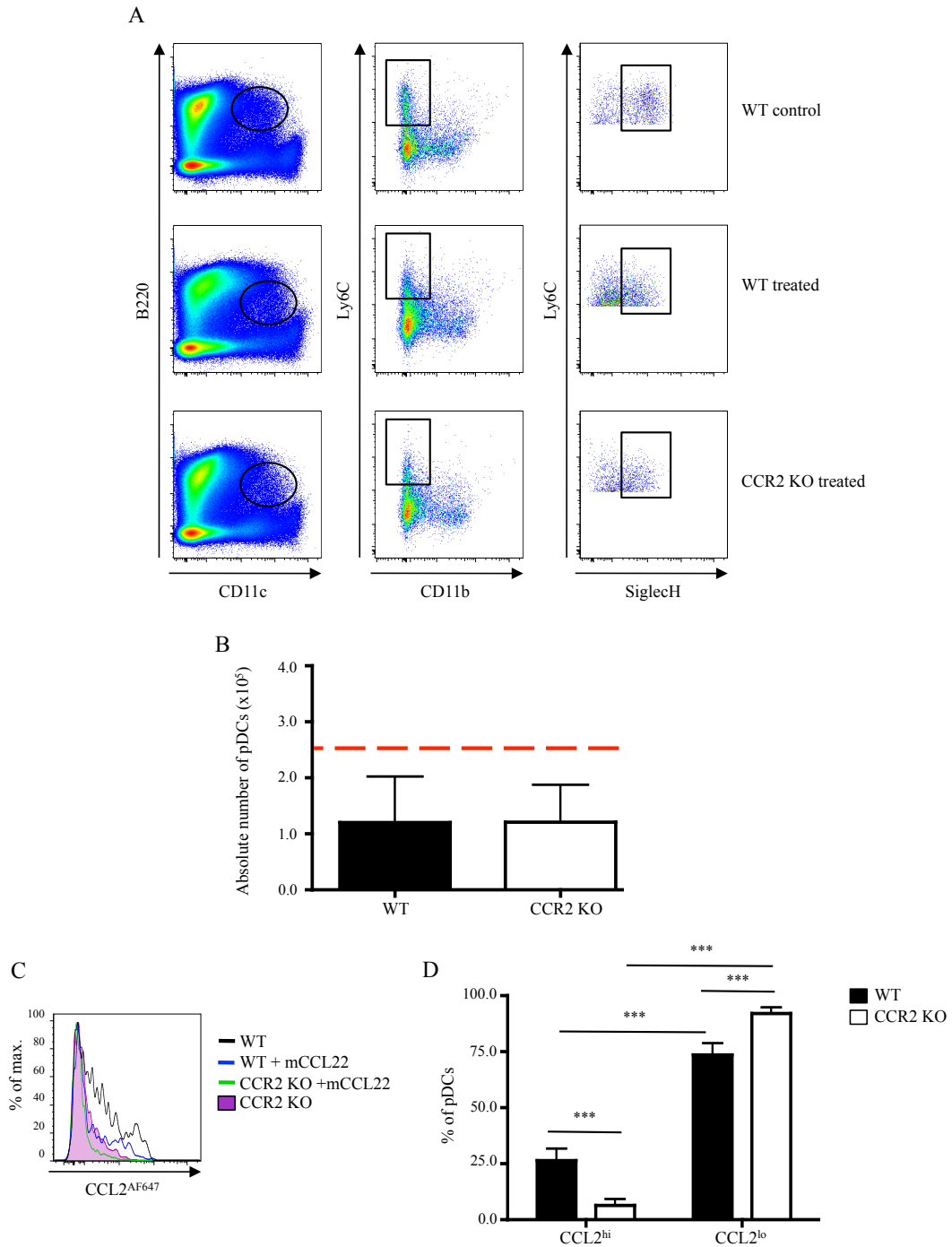


Figure 5-36: Effect of imiquimod treatment on splenic pDCs.

The dorsal skin of WT and CCR2 KO animals was treated topically with imiquimod for 7 days before harvest on the 8th day. (A) Following exclusion of doublets, live cells were gated as B220⁺CD11c⁺, Ly6C⁺CD11b⁻ and finally SiglecH⁺. (A) Representative plots of pDC gating in WT control (untreated) animals and imiquimod treated animals. (B) The absolute number of splenic pDCs was determined in imiquimod treated WT and CCR2 KO animals, and the red line illustrates absolute number of splenic pDCs in a WT control animal. (C) Representative histograms of CCL2^{AF647} uptake by pDCs from imiquimod treated WT (black line) and CCR2 KO cells (shaded purple area without competition, and WT (blue line) and CCR2 KO (green line) samples competed with 10-fold molar excess of mCCL22. (D) The proportion of CCL2^{hi} and CCL2^{lo} pDCs was determined (n=9 mean + SD). Data were analysed by Mann Whitney T-test (B) or two-way ANOVA with Bonferroni post-test (D) p<0.001 ***.

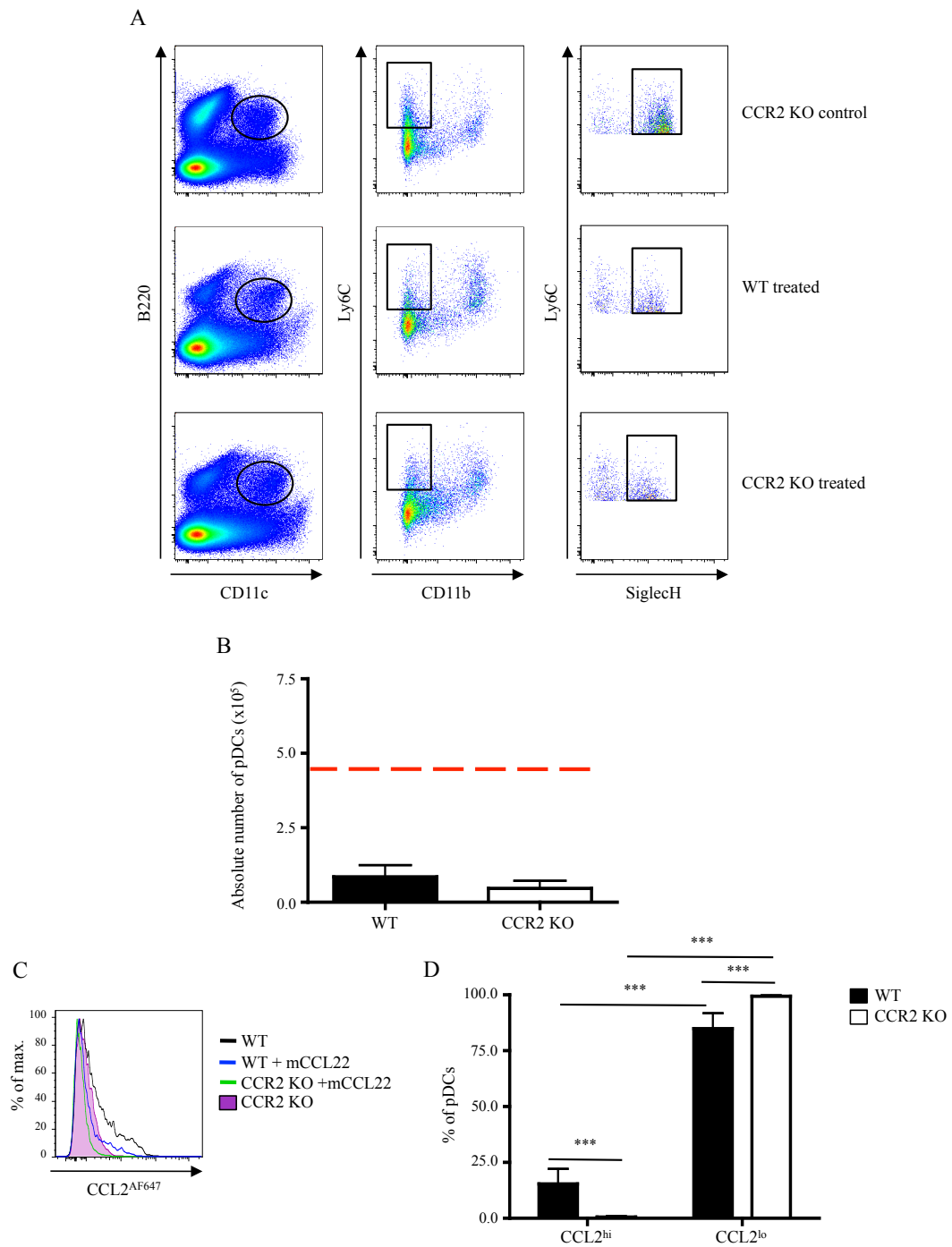


Figure 5-37: Effect of imiquimod treatment on BM pDCs.

The dorsal skin of WT and CCR2 KO animals was treated topically with imiquimod for 7 days before harvest on the 8th day. (A) Following exclusion of doublets, live cells were gated as B220⁺CD11c⁺, Ly6C⁺CD11b⁻ and finally SiglecH⁺. (A) Representative plots of pDC gating in CCR2 KO control (untreated) animals and imiquimod treated animals. (B) The absolute number of BM pDCs was determined in imiquimod treated WT and CCR2 KO animals, and the red line illustrates absolute number of BM pDCs in a CCR2 KO control animal. (C) Representative histograms of CCL2^{AF647} uptake by pDCs from imiquimod treated WT (black line) and CCR2 KO cells (shaded purple area without competition, and WT (blue line) and CCR2 KO (green line) samples competed with 10-fold molar excess of mCCL22. (D) The proportion of CCL2^{hi} and CCL2^{lo} pDCs (n=5 mean + SD). Data were analysed by unpaired T-test (B) or two-way ANOVA with Bonferroni post-test (D) p<0.001 ***.

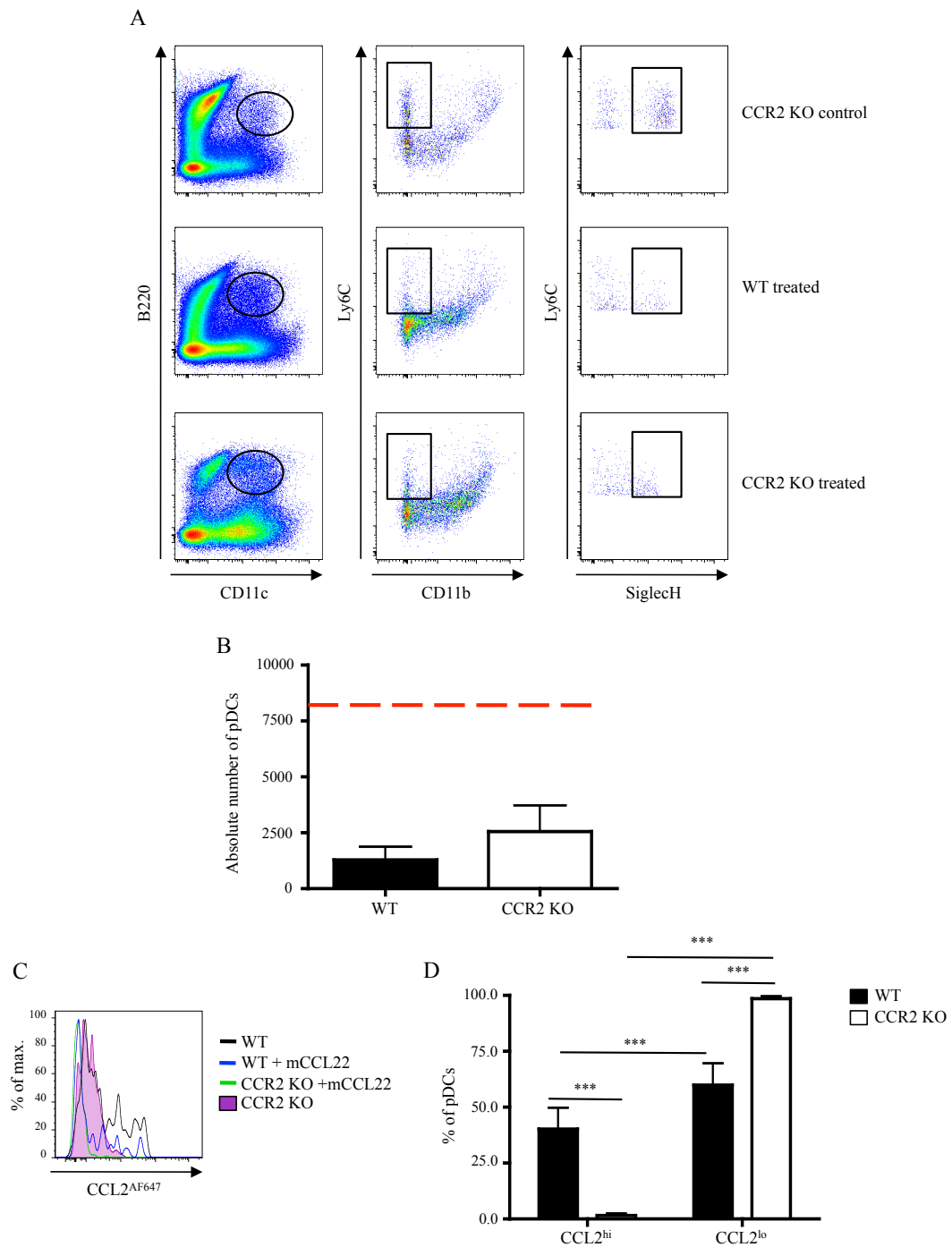


Figure 5-38: Effect of imiquimod treatment on blood pDCs.

The dorsal skin of WT and CCR2 KO animals was treated topically with imiquimod for 7 days before harvest on the 8th day. (A) Following exclusion of doublets, live cells were gated as B220⁺CD11c⁺, Ly6C⁺CD11b⁻ and finally SiglecH⁺. (A) Representative plots of pDC gating in CCR2 KO control (untreated) animals and imiquimod treated animals. (B) The absolute number of blood pDCs was determined in imiquimod treated WT and CCR2 KO animals, and the red line illustrates absolute number of blood pDCs in a CCR2 KO control animal. (C) Representative histograms of CCL2^{AF647} uptake by pDCs from imiquimod treated WT (black line) and CCR2 KO cells (shaded purple area without competition, and WT (blue line) and CCR2 KO (green line) samples competed with 10-fold molar excess of mCCL22. (D) The proportion of CCL2^{hi} and CCL2^{lo} pDCs (n=5 mean + SD). Data were analysed by unpaired T-test (B) or two-way ANOVA with Bonferroni post-test (D) p<0.001 ***.

Chapter 6 – Discussion

6.1 Introduction

The immune system is continually responding to challenges by pathogens and tissue damage through direct interactions with both self and foreign Ag. The location of the immune cells facilitates and coordinates such responses, and plays an important role in dictating their outcome. The migration and organisation of immune cells is tightly policed by the chemokine system, which is broadly divided into two functional groups, homeostatic and inflammatory chemokines. Homeostatic chemokines are involved in the development of the immune system, and its maintenance. They also facilitate the migration of cells around resting tissues. In contrast, inflammatory chemokines mediate the migration of immune cells to sites of inflammation. Produced upon inflammatory insult, they aid in the initiation of the immune response and its resolution. However, some inflammatory chemokine receptors, such as CCR2, also possess homeostatic roles e.g. mobilisation of Ly6C^{hi} monocytes from the BM (Serbina and Pamer, 2006). These specialised and fundamental roles of chemokines demonstrate the importance of accurately profiling chemokine receptor expression. With a detailed and reliable picture of receptor expression we can further the understanding of the function of particular immune cells. However, in the case of many murine receptors, including CCR2 and D6, there is limited knowledge of their expression profiles mainly due to poor sensitivity of available reagents. Therefore, to achieve the original aim of this project (determining how CCR2 contributes to the regulation of its ligands through chemokine scavenging), a comprehensive flow cytometric characterisation of CCR2 and D6 expression by mouse leukocytes was required. The data generated from these experiments altered the direction of my project, and my subsequent aims were to explore the regulation, specificity and function of CCR2 receptors on these cell populations.

6.2 Expression of CCR2 in steady-state animals

Most studies that provide information about CCR2 expression do so by monitoring transcript levels or by detecting cell surface levels of CCR2 protein using antibodies. Determining the level of transcript provides some indication about

where CCR2 is expressed, however without quantification of expression it is difficult to determine relative level of expression between tissues or cell types. Data generated by the Immunological Genome Project can provide details of CCR2 transcript levels in cell populations relative to others. Alternatively, numerous studies published throughout the duration of this PhD have been conducted using CCR2 reporter mice, CCR2-GFP or CCR2-RFP, these have provided information about CCR2 expression on individual cells by both flow cytometry and analysis of tissue sections (Saederup et al., 2010; Mizutani et al., 2011; Shi et al., 2011; Jarchum et al., 2012).

6.2.1 Antibody mediated detection of CCR2

In the initial experiments described in Chapter 3, the surface levels of CCR2 was defined using two commercially available antibodies and the most commonly used anti-mouse CCR2 antibody, MC-21. Both commercial antibodies were tested at a range of concentrations and incubation times, but they failed to detect CCR2 on BM cells (Figure 3-1). In contrast, MC-21 could detect CCR2 expression in the spleen, BM and blood. The majority of CCR2 specific staining was limited to Ly6C⁺ cell populations (Figure 3-3). The antibody had high levels of non-specific background staining, as staining profiles of WT and CCR2 KO samples were very similar in most cell populations. This was despite the low level of staining with isotype control antibodies suggesting that many of these populations contained MC-21⁺ (i.e. CCR2⁺) subsets (Figure 3-4). Thus, a comparison of MC-21 staining of WT cells to isotype staining alone, without the use of MC-21-stained CCR2 KO controls, could lead to the generation of false positives. For example, BM and blood neutrophils, in the absence of CCR2 KO samples, would be considered to be CCR2⁺. This could perhaps explain some of discrepancies that have been reported in CCR2 expression by neutrophils, with some groups reporting neutrophils to be CCR2⁺ and others CCR2⁻ (Maus et al., 2003; Reichel et al., 2006; Souto et al., 2011).

MC-21 has been used in many studies to assess CCR2 expression, including studies that included the necessary CCR2 KO controls. For example, Maus *et al.* showed that F4/80⁺ cells in the peripheral blood of mice had specific staining of CCR2, which was absent in CCR2 KOs (Maus et al., 2003). Therefore, even though MC-21 was tested at a number of different concentrations, there is a possibility

that the poor surface CCR2 detection revealed by the WT/CCR2 KO comparison might result from the suboptimal performance of the batch of MC-21 utilised in these experiments. To resolve this issue, further experiments with new MC-21 batches would be required. The difficulties encountered using this non-commercially available antibody, highlights the requirement of a new technique for the robust and reliable detection of CCR2.

6.2.2 Profiling CCL2 receptor activity using the CCL2^{AF647} assay

The failure of commercial antibodies to reliably detect CCR2, plus the apparent risk of generating false positives using MC-21, meant that previous profiling completed in the absence of CCR2 KO controls might have painted a false picture of CCR2 expression within the immune system. Furthermore, MC-21 has also been used to validate both the CCR2-GFP and CCR2-RFP reporter mice, illustrating that the majority, but not all, GFP⁺ or RFP⁺ cells were also positive for staining with MC-21 (Hohl et al., 2009; Saederup et al., 2010). This means that CCR2 transcript levels might not fully correlate with CCR2 surface levels. I developed a novel approach using fluorescently labelled human CCL2 that would facilitate the accurate identification of CCR2⁻, CCR2^{lo} and CCR2^{hi} cells. CCR2 is not the only CCL2 binding receptor, as the atypical chemokine receptor D6 can also bind CCL2. Thus appropriate controls are required to distinguish CCR2 activity from D6. The use of mCCL22 to compete D6 activity was specific and not simply due to the addition of surplus chemokine, as competition with a non-D6 ligand, mCCL19 had no effect on D6 dependent uptake of CCL2^{AF647} (Figure 3-6). mCCL7 competition on the other hand can be used to specifically identify CCR2 mediated uptake, as it is a ligand for CCR2 but not D6. However, as I shall discuss later in section 6.4.1, CCR2 on different cell types can have different affinities for mCCL7. The assay also determined that in all tested tissues, including the spleen, BM, LN and blood, the majority of CCL2^{AF647} uptake was CCR2 dependent, with only low levels of D6 activity detected.

Within the BM and blood samples of the CCR2 KO mice there was a population of cells, defined as Ly6C⁺CCL2^{lo} (BM) or Ly6C⁺CCL2⁺ (blood) that exhibited some non-specific uptake of CCL2^{AF647}, in that it could not be completely competed by mCCL22 (Figure 3-7) or numerous other CC ligands, including mCCL2 (Figure 3-8). D6 ligands caused a small reduction in CCL2^{AF647} uptake that was not present

when uptake was competed with non-D6 ligands, such as mCCL7, mCCL8, mCCL19 or mCCL21. DARC has also been shown to strongly bind CCL2, however it is unlikely to be responsible for the CCR2/D6 independent uptake of CCL2^{AF647}, as mCCL7, the only tested DARC ligand that does not also bind to D6, did not compete CCL2^{AF647} uptake (Hansell et al., 2011a). Therefore, the remaining uptake present in CCR2 KO samples following competition with a D6 ligand is probably non-specific uptake, perhaps involving pinocytosis. This indicates a caveat of the assay design, as some cells, particularly myeloid cells with phagocytic capabilities, might internalise CCL2^{AF647} non-specifically, i.e. independently of CCR2, D6 or other unknown CCL2 receptors that might exist. Although this might complicate the issue of detecting CCR2 and D6 activity on highly phagocytic cells, with the appropriate controls (e.g. CCR2 KO and mCCL22 competition) it should still be feasible to detect both CCR2 and D6. We would expect the level of inhibition of CCL2^{AF647} uptake to vary between cell types, with cells with phagocytic potential possessing higher background levels of CCL2^{AF647} uptake.

Using this methodology I have completed a comprehensive analysis of CCR2 and D6 expression in cells of the spleen, PLNs, BM and blood. This data is summarised in Tables 6-1 to 6-4 and discussed in more detail in the following sections.

Name	Identification	CCR2	D6		Systemic Inflammation
			WT	KO	
Monocytes	Ly6C ^{hi} Gr1 ^{lo} CD11b ⁺	++++	-	-	
Neutrophils	Ly6C ^{lo} Gr1 ^{hi} CD11b ⁺	-	-	-	↑ D6 in WT and KO 48 and 72 hrs after LPS.
NK cells	DX5 ⁺	+++	-	-	D6 activity in both WT and KO 48 hrs after LPS.
pDCs	B220 ⁺ CD11c ⁺ Ly6C ⁺ CD11b ⁻	+++	+	+	↑ D6 in WT and KO 48 and 72 hrs after LPS. No CCR2 activity at 72 hrs.
CD11b ⁺ cDCs	CD11c ^{hi} MHCII ^{hi} CD8α ⁻ CD11b ⁺	++	-	-	
CD8α ⁺ cDCs	CD11c ^{hi} MHCII ^{hi} CD8α ⁺ CD11b ⁻	++	+	-	D6 activity in both WT and KO 48 hrs after LPS.
Macrophages*	CD11b ⁺ F4/80 ⁺	+	ND	+	
CD4 ⁺ T cells*	CD3 ⁺ CD8 ⁻	+	ND	-	
CD8 ⁺ T cells*	CD3 ⁺ CD8 ⁺	+	ND	-	
γδ T cells*	γδ ⁺	+	ND	-	
MZ-B cells	CD19 ⁺ IgM ^{hi} IgD ^{lo} CD21 ⁺	-	+	+	↑ D6 in WT and KO 48 and 72 hrs after LPS.
B cells*	CD19 ⁺	-	ND	+	

Table 6-1: CCR2 and D6 activity of splenic leukocyte populations.

Expression of CCR2 was examined by comparing CCL2^{AF647} uptake profiles in WT and CCR2 KO. Expression of D6 was examined in both WT and CCR2 KO cells by competition of CCL2^{AF647} uptake with mCCL22. Expression of CCR2 and D6 is denoted by +, whereby + signifies low levels and ++++ signifies high levels; - denotes lack of activity; ND indicates that D6 activity was not determined on WT cells. Splenic populations were also examined for the effect of LPS on CCR2 and D6 activity. * indicates populations that were not examined for the effect of LPS on CCL2 receptor activity. All analysed CCR2⁺ populations, except pDCs had a decrease in CCR2 activity 24 hrs after LPS, which was restored or upregulated 48 hrs after LPS treatment. In addition, in the absence of CCR2 all populations had a significant upregulation of D6, which was limited to 48 hrs after LPS treatment. Comments in the systemic inflammation column describe alterations to D6 activity following LPS treatment.

Name	Identification	CCR2	D6	
			WT	KO
γδ T cells	CD3 ⁻ CD19 ⁻ γδ ⁺	+	ND	-
αβ T cells	CD3 ⁺ CD19 ⁻	-	ND	-
B cells	CD19 ⁺ MHCII ⁺	-	ND	-
Migratory cDCs	CD11c ⁺ MHCII ^{hi}	-	ND	-
Resident cDCs	CD11c ⁺ MHCII ^{lo}	+++	ND	-
pDCs	B220 ⁺ CD11c ⁺ Ly6C ⁺ CD11b ⁻	+++	+	+

Table 6-2: CCR2 and D6 activity of PLN leukocyte populations.

Expression of CCR2 was examined by comparing CCL2^{AF647} uptake profiles in WT and CCR2 KO. Expression of D6 was examined in both WT and CCR2 KO cells by competition of CCL2^{AF647} uptake with mCCL22. Expression of CCR2 and D6 is denoted by +, whereby + signifies low levels and ++++ signifies high levels; - denotes lack of CCL2 receptor activity; ND indicates that D6 activity was not determined on WT cells.

Name	Identification	CCR2	D6	
			WT	KO
Monocytes	Ly6C ⁺ Gr1 ^{lo} CD11b ⁺ CD115 ⁺	++++	+	+
Neutrophils	Ly6C ⁺ Gr1 ^{hi} CD11b ⁺ CD115 ⁻	-	ND	-
Population A	Ly6C ^{lo} Gr1 ^{lo} CD11b ⁺ CD115 ⁺	++++	ND	+
Population B	Ly6C ⁺ Gr1 ^{lo} CD11b ⁺ CD115 ⁻	-	ND	-
Population C	Ly6C ^{lo} Gr1 ^{lo} CD11b ⁺ CD115 ⁻	-	ND	-
B cells	B220 ⁺ CD11c ⁻	-	ND	-
pDCs	B220 ⁺ CD11c ⁺ Ly6C ⁺ CD11b ⁻	+++	+	+
CD11c ⁺ cells	B220 ⁻ CD11c ⁺	++	ND	+

Table 6-3: CCR2 and D6 activity of BM leukocyte populations.

Expression of CCR2 was examined by comparing CCL2^{AF647} uptake profiles in WT and CCR2 KO. Expression of D6 was examined in both WT and CCR2 KO cells by competition of CCL2^{AF647} uptake with mCCL22. Expression of CCR2 and D6 is denoted by +, whereby + signifies low levels and ++++ signifies high levels; - denotes lack of CCL2 receptor activity; ND indicates that D6 activity was not determined on WT cells.

Name	Identification	CCR2	D6	
			WT	KO
Monocytes	Ly6C ⁺ Gr1 ^{lo} CD11b ⁺ CD115 ⁺	++++	-	-
Neutrophils	Ly6C ⁺ Gr1 ^{hi} CD11b ⁺ CD115 ⁻	-	ND	-
Population A	Ly6C ^{lo} Gr1 ^{lo} CD11b ⁺ CD115 ⁺	+++	ND	-
Population B	Ly6C ⁺ Gr1 ^{lo} CD11b ⁺ CD115 ⁻	++++	ND	-
Population C	Ly6C ^{lo} Gr1 ^{lo} CD11b ⁺ CD115 ⁻	-	ND	-
B cells	B220 ⁺ CD11c ⁻	-	ND	-
pDCs	B220 ⁺ CD11c ⁺ Ly6C ⁺ CD11b ⁻	+++	+	+
CD11c ⁺ cells	B220 ⁻ CD11c ⁺	+++	ND	-

Table 6-4: CCR2 and D6 activity of blood leukocyte populations.

Expression of CCR2 was examined by comparing CCL2^{AF647} uptake profiles in WT and CCR2 KO. Expression of D6 was examined in both WT and CCR2 KO cells by competition of CCL2^{AF647} uptake with mCCL22. Expression of CCR2 and D6 is denoted by +, whereby + signifies low levels and ++++ signifies high levels; - denotes lack of CCL2 receptor activity; ND indicates that D6 activity was not determined on WT cells.

6.2.2.1 Myeloid cells

The majority of CCR2 dependent uptake was associated with cells of the innate immune system CCR2 activity was highest on Ly6C^{hi} monocytes in all tested tissues and, consistent with published observations using CCR2 reporter mice, these cells were uniformly positive for CCR2 (Serbina et al., 2009; Saederup et al., 2010; Lewis et al., 2011). In all other cell populations none, or only a fraction of cells, became CCL2⁺ after CCL2^{AF647} uptake. This is consistent with

published results and data presented in this thesis using the MC-21 antibody (Mack et al., 2001). The expression of a chemokine receptor by a proportion of a cell population has often segregated that cell population into functionally distinct subsets. For example, CCR2 expression by monocytes can delineate the inflammatory and “resident” monocyte populations (Geissmann et al., 2003; Serbina and Pamer, 2006) and CCR9 is used as a marker of tolerogenic pDCs (Hadeiba et al., 2008; Björck et al., 2011; Schlitzer et al., 2011). Therefore, the presence of CCR2 activity on a proportion of each population might delineate a functionally distinct subset of these cells. Furthermore, expression of CCR2 might lead to differences in the migratory potential of the two subsets of cells, and perhaps the presence of CCR2 alters their localisation in the spleen and LN before or during inflammation.

Both the Ly6C^{hi} and Ly6C^{lo} populations of monocytes have been reported to give rise to macrophages (Yona and Jung, 2010). Inflammatory Ly6C^{hi} monocytes express CCR2 and are recruited to sites of inflammation, where they differentiate into macrophages that are important in the clearance of pathogens. The differentiation of human peripheral blood CCR2⁺CD14⁺ inflammatory monocytes into macrophages has been reported to cause a decrease in CCR2 expression, both at the level of mRNA and surface protein. The decrease in CCR2 was associated with a parallel decrease in functional responses to CCL2, such as chemotaxis (Fantuzzi et al., 1999). However, splenic macrophages and other tissue resident macrophages, such as microglia are reported to arise from the differentiation of Ly6C^{lo}CCR2⁻ monocytes (Gordon and Taylor, 2005). In addition, a recent report indicates that many macrophages develop independently of haematopoietic stem cells, as they originate from the yolk sac (Schulz et al., 2012). Examination of CCR2 transcript levels showed that yolk sac macrophages are CCR2⁻, and only a proportion of haematopoietic stem cell derived macrophages are CCR2⁺ (Schulz et al., 2012). Consistent with these observations, my results indicate that only a small proportion of splenic macrophages (~12%) are CCL2⁺ (Figure 3-10), which is significantly lower than the percentage of CCL2⁺ monocytes (~85%). Furthermore, in contrast to monocytes, splenic macrophages also possessed low levels of D6 activity (Figure 3-10).

Results presented in this thesis demonstrate that neutrophils in unchallenged animals in the tested tissues do not internalise CCL2^{AF647} indicating that they do not possess active CCR2 or D6 (Figures 3-10, 3-12 and 3-14). However, neutrophils were the only splenic cell population to show no CCL2 uptake activity at all, and even small numbers of lymphocytes including B and T cells internalised CCL2^{AF647} via CCR2. However, it should be noted that the assay only provides information about functionally active receptors, as CCL2^{AF647} must be both bound and internalised by CCR2, therefore it cannot be excluded that neutrophils express inactive CCR2 that does not internalise CCL2^{AF647}.

6.2.2.2 B cells

In accordance with observations published from the Nibbs lab during the course of my studies (Appendix 2), a large proportion, if not all of the observed splenic D6 dependent uptake was associated with MZ-B cells (Hansell et al., 2011b). PLN B cells did not possess detectable D6 activity, presumably due to the low abundance and absence of D6 expressing B1 B cells and MZ-B cells, respectively in the LN (Hansell et al., 2011b) (Figure 3-13). However, in contrast to published observations (Hansell et al., 2011b) D6 activity was not detected on BM (Figure 3-12) and blood (Figure 3-14) B cells. The inconsistency between the published observations and my results might be due to a strain difference. Here I examined D6 activity in the total B cell population in CCR2 KO animals and found that B1 B cells in the blood and BM of CCR2 KO mice do not possess D6 activity, whereas Hansell *et al.* examined D6 activity in WT mice (Hansell et al., 2011b). However, further work to delineate the B cell populations in the BM and blood of CCR2 KO animals would need to be performed in order to confirm this. Although D6 activity was not found on B cells in any tissue, other than the spleen, there were significant levels of D6 detected on other cell populations in each tissue e.g. pDCs in each tissue possessed both CCR2 and D6 (Figure 5-3).

There was a very small population of CCR2⁺ B cells within the spleen (Figure 3-6), BM (Figure 3-12) and blood (Figure 3-13), which was not present in the LNs (Figure 3-13). Upon examination of the physical properties of these cells they were much larger than typical lymphocytes. Doublet cells had been excluded from the analysis so it is unlikely that they were doublets consisting of a B cell and a CCR2⁺ cell. One possibility is that they could be plasmablasts, due to

previous evidence of CCR2 expression by plasma cells (Delogu et al., 2006). In fact, CCR2 has been reported to play a vital role in plasma cell differentiation. Pax5 is a transcription factor that represses lineage inappropriate genes, including CCR2, whilst activating B cell specific genes in B cells. Deletion of Pax5 leads to a deficiency in B cells, as in its absence lineage inappropriate genes, such as myeloid and T cell genes are reactivated. Using chimeric mice that were reconstituted with a 1:1 mixture of BM from mice deficient in CCR2 and Pax5, Delogu *et al.* showed that mice formed normal germinal centres, but had impaired immune responses, demonstrated by a decrease in Ag specific IgG1 in serum, indicating a requirement of CCR2 for normal plasma cell function (Delogu et al., 2006). However, it should be noted that in this study there were only 2 CCR2 KO biological replicates (Delogu et al., 2006). Plasmablasts have low expression of CD19 (Delogu et al., 2006), however I found that total B cells and the CCR2⁺ B cell population did not possess any significant differences in their CD19 expression, as quantified by comparison of CD19 Δ MFI (data not shown). This would suggest that these cells are not plasmablasts.

6.2.2.3 Populations A, B and C

Several populations of cells of uncertain origin, and designated Population A, B and C, were identified in the BM (Figure 3-12) and blood (Figure 3-13) of WT and CCR2 KO mice. Each population was characterised by differences in the expression of four markers: Ly6C, CD11b, Gr1 and CD115. Population A was identified as CD115⁺CD11b⁺Ly6C^{lo}Gr1^{lo} in both the BM and blood. In these tissues Population A had high levels of CCR2 dependent uptake of CCL2^{AF647}, but CCR2 activity was lower in the blood (~50% CCL2⁺) than the BM (~85% CCL2⁺), with an overall decrease in the level of CCL2^{AF647} uptake observed on a cell-by-cell basis. BM and blood Population A cells had similar physical properties to Ly6C^{hi} monocytes. Their expression of CD115 firmly points to a monocytic origin, indicating that they could Ly6C^{lo} monocytes or monocytes of intermediary phenotype (Ly6C^{inter} monocytes), which are produced during the conversion of Ly6C^{hi} monocytes into Ly6C^{lo} monocytes. This conversion results in the downregulation of both CCR2 and Ly6C, and the parallel acquisition of higher levels of CX₃CR1 (Sunderkötter et al., 2004; Serbina and Pamer, 2006; Tacke and Randolph, 2006). There is controversy surrounding the tissue in which this conversion occurs. Some groups report that Ly6C^{hi} monocytes, in the absence of

inflammation, traffic back to the BM where they are converted into Ly6C^{lo} monocytes (Varol et al., 2007; Shi and Pamer, 2011). In contrast, others report that this conversion occurs in the blood, and that the BM monocyte population is almost exclusively composed of Ly6C^{hi} monocytes (Sunderkötter et al., 2004; Gordon and Taylor, 2005). The data presented here supports the second observation, as limited numbers of cells from Population A were observed in the BM, while their numbers increased in the blood. Furthermore, CCR2 activity of the population, although reduced in comparison to BM Ly6C^{hi} monocytes, was further reduced in the blood.

Cells from Population B were Gr1^{lo}CD115⁻CD11b⁺Ly6C⁺. The expression of Gr1 increases with maturation of neutrophils, thus immature neutrophils can be identified as Gr1^{lo}CD115⁻ (Hestdal et al., 1991). In the BM, Population B cells may represent immature neutrophils, as this population had little CCR2 activity, which is consistent with the absence of CCR2 activity on mature neutrophils. However, the physical properties of these cells suggest they are more monocyte-like than neutrophil-like. Furthermore, Population B in the blood had high levels of CCR2 activity, similar to the profiles produced by Ly6C^{hi} monocytes. The only observed difference in the surface immunophenotype of Population B in the blood and Ly6C^{hi} monocytes was their expression of CD115. I was unable to identify this population in the spleen, as, in my hands, anti-CD115 did not stain splenic monocytes. Anti-CD115 antibodies have been used by others to successfully identify resting (Swirski et al., 2009) or activated (Drutman et al., 2012) splenic Ly6C^{hi} monocytes, but my data would at least suggest that CD115 is reduced on splenic Ly6C^{hi} monocytes.

CD115 is typically considered to be a monocyte marker, as it is crucially involved in their development (Auffray et al., 2009). However, recently Rose *et al.* described the identification of a population of CD115⁻ splenic monocytes/macrophages (Rose et al., 2011). Therefore, it is possible that Population B are CD115⁻ monocytes, and that their emigration from the BM is accompanied by a large increase in CCR2 activity. Alternatively, these cells might not be monocytes, but a precursor that upon entry in the periphery mature and acquire CCR2 activity. The splenic pre-cDC population that was discussed in the Introduction (section 1.5.1) has a similar surface phenotype. Splenic pre-cDCs have been identified as CD11c⁺CD11b^{lo}F4/80^{lo}Ly6C⁺Ly6G⁻ and

the same population was shown to exist in the blood (Naik et al., 2006). The pre-cDCs were not examined for CD115 expression, or Gr1. However, anti-Gr1 binds to both Ly6C and Ly6G, expressed by monocytes and neutrophils, respectively (Daley et al., 2008). Naik *et al.* illustrated that the pre-cDCs were Ly6C⁺ and Ly6G⁻ (Naik et al., 2006), thus perhaps the low expression of Gr1 detected on Population B is explained by the presence of only Ly6C on these cells. Both of these theories suggest that BM Population B cells are developmental precursors of blood Population B cells and that their maturation is accompanied by an increase in CCR2 activity. Si *et al.* have examined surface expression of CCR2 during the differentiation of BM haematopoietic stem cells and haematopoietic progenitors (Si et al., 2010). According to staining with MC-21, BM haematopoietic stem cells and haematopoietic progenitor cells express CCR2 and their differentiation along the myeloid lineage is accompanied by an increase in CCR2 expression (Si et al., 2010). These observations, and the lack of CD115 expression by BM Population B, make it unlikely that they are of myeloid lineage. Therefore, BM and blood Population B cells might not be linked developmentally. Population B in the blood might derive from Ly6C^{hi} monocytes that have lost their expression of CD115. Further investigations into the surface phenotype and function of these cells are required to prove the identity of cells within Population B.

Population C was identified in the blood and BM as Ly6C^{lo}CD11b⁺Gr1^{lo}CD115⁻. These cells did not possess significant levels of CCR2 or D6 activity in either tissue or possess physical characteristic that were similar to monocytes, neutrophils or lymphocytes. They were very large granular cells. The physical properties and surface phenotype of these cells suggest that they might be eosinophils, as Rose *et al.* have identified eosinophils as SSC^{hi}CD11b⁺Ly6C^{inter}Gr1^{inter} cells (Rose et al., 2011). Confirmation of the identity of these cells as eosinophils could be gained by examining their expression of the eosinophil specific marker SiglecF (Zhang et al., 2007).

6.2.2.4 Population D and CD11c⁺MHCII⁻ cells

Two additional populations of cells whose identity was uncertain were found in the spleen of both WT and CCR2 KO animals. These were named Population D (Figure 5-1) and CD11c⁺MHCII⁻ cells (Figure 3-11). Both populations had high

levels of CCR2 dependent CCL2^{AF647} uptake and Population D also possessed low levels of D6. In Chapter 5 I have already speculated over the identity of Population D, suggesting that it might contain a subset of NK cells. Blasius *et al.* have identified an NK cell subset that is B220⁺CD11c⁺NK1.1⁺CD11b⁺ (Blasius *et al.*, 2007). Population D cells were identified as B220⁺CD11c⁺Ly6C⁺/CD11b⁺/ cells (i.e. heterogeneous for CD11b and Ly6C) but importantly were negative for the pDC markers, PDCA1 and SiglecH. These observations have important implications in the identification of pDCs, because they indicate that B220⁺CD11c⁺ gating alone is not sufficient to identify pDCs. Such a population would be substantially contaminated by cells lacking SiglecH and PDCA1, which I would not consider to be pDCs. The results presented in Chapter 3 have illustrated that NK cells have high levels of CCR2 activity (Figure 3-9), a feature that fits with the description of Population D. However, NK cells identified as simply DX5⁺ did not possess any D6 activity. Therefore, D6 activity might be limited to the B220⁺CD11c⁺NK1.1⁺ subset of NK cells. DX5 was originally considered to be a pan-NK cell marker but has also been shown to be expressed by basophils (Arase *et al.*, 2001; Obata *et al.*, 2007). However, the observed uptake can be assigned to NK cells due to the physical properties of the cells, as they were similar in size to lymphocytes, rather than the larger basophils.

Initial investigations into the surface phenotype of CD11c⁺MHCII⁻ cells suggest the population contains a mix of several cell types. The cells were examined for the expression of a number of surface markers, such as F4/80, Gr1, CD11b, DX5 and B220. By process of elimination I was able to surmise that the population does not contain B cells, T cells or NK cells, as all were excluded at the time of live cell gating. However, the presence of a proportion of DX5⁺ cells within this population suggests not all NK cells were excluded from the analysis and could account for some of the CCR2 activity. The cells were also B220⁻ and CD11b⁺, indicating that they are not pDCs. The expression of CD11b⁺ and differential expression of Gr1 by the population suggests that it might contain Ly6C^{hi} monocytes, but their uptake is not as pronounced as Ly6C^{hi} monocytes. Further work is needed to confirm the identity of this population, but their physical properties indicate that the cells are of a lymphocytic origin, having FSC and SSC lower than neutrophils. CD11c is typically considered to be a marker of DCs, however these results clearly indicate additional markers are required to

accurately identify DC populations. Gating on the basis of CD11c alone would segregate a population of cells that includes DCs, but this population would be heavily contaminated with cells of various origins (e.g. B cells, NK cells and macrophages). Therefore, care must be taken when interpreting results produced using CD11c-DTR mice, which have DTR under the control of the CD11c promoter. CD11c-DTR mice have been used to examine cDC biology and determine the affects of depletion of cDCs in numerous models (Hochweller et al., 2009; Jung et al., 2002). However, treatment of CD11c-DTR mice with diphtheria toxin does not lead to a specific depletion of cDCs, as it also leads to partial depletion of B cells, T cells and NK cells (Hochweller et al., 2008).

6.2.2.5 T cells

Mack *et al.* reported that 5-15% CD4⁺ T cells and 2-10% CD8⁺ T cells expressed CCR2, as determined by using the MC-21 antibody (Mack et al., 2001). When the percentage of CCL2⁺ cells found in CCR2 KO T cell populations was subtracted from the percentage of CCL2⁺ in WT mice, it was observed that similar frequencies of CD4⁺ (13.27%) and CD8 α ⁺ (6.82%) T cells possessed CCR2 activity. In Figure 3-9, CD4⁺ T cells were not identified by their expression of CD4, but by their absence of CD8 α , therefore it might be considered inaccurate to characterise these cells as CD4⁺ T cells. However, experiments conducted by Chris Hansell (personal communication) have illustrated the CD3⁺CD4⁺ cells have similar profiles to the ones shown in Figure 3-9. Furthermore, the proportions of CD8 α ⁺CCR2⁺ (2-10% Mack paper vs. 6.82%) and CD4⁺CCR2⁺ (5-15% Mack paper vs. 13.27%) T cells that were measured using either technique were similar, with there being a greater proportion of CD4⁺CCR2⁺ than CD8 α ⁺CCR2⁺ (Mack et al., 2001). In contrast to splenic T cells, TCR $\alpha\beta$ ⁺ T cells (gated as CD3⁺) in the LN had virtually no CCR2 dependent uptake of CCL2^{AF647}. This might be explained by a difference in the phenotype of the T cell population between the spleen and LN (Weninger et al., 2001). The spleen is a rich source of effector and memory T cells, which have downregulated CCR7 expression and express inflammatory chemokine receptors, including CCR2 (Sallusto et al., 1999; Weninger et al., 2001). The LN T cell population may possess more naïve T cells that are rich in expression of CCR7, but lack expression of inflammatory chemokine receptors (Sallusto et al., 1999; Weninger et al., 2001). Work by Ross Kinstrie and Eric Cruikshank in our group has shown that that CCR5 and CXCR3 are restricted to

CD44⁺ memory T cells (CD4⁺ and particularly CD8 α ⁺) (personal communication). It would be interesting to determine whether CCL2^{AF647} uptake by CD4⁺ and CD8 α ⁺ T cells correlated with expression of CD44, and other markers of T cell phenotypes, such as CD62L and CD25.

Splenic and LN $\gamma\delta$ T cells had a higher proportion of CCR2⁺ cells than the TCR $\alpha\beta$ ⁺ T cells. Similar to cells of the innate immune system, $\gamma\delta$ T cells contribute to the early defence against pathogens, as in addition to their ability to recognise Ag via MHC, they can also recognise Ag in the absence of processing and presentation by MHC (Kozbor et al., 1989; Matis et al., 1989; Holoshitz et al., 1992). Thus, akin to other cells of innate immune systems $\gamma\delta$ T cells use CCR2 to mobilise to sites of inflammation and provide the first line of defence against invading pathogens (Penido et al., 2008).

6.2.2.6 cDCs

In a resting animal most cDCs within the secondary lymphoid organs are phenotypically immature, as characterised by their low expression of MHCII and the costimulatory molecule, CD86 (Wilson et al., 2003). Immature cDCs are reported to express inflammatory chemokine receptors, such as CCR2, which are downregulated upon cDC maturation and CCR7 is upregulated (Dieu et al., 1998; Sallusto et al., 1998; Sozzani et al., 1999; 2000; Alvarez et al., 2008). Therefore, although Wilson *et al.* did not study the expression of chemokine receptors by splenic cDCs their immature phenotype might indicate that they possess inflammatory chemokine receptors (Wilson et al., 2003). In accordance with this hypothesis, data presented in this thesis shows that both CD8 α ⁺ and CD11b⁺ splenic cDCs possess CCR2 activity, with a larger proportion of CD8 α ⁺ cDCs showing CCR2 activity (Figure 3-11). Consistent with my observations, work conducted by Lewis *et al.* illustrated that in the spleen of CCR2-RFP mice, CD8 α ⁺ cDCs had high levels of RFP/CCR2 (Lewis et al., 2011). Furthermore, they defined two subsets of CD11b⁺ cDCs based on the expression of the C-type lectin Clec12a. CD11b⁺Clec12a⁺ cDCs were RFP/CCR2⁺, whereas CD11b⁺Clec12a⁻ cDCs expressed little RFP/CCR2⁺ (Lewis et al., 2011). Therefore, within the population of CD11b⁺ cDCs that I gated there exists two populations of cDCs, which possess differences in their CCR2 expression. In future experiments, it would be

interesting to determine if CCL2^{AF647} uptake correlates with expression of Clec12a by CD11b⁺ cDCs.

In PLNs only resident cDCs were found to have CCR2 activity, as migratory cDC populations contained very few CCL2⁺ cells. Similar to the spleen, LN resident cDCs are typically immature cDCs (Wilson et al., 2003; Sixt et al., 2005), thus the expression of CCR2 by an immature cDC population is not surprising. However, resident cDCs, gated as CD11c⁺MHCII^{lo}, would also include pDCs, which have been shown to possess high levels of CCR2 in several tissues, including LNs (Figure 5-3). Therefore, since the CD11c⁺MHCII^{lo} population contains cDCs in addition to pDCs, we can conclude that CCL2^{AF647} uptake by CD11c⁺MHCII^{lo} cells is not exclusively due to pDCs. It would suggest in fact that non-pDC CD11c⁺MHCII^{lo} cells, most of which are likely to be cDCs, are capable of CCR2-dependent CCL2^{AF647} uptake. This would be consistent with data from the spleen where a substantial subset of cDCs have CCR2 activity.

The lack of CCR2 activity amongst migratory cDCs was expected, because their arrival from peripheral tissues is associated with their maturation and the downregulation of inflammatory chemokine receptors, with a parallel upregulation of CCR7 (Dieu et al., 1998; Sallusto et al., 1998). Migratory cDCs had significantly higher background levels of CCL2^{AF647} uptake than resident cDCs, perhaps indicating that they possess a high phagocytic capacity. However, migratory cDCs are mature cDCs that should demonstrate a decreased phagocytic potential compared to immature cDCs, such as LN resident cDCs (Cella et al., 1997; Kamath et al., 2000; Sallusto and Lanzavecchia, 2002; Wilson et al., 2003).

Sixt *et al.* have reported that immature LN resident cDCs are immobilised on the basement membrane of the fibroblastic reticular cell network. It is only following their maturation that they become highly motile (Sixt et al., 2005). However, CCR2 might allow a subset of LN resident cDCs to respond to CCR2 ligands present in the LN during homeostasis and inflammation. During inflammation, inflammatory chemokines such as CCL2 are produced at peripheral inflammatory sites, which can be transported in lymph to the subcapsular sinus of the draining LN. The fibroblastic reticular cell network can channel CCL2 from the subcapsular sinus to HEVs (Gretz et al., 2000; Andrian

and Mempel, 2003). Therefore, immobilised CCR2⁺ resident cDCs might be provided with cues for migration by exposure to CCL2 present within the fibroblastic reticular cell network. Interestingly, according to data on the Immgen website (<http://www.immgen.org>), CCL2 and CCL7 transcripts, but not those encoding CCL12, are produced at high levels by fibroblast reticular cells isolated from resting skin-draining and mesenteric LNs. Thus, CCR2 expression by LN DCs might be significant even in the absence of inflammation.

The three methods that are now used to detect CCR2 i.e. transcript levels, CCR2 reporter mice and MC-21 antibody, have produced some conflicting results with regards to CCR2 expression by individual cell populations (Mack et al., 2001; Saederup et al., 2010; Yamaski et al., 2012). My data might help to clarify some of these inconsistencies. Saederup *et al.* reported that expression of detectable CCR2 protein was more restricted than CCR2 mRNA, so some cells that were found to be CCR2⁺ at the transcript level, did not possess surface CCR2. Likewise, a percentage of GFP⁺ cells within CCR2-GFP reporter mice did not possess detectable CCR2 surface protein (Hohl et al., 2009). Analysis of RFP expression by flow cytometry illustrated that 5-10% of T cells and 85-95% of NK cells were RFP⁺. However, Saederup *et al.* did not detect any surface expression of CCR2 on NK cells or T cells, according to staining with MC-21 (Saederup et al., 2010). This is in contrast to Mack *et al.* that reported surface CCR2 protein was expressed by a small number of CD4⁺ and CD8⁺ T cells (Mack et al., 2001). Yamaski *et al.* summarised these inconsistencies, reporting that although several cell types, such as monocytes, basophils and immature cDCs have been found to express CCR2 both at transcript and protein level, other populations have only been found to express CCR2 mRNA and their surface levels of CCR2 has yet to be definitively confirmed (Yamaski et al., 2012). Immature B cells, T cells and NK cells have all been reported to express CCR2 at the transcript level: however their level of CCR2 surface protein has not been confirmed (Yamaski et al., 2012). Data presented in this thesis has shown that low numbers of both CD4⁺ and CD8 α ⁺ T cells possess low levels of CCR2 activity and NK cells possess significant levels CCR2 activity. CCR2 activity was only found on a very small number of B cells (Figure 3-9). Furthermore, splenic macrophages possessed low levels of CCR2 activity, whereas use of CCR2-GFP mice illustrated that lung

macrophages were negative for CCR2⁻ (Hohl et al., 2009). This difference might be due to tissue-specific differences in CCR2 expression.

Each cell population had varying levels of CCR2 activity, ranging from CCR2⁻, CCR2^{lo} to CCR2^{hi}. Where the presence of high or low levels of CCR2 might have a functional significance. Volpe *et al.* have shown that upon binding of ligand, CCR2 on Ly6C^{hi} monocytes was rapidly internalised. However, this internalisation of CCR2 did not affect the responsiveness of Ly6C^{hi} monocytes to further CCR2 ligands, as monocytes were still able to migrate in response to CCR2 ligands. Thus, CCR2 must either be rapidly recycled back to the surface where it can bind more ligand, or there are sufficient numbers of CCR2 receptors on the surface of Ly6C^{hi} monocytes to maintain high levels of responsiveness following the internalisation of some receptors (Volpe et al., 2012). This feature might be limited to cell populations with high CCR2 activity, as internalisation of CCR2 in response to CCR2 ligands might render populations with low CCR2 activity unresponsive to further ligand, both in terms of migration and signalling. *In vitro* transwell migration assays or calcium ion flux assays could be used to determine the migratory and signalling potential of both CCR2^{hi} and CCR2^{lo} populations in response to varying concentrations of CCR2 ligands.

6.3 Effect of systemic inflammation induced by LPS on CCR2 and D6 activity

LPS mediated activation of TLR4 has previously been described to downregulate CCR2 expression in human (Xu et al., 2000; Parker et al., 2004) and murine (Zhou et al., 1999) monocytes, as measured by antibody mediated detection of surface CCR2 levels. Results presented in Chapter 4 firmly support this observation, as both splenic (Figure 4-1) and BM (Figure 4-11) Ly6C^{hi} monocytes showed a substantial reduction in CCR2 dependent uptake of CCL2^{AF647} 24 hrs after LPS treatment. Furthermore, CD11b⁺ and CD8 α ⁺ cDCs, both of which are reported to express TLR4 (Mazzoni and Segal, 2004), were shown to have a complete loss of CCR2 activity 24 hrs after LPS administration (Figure 4-7 and Figure 4-8). This might be explained by cDC maturation, which is associated with downregulation of inflammatory chemokine receptors and the upregulation of CCR7 (Dieu et al., 1998; Sallusto et al., 1998; Alvarez et al., 2008). Indeed, reduction of CCR2 dependent uptake of CCL2^{AF647} was coincident with acquisition

of the activation marker CD86 (Figure 4-9). The expression of TLR4 by NK cells and pDCs is controversial. NK cells have been shown to possess TLR4 at the transcript level and to carry intracellular TLR4 protein, but they have been reported to express little surface TLR4 protein (Souza-Fonseca-Guimaraes et al., 2012). Several conflicting results have also been published with regards to TLR4 expression by pDCs. Boonstra *et al.* found that BM-derived pDCs and splenic pDCs did not express TLR4 (Boonstra et al., 2002), whereas Edwards *et al.* reported that splenic pDCs did (Edwards et al., 2003). Both groups determined expression only at the transcript level (Boonstra et al., 2002; Edwards et al., 2003).

Regardless of the controversies in expression of TLR4 by NK cells and pDCs, my results suggest that the CCR2 activity of both cell populations is affected by LPS treatment, as 24 hrs after LPS administration both NK cells (Figure 4-3) and pDCs (Figure 4-6) had a large reduction in CCR2 dependent uptake of CCL2^{AF647}.

Interestingly, at the 24 hr time-point, LPS did not appear to affect the D6 activity of cell populations that were shown to exhibit D6 dependent uptake of CCL2^{AF647} in untreated animals. For example, splenic MZ-B cells (Figure 4-5), splenic pDCs (Figure 4-6) and BM monocytes (Figure 4-11) maintained D6 activity 24 hrs after LPS treatment.

Neutrophils did not possess CCR2 activity in resting animals, or at any time-point after LPS administration (Figure 4-4). In contrast to results presented here, another group has illustrated that BM neutrophils are dependent on CCR2 for their infiltration into organs during a model of sepsis induced by caecal puncture (Souto et al., 2011). Souto *et al.* confirmed CCR2 expression by flow cytometry using the anti-CCR2 antibody from Novus (Souto et al., 2011), which in my hands was unable to detect CCR2 (Figure 3-1). The group reported very low levels of expression of CCR2 on untreated neutrophils, but after treatment with LPS for 2 hrs surface CCR2 was upregulated, but was still expressed at low levels. They also illustrated that LPS exposed neutrophils isolated from BM of WT animals could respond in chemotactic assays to CCR2 ligands. Migration towards CCL2 and CCL7 by LPS activated neutrophils was mediated by CCR2, as no migration was observed by CCR2 deficient animals (Souto et al., 2011). Therefore, perhaps neutrophils rapidly upregulate CCR2 following exposure to LPS, but by 24 hrs CCR2 activity is lost. In addition, although neutrophils did not possess D6 dependent uptake of CCL2^{AF647} in a resting animal, my results suggest that

activation of TLR4 on neutrophils by LPS exposure results in significant upregulation of D6 activity 48 and 72 hrs after LPS treatment (Figure 4-4). Work conducted in Gerry Graham's lab suggests that D6 expression by neutrophils controls the positioning of neutrophils within inflamed tissues by regulating their migrational responses to inflammatory CC chemokines (personal communication from Gerry Graham and Rob Nibbs). In the absence of D6, neutrophils had enhanced migratory responses to the CCR1 ligand, CCL3 in chemotaxis assays. Furthermore, neutrophil accumulation in TPA induced skin inflammation is exaggerated in the absence of D6, which leads to exacerbated skin inflammation. However, neutrophil accumulation was blocked by the antagonism of CCR1 (Gerry Graham and Rob Nibbs personal communication). Thus, upregulation of D6, 48 and 72 hrs after LPS administration might function to regulate neutrophil migration to sites of inflammation by controlling their migratory responses to inflammatory chemokines.

Following the downregulation of CCR2 dependent uptake by 24 hrs, CCR2 activity was restored or upregulated in the majority of cases. For example, BM and splenic monocytes, NK cells, and CD11b⁺ and CD8 α ⁺ cDCs all restored or upregulated CCR2 activity at the later time-points in the LPS time-course. Interestingly, pDCs, which possess CCR2 and low levels of D6 activity in a resting animal, did not restore CCR2 activity following its downregulation at 24 hrs, but instead had a significant upregulation of D6 dependent CCL2^{AF647} uptake 72 hrs after LPS administration (Figure 4-6). In contrast, 48 hrs after LPS treatment, WT pDCs did not possess significant levels of D6, but CCL2^{AF647} uptake was mediated by CCR2. CCR2 might therefore be important for pDC migration at this time-point, but there was no affect on the frequency of pDCs, so it is not required for the entry or exit of pDCs from the spleen. However, pDCs might exhibit intra-splenic migration that is CCR2 dependent. CCR2 might facilitate pDC localisation to an area in spleen where the later upregulated D6 can sequester inflammatory chemokines. To test this hypothesis, distribution of WT and CCR2 KO pDCs 48 hrs after LPS injection could be examined in splenic tissue sections stained with antibodies against PDCA1 or SiglecH.

These later time-points in the LPS time-course may be part of the resolution phase of inflammation, and CCR2 and D6 may participate in this process. My

results and other published work for D6 (Hansell et al., 2011b) and CCR2 (Volpe et al., 2012) have shown that both receptors possess scavenging activity. Therefore, upregulation of CCR2 or D6 activity at the later time-points might aid in the resolution of inflammation by sequestering remaining proinflammatory chemokines produced during times of inflammation (Kopydlowski et al., 1999; Xu et al., 2000). Calculation of the percentage of CCL2⁺ cells within each cell population illustrated a striking phenotype. In the CCR2 KO samples, each cell population at the 48 hr time point was found to have a proportion of cells that had taken up CCL2^{AF647} in a D6 dependent manner. This appeared to be limited to the 48 hr time-point, as by 72 hrs all populations, except pDCs, neutrophils and MZ-B cells had lost D6 activity. In the majority of cell types this phenomenon was only detectable in CCR2 KOs. In addition, although not shown here, data produced by Chris Hansell and I suggest that splenic pDCs from D6 KO animals have increased CCR2 activity at later time-points in the LPS time-course. These results suggest that in the absence of one CCL2 binding receptor the other receptor plays a more important role in scavenging CCR2 ligands. Maus *et al.* have illustrated that intratracheal administration of LPS in CCR2 KO animals is associated with increased levels of CCL2 in bronchial alveolar lavage fluid compared to WT animals (Maus et al., 2005). They performed a dose response curve of LPS, and found that each concentration of LPS produced different profiles of CCL2 production in bronchial alveolar lavage fluid. At the two highest concentrations of LPS (10 or 20 µg), peak CCL2 production was 72 or 48 hrs after LPS administration, respectively (Maus et al., 2005). These concentrations are similar to the amount of LPS administered intravenously in my study, therefore perhaps the upregulation of D6 by CCR2 KO cells can be coordinated with peak production of CCL2. Upregulation of D6 might serve to scavenge excess CCL2, which could aid in the resolution of inflammation. This can be explored in future experiments by examining the level of CCL2 (and the other CCR2/D6 ligand CCL12) present in the serum at each time-point of the LPS time-course in CCR2 KO, D6 KO and CCR2/D6 double KO mice.

These results have helped to expand our current understanding of D6 expression. It has been observed that several populations of cells in WT spleens, such as pDCs and CD8α⁺ cDCs, along with BM Ly6C^{hi} monocytes possess significant levels of CCR2 and D6 activity. The expression of D6 on B1 B cells has been shown to

regulate their sensitivity to the CXCR5 ligand, CXCL13 (Hansell et al., 2011b). The co-expression of D6 and CXCR5 by B1 B cells can lead to decreased CXCL13 induced migration of B1 B cells, as in the absence of D6 migratory responses to CXCL13 were significantly enhanced (Hansell et al., 2011b). D6 deletion did not affect the surface expression of CXCR5, and the effects of D6 on CXCR5 activity were hypothesised to arise via chemokine-independent phosphorylation of D6 which drives the redistribution of β -arrestins from the cytoplasm to the membrane (McCulloch et al., 2008; Hansell et al., 2011; Gerry Graham and Rob Nibbs personal communication). This is not required for D6 mediated chemokine scavenging, but could theoretically influence the activity of chemokine receptors co-expressed with D6 (McCulloch et al., 2008; Hansell et al., 2011b; Gerry Graham and Rob Nibbs personal communication). Therefore, perhaps D6 can regulate the function of CCR2 by either altering the migration potential of cells by scavenging ligands to reduce chemotactic signals, or, akin to D6 and CXCR5, by regulating the sensitivity of CCR2 for its ligands. This hypothesis might explain the reported increase in Ly6C^{hi} monocytes in the secondary lymphoid organs of animals deficient in D6 (Savino et al., 2012). Savino *et al.* have reported that during inflammation D6 might be important in the regulation of CCR2 dependent Ly6C^{hi} monocyte egress from the BM (Savino et al., 2012). Data shown in Figure 4-11 suggests that BM Ly6C^{hi} monocytes possess CCR2 and D6. Therefore, perhaps within the BM, D6 sequesters CCR2 ligands and in doing so, might regulate CCR2 dependent mobilisation of Ly6C^{hi} monocytes from the BM during inflammation. In the absence of D6 there would be less scavenging of CCR2 ligands and as a consequence, egress of Ly6C^{hi} monocytes would be increased.

6.4 Advantages and disadvantages of the CCL2^{AF647} assay

6.4.1 CCL2^{AF647} assay versus antibodies

Data presented in this thesis establish CCL2^{AF647} uptake assay as a reliable, sensitive and specific method to detect CCL2 receptors. Consistent with published observations high levels of D6 activity was observed on MZ-B cells (Figure 3-9) (Hansell et al., 2011b), and all populations possessing CCR2 activity in the CCL2^{AF647} uptake assay have previously been reported to express CCR2 at

either the transcript level or by antibody mediated detection of surface CCR2. However, the proportion of CCR2⁺ cells of each population differs depending on which detection method was utilised. Typically a greater number of CCR2⁺ cells were found when using the CCL2^{AF647} assay. Prime examples are the CD8 α ⁺ cDCs, pDCs and NK cells. Thus, the CCL2^{AF647} assay appears to be more sensitive than the anti-CCR2 antibody MC-21, as the assay was able to detect CCR2^{hi}, CCR2^{lo} and CCR2⁻ populations.

Another advantage of the assay over the use of antibodies is that in addition to the simple role of detecting surface CCL2 receptors, it also provides information about their activity. However, the assay fails to distinguish if the observed CCL2^{AF647} uptake is facilitated by small amounts of receptors highly active for uptake, or large numbers of receptors with low overall uptake capacity. Therefore, levels of CCR2/D6 activity detected using the CCL2^{AF647} assay might not reflect the surface expression level of CCR2 or D6. Nonetheless the comparison of my results to published profiles of CCR2 expression produced using the MC-21 antibody indicate that in mice it probably does, at least to some extent, correlate with CCR2 surface levels. The lack of a reliable anti-murine D6 antibody means that a similar comparison cannot be conducted. As discussed earlier (section 3.2), a caveat associated with the CCL2^{AF647} assay is that it only provides information about functionally active receptors. Therefore CCR2 might be present on a cell, but if it does not bind and internalise CCL2^{AF647} it would be reported as being CCR2⁻. The functional significance of the presence of CCR2/D6 on the cell surface when the receptor cannot internalise CCL2^{AF647} is unclear.

There are many other variables that might affect the cell specific differences in CCR2/D6 activity. For example, CCL2 receptors might have different affinities for CCL2^{AF647} depending on the cell it is expressed on. Indeed, my data provides evidence of cell-type specific interactions of CCR2 with its ligands and these shall be discussed later in this section. The capacity of CCR2 to signal in response to its ligands might also be subject to cell-type specific differences. The ability of cell populations to internalise CCL2^{AF647} might be affected by cell specific differences in the rate of receptor recycling, which would influence the number of available receptors, and as a consequence alter the cells ability to internalise CCL2^{AF647}. In addition, the rate of CCL2^{AF647} internalisation and

subsequent degradation may well differ between cell populations. Therefore, altering the length of the 1 hr incubation with CCL2^{AF647} could generate different results. Some cell populations might be able to rapidly internalise CCL2^{AF647} and would be CCL2⁺ even during short incubation periods, whereas other populations requiring longer periods of time to internalise CCL2^{AF647} would appear CCL2⁻. This might also apply to the rate of CCL2^{AF647} degradation, as cell populations that rapidly degrade CCL2^{AF647} following its internalisation might appear CCL2⁻ at later time-points. In contrast, cell populations that possess a slower CCL2^{AF647} degradation rate would still appear CCL2⁺.

Similar to reliable antibodies against chemokine receptors that can be used to measure downregulation of receptor level in response to inflammatory stimuli, or stimulation with chemokine, the CCL2^{AF647} assay can measure downregulation of CCL2 receptor activity. Furthermore, the use of competitor ligands to compete CCL2^{AF647} uptake provided information about receptor specificity and potentially receptor occupancy. A range of CCR2 ligands were used to compete CCR2 dependent uptake of CCL2^{AF647}, including mCCL2, mCCL7 and mCCL12 (Figure 3-17). mCCL8 was not included, as although it was originally considered to be a CCR2 ligand, this is now known to be false, as CCL8 in mice is in fact a ligand of CCR8 (Islam et al., 2011). This fits with results produced by the Nibbs lab demonstrating that CCL8 had no action on either CCR2 or D6 mediated uptake of CCL2^{AF647} (Hansell et al., 2011b). Traditionally, CCL3 is not considered to be a CCR2 ligand, and was included in competition experiments as a negative control, as it should compete D6 but not CCR2 dependent uptake. However, recent data from our lab has shown that mCCL3, although less effective than other CCR2 ligands, can also inhibit CCR2 dependent uptake by peritoneal T cells and splenic Ly6C^{hi} monocytes (Hansell et al., 2011b). I found that mCCL3 had minimal effects on CCR2 dependent CCL2^{AF647} uptake by Ly6C⁺ cells. This discrepancy in results might be explained by differences in the concentration of mCCL3 used. Hansell *et al.* used 100 nM of mCCL3 to partially block CCR2 dependent CCL2^{AF647} uptake (Hansell et al., 2011b), whereas the highest concentration used in my co-incubation competition experiments was 25 nM (Figure 3-17). Perhaps mCCL3 has lower affinity for CCR2 than other CCR2 ligands, thus higher concentrations of mCCL3 are required to inhibit CCL2^{AF647} uptake. However, these lower doses of mCCL3 did cause a decrease in D6

dependent uptake by the Ly6C⁻ fraction of cells, which contains D6⁺ MZ-B cells. Likewise, both mCCL2 and mCCL12 were also able to compete D6 dependent uptake by Ly6C⁻ cells, but the non-D6 ligand CCL7 was not. All three ligands were, however, able to compete CCL2^{AF647} uptake by Ly6C^{hi} monocytes and Ly6C⁻ CD11b⁺ cells in a dose-dependent manner. At the highest concentration tested (25 nM) mCCL2 was nearly able to completely block CCL2^{AF647} uptake, which might indicate that at this concentration most receptors are occupied. Interestingly, although there were no significant differences in the ability of mCCL2, mCCL7 and mCCL12 to compete CCL2^{AF647} uptake by Ly6C^{hi} monocytes, mCCL7 and mCCL12 were much less effective at inhibiting CCL2^{AF647} uptake by Ly6C⁻ CD11b⁺ cells than mCCL2. These results suggest that CCR2 on different cells has different interactions with its ligands.

The assay can also be used to test the ability of ligands to desensitise CCR2, by monitoring CCR2 activity following exposure of WT splenocytes to an excess of unlabelled CCR2 ligands, such as mCCL2, mCCL7 or mCCL12, or the control ligand mCCL3 (Figure 3-18). Similar to co-incubation experiments each chemokine produced distinct profiles of uninhibited CCL2^{AF647} uptake. Prior exposure to mCCL3 did not appear to have any effect on CCR2 activity, whereas mCCL2, mCCL7 and mCCL12 were all able to desensitise CCR2 on Ly6C^{hi} monocytes in a concentration dependent manner. CCL2 was superior at desensitising CCR2 on Ly6C^{hi} monocytes, particularly at higher concentrations. This observation was more striking in Ly6C⁻ CD11b⁺ cells, as mCCL7 and mCCL12 were unable to inhibit CCL2^{AF647} uptake at all concentrations, other than at 250nM when minimal inhibition was observed. These results were not entirely surprising as other chemokine ligands have been shown to have differential effects on the desensitisation of their receptor, for example CCR5 and its ligands (Oppermann et al., 1999). Desensitisation of chemokine receptors is controlled by the phosphorylation of the receptor by GRKs, which leads to the recruitment of β -arrestin proteins. Binding of the β -arrestin proteins to the receptor prevents the interaction of G proteins to the receptor, thereby inhibiting further signalling from the receptor and can also mediate internalisation of the receptor (Rot and Andrian, 2004; Neel et al., 2009). Each CCR5 ligand activates GRKs, but do so with different efficiency. This can lead to alterations in the phosphorylation of the receptor, thereby modulating the number of functional

receptors on the surface (Oppermann et al., 1999). Accordingly, CCR2 ligands may also have differential effects on the phosphorylation of CCR2, and consequently on the desensitisation of the receptor, as determined by receptor silencing or internalisation. Therefore, the ability of a CCR2⁺ cell to migrate in response to a particular CCR2 ligand might be affected by prior exposure to other CCR2 ligands.

Desensitisation of CCR2 required considerably higher concentrations of ligand relative to the low amounts necessary for competition during co-incubation. As mentioned earlier, co-incubation experiments might give an indication of receptor occupancy, as it appeared that 25 nM of mCCL2 could nearly completely prevent uptake of CCL2^{AF647} by Ly6C^{hi} monocytes and Ly6C^{lo}CD11b⁺ cells (Figure 3-17). Thus, only low concentrations of ligands were required to occupy most CCR2 receptors. In contrast, pre-incubation of splenocytes with 25 nM of mCCL2 only caused partial desensitisation of CCR2, as further reductions in CCL2^{AF647} uptake were observed when splenocytes were pre-incubated with higher concentrations of mCCL2. The observations by Volpe *et al.* (described in section 6.2.2.6) provide some insight into CCR2 desensitisation and perhaps explain the requirement of high concentrations of ligands to do so. The group showed that Ly6C^{hi} monocytes have a uniform expression of CCR2 on their surface, which helps to maintain responsiveness to ligands following internalisation of some receptors (Volpe et al., 2012). Therefore, in order to desensitise CCR2 on Ly6C^{hi} monocytes an excess of ligand would be required to inundate all available CCR2. My earlier results illustrated that of the analysed cell populations, Ly6C^{hi} monocytes possessed the greater level of CCR2 activity. Thus, perhaps monocytes behave differently to other cells because of their high CCR2 activity. My data provide support for this hypothesis because they suggest that the interaction of CCR2 with its ligands is cell-type specific, as although mCCL2, mCCL7 and mCCL12 were all able to desensitise CCR2 on Ly6C^{hi} monocytes, only mCCL2 was able to desensitise CCR2 on Ly6C^{lo}CD11b⁺ cells. Further investigations are needed to confirm this observation, and it would be interesting to repeat the competition and pre-incubation experiments with some of the other CCR2^{hi} populations, such as NK cells and pDCs to determine whether they also generate cell specific CCR2 ligand binding profiles.

An advantage of using antibodies over fluorescent chemokines relates to cost. CCL2^{AF647} is a relatively expensive reagent, so some groups might elect to use antibodies over the more sensitive CCL2^{AF647} uptake assay. However, there are limited numbers of reliable antibodies targeted against murine CCR2 and no reliable anti-murine D6 antibodies exist. Furthermore, with the exception of humans, even fewer antibodies are targeted against CCR2/D6 in other mammalian and non-mammalian species. Some antibodies targeted against murine or human CCR2 have been reported to possess cross-reactivity to rat CCR2, and Yrlid *et al.* described CCR2 expression on rat monocytes using an anti-rat CCR2 antibody (Yrlid *et al.*, 2006). However, to my knowledge no antibody has been generated that specifically identifies CCR2 on primary cells in species other than mouse, rat and humans. The final advantage of the CCL2^{AF647} assay is that due to the highly conserved nature of chemokines and their receptors (Allen *et al.*, 2007), the assay is not subject to the same species restrictions as antibodies and is likely to work in multiple mammals. The results presented in Chapter 3, demonstrate that the assay works cross-species, and is able to detect human and rat CCR2 (Figure 3-16). Amanda Guth (Colorado State University, USA) has also demonstrated that the assay can detect CCR2 on canine cells (personal communication). However, it failed to detect D6 activity on pDCs from human peripheral blood or rat spleen, which are a population of cells shown to express D6 both in the spleen and blood of mice (Figures 3-11 and 3-13). Consistent with murine data (Figure 3-13), D6 activity was not detected on human blood B cells (Figure 3-16). No rat CCL22 was available commercially, thus CCL2^{AF647} uptake in the rat samples was competed with mCCL22. It is unknown whether mCCL22 is bioactive on rat D6, therefore the use of mCCL22 is an imperfect control to detect D6 as it might not actually be able to compete with CCL2^{AF647} for binding to D6. These results also suggested that expression of chemokine receptors by specific cell populations might differ between species. Murine splenic NK cells possessed high CCR2 activity, whereas human peripheral blood NK cells had minimal levels of CCR2 activity. These data also suggested that a proportion of CD43⁻ monocytes in the rat, the equivalent of Ly6C^{hi}CCR2^{hi} monocytes in mice, did not uptake CCL2^{AF647}, indicating that perhaps not all rat CD43⁻ monocytes are like murine Ly6C^{hi} monocytes. The CCL2⁻ population are unlikely to be functional equivalents of murine Ly6C^{lo} cells, as in mice these cells also possess appreciable levels of CCR2 activity. Furthermore, in rats only

one homogenous population of pDCs based on their CCR2 activity was identified, rather than the two populations found in mice and humans. This might indicate that the role of CCR2 on these cells is different in each species, or that the method used to identify rat pDCs does not include all pDC subsets.

Our lab has optimised the use of several fluorescent chemokine assays to detect a range of receptors, such as D6, CXCR2, CXCR3, CCR7, CCX-CKR, CCR4, CCR1 and CCR5 (Bordon et al., 2009; Hansell et al., 2011b; Rob Nibbs personal communication). Two such assays using CCL2^{AF647} or CCL22^{AF647} to detect D6 activity have been published. One assesses the role of D6 in the development and resolution of DSS-induced colitis, illustrating D6 activity was present on colonic B cells (Bordon et al., 2009). This paper also showed expression of CCR4 by colonic T cells (Bordon et al., 2009). The second and most recent paper, to which I made a contribution (Appendix 2), described D6 activity on innate-like B cells (Hansell et al., 2011b). Other assays that have been optimised by the lab are the CXCL8^{AF647} assay, which we have found can detect CXCR2 in mice, humans and rats. This assay demonstrated high CXCR2 activity on neutrophils in each species. CCR7 activity was examined using CCL19^{AF647} by a previous member of our lab, Catherine Hurson (Hurson, 2011), and has recently been adapted by Darren Asquith to confirm expression of CCX-CKR by LN lymphatic endothelial cells (confirmed by recent microarray data from Immgen, Malhotra et al., 2012). Lastly, the presence of CCR5 activity and other CCL5 receptors on a range of cells has been analysed using a CCL5^{AF647} assay. All of this work, and the data presented in this thesis help to establish the use of fluorescent chemokines as a reliable and sensitive means to detect chemokine receptors in mice and other mammalian species. Furthermore, they illustrate some of the additional applications of fluorescent chemokine assays, such as determining receptor specificity, regulation and occupancy.

6.4.2 CCL2^{AF647} assay versus knock-in reporter mice

Despite the numerous applications of fluorescent chemokine assays, they are subject to several functional limitations when compared to knock-in mice, such as CCR2-GFP and CCR2-RFP. Fluorescent chemokines cannot currently be used to establish CCR2 activity within tissue sections, thus they are incapable of determining localisation of CCR2⁺ cells within a tissue. In contrast, both CCR2-

GFP and CCR2-RFP mice have been used in numerous studies to establish localisation of cells via immunohistochemistry. For example, Saederup *et al.* elegantly showed the distribution of CCR2 and/or CX₃CR1 in sections of naïve and inflamed brains using CCR2-RFP mice crossed with CX₃CR1-GFP mice (Saederup *et al.*, 2010). In resting brains there were very few CCR2-RFP⁺ cells in the brain parenchyma of CCR2^{RFP/+}CX₃CR1^{GFP/+} mice. In contrast, following induction of EAE, CCR2-RFP⁺ cells were found in parenchymal and perivascular regions of the brain at peak disease severity. These cells were found to be Ly6C^{hi} inflammatory monocytes, as they were absent in mice deficient in CCR2, but not CX₃CR1 (CCR2^{RFP/RFP}CX₃CR1^{GFP/+}), and were positively stained with 7/4, a marker of Ly6C^{hi} monocytes (Saederup *et al.*, 2010). CCR2^{RFP/+}CX₃CR1^{GFP/+} knock-in reporter mice have also been used to examine CCR2 and CX₃CR1 expression in neuronal tissues of a developing embryo (Mizutani *et al.*, 2011). CCR2-GFP mice have been used to examine localisation of Ly6C^{hi} monocytes within sections of colonic lamina propria during *Clostridium difficile* induced colitis (Jarchum *et al.*, 2012). This study revealed that although Ly6C^{hi} monocytes are recruited to colonic lamina propria they do not enter gut lumen, and that neutrophils are crucial for the early defence against *Clostridium difficile* (Jarchum *et al.*, 2012). CCR2-GFP mice have also been used to examine recruitment and localisation of Ly6C^{hi} monocytes in the liver of mice infected with *Listeria monocytogenes* (Shi *et al.*, 2010). Within the liver, Ly6C^{hi} monocytes surrounded the foci of infection and formed lesions. It was within these foci that monocytes differentiated into TipDCs, and CCR2-GFP⁺ cells could be colocalised with immunofluorescent staining for iNOS (Shi *et al.*, 2010). This study also highlighted another advantage of knock-in reporter mice compared to fluorescent chemokines, as knock-in reporter mice, such as CCR2-GFP can facilitate the analysis of cell trafficking by intravital microscopy. For example, Shi *et al.* monitored trafficking of Ly6C^{hi} monocytes into livers of infected CCR2-GFP mice (Shi *et al.*, 2010). Therefore, although fluorescent chemokines are a sensitive and reliable method to detect receptor activity, they are severely limited in their ability to detect receptors *in situ*.

6.5 Cellularity of lymphoid organs and blood in CCR2 KO

6.5.1 Steady-state

The cellularity of the lymphoid organs and the blood of steady-state CCR2 KO animals was similar to WT animals (Figure 3-15). However, consistent with published observations (Sunderkötter et al., 2004; Serbina and Pamer, 2006; Tacke and Randolph, 2006), CCR2 KOs had a significantly decreased frequency of Ly6C^{hi} monocytes in spleen and blood, with a parallel increase in Ly6C^{hi} monocytes detected in the BM. Furthermore, there was a significant reduction in the frequency of Population B cells detected in the blood of CCR2 KO animals (Figure 3-15C). Earlier in section 6.2.2.3 it was proposed that Population B might represent a population of CD115⁻ monocytes or pre-cDCs. Therefore, perhaps akin to the highly CCR2 dependent mobilisation of Ly6C^{hi} monocytes from the BM, the decrease in Population B cells in the blood of CCR2 KO animals might be explained by an increase in the BM. However, there was no corresponding increase in the BM of CCR2 KOs, which suggests that Population B are not dependent on CCR2 for their emigration from the BM, unless any excess cells in this population die in the BM. Interestingly, these cells do not appear to acquire CCR2 activity until they are in the blood. An alternative explanation is that CCR2 might play a role in their retention in the spleen, and it will be of interest in future experiments to try to identify Population B cells within the spleen and determine their relative frequency in the spleens of WT and CCR2 KO animals. Another theory to explain the decrease in Population B in the blood of CCR2 KOs is that the absence of CCR2 effects their survival. CCR2 deletion has been associated with enhanced turnover and apoptosis of BM myeloid cell progenitors (Reid et al., 1999). Reid *et al.* did not elucidate the exact mechanism of CCR2 induced survival, but their results suggest that CCR2 signals enhance the survival of BM myeloid cell progenitors (Reid et al., 1999). Thus, in the absence of CCR2, perhaps Population B cells do not receive a survival signal and are subject to apoptosis. A final explanation is that Population B cells in blood are derived from Ly6C^{hi} monocytes. These CD115⁻ cells might have a different function from CD115⁺ Ly6C^{hi} monocytes *in vivo*, such as the regeneration of cDCs in response to inflammation-induced cDC death. If so, their paucity in CCR2 KO blood might underlie the deficit in CD11b⁺ and CD8 α ⁺ cDCs 24 hrs after LPS administration. Clearly, further experiments are required to assess these ideas.

There was also a significant increase in the frequency of B cells and decrease in T cell frequency detected in the PLNs of CCR2 KO mice compared to WT (Figure 3-15). T and B cells from PLNs were negative for CCR2 activity (Figure 3-14). Therefore, it is unlikely that a deficiency in CCR2 affected their ability to migrate to or from LNs, or caused any other cell autonomous defects in these cells. Instead, the effect of CCR2 deletion on T and B cell frequency might be secondary to structural changes in LNs or changes in the distribution of other cell types.

6.5.2 Systemic inflammation

The absence of CCR2 in steady-state animals only affected the frequency of one splenic cell population, namely Ly6C^{hi} monocytes. In contrast, treatment of WT and CCR2 KO animals with 15 µg LPS led to marked alterations in the frequency of several populations in the spleen.

6.5.2.1 Neutrophils

Peak accumulation of neutrophils in inflammatory exudate occurs 6 to 24 hrs after LPS administration (Ulich et al., 1991). In the WT spleen, however, neutrophil abundance did not peak until 48 hrs after LPS injection.

Unexpectedly, neutrophils peaked in the CCR2 KO at 24 hrs when they were more abundant than in WT. This is in contrast to observations by Souto *et al.* who reported that LPS induced infiltration of neutrophils into lungs, heart and kidney was dependent on CCR2 (Souto et al., 2011). Other receptors have been reported to coordinate neutrophil mobilisation into the spleen during LPS induced inflammation, such as CXCR4. CXCR4 is upregulated on splenic Gr1⁺CD11b⁺ granulocytes 12 hrs after induction of systemic inflammation by caecal ligation. The mobilisation of neutrophils into the spleen was inhibited by blockade of the CXCR4 ligand, CXCL12 (Delano et al., 2011). Therefore, perhaps CXCR4 can over-compensate for the loss of CCR2, and in the absence of CCR2 plays a greater role in neutrophil migration to the spleen than observed in WT animals, explaining the increased neutrophil frequency in the spleen of CCR2 KO animals. Alternatively, LPS treatment might cause the release of more neutrophils from CCR2 KO BM, as in the absence of CCR2 the BM has been

described to have defects, such as retention of Ly6C^{hi} monocytes (Serbina et al., 2006)

6.5.2.2 Monocytes

Serbina *et al.* have illustrated that during the early stages of infection with *Listeria monocytogenes* pre-existing BM Ly6C^{hi} monocytes are recruited to the spleen (Serbina et al., 2009). In contrast, at later stages of infection the frequency of BM Ly6C^{hi} monocytes increased rather than decreased, as robust expansion of BM monocyte precursors supported continuous recruitment of Ly6C^{hi} monocytes to the spleen (Serbina et al., 2009). Consistent with these observations, results presented in Chapter 4 illustrated that LPS treatment resulted in an increase in the frequency of Ly6C^{hi} monocytes in spleen (Figure 4-2) and BM (Figure 4-11) of WT mice. However, there appeared to be no preliminary decrease in Ly6C^{hi} monocytes in the BM (Figure 4-11). The use of different mice models of inflammation might account for this discrepancy, as results by Shi *et al.* suggest that LPS induced monocyte mobilisation is very rapid occurring within hrs, rather than days (Shi et al., 2011).

Using a combination of CCR2-GFP and CCL2-GFP reporter mice, Shi et al have examined Ly6C^{hi} monocytes emigration from the BM in response to low doses of TLR ligands (Shi et al., 2011). The study illustrated that very low amounts of LPS (2 ng) delivered i.p. induced rapid monocyte mobilisation (Shi et al., 2011). 3 hrs after LPS treatment there was a significant reduction in the frequency of BM Ly6C^{hi} monocytes, which coincided with an increase in the blood (Shi et al., 2011). Rapid release of monocytes from the BM in response to low doses of LPS is CCR2 dependent. Moreover, conditional deletion of CCL2 from BM mesenchymal cells led to a significant decrease in circulating monocytes 4 hrs after treatment with 20 ng LPS, indicating that Ly6C^{hi} monocyte emigration from the BM is mediated by CCL2 production by BM mesenchymal cells (Shi et al., 2011). It is possible that this rapid CCR2-dependent monocyte release also happened in response to the 15 µg dose of LPS that I used, and that it was missed because of analysing too late after LPS administration (i.e. 24 hrs).

Interestingly, 24 hrs after treatment with 15 µg LPS the resting deficit in peripheral Ly6C^{hi} monocytes in CCR2 KO animals was absent (Figure 4-2), and

was accompanied by a marked decrease in the frequency of CCR2 KO BM Ly6C^{hi} monocytes that was not seen in WT mice (Figure 4-11). The deficit in peripheral monocytes was restored at the later time-points (Figure 4-2). Thus, LPS treatment led to CCR2-independent mobilisation of Ly6C^{hi} monocytes from the BM into the periphery. Monocyte mobilisation in CCR2 KOs induced by treatment with 15 µg LPS may occur via another inflammatory chemokine receptor. There is a high degree of redundancy in chemokine receptors, and in the absence of one receptor, another can compensate for its loss and perform similar roles to that of the missing receptor (Krueger et al., 2010). I theorised that other inflammatory chemokine receptors expressed by Ly6C^{hi} monocytes might be responsible for the observed LPS driven CCR2 independent mobilisation. Our lab and others have shown that BM Ly6C^{hi} monocytes express CXCR2 (Traves et al., 2004; Boisvert et al., 2006), however CXCR2 antagonism had no effect on LPS induced monocyte mobilisation in the CCR2 KO (Figure 4-12). Thus, the mechanisms responsible for LPS induced loss of CCR2 dependence for monocyte release from the BM remains to be defined.

6.5.2.3 cDCs

In accordance with published observations (Zanoni et al., 2009), treatment with 15 µg of LPS resulted in a significant reduction in the abundance of cDCs in WT and CCR2 KO spleens (Figure 4-10). The frequency of cDCs did not recover within the time-scale of the experiment. 72 hrs after LPS administration CD11b⁺ and CD8α⁺ cDCs were significantly reduced in WT and CCR2 KO animals compared to PBS controls. cDCs were gated as CD11c^{hi}MHCII^{hi} cells, but Singh-Jasuja *et al.* have demonstrated that LPS activated cDCs downregulate their expression of CD11c (Singh-Jasuja et al., 2012). Therefore, the decreased cDC frequency might be explained by the downregulation of CD11c and the absence of cDCs from the CD11c^{hi}MHCII^{hi} gate. However, other groups have reported that LPS induced activation of cDCs causes an increase in their turnover rate (Kamath et al., 2000; 2002) and results in their death by apoptosis, and as a consequence decreases the number of splenic cDCs (Zanoni et al., 2009). Therefore, the observed decrease in cDC abundance may be a result of cDC death following their activation by LPS. LPS treatment also resulted in a significant decrease in the frequency of CD11b⁺ and CD8α⁺ cDCs detected in CCR2 KO spleens compared

with those of the WT. This suggests that CCR2 KO cDCs may have an increased rate of death compared to WT cDCs.

A decrease in splenic cDC numbers triggers the differentiation of splenic cDC precursors. Depletion or reduction of the splenic cDC frequency is associated with an increase in Flt3L, which was reported to trigger differentiation of cDC precursors. Upon restoration of cDC numbers Flt3L availability is decreased and cDC precursor differentiation is reduced (Hochweller et al., 2009). Splenic cDC numbers in WT animals are reported to recover 5 days after LPS administration (Zanoni et al., 2009). It would be interesting to establish whether CCR2 KO cDCs recover within the same time-scale, and to define the affect of LPS on the frequency of Population B in the blood and spleen. If Population B is truly a population of pre-cDCs, one might expect that as the frequency of cDCs decreases, there would be a parallel increase in the differentiation of the cells within this population and perhaps their frequency within the spleen. However, CCR2 KOs have a deficit in blood Population B, so the number of cells present that could differentiate into cDCs might be substantially reduced in comparison to WT animals. CCR2 KOs might therefore exhibit delays in the restoration of their splenic cDC populations. This might also explain the CCR2 KO specific decrease in cDC frequency 24 hrs after LPS (Figure 4-10). The decrease in cDCs would trigger Flt3L production, which would drive differentiation of precursors to replace the diminishing cDC population. However, the reduction in Population B cells in CCR2 KOs would mean that there are fewer precursors available to differentiate and as a consequence, compared to a WT population there would be a decrease in the cDC population.

An alternative hypothesis that might explain the CCR2 KO specific decrease in cDC frequency 24 hrs after LPS is an indirect effect of the absence of peripheral Ly6C^{hi} monocytes in CCR2 KO animals. During inflammatory conditions, Ly6C^{hi} monocytes can differentiate into inflammatory cDCs (Tam and Wick, 2004; Naik et al., 2006; Shortman and Naik, 2007). The resting defect in Ly6C^{hi} monocytes in CCR2 KO mice might lead to a peripheral deficit in inflammatory cDCs 24 hrs after LPS (Tam and Wick, 2004; Naik et al., 2006; Serbina and Pamer, 2006; Shortman and Naik, 2007). To examine whether the deficit in Population B or Ly6C^{hi} monocytes are responsible for the CCR2 KO specific decrease in cDCs 24 hrs after LPS, we could transfer either WT Population B cells or WT Ly6C^{hi}

monocytes into CCR2 KO animals before the start of the LPS time-course and determine whether either cell type restores the reduction in cDC numbers at 24 hrs.

The observed LPS induced decrease in cDC frequency was subsequent to the acquisition of the activation marker CD86 in WT cells, or simultaneous in the case of CCR2 KOs, as CD86 was specifically upregulated 24 hrs after LPS treatment (Figure 4-9). CCR2 KO splenic cDCs have been reported to have lower expression levels of activation markers (Fiorina et al., 2008). However, my results using CD86 did not reveal any noticeable differences in expression. This is consistent with published results as Fiorina *et al.* showed that only CD80 and not CD86 was affected by loss of CCR2 (Fiorina et al., 2008). CD80 and CD86 have distinct functions in the activation of T cells. CD86 is thought to be the initial costimulatory ligand as it is expressed earlier than CD80 and is more abundant, whereas CD80 ligation supports the generation of T cells with regulatory functions (Hathcock et al., 1994; Sharpe and Freeman, 2002; Sansom et al., 2003). The defective maturation of CCR2 KO cDCs, as characterised by expression of the activation marker CD80 might also correlate specifically with the decrease in CCR2 KO cDC numbers.

Decreased cDC frequency in WT mice was associated with increased or recovery of CCR2 activity in the cDC subsets (Figures 4-7 and 4-8). Therefore, very low numbers of cDCs compared to the PBS control are responsible for the restoration of CCR2 dependent $CCL2^{AF647}$ uptake. As LPS treatment potentially results in the apoptosis of the original cDC population, newly recruited or recently differentiated pre-cDCs are likely to be responsible for the high levels of CCR2 activity detected at the later time-points in the LPS time-course. In accordance with this hypothesis, Population B and $Ly6C^{hi}$ monocytes in the blood have high levels of CCR2 activity (Figure 3-13) coincident with the re-emergence of CCR2 activity of cDCs.

Collectively, these results have shown that in resting mice there is little effect of CCR2 deletion on the frequency of the majority of $CCL2^+$ cell populations, with the notable exception of $Ly6C^{hi}$ monocytes and closely related Population B cells. During systemic inflammation, CCR2 deficiency drastically affected the frequency of $Ly6C^{hi}$ monocytes and cDCs. There were no apparent effects of

CCR2 deletion on the splenic frequency of the other CCL2⁺ populations, both during homeostasis and inflammation. This might indicate that CCR2 is not required for their migration to or from the spleen, or their survival in this organ. However, CCR2 might be involved in their intra-splenic migration. By examining the localisation of cells within resting or inflamed spleens of WT and CCR2 KO animals via immunohistochemistry, we might find that inflammation induces CCR2 dependent migration of CCL2⁺ populations within the spleen.

6.6 CCL2 receptors and pDCs

Chapter 5 details the characterisation of two subsets of pDCs that were identified based on CCR2 activity. The difference in CCR2 expression was demonstrated both by CCL2^{AF647} uptake activity and variation in CCR2 transcripts. Both CCR2^{hi/lo} pDC subsets were shown to have no differences in the expression of the pDC markers, PDCA1 and Siglech in resting animals (Figure 5-2).

Approximately 50% of pDCs in the majority of the tested lymphoid organs and blood had high levels of CCR2 activity (Figure 5-3). This is in sharp contrast to results produced using the MC-21 antibody: both others and myself found only very low levels of MC-21⁺ pDCs. Wendland *et al.* reported that only 25% of WT BM pDCs were MC-21⁺ when compared to isotype control stained WT cells (Wendland *et al.*, 2007). Furthermore, within each tested tissue, competition with mCCL22 provided evidence of D6 activity in WT and CCR2 KO pDCs. In addition, the microarray of splenic pDCs demonstrated that there were no differences in D6 expression at the transcript level between the two subsets (Figure 5-23). However, the relative proportion of pDCs possessing CCR2 and D6 activity was different within each tissue. The tissue specific differences in expression of both of these inflammatory chemokine receptors might be explained by differences in the maturation or activation state of the two subsets. The BM is a rich source of pDC progenitors and immature pDCs, so CCR2 might be a marker of more terminally differentiated pDCs. However, comparison of the surface phenotype of splenic and BM WT pDCs did not indicate any major differences in the expression of a range of markers, including activation and maturation markers (Figure 5-31 and 5-32).

6.6.1 Surface phenotype of CCL2^{hi} and CCL2^{lo} pDCs

As summarised in the Introduction, many groups have described subsets of pDCs based on their maturation status. In brief, O’Keeffe *et al.* have reported that CD4⁺ pDCs are terminal differentiated mature pDCs and approximately 66% of splenic pDCs identified as B220⁺CD11c⁺ cells are CD4⁺ (O’Keeffe *et al.*, 2002). Furthermore, mature pDCs (gated as B220⁺CD11c⁺ cells following exclusion of lymphocytes and myeloid cells) are also reportedly CD9⁻, with CD9 downregulated upon differentiation into mature pDCs (Björck *et al.*, 2011). Consistent with these results and despite the inadequacy of using B220⁺CD11c⁺ to identify pDCs, it was found that a high proportion of both CCL2^{hi} and CCL2^{lo} expressed CD4 (Figure 5-12), and that approximately 64% of total WT splenic pDCs expressed CD4 (Figure 5-32). My results also illustrated that the majority of splenic pDCs were CD9⁻, with a minor proportion (~8%) being immature CD9⁺ pDCs (Figure 5-31), and there were no significant differences in CD9 expression between the two subsets (Figure 5-12). These results suggest that there are no major differences in the maturation state of the two subsets, and that most pDCs identified would be classified as mature. Ly49Q is also considered to be a marker of pDC maturation, as pDCs acquire expression of Ly49Q before exiting the BM, and approximately 87% of splenic pDCs are Ly49Q⁺ (Omatsu *et al.*, 2005; Toma-Hirano *et al.*, 2007). In my hands, both the CCL2 subsets (Figure 5-12) and total splenic pDCs (Figure 5-31) were Ly49Q⁻. However, this is likely a false negative due to the poor sensitivity of the anti-Ly49Q antibody, as it failed to detect Ly49Q on any splenic cells (Figure 5-12C).

The gut homing chemokine receptor CCR9 has been described by three groups to be a marker of mature pDCs (Hadeiba *et al.*, 2008; Björck *et al.*, 2011; Schlitzer *et al.*, 2011). These groups illustrated that the majority of splenic pDCs (identified as simply B220⁺CD11c⁺ cells (Hadeiba *et al.*, 2008); B220⁺CD11c⁺ cells after the exclusion of myeloid and lymphocyte cells (Björck *et al.*, 2011); or PDCA1⁺CD11c⁺ cells (Schlitzer *et al.*, 2011)) were CCR9⁺. However, Schlitzer *et al.* (Schlitzer *et al.*, 2011) and Björck *et al.* (Björck *et al.*, 2011) reported that a small population of splenic pDCs ~11-12% were CCR9⁻. I also found that the majority (~87%) of splenic pDCs were CCR9⁺ (Figure 5-31). Significantly, more CCL2^{lo} pDCs expressed CCR9. A small population, representing approximately 25% of CCL2^{hi} pDCs were CCR9⁻, and essentially all CCR9⁻ pDCs were in the CCL2^{hi}

subset (Figure 5-11). This might indicate that a small proportion of CCL2^{hi} pDCs are immature pDCs. Recently, Schlitzer *et al.* proposed that CCR9⁻ pDCs are in fact a SiglecH⁺PDCA1⁺ intermediary precursor of pDCs and that they are mainly found in the BM. In contrast, I found that nearly all BM WT pDCs were CCR9⁺ (~86%) compared to the reported ~66% (Schlitzer *et al.*, 2011).

In the BM, CCR9⁻ precursors preferentially give rise to pDCs (Schlitzer *et al.*, 2012). However, in the periphery they have the potential to give rise to both pDCs and cDCs (Schlitzer *et al.*, 2012). Furthermore, CCR9⁻ precursors spontaneously gave rise to fully differentiated CCR9⁺ pDCs *in vitro* when cultured in media alone or media supplemented with Flt3L. However, when cultured with media supplemented with granulocyte macrophage-colony stimulating factor (GM-CSF) they differentiated into cDCs (Schlitzer *et al.*, 2011; 2012). A similar experiment could be performed to examine whether purified CCR9⁻CCL2^{hi} pDCs possess the ability to differentiate into fully differentiated CCR9⁺ pDCs or cDCs. Interestingly, CCR9⁻ pDCs have also been reported to be proinflammatory, producing high levels of the IL-6, IL-12 and TNF α compared to CCR9⁺ pDCs (Hadeiba *et al.*, 2008; Björck *et al.*, 2011). Therefore, this small population of splenic pDCs might perform the proinflammatory roles of pDCs and CCR2 might coordinate their migration.

CCR9⁺ pDCs are described to possess tolerogenic properties (Hadeiba *et al.*, 2008; Björck *et al.*, 2011; Schlitzer *et al.*, 2011), as are CD8 α ⁺ pDCs (Lombardi *et al.*, 2012). Tolerogenic pDCs are thought to induce generation of Tregs that secrete the anti-inflammatory cytokine, IL-10 (Colonna *et al.*, 2004; Ito *et al.*, 2007; Baba *et al.*, 2009; Matta *et al.*, 2010). The majority of CCL2^{hi/lo} pDCs were found to express both CCR9 and CD8 α , indicating that both subsets are likely to contain tolerogenic pDCs.

The expression of several other chemokine receptors was also examined in these two CCL2 pDC subsets (Figure 5-11). The two subsets had relatively minor, but statistically significant differences in expression of CX₃CR1. Furthermore, consistent to published observations which illustrated that pDCs possess CCR1 and CCR5 transcripts (Yoneyama *et al.*, 2004; Wendland *et al.*, 2007), the total pDC population internalised CCL5^{AF647} in a receptor-mediated fashion by one or more of the CCL5 binding receptors, CCR1, CCR3, CCR5 or D6. Competition with

mCCL4 indicated that pDCs possessed significant levels of either D6 or CCR5, as it caused a significant decrease in CCL5^{AF647} uptake. mCCL5 provided more extensive inhibition of CCL5^{AF647} uptake suggesting that other CCL5 receptors, most likely CCR1, are also present (Figure 5-11D). I could not determine the relative proportions of each subset that possessed CCL5 receptor activity, as both chemokines, CCL5 and CCL2 were labelled with the same fluorophore, AF647. However, no differences in expression of CCL5 receptors were seen in the microarray data (Figure 5-24). I also examined the expression of two integrins, CD62L and $\alpha 4\beta 7$ (Figure 5-12), both of which have been shown to be involved in pDC migration (Wendland et al., 2007; Seth et al., 2011). Both were expressed at very low levels by the CCL2 pDC subsets, however there was a significant decrease in CD62L expression by CCL2^{lo} pDCs compared to CCL2^{hi} pDCs. CD62L, like CCR7 is involved in the transmigration of pDCs into PLNs (Nakano et al., 2001; Diacovo et al., 2005; Seth et al., 2011). This might indicate that CCL2^{lo} pDCs are less efficient at entry into PLNs. However, there were no differences in the proportion of CCL2^{hi} to CCL2^{lo} pDCs in PLNs (Figure 5-3).

Interestingly, following activation with CpG-C, a small proportion (~15%) of each subset upregulated SiglecH, but again there were no differences in expression between the two subsets (Figure 5-29). To my knowledge, the upregulation of SiglecH by activated pDCs has not been described. However, Björck *et al.* associated the maturation of CD9⁺ into the terminally differentiated CD9⁻ pDCs with an increase in SiglecH expression (Björck et al., 2011). The majority of the CCL2^{hi} and CCL2^{lo} pDCs did not express CD9, indicating that they are mature fully differentiated pDCs. Furthermore, Björck *et al.* reported that upregulation of SiglecH occurred as a natural part of their maturation and did not require activation of the cells (Björck et al., 2011). Therefore, I do not believe that the observed upregulation of SiglecH expression following activation of pDCs with CpG-C was due to the maturation of the cells. The expression of the activation markers CD86 and ICOS-L was limited to the SiglecH^{hi} population of each of the CCL2 subsets. This might indicate that activation of pDCs results in an increase in SiglecH expression. SiglecH can function as an endocytic receptor mediating Ag uptake, which can then be cross-presented by pDCs to CD8 α ⁺ T cells (Zhang et al., 2006). Furthermore, Takagi *et al.* have shown that SiglecH modulates pDC function, and in its absence pDCs have an altered capacity to prime CD4⁺ and

CD8 α^+ T cells (Takagi et al., 2011). Therefore, in future it would be interesting to compare the relative abilities of CpG-induced SiglecH^{hi} and SiglecH^{lo} pDCs to cross-present Ag to CD8 α^+ T cells. Data presented in Chapter 5 illustrates that unstimulated Ag loaded pDCs were able to induce naïve Ag-specific CD8 α^+ T cell proliferation (Figure 5-17) and furthermore, TLR7 mediated activation of pDCs enhanced their ability to prime and stimulate proliferation of naïve CD8 α^+ T cells (Figure 5-19). Based on these results it can be hypothesised that the enhanced proliferative stimulatory capacity of TLR7 activated pDC might be due to the presence of a SiglecH^{hi} population of pDCs. By purifying SiglecH^{hi} and SiglecH^{lo} pDCs it would be possible to determine which population was responsible for the observed proliferation. The Ag presenting properties of the two subsets shall be discussed in more detail in section 6.7.

6.6.2 CCR2- or D6-deficiency affects pDCs phenotype

The impact of CCR2- or D6-deficiency on the pDC subsets was examined next (Figure 5-30 to 5-33). One of the most striking phenotypes, although not consistent between repeat experiments, was observed in the D6 KO animals. Often these animals only possessed CCL2^{hi} pDCs and lacked CCL2^{lo} pDCs (Figure 5-30). As discussed earlier, there is a high degree of redundancy in chemokine receptors, and in the absence of one receptor, another receptor can compensate for its lost (Krueger et al., 2010). As such, CCR2 might compensate for loss of D6. Both D6 and CCR2 possess scavenging capabilities (Hansell et al., 2006; Volpe et al., 2012) and perhaps in the absence of D6, CCR2 is upregulated to increase a cells scavenging capacity, through binding and internalising more CCL2. In contrast, CCR2 KO pDCs only internalised low levels of CCL2^{AF647} in a D6 dependent manner. There were no difference in the absolute number of pDCs in the spleen of each mouse strain (Figure 5-33) and there were relatively few alterations in the expression of all the tested surface markers (Figure 5-31 and 5-32). A significantly higher proportion of CCR2 KO BM pDCs expressed CCR9, but there were no significant differences in the expression of another tolerogenic marker CD8 α (Lombardi et al., 2012) (Figure 5-32). These data suggest that CCR9⁻ pDCs might be absent from animals deficient in CCR2. The potential roles of CCR9⁻ pDCs as immature proinflammatory pDCs have already been discussed. Therefore, CCR2 KO animals might be deficient in proinflammatory pDCs, and all pDCs within these animals appear to be tolerogenic CCR9⁺ pDCs. This might have

significant consequences on the ability of CCR2 KO animals to mount protective proinflammatory responses against viral pathogens. CCR9 is also a marker of mature pDCs (Hadeiba et al., 2008; Björck et al., 2011; Schlitzer et al., 2011), and notably, a significantly higher proportion of CCR2 KO BM pDCs expressed the maturation marker CD4 (O'Keeffe et al., 2002). Immature pDCs can also be characterised by the expression of CD9, as maturation is accompanied by a downregulation of this proteins expression (Björck et al., 2011). Significantly fewer CCR2 KO BM pDCs were found to express CD9 compared to WT pDCs. Collectively, these results indicate that a greater proportion of pDCs in the BM of CCR2 KOs are terminally differentiated in comparison to WT and D6 KO animals.

CCR2 KO and D6 KO BM pDCs had significantly lower expression of the integrin $\alpha 4\beta 7$ compared to WT pDCs. $\alpha 4\beta 7$ is involved in pDC migration to the small intestine and MLNs (Hadeiba et al., 2008). This might indicate that CCR2 KO and D6 KO pDCs are less efficient at entry into small intestine and MLNs. However, CCR2 KO and D6 KO pDCs had significantly higher expression of the gut homing chemokine receptor CCR9. It would be interesting to determine whether deficiency in CCR2 or D6 affected pDC migration to MLNs or small intestine. The most striking observation was that D6 KO BM contained over 12-fold more CD9⁺ pDCs compared to WT, and a 100-fold more than CCR2 KO BM. This might indicate that surface expression of CD9 is suppressed in the presence of D6. Furthermore, CD9 is a marker of immature pDCs, thus D6 KO BM pDCs are likely to be immature. However, there were no significant differences in the expression of CD9 by splenic pDCs in the three mice strains, as relatively few splenic pDCs expressed CD9. This might indicate that the absence of D6 alters the maturation process of BM pDCs, perhaps D6 is required for optimal terminal differentiation of BM pDCs. This could be determined by examining downregulation of CD9 by purified BM pDCs from each mouse strain in the presence of media or media supplemented with Flt3L. In addition to being a marker for immature pDCs, CD9 is a tetraspanin protein that has reported to regulate integrin-dependent cell migration and can promote clustering of ICAM1 and VCAM1 on leukocytes (Barriero et al., 2005; Powner et al., 2011). This might indicate that increased CD9 expression by D6 KO BM pDCs modulates their adhesion and migration properties. However, analysis of all the phenotypes identified in D6 KO pDCs must be interpreted with some caution. I have

illustrated that pDCs from animals deficient in D6 can present with two CCL2^{AF647} uptake profiles: one similar to WT animals, while in the second all pDCs are CCL2^{hi}. The reason for this is not known, but it suggests that there is marked variability in pDCs from D6 KO animals, which cannot be explained by differences in the age, gender or housing conditions of the animals.

6.6.3 Microarray analysis

Microarray analysis facilitated a comprehensive comparison of transcript levels between the two CCL2 pDC subsets (Figure 5-24), and revealed that the pDC subsets were very similar in terms of their expression of a broad range of genes. The subsets did not differ in their expression of pDC specific genes (Figure 5-27) and flow cytometry also confirmed that there were no differences in their expression of pDC specific cell surface molecules Siglech and PDCA1 (Figure 5-2). Consistent with T cell stimulatory data, the two subsets did not differ in their expression of Ag presentation genes, such as *CD86* and *MHCII*. However, and most importantly, microarray analysis showed that *CCR2* was differentially expressed between the two subsets, although there was no difference in D6 expression (Figure 5-24). Other genes that were differentially expressed between the two subsets could not be clustered based on functional categorisation i.e. inflammatory vs. tolerance. However, several tumour suppressor genes were upregulated in CCL2^{lo} pDCs. Furthermore, two *ifitm* genes, *ifitm-1* and *3*, involved in viral defence were expressed at higher levels in CCL2^{hi} pDCs. This might be consistent with the presence of the CCR9⁺ proinflammatory immature pDCs within this subset. Several surface receptors, such as IL-13Ra1 and CD200R, were differentially expressed between the two subsets. These receptors were of interest as engagement of either receptor on pDCs has been shown to modulate pDC function. Activation of CD200R1 on pDCs by cells expressing its ligand CD200 has been shown to induce IFN α release (Manlapat et al., 2007). Tel *et al.* have shown that TLR9 mediated activation of pDCs can be modulated by the addition of IL-13, which causes a decrease in the expression of costimulatory molecules, CD83 and CD86 (Tel et al., 2010).

Validation of the microarray results was initially performed via QPCR. However, the QPCR malfunctioned and no accurate readings could be determined for gene expression. The QPCR was not repeated as it used all remaining pDC RNA that

was generated for the microarray and time restrictions of this PhD meant that it could not be repeated due to the required cell sorting experiments to obtain more RNA. As an alternative method to perform qualitative analysis of the microarray data, flow cytometry was utilised in an effort to confirm expression of some of the surface receptor markers shown to be differentially expressed at the transcript level on the microarray between the two subsets (Figure 5-28). Antibody staining of the CCL2^{hi/lo} pDC subsets revealed no significant differences in the expression of CD200R1. Furthermore, CD200R1 KO animals had similar expression to WT animals, indicating that there was a high degree of non-specific staining with the anti-CD200R1 antibody. The lack of a reliable antibody to examine CD200R1 hindered this analysis. However, in the future, it would be interesting to determine if CD200R1 engagement led to differences in IFN α production by the two pDC subsets.

The microarray and the later antibody staining of IL-13Ra1 illustrated that the IL-13 receptor is differentially expressed by the two pDC subsets, with CCL2^{hi} pDCs having greater expression (Figures 5-27 and 5-28). However, my results showed that there was no effect on the CpG-C induced activation of pDCs, quantified by the expression of costimulatory molecules CD86 and ICOS-L, following the addition of IL-13 (Figure 5-29). Tel *et al.* did not describe any effect of IL-13 on ICOS-L: it was decided to use ICOS-L because it has been shown to be expressed at significantly higher levels on CpG activated pDCs than CD86 (Ito *et al.*, 2007).

The microarray analysis also illustrated that incubation of pDCs at 37°C in CCL2^{AF647} caused a substantial change in gene expression in pDCs (Figure 5-26). The majority of genes that were affected by culture were those reported to be highly expressed by Langerhans cells and cDCs. As the FACS-purified pDC populations had >95% purity at the start of the incubation, these results might indicate that culture *in vitro* initiated some form of differentiation of pDCs towards LC/cDC-like cells. Schlitzer *et al.* have illustrated that purified CCR9⁻ pre-pDCs could differentiate into cDCs when cultured with GM-CSF for 48 hrs (Schlitzer *et al.*, 2011; 2012). CCR9⁻ pDCs cultured in media alone differentiated into CCR9⁺ pDCs. CCR9⁺ pDCs, as previously discussed are terminally differentiated pDCs, which do not possess the ability to differentiate into cDCs

in response to GM-CSF (Schlitzer et al., 2011; 2012). Interestingly, my results suggest that splenic pDCs, the majority of which are CCR9⁺, did undergo some differentiation in response to culture at 37°C.

Recently, a core cDC signature that distinguishes cDCs from pDCs and macrophages at the transcript level has been identified. This signature is composed of 24 genes that were expressed 2-fold higher in cDCs than macrophages (Miller et al., 2012). This signature could not be identified in the list of genes upregulated as a consequence of culture (Appendix 1). Furthermore, lymphoid and non-lymphoid tissue cDCs were found to express 125 genes that are absent from pDCs (Miller et al., 2012). Of these 125 genes, only 6 (*atf3*, *cd83*, *ifitm2*, *lfng*, *nr4a3* and *rasgef1b*) were present in the list of genes affected by culture (Appendix 1). These results indicate that incubation for 1 hr at 37°C in CCL2^{AF647} did cause upregulation of several cDC specific genes. However, and not unexpectedly, this short incubation period did not cause full differentiation of pDCs into cDCs. Therefore, a longer incubation period of cells with CCL2^{AF647} at 37°C might trigger full differentiation of pDCs into cDCs. Despite the alteration in genetic profiles, antibody staining of the pDC specific markers, PDCA1 and SiglecH indicated that the two subsets were still positive for pDC markers following the incubation, thus although many genes are altered, it appears that the pDC specific genes are not. Furthermore, regardless of the upregulation of cDC and Langerhans cell specific genes, CCL2^{hi} and CCL2^{lo} pDCs maintain many hallmark features of pDCs (i.e. ability to response to TLR7/9 agonists and IFN α production), but they may contain a small proportion of cells that are starting to become cDC-like.

pDCs represent only a small proportion of the splenic cell populations. Thus in many of my experiments, including sorting of pDCs for the microarray, Flt3L was used to expand the number of pDCs in the periphery. Reizis *et al.* have discouraged the use of Flt3L to expand the pDC pool or to drive the *in vitro* generation of BM-pDCs, stating that the tumour and the above physiological Flt3L levels might lead to alterations in the profiles and functions of pDCs (Reizis et al., 2011b). However, as shown in Figure 5-8, B16FL treated animals had no apparent alterations in their CCR2 activity, with CCL2^{hi} pDCs comprising ~50% of the pDC population in both the spleen and PLNs. This is in contrast to Wendland

et al. who reported that pDCs from the spleen of a Flt3L treated animal possessed significantly more MC-21 immunoreactivity than BM pDCs from an untreated animal (Wendland *et al.*, 2007). Flt3L exposure did, however, lead to differences in IL-13Ra1 expression (Figure 5-28). Nonetheless, the method of pDC expansion, a necessary step to generate enough pDCs to do the work, must be borne in mind when interpreting the data.

6.7 What role does CCR2 play on pDCs?

My results showed that pDCs can migrate *in vitro* in response to CCL2 (Figure 5-10), which is in sharp contrast to Penna *et al.* that showed that human steady-state pDCs do not migrate in response to inflammatory chemokines (Penna *et al.*, 2001), which is surprising given that all human peripheral blood pDCs are highly active for CCL2^{AF647} uptake (Figure 3-16). The migration of the subsets to CCL2 could not be examined, as the segregation of the two subsets requires exposure to CCL2^{AF647}, which will desensitise CCR2 to further exposure of CCR2 ligands (Figures 3-17 and 3-18). CCR2 is unlikely to be required for pDC migration from the BM or into the spleen, as there were no significant differences in the absolute number of pDCs detected in WT and CCR2 KO animals (Figure 5-33). Furthermore, LPS induced inflammation did not significantly affect the frequency of splenic pDCs in WT and CCR2 KO animals, indicating that CCR2 was not required during inflammation (Figure 4-6). However, there is controversy about whether pDCs express TLR4, thus it is not known whether LPS would act directly or indirectly on pDCs (Krug *et al.*, 2001; Edwards *et al.*, 2003). Therefore, CCR2 might only play a role in pDC migration following direct activation of pDCs via TLR7 or TLR9.

The application of a TLR7 agonist, imiquimod to the skin has been reported to cause CCL2 dependent recruitment of pDCs to the inflamed skin (Drobits *et al.*, 2012). Shortly after imiquimod treatment (24 hrs) of the skin, CCL2 production was induced in a TLR7 and IFN α/β receptor 1 dependent fashion. In the absence of TLR7, CCL2 production was significantly reduced and pDC recruitment to the skin was diminished. Likewise, animals deficient in CCL2 did not recruit pDCs to the skin (Drobits *et al.*, 2012). Drobits *et al.* proposed that TLR7⁺ mast cells in the dermis were responsible for the imiquimod induced CCL2 release, as they illustrated that BM-derived mast cells produced significant levels of CCL2

following incubation with imiquimod (Drobits et al., 2012). Here I showed CCR2 KO animals had significantly more, rather than fewer, pDCs recruited to imiquimod treated skin compared to WT mice (Figure 5-34). Furthermore, there were no significant differences in the number of pDCs in the draining inguinal LN, spleen, BM or blood of CCR2 KO mice treated with imiquimod compared to similarly treated WT controls (Figure 5-35 to 5-38). Thus, CCR2 was not required for pDC migration to the skin. The low number of cells retrieved from skin preparations meant that pDCs could not be examined for their CCR2 activity, thus the relative contributions of the CCL2^{hi/lo} subsets to the skin pDC population could not be determined. Furthermore, in contrast to Langerhans cells, which are highly dependent on CCR2 for their migration from the skin to the draining LNs (Sato et al., 2000), pDCs did not appear to require CCR2 for escape to the draining inguinal LNs (Figure 5-35). Therefore, regardless of their ability to migrate *in vitro* in response to CCL2 (Figure 5-10), in an *in vivo* model in which pDCs are reported to exhibit CCL2 dependent migration into the skin (Drobits et al., 2012), my results suggest that they did not require CCR2 to migrate.

The CCL2 dependent migration of pDCs might be due to an indirect effect. Perhaps pDCs do not migrate to inflamed skin in a CCR2 or CCL2 dependent manner, but CCL2 recruits an intermediary cell population that once activated in the skin produces pDC-recruiting chemokines. For example, Jimenez *et al.* have reported that CCR2 KO mice have reduced levels of the CCR7 ligand, CCL19, and hypothesised that a link exists between CCR2 and activation of the CCR7-CCL19 axis (Jimenez et al., 2010). However, if this hypothesis were true, a decrease in pDCs would still be expected, as a consequence of the loss of the intermediary cell population. These results might indicate that CCL2 is functioning independently of CCR2. In section 1.6.1.4 some of the divergent phenotypes of CCR2 KO and CCL2 KO animals were described. CCR2 KO mice have diminished Th1 responses (Boring et al., 1997; Peters et al., 2000; Chiu et al., 2004), whereas CCL2 KO mice have diminished Th2 responses (Boring et al., 1997; deSchoolmeester et al., 2003). Therefore, an alternative conclusion is that the CCR2 independent CCL2 dependent migration of pDCs might be another divergent phenotype of animals deficient in the receptor or its ligand.

A consistent phenotype observed in each tissue was that following imiquimod treatment, pDCs lost CCR2 activity, and there was a significant reduction in the

proportion of CCL2^{hi} pDCs in the inguinal LNs, spleen and BM (Figure 5-35 to 5-37). However, similar to results produced with LPS, D6 activity was not affected, as pDCs within each tissue maintained D6 activity. The loss of CCR2 activity might indicate that, similar to cDCs, following activation, pDCs downregulate inflammatory chemokine receptors and upregulate CCR7 (Dieu et al., 1998; Sallusto et al., 1998). Thus, perhaps CCR2 is not involved in the migration of pDCs to a specific organ, but may coordinate their migration within the organ itself. It would be of interest to establish the location of each subset within splenic tissue sections. However, CCL2^{AF647} cannot be used to distinguish the two subsets in tissue sections and no other marker has fully coordinated with CCR2 expression, therefore to confirm the location of the two subsets within the section the CCL2 subsets would need to be purified and each subset individually labelled. Following adoptive transfer of the labelled cells it should be possible to assess their distribution within the tissues.

I have shown that there are no substantial functional differences between CCL2^{hi} and CCL2^{lo} pDCs. They do not possess gross morphological differences, except that some CCL2^{lo} pDCs have vacuoles present in their nuclei (Figure 5-14). The presence of vacuoles within the nuclei of CCL2^{lo} pDCs could be due to apoptosis induced by the stress of sorting. However, they were not present in CCL2^{hi} pDCs and no differences in the viability of either subset (Figure 5-29) or in the expression of apoptosis associated genes in the microarray data were observed (Figure 5-24). Furthermore, the vacuoles in the nuclei of CCL2^{lo} pDCs were not detrimental to pDC function, as both subsets were able to produce IFN α/β in response to CpG or R848 stimulation (Figure 5-21). pDCs possess the ability to produce high levels of IFN α/β in response to TLR7 (R848) or TLR9 (CpG) stimulation (Naik et al., 2005; Reizis et al., 2011a). However, similar to results by Ito *et al.* CCL2^{hi/lo} pDCs stimulated with CpG-A made significantly more IFN α than R848 stimulated pDCs (Ito et al., 2006). Most groups have demonstrated both mature and immature pDCs can produce IFN α/β (O'Keeffe et al., 2002; Omatsu et al., 2005; Toma-Hirano et al., 2007). However, Björck *et al.* showed that BM CD9⁺ immature pDCs had a greater capacity to produce IFN α than mature peripheral CD9⁻ pDCs (Björck et al., 2011). In contradiction to these observations, splenic CCL2^{hi/lo} subsets were CD9⁻ and capable of producing IFN α in response to TLR7 and TLR9 stimulation. However, a positive control of

immature pDCs to compare the capacity of immature ($CD9^+$) and the two $CCL2^{hi/lo} CD9^-$ subsets to produce $IFN\alpha$ was not included. Thus, the two $CCL2^{hi/lo} CD9^-$ subsets might have a lower capacity to produce $IFN\alpha$ than the $CD9^+$ immature pDCs.

There were no differences in the T cell stimulatory capacity of the two CCL2 pDC subsets (Figures 5-15 to 5-20) and consistent with published observations (Asselin-Paturel et al., 2001; Blasius and Colonna, 2006; Villadangos and Young, 2008), the pDCs were far less efficient at processing and presenting Ag to T cells than cDCs. However, both CCL2 subsets were able to stimulate T cell proliferation in similar capacities. Many groups have investigated the T cell stimulatory capacity of pDCs. Some reported that pDCs can stimulate memory $CD8^+$ and effector Th1 cells (Colonna, 2003; Fonteneau et al., 2003), whereas other groups have reported that pDCs possess the ability to prime naïve T cells (Asselin-Paturel et al., 2001; Mouriès et al., 2008). Similar to results generated by Asselin-Paturel *et al.* (Asselin-Paturel et al., 2001), total pDCs and the two CCL2 pDC subsets were only able to prime and stimulate minimal proliferation of naïve $CD4^+$ T cells (Figure 5-15 and 5-16). In contrast, both subsets were significantly more efficient at processing and cross-presenting OVA to $CD8\alpha^+$ T cells (Figure 5-18). This is also consistent with published observations, as pDCs are reported to be efficient at priming and stimulating proliferation of naïve $CD8^+$ T cells by cross-presentation of exogenous Ag on MHC I (Mouriès et al., 2008). I initially wanted to confirm the tolerogenic properties of the subsets, both have been shown to express CCR9 and $CD8\alpha$, markers of tolerogenic pDCs. My aim was to examine the expression of FoxP3, the key transcription factor expressed by Tregs (Boehmer and Nolting, 2008). However, the inferior $CD4^+$ stimulatory capacity of the pDCs and the resulting low T cell numbers made this extremely difficult.

Resting non-stimulated pDCs express low levels of MHCII and costimulatory molecules, and imaging studies have shown that their interaction with T cells is not stable and are only transient contacts (Mittelbrunn et al., 2009). In contrast, following their activation pDCs can maintain sustained contacts with T cells and have a higher immunogenic capacity than resting pDCs (Mittelbrunn et al., 2009). Accordingly, many groups have reported that the T cell stimulatory

capacity of pDCs is enhanced by their activation (Asselin-Paturel et al., 2001; Boonstra et al., 2002; Colonna et al., 2004; Salio et al., 2004; Mouriès et al., 2008). For example, Mouriès *et al.* reported that CpG or R848 activated pDCs have significantly enhanced ability to cross-present and prime naïve CD8⁺ T cells (Mouriès et al., 2008). Consistent with these observations, following activation with R848, CCL2^{hi} and CCL2^{lo} pDCs had increased CD8α⁺ T cell stimulatory capacity, as there was a significant increase in the proportion of T cells that have divided. Furthermore, there was a significant increase in the number of T cells in the later division generations following activation of pDCs with R848 (Figure 5-19). I also found that following activation with CpG-C, both subsets upregulated costimulatory molecules CD86 and ICOS-L, which may in part explain their enhanced T cell stimulatory capacity (Figure 5-29).

These results also suggest that activation of CCR2 signalling does not affect the T cell stimulatory capacity of the two subsets, as addition of exogenous CCL2 to co-cultures had no effect on their T cell stimulatory capacity (Figure 5-20). Exposure of pDCs to CCL2^{AF647} was required to facilitate purification of the two pDC subsets. This prior exposure to CCL2 might have desensitised CCR2. However, the co-culture experiments were performed over a three day period, therefore it was expected that CCR2 activity would be restored within this time. An alternative method to examine whether CCR2 affects the T cell stimulatory capacity of the two subsets would be to determine the ability of total pDCs to prime T cell proliferation in the presence and absence of CCL2. T cell stimulatory capacity could also be compared between total pDCs from WT and CCR2 KO animals.

6.8 Conclusions and future directions

These studies have helped to establish the use of the CCL2^{AF647} assay as a reliable, sensitive and versatile method for CCR2 detection. They have also furthered our understanding about CCR2 and D6 expression and regulation. Furthermore, the assay facilitated the identification of two distinct pDC subsets based on CCR2 expression. The microarray analysis of the two subsets confirmed the difference in CCR2 expression, in addition to the identification of several other genes that were differentially expressed by the subsets. For example, IL-13Ra1 was expressed at higher levels in CCL2^{hi} pDCs, as confirmed by microarray

results and antibody staining. However, addition of IL-13 did not appear to have any effect on CpG induced pDC maturation. Subsequent to a further attempt at validating the microarray results by QPCR it would be of interest to determine the role that differentially expressed genes may have in the pDC subsets.

My preliminary investigations have not revealed any indispensable role for CCR2 in pDC function or an association of CCR2 activity with a particular pDC phenotype. The two subsets had similar T cell stimulatory and IFN α production capacity. Furthermore, although my *in vitro* data shows that mouse pDCs can migrate in response to CCL2, CCR2 was not required for the CCL2 dependent migration of pDCs to imiquimod inflamed skin. The time-restrictions of this PhD have meant that I have only been able to examine the role of CCR2 in pDC migration in one model of inflammation and although CCR2 was not found to function in pDC migration within this model, a role for CCR2 in the migration of pDCs should not be discounted. CCR2 expression by Ly6C^{hi} monocytes has been shown to be crucial in the defence against *Listeria monocytogenes* (Serbina and Pamer, 2006), and perhaps similarly CCL2^{hi} pDCs might play a central role in defence against other specific pathogens.

By establishing a role of CCR2 on pDCs, it may help us to determine why CCR2 is expressed at a higher level on a proportion of pDCs, as the mechanism by which this occurs is as yet unknown. My early results provide evidence that differences in chemokine receptor expression are not a consequence of differences in the activation or maturation states of the subsets. I have shown that CCL2^{hi} pDCs can downregulate their CCR2 activity in response to inflammation, either directly mediated by TLR7 stimulation or indirectly by TLR4 stimulation. However, it has yet to be confirmed whether the two subsets can interconvert i.e. can CCL2^{lo} pDCs become CCL2^{hi}, or vice versa. This could be done either *in vitro*, by purifying the two subsets and incubating them with Flt3L or alternatively, purified CCL2^{hi/lo} subsets could be labelled and injected i.v. into steady-state and/or inflamed mice. After a short incubation period of 24-48 hrs the relative proportions of labelled CCL2^{hi/lo} pDCs in peripheral lymphoid organs could be determined. If the two subsets can indeed interconvert it may not occur within this short time-period. Long-term transfers might be achieved by purifying CCL2^{hi/lo} pDCs from mice expressing one of the two identifiable alleles of CD45,

CD45.1 or CD45.2. The purified cells can then be injected i.v. into mice expressing the other allele, which would allow for the later identification of the transferred cells by flow cytometry.

Collectively these results have helped enhance our understanding of CCR2 and D6 expression within the immune system. Further to this, I have identified a previously uncharacterised subset of pDCs that express CCR2 and have provided initial observations of their function in steady-state and inflammatory settings. Finally, understanding the consequences of CCR2 and D6 expression on pDCs is of paramount importance, as it will provide further insight into pDC biology and their roles in inflammatory disease.

Appendices

Gene Symbol	FC CCL2 ^{hi} pDCs vs. total pDCs	FC CCL2 ^{lo} pDCs vs. total pDCs	FC CCL2 ^{hi} pDCs vs. CCL2 ^{lo} pDCs
Hspb1	29.3394	22.7519	1.28954
Cdkn1a	9.3763	6.45646	1.45224
Il1r2	9.29091	4.80465	1.93373
Hsph1	8.81644	8.38109	1.05194
Vdr	8.72108	5.01912	1.73757
Atf3	7.41372	5.57453	1.32993
Bag3	6.93039	4.8588	1.42636
Tnip3	6.80021	2.85079	2.38538
Cables1	6.66265	7.60426	-1.14133
Plk2	6.5466	2.7754	2.3588
Tnfsf9	6.35579	3.11829	2.03823
Nr4a2	6.28692	2.86412	2.19506
Pde3b	6.2139	5.46505	1.13703
Nr4a3	6.14912	4.59796	1.33736
Bcl2l11	6.10685	5.7635	1.05957
Rasgef1b	6.05559	4.06192	1.49082
Ramp3	5.8075	4.05765	1.43125
Id3	5.66284	6.86889	-1.21298
Gcnt2	5.61535	3.62012	1.55115
Gla	5.50683	6.59929	-1.19838
Emp1	5.46121	2.6863	2.03299
Dennd4a	5.43378	4.46489	1.217
Hspa1a	5.427	5.22977	1.03771
Trp53inp2	5.38456	5.00378	1.0761
Hspa1a	5.22672	5.16817	1.01133
Galnt6	5.13271	2.22194	2.31001
Fam129b	5.0343	2.74365	1.83489
Lmna	4.98433	4.76647	1.04571
Celsr1	4.82361	3.55044	1.3586
Plk3	4.76339	3.94427	1.20767
Cd83	4.6511	3.24859	1.43173
Dnajb1	4.58822	4.31528	1.06325
Ppp1r16b	4.43456	4.0806	1.08674
Hspa1a	4.41382	4.01133	1.10034
Chst11	4.39513	4.85164	-1.10387
Cenpa	4.19494	3.86498	1.08537
Ifrd1	4.16067	3.45817	1.20314
Gprc5a	4.10197	2.70364	1.5172
B3gnt5	4.06822	2.95382	1.37727
Lfng	4.02826	2.32985	1.72898
Gp49a	3.9923	2.1546	1.85292
Crip2	3.96321	2.51599	1.57521
Hspd1	3.9097	3.45377	1.13201
Ccl3	3.9048	4.19582	-1.07453
Ifitm2	3.88561	1.48872	2.61003
Dusp8	3.8822	3.82797	1.01417
Dnaja1	3.8725	3.63439	1.06552

Phlpp1	3.87027	3.30063	1.17259
Nfil3	3.80038	2.55519	1.48731
Stat4	3.77151	2.871	1.31366
Grhl3	3.76737	4.94526	-1.31265
Grasp	3.74881	3.57292	1.04923
Hspa1l	3.73597	2.44837	1.5259
Spsb1	3.69163	5.48259	-1.48514
Hspd1	3.68323	3.26767	1.12717
Vps37b	3.61875	3.16576	1.14309
Klrb1b	3.57996	1.3344	2.68282
Erf	3.56601	3.60638	-1.01132
Jup	3.5653	1.69426	2.10434
Uck2	3.51091	2.27667	1.54213
5430435G22Rik	3.50327	2.47347	1.41634
Fam46c	3.49869	4.16328	-1.18995
Odc1	3.4286	3.41412	1.00424
Ppp1r15a	3.3956	3.44792	-1.01541
Kcnn4	3.39427	2.97902	1.13939
Dennd4a	3.3351	2.86955	1.16224
Itga5	3.28626	1.74703	1.88105
Slc5a3	3.26697	2.42071	1.34959
Lzts1	3.24352	3.24243	1.00034
Vegfa	3.23476	2.56818	1.25955
Mir22	3.22557	2.65768	1.21368
Smad3	3.14949	3.28379	-1.04264
Dusp16	3.14569	2.74328	1.14669
Kdm6b	3.13961	3.29647	-1.04996
Zfand2a	3.13943	2.62853	1.19437
Dennd4a	3.13292	2.82385	1.10945
Gfod1	3.08547	2.889	1.06801
Klf10	3.0764	2.57153	1.19633
Ier3	3.06985	2.68807	1.14203
Dennd4a	3.06708	2.56484	1.19582
Lrrc8d	3.04231	3.00515	1.01237
Pvr	3.03921	2.19614	1.38389
Hsp90aa1	3.03691	3.08098	-1.01451
Mir155	3.03072	2.2659	1.33753
Ets2	3.01579	2.45296	1.22945
Rhobtb2	-3.00233	-1.7683	-1.69786
Gm10790	-3.01111	-2.53447	-1.18806
Cyp2r1	-3.02515	-1.82511	-1.65751
Gm12250	-3.21138	-2.52557	-1.27155
Ppm1e	-3.39078	-2.26043	-1.50006
Mlh3	-3.41029	-2.08797	-1.6333

Appendix 1: List of genes examined for alterations in expression as an effect of incubation in Figure 5-26.

The FC differences between CCL2^{hi} pDC vs. total pDCs, CCL2^{lo} pDCs vs. total pDCs and CCL2^{hi} vs. CCL2^{lo} pDCs for all genes with a FC of <-3.0 or >3.0 and p value of p<0.005 between the CCL2^{hi} pDCs and total pDCs. Each gene was examined for its relative expression in cell types using Immgen. Genes with high expression in Langerhan cells (LCs) are shown in blue, high expression in cDCs (red) and high expression in cells other than LCs, pDCs and cDCs (black). Furthermore, genes that were expressed at a higher level in pDCs than LCs are shown in pink and genes with similar expression in pDCs and LCs are shown in green.

- 1 Title: The atypical chemokine receptor CCX-CKR regulates CCL19
· and CCL21, and fine-tunes immune responses in the lung.
Author(s): Asquith, D.; Mirchandani, A.; Anderson, E.; et al.
Conference: European Congress of Immunology Location: Glasgow,
SCOTLAND Date: SEP 05-08, 2012
Source: IMMUNOLOGY Volume: 137 Special Issue: SI Supplement: 1
Pages: 66-66 Published: SEP 2012
Times Cited: 0 (from All Databases)

- 2 Title: Universal expression and dual function of the chemokine
· scavenger D6 on innate-like B cells
Author(s): Hansell, C.; Schiering, C.; Kinstrie, R.; et al.
Conference: Annual Congress of the British-Society-for-Immunology
Location: Liverpool, ENGLAND Date: DEC 06-10, 2010
Sponsor(s): British Soc Immunol
Source: IMMUNOLOGY Volume: 131 Supplement: 1 Pages: 32-32
Published: DEC 2010
Times Cited: 0 (from All Databases)

- 3 Title: Sensitive flow cytometric detection of the chemokine
· receptor CCR2 on mouse leukocytes
Author(s): Ford, L.; Hansell, C.; Nibbs, R.
Conference: Annual Congress of the British-Society-for-Immunology
Location: Liverpool, ENGLAND Date: DEC 06-10, 2010
Sponsor(s): British Soc Immunol
Source: IMMUNOLOGY Volume: 131 Supplement: 1 Pages: 140-141
Published: DEC 2010
Times Cited: 0 (from All Databases)

Appendix 2: List of published abstracts that I contributed to.

1. Using fluorescent chemokine uptake to detect chemokine receptors by Fluorescent Activated Cell Sorting.

Laura B Ford, Chris A H Hansell & Robert J B Nibbs.

Methods in Molecular Biology (In Press 2012).

2. Fluorescent CCL2 uptake: a specific, sensitive and versatile method for the detection of CCL2 receptors in mammals.

L Ford, R Kinstrie, M Clarke, C Hurson, E Anderson, V Cerovic, C Hansell, R Nibbs.

In preparation (2012)

Appendix 4: List of my manuscripts in press or preparation.

References

- Aiuti, A., Springer, T., Webb, I.J., and Gutierrez-Ramos, J.C. (1997). The Chemokine SDF-1 Is a Chemoattractant for Human CD34 Hematopoietic Progenitor Cells and Provides a New Mechanism to Explain the Mobilization of CD34 Progenitors to Peripheral Blood. *J Exp Med* 185, 111-120.
- Allavena, P., Sica, A., Vecchi, A., Locati, M., Sozzani, S., and Mantovani, A. (2000). The chemokine receptor switch paradigm and dendritic cell migration: its significance in tumor tissues. *Immunol Rev* 177, 141-149.
- Allen, S.J., Crown, S.E., and Handel, T.M. (2007). Chemokine: receptor structure, interactions, and antagonism. *Annu. Rev. Immunol.* 25, 787-820.
- Alon, R., and Feigelson, S. (2002). From rolling to arrest on blood vessels: leukocyte tap dancing on endothelial integrin ligands and chemokines at sub-second contacts. *Semin Immunol* 14, 93-104.
- Alon, R., and Feigelson, S.W. (2009). Chemokine Signaling to Lymphocyte Integrins Under Shear Flow. *Microcirculation* 16, 3-16.
- Alvarez, D., Vollmann, E.H., and von Andrian, U.H. (2008). Mechanisms and consequences of dendritic cell migration. *Immunity* 29, 325-342.
- Anandarajah, A.P., and Ritchlin, C.T. (2004). Pathogenesis of psoriatic arthritis. *Curr Opin Rheumatol* 16, 338-343.
- Anderson, E.J.R. (2011). The Role of the CCX-CKR Chemokine Receptor in Immunity and Tolerance. Thesis 1-243.
- Ansel, K.M., and Cyster, J.G. (2001). Chemokines in lymphopoiesis and lymphoid organ development. *Curr Opin Immunol* 13, 172-179.
- Ansel, K.M., Ngo, V.N., Hyman, P.L., Luther, S.A., Förster, R., Sedgwick, J.D., Browning, J.L., Lipp, M., and Cyster, J.G. (2000). A chemokine-driven positive feedback loop organizes lymphoid follicles. *Nature* 406, 309-314.
- Arase, H., Saito, T., Phillips, J.H., and Lanier, L.L. (2001). Cutting edge: the mouse NK cell-associated antigen recognized by DX5 monoclonal antibody is CD49b (alpha 2 integrin, very late antigen-2). *J Immunol* 167, 1141-1144.
- Ardavín, C. (2003). Origin, precursors and differentiation of mouse dendritic cells. *Nat Rev Immunol* 3, 582-590.
- Ardavín, C., Wu, L., Li, C.L., and Shortman, K. (1993). Thymic dendritic cells and T cells develop simultaneously in the thymus from a common precursor population. *Nature* 362, 761-763.
- Asselin-Paturel, C., Boonstra, A., Dalod, M., Durand, I., Yessaad, N., Dezutter-Dambuyant, C., Vicari, A., O'Garra, A., Biron, C., Brière, F., et al. (2001). Mouse type I IFN-producing cells are immature APCs with plasmacytoid morphology. *Nat Immunol* 2, 1144-1150.
- Asselin-Paturel, C., Brizard, G., Chemin, K., Boonstra, A., O'Garra, A., Vicari, A., and Trinchieri, G. (2005). Type I interferon dependence of plasmacytoid dendritic cell activation and migration. *J Exp Med* 201, 1157-1167.
- Asselin-Paturel, C., Brizard, G., Pin, J.-J., Brière, F., and Trinchieri, G. (2003). Mouse strain differences in plasmacytoid dendritic cell frequency and function revealed by a novel monoclonal antibody. *J Immunol* 171, 6466-6477.
- Auffray, C., Fogg, D., Garfa, M., Elain, G., Join-Lambert, O., Kayal, S., Sarnacki, S., Cumano, A., Lauvau, G., and Geissmann, F. (2007). Monitoring of Blood Vessels and Tissues by a Population of Monocytes with Patrolling Behavior. *Science* 317, 666-670.
- Auffray, C., Fogg, D.K., Narni-Mancinelli, E., Senechal, B., Trouillet, C., Saederup, N., Leemput, J., Bigot, K., Campisi, L., Abitbol, M., et al. (2009a). CX3CR1⁺ CD115⁺ CD135⁺ common macrophage/DC precursors and the role of CX3CR1 in their response to inflammation. *J Exp Med* 206, 595-606.
- Auffray, C., Sieweke, M.H., and Geissmann, F. (2009b). Blood monocytes: development, heterogeneity, and relationship with dendritic cells. *Annu. Rev. Immunol.* 27, 669-692.

- Baba, T., Nakamoto, Y., and Mukaida, N. (2009). Crucial contribution of thymic Sirp alpha+ conventional dendritic cells to central tolerance against blood-borne antigens in a CCR2-dependent manner. *J Immunol* *183*, 3053-3063.
- Baekkevold, E.S., Yamanaka, T., Palframan, R.T., Carlsen, H.S., Reinholt, F.P., von Andrian, U.H., Brandtzaeg, P., and Haraldsen, G. (2001). The CCR7 ligand elc (CCL19) is transcytosed in high endothelial venules and mediates T cell recruitment. *J Exp Med* *193*, 1105-1112.
- Bajénoff, M., Egen, J.G., Koo, L.Y., Laugier, J.P., Brau, F., Glaichenhaus, N., and Germain, R.N. (2006). Stromal Cell Networks Regulate Lymphocyte Entry, Migration, and Territoriality in Lymph Nodes. *Immunity* *25*, 989-1001.
- Bajénoff, M., Glaichenhaus, N., and Germain, R.N. (2008). Fibroblastic reticular cells guide T lymphocyte entry into and migration within the splenic T cell zone. *The Journal of Immunology* *181*, 3947-3954.
- Ballantyne, S.J., Barlow, J.L., Jolin, H.E., Nath, P., Williams, A.S., Chung, K.F., Sturton, G., Wong, S.H., and McKenzie, A.N.J. (2007). Blocking IL-25 prevents airway hyperresponsiveness in allergic asthma. *J. Allergy Clin. Immunol.* *120*, 1324-1331.
- Banchereau, J., Brière, F., Caux, C., Davoust, J., Lebecque, S., Liu, Y.J., Pulendran, B., and Palucka, K. (2000). Immunobiology of dendritic cells. *Annu. Rev. Immunol.* *18*, 767-811.
- Banchereau, J., and Pascual, V. (2006). Type I interferon in systemic lupus erythematosus and other autoimmune diseases. *Immunity* *25*, 383-392.
- Banchereau, J., and Steinman, R.M. (1998). Dendritic cells and the control of immunity. *Nature* *392*, 245-252.
- Barreiro, O., Yáñez-Mó, M., Sala-Valdés, M., Gutiérrez-López, M.D., Ovalle, S., Higginbottom, A., Monk, P.N., Cabañas, C., and Sánchez-Madrid, F. (2005). Endothelial tetraspanin microdomains regulate leukocyte firm adhesion during extravasation. *Blood* *105*, 2852-2861.
- Benoist, C., Lanier, L., Merad, M., and Mathis, D. (2012). Consortium biology in immunology: the perspective from the Immunological Genome Project. *Nat Rev Immunol* *12*, 734-740.
- Bento, A.F., Leite, D.F.P., Claudino, R.F., Hara, D.B., Leal, P.C., and Calixto, J.B. (2008). The selective nonpeptide CXCR2 antagonist SB225002 ameliorates acute experimental colitis in mice. *J Leukoc Biol* *84*, 1213-1221.
- Berghöfer, B., Haley, G., Frommer, T., Bein, G., and Hackstein, H. (2007). Natural and synthetic TLR7 ligands inhibit CpG-A- and CpG-C-oligodeoxynucleotide-induced IFN-alpha production. *J Immunol* *178*, 4072-4079.
- Bezman, N.A., Kim, C.C., Sun, J.C., Min-Oo, G., Hendricks, D.W., Kamimura, Y., Best, J.A., Goldrath, A.W., and Lanier, L.L. (2011). Molecular definition of the identity and activation of natural killer cells. *Nat Immunol* *11*, 1-11.
- Binder, N.B., Niederreiter, B., Hoffmann, O., Stange, R., Pap, T., Stulnig, T.M., Mack, M., Erben, R.G., Smolen, J.S., and Redlich, K. (2009). Estrogen-dependent and C-C chemokine receptor-2-dependent pathways determine osteoclast behavior in osteoporosis. *Nat Med* *15*, 417-424.
- Björck, P., Leong, H.X., and Engleman, E.G. (2011). Plasmacytoid dendritic cell dichotomy: identification of IFN-alpha producing cells as a phenotypically and functionally distinct subset. *J Immunol* *186*, 1477-1485.
- Blasius, A.L., Barchet, W., Cella, M., and Colonna, M. (2007). Development and function of murine B220+CD11c+NK1.1+ cells identify them as a subset of NK cells. *J Exp Med* *204*, 2561-2568.
- Blasius, A.L., Cella, M., Maldonado, J., Takai, T., and Colonna, M. (2006a). Siglec-H is an IPC-specific receptor that modulates type I IFN secretion through DAP12. *Blood* *107*, 2474-2476.
- Blasius, A.L., and Colonna, M. (2006). Sampling and signaling in plasmacytoid dendritic cells: the potential roles of Siglec-H. *Trends Immunol* *27*, 255-260.

- Blasius, A.L., Giurisato, E., Cella, M., Schreiber, R.D., Shaw, A.S., and Colonna, M. (2006b). Bone marrow stromal cell antigen 2 is a specific marker of type I IFN-producing cells in the naive mouse, but a promiscuous cell surface antigen following IFN stimulation. *J Immunol* *177*, 3260-3265.
- Blasius, A., Vermi, W., Krug, A., Facchetti, F., Cella, M., and Colonna, M. (2004). A cell-surface molecule selectively expressed on murine natural interferon-producing cells that blocks secretion of interferon-alpha. *Blood* *103*, 4201-4206.
- Boehmer, von, H., and Nolting, J. (2008). What turns on Foxp3? *Nat Immunol* *9*, 121-122.
- Boisvert, W.A., Rose, D.M., Johnson, K.A., Fuentes, M.E., Lira, S.A., Curtiss, L.K., and Terkeltaub, R.A. (2006). Up-regulated expression of the CXCR2 ligand KC/GRO-alpha in atherosclerotic lesions plays a central role in macrophage accumulation and lesion progression. *Am J Pathol* *168*, 1385-1395.
- Boldajipour, B., Mahabaleswar, H., Kardash, E., Reichman-Fried, M., Blaser, H., Minina, S., Wilson, D., Xu, Q., and Raz, E. (2008). Control of Chemokine-Guided Cell Migration by Ligand Sequestration. *Cell* *132*, 463-473.
- Bonecchi, R., Locati, M., Galliera, E., Vulcano, M., Sironi, M., Fra, A.M., Gobbi, M., Vecchi, A., Sozzani, S., Haribabu, B., et al. (2004). Differential recognition and scavenging of native and truncated macrophage-derived chemokine (macrophage-derived chemokine/CC chemokine ligand 22) by the D6 decoy receptor. *J Immunol* *172*, 4972-4976.
- Bonini, J.A., and Steiner, D.F. (1997). Molecular cloning and expression of a novel rat CC-chemokine receptor (rCCR10rR) that binds MCP-1 and MIP-1beta with high affinity. *DNA Cell Biol.* *16*, 1023-1030.
- Boonstra, A., Asselin-Paturel, C., Gilliet, M., Crain, C., Trinchieri, G., Liu, Y.J., and O'Garra, A. (2002). Flexibility of Mouse Classical and Plasmacytoid-derived Dendritic Cells in Directing T Helper Type 1 and 2 Cell Development: Dependency on Antigen Dose and Differential Toll-like Receptor Ligation. *Journal of Experimental Medicine* *197*, 101-109.
- Bordon, Y., Hansell, C.A.H., Sester, D.P., Clarke, M., Mowat, A.M., and Nibbs, R.J.B. (2009). The Atypical Chemokine Receptor D6 Contributes to the Development of Experimental Colitis. *The Journal of Immunology* *182*, 5032-5040.
- Boring, L., Gosling, J., Chensue, S.W., Kunkel, S.L., Farese, R.V., Broxmeyer, H.E., and Charo, I.F. (1997). Impaired monocyte migration and reduced type 1 (Th1) cytokine responses in C-C chemokine receptor 2 knockout mice. *J Clin Invest* *100*, 2552-2561.
- Borrow, P., Martínez-Sobrido, L., and de la Torre, J.C. (2010). Inhibition of the Type I Interferon Antiviral Response During Arenavirus Infection. *Viruses* *2*, 2443-2480.
- Boudakov, I., Liu, J., Fan, N., Gulay, P., Wong, K., and Gorkzynski, R.M. (2007). Mice Lacking CD200R1 Show Absence of Suppression of Lipopolysaccharide-Induced Tumor Necrosis Factor-alpha and Mixed Leukocyte Culture Responses by CD200. *Transplantation* *84*, 251-257.
- Braun, A., Worbs, T., Moschovakis, G.L., Halle, S., Hoffmann, K., Bölter, J., Münk, A., and Förster, R. (2011). Afferent lymph-derived T cells and DCs use different chemokine receptor CCR7-dependent routes for entry into the lymph node and intranodal migration. *Nat Immunol* *12*, 879-887.
- Brawand, P., Fitzpatrick, D.R., Greenfield, B.W., Brasel, K., Maliszewski, C.R., and De Smedt, T. (2002). Murine plasmacytoid pre-dendritic cells generated from Flt3 ligand-supplemented bone marrow cultures are immature APCs. *J Immunol* *169*, 6711-6719.
- Britschgi, M.R., Link, A., Lissandrin, T.K.A., and Luther, S.A. (2008). Dynamic modulation of CCR7 expression and function on naive T lymphocytes in vivo. *The Journal of Immunology* *181*, 7681-7688.
- Brühl, H., Cihak, J., Schneider, M.A., Plachý, J., Rupp, T., Wenzel, I., Shakarami, M., Milz, S., Ellwart, J.W., Stangassinger, M., et al. (2004). Dual role of CCR2 during initiation and progression of collagen-induced arthritis: evidence for regulatory activity of CCR2+ T cells. *J Immunol* *172*, 890-898.

- Campbell, D.J., and Butcher, E.C. (2002). Rapid acquisition of tissue-specific homing phenotypes by CD4(+) T cells activated in cutaneous or mucosal lymphoid tissues. *J Exp Med* 195, 135-141.
- Cardona, A.E., Sasse, M.E., Liu, L., Cardona, S.M., Mizutani, M., Savarin, C., Hu, T., and Ransohoff, R.M. (2008). Scavenging roles of chemokine receptors: chemokine receptor deficiency is associated with increased levels of ligand in circulation and tissues. *Blood* 112, 256-263.
- Cascalho, M., Wong, J., Brown, J., Jäck, H.M., Steinberg, C., and Wabl, M. (2000). A B220(-), CD19(-) population of B cells in the peripheral blood of quasimonoclonal mice. *Int Immunol* 12, 29-35.
- Cella, M., Engering, A., Pinet, V., Pieters, J., and Lanzavecchia, A. (1997). Inflammatory stimuli induce accumulation of MHC class II complexes on dendritic cells. *Nature* 388, 782-787.
- Cervantes-Barragan, L., Lewis, K.L., Firner, S., Thiel, V., Hugues, S., Reith, W., Ludewig, B., and Reizis, B. (2012). Plasmacytoid dendritic cells control T-cell response to chronic viral infection. *Proceedings of the National Academy of Sciences of the United States of America* 109, 3012-3017.
- Cesta, M.F. (2006). Normal structure, function, and histology of the spleen. *Toxicol Pathol* 34, 455-465.
- Chandra, R., Villanueva, E., Feketova, E., Machiedo, G.W., Hasko, G., Deitch, E.A., and Spolarics, Z. (2008). Endotoxemia down-regulates bone marrow lymphopoiesis but stimulates myelopoiesis: the effect of G6PD deficiency. *J Leukoc Biol* 83, 1541-1550.
- Charo, I.F., and Ransohoff, R.M. (2006). The many roles of chemokines and chemokine receptors in inflammation. *N. Engl. J. Med.* 354, 610-621.
- Chiu, B.-C., Freeman, C.M., Stolberg, V.R., Hu, J.S., Zeibecoglou, K., Lu, B., Gerard, C., Charo, I.F., Lira, S.A., and Chensue, S.W. (2004). Impaired lung dendritic cell activation in CCR2 knockout mice. *Am J Pathol* 165, 1199-1209.
- Cisse, B., Caton, M.L., Lehner, M., Maeda, T., Scheu, S., Locksley, R., Holmberg, D., Zweier, C., Hollander, den, N.S., Kant, S.G., et al. (2008). Transcription factor E2-2 is an essential and specific regulator of plasmacytoid dendritic cell development. *Cell* 135, 37-48.
- Cochain, C., Auvynet, C., Poupel, L., Vilar, J., Dumeau, E., Richart, A., Recalde, A., Zouggar, Y., Yin, K.Y.H.W., Bruneval, P., et al. (2012). The Chemokine Decoy Receptor D6 Prevents Excessive Inflammation and Adverse Ventricular Remodeling After Myocardial Infarction. *Arteriosclerosis, Thrombosis, and Vascular Biology* 32, 2206-2213.
- Collington, S.J., Hallgren, J., Pease, J.E., Jones, T.G., Rollins, B.J., Westwick, J., Austen, K.F., Williams, T.J., Gurish, M.F., and Weller, C.L. (2010). The role of the CCL2/CCR2 axis in mouse mast cell migration in vitro and in vivo. *The Journal of Immunology* 184, 6114-6123.
- Colonna, M. (2003). Plasmacytoid dendritic cells: are they professional antigen-presenting cells? *Blood* 101, 3342a-3342.
- Colonna, M., Trinchieri, G., and Liu, Y.-J. (2004). Plasmacytoid dendritic cells in immunity. *Nat Immunol* 5, 1219-1226.
- Comerford, I., and Nibbs, R.J.B. (2005). Post-translational control of chemokines: a role for decoy receptors? *Immunol Lett* 96, 163-174.
- Cotton, M., and Claing, A. (2009). G protein-coupled receptors stimulation and the control of cell migration. *Cellular Signalling* 21, 1045-1053.
- Crane, M.J., Hokeness-Antonelli, K.L., and Salazar-Mather, T.P. (2009). Regulation of inflammatory monocyte/macrophage recruitment from the bone marrow during murine cytomegalovirus infection: role for type I interferons in localized induction of CCR2 ligands. *J Immunol* 183, 2810-2817.
- Cronshaw, D.G., Kouroumalis, A., Parry, R., Webb, A., Brown, Z., and Ward, S.G. (2006). Evidence that phospholipase-C-dependent, calcium-independent mechanisms are required for directional migration of T-lymphocytes in response to the CCR4 ligands CCL17 and CCL22. *J Leukoc Biol* 79, 1369-1380.

- Crown, S.E., Yu, Y., Sweeney, M.D., Leary, J.A., and Handel, T.M. (2006). Heterodimerization of CCR2 chemokines and regulation by glycosaminoglycan binding. *J Biol Chem* **281**, 25438-25446.
- Cupedo, T., and Mebius, R.E. (2003). Role of chemokines in the development of secondary and tertiary lymphoid tissues. *Semin Immunol* **15**, 243-248.
- Cyster, J.G. (1999). Chemokines and cell migration in secondary lymphoid organs. *Science* **286**, 2098-2102.
- Cyster, J.G. (2005). Chemokines, sphingosine-1-phosphate, and cell migration in secondary lymphoid organs. *Annu. Rev. Immunol.* **23**, 127-159.
- Cyster, J.G., and Goodnow, C.C. (1995). Pertussis toxin inhibits migration of B and T lymphocytes into splenic white pulp cords. *J Exp Med* **182**, 581-586.
- Daley, J.M., Thomay, A.A., Connolly, M.D., Reichner, J.S., and Albina, J.E. (2008). Use of Ly6G-specific monoclonal antibody to deplete neutrophils in mice. *J Leukoc Biol* **83**, 64-70.
- D'Amico, A., and Wu, L. (2003). The early progenitors of mouse dendritic cells and plasmacytoid predendritic cells are within the bone marrow hemopoietic precursors expressing Flt3. *J Exp Med* **198**, 293-303.
- D'Apuzzo, M., Rolink, A., Loetscher, M., Hoxie, J.A., Clark-Lewis, I., Melchers, F., Baggiolini, M., and Moser, B. (1997). The chemokine SDF-1, stromal cell-derived factor 1, attracts early stage B cell precursors via the chemokine receptor CXCR4. *Eur J Immunol* **27**, 1788-1793.
- Davalos-Misslitz, A.C.M., Rieckenberg, J., Willenzon, S., Worbs, T., Kremmer, E., Bernhardt, G., and Förster, R. (2007). Generalized multi-organ autoimmunity in CCR7-deficient mice. *Eur J Immunol* **37**, 613-622.
- Décaillot, F.M., Kazmi, M.A., Lin, Y., Ray-Saha, S., Sakmar, T.P., and Sachdev, P. (2011). CXCR7/CXCR4 heterodimer constitutively recruits beta-arrestin to enhance cell migration. *J Biol Chem* **286**, 32188-32197.
- Delano, M.J., Kelly-Scumpia, K.M., Thayer, T.C., Winfield, R.D., Scumpia, P.O., Cuenca, A.G., Harrington, P.B., O'Malley, K.A., Warner, E., Gabilovich, S., et al. (2011). Neutrophil Mobilization from the Bone Marrow during Polymicrobial Sepsis Is Dependent on CXCL12 Signaling. *The Journal of Immunology* **187**, 911-918.
- Delogu, A., Schebesta, A., Sun, Q., Aschenbrenner, K., Perlot, T., and Busslinger, M. (2006). Gene Repression by Pax5 in B Cells Is Essential for Blood Cell Homeostasis and Is Reversed in Plasma Cells. *Immunity* **24**, 269-281.
- deSchoolmeester, M.L., Little, M.C., Rollins, B.J., and Else, K.J. (2003). Absence of CC chemokine ligand 2 results in an altered Th1/Th2 cytokine balance and failure to expel *Trichuris muris* infection. *J Immunol* **170**, 4693-4700.
- Deshmane, S.L., Kremlev, S., Amini, S., and Sawaya, B.E. (2009). Monocyte chemoattractant protein-1 (MCP-1): an overview. *Journal of Interferon & Cytokine Research* **29**, 313-326.
- De Smedt, T., Pajak, B., Klaus, G.G., Noelle, R.J., Urbain, J., Leo, O., and Moser, M. (1998). Antigen-specific T lymphocytes regulate lipopolysaccharide-induced apoptosis of dendritic cells in vivo. *J Immunol* **161**, 4476-4479.
- De Smedt, T., Pajak, B., Muraille, E., Lespagnard, L., Heinen, E., De Baetselier, P., Urbain, J., Leo, O., and Moser, M. (1996). Regulation of dendritic cell numbers and maturation by lipopolysaccharide in vivo. *J Exp Med* **184**, 1413-1424.
- de St Groth, B.F. (2001). DCs and peripheral T cell tolerance. *Semin Immunol* **13**, 311-322.
- Diacovo, T.G., Blasius, A.L., Mak, T.W., Cella, M., and Colonna, M. (2005). Adhesive mechanisms governing interferon-producing cell recruitment into lymph nodes. *J Exp Med* **202**, 687-696.
- Dieu, M.C., Vanbervliet, B., Vicari, A., Bridon, J.M., Oldham, E., Ait-Yahia, S., Brière, F., Zlotnik, A., Lebecque, S., and Caux, C. (1998). Selective recruitment of immature and mature dendritic cells by distinct chemokines expressed in different anatomic sites. *J Exp Med* **188**, 373-386.

- Di Liberto, D., Locati, M., Caccamo, N., Vecchi, A., Meraviglia, S., Salerno, A., Sireci, G., Nebuloni, M., Caceres, N., Cardona, P.J., et al. (2008). Role of the chemokine decoy receptor D6 in balancing inflammation, immune activation, and antimicrobial resistance in *Mycobacterium tuberculosis* infection. *Journal of Experimental Medicine* 205, 2075-2084.
- Dorner, B.G., Dorner, M.B., Zhou, X., Opitz, C., Mora, A., GÜttler, S., Hutloff, A., Mages, H.W., Ranke, K., Schaefer, M., et al. (2009). Selective Expression of the Chemokine Receptor XCR1 on Cross-presenting Dendritic Cells Determines Cooperation with CD8+ T Cells. *Immunity* 31, 823-833.
- Douillard, P., Stoitzner, P., Tripp, C.H., Clair-Moninot, V., Ait-Yahia, S., McLellan, A.D., Eggert, A., Romani, N., and Saeland, S. (2005). Mouse Lymphoid Tissue Contains Distinct Subsets of Langerin/CD207+ Dendritic Cells, Only One of Which Represents Epidermal-Derived Langerhans Cells. *Journal of Investigative Dermatology* 125, 983-994.
- Drobits, B., Holcman, M., Amberg, N., Swiecki, M., Grundtner, R., Hammer, M., Colonna, M., and Sibilica, M. (2012). Imiquimod clears tumors in mice independent of adaptive immunity by converting pDCs into tumor-killing effector cells. *J Clin Invest*.
- Drutman, S.B., Kendall, J.C., and Trombetta, E.S. (2012). Inflammatory Spleen Monocytes Can Upregulate CD11c Expression Without Converting into Dendritic Cells. *The Journal of Immunology* 188, 3603-3610.
- Eash, K.J., Greenbaum, A.M., Gopalan, P.K., and Link, D.C. (2010). CXCR2 and CXCR4 antagonistically regulate neutrophil trafficking from murine bone marrow. *J Clin Invest* 120, 2423-2431.
- Edwards, A.D., Diebold, S.S., Slack, E.M.C., Tomizawa, H., Hemmi, H., Kaisho, T., Akira, S., and E Sousa, C.R. (2003). Toll-like receptor expression in murine DC subsets: lack of TLR7 expression by CD8 alpha+ DC correlates with unresponsiveness to imidazoquinolines. *Eur J Immunol* 33, 827-833.
- Fantuzzi, L., Borghi, P., Ciolli, V., Pavlakis, G., Belardelli, F., and Gessani, S. (1999). Loss of CCR2 expression and functional response to monocyte chemotactic protein (MCP-1) during the differentiation of human monocytes: role of secreted MCP-1 in the regulation of the chemotactic response. *Blood* 94, 875-883.
- Fazilleau, N., Mark, L., McHeyzer-Williams, L.J., and McHeyzer-Williams, M.G. (2009). Follicular Helper T Cells: Lineage and Location. *Immunity* 30, 324-335.
- Finlay, B.B., and McFadden, G. (2006). Anti-Immunology: Evasion of the Host Immune System by Bacterial and Viral Pathogens. *Cell* 124, 767-782.
- Fiorina, P., Jurewicz, M., Vergani, A., Augello, A., Paez, J., Ricchiuti, V., Tchirpachvili, V., Sayegh, M.H., and Abdi, R. (2008). Phenotypic and functional differences between wild-type and CCR2-/- dendritic cells: implications for islet transplantation. *Transplantation* 85, 1030-1038.
- Flaishon, L., Becker-Herman, S., Hart, G., Levo, Y., Kuziel, W.A., and Shachar, I. (2004). Expression of the chemokine receptor CCR2 on immature B cells negatively regulates their cytoskeletal rearrangement and migration. *Blood* 104, 933-941.
- Fonteneau, J.-F., Gilliet, M., Larsson, M., Dasilva, I., Münz, C., Liu, Y.-J., and Bhardwaj, N. (2003). Activation of influenza virus-specific CD4+ and CD8+ T cells: a new role for plasmacytoid dendritic cells in adaptive immunity. *Blood* 101, 3520-3526.
- Förster, R., Davalos-Miszlitz, A.C., and Rot, A. (2008). CCR7 and its ligands: balancing immunity and tolerance. *Nat Rev Immunol* 8, 362-371.
- Förster, R., Mattis, A.E., Kremmer, E., Wolf, E., Brem, G., and Lipp, M. (1996). A putative chemokine receptor, BLR1, directs B cell migration to defined lymphoid organs and specific anatomic compartments of the spleen. *Cell* 87, 1037-1047.
- Förster, R., Schubel, A., Breitfeld, D., Kremmer, E., Renner-Müller, I., Wolf, E., and Lipp, M. (1999). CCR7 coordinates the primary immune response by establishing functional microenvironments in secondary lymphoid organs. *Cell* 99, 23-33.
- Fra, A.M., Locati, M., Otero, K., Sironi, M., Signorelli, P., Massardi, M.L., Gobbi, M., Vecchi, A., Sozzani, S., and Mantovani, A. (2003). Cutting edge: scavenging of

- inflammatory CC chemokines by the promiscuous putatively silent chemokine receptor D6. *J Immunol* **170**, 2279-2282.
- Friedman, R.S., Jacobelli, J., and Krummel, M.F. (2006). Surface-bound chemokines capture and prime T cells for synapse formation. *Nat Immunol* **7**, 1101-1108.
- Fuchsberger, M., Hochrein, H., and O'Keefe, M. (2005). Activation of plasmacytoid dendritic cells. *Immunol Cell Biol* **83**, 571-577.
- Gabrilovich, D.I., Ostrand-Rosenberg, S., and Bronte, V. (2012). Coordinated regulation of myeloid cells by tumours. *Nat Rev Immunol* **12**, 253-268.
- Galliera, E., Jala, V.R., Trent, J.O., Bonecchi, R., Signorelli, P., Lefkowitz, R.J., Mantovani, A., Locati, M., and Haribabu, B. (2004). beta-Arrestin-dependent constitutive internalization of the human chemokine decoy receptor D6. *J Biol Chem* **279**, 25590-25597.
- Gatto, D., Wood, K., and Brink, R. (2011). EBI2 Operates Independently of but in Cooperation with CXCR5 and CCR7 To Direct B Cell Migration and Organization in Follicles and the Germinal Center. *The Journal of Immunology* **187**, 4621-4628.
- Gaupp, S., Pitt, D., Kuziel, W.A., Cannella, B., and Raine, C.S. (2003). Experimental autoimmune encephalomyelitis (EAE) in CCR2(-/-) mice: susceptibility in multiple strains. *Am J Pathol* **162**, 139-150.
- Geissmann, F., Jung, S., and Littman, D.R. (2003). Blood Monocytes Consist of Two Principal Subsets with Distinct Migratory Properties. *Immunity* **19**, 71-82.
- Ghosh, H.S., Cisse, B., Bunin, A., Lewis, K.L., and Reizis, B. (2010). Continuous Expression of the Transcription Factor E2-2 Maintains the Cell Fate of Mature Plasmacytoid Dendritic Cells. *Immunity* **33**, 905-916.
- Giagulli, C., Scarpini, E., Ottoboni, L., Narumiya, S., Butcher, E.C., Constantin, G., and Laudanna, C. (2004). RhoA and zeta PKC control distinct modalities of LFA-1 activation by chemokines: critical role of LFA-1 affinity triggering in lymphocyte in vivo homing. *Immunity* **20**, 25-35.
- Gibson, S.J., Lindh, J.M., Riter, T.R., Gleason, R.M., Rogers, L.M., Fuller, A.E., Oesterich, J.L., Gorden, K.B., Qiu, X., McKane, S.W., et al. (2002). Plasmacytoid dendritic cells produce cytokines and mature in response to the TLR7 agonists, imiquimod and resiquimod. *Cell Immunol* **218**, 74-86.
- Gilliet, M., Boonstra, A., Paturel, C., Antonenko, S., Xu, X.-L., Trinchieri, G., O'Garra, A., and Liu, Y.-J. (2002). The development of murine plasmacytoid dendritic cell precursors is differentially regulated by FLT3-ligand and granulocyte/macrophage colony-stimulating factor. *J Exp Med* **195**, 953-958.
- Gilliet, M., Cao, W., and Liu, Y.-J. (2008). Plasmacytoid dendritic cells: sensing nucleic acids in viral infection and autoimmune diseases. *Nat Rev Immunol* **8**, 594-606.
- Gilliet, M., and Lande, R. (2008). Antimicrobial peptides and self-DNA in autoimmune skin inflammation. *Curr Opin Immunol* **20**, 401-407.
- Ginhoux, F., Tacke, F., Angeli, V., Bogunovic, M., Loubreau, M., Dai, X.-M., Stanley, E.R., Randolph, G.J., and Merad, M. (2006). Langerhans cells arise from monocytes in vivo. *Nat Immunol* **7**, 265-273.
- Gonzalez, E., Kulkarni, H., Bolivar, H., Mangano, A., Sanchez, R., Catano, G., Nibbs, R.J., Freedman, B.I., Quinones, M.P., Bamshad, M.J., et al. (2005). The influence of CCL3L1 gene-containing segmental duplications on HIV-1/AIDS susceptibility. *Science* **307**, 1434-1440.
- González-Navajas, J.M., Fine, S., Law, J., Datta, S.K., Nguyen, K.P., Yu, M., Corr, M., Katakura, K., Eckman, L., Lee, J., et al. (2010). TLR4 signaling in effector CD4+ T cells regulates TCR activation and experimental colitis in mice. *J Clin Invest* **120**, 570-581.
- Gordon, S., and Taylor, P.R. (2005). Monocyte and macrophage heterogeneity. *Nat Rev Immunol* **5**, 953-964.
- Graham, G.J. (2009). D6 and the atypical chemokine receptor family: Novel regulators of immune and inflammatory processes. *Eur J Immunol* **39**, 342-351.

- Grailer, J.J., Koderer, M., and Steeber, D.A. (2009). L-selectin: Role in regulating homeostasis and cutaneous inflammation. *Journal of Dermatological Science* 56, 141-147.
- Grakoui, A., Bromley, S.K., Sumen, C., Davis, M.M., Shaw, A.S., Allen, P.M., and Dustin, M.L. (1999). The immunological synapse: a molecular machine controlling T cell activation. *Science* 285, 221-227.
- Gregorio, J., Meller, S., Conrad, C., Di Nardo, A., Homey, B., Lauerma, A., Arai, N., Gallo, R.L., Digiovanni, J., and Gilliet, M. (2010). Plasmacytoid dendritic cells sense skin injury and promote wound healing through type I interferons. *J Exp Med* 207, 2921-2930.
- Gretz, J.E., Norbury, C.C., Anderson, A.O., Proudfoot, A.E., and Shaw, S. (2000). Lymph-borne chemokines and other low molecular weight molecules reach high endothelial venules via specialized conduits while a functional barrier limits access to the lymphocyte microenvironments in lymph node cortex. *J Exp Med* 192, 1425-1440.
- Guiducci, C., Tripodo, C., Gong, M., Sangaletti, S., Colombo, M.P., Coffman, R.L., and Barrat, F.J. (2010). Autoimmune skin inflammation is dependent on plasmacytoid dendritic cell activation by nucleic acids via TLR7 and TLR9. *J Exp Med* 207, 2931-2942.
- Guillerey, C., Mouriès, J., Polo, G., Doyen, N., Law, H.K.W., Chan, S., Kastner, P., Leclerc, C., and Dadaglio, G. (2012). Pivotal role of plasmacytoid dendritic cells in inflammation and NK-cell responses after TLR9 triggering in mice. *Blood* 120, 90-99.
- Gunn, M.D., Kyuwa, S., Tam, C., Kakiuchi, T., Matsuzawa, A., Williams, L.T., and Nakano, H. (1999). Mice lacking expression of secondary lymphoid organ chemokine have defects in lymphocyte homing and dendritic cell localization. *J Exp Med* 189, 451-460.
- Gururajan, M., Jacob, J., and Pulendran, B. (2007). Toll-Like Receptor Expression and Responsiveness of Distinct Murine Splenic and Mucosal B-Cell Subsets. *PLoS ONE* 2, e863.
- Gutiérrez, J., Kremer, L., Zaballos, A., Goya, I., Martínez-A, C., and Márquez, G. (2004). Analysis of post-translational CCR8 modifications and their influence on receptor activity. *J Biol Chem* 279, 14726-14733.
- Haan, den, J.M., Lehar, S.M., and Bevan, M.J. (2000). CD8(+) but not CD8(-) dendritic cells cross-prime cytotoxic T cells in vivo. *J Exp Med* 192, 1685-1696.
- Hadeiba, H., Sato, T., Habtezion, A., Oderup, C., Pan, J., and Butcher, E.C. (2008). CCR9 expression defines tolerogenic plasmacytoid dendritic cells able to suppress acute graft-versus-host disease. *Nat Immunol* 9, 1253-1260.
- Handel, T.M., Johnson, Z., Crown, S.E., Lau, E.K., and Proudfoot, A.E. (2005). Regulation of protein function by glycosaminoglycans--as exemplified by chemokines. *Annu. Rev. Biochem.* 74, 385-410.
- Hansell, C.A.H., Hurson, C.E., and Nibbs, R.J.B. (2011a). DARC and D6: silent partners in chemokine regulation? *Immunol Cell Biol* 89, 197-206.
- Hansell, C.A.H., Schiering, C., Kinstrie, R., Ford, L., Bordon, Y., McInnes, I.B., Goodyear, C.S., and Nibbs, R.J.B. (2011b). Universal expression and dual function of the atypical chemokine receptor D6 on innate-like B cells in mice. *Blood* 117, 5413-5424.
- Hansell, C.A.H., Simpson, C.V., and Nibbs, R.J.B. (2006). Chemokine sequestration by atypical chemokine receptors. *Biochem. Soc. Trans.* 34, 1009-1013.
- Hargreaves, D.C., Hyman, P.L., Lu, T.T., Ngo, V.N., Bidgol, A., Suzuki, G., Zou, Y.R., Littman, D.R., and Cyster, J.G. (2001). A coordinated change in chemokine responsiveness guides plasma cell movements. *J Exp Med* 194, 45-56.
- Haringman, J.J., Gerlag, D.M., Smeets, T.J.M., Baeten, D., van den Bosch, F., Bresnihan, B., Breedveld, F.C., Dinant, H.J., Legay, F., Gram, H., et al. (2006). A randomized controlled trial with an anti-CCL2 (anti-monocyte chemotactic protein 1) monoclonal antibody in patients with rheumatoid arthritis. *Arthritis Rheum* 54, 2387-2392.
- Hart, D.N. (1997). Dendritic cells: unique leukocyte populations which control the primary immune response. *Blood* 90, 3245-3287.

- Hartmann, T.N., Grabovsky, V., Pasvolsky, R., Shulman, Z., Buss, E.C., Spiegel, A., Nagler, A., Lapidot, T., Thelen, M., and Alon, R. (2008). A crosstalk between intracellular CXCR7 and CXCR4 involved in rapid CXCL12-triggered integrin activation but not in chemokine-triggered motility of human T lymphocytes and CD34+ cells. *J Leukoc Biol* 84, 1130-1140.
- Hathcock, K.S., Laszlo, G., Pucillo, C., Linsley, P., and Hodes, R.J. (1994). Comparative analysis of B7-1 and B7-2 costimulatory ligands: expression and function. *J Exp Med* 180, 631-640.
- Heino, M., Peterson, P., Kudoh, J., Nagamine, K., Lagerstedt, A., Ovod, V., Ranki, A., Rantala, I., Nieminen, M., Tuukkanen, J., et al. (1999). Autoimmune regulator is expressed in the cells regulating immune tolerance in thymus medulla. *Biochem Biophys Res Commun* 257, 821-825.
- Hestdal, K., Ruscetti, F.W., Ihle, J.N., Jacobsen, S.E., Dubois, C.M., Kopp, W.C., Longo, D.L., and Keller, J.R. (1991). Characterization and regulation of RB6-8C5 antigen expression on murine bone marrow cells. *J Immunol* 147, 22-28.
- Hochweller, K., Miloud, T., Striegler, J., Naik, S., Hämmerling, G.J., and Garbi, N. (2009). Homeostasis of dendritic cells in lymphoid organs is controlled by regulation of their precursors via a feedback loop. *Blood* 114, 4411-4421.
- Hochweller, K., Striegler, J., Hämmerling, G.J., and Garbi, N. (2008). A novel CD11c.DTR transgenic mouse for depletion of dendritic cells reveals their requirement for homeostatic proliferation of natural killer cells. *Eur J Immunol* 38, 2776-2783.
- Hogquist, K.A., Jameson, S.C., Heath, W.R., Howard, J.L., Bevan, M.J., and Carbone, F.R. (1994). T cell receptor antagonist peptides induce positive selection. *Cell* 76, 17-27.
- Hohl, T.M., Rivera, A., Lipuma, L., Gallegos, A., Shi, C., Mack, M., and Pamer, E.G. (2009). Inflammatory Monocytes Facilitate Adaptive CD4 T Cell Responses during Respiratory Fungal Infection. *Cell Host and Microbe* 6, 470-481.
- Hokeness, K.L., Kuziel, W.A., Biron, C.A., and Salazar-Mather, T.P. (2005). Monocyte chemoattractant protein-1 and CCR2 interactions are required for IFN-alpha/beta-induced inflammatory responses and antiviral defense in liver. *J Immunol* 174, 1549-1556.
- Holoshitz, J., Vila, L.M., Keroack, B.J., McKinley, D.R., and Bayne, N.K. (1992). Dual antigenic recognition by cloned human gamma delta T cells. *J Clin Invest* 89, 308-314.
- Horuk, R. (2009). Chemokine receptor antagonists: overcoming developmental hurdles. *Nat Rev Drug Discov* 8, 23-33.
- Huang, I.-C., Bailey, C.C., Weyer, J.L., Radoshitzky, S.R., Becker, M.M., Chiang, J.J., Brass, A.L., Ahmed, A.A., Chi, X., Dong, L., et al. (2011). Distinct Patterns of IFITM-Mediated Restriction of Filoviruses, SARS Coronavirus, and Influenza A Virus. *PLoS Pathog* 7, e1001258.
- Hubert, F.-X., Voisine, C., Louvet, C., Heslan, J.-M., Ouabed, A., Heslan, M., and Josien, R. (2006). Differential pattern recognition receptor expression but stereotyped responsiveness in rat spleen dendritic cell subsets. *J Immunol* 177, 1007-1016.
- Hume, D.A. (2008). Macrophages as APC and the dendritic cell myth. *The Journal of Immunology* 181, 5829-5835.
- Hurson, C.E. (2011). Expression and function of the atypical chemokine receptor CCX-CKR. (PhD thesis, University of Glasgow.).
- Hu, Y., Wang, J., Yang, B., Zheng, N., Qin, M., Ji, Y., Lin, G., Tian, L., Wu, X., Wu, L., et al. (2011). Guanylate binding protein 4 negatively regulates virus-induced type I IFN and antiviral response by targeting IFN regulatory factor 7. *The Journal of Immunology* 187, 6456-6462.
- Inngjerdigen, M., Damaj, B., and Maghazachi, A.A. (2001). Expression and regulation of chemokine receptors in human natural killer cells. *Blood* 97, 367-375.
- Irizarry, R.A., Bolstad, B.M., Collin, F., Cope, L.M., Hobbs, B., and Speed, T.P. (2003). Summaries of Affymetrix GeneChip probe level data. *Nucleic Acids Res.* 31, e15.

- Irla, M., Küpfer, N., Suter, T., Lissilaa, R., Benkhoucha, M., Skupsky, J., Lalive, P.H., Fontana, A., Reith, W., and Hugues, S. (2010). MHC class II-restricted antigen presentation by plasmacytoid dendritic cells inhibits T cell-mediated autoimmunity. *Journal of Experimental Medicine* 207, 1891-1905.
- Islam, S.A., Chang, D.S., Colvin, R.A., Byrne, M.H., McCully, M.L., Moser, B., Lira, S.A., Charo, I.F., and Luster, A.D. (2011). Mouse CCL8, a CCR8 agonist, promotes atopic dermatitis by recruiting IL-5⁺ TH2 cells. *Nat Immunol* 12, 167-177.
- Ito, T., Kanzler, H., Duramad, O., Cao, W., and Liu, Y.-J. (2006). Specialization, kinetics, and repertoire of type 1 interferon responses by human plasmacytoid predendritic cells. *Blood* 107, 2423-2431.
- Ito, T., Yang, M., Wang, Y.-H., Lande, R., Gregorio, J., Perng, O.A., Qin, X.-F., Liu, Y.-J., and Gilliet, M. (2007). Plasmacytoid dendritic cells prime IL-10-producing T regulatory cells by inducible costimulator ligand. *J Exp Med* 204, 105-115.
- Iwata, M., Hirakiyama, A., Eshima, Y., Kagechika, H., Kato, C., and Song, S.-Y. (2004). Retinoic Acid Imprints Gut-Homing Specificity on T Cells. *Immunity* 21, 527-538.
- Jamieson, T., Cook, D.N., Nibbs, R.J.B., Rot, A., Nixon, C., McLean, P., Alcami, A., Lira, S.A., Wiekowski, M., and Graham, G.J. (2005). The chemokine receptor D6 limits the inflammatory response in vivo. *Nat Immunol* 6, 403-411.
- Jarchum, I., Liu, M., Shi, C., Equinda, M., and Pamer, E.G. (2012). Critical role for MyD88-mediated neutrophil recruitment during *Clostridium difficile* colitis. *Infect Immun* 80, 2989-2996.
- Jego, G., Palucka, A.K., Blanck, J.-P., Chalouni, C., Pascual, V., and Banchereau, J. (2003). Plasmacytoid Dendritic Cells Induce Plasma Cell Differentiation through Type I Interferon and Interleukin 6. *Immunity* 19, 225-234.
- Jiang, N., Leach, L.J., Hu, X., Potokina, E., Jia, T., Druka, A., Waugh, R., Kearsey, M.J., and Luo, Z.W. (2008). Methods for evaluating gene expression from Affymetrix microarray datasets. *BMC Bioinformatics* 9, 284.
- Jimenez, F., Quinones, M.P., Martinez, H.G., Estrada, C.A., Clark, K., Garavito, E., Ibarra, J., Melby, P.C., and Ahuja, S.S. (2010). CCR2 plays a critical role in dendritic cell maturation: possible role of CCL2 and NF-kappa B. *The Journal of Immunology* 184, 5571-5581.
- Jin, B., Sun, T., Yu, X.-H., Yang, Y.-X., and Yeo, A.E.T. (2012). The Effects of TLR Activation on T-Cell Development and Differentiation. *Clinical and Developmental Immunology* 2012, 1-32.
- Jung, S., Aliberti, J., Graemmel, P., Sunshine, M.J., Kreutzberg, G.W., Sher, A., and Littman, D.R. (2000). Analysis of fractalkine receptor CX(3)CR1 function by targeted deletion and green fluorescent protein reporter gene insertion. *Mol Cell Biol* 20, 4106-4114.
- Jung, S., Unutmaz, D., Wong, P., Sano, G.-I., De los Santos, K., Sparwasser, T., Wu, S., Vuthoori, S., Ko, K., Zavala, F., et al. (2002). In vivo depletion of CD11c⁺ dendritic cells abrogates priming of CD8⁺ T cells by exogenous cell-associated antigens. *Immunity* 17, 211-220.
- Juskewitch, J.E., Knudsen, B.E., Platt, J.L., Nath, K.A., Knutson, K.L., Brunn, G.J., and Grande, J.P. (2012). LPS-induced murine systemic inflammation is driven by parenchymal cell activation and exclusively predicted by early MCP-1 plasma levels. *Am J Pathol* 180, 32-40.
- Kabashima, K., Murata, T., Tanaka, H., Matsuoka, T., Sakata, D., Yoshida, N., Katagiri, K., Kinashi, T., Tanaka, T., Miyasaka, M., et al. (2003). Thromboxane A2 modulates interaction of dendritic cells and T cells and regulates acquired immunity. *Nat Immunol* 4, 694-701.
- Kamath, A.T., Henri, S., Battye, F., Tough, D.F., and Shortman, K. (2002). Developmental kinetics and lifespan of dendritic cells in mouse lymphoid organs. *Blood* 100, 1734-1741.

- Kamath, A.T., Pooley, J., O'Keeffe, M.A., Vremec, D., Zhan, Y., Lew, A.M., D'amico, A., Wu, L., Tough, D.F., and Shortman, K. (2000). The development, maturation, and turnover rate of mouse spleen dendritic cell populations. *J Immunol* *165*, 6762-6770.
- Kamogawa-Schifter, Y., Ohkawa, J., Namiki, S., Arai, N., Arai, K.-I., and Liu, Y. (2005). Ly49Q defines 2 pDC subsets in mice. *Blood* *105*, 2787-2792.
- Kandouz, M., Haidara, K., Zhao, J., Brisson, M.-L., and Batist, G. (2010). The EphB2 tumor suppressor induces autophagic cell death via concomitant activation of the ERK1/2 and PI3K pathways. *Cell Cycle* *9*, 398-407.
- Karsunky, H., Merad, M., Cozzio, A., Weissman, I.L., and Manz, M.G. (2003). Flt3 Ligand Regulates Dendritic Cell Development from Flt3+ Lymphoid and Myeloid-committed Progenitors to Flt3+ Dendritic Cells In Vivo. *Journal of Experimental Medicine* *198*, 305-313.
- Kerkmann, M., Rothenfusser, S., Hornung, V., Towarowski, A., Wagner, M., Sarris, A., Giese, T., Endres, S., and Hartmann, G. (2003). Activation with CpG-A and CpG-B oligonucleotides reveals two distinct regulatory pathways of type I IFN synthesis in human plasmacytoid dendritic cells. *J Immunol* *170*, 4465-4474.
- Kim, R., Emi, M., Tanabe, K., and Arihiro, K. (2007). Potential functional role of plasmacytoid dendritic cells in cancer immunity. *Immunology* *121*, 149-157.
- Kinashi, T. (2005). Intracellular signalling controlling integrin activation in lymphocytes. *Nat Rev Immunol* *5*, 546-559.
- Kissenpfennig, A., Henri, S., Dubois, B., Laplace-Builhé, C., Perrin, P., Romani, N., Tripp, C.H., Douillard, P., Leserman, L., Kaiserlian, D., et al. (2005). Dynamics and Function of Langerhans Cells In Vivo. *Immunity* *22*, 643-654.
- Kohrgruber, N., Gröger, M., Meraner, P., Kriehuber, E., Petzelbauer, P., Brandt, S., Stingl, G., Rot, A., and Maurer, D. (2004). Plasmacytoid dendritic cell recruitment by immobilized CXCR3 ligands. *J Immunol* *173*, 6592-6602.
- Kool, M., GeurtsVanKessel, C., Muskens, F., Madeira, F.B., van Nimwegen, M., Kuipers, H., Thielemans, K., Hoogsteden, H.C., Hammad, H., and Lambrecht, B.N. (2011). Facilitated antigen uptake and timed exposure to TLR ligands dictate the antigen-presenting potential of plasmacytoid DCs. *J Leukoc Biol* *90*, 1177-1190.
- Kopydlowski, K.M., Salkowski, C.A., Cody, M.J., van Rooijen, N., Major, J., Hamilton, T.A., and Vogel, S.N. (1999). Regulation of macrophage chemokine expression by lipopolysaccharide in vitro and in vivo. *J Immunol* *163*, 1537-1544.
- Kozbor, D., Trinchieri, G., Monos, D.S., Isobe, M., Russo, G., Haney, J.A., Zmijewski, C., and Croce, C.M. (1989). Human TCR-gamma+/delta+, CD8+ T lymphocytes recognize tetanus toxoid in an MHC-restricted fashion. *J Exp Med* *169*, 1847-1851.
- Krueger, A., Willenzon, S., Lyszkiewicz, M., Kremmer, E., and Förster, R. (2010). CC chemokine receptor 7 and 9 double-deficient hematopoietic progenitors are severely impaired in seeding the adult thymus. *Blood* *115*, 1906-1912.
- Krug, A., Rothenfusser, S., Hornung, V., Jahrsdörfer, B., Blackwell, S., Ballas, Z.K., Endres, S., Krieg, A.M., and Hartmann, G. (2001a). Identification of CpG oligonucleotide sequences with high induction of IFN-alpha/beta in plasmacytoid dendritic cells. *Eur J Immunol* *31*, 2154-2163.
- Krug, A., Towarowski, A., Britsch, S., Rothenfusser, S., Hornung, V., Bals, R., Giese, T., Engelmann, H., Endres, S., Krieg, A.M., et al. (2001b). Toll-like receptor expression reveals CpG DNA as a unique microbial stimulus for plasmacytoid dendritic cells which synergizes with CD40 ligand to induce high amounts of IL-12. *Eur J Immunol* *31*, 3026-3037.
- Kurobe, H., Liu, C., Ueno, T., Saito, F., Ohgashi, I., Seach, N., Arakaki, R., Hayashi, Y., Kitagawa, T., Lipp, M., et al. (2006). CCR7-Dependent Cortex-to-Medulla Migration of Positively Selected Thymocytes Is Essential for Establishing Central Tolerance. *Immunity* *24*, 165-177.
- Kwan, J., and Killeen, N. (2004). CCR7 directs the migration of thymocytes into the thymic medulla. *J Immunol* *172*, 3999-4007.

- Lanzavecchia, A., and Sallusto, F. (2005). Understanding the generation and function of memory T cell subsets. *Curr Opin Immunol* 17, 326-332.
- Lau, E.K., Paavola, C.D., Johnson, Z., Gaudry, J.-P., Geretti, E., Borlat, F., Kungl, A.J., Proudfoot, A.E., and Handel, T.M. (2004). Identification of the glycosaminoglycan binding site of the CC chemokine, MCP-1: implications for structure and function in vivo. *J Biol Chem* 279, 22294-22305.
- Le, Y., Zhou, Y., Iribarren, P., and Wang, J. (2004). Chemokines and chemokine receptors: their manifold roles in homeostasis and disease. *Cell Mol Immunol* 1, 95-104.
- Le, Y., Zhu, B.-M., Harley, B., Park, S.-Y., Kobayashi, T., Manis, J.P., Luo, H.R., Yoshimura, A., Hennighausen, L., and Silberstein, L.E. (2007). SOCS3 Protein Developmentally Regulates the Chemokine Receptor CXCR4-FAK Signaling Pathway during B Lymphopoiesis. *Immunity* 27, 811-823.
- Lee, K.M., McKimmie, C.S., Gilchrist, D.S., Pallas, K.J., Nibbs, R.J., Garside, P., McDonald, V., Jenkins, C., Ransohoff, R., Liu, L., et al. (2011). D6 facilitates cellular migration and fluid flow to lymph nodes by suppressing lymphatic congestion. *Blood* 118, 6220-6229.
- Leenen, P.J., Radosević, K., Voerman, J.S., Salomon, B., van Rooijen, N., Klatzmann, D., and van Ewijk, W. (1998). Heterogeneity of mouse spleen dendritic cells: in vivo phagocytic activity, expression of macrophage markers, and subpopulation turnover. *J Immunol* 160, 2166-2173.
- Lei, Y., Ripen, A.M., Ishimaru, N., Ohigashi, I., Nagasawa, T., Jeker, L.T., Bosl, M.R., Hollander, G.A., Hayashi, Y., de Waal Malefyt, R., et al. (2011). Aire-dependent production of XCL1 mediates medullary accumulation of thymic dendritic cells and contributes to regulatory T cell development. *Journal of Experimental Medicine* 208, 383-394.
- León, B., Ballesteros-Tato, A., Browning, J.L., Dunn, R., Randall, T.D., and Lund, F.E. (2012). Regulation of TH2 development by CXCR5+ dendritic cells and lymphotoxin-expressing B cells. *Nat Immunol* 13, 681-690.
- Lewis, K.L., Caton, M.L., Bogunovic, M., Greter, M., Grajkowska, L.T., Ng, D., Klinakis, A., Charo, I.F., Jung, S., Gommerman, J.L., et al. (2011). Notch2 Receptor Signaling Controls Functional Differentiation of Dendritic Cells in the Spleen and Intestine. *Immunity* 35, 780-791.
- Liao, W., Lin, J.-X., Wang, L., Li, P., and Leonard, W.J. (2011). Modulation of cytokine receptors by IL-2 broadly regulates differentiation into helper T cell lineages. *Nat Immunol* 12, 551-559.
- Link, A., Vogt, T.K., Favre, S., Britschgi, M.R., Acha-Orbea, H., Hinz, B., Cyster, J.G., and Luther, S.A. (2007). Fibroblastic reticular cells in lymph nodes regulate the homeostasis of naive T cells. *Nat Immunol* 8, 1255-1265.
- Liu, C., Lou, Y., Lizée, G., Qin, H., Liu, S., Rabinovich, B., Kim, G.J., Wang, Y.-H., Ye, Y., Sikora, A.G., et al. (2008). Plasmacytoid dendritic cells induce NK cell-dependent, tumor antigen-specific T cell cross-priming and tumor regression in mice. *J Clin Invest*.
- Liu, C., Saito, F., Liu, Z., Lei, Y., Uehara, S., Love, P., Lipp, M., Kondo, S., Manley, N., and Takahama, Y. (2006). Coordination between CCR7- and CCR9-mediated chemokine signals in prevascular fetal thymus colonization. *Blood* 108, 2531-2539.
- Liu, K., and Nussenzweig, M.C. (2010). Origin and development of dendritic cells. *Immunol Rev* 234, 45-54.
- Liu, K., Victora, G.D., Schwickert, T.A., Guermontprez, P., Meredith, M.M., Yao, K., Chu, F.-F., Randolph, G.J., Rudensky, A.Y., and Nussenzweig, M. (2009). In vivo analysis of dendritic cell development and homeostasis. *Science* 324, 392-397.
- Liu, K., Waskow, C., Liu, X., Yao, K., Hoh, J., and Nussenzweig, M. (2007). Origin of dendritic cells in peripheral lymphoid organs of mice. *Nat Immunol* 8, 578-583.
- Liu, Y.-J. (2005). IPC: professional type 1 interferon-producing cells and plasmacytoid dendritic cell precursors. *Annu. Rev. Immunol.* 23, 275-306.
- Li, Y., Zhao, L.-D., Tong, L.-S., Qian, S.-N., Ren, Y., Zhang, L., Ding, X., Chen, Y., Wang, Y.-X., Zhang, W., et al. (2012). Aberrant CD200/CD200R1 expression and function

- in systemic lupus erythematosus contributes to abnormal T-cell responsiveness and dendritic cell activity. *Arthritis Research & Therapy* 14, R123.
- Lloyd, C.M., Phillips, A.R.J., Cooper, G.J.S., and Dunbar, P.R. (2008). Three-colour fluorescence immunohistochemistry reveals the diversity of cells staining for macrophage markers in murine spleen and liver. *J Immunol Methods* 334, 70-81.
- Lombardi, V., Speak, A.O., Kerzerho, J., Szely, N., and Akbari, O. (2012). CD8 α +beta- and CD8 α +beta+ plasmacytoid dendritic cells induce Foxp3+ regulatory T cells and prevent the induction of airway hyper-reactivity. *5*, 432-443.
- Lopes-Carvalho, T., and Kearney, J.F. (2004). Development and selection of marginal zone B cells. *Immunol Rev* 197, 192-205.
- Lucas, A.D., and Greaves, D.R. (2001). Atherosclerosis: role of chemokines and macrophages. *Expert Rev Mol Med* 3, 1-18.
- Luther, S.A., Ansel, K.M., and Cyster, J.G. (2003). Overlapping Roles of CXCL13, Interleukin 7 Receptor , and CCR7 Ligands in Lymph Node Development. *Journal of Experimental Medicine* 197, 1191-1198.
- Luther, S.A., and Cyster, J.G. (2001). Chemokines as regulators of T cell differentiation. *Nat Immunol* 2, 102-107.
- Luther, S.A., Tang, H.L., Hyman, P.L., Farr, A.G., and Cyster, J.G. (2000). Coexpression of the chemokines ELC and SLC by T zone stromal cells and deletion of the ELC gene in the plt/plt mouse. *Proceedings of the National Academy of Sciences of the United States of America* 97, 12694-12699.
- Lutz, M.B., and Schuler, G. (2002). Immature, semi-mature and fully mature dendritic cells: which signals induce tolerance or immunity? *Trends Immunol* 23, 445-449.
- Ma, Q., Jones, D., Borghesani, P.R., Segal, R.A., Nagasawa, T., Kishimoto, T., Bronson, R.T., and Springer, T.A. (1998). Impaired B-lymphopoiesis, myelopoiesis, and derailed cerebellar neuron migration in CXCR4 and SDF-1-deficient mice. *Proceedings of the National Academy of Sciences of the United States of America* 95, 1-6.
- Mach, N., Gillessen, S., Wilson, S.B., Sheehan, C., Mihm, M., and Dranoff, G. (2000). Differences in dendritic cells stimulated in vivo by tumors engineered to secrete granulocyte-macrophage colony-stimulating factor or Flt3-ligand. *Cancer Res* 60, 3239-3246.
- Mack, M., Cihak, J., Simonis, C., Luckow, B., Proudfoot, A.E., Plachý, J., Brühl, H., Frink, M., Anders, H.J., Vielhauer, V., et al. (2001). Expression and characterization of the chemokine receptors CCR2 and CCR5 in mice. *J Immunol* 166, 4697-4704.
- MacLennan, I.C.M., Toellner, K.-M., Cunningham, A.F., Serre, K., Sze, D.M.-Y., Zúñiga, E., Cook, M.C., and Vinuesa, C.G. (2003). Extrafollicular antibody responses. *Immunol Rev* 194, 8-18.
- Madigan, J., Freeman, D.J., Menzies, F., Forrow, S., Nelson, S.M., Young, A., Sharkey, A., Moffett, A., Graham, G.J., Greer, I.A., et al. (2010). Chemokine Scavenger D6 Is Expressed by Trophoblasts and Aids the Survival of Mouse Embryos Transferred into Allogeneic Recipients. *The Journal of Immunology* 184, 3202-3212.
- Malhotra, D., Fletcher, A.L., Astarita, J., Lukacs-Kornek, V., Tayalia, P., Gonzalez, S.F., Elpek, K.G., Chang, S.K., Knoblich, K., Hemler, M.E., et al. (2012). Transcriptional profiling of stroma from inflamed and resting lymph nodes defines immunological hallmarks. *Nat Immunol* 13, 499-510.
- Manlapat, A.K., Kahler, D.J., Chandler, P.R., Munn, D.H., and Mellor, A.L. (2007). Cell-autonomous control of interferon type I expression by indoleamine 2,3-dioxygenase in regulatory CD19+ dendritic cells. *Eur J Immunol* 37, 1064-1071.
- Mangini, A.J., Lafyatis, R., and Van Seventer, J.M. (2007). Type I interferons inhibition of inflammatory T helper cell responses in systemic lupus erythematosus. *Ann N Y Acad Sci* 1108, 11-23.
- Mantovani, A. (1999). The chemokine system: redundancy for robust outputs. *Immunol Today* 20, 254-257.
- Mantovani, A., Bonecchi, R., and Locati, M. (2006). Tuning inflammation and immunity by chemokine sequestration: decoys and more. *Nat Rev Immunol* 6, 907-918.

- Manz, M.G., Traver, D., Miyamoto, T., Weissman, I.L., and Akashi, K. (2001). Dendritic cell potentials of early lymphoid and myeloid progenitors. *Blood* 97, 3333-3341.
- Mao, H., Qu, X., Yang, Y., Zuo, W., Bi, Y., Zhou, C., Yin, H., Deng, B., Sun, J., and Zhang, L. (2009). A novel tumor suppressor gene RhoBTB2 (DBC2): Frequent loss of expression in sporadic breast cancer. *Mol. Carcinog.* n/a-n/a.
- Maraskovsky, E., Brasel, K., Teepe, M., Roux, E.R., Lyman, S.D., Shortman, K., and McKenna, H.J. (1996). Dramatic increase in the numbers of functionally mature dendritic cells in Flt3 ligand-treated mice: multiple dendritic cell subpopulations identified. *J Exp Med* 184, 1953-1962.
- Martinez de la Torre, Y., Buracchi, C., Borroni, E.M., Dupor, J., Bonecchi, R., Nebuloni, M., Pasqualini, F., Doni, A., Lauri, E., Agostinis, C., et al. (2007). Protection against inflammation- and autoantibody-caused fetal loss by the chemokine decoy receptor D6. *Proceedings of the National Academy of Sciences of the United States of America* 104, 2319-2324.
- Martin, F., and Kearney, J.F. (2000). B-cell subsets and the mature preimmune repertoire. Marginal zone and B1 B cells as part of a "natural immune memory". *Immunol Rev* 175, 70-79.
- Martín, P., del Hoyo, G.M., Anjuère, F., Ruiz, S.R., Arias, C.F., Marín, A.R., and Ardavín, C. (2000). Concept of lymphoid versus myeloid dendritic cell lineages revisited: both CD8alpha(-) and CD8alpha(+) dendritic cells are generated from CD4(low) lymphoid-committed precursors. *Blood* 96, 2511-2519.
- Matis, L.A., Fry, A.M., Cron, R.Q., Cotterman, M.M., Dick, R.F., and Bluestone, J.A. (1989). Structure and specificity of a class II MHC alloreactive gamma delta T cell receptor heterodimer. *Science* 245, 746-749.
- Matta, B.M., Castellaneta, A., and Thomson, A.W. (2010). Tolerogenic plasmacytoid DC. *Eur J Immunol* 40, 2667-2676.
- Maus, U., Grote, von, K., Kuziel, W.A., Mack, M., Miller, E.J., Cihak, J., Stangassinger, M., Maus, R., Schlöndorff, D., Seeger, W., et al. (2002). The role of CC chemokine receptor 2 in alveolar monocyte and neutrophil immigration in intact mice. *Am J Respir Crit Care Med* 166, 268-273.
- Maus, U.A., Waelsch, K., Kuziel, W.A., Delbeck, T., Mack, M., Blackwell, T.S., Christman, J.W., Schlöndorff, D., Seeger, W., and Lohmeyer, J. (2003). Monocytes are potent facilitators of alveolar neutrophil emigration during lung inflammation: role of the CCL2-CCR2 axis. *J Immunol* 170, 3273-3278.
- Maus, U.A., Wellmann, S., Hampl, C., Kuziel, W.A., Srivastava, M., Mack, M., Everhart, M.B., Blackwell, T.S., Christman, J.W., Schlöndorff, D., et al. (2005). CCR2-positive monocytes recruited to inflamed lungs downregulate local CCL2 chemokine levels. *Am J Physiol Lung Cell Mol Physiol* 288, L350-L358.
- Mazzoni, A., and Segal, D.M. (2004). Controlling the Toll road to dendritic cell polarization. *J Leukoc Biol* 75, 721-730.
- McDonald, B., Pittman, K., Menezes, G.B., Hirota, S.A., Slaba, I., Waterhouse, C.C.M., Beck, P.L., Muruve, D.A., and Kubes, P. (2010). Intravascular danger signals guide neutrophils to sites of sterile inflammation. *Science* 330, 362-366.
- McKenna, H.J., Stocking, K.L., Miller, R.E., Brasel, K., De Smedt, T., Maraskovsky, E., Maliszewski, C.R., Lynch, D.H., Smith, J., Pulendran, B., et al. (2000). Mice lacking flt3 ligand have deficient hematopoiesis affecting hematopoietic progenitor cells, dendritic cells, and natural killer cells. *Blood* 95, 3489-3497.
- McKenna, K., Beignon, A.-S., and Bhardwaj, N. (2005). Plasmacytoid dendritic cells: linking innate and adaptive immunity. *J Virol* 79, 17-27.
- McKimmie, C.S., Fraser, A.R., Hansell, C., Gutiérrez, L., Philipsen, S., Connell, L., Rot, A., Kurowska-Stolarska, M., Carreno, P., Pruenster, M., et al. (2008). Hemopoietic cell expression of the chemokine decoy receptor D6 is dynamic and regulated by GATA1. *The Journal of Immunology* 181, 3353-3363.

- McCulloch, C.V., Morrow, V., Milasta, S., Comerford, I., Milligan, G., Graham, G.J., Isaacs, N.W., and Nibbs, R.J.B. (2008). Multiple roles for the C-terminal tail of the chemokine scavenger D6. *J Biol Chem* 283, 7972-7982.
- McLellan, A.D., Kapp, M., Eggert, A., Linden, C., Bommhardt, U., Bröcker, E.-B., Kämmerer, U., and Kämpgen, E. (2002). Anatomic location and T-cell stimulatory functions of mouse dendritic cell subsets defined by CD4 and CD8 expression. *Blood* 99, 2084-2093.
- Mebius, R.E., and Kraal, G. (2005). Structure and function of the spleen. *Nat Rev Immunol* 5, 606-616.
- Mellado, M., Rodríguez-Frade, J.M., Mañes, S., and Martínez-A, C. (2001). Chemokine signaling and functional responses: the role of receptor dimerization and TK pathway activation. *Annu. Rev. Immunol.* 19, 397-421.
- Mestas, J., and Hughes, C.C.W. (2004). Of mice and not men: differences between mouse and human immunology. *J Immunol* 172, 2731-2738.
- Metzger, T.C., and Anderson, M.S. (2011). Control of central and peripheral tolerance by Aire. *Immunol Rev* 241, 89-103.
- Middleton, J., Patterson, A.M., Gardner, L., Schmutz, C., and Ashton, B.A. (2002). Leukocyte extravasation: chemokine transport and presentation by the endothelium. *Blood* 100, 3853-3860.
- Mildner, A., Mack, M., Schmidt, H., Brück, W., Djukic, M., Zabel, M.D., Hille, A., Priller, J., and Prinz, M. (2009). CCR2+Ly-6Chi monocytes are crucial for the effector phase of autoimmunity in the central nervous system. *Brain* 132, 2487-2500.
- Miller, J.C., Brown, B.D., Shay, T., Gautier, E.L., Jojic, V., Cohain, A., Pandey, G., Leboeuf, M., Elpek, K.G., Helft, J., et al. (2012). Deciphering the transcriptional network of the dendritic cell lineage. *Nat Immunol* 13, 888-899.
- Miloud, T., Hämmerling, G.J., and Garbi, N. (2010). Review of murine dendritic cells: types, location, and development. *Methods Mol Biol* 595, 21-42.
- Misslitz, A., Pabst, O., Hintzen, G., Ohl, L., Kremmer, E., Petrie, H.T., and Förster, R. (2004). Thymic T cell development and progenitor localization depend on CCR7. *J Exp Med* 200, 481-491.
- Mitchell, J. (1973). Lymphocyte circulation in the spleen. Marginal zone bridging channels and their possible role in cell traffic. *Immunology* 24, 93-107.
- Mittelbrunn, M., del Hoyo, G.M., Lopez-Bravo, M., Martin-Cofreces, N.B., Scholer, A., Hugues, S., Fetler, L., Amigorena, S., Ardavin, C., and Sánchez-Madrid, F. (2009). Imaging of plasmacytoid dendritic cell interactions with T cells. *Blood* 113, 75-84.
- Miyasaka, M., and Tanaka, T. (2004). Lymphocyte trafficking across high endothelial venules: dogmas and enigmas. *Nat Rev Immunol* 4, 360-370.
- Mizutani, M., Pino, P.A., Saederup, N., Charo, I.F., Ransohoff, R.M., and Cardona, A.E. (2011). The Fractalkine Receptor but Not CCR2 Is Present on Microglia from Embryonic Development throughout Adulthood. *The Journal of Immunology* 188, 29-36.
- Morrison, B.E., Park, S.J., Mooney, J.M., and Mehrad, B. (2003). Chemokine-mediated recruitment of NK cells is a critical host defense mechanism in invasive aspergillosis. *J Clin Invest* 112, 1862-1870.
- Mouriès, J., Moron, G., Schlecht, G., Escriou, N., Dadaglio, G., and Leclerc, C. (2008). Plasmacytoid dendritic cells efficiently cross-prime naive T cells in vivo after TLR activation. *Blood* 112, 3713-3722.
- Mueller, A., Mahmoud, N.G., and Strange, P.G. (2006). Diverse signalling by different chemokines through the chemokine receptor CCR5. *Biochemical Pharmacology* 72, 739-748.
- Muppidi, J.R., Arnon, T.I., Bronevetsky, Y., Veerapen, N., Tanaka, M., Besra, G.S., and Cyster, J.G. (2011). Cannabinoid receptor 2 positions and retains marginal zone B cells within the splenic marginal zone. *Journal of Experimental Medicine* 208, 1941-1948.
- Murdoch, C., and Finn, A. (2000). Chemokine receptors and their role in inflammation and infectious diseases. *Blood* 95, 3032-3043.

- Murphy, P.M., Baggiolini, M., Charo, I.F., Hébert, C.A., Horuk, R., Matsushima, K., Miller, L.H., Oppenheim, J.J., and Power, C.A. (2000). International union of pharmacology. XXII. Nomenclature for chemokine receptors. *Pharmacol. Rev.* 52, 145-176.
- Murphy, K.M., Heimberger, A.B., and Loh, D.Y. (1990). Induction by antigen of intrathymic apoptosis of CD4+CD8+TCRlo thymocytes in vivo. *Science* 250, 1720-1723.
- Naik, S.H., Corcoran, L.M., and Wu, L. (2005a). Development of murine plasmacytoid dendritic cell subsets. *Immunol Cell Biol* 83, 563-570.
- Naik, S.H., Metcalf, D., van Nieuwenhuijze, A., Wicks, I., Wu, L., O'Keeffe, M., and Shortman, K. (2006). Intrasplenic steady-state dendritic cell precursors that are distinct from monocytes. *Nat Immunol* 7, 663-671.
- Naik, S.H., O'Keeffe, M., and Wu, L. (2010). CD8+, CD8-, and plasmacytoid dendritic cell generation in vitro using flt3 ligand. *Methods Mol Biol* 595, 167-176.
- Naik, S.H., Proietto, A.I., Wilson, N.S., Dakic, A., Schnorrer, P., Fuchsberger, M., Lahoud, M.H., O'Keeffe, M., Shao, Q.-X., Chen, W.-F., et al. (2005b). Cutting edge: generation of splenic CD8+ and CD8- dendritic cell equivalents in Fms-like tyrosine kinase 3 ligand bone marrow cultures. *J Immunol* 174, 6592-6597.
- Naik, S.H., Sathe, P., Park, H.-Y., Metcalf, D., Proietto, A.I., Dakic, A., Carotta, S., O'Keeffe, M., Bahlo, M., Papenfuss, A., et al. (2007). Development of plasmacytoid and conventional dendritic cell subtypes from single precursor cells derived in vitro and in vivo. *Nat Immunol* 8, 1217-1226.
- Nakano, H., Lin, K.L., Yanagita, M., Charbonneau, C., Cook, D.N., Kakiuchi, T., and Gunn, M.D. (2009). Blood-derived inflammatory dendritic cells in lymph nodes stimulate acute T helper type 1 immune responses. *Nat Immunol* 10, 394-402.
- Nakano, H., Yanagita, M., and Gunn, M.D. (2001). CD11c(+)B220(+)Gr-1(+) cells in mouse lymph nodes and spleen display characteristics of plasmacytoid dendritic cells. *J Exp Med* 194, 1171-1178.
- Nansen, A., Marker, O., Bartholdy, C., and Thomsen, A.R. (2000). CCR2+ and CCR5+ CD8+ T cells increase during viral infection and migrate to sites of infection. *Eur J Immunol* 30, 1797-1806.
- Neel, N.F., Schutyser, E., Sai, J., Fan, G.-H., and Richmond, A. (2009). Chemokine receptor internalization and intracellular trafficking. *Cytokine Growth Factor Rev* 16, 637-658.
- Nibbs, R.J.B., Gilchrist, D.S., King, V., Ferrar, A., Forrow, S., Hunter, K.D., and Graham, G.J. (2007). The atypical chemokine receptor D6 suppresses the development of chemically induced skin tumors. *J Clin Invest* 117, 1884-1892.
- Nibbs, R., Graham, G., and Rot, A. (2003). Chemokines on the move: control by the chemokine "interceptors" Duffy blood group antigen and D6. *Semin Immunol* 15, 287-294.
- Nibbs, R.J.B., Kriehuber, E., Ponath, P.D., Parent, D., Qin, S., Campbell, J.D.M., Henderson, A., Kerjaschki, D., Maurer, D., Graham, G.J., et al. (2001). The B-Chemokine Receptor D6 Is Expressed by Lymphatic Endothelium and a Subset of Vascular Tumors. *Am J Pathol* 158, 867-877.
- Nibbs, R.J., Wylie, S.M., Pragnell, I.B., and Graham, G.J. (1997a). Cloning and characterization of a novel murine beta chemokine receptor, D6. Comparison to three other related macrophage inflammatory protein-1alpha receptors, CCR-1, CCR-3, and CCR-5. *J Biol Chem* 272, 12495-12504.
- Nibbs, R.J., Wylie, S.M., Yang, J., Landau, N.R., and Graham, G.J. (1997b). Cloning and characterization of a novel promiscuous human beta-chemokine receptor D6. *J Biol Chem* 272, 32078-32083.
- Nieto, M., Frade, J.M., Sancho, D., Mellado, M., Martínez-A, C., and Sánchez-Madrid, F. (1997). Polarization of chemokine receptors to the leading edge during lymphocyte chemotaxis. *J Exp Med* 186, 153-158.
- Nitta, T., Murata, S., Ueno, T., Tanaka, K., and Takahama, Y. (2008). Thymic microenvironments for T-cell repertoire formation. *Adv. Immunol.* 99, 59-94.

- Obata, K., Mukai, K., Tsujimura, Y., Ishiwata, K., Kawano, Y., Minegishi, Y., Watanabe, N., and Karasuyama, H. (2007). Basophils are essential initiators of a novel type of chronic allergic inflammation. *Blood* *110*, 913-920.
- Ohl, L., Bernhardt, G., Pabst, O., and Förster, R. (2003a). Chemokines as organizers of primary and secondary lymphoid organs. *Semin Immunol* *15*, 249-255.
- Ohl, L., Henning, G., Krautwald, S., Lipp, M., Hardtke, S., Bernhardt, G., Pabst, O., and Förster, R. (2003b). Cooperating Mechanisms of CXCR5 and CCR7 in Development and Organization of Secondary Lymphoid Organs. *Journal of Experimental Medicine* *197*, 1199-1204.
- Ohl, L., Mohaupt, M., Czeloth, N., Hintzen, G., Kiafard, Z., Zwirner, J., Blankenstein, T., Henning, G., and Förster, R. (2004). CCR7 Governs Skin Dendritic Cell Migration under Inflammatory and Steady-State Conditions. *Immunity* *21*, 279-288.
- Okada, T., Ngo, V.N., Ekland, E.H., Förster, R., Lipp, M., Littman, D.R., and Cyster, J.G. (2002). Chemokine Requirements for B Cell Entry to Lymph Nodes and Peyer's Patches. *Journal of Experimental Medicine* *196*, 65-75.
- O'Keeffe, M., Hochrein, H., Vremec, D., Caminschi, I., Miller, J.L., Anders, E.M., Wu, L., Lahoud, M.H., Henri, S., Scott, B., et al. (2002). Mouse Plasmacytoid Cells: Long-lived Cells, Heterogeneous in Surface Phenotype and Function, that Differentiate Into CD8⁺ Dendritic Cells Only after Microbial Stimulus. *Journal of Experimental Medicine* *196*, 1307-1319.
- Omatsu, Y., Iyoda, T., Kimura, Y., Maki, A., Ishimori, M., Toyama-Sorimachi, N., and Inaba, K. (2005). Development of murine plasmacytoid dendritic cells defined by increased expression of an inhibitory NK receptor, Ly49Q. *J Immunol* *174*, 6657-6662.
- Oppermann, M., Mack, M., Proudfoot, A.E., and Olbrich, H. (1999). Differential effects of CC chemokines on CC chemokine receptor 5 (CCR5) phosphorylation and identification of phosphorylation sites on the CCR5 carboxyl terminus. *J Biol Chem* *274*, 8875-8885.
- Osterholzer, J.J., Ames, T., Polak, T., Sonstein, J., Moore, B.B., Chensue, S.W., Toews, G.B., and Curtis, J.L. (2005). CCR2 and CCR6, but not endothelial selectins, mediate the accumulation of immature dendritic cells within the lungs of mice in response to particulate antigen. *J Immunol* *175*, 874-883.
- Osterholzer, J.J., Chen, G.-H., Olszewski, M.A., Curtis, J.L., Huffnagle, G.B., and Toews, G.B. (2009). Accumulation of CD11b⁺ lung dendritic cells in response to fungal infection results from the CCR2-mediated recruitment and differentiation of Ly-6Chigh monocytes. *The Journal of Immunology* *183*, 8044-8053.
- Osterholzer, J.J., Curtis, J.L., Polak, T., Ames, T., Chen, G.-H., McDonald, R., Huffnagle, G.B., and Toews, G.B. (2008). CCR2 mediates conventional dendritic cell recruitment and the formation of bronchovascular mononuclear cell infiltrates in the lungs of mice infected with *Cryptococcus neoformans*. *J Immunol* *181*, 610-620.
- Palamara, F., Meindl, S., Holcmann, M., Lühns, P., Stingl, G., and Sibilina, M. (2004). Identification and characterization of pDC-like cells in normal mouse skin and melanomas treated with imiquimod. *J Immunol* *173*, 3051-3061.
- Palframan, R.T., Jung, S., Cheng, G., Weninger, W., Luo, Y., Dorf, M., Littman, D.R., Rollins, B.J., Zweerink, H., Rot, A., et al. (2001). Inflammatory chemokine transport and presentation in HEV: a remote control mechanism for monocyte recruitment to lymph nodes in inflamed tissues. *J Exp Med* *194*, 1361-1373.
- Palmer, E. (2003). Cell death and immunity: Negative selection – clearing out the bad apples from the T-cell repertoire. *Nat Rev Immunol* *3*, 383-391.
- Panopoulos, A.D., Zhang, L., Snow, J.W., Jones, D.M., Smith, A.M., Kasmi, El, K.C., Liu, F., Goldsmith, M.A., Link, D.C., Murray, P.J., et al. (2006). STAT3 governs distinct pathways in emergency granulopoiesis and mature neutrophils. *Blood* *108*, 3682-3690.
- Pappu, R., Schwab, S.R., Cornelissen, I., Pereira, J.P., Regard, J.B., Xu, Y., Camerer, E., Zheng, Y.W., Huang, Y., Cyster, J.G., et al. (2007). Promotion of Lymphocyte Egress into Blood and Lymph by Distinct Sources of Sphingosine-1-Phosphate. *Science* *316*, 295-298.

- Parker, L.C., Whyte, M.K.B., Vogel, S.N., Dower, S.K., and Sabroe, I. (2004). Toll-like receptor (TLR)2 and TLR4 agonists regulate CCR expression in human monocytic cells. *J Immunol* 172, 4977-4986.
- Pascual, V., Farkas, L., and Banchereau, J. (2006). Systemic lupus erythematosus: all roads lead to type I interferons. *Curr Opin Immunol* 18, 676-682.
- Penido, C., Costa, M.F.S., Souza, M.C., Costa, K.A., Candéa, A.L.P., Benjamim, C.F., and Henriques, M.D.G.M.O. (2008). Involvement of CC chemokines in gammadelta T lymphocyte trafficking during allergic inflammation: the role of CCL2/CCR2 pathway. *Int Immunol* 20, 129-139.
- Penna, G., Sozzani, S., and Adorini, L. (2001). Cutting edge: selective usage of chemokine receptors by plasmacytoid dendritic cells. *J Immunol* 167, 1862-1866.
- Peters, W., Cyster, J.G., Mack, M., Schlöndorff, D., Wolf, A.J., Ernst, J.D., and Charo, I.F. (2004). CCR2-dependent trafficking of F4/80dim macrophages and CD11cdim/intermediate dendritic cells is crucial for T cell recruitment to lungs infected with *Mycobacterium tuberculosis*. *J Immunol* 172, 7647-7653.
- Peters, W., Dupuis, M., and Charo, I.F. (2000). A mechanism for the impaired IFN-gamma production in C-C chemokine receptor 2 (CCR2) knockout mice: role of CCR2 in linking the innate and adaptive immune responses. *J Immunol* 165, 7072-7077.
- Pettit, E.J., and Fay, F.S. (1998). Cytosolic free calcium and the cytoskeleton in the control of leukocyte chemotaxis. *Physiol. Rev.* 78, 949-967.
- Pillai, S., and Cariappa, A. (2009). The follicular versus marginal zone B lymphocyte cell fate decision. *Nat Rev Immunol* 9, 767-777.
- Pillai, S., Cariappa, A., and Moran, S.T. (2005). Marginal zone B cells. *Annu. Rev. Immunol.* 23, 161-196.
- Powner, D., Kopp, P.M., Monkley, S.J., Critchley, D.R., and Berditchevski, F. (2011). Tetraspanin CD9 in cell migration. *Biochem. Soc. Trans.* 39, 563-567.
- Premont, R.T., and Gainetdinov, R.R. (2007). Physiological roles of G protein-coupled receptor kinases and arrestins. *Annu. Rev. Physiol.* 69, 511-534.
- Preobrazhensky, A.A., Dragan, S., Kawano, T., Gavrilin, M.A., Gulina, I.V., Chakravarty, L., and Kolattukudy, P.E. (2000). Monocyte chemotactic protein-1 receptor CCR2B is a glycoprotein that has tyrosine sulfation in a conserved extracellular N-terminal region. *J Immunol* 165, 5295-5303.
- Prinz, M., and Priller, J. (2010). Tickets to the brain: role of CCR2 and CX3CR1 in myeloid cell entry in the CNS. *J. Neuroimmunol.* 224, 80-84.
- Pulendran, B., Lingappa, J., Kennedy, M.K., Smith, J., Teepe, M., Rudensky, A., Maliszewski, C.R., and Maraskovsky, E. (1997). Developmental pathways of dendritic cells in vivo: distinct function, phenotype, and localization of dendritic cell subsets in FLT3 ligand-treated mice. *J Immunol* 159, 2222-2231.
- Rahman, A.H., Taylor, D.K., and Turka, L.A. (2009). The contribution of direct TLR signaling to T cell responses. *Immunol Res* 45, 25-36.
- Rajagopalan, L., and Rajarathnam, K. (2006). Structural Basis of Chemokine Receptor Function—A Model for Binding Affinity and Ligand Selectivity. *Biosci Rep* 26, 325-339.
- Raman, D., Sobolik-Delmaire, T., and Richmond, A. (2011). Chemokines in health and disease. *Exp Cell Res* 317, 575-589.
- Randall, T.D., Carragher, D.M., and Rangel-Moreno, J. (2008). Development of Secondary Lymphoid Organs. *Annu. Rev. Immunol.* 26, 627-650.
- Randolph, G.J., Ochoa, J., and Partida-Sánchez, S. (2008). Migration of dendritic cell subsets and their precursors. *Annu. Rev. Immunol.* 26, 293-316.
- Raz, E., and Reichman-Fried, M. (2006). Attraction rules: germ cell migration in zebrafish. *Current Opinion in Genetics & Development* 16, 355-359.
- Reichel, C.A., Khandoga, A., Anders, H.-J., Schlöndorff, D., Luckow, B., and Krombach, F. (2006). Chemokine receptors Ccr1, Ccr2, and Ccr5 mediate neutrophil migration to postischemic tissue. *J Leukoc Biol* 79, 114-122.

- Reid, S., Ritchie, A., Boring, L., Gosling, J., Cooper, S., Hangoc, G., Charo, I.F., and Broxmeyer, H.E. (1999). Enhanced myeloid progenitor cell cycling and apoptosis in mice lacking the chemokine receptor, CCR2. *Blood* 93, 1524-1533.
- Reiss, Y., Proudfoot, A.E., Power, C.A., Campbell, J.J., and Butcher, E.C. (2001). CC chemokine receptor (CCR)4 and the CCR10 ligand cutaneous T cell-attracting chemokine (CTACK) in lymphocyte trafficking to inflamed skin. *J Exp Med* 194, 1541-1547.
- Reizis, B. (2010). Regulation of plasmacytoid dendritic cell development. *Curr Opin Immunol* 22, 206-211.
- Reizis, B., Bunin, A., Ghosh, H.S., Lewis, K.L., and Sisirak, V. (2011a). Plasmacytoid dendritic cells: recent progress and open questions. *Annu. Rev. Immunol.* 29, 163-183.
- Reizis, B., Colonna, M., Trinchieri, G., Barrat, F., and Gilliet, M. (2011b). Plasmacytoid dendritic cells: one-trick ponies or workhorses of the immune system? *Nat Rev Immunol.*
- Rickel, E.A., Siegel, L.A., Yoon, B.-R.P., Rottman, J.B., Kugler, D.G., Swart, D.A., Anders, P.M., Tocker, J.E., Comeau, M.R., and Budelsky, A.L. (2008). Identification of functional roles for both IL-17RB and IL-17RA in mediating IL-25-induced activities. *The Journal of Immunology* 181, 4299-4310.
- Rodewald, H.-R. (2008). Thymus Organogenesis. *Annu. Rev. Immunol.* 26, 355-388.
- Rodríguez-Frade, J.M., Vila-Coro, A.J., de Ana, A.M., Albar, J.P., Martínez-A, C., and Mellado, M. (1999). The chemokine monocyte chemoattractant protein-1 induces functional responses through dimerization of its receptor CCR2. *Proceedings of the National Academy of Sciences of the United States of America* 96, 3628-3633.
- Rönnblom, L., and Pascual, V. (2008). The innate immune system in SLE: type I interferons and dendritic cells. *Lupus* 17, 394-399.
- Roosendaal, R., Mebius, R.E., and Kraal, G. (2008). The conduit system of the lymph node. *Int Immunol* 20, 1483-1487.
- Rose, S., Misharin, A., and Perlman, H. (2011). A novel Ly6C/Ly6G-based strategy to analyze the mouse splenic myeloid compartment. *Cytometry* 81A, 343-350.
- Rossi, D., and Zlotnik, A. (2000). The biology of chemokines and their receptors. *Annu. Rev. Immunol.* 18, 217-242.
- Rot, A., and von Andrian, U.H. (2004). Chemokines in innate and adaptive host defense: basic chemokines grammar for immune cells. *Annu. Rev. Immunol.* 22, 891-928.
- Sabroe, I., Parker, L., Dower, S., and Whyte, M. (2008). The role of TLR activation in inflammation. *J. Pathol.* 214, 126-135.
- Saederup, N., Cardona, A.E., Croft, K., Mizutani, M., Cotleur, A.C., Tsou, C.-L., Ransohoff, R.M., and Charo, I.F. (2010). Selective chemokine receptor usage by central nervous system myeloid cells in CCR2-red fluorescent protein knock-in mice. *PLoS ONE* 5, e13693.
- Salanga, C.L., and Handel, T.M. (2011). Chemokine oligomerization and interactions with receptors and glycosaminoglycans: The role of structural dynamics in function. *Exp Cell Res* 317, 590-601.
- Salanga, C.L., O'Hayre, M., and Handel, T. (2009). Modulation of chemokine receptor activity through dimerization and crosstalk. *Cell Mol Life Sci* 66, 1370-1386.
- Salio, M., Palmowski, M.J., Atzberger, A., Hermans, I.F., and Cerundolo, V. (2004). CpG-matured murine plasmacytoid dendritic cells are capable of in vivo priming of functional CD8 T cell responses to endogenous but not exogenous antigens. *J Exp Med* 199, 567-579.
- Sallusto, F., Geginat, J., and Lanzavecchia, A. (2004). Central Memory and Effector Memory T Cell Subsets: Function, Generation, and Maintenance. *Annu. Rev. Immunol.* 22, 745-763.
- Sallusto, F., Kremmer, E., Palermo, B., Hoy, A., Ponath, P., Qin, S., Förster, R., Lipp, M., and Lanzavecchia, A. (1999). Switch in chemokine receptor expression upon TCR stimulation reveals novel homing potential for recently activated T cells. *Eur J Immunol* 29, 2037-2045.

- Sallusto, F., and Lanzavecchia, A. (2002). The instructive role of dendritic cells on T-cell responses. *Arthritis Res. 4 Suppl 3*, S127-S132.
- Sallusto, F., Schaerli, P., Loetscher, P., Schaniel, C., Lenig, D., Mackay, C.R., Qin, S., and Lanzavecchia, A. (1998). Rapid and coordinated switch in chemokine receptor expression during dendritic cell maturation. *Eur J Immunol* 28, 2760-2769.
- Sansom, D.M., Manzotti, C.N., and Zheng, Y. (2003). What's the difference between CD80 and CD86? *Trends Immunol* 24, 313-318.
- Santiago-Raber, M.-L., Baudino, L., and Izui, S. (2009). Emerging roles of TLR7 and TLR9 in murine SLE. *J Autoimmun* 33, 231-238.
- Sapozhnikov, A., Fischer, J.A.A., Zaft, T., Krauthgamer, R., Dzionek, A., and Jung, S. (2007). Organ-dependent in vivo priming of naive CD4+, but not CD8+, T cells by plasmacytoid dendritic cells. *Journal of Experimental Medicine* 204, 1923-1933.
- Sartor, R.B. (2006). Mechanisms of Disease: pathogenesis of Crohn's disease and ulcerative colitis. *Nat Clin Pract Gastroenterol Hepatol* 3, 390-407.
- Sathe, P., and Shortman, K. (2008). The steady-state development of splenic dendritic cells. *Mucosal Immunology* 1, 425-431.
- Sánchez-Alcañiz, J.A., Haege, S., Mueller, W., Pla, R., Mackay, F., Schulz, S., López-Bendito, G., Stumm, R., and Marín, O. (2011). Cxcr7 Controls Neuronal Migration by Regulating Chemokine Responsiveness. *Neuron* 69, 77-90.
- Sato, N., Ahuja, S.K., Quinones, M., KostECKI, V., Reddick, R.L., Melby, P.C., Kuziel, W.A., and Ahuja, S.S. (2000). CC chemokine receptor (CCR)2 is required for langerhans cell migration and localization of T helper cell type 1 (Th1)-inducing dendritic cells. Absence of CCR2 shifts the Leishmania major-resistant phenotype to a susceptible state dominated by Th2 cytokines, b cell outgrowth, and sustained neutrophilic inflammation. *J Exp Med* 192, 205-218.
- Savino, B., Castor, M.G., Caronni, N., Sarukhan, A., Anselmo, A., Buracchi, C., Benvenuti, F., Pinho, V., Teixeira, M.M., Mantovani, A., et al. (2012). Control of murine Ly6Chigh monocyte traffic and immunosuppressive activities by atypical chemokine receptor D6. *Blood* 119, 5250-5260.
- Schlitzer, A., Heiseke, A.F., Einwächter, H., Reindl, W., Schiemann, M., Manta, C.-P., See, P., Niess, J.-H., Suter, T., Ginhoux, F., et al. (2012). Tissue-specific differentiation of a circulating CCR9- pDC-like common dendritic cell precursor. *Blood* 119, 6063-6071.
- Schlitzer, A., Loschko, J., Mair, K., Vogelmann, R., Henkel, L., Einwächter, H., Schiemann, M., Niess, J.-H., Reindl, W., and Krug, A. (2011). Identification of CCR9-murine plasmacytoid DC precursors with plasticity to differentiate into conventional DCs. *Blood* 117, 6562-6570.
- Schneider, M.A., Meingassner, J.G., Lipp, M., Moore, H.D., and Rot, A. (2007). CCR7 is required for the in vivo function of CD4+ CD25+ regulatory T cells. *Journal of Experimental Medicine* 204, 735-745.
- Schroeder, A., Mueller, O., Stocker, S., Salowsky, R., Leiber, M., Gassmann, M., Lightfoot, S., Menzel, W., Granzow, M., and Ragg, T. (2006). The RIN: an RNA integrity number for assigning integrity values to RNA measurements. *BMC Mol. Biol.* 7, 3.
- Schulz, C., Perdiguero, E.G., Chorro, L., Szabo-Rogers, H., Cagnard, N., Kierdorf, K., Prinz, M., Wu, B., Jacobsen, S.E.W., Pollard, J.W., et al. (2012). A Lineage of Myeloid Cells Independent of Myb and Hematopoietic Stem Cells. *Science* 336, 86-90.
- Schumann, K., Lämmermann, T., Bruckner, M., Legler, D.F., Polleux, J., Spatz, J.P., Schuler, G., Förster, R., Lutz, M.B., Sorokin, L., et al. (2010). Immobilized chemokine fields and soluble chemokine gradients cooperatively shape migration patterns of dendritic cells. *Immunity* 32, 703-713.
- Schwab, S.R., and Cyster, J.G. (2007). Finding a way out: lymphocyte egress from lymphoid organs. *Nat Immunol* 8, 1295-1301.
- Schwab, S.R., Pereira, J.P., Matloubian, M., Xu, Y., Huang, Y., and Cyster, J.G. (2005). Lymphocyte sequestration through S1P lyase inhibition and disruption of S1P gradients. *Science* 309, 1735-1739.

- Serbina, N.V., Hohl, T.M., Cherny, M., and Pamer, E.G. (2009). Selective expansion of the monocytic lineage directed by bacterial infection. *J Immunol* *183*, 1900-1910.
- Serbina, N.V., Jia, T., Hohl, T.M., and Pamer, E.G. (2008). Monocyte-mediated defense against microbial pathogens. *Annu. Rev. Immunol.* *26*, 421-452.
- Serbina, N.V., and Pamer, E.G. (2006). Monocyte emigration from bone marrow during bacterial infection requires signals mediated by chemokine receptor CCR2. *Nat Immunol* *7*, 311-317.
- Serra, H.M., Baena-Cagnani, C.E., and Eberhard, Y. (2004). Is secondary lymphoid-organ chemokine (SLC/CCL21) much more than a constitutive chemokine? *Allergy* *59*, 1219-1223.
- Seth, S., Oberdörfer, L., Hyde, R., Hoff, K., Thies, V., Worbs, T., Schmitz, S., and Förster, R. (2011). CCR7 essentially contributes to the homing of plasmacytoid dendritic cells to lymph nodes under steady-state as well as inflammatory conditions. *J Immunol* *186*, 3364-3372.
- Sharma, M., Afrin, F., Satija, N., Tripathi, R.P., and Gangenahalli, G.U. (2011). Stromal-derived factor-1/CXCR4 signaling: indispensable role in homing and engraftment of hematopoietic stem cells in bone marrow. *Stem Cells Dev.* *20*, 933-946.
- Sharpe, A.H., and Freeman, G.J. (2002). The B7-CD28 superfamily. *Nat Rev Immunol* *2*, 116-126.
- Shi, C., Jia, T., Mendez-Ferrer, S., Hohl, T.M., Serbina, N.V., Lipuma, L., Leiner, I., Li, M.O., Frenette, P.S., and Pamer, E.G. (2011). Bone marrow mesenchymal stem and progenitor cells induce monocyte emigration in response to circulating toll-like receptor ligands. *Immunity* *34*, 590-601.
- Shi, C., and Pamer, E.G. (2011). Monocyte recruitment during infection and inflammation. *Nat Rev Immunol* *11*, 762-774.
- Shi, C., Velázquez, Hohl, T.M., Leiner, I., Dustin, M.L., and Pamer, E.G. (2010). Monocyte trafficking to hepatic sites of bacterial infection is chemokine independent and directed by focal intercellular adhesion molecule-1 expression. *The Journal of Immunology* *184*, 6266-6274.
- Shortman, K., and Heath, W.R. (2010). The CD8⁺ dendritic cell subset. *Immunol Rev* *234*, 18-31.
- Shortman, K., and Naik, S.H. (2007). Steady-state and inflammatory dendritic-cell development. *Nat Rev Immunol* *7*, 19-30.
- Shulman, Z., Cohen, S.J., Roediger, B., Kalchenko, V., Jain, R., Grabovsky, V., Klein, E., Shinder, V., Stoler-Barak, L., Feigelson, S.W., et al. (2011). Transendothelial migration of lymphocytes mediated by intraendothelial vesicle stores rather than by extracellular chemokine depots. *Nat Immunol* *13*, 67-76.
- Sierro, F., Biben, C., Martínez-Muñoz, L., Mellado, M., Ransohoff, R.M., Li, M., Woehl, B., Leung, H., Groom, J., Batten, M., et al. (2007). Disrupted cardiac development but normal hematopoiesis in mice deficient in the second CXCL12/SDF-1 receptor, CXCR7. *Proceedings of the National Academy of Sciences of the United States of America* *104*, 14759-14764.
- Sigmundsdottir, H., Pan, J., Debes, G.F., Alt, C., Habtezion, A., Soler, D., and Butcher, E.C. (2007). DCs metabolize sunlight-induced vitamin D3 to “program” T cell attraction to the epidermal chemokine CCL27. *Nat Immunol* *8*, 285-293.
- Singh-Jasuja, H., Thiolat, A., Ribon, M., Boissier, M.-C., Bessis, N., Rammensee, H.-G., and Decker, P. (2012). The mouse dendritic cell marker CD11c is down-regulated upon cell activation through Toll-like receptor triggering. *Immunobiology* *1-12*.
- Sisirak, V., Faget, J., Gobert, M., Goutagny, N., Vey, N., Treilleux, I., Renaudineau, S., Poyet, G., Labidi-Galy, S.I., Goddard-Leon, S., et al. (2012). Impaired IFN- α production by Plasmacytoid dendritic cells favors regulatory T cell expansion and contributes to breast cancer progression. *Cancer Res.*
- Si, Y., Tsou, C.-L., Croft, K., and Charo, I.F. (2010). CCR2 mediates hematopoietic stem and progenitor cell trafficking to sites of inflammation in mice. *J Clin Invest* *120*, 1192-1203.

- Sixt, M., Kanazawa, N., Selg, M., Samson, T., Roos, G., Reinhardt, D.P., Pabst, R., Lutz, M.B., and Sorokin, L. (2005). The Conduit System Transports Soluble Antigens from the Afferent Lymph to Resident Dendritic Cells in the T Cell Area of the Lymph Node. *Immunity* 22, 19-29.
- Smit, J.J., Rudd, B.D., and Lukacs, N.W. (2006). Plasmacytoid dendritic cells inhibit pulmonary immunopathology and promote clearance of respiratory syncytial virus. *J Exp Med* 203, 1153-1159.
- Sorrentino, R., Morello, S., Luciano, A., Crother, T.R., Maiolino, P., Bonavita, E., Arra, C., Adcock, I.M., Arditi, M., and Pinto, A. (2010). Plasmacytoid Dendritic Cells Alter the Antitumor Activity of CpG-Oligodeoxynucleotides in a Mouse Model of Lung Carcinoma. *The Journal of Immunology* 185, 4641-4650.
- Souto, F.O., Alves-Filho, J.C., Turato, W.M., Auxiliadora-Martins, M., Basile-Filho, A., and Cunha, F.Q. (2011). Essential Role of CCR2 in Neutrophil Tissue Infiltration and Multiple Organ Dysfunction in Sepsis. *Am J Respir Crit Care Med* 183, 234-242.
- Souza-Fonseca-Guimaraes, F., Parlato, M., Fitting, C., Cavillon, J.M., and Adib-Conquy, M. (2012). NK Cell Tolerance to TLR Agonists Mediated by Regulatory T Cells after Polymicrobial Sepsis. *The Journal of Immunology* 188, 5850-5858.
- Sozzani, S., Allavena, P., Vecchi, A., and Mantovani, A. (1999). The role of chemokines in the regulation of dendritic cell trafficking. *J Leukoc Biol* 66, 1-9.
- Sozzani, S., Allavena, P., Vecchi, A., and Mantovani, A. (2000). Chemokines and dendritic cell traffic. *J Clin Immunol* 20, 151-160.
- Sozzani, S., Vermi, W., Del Prete, A., and Facchetti, F. (2010). Trafficking properties of plasmacytoid dendritic cells in health and disease. *Trends Immunol* 31, 270-277.
- Steinman, R.M., Hawiger, D., Liu, K., Bonifaz, L., Bonnyay, D., Mahnke, K., Iyoda, T., Ravetch, J., Dhodapkar, M., Inaba, K., et al. (2003). Dendritic cell function in vivo during the steady state: a role in peripheral tolerance. *Ann N Y Acad Sci* 987, 15-25.
- Stein, J.V., Rot, A., Luo, Y., Narasimhaswamy, M., Nakano, H., Gunn, M.D., Matsuzawa, A., Quackenbush, E.J., Dorf, M.E., and von Andrian, U.H. (2000). The CC chemokine thymus-derived chemotactic agent 4 (TCA-4, secondary lymphoid tissue chemokine, 6Ckine, exodus-2) triggers lymphocyte function-associated antigen 1-mediated arrest of rolling T lymphocytes in peripheral lymph node high endothelial venules. *J Exp Med* 191, 61-76.
- Stevenson, N.J., McFarlane, C., Ong, S.T., Nahlik, K., Kelvin, A., Addley, M.R., Long, A., Greaves, D.R., O'Farrelly, C., and Johnston, J.A. (2010). Suppressor of cytokine signalling (SOCS) 1 and 3 enhance cell adhesion and inhibit migration towards the chemokine eotaxin/CCL11. *FEBS Lett* 584, 4469-4474.
- Strauss-Ayali, D., Conrad, S.M., and Mosser, D.M. (2007). Monocyte subpopulations and their differentiation patterns during infection. *J Leukoc Biol* 82, 244-252.
- Sugimoto, Y., Katayama, N., Masuya, M., Miyata, E., Ueno, M., Ohishi, K., Nishii, K., Takakura, N., and Shiku, H. (2006). Differential cell division history between neutrophils and macrophages in their development from granulocyte-macrophage progenitors. *Br J Haematol* 135, 725-731.
- Sunderkötter, C., Nikolic, T., Dillon, M.J., van Rooijen, N., Stehling, M., Drevets, D.A., and Leenen, P.J.M. (2004). Subpopulations of mouse blood monocytes differ in maturation stage and inflammatory response. *J Immunol* 172, 4410-4417.
- Swiecki, M., and Colonna, M. (2010). Unraveling the functions of plasmacytoid dendritic cells during viral infections, autoimmunity, and tolerance. *Immunol Rev* 234, 142-162.
- Swiecki, M., Wang, Y., Gilfillan, S., Lenschow, D.J., and Colonna, M. (2012). Cutting Edge: Paradoxical Roles of BST2/Tetherin in Promoting Type I IFN Response and Viral Infection. *The Journal of Immunology* 188, 2488-2492.
- Swirski, F.K., Nahrendorf, M., Etzrodt, M., Wildgruber, M., Cortez-Retamozo, V., Panizzi, P., Figueiredo, J.-L., Kohler, R.H., Chudnovskiy, A., Waterman, P., et al. (2009). Identification of splenic reservoir monocytes and their deployment to inflammatory sites. *Science* 325, 612-616.

Tacke, F., Alvarez, D., Kaplan, T.J., Jakubzick, C., Spanbroek, R., Llodra, J., Garin, A., Liu, J., Mack, M., van Rooijen, N., et al. (2007). Monocyte subsets differentially employ CCR2, CCR5, and CX3CR1 to accumulate within atherosclerotic plaques. *J Clin Invest* 117, 185-194.

Tacke, F., and Randolph, G.J. (2006). Migratory fate and differentiation of blood monocyte subsets. *Immunobiology* 211, 609-618.

Takagi, H., Fukaya, T., Eizumi, K., Sato, Y., Sato, K., Shibasaki, A., Otsuka, H., Hijikata, A., Watanabe, T., Ohara, O., et al. (2011). Plasmacytoid Dendritic Cells Are Crucial for the Initiation of Inflammation and T Cell Immunity In Vivo. *Immunity* 35, 958-971.

Takeda, K., Kaisho, T., and Akira, S. (2003). Toll-like receptors. *Annu. Rev. Immunol.* 21, 335-376.

Tam, M.A., and Wick, M.J. (2004). Dendritic cells and immunity to *Listeria*: TipDCs are a new recruit. *Trends Immunol* 25, 335-339.

Tan, J.K.H., and O'Neill, H.C. (2007). Concise review: Dendritic cell development in the context of the spleen microenvironment. *Stem Cells* 25, 2139-2145.

Tel, J., Torensma, R., Figdor, C.G., and de Vries, I.J.M. (2010). IL-4 and IL-13 Alter Plasmacytoid Dendritic Cell Responsiveness to CpG DNA and Herpes Simplex Virus-1. *Journal of Investigative Dermatology* 131, 900-906.

Toma-Hirano, M., Namiki, S., Miyatake, S., Arai, K.-I., and Kamogawa-Schifter, Y. (2007). Type I interferon regulates pDC maturation and Ly49Q expression. *Eur J Immunol* 37, 2707-2714.

Townson, J.R., Barcellos, L.F., and Nibbs, R.J.B. (2002). Gene copy number regulates the production of the human chemokine CCL3-L1. *Eur J Immunol* 32, 3016-3026.

Toyama-Sorimachi, N.N., Tsujimura, Y.Y., Maruya, M.M., Onoda, A.A., Kubota, T.T., Koyasu, S.S., Inaba, K.K., and Karasuyama, H.H. (2004). Ly49Q, a member of the Ly49 family that is selectively expressed on myeloid lineage cells and involved in regulation of cytoskeletal architecture. *Proceedings of the National Academy of Sciences of the United States of America* 101, 1016-1021.

Traver, D., Akashi, K., Manz, M., Merad, M., Miyamoto, T., Engleman, E.G., and Weissman, I.L. (2000). Development of CD8alpha-positive dendritic cells from a common myeloid progenitor. *Science* 290, 2152-2154.

Traves, S.L., Smith, S.J., Barnes, P.J., and Donnelly, L.E. (2004). Specific CXC but not CC chemokines cause elevated monocyte migration in COPD: a role for CXCR2. *J Leukoc Biol* 76, 441-450.

Tsou, C.-L., Peters, W., Si, Y., Slaymaker, S., Aslanian, A.M., Weisberg, S.P., Mack, M., and Charo, I.F. (2007). Critical roles for CCR2 and MCP-3 in monocyte mobilization from bone marrow and recruitment to inflammatory sites. *J Clin Invest* 117, 902-909.

Tylaska, L.A., Boring, L., Weng, W., Aiello, R., Charo, I.F., Rollins, B.J., and Gladue, R.P. (2002). *Ccr2* regulates the level of MCP-1/CCL2 in vitro and at inflammatory sites and controls T cell activation in response to alloantigen. *Cytokine* 18, 184-190.

Uehara, S., Grinberg, A., Farber, J.M., and Love, P.E. (2002). A role for CCR9 in T lymphocyte development and migration. *J Immunol* 168, 2811-2819.

Ueno, T., Saito, F., Gray, D.H.D., Kuse, S., Hieshima, K., Nakano, H., Kakiuchi, T., Lipp, M., Boyd, R.L., and Takahama, Y. (2004). CCR7 signals are essential for cortex-medulla migration of developing thymocytes. *J Exp Med* 200, 493-505.

Ulich, T.R., Watson, L.R., Yin, S.M., Guo, K.Z., Wang, P., Thang, H., and del Castillo, J. (1991). The intratracheal administration of endotoxin and cytokines. I. Characterization of LPS-induced IL-1 and TNF mRNA expression and the LPS-, IL-1-, and TNF-induced inflammatory infiltrate. *Am J Pathol* 138, 1485-1496.

Ulvmar, M.H., Hub, E., and Rot, A. (2011). Atypical chemokine receptors. *Exp Cell Res* 317, 556-568.

Umamoto, E., Otani, K., Ikeno, T., Verjan Garcia, N., Hayasaka, H., Bai, Z., Jang, M.H., Tanaka, T., Nagasawa, T., Ueda, K., et al. (2012). Constitutive Plasmacytoid Dendritic

Cell Migration to the Splenic White Pulp Is Cooperatively Regulated by CCR7- and CXCR4-Mediated Signaling. *The Journal of Immunology* **189**, 191-199.

Vanbervliet, B., Bendriss-Vermare, N., Massacrier, C., Homey, B., de Bouteiller, O., Brière, F., Trinchieri, G., and Caux, C. (2003). The Inducible CXCR3 Ligands Control Plasmacytoid Dendritic Cell Responsiveness to the Constitutive Chemokine Stromal Cell-derived Factor 1 (SDF-1)/CXCL12. *Journal of Experimental Medicine* **198**, 823-830.

Varol, C., Landsman, L., Fogg, D.K., Greenshtein, L., Gildor, B., Margalit, R., Kalchenko, V., Geissmann, F., and Jung, S. (2007). Monocytes give rise to mucosal, but not splenic, conventional dendritic cells. *Journal of Experimental Medicine* **204**, 171-180.

Vecchi, A., Massimiliano, L., Ramponi, S., Luini, W., Bernasconi, S., Bonecchi, R., Allavena, P., Parmentier, M., Mantovani, A., and Sozzani, S. (1999). Differential responsiveness to constitutive vs. inducible chemokines of immature and mature mouse dendritic cells. *J Leukoc Biol* **66**, 489-494.

Veenstra, M., and Ransohoff, R.M. (2012). Chemokine receptor CXCR2: Physiology regulator and neuroinflammation controller? *J. Neuroimmunol.* **246**, 1-9.

Vergunst, C.E., Gerlag, D.M., Lopatinskaya, L., Klareskog, L., Smith, M.D., van den Bosch, F., Dinant, H.J., Lee, Y., Wyant, T., Jacobson, E.W., et al. (2008). Modulation of CCR2 in rheumatoid arthritis: A double-blind, randomized, placebo-controlled clinical trial. *Arthritis Rheum* **58**, 1931-1939.

Vermi, W., Riboldi, E., Wittamer, V., Gentili, F., Luini, W., Marrelli, S., Vecchi, A., Franssen, J.-D., Communi, D., Massardi, L., et al. (2005). Role of ChemR23 in directing the migration of myeloid and plasmacytoid dendritic cells to lymphoid organs and inflamed skin. *J Exp Med* **201**, 509-515.

Vetrano, S., Borroni, E.M., Sarukhan, A., Savino, B., Bonecchi, R., Correale, C., Arena, V., Fantini, M., Roncalli, M., Malesci, A., et al. (2010). The lymphatic system controls intestinal inflammation and inflammation-associated colon cancer through the chemokine decoy receptor D6. *Gut* **59**, 197-206.

Vicente-Manzanares, M., Choi, C.K., and Horwitz, A.R. (2009). Integrins in cell migration--the actin connection. *J. Cell. Sci.* **122**, 199-206.

Villadangos, J.A., and Young, L. (2008). Antigen-presentation properties of plasmacytoid dendritic cells. *Immunity* **29**, 352-361.

Volpe, S., Cameroni, E., Moepps, B., Thelen, S., Apuzzo, T., and Thelen, M. (2012). CCR2 Acts as Scavenger for CCL2 during Monocyte Chemotaxis. *PLoS ONE* **7**, e37208.

von Andrian, U.H., and Mempel, T.R. (2003). Homing and cellular traffic in lymph nodes. *Nat Rev Immunol* **3**, 867-878.

Vremec, D., Pooley, J., Hochrein, H., Wu, L., and Shortman, K. (2000). CD4 and CD8 expression by dendritic cell subtypes in mouse thymus and spleen. *J Immunol* **164**, 2978-2986.

Vremec, D., and Shortman, K. (1997). Dendritic cell subtypes in mouse lymphoid organs: cross-correlation of surface markers, changes with incubation, and differences among thymus, spleen, and lymph nodes. *J Immunol* **159**, 565-573.

Vroon, A., Heijnen, C.J., and Kavelaars, A. (2006). GRKs and arrestins: regulators of migration and inflammation. *J Leukoc Biol* **80**, 1214-1221.

Wang, Y., Li, G., Stanco, A., Long, J.E., Crawford, D., Potter, G.B., Pleasure, S.J., Behrens, T., and Rubenstein, J.L.R. (2011). CXCR4 and CXCR7 Have Distinct Functions in Regulating Interneuron Migration. *Neuron* **69**, 61-76.

Warnock, R.A., Askari, S., Butcher, E.C., and von Andrian, U.H. (1998). Molecular mechanisms of lymphocyte homing to peripheral lymph nodes. *J Exp Med* **187**, 205-216.

Weber, M., Blair, E., Simpson, C.V., O'Hara, M., Blackburn, P.E., Rot, A., Graham, G.J., and Nibbs, R.J.B. (2004). The chemokine receptor D6 constitutively traffics to and from the cell surface to internalize and degrade chemokines. *Mol. Biol. Cell* **15**, 2492-2508.

Wei, S., Kryczek, I., Zou, L., Daniel, B., Cheng, P., Mottram, P., Curiel, T., Lange, A., and Zou, W. (2005). Plasmacytoid dendritic cells induce CD8⁺ regulatory T cells in human ovarian carcinoma. *Cancer Res* **65**, 5020-5026.

- Weinlich, G., Heine, M., Stössel, H., Zanella, M., Stoitzner, P., Ortner, U., Smolle, J., Koch, F., Sepp, N.T., Schuler, G., et al. (1998). Entry into afferent lymphatics and maturation in situ of migrating murine cutaneous dendritic cells. *J Invest Dermatol* *110*, 441-448.
- Wells, T.N., Power, C.A., and Proudfoot, A.E. (1998). Definition, function and pathophysiological significance of chemokine receptors. *Trends Pharmacol. Sci.* *19*, 376-380.
- Wendland, M., Czeloth, N., Mach, N., Malissen, B., Kremmer, E., Pabst, O., and Förster, R. (2007). CCR9 is a homing receptor for plasmacytoid dendritic cells to the small intestine. *Proceedings of the National Academy of Sciences of the United States of America* *104*, 6347-6352.
- Wendland, M., Willenzon, S., Kocks, J., Davalos-Misnitz, A.C., Hammerschmidt, S.I., Schumann, K., Kremmer, E., Sixt, M., Hoffmeyer, A., Pabst, O., et al. (2011). Lymph node T cell homeostasis relies on steady state homing of dendritic cells. *Immunity* *35*, 945-957.
- Weninger, W., Crowley, M.A., Manjunath, N., and von Andrian, U.H. (2001). Migratory properties of naive, effector, and memory CD8(+) T cells. *J Exp Med* *194*, 953-966.
- Whitehead, G.S., Wang, T., DeGraff, L.M., Card, J.W., Lira, S.A., Graham, G.J., and Cook, D.N. (2006). The Chemokine Receptor D6 Has Opposing Effects on Allergic Inflammation and Airway Reactivity. *Am J Respir Crit Care Med* *175*, 243-249.
- Wilson, H.L., and O'Neill, H.C. (2003). Murine dendritic cell development: difficulties associated with subset analysis. *Immunol Cell Biol* *81*, 239-246.
- Wilson, N.S., El-Sukkari, D., Belz, G.T., Smith, C.M., Steptoe, R.J., Heath, W.R., Shortman, K., and Villadangos, J.A. (2003). Most lymphoid organ dendritic cell types are phenotypically and functionally immature. *Blood* *102*, 2187-2194.
- Witt, C.M., and Robey, E.A. (2004). The ins and outs of CCR7 in the thymus. *J Exp Med* *200*, 405-409.
- Worbs, T., and Förster, R. (2009). T cell migration dynamics within lymph nodes during steady state: an overview of extracellular and intracellular factors influencing the basal intranodal T cell motility. *Curr. Top. Microbiol. Immunol.* *334*, 71-105.
- Worbs, T., Bode, U., Yan, S., Hoffmann, M.W., Hintzen, G., Bernhardt, G., Förster, R., and Pabst, O. (2006). Oral tolerance originates in the intestinal immune system and relies on antigen carriage by dendritic cells. *J Exp Med* *203*, 519-527.
- Worbs, T., Mempel, T.R., Bolter, J., von Andrian, U.H., and Förster, R. (2007). CCR7 ligands stimulate the intranodal motility of T lymphocytes in vivo. *Journal of Experimental Medicine* *204*, 489-495.
- Workman, C.J., Szymczak-Workman, A.L., Collison, L.W., Pillai, M.R., and Vignali, D.A.A. (2009). The development and function of regulatory T cells. *Cell Mol Life Sci* *66*, 2603-2622.
- Wu, L., D'amico, A., Hochrein, H., O'Keeffe, M., Shortman, K., and Lucas, K. (2001). Development of thymic and splenic dendritic cell populations from different hemopoietic precursors. *Blood* *98*, 3376-3382.
- Wu, L., and Liu, Y.-J. (2007). Development of dendritic-cell lineages. *Immunity* *26*, 741-750.
- Xia, M., and Sui, Z. (2009). Recent developments in CCR2 antagonists. *Expert Opin Ther Pat* *19*, 295-303.
- Xu, L., Khandaker, M.H., Barlic, J., Ran, L., Borja, M.L., Madrenas, J., Rahimpour, R., Chen, K., Mitchell, G., Tan, C.M., et al. (2000). Identification of a novel mechanism for endotoxin-mediated down-modulation of CC chemokine receptor expression. *Eur J Immunol* *30*, 227-235.
- Yamaski, R., Liu, L., Lin, J., and Ransohoff, R.M. (2012). Role of CCR2 in immunobiology and neurobiology. *Clinical and Experimental Neuroimmunology* *3*, 16-29.
- Yanagawa, Y. (2002). CCL19 induces rapid dendritic extension of murine dendritic cells. *Blood* *100*, 1948-1956.

- Yona, S., and Jung, S. (2010). Monocytes: subsets, origins, fates and functions. *Current Opinion in Hematology* 17, 53-59.
- Yoneyama, H., Matsuno, K., Zhang, Y., Nishiwaki, T., Kitabatake, M., Ueha, S., Narumi, S., Morikawa, S., Ezaki, T., Lu, B., et al. (2004). Evidence for recruitment of plasmacytoid dendritic cell precursors to inflamed lymph nodes through high endothelial venules. *Int Immunol* 16, 915-928.
- Yrlid, U., Jenkins, C.D., and MacPherson, G.G. (2006). Relationships between distinct blood monocyte subsets and migrating intestinal lymph dendritic cells in vivo under steady-state conditions. *J Immunol* 176, 4155-4162.
- Yu, P., Wang, Y., Chin, R.K., Martinez-Pomares, L., Gordon, S., Kosco-Vibois, M.H., Cyster, J., and Fu, Y.-X. (2002). B cells control the migration of a subset of dendritic cells into B cell follicles via CXC chemokine ligand 13 in a lymphotoxin-dependent fashion. *J Immunol* 168, 5117-5123.
- Zachariah, M., and Cyster, J. (2009). Thymic egress: S1P of 1000. *F1000 Biol Rep.*
- Zanoni, I., and Granucci, F. (2010). Differences in lipopolysaccharide-induced signaling between conventional dendritic cells and macrophages. *Immunobiology* 215, 709-712.
- Zanoni, I., Ostuni, R., Capuano, G., Collini, M., Caccia, M., Ronchi, A.E., Rocchetti, M., Mingozzi, F., Foti, M., Chirico, G., et al. (2009). CD14 regulates the dendritic cell life cycle after LPS exposure through NFAT activation. *Nature* 1-6.
- Zhang, J., Raper, A., Sugita, N., Hingorani, R., and Crocker, P.R. (2006). Characterization of Siglec-H as a novel endocytic receptor expressed on murine plasmacytoid dendritic cell precursors. *Blood* 107, 3600-3608.
- Zhang, M., Angata, T., Cho, J.Y., Miller, M., Broide, D.H., and Varki, A. (2007). Defining the in vivo function of Siglec-F, a CD33-related Siglec expressed on mouse eosinophils. *Blood* 109, 4280-4287.
- Zhou, M.I., Foy, R.L., Chitalia, V.C., Zhao, J., Panchenko, M.V., Wang, H., and Cohen, H.T. (2005). Jade-1, a candidate renal tumor suppressor that promotes apoptosis. *Proceedings of the National Academy of Sciences of the United States of America* 102, 11035-11040.
- Zhou, Y., Yang, Y., Warr, G., and Bravo, R. (1999). LPS down-regulates the expression of chemokine receptor CCR2 in mice and abolishes macrophage infiltration in acute inflammation. *J Leukoc Biol* 65, 265-269.
- Zhu, J., and Paul, W.E. (2008). CD4 T cells: fates, functions, and faults. *Blood* 112, 1557-1569.
- Zhu, J., Yamane, H., and Paul, W.E. (2010). Differentiation of Effector CD4 T Cell Populations *. *Annu. Rev. Immunol.* 28, 445-489.
- Zlotoff, D.A., Sambandam, A., Logan, T.D., Bell, J.J., Schwarz, B.A., and Bhandoola, A. (2010). CCR7 and CCR9 together recruit hematopoietic progenitors to the adult thymus. *Blood* 115, 1897-1905.